Advanced Textbooks in Control and Signal Processing

Nhan T. Nguyen

Model-Reference Adaptive Control

A Primer

Springer

Advanced Textbooks in Control and Signal Processing

More information about this series at http://www.springer.com/series/4045

Nhan T. Nguyen

Model-Reference Adaptive Control

A Primer

Springer

Nhan T. Nguyen
Intelligent Systems
NASA Ames Research Center
Moffett Field, CA
USA

ISSN 1439-2232 ISSN 2510-3814 (electronic)
Advanced Textbooks in Control and Signal Processing
ISBN 978-3-319-56392-3 ISBN 978-3-319-56393-0 (eBook)
https://doi.org/10.1007/978-3-319-56393-0

Library of Congress Control Number: 2017953807

Printed on acid-free paper

This Springer imprint is published by Springer Nature
The registered company is Springer International Publishing AG
The registered company address is: Gewerbestrasse 11, 6330 Cham, Switzerland

To my wife Rosa and my children Daniel and Natalia

Series Editors' Foreword

The *Advanced Textbooks in Control and Signal Processing* series is designed as a vehicle for the systematic textbook presentation of both fundamental and innovative topics in the control and signal processing disciplines. It is hoped that prospective authors will welcome the opportunity to publish a more rounded and structured presentation of some of the newer emerging control and signal processing technologies in this textbook series. However, it is useful to note that there will always be a place in the series for contemporary presentations of foundational material in these important engineering areas.

The science of adaptive control design and implementation, as presented in this textbook, is motivated by some very practical problems found in real-world control applications. Probably the most important issue is maintaining the desired performance specifications and closed-loop system stability in the presence of changing process dynamics. The way a real system can change is an interesting topic in itself. A system may operate for long periods with unchanging parameters or characteristics and then change both significantly and rapidly when, for example, a new operating regime begins. Alternatively, a system may be changing all the time, sometimes slowly, as in the case of long-term component wear and degradation, and sometimes more rapidly as a product evolves or new operating regimes are entered.

When system change is predictable, the most widely applied forms of adaptive control are probably the controller gain schedule and the controller schedule *per se*. These technologies have the advantages of application transparency and, in safety-critical situations, verifiability. This approach has links to the methods of multimodel control design.

Another approach to adaptive control is that of online updates and improvements to linear parameter varying control designs when the underlying system is nonlinear, partially uncertain, or slowly changing. A technique that found much favor was that of self-tuning control. Although this technique has a very transparent architecture, it was soon realized that, even when plants were linear, these types of adaptive control problems are nonlinear systems that need nonlinear systems analysis for their study.

The other theme in this textbook is the use of a model-reference control framework. In the literature of deterministic control designs, such schemes are more likely to be termed "model-following" control systems. This class of techniques is an interesting field in its own right. Quite a few contributions focus on the use of classical PID controllers in the model-following framework to achieve additional robustness and performance gains in the presence of process uncertainty. A fundamental purpose of the model in these schemes is to instil the desired control system performance specifications such as overshoot, rise time, zero steady-state error, and prescribed stability margins. An important art in this method is to specify the model so that the closed-loop process can actually achieve the desired performance specifications.

Combining adaptive control with model-following design yields the class of methods known as model-reference adaptive control (MRAC). To understand such methods requires a good grounding in nonlinear systems methods and Lyapunov stability theory. This is where the text *Model-Reference Adaptive Control: A Primer* by Nhan T. Nguyen begins. Dr. Nguyen has distilled his many years of experience into this textbook for which the material has been tested on lecture courses given by the author. The material is presented in sharply focussed sections with examples, chapter exercises, and supporting references. Dr. Nguyen is a leading research scientist at the NASA Ames Research Center at Moffett Field, California, USA, and his extensive research has included an exploration of the potential of MRAC in aerospace applications. This experience is reflected in the textbook through the discussions he presents on the certification and validation of adaptive control methods in safety-critical systems and high-risk human aerospace applications. Outcomes from Dr. Nguyen's experiences are also evident in the final chapter of the textbook that contains the details of a number of case studies mostly drawn from the aerospace field. The Series Editors are pleased to welcome this application-orientated textbook to the *Advanced Textbooks in Control and Signal Processing* series and believe it will find a wide readership in the control and aerospace communities.

January 2017

M. J. Grimble
M. A. Johnson
Industrial Control Centre
Glasgow, Scotland, UK

Preface

This textbook is developed from a series of lecture notes for graduate courses that the author has taught. The textbook includes new research materials that the author developed during his research at NASA Ames Research Center. The intended readers of this book are masters-level graduate students and beginning doctoral students. The author notes that there exist many excellent advanced adaptive control textbooks that provide in-depth rigorous mathematical control theory aimed at doctoral and post-doctoral researchers. This textbook is aimed at applied control theory and applications intended to provide the readers a sufficient working understanding of adaptive control theory through applications. Examples and problem sets are used to reinforce the materials and aid the understanding through applications of adaptive control techniques. A solutions manual for many of the problems, available free of charge to instructors who adopt this textbook for use in teaching their courses, can be downloaded from http://www.springer.com/book/9783319563923. During the course of teaching, the author feels that such a textbook could help beginning graduate students to better understand and appreciate the richness of adaptive control without feeling being overwhelmed by the mathematics of real analysis required in adaptive control theory. It is with this objective in mind that the author decided to compose this manuscript.

Adaptive control is a well-researched subject, and as such, the subject is enriched by a voluminous body of research literature. Many new advancements in adaptive control theory are still being developed in the present time. The textbook does not attempt to incorporate all of the latest developments in adaptive control theory, for this would require an extensive endeavor which would be exceedingly beyond the scope of this textbook. Rather, the book tries to provide a foundation in the model-reference adaptive control with basic well-accepted adaptive control techniques. Parameter estimation by least-squares techniques and uncertainty approximation by neural networks are covered. The second half of the book is devoted to the subject of robust adaptive control. Robustness issues with model-reference adaptive control are discussed. Standard methods to improve robustness are covered in the remainder of the second half of the textbook. These include well-established methods, such as the dead zone, projection, σ modification, and e modification.

More recent robust adaptive control methods are also covered. These include the author's work in optimal control modification and bi-objective optimal control modification, as well as two recent well-known adaptive control methods: the adaptive loop recovery and $\mathcal{L}_1$ adaptive control. The author well recognizes that this is by no means a complete exposition of all the latest advancements in robust adaptive control theory. The readers will be referred to a list of references provided in the bibliography for other adaptive control methods. Finally, this book includes a chapter on applications. In particular, the applications on adaptive flight control are exhibited from the author's body of research in this field.

Acknowledgements

The author wishes to acknowledge NASA Aeronautics Research Mission Directorate for providing the author with the opportunity to conduct research in adaptive control theory in the course of conducting aviation safety research. The author is appreciative of all the support from his colleagues at NASA Ames Research Center and NASA Armstrong (formerly Dryden) Flight Research Center during the course of research and flight testing of adaptive flight controllers on NASA research aircraft. In particular, the author wants to thank Joseph Totah and Kalmanje Krishnakumar of NASA Ames Research Center for their organizational support to allow the pursuit of this research. The author is appreciative of the friendly collaboration with John Bosworth, Curtis Hanson, and in particular John Burken of NASA Armstrong Flight Research Center on flight test validation of adaptive control. The author would like to acknowledge Prof. Anthony Calise, Prof. Naira Hovakimyan, and Prof. Kumpati Narendra for allowing their work to be included in the manuscript. The author also would like to acknowledge Stephen Jacklin at NASA Ames Research Center for his thorough and insightful input on the certification of adaptive control. Finally, the author would be remiss without acknowledging the support of the author's family that allows him the personal freedom to pursue the research that goes into this manuscript.

Santa Clara, CA, USA Nhan T. Nguyen
November 2016

Contents

1 Introduction 1
1.1 Overview 2
1.2 Verification and Validation Challenges for Adaptive Flight Control Systems 6
1.2.1 Verification by Simulation of Adaptive Flight Control Systems 7
1.2.2 Adaptive Control Metrics 8
1.3 Summary 9
References 9

2 Nonlinear Systems 17
2.1 Equilibrium and Linearization 21
2.2 Local Stability and Phase Plane Analysis 24
2.3 Other Nonlinear Behaviors 27
2.4 Summary 28
2.5 Exercises 29
Reference 30

3 Mathematical Preliminaries 31
3.1 Vector and Matrix Norms 31
3.1.1 Vector Norms 31
3.1.2 Matrix Norms 35
3.2 Compact Set 37
3.3 Existence and Uniqueness 38
3.3.1 Cauchy Theorem 38
3.3.2 Global Lipschitz Condition 39
3.3.3 Local Lipschitz Condition 40

3.4 Positive Definite, Symmetric and Anti-Symmetric Matrices . . . 41
3.4.1 Positive-Definite Matrix and Function 41
3.4.2 Anti-Symmetric Matrix 43
3.5 Summary 45
3.6 Exercises 45

4 Lyapunov Stability Theory 47
4.1 Stability Concepts 48
4.1.1 Stability Definition 49
4.1.2 Asymptotic Stability 50
4.1.3 Exponential Stability 51
4.2 Lyapunov's Direct Method 52
4.2.1 Motivation 52
4.2.2 Lyapunov Theorem for Local Stability 57
4.2.3 Lyapunov Theorem for Exponential Stability 60
4.2.4 Radially Unbounded Functions 61
4.2.5 Barbashin–Krasovskii Theorem for Global Asymptotic Stability 61
4.2.6 LaSalle's Invariant Set Theorem 63
4.2.7 Differential Lyapunov Equation 67
4.3 Stability of Non-Autonomous Systems 69
4.3.1 Uniform Stability 70
4.3.2 Uniform Boundedness 71
4.3.3 Barbalat's Lemma 74
4.4 Summary 78
4.5 Exercises 78
References 81

5 Model-Reference Adaptive Control 83
5.1 Composition of a Model-Reference Adaptive Control System 86
5.1.1 Uncertain Plant 86
5.1.2 Reference Model 88
5.1.3 Controller 89
5.1.4 Adaptive Law 89
5.2 Direct MRAC for First-Order SISO Systems 90
5.2.1 Case I: a and b Unknown but Sign of b Known 90
5.2.2 Case II: a and b Known 93
5.3 Indirect MRAC for First-Order SISO Systems 95
5.4 Direct MRAC for Second-Order SISO Systems 99
5.4.1 Case I: A and B Unknown but Sign of b known 99
5.4.2 Case II: A and B Known 105
5.5 Indirect MRAC for Second-Order SISO Systems 106

5.6 Direct MRAC for MIMO Systems . . . 110
5.6.1 Case I: A and Λ Unknown, but B and Sign of Λ Known . . . 111
5.6.2 Case II: A, B, $\Lambda = I$ Known . . . 117
5.7 Indirect MRAC for MIMO Systems . . . 118
5.8 Summary . . . 120
5.9 Exercises . . . 121
References . . . 123

6 Least-Squares Parameter Identification . . . 125
6.1 Least-Squares Regression . . . 126
6.2 Convex Optimization and Least-Squares Gradient Method . . . 128
6.3 Persistent Excitation and Parameter Convergence . . . 130
6.4 Recursive Least-Squares . . . 134
6.5 Indirect Adaptive Control with Least-Squares Parameter Identification . . . 137
6.6 Estimation of Time Derivative Signals . . . 146
6.7 Summary . . . 147
6.8 Exercises . . . 148
References . . . 149

7 Function Approximation and Adaptive Control with Unstructured Uncertainty . . . 151
7.1 Polynomial Approximation by Least-Squares . . . 152
7.2 Neural Network Approximation . . . 154
7.3 Adaptive Control with Unstructured Uncertainty . . . 159
7.3.1 Recursive Least-Squares Direct Adaptive Control with Matrix Inversion . . . 160
7.3.2 Modified Recursive Least-Squares Direct Adaptive Control without Matrix Inversion . . . 164
7.3.3 Least-Squares Gradient Direct Adaptive Control . . . 168
7.3.4 Least-Squares Gradient Direct Adaptive Control with Neural Network Approximation . . . 173
7.3.5 MRAC with Neural Network Approximation . . . 175
7.4 Summary . . . 182
7.5 Exercises . . . 183
References . . . 184

8 Robustness Issues with Adaptive Control . . . 185
8.1 Parameter Drift . . . 186
8.2 Non-minimum Phase Systems . . . 190
8.3 Time-Delay Systems . . . 193
8.4 Unmodeled Dynamics . . . 195
8.5 Fast Adaptation . . . 200

8.6 Summary . . . 205
8.7 Exercises . . . 206
References . . . 207

9 Robust Adaptive Control . . . 209
9.1 Dead-Zone Method . . . 212
9.2 Projection Method . . . 213
9.3 σ Modification . . . 220
9.4 e Modification . . . 228
9.5 Optimal Control Modification . . . 234
9.5.1 Optimal Control . . . 234
9.5.2 Derivation of Optimal Control Modification . . . 240
9.5.3 Lyapunov Stability Analysis . . . 247
9.5.4 Linear Asymptotic Property . . . 254
9.6 Adaptive Loop Recovery Modification . . . 261
9.7 $\mathscr{L}_1$ Adaptive Control . . . 267
9.8 Normalization . . . 274
9.9 Covariance Adjustment of Adaptation Rate . . . 280
9.10 Optimal Control Modification for Systems with Control Input Uncertainty . . . 286
9.11 Bi-Objective Optimal Control Modification for Systems with Control Input Uncertainty . . . 291
9.12 Adaptive Control for Singularly Perturbed Systems with First-Order Slow Actuator Dynamics . . . 307
9.13 Optimal Control Modification for Linear Uncertain Systems with Unmodeled Dynamics . . . 314
9.14 Adaptive Control of Non-Minimum Phase Plants with Relative Degree 1 . . . 322
9.14.1 Minimum Phase Plant . . . 323
9.14.2 Non-Minimum Phase Plant . . . 325
9.15 Summary . . . 339
9.16 Exercises . . . 340
References . . . 345

10 Aerospace Applications . . . 349
10.1 Inverted Pendulum . . . 351
10.2 Double Pendulum in Robotic Applications . . . 354
10.3 Adaptive Control of Aircraft Longitudinal Dynamics . . . 359
10.4 Recursive Least-Squares and Neural Network Pitch Attitude Adaptive Flight Control . . . 366
10.5 Adaptive Control of Flexible Aircraft . . . 374

10.6 Adaptive Linear Quadratic Gaussian Flutter Suppression Control . . . 385
10.7 Adaptive Flight Control . . . 406
10.8 Hybrid Adaptive Flight Control . . . 414
10.9 Adaptive Flight Control for F-18 Aircraft with Optimal Control Modification . . . 417
10.10 Summary . . . 425
10.11 Exercises . . . 426
References . . . 427

Suggested Exam Questions . . . 431

Index . . . 441

About the Author

Dr. Nhan Nguyen is a senior research scientist at NASA Ames Research Center with over 31 years of experience. He is the technical group lead of the Advanced Control and Evolvable Systems research group in the Intelligent Systems Division with 22 researchers conducting aerospace flight control research. He is currently leading a project team to conduct research and development of advanced aeroservoelastic control technologies for flexible aircraft. He served as the Project Scientist in the NASA Integrated Resilient Aircraft Control (IRAC) Project from 2007 to 2010 with an annual budget of $21 million that funded advanced research in adaptive control conducted by NASA, industry, and academia. His prior position was the Deputy Principal Investigator of the IRAC project from 2005 to 2006. His work on optimal control modification adaptive control culminated in a successful flight validation experiment on NASA F-18 research aircraft in 2010. He has received several prestigious awards including the NASA Exceptional Scientific Achievement Medal, NASA Exceptional Achievement Medal, two-time NASA Ames Honors for Excellence as Engineer, and more than 50 other NASA career awards. He has four US patents and two other patents in pending. He has over 15 NASA invention disclosures. He has published over 200 peer-reviewed technical publications. He is the chair of the American Institute of Aeronautics and Astronautics (AIAA) Intelligent Systems Technical Committee with 50 professional members. He has received two AIAA Distinguished Services Awards.

Chapter 1
Introduction

Abstract This chapter provides a brief summary of the recent advancements made in model-reference adaptive control theory. Adaptive control is a promising technology that can improve the performance of control systems in the presence of uncertainty due to a variety of factors such as degradation and modeling uncertainty. During the past decade, the adaptive control research community has produced several advancements in adaptive control theory along with many novel adaptive control methods as a result of the increased government research funding. Many of these new adaptive control methods have added new capabilities in terms of improved performance and robustness that further increase the viability of model-reference adaptive control as a future technology. Flight test validation of adaptive control on full-scale aircraft and unmanned arial vehicles has increased the confidence in model-reference adaptive control as a possible new flight control technology for aerospace vehicles in the near future. In spite of the five decades of research in adaptive control, the fact still remains that currently no adaptive control system has ever been deployed on any safety-critical or human-rated production systems. Many technical problems remain unresolved. As a nonlinear control method, the lack of well-accepted metrics for adaptive control system design presents a major hurdle for certification. The development of certifiable adaptive control systems is viewed as a major technical challenge for the adaptive control research community to address in the current research.

Adaptive control is a well-researched topic in control theory that spans several decades. Many adaptive control applications can be found in aerospace and other settings, but very few or none have been deployed on safety-critical production systems. In this chapter, the learning objectives are:

- To understand a brief history of adaptive control research and the extensive on-going research in this topic;

N.T. Nguyen, *Model-Reference Adaptive Control*, Advanced Textbooks
in Control and Signal Processing, https://doi.org/10.1007/978-3-319-56393-0_1

- To recognize the fact that, in spite of the many advancements in the field, adoption of adaptive control technologies is not widespread and its applications are limited in scope; and
- To recognize that verification, validation, and certification are viewed as significant technical barriers that need to be further researched in order to increase the confidence in and the trustworthiness of adaptive control technologies, which would enable future adoption.

1.1 Overview

Adaptive control is a study of a class of nonlinear control methods that deal with systems with uncertainty. The uncertainty can be due to unforeseen internal changes in system dynamics or external disturbances. An adaptive control system can be broadly described as any control system that has the ability to adjust control design parameters such as control gains online based on inputs received by the plant in order to accommodate system uncertainty as illustrated in Fig. 1.1. The adjustable parameters are called adaptive parameters, and the adjusting mechanism, which is described by a set of mathematical equations, is called an adaptive law. In most cases, a typical adaptive law is nonlinear. This nonlinearity makes adaptive control inherently difficult to design and analyze since many traditional design and analysis methods for linear time-invariant (LTI) control systems such as bode plot, phase and gain margins, eigenvalue analysis are not applicable.

Adaptive control has a long history dated back to the early 1950s when there was an extensive research interest in designing advanced autopilots for high-performance aircraft that operated over a wide range of flight conditions [1]. After a significant research and development effort, gain-scheduling control was gaining acceptance over adaptive control due to the inherent difficulty associated with nonlinearity of adaptive control. On the other hand, gain-scheduling control can take advantage of classical control techniques in the design selection of suitable control gains that are scheduled as a function of aircraft operating conditions.

The 1960s saw the emergence of the modern control theory and Lyapunov stability theory that also contributed to adaptive control theory. Whitaker et al. developed model-reference adaptive control with the sensitivity method and MIT rule. During this development phase, there was a lack of stability proofs and good understanding of the properties of adaptive control. In 1967, an adaptive flight controller was flight-tested by NASA on one of the three X-15 experimental hypersonic aircrafts [2, 3]. Several successful test flights were made before an ill-fated test flight occurred that resulted in a fatal crash of one of these vehicles. This event and the technical difficulties led to a diminished interest in adaptive control.

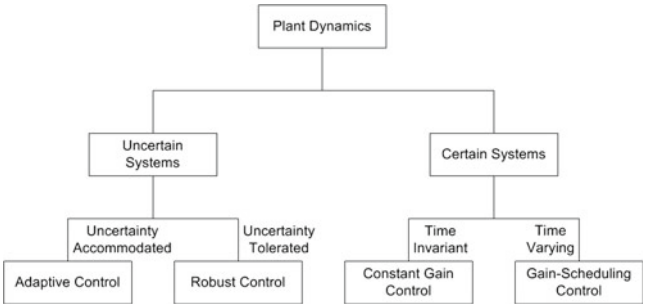

Fig. 1.1 Classes of automatic control for dynamical systems

In the 1970s, the Lyapunov stability theory was established as a foundation for model-reference adaptive control. This represented a breakthrough in adaptive control as it led to the development of improved model-reference adaptive control schemes with the accompanied Lyapunov stability theory. The excitements soon gave way to a realization in the 1980s that, in spite of the Lyapunov stability theory, adaptive control can exhibit unstable behaviors in the presence of small disturbances or unmodeled dynamics [4]. This led to the recognition that model-reference adaptive control was sensitive to system modeling accuracy and the resultant mismatch between a real system and a plant model of the system. This lack of robustness led to the development of the σ modification [5] and e modification to improve the stability properties of adaptive control [6]. These robust modification schemes represent a new class of "robust adaptive control."

In the 1990s and up to the present time, research in adaptive control remains highly active. Neural networks were introduced as a mechanism for adaptation [7–12]. This led to the development of a class of adaptive control called "intelligent control" or "neural network adaptive control" which utilizes neural networks to approximate model uncertainties, but the basic framework remains to be the same as model-reference adaptive control [13–21].

The following decade saw a resurgence of interest in adaptive control research. This also coincided with a period of increased research funding made possible by NASA [22] and other US government agencies. In particular, NASA has been an active key player in adaptive control technology development as illustrated on the time line in Fig. 1.2. During this period, the adaptive control research community produced several advancements in adaptive control theory along with many novel adaptive control methods as a result of the increased research funding. The list of these new advancements is long, and it would not do justice to include all of these new methods in this limited space. The reader is referred to a subset of this list from which those novel adaptive control methods that were funded by NASA during this decade can be found. These methods include: adaptive control based on retrospective cost optimization by Santillo and Bernstein [23, 24], adaptive control with reference model modification by Stepanyan and Krishnakumar [25, 26], adaptive loop recov-

ery by Calise and Yucelen [27, 28], bounded linear stability analysis metric-driven adaptive control by Nguyen [29, 30], combined/composite model-reference adaptive control by Lavretsky [31, 32], derivative-free model-reference adaptive control by Yucelen and Calise [33, 34], hybrid adaptive control by Nguyen [35–37], K modification by Kim et al. [38], Kalman filter modification by Yucelen and Calise [39, 40], $\mathcal{L}_1$ adaptive control by Hovakimyan and Cao [41–43], least-squares adaptive control by Nguyen [44, 45], concurrent learning least-squares adaptive control by Chowdhary and Johnson [46, 47], modified state observer adaptive control by Balaskrishnan [48], multivariable model-reference adaptive control by Guo and Tao [49], optimal control modification [50, 51] and multiobjective optimal control modification by Nguyen [52, 53], Q modification by Volyanskyy et al. [54, 55], and parameter-dependent Riccati equation adaptive control by Kim et al. [56]. Many of these new adaptive control methods have added new capabilities in terms of improved performance and robustness that further increase the viability of model-reference adaptive control as a future technology.

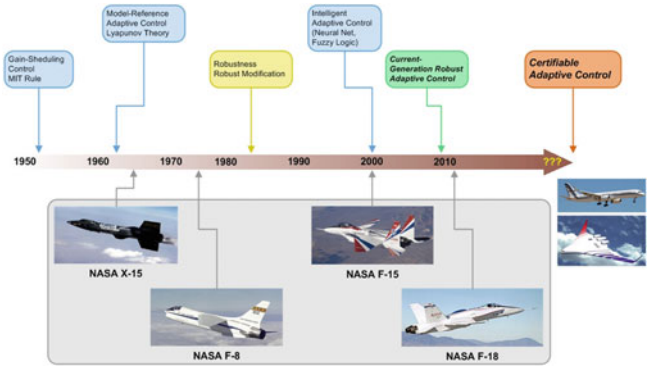

Fig. 1.2 Adaptive control research time line

In terms of flight validation, an intelligent flight control system based on the sigma-pi neural network adaptive control by Calise and Rysdyk [13] was developed and flight-tested by NASA on a F-15 aircraft at NASA Armstrong (former Dryden) Flight Research Center in the early 2000s to demonstrate the capability of neural network adaptive control [57, 58]. In 2010, another flight test program was conducted on a F/A-18 aircraft at NASA Armstrong Flight Research Center to demonstrate a new simplified adaptive flight controller based on the optimal control modification [59–62]. A pilot-in-the-loop high-fidelity flight simulation study of several adaptive control methods was conducted at NASA Ames Research Center in 2009 [63, 64]. A flight experiment of the $\mathcal{L}_1$ adaptive control was conducted on NASA AirSTAR flight test vehicle at NASA Langley Research Center in 2009 [65]. Another flight experiment of the $\mathcal{L}_1$ adaptive control was conducted on a UAV (unmanned arial vehicle) at the Naval Postgraduate School in 2009 [66]. Model-reference adaptive

control was also evaluated for fight testing on a Beechcraft Bonanza fly-by-wire testbed in 2010 [67]. These flight experiments and many others that followed have increased the confidence in model-reference adaptive control as a possible new flight control technology for aerospace vehicles in the near future. They also revealed that further flight validation for adaptive control is still needed to mature this technology.

Research in adaptive control continues at the present time. It would be well beyond the scope of this book to include all current research activities. The interested reader is referred to the references for more information on numerous applications for aircraft [68–79], spacecraft [21, 80–83], UAVs [15, 47, 65, 66, 84], aerospace structures [85, 86], robotic systems [18, 87], munition systems [88], fluid systems [89], and many others.

The current research in adaptive control generally lacks the ability to deal with integrated effects that exist in many different system designs and operations. These include but are not limited to: complex uncertainties due to unmodeled dynamics [4, 90], gross changes in system dynamics resulting from unintended operations and structural damage [36, 76, 91], unknown component failures and anomalies [80, 92–94], high degree of design complexity [59], novel actuators and sensors [79, 95], multiphysics interactions [85, 86, 96–98], and many other effects.

Adaptive control plays a major role in the aerospace domain. In aerospace vehicles with damaged structures or failed flight control surfaces or operating in off-nominal flight events, the vehicles can exhibit numerous coupled effects such as aerodynamics, vehicle dynamics, structural dynamics, and propulsion. These coupled effects can impose a wide range of uncertainties on the performance of a flight control system. Thus, even though an adaptive control system may be shown to be stable in a nominal flight condition, it may fail to provide enough stability in the presence of these uncertainties [99, 100]. For example, conventional aircraft flight control systems incorporate aeroservoelastic (ASE) notch filters to prevent control signals from exciting aeroelastic wing modes. However, if changes in aircraft dynamics are significant, the frequencies of the aeroelastic modes may change enough to render the ASE notch filters ineffective. This could cause the control signals to excite wing modes which could lead to problems for a pilot to control an aircraft. Another problem faced by adaptive control is the ability of adaptive control systems to accommodate slow or degraded flight control actuators such an impaired flight control surface or engine as a flight control effector [79, 101]. The dissimilar actuator rates due to slow actuator dynamics can cause problems with adaptive control and can potentially lead to pilot-induced oscillations (PIO) [102].

To adequately deal with these coupled effects, integrated approaches in adaptive control research need to be developed. These integrated approaches will be required to develop new fundamental multidisciplinary methods in adaptive control and system modeling. Unmodeled dynamics are a significant source of uncertainty and a causal factor of instability of adaptive control systems in high-gain adaptation situations. Future research in adaptive control should leverage fundamental understanding of the structures of these secondary dynamics by incorporating multidisciplinary methods into the design of an adaptive control system. With a better understanding of the

system uncertainties, more effective adaptive control methods may be developed to achieve improved robustness in the presence of uncertainties.

1.2 Verification and Validation Challenges for Adaptive Flight Control Systems

In spite of the five decades of research in adaptive control, the fact still remains that currently no adaptive control system has ever been deployed on any safety-critical or human-rated production systems such as passenger transport aircraft [99, 103–106]. It should be noted that adaptive control has been successfully developed and deployed in munition production systems [88]. The problem lies in the difficulty with the certification of adaptive control systems since existing certification methods for linear time-invariant (LTI) control systems cannot readily be used for nonlinear adaptive control systems. Research to address the notion of metrics for adaptive control began to appear during the first decade of the twenty-first century [14, 107–115]. The goal of this research is to develop performance and stability metrics for adaptive control similar to overshoot, settling time, phase and gain margins for LTI control systems. These metrics, if accepted, could pave a path toward certification that would potentially lead to the adoption of adaptive control as a future control technology for safety-critical and human-rated production systems.

Development of certifiable adaptive control systems represents a major challenge to overcome. Adaptive control systems with learning algorithms will never become part of the future unless it can be proven that they are highly safe and reliable. Rigorous methods for adaptive control software verification and validation must therefore be developed to ensure that adaptive control system software failures will not occur to verify that the adaptive control system functions as required, to eliminate unintended functionality, and to demonstrate that certification requirements imposed by regulatory bodies such as the Federal Aviation Administration (FAA) can be satisfied [104, 105].

The ability of an adaptive control system to modify a pre-designed flight control system is a strength and a weakness at the same time. On the one hand, the ability of adaptive control systems to accommodate system degradation is considered as a major advantage since traditional gain-scheduling control methods tend to be less capable of handling off-nominal flight conditions outside their design operating envelopes. On the other hand, serious problems with adaptive control can still exist with regard to unmodeled dynamics and high-gain adaptation. Adaptive control systems are sensitive to these potential problems as well as many others including actuator dynamics and exogenous disturbances. To be certifiable, an adaptive flight control system must be able to prove that these effects as well as other factors such as time delay, system constraints, and measurement noise are handled in a globally satisfactory manner.

1.2.1 *Verification by Simulation of Adaptive Flight Control Systems*

Simulation is an integral part of the verification of adaptive control systems [104, 105, 116, 117]. Many aspects of adaptive control systems, in particular convergence and stability, can only be analyzed with simulations that provide enough detail and fidelity to model significant nonlinear dynamics. For example, stall upset of an aircraft cannot be expressed as a linear model since this effect is highly nonlinear and unsteady. Simulation provides a fairly rapid way to accomplish the following tasks:

- Evaluation and comparison of different adaptive control algorithms;
- Tuning control gains and weight update laws;
- Determination of progress of adaptation at each step;
- Evaluation of the effects of process and measurement noise on convergence of adaptive parameters;
- Determination of stability boundaries;
- Validation with actual flight computer hardware;
- Conducting piloted evaluation of adaptive control in a flight simulator;
- Simulating ad hoc techniques of improving the adaptation process, such as adding persistent excitation to improve identification and convergence, or stopping the adaptation process after the tracking error converges to within a specified tolerance or after a specified number of iterations.

Simulations differ primarily in the fidelity with which the plant is modeled. Higher fidelity simulations require more complicated mathematical models of the adaptive control system and also a greater use of actual (and expensive) controller hardware. The behavior of simple linear models is compared to that of higher fidelity nonlinear models when they are available to ensure that analyses performed using the linear models still apply. In order to be cost effective, the lowest fidelity testbed is usually used as much as possible.

The lowest fidelity simulations are usually run on a desktop computer. This simulation typically includes the control laws and a linear or nonlinear plant of the system dynamics. A linear model is most often used in early control law design and analysis or to calculate linear gain and phase margins. Changes to the plant model can be simulated by changing the system transfer function from one matrix to another with varying frequency. By varying the amount of change, the stability boundaries of the system can be determined. Concomitant with this process is an evaluation of the system tuning parameters that are used in the adaptive control algorithms. The desktop simulation environment provides a quick way to compare different adaptive control algorithms and controller architectures. Only the most promising designs need to be simulated using higher fidelity simulations.

Higher fidelity simulation testbeds use actual flight hardware (or even aircraft) in the simulation of the control loop and are often run in dedicated computing environments with a cockpit and out-the-window graphics [117, 118]. These simulations may include a cockpit to interface with the pilot and can either be fixed-base or

motion-base. Motion-base simulators additionally provide the pilot with simulations of physical (motion and visual) cues of the actual flight [63]. Typically, they contain software models of nonlinear aircraft dynamics, actuator models, and sensor models. Using the actual aircraft flight computer is a particularly important advantage of this simulation, since all computers tend to handle exceptions differently and may have differences in their computational processes. Either an actual or iron-bird aircraft may be used in a higher fidelity simulation to provide realistic actuator dynamics, sensor noise, actual flight wiring, and some structural interactions. These testbeds allow for a complete check out of all interfaces to the flight hardware, timing tests, and various failure modes and effects analysis (FMEA) testing, which is not possible in a low fidelity simulation.

1.2.2 Adaptive Control Metrics

In spite of the many advancements made in adaptive control research and the potential benefits of adaptive control systems, the absence of verification and validation methods for adaptive control systems remains a major hurdle to the implementation of adaptive control in safety-critical or human-rated production systems. This hurdle can be traced to the lack of performance and stability metrics for adaptive control. The development of verifiable metrics for adaptive control is an important aspect of adaptive control research in order to mature adaptive control technology for use in future safety-critical and human-rated production systems. Stability metrics of adaptive control are an important consideration for assessing system robustness to unmodeled dynamics, time delay, high-gain learning, and exogenous disturbances. Therefore, it is imperative to define a proper set of stability and performance metrics for adaptive systems as a first step in the development of reliable verification and validation methods that could lead to the certification of adaptive control software.

Another potential benefit of metrics for adaptive control is the consideration for metrics-driven adaptive control. Metrics-driven adaptive control is the notion that adaptation in certain cases should be driven by the need to trade off between stability and performance to maintain operational safety of a control system [30]. Research in this area has resulted in some initial analysis methods for computing stability metrics online that could be used to adjust the adaptive parameters of an adaptive control system to improve stability margins of the closed-loop system [29].

Generally, the classical gain and phase margins for LTI systems are not applicable to adaptive control systems which are nonlinear. Some results began to appear in the literature on the definition and evaluation of candidate metrics for adaptive control systems [14, 109, 110, 112, 115]. The use of a parameter sensitivity as a metric for the output of neural networks has been investigated [103]. Stability metrics based on the Lyapunov analysis and passivity theory have been studied [108]. Metrics for evaluation of stability and robustness of adaptive control systems can also be obtained from optimization frameworks [107, 119]. The notion of time-delay margin as a stability metric has been studied by many authors [120, 121].

There are several unaddressed issues related to the implementation of adaptive control technology in aerospace vehicles to accommodate uncertainty in adverse events. These issues include but are not limited to: (1) achievable stability metrics of adaptive control as related to uncertainty bounds; (2) adaptation in the presence of static and dynamic saturation of actuators; (3) cross-coupling between longitudinal and lateral-directional axes due to failures, damage, and different rates of adaptation in each axis; (4) online reconfiguration and control reallocation using nontraditional control effectors such as engines; and (5) timescale separation in actuator systems with different time latencies such as conventional control surfaces and engines.

1.3 Summary

Adaptive control is a well-researched subject over the past several decades. Adaptive control is a promising technology that could provide improved performance of control systems in the presence of uncertainty due to a variety of factors such as degradation and modeling uncertainty. During the past decade, advancements in adaptive control theory along with many novel adaptive control methods have been made by researchers in the field. Many of these new adaptive control methods have added new capabilities in terms of improved performance and robustness that further increase the viability of model-reference adaptive control as a future technology. Flight test validation of adaptive control on full-scale aircraft and unmanned arial vehicles has increased the confidence in model-reference adaptive control as a possible new flight control technology for aerospace vehicles in the near future.

In spite of this, adaptive control is not well-accepted for applications in safety-critical or human-rated production systems. Many technical problems remain unresolved. As a nonlinear control method, the lack of well-accepted metrics for adaptive control system design as opposed to linear control systems presents a major hurdle for certification.

References

1. Åström, K. J., & Wittenmark, B. (2008). *Adaptive control*: Dover Publications Inc.
2. Jenkins, D. R. (2000). Hypersonics Before the Shuttle: A Concise History of the X-15 Research Airplane, NASA SP-2000-4518.
3. Staff of the Flight Research Center. (1971). Experience with the X-15 Adaptive Flight Control System, NASA TN D-6208.
4. Rohrs, C. E., Valavani, L., Athans, M., & Stein, G. (1985). Robustness of continuous-time adaptive control algorithms in the presence of unmodeled dynamics. *IEEE Transactions on Automatic Control*, *AC-30*(9), 881–889.
5. Ioannou, P., & Kokotovic, P. (1984). Instability analysis and improvement of robustness of adaptive control. *Automatica*, *20*(5), 583–594.
6. Narendra, K. S. & Annaswamy, A. M. (1987). A new adaptive law for robust adaptation without persistent excitation. *IEEE Transactions on Automatic Control*, *AC-32*(2), 134–145.

7. Cybenko, G. (1989). Approximation by superpositions of a sigmoidal function. *Mathematics of Control Signals Systems*, *2*, 303–314.
8. Lee, T., & Jeng, J. (1998). The Chebyshev-Polynomials-based unified model neural networks for function approximation. *IEEE Transactions on Systems, Man, and Cybernetics, Part B: Cybernetics*, *28*(6), 925–935.
9. Micchelli, C. A. (1986). Interpolation of scattered data: distance matrices and conditionally positive definite functions. *Constructive Approximation*, *2*, 11–12.
10. Moody, J. (1992). *The effective number of parameters: An analysis of generalization and regularization in nonlinear learning systems*. Advances in Neural Information Processing Systems (Vol. 4). San Mateo: Morgan Kaufmann Publishers.
11. Suykens, J., Vandewalle, J., & deMoor, B. (1996). *Artificial neural networks for modeling and control of non-linear systems*: Dordrecht: Kluwer Academic Publisher.
12. Wang, X., Huang, Y., & Nguyen, N. (2010). Robustness quantification of recurrent neural network using unscented transform. *Elsevier Journal of Neural Computing*, *74*(1–3),
13. Calise, A. J., & Rysdyk, R. T. (1998). Nonlinear adaptive flight control using neural networks. *IEEE Control System Magazine*, *18*(6), 1425.
14. Ishihara, A., Ben-Menahem, S., & Nguyen, N. (2009). Protection ellipsoids for stability analysis of feedforward neural-net controllers. In *International Joint Conference on Neural Networks*.
15. Johnson, E. N., Calise, A. J., El-Shirbiny, H. A., & Rysdyk, R. T. (2000). Feedback linearization with neural network augmentation applied to X-33 attitude control. In *AIAA Guidance, Navigation, and Control Conference, AIAA-2000-4157, August, 2000*.
16. Kim, B. S., & Calise, A. J. (1997). Nonlinear flight control using neural networks. *Journal of Guidance, Control, and Dynamics*, *20*(1), 26–33.
17. Lam, Q., Nguyen, N., & Oppenheimer, M. (2012). Intelligent adaptive flight control using optimal control modification and neural network as control augmentation layer and robustness enhancer. In *AIAA Infotech@Aerospace conference, AIAA-2012-2519, June, 2012*.
18. Lewis, F. W., Jagannathan, S., & Yesildirak, A. (1998). *Neural network control of robot manipulators and non-linear systems*. Boca Raton: CRC.
19. Rysdyk, R. T., Nardi, F., & Calise, A. J. (1999). Robust adaptive nonlinear flight control applications using neural networks. In *American Control Conference*.
20. Steinberg, M. L. (1999). A comparison of intelligent, adaptive, and nonlinear flight control laws. In *AIAA Guidance, Navigation, and Control Conference, AIAA-1999-4044, August, 1999*.
21. Zou, A., Kumar, K., & Hou, Z. (2010). Attitude control of spacecraft using chebyshev neural networks. *IEEE Transactions on Neural Networks*, *21*(9), 1457–1471.
22. Krishnakumar, K., Nguyen, N., & Kaneshige, J. (2010, December). Integrated resilient aircraft control. In *Encyclopedia of Aerospace Engineering* (Vol. 8). New Jersey: Wiley. ISBN: 978-0-470-75440-5.
23. Santillo, M. A. & Bernstein, D. S. (2008). A retrospective correction filter for discrete-time adaptive control of non-minimum phase systems. In *IEEE Conference on Decision and Control, December, 2008*.
24. Santillo, M. A., & Bernstein, D. S. (2010). Adaptive control based on retrospective cost optimization. *AIAA Journal of Guidance, Control, and Dynamics*, *33*(2), 289–304.
25. Stepanyan V. & Krishnakumar, K. (2010). MRAC revisited: Guaranteed performance with reference model modification. In *American Control Conference*.
26. Stepanyan, V., & Krishnakumar, K. (2012). Adaptive control with reference model modification. *AIAA Journal of Guidance, Control, and Dynamics*, *35*(4), 1370–1374.
27. Calise, A. J., Yucelen, T., Muse, J., & Yang, B. (2009). A loop recovery method for adaptive control. In *AIAA Guidance, Navigation, and Control Conference, AIAA-2009-5967, August 2009*.
28. Calise, A. J., & Yucelen, T. (2012). Adaptive loop transfer recovery. *AIAA Journal of Guidance, Control, and Dynamics*, *35*(3), 807–815.

29. Nguyen, N., Bakhtiari-Nejad, M., & Huang, Y. (2007). Hybrid adaptive flight control with bounded linear stability analysis. In *AIAA Guidance, Navigation, and Control Conference, AIAA-2007-6422, August 2007*.
30. Bakhtiari-Nejad, M., Nguyen, N., & Krishnakumar, K. (2009). Adjustment of adaptive gain with bounded linear stability analysis to improve time-delay margin for metrics-driven adaptive control. In *AIAA Infotech@Aerospace Conference, AIAA-2009-1801, April 2009*.
31. Lavretsky, E. (2009). Combined/composite model reference adaptive control. In *AIAA Guidance, Navigation, and Control Conference, AIAA-2009-6065, August 2009*.
32. Lavretsky, E. (2009). Combined/composite model reference adaptive control. *IEEE Transactions on Automatic Control*, *54*(11), 2692–2697.
33. Yucelen, T., & Calise, A. J. (2010). Derivative-free model reference adaptive control. In *AIAA Guidance, Navigation, and [11, 5] Control Conference, AIAA-2009-5858, August 2010*.
34. Yucelen, T., & Calise, A. J. (2011). Derivative-free model reference adaptive control. *AIAA Journal of Guidance, Control, and Dynamics*, *34*(4), 933–950.
35. Nguyen, N., Krishnakumar, K., Kaneshige, J., & Nespeca, P. (2006). Dynamics and adaptive control for stability recovery of damaged asymmetric aircraft. In *AIAA Guidance, Navigation, and Control Conference, AIAA-2006-6049, August 2006*.
36. Nguyen, N., Krishnakumar, K., Kaneshige, J., & Nespeca, P. (2008). Flight dynamics modeling and hybrid adaptive control of damaged asymmetric aircraft. *AIAA Journal of Guidance, Control, and Dynamics*, *31*(3), 751–764.
37. Nguyen, N. (2011). *Hybrid adaptive flight control with model inversion adaptation*. In Advances in Flight Control Systems. Croatia: Intech Publishing. ISBN 978-953-307-218-0.
38. Kim, K., Yucelen, T., & Calise, A. J. (2010). $\mathcal{K}$-modification in adaptive control. In *AIAA Infotech@Aerospace Conference, AIAA-2010-3321, April 2010*.
39. Yucelen, T., & Calise, A. J. (2009). A Kalman filter optimization approach to direct adaptive control. In *AIAA Guidance, Navigation, and Control Conference, AIAA-2010-7769, August 2009*.
40. Yucelen, T., & Calise, A. J. (2010). A Kalman filter modification in adaptive control. *AIAA Journal of Guidance, Control, and Dynamics*, *33*(2), 426–439.
41. Cao, C., & Hovakimyan, N. (2007). Guaranteed transient performance with $\mathcal{L}_1$ adaptive controller for systems with unknown time-varying parameters and bounded disturbances: Part I. In *American Control Conference, July 2007*.
42. Cao, C., & Hovakimyan, N. (2008). Design and analysis of a novel $\mathcal{L}_1$ adaptive control architecture with guaranteed transient performance. *IEEE Transactions on Automatic Control*, *53*(2), 586–591.
43. Hovakimyan, N., & Cao, C. (2010). $\mathcal{L}_1$ *Adaptive control theory: Guaranteed robustness with fast adaptation*. Society for Industrial and Applied Mathematics.
44. Nguyen, N., Burken, J., & Ishihara, A. (2011). Least-squares adaptive control using Chebyshev orthogonal polynomials. In *AIAA Infotech@Aerospace Conference, AIAA-2011-1402, March 2011*.
45. Nguyen, N. (2013). Least-squares model reference adaptive control with Chebyshev orthogonal polynomial approximation. *AIAA Journal of Aerospace Information Systems*, *10*(6), 268–286.
46. Chowdhary, G., & Johnson, E. (2010). Least squares based modification for adaptive control. In *IEEE Conference on Decision and Control, December 2010*.
47. Chowdhary, G., & Johnson, E. (2011). Theory and flight-test validation of a concurrent-learning adaptive controller. *AIAA Journal of Guidance, Control, and Dynamics*, *34*(2), 592–607.
48. Balakrishnan, S. N., Unnikrishnan, N., Nguyen, N., & Krishnakumar, K. (2009). Neuroadaptive model following controller design for non-affine and non- square aircraft systems. In *AIAA Guidance, Navigation, and Control Conference, AIAA-2009-5737, August 2009*.
49. Guo, J., & Tao, G. (20011). A Multivariable MRAC design for aircraft systems under failure and damage conditions. In *American Control Conference, June 2011*.

50. Nguyen, N., Krishnakumar, K., & Boskovic, J. (2008). An optimal control modification to model-reference adaptive control for fast adaptation. In *AIAA Guidance, Navigation, and Control Conference, AIAA 2008-7283, August 2008*.
51. Nguyen, N. (2012). Optimal control modification for robust adaptive control with large adaptive gain. *Systems and Control Letters*, *61*(2012), 485–494.
52. Nguyen, N. (2014). Multi-objective optimal control modification adaptive control method for systems with input and unmatched uncertainties. In *AIAA Guidance, Navigation, and Control Conference, AIAA-2014-0454, January 2014*.
53. Nguyen, N., & Balakrishnan, S. N. (2014). Bi-objective optimal control modification adaptive control for systems with input uncertainty. *IEEE/CAA Journal of Automatica Sinica*, *1*(4), 423–434.
54. Volyanskyy, K. Y., & Calise, A. J. (2006). A novel q-modification term for adaptive control. In *American Control Conference, June 2006*.
55. Volyanskyy, K. Y., Haddad, W. M., & Calise, A. J. (2009). A new neuroadaptive control architecture for nonlinear uncertain dynamical systems: Beyond σ- and *e*-modifications. *IEEE Transactions on Neural Networks*, *20*, 1707–1723.
56. Kim, K., Yucelen, T., Calise, A.J., & Nguyen, N. (2011). Adaptive output feedback control for an aeroelastic generic transport model: A parameter dependent Riccati equation approach. In *AIAA Guidance, Navigation, and Control Conference, AIAA-2011-6456, August 2011*.
57. Bosworth, J., & Williams-Hayes, P. S. (2007). Flight test results from the NF-15B IFCS project with adaptation to a simulated stabilator failure. In *AIAA Infotech@Aerospace Conference, AIAA-2007-2818, May 2007*.
58. Williams-Hayes, P. S. Flight test implementation of a second generation intelligent flight control system. In *NASA TM-2005-213669*.
59. Hanson, C., Johnson, M., Schaefer, J., Nguyen, N., & Burken, J. (2011). Handling qualities evaluations of low complexity model reference adaptive controllers for reduced pitch and roll damping scenarios. In *AIAA Guidance, Navigation, and Control Conference, AIAA-2011-6607, August 2011*.
60. Hanson, C., Schaefer, J., Johnson, M., & Nguyen, N. Design of low complexity model reference adaptive controllers. In *NASA-TM-215972*.
61. Nguyen, N., Hanson, C., Burken, J., & Schaefer, J. (2016). Normalized optimal control modification and flight experiments on NASA F/A-18 aircraft. *AIAA Journal of Guidance, Control, and Dynamics*.
62. Schaefer, J., Hanson , C., Johnson, M., & Nguyen, N. (2011). Handling qualities of model reference adaptive controllers with varying complexity for pitch-roll coupled failures. In *IAA Guidance, Navigation, and Control Conference, AIAA-2011-6453, August 2011*.
63. Campbell, S., Kaneshige, J., Nguyen, N., & Krishnakumar, K. (2010). An adaptive control simulation study using pilot handling qualities evaluations. In *AIAA Guidance, Navigation, and Control Conference, AIAA-2010-8013, August 2010*.
64. Campbell, S., Kaneshige, J., Nguyen, N., & Krishnakumar, K. (2010). Implementation and evaluation of multiple adaptive control technologies for a generic transport aircraft simulation. In *AIAA Infotech@Aerospace Conference, AIAA-2010-3322, April 2010*.
65. Gregory, I. M, Cao, C., Xargay, E., Hovakimyan, N., & Zou, X. (2009). $\mathcal{L}_1$ adaptive control design for NASA AirSTAR flight test vehicle. In *AIAA Guidance, Navigation, and Control Conference, AIAA-2009-5738, August 2009*.
66. Kitsios, I., Dobrokhodov, V., Kaminer, I., Jones, K., Xargay, E., Hovakimyan, N., Cao, C., Lizarraga, M., Gregory, I., Nguyen, N., & Krishnakumar, K. (2009). Experimental validation of a metrics driven $\mathcal{L}_1$ adaptive control in the presence of generalized unmodeled dynamics. In *AIAA Guidance, Navigation, and Control Conference, AIAA-2009-6188, August 2009*.
67. Steck, J., Lemon, K., Hinson, B., Kimball, D., & Nguyen, N. (2010). Model reference adaptive fight control adapted for general aviation: Controller gain simulation and preliminary flight testing on a bonanza fly-by-wire Testbed. In *AIAA Guidance, Navigation, and Control Conference, AIAA-2010-8278, August 2010*.

68. Bhattacharyya, S., Krishnakumar, K., & Nguyen, N. (2012). Adaptive autopilot designs for improved tracking and stability. In *AIAA Infotech@Aerospace Conference, AIAA-2012-2494, June 2012*.
69. Burken, J., Nguyen, N., & Griffin, B. (2010). Adaptive flight control design with optimal control modification for F- 18 aircraft model. In *AIAA Infotech@Aerospace Conference, AIAA-2010-3364, April 2010*.
70. Campbell, S., Nguyen, N., Kaneshige, J., & Krishnakumar, K. (2009). Parameter estimation for a hybrid adaptive flight controller. In *AIAA Infotech@Aerospace Conference, AIAA-2009-1803, April 2009*.
71. Chen, S., Yang, Y., Balakrishnan, S. N., Nguyen, N., & Krishnakumar, K. (2009). SNAC convergence and use in adaptive autopilot design. In *International Joint Conference on Neural Networks, June 2009*.
72. Eberhart, R. L., & Ward, D. G. (1999). Indirect adaptive flight control system interactions. *International Journal of Robust and Nonlinear Control*, *9*, 1013–1031.
73. Hinson, B., Steck, J., Rokhsaz, K., & Nguyen, N. (2011). Adaptive control of an elastic general aviation aircraft. In *AIAA Guidance, Navigation, and Control Conference, AIAA-2011-6560, August 2011*.
74. Lemon, K., Steck, J., Hinson, B., Rokhsaz, K., & Nguyen, N. (2011). Application of a six degree of freedom adaptive controller to a general aviation aircraft. In *AIAA Guidance, Navigation, and Control Conference, AIAA-2011-6562, August 2011*.
75. Nguyen, N., Tuzcu, I., Yucelen, T., & Calise, A. (2011). Longitudinal dynamics and adaptive control application for an aeroelastic generic transport model. In *AIAA Atmospheric Flight Mechanics Conference, AIAA-2011-6319, August 2011*.
76. Rajagopal, K., Balakrishnan, S.N., Nguyen, N., & Krishnakumar, K. (2010). Robust adaptive control of a structurally damaged aircraft. In *AIAA Guidance, Navigation, and Control Conference, AIAA-2010-8012, August 2010*.
77. Reed, S., Steck, J., & Nguyen, N. (2011). Demonstration of the optimal control modification for general aviation: Design and simulation. In *AIAA Guidance, Navigation, and Control Conference, AIAA-2011-6254, August 2011*.
78. Reed, S., Steck, J., & Nguyen, N. (2014). Demonstration of the optimal control modification for 6-DOF control of a general aviation aircraft. In *AIAA Guidance, Navigation, and Control Conference, AIAA-2014-1292, January 2014*.
79. Stepanyan, V., , Nguyen, N., & Krishnakumar, K. (2009). Adaptive control of a transport aircraft using differential thrust. In *AIAA Guidance, Navigation, and Control Conference, AIAA-2009-5741, August 2009*.
80. Boskovic, J., Jackson, J., Mehra, R., & Nguyen, N. (2009). Multiple-model adaptive fault-tolerant control of a planetary lander. *AIAA Journal of Guidance, Control, and Dynamics*, *32*(6), 1812–1826.
81. Lam, Q., & Nguyen, N. (2013). Pointing control accuracy and robustness enhancement of an optical payload system using a direct adaptive control combined with an optimal control modification. In *AIAA Infotech@Aerospace Conference, AIAA-2013-5041, August 2013*.
82. Lefevre B., & Jha, R. (2009). Hybrid adaptive launch vehicle ascent flight control. In *AIAA Guidance, Navigation, and Control Conference, AIAA-2009-5958, August 2009*.
83. Swei, S., & Nguyen, N. (2016). Adaptive estimation of disturbance torque for orbiting spacecraft using recursive least squares method. In *AIAA Infotech@Aerospace Conference, AIAA-2016-0399, January 2016*.
84. Hovakimyan, N., Kim, N., Calise, A. J., Prasad, J. V. R., & Corban, E. J. (2001). Adaptive output feedback for high-bandwidth control of an unmanned helicopter. In *AIAA Guidance, Navigation and Control Conference, AIAA-2001-4181, August 2001*.
85. Nguyen, N., Swei, S., & Ting, E. (2015). Adaptive linear quadratic gaussian optimal control modification for flutter suppression of adaptive wing. In *AIAA Infotech@Aerospace Conference, AIAA 2015-0118, January 2015*.
86. Kumar, M., Rajagopal, K., Balakrishnan, S. N., & Nguyen, N. (2014). Reinforcement learning based controller synthesis for flexible aircraft wings. *IEEE/CAA Journal of Automatica Sinica*, *1*(4), 435–448.

87. Ishihara, A., Al-Ali, K., Kulkarni, N., & Nguyen, N. (2009). Modeling Error Driven Robot Control. In *AIAA Infotech@Aerospace Conference, AIAA-2009-1974, April 2009*.
88. Sharma, M., Calise, A., & Corban, J. E. (2000). Application of an adaptive autopilot design to a family of guided munitions. In *AIAA Guidance, Navigation, and Control Conference, AIAA-2000-3969, August 2000*.
89. Nguyen, N., Bright, M., & Culley, D. (2007). Adaptive feedback optimal control of flow separation on stators by air injection. *AIAA Journal*, *45*(6),
90. Nguyen, N. (2013). Adaptive control for linear uncertain systems with unmodeled dynamics revisited via optimal control modification. In *AIAA Guidance, Navigation, and Control Conference, AIAA-2013-4988, August 2013*.
91. Lemaignan, B. (2005). Flying with no flight controls: handling qualities analyses of the baghdad event. In *AIAA Atmospheric Flight Mechanics Conference, AIAA-2005-5907, August 2005*.
92. Nguyen, N. (2012). Bi-objective optimal control modification adaptive control for systems with input uncertainty. In *AIAA Guidance, Navigation, and Control Conference, AIAA-2012-4615, August 2012*.
93. Nguyen, N. (2010). Optimal control modification adaptive law for time-scale separated systems. In *American Control Conference, June 2010*.
94. Stepanyan, V., & Nguyen, N. (2009). Control of systems with slow actuators using time scale separation. In *AIAA Guidance, Navigation, and Control Conference, AIAA-2009-6272, August 2009*.
95. Nguyen, N., & Stepanyan, V. (2010). Flight-propulsion response requirements for directional stability and control. In *AIAA Infotech@Aerospace Conference, AIAA-2010-3471, April 2010*.
96. Tuzcu, I., & Nguyen, N. (2009). Aeroelastic modeling and adaptive control of generic transport model. In AIAA Atmospheric Flight Mechanics, AIAA-2010-7503, August 2010.
97. Tuzcu, I., & Nguyen, N. (2010). Modeling and control of generic transport model. In *51st AIAA/ASME/ASCE/AHS/ASC Structures, Structural Dynamics, and Materials Conference, AIAA-2010-2622, April 2010*.
98. Yucelen, T., Kim, K., Calise, A., & Nguyen, N. (2011). Derivative-free output feedback adaptive control of an aeroelastic generic transport model. In *AIAA Guidance, Navigation, and Control Conference, AIAA-2011-6454, August 2011*.
99. Nguyen, N., & Jacklin, S. (2010). Stability, convergence, and verification and validation challenges of neural net adaptive flight control. In *Applications of Neural Networks in High Assurance Systems Studies in Computational Intelligence* (Vol. 268, pp. 77–110). Berlin: Springer.
100. Nguyen, N., & Jacklin, S. (2007). Neural net adaptive flight control stability, verification and validation challenges, and future research. In *International Joint Conference on Neural Networks, August 2007*.
101. Nguyen, N., Ishihara, A., Stepanyan, V., & Boskovic, J. (2009). Optimal control modification for robust adaptation of singularly perturbed systems with slow actuators. In *AIAA Guidance, Navigation, and Control Conference, AIAA-2009-5615, August 2009*.
102. Gilbreath, G. P. (2001). Prediction of Pilot-Induced Oscillations (PIO) due to Actuator Rate Limiting Using the Open-Loop Onset Point (OLOP) Criterion. In M.S. Thesis, Air Force Institute of Technology, Wright-Patterson Air Force Base, Ohio, 2001.
103. Schumann, J., & Liu, Y. (2007). Tools and methods for the verification and validation of adaptive aircraft control systems. In *IEEE Aerospace Conference, March 2007*.
104. Jacklin, S. (2009). Closing the certification gaps in adaptive flight control software. In *AIAA Guidance, Navigation, and Control Conference, AIAA-2008-6988, August 2008*.
105. Jacklin, S. A., Schumann, J. M., Gupta, P. P., Richard, R., Guenther, K., & Soares, F. (2005). Development of advanced verification and validation procedures and tools for the certification of learning systems in aerospace applications. In *AIAA Infotech@aerospace Conference, September 2005*.
106. Jacklin, S. A. (2015). Survey of verification and validation techniques for small satellite software development. In *Space Tech Expo Conference, May 2015*.

107. Crespo, L. G., Kenny, S. P., & Giesy, D. P. (2008). Figures of merit for control verification. In *AIAA Guidance, Navigation, and Control Conference, AIAA 2008-6339, August 2008*.
108. Hodel, A. S., Whorton, M., & Zhu, J. J. (2008). Stability metrics for simulation and flight-software assessment and monitoring of adaptive control assist compensators. In *AIAA Guidance, Navigation, and Control Conference, AIAA 2008-7005, August 2008*.
109. Ishihara, A., Ben-Menahem, S., & Nguyen, N. (2009). Time delay margin computation via the Razumikhin method for an adaptive control system. In *AIAA Guidance, Navigation, and Control Conference, AIAA-2009-5969, August 2009*.
110. Ishihara, A., Ben-Menahem, S., & Nguyen, N. (2009). Time delay margin estimation for direct adaptive control of a linear system. In *IASTED International Conference on Identification, Control and Applications, August 2009*.
111. Ishihara, A., Nguyen, N., & Stepanyan, V. (2010). Time delay margin estimation for adaptive outer- loop longitudinal aircraft control. In *AIAA Infotech@Aerospace Conference, AIAA-2010-3455, April 2010*.
112. Nguyen, N., & Summers, E. (2011). On time delay margin estimation for adaptive control and robust modification adaptive laws. In *AIAA Guidance, Navigation, and Control Conference, AIAA-2011-6438, August 2011*.
113. Nguyen, N., & Boskovic, J. (2008). Bounded linear stability margin analysis of nonlinear hybrid adaptive control. In *American Control Conference, June 2008*.
114. Rajagopal, K., Balakrishnan, S. N., Nguyen, N., & Krishnakumar, K. (2013). Time delay margin analysis of modified state observer based adaptive control. In *AIAA Guidance, Navigation, and Control Conference, AIAA-2013-4755, August 2013*.
115. Stepanyan, V., Krishnakumar, K., Nguyen, N., & Van Eykeren, L. (2009). Stability and performance metrics for adaptive flight control. In *AIAA Guidance, Navigation, and Control Conference, AIAA-2009-5965, August 2009*.
116. Belcastro, C., & Belcastro, C. (2003). On the validation of safety critical aircraft systems, part I: Analytical and simulation methods. In *AIAA Guidance, Navigation, and Control Conference, AIAA-2003-5559, August 2003*.
117. Belcastro, C., & Belcastro, C. (2003). On the validation of safety critical aircraft systems, Part II: Analytical and simulation methods. In *AIAA Guidance, Navigation, and Control Conference, AIAA-2003-5560, August 2003*.
118. Duke, E. L., Brumbaugh, R. W., & Disbrow, D. (1989). A rapid prototyping facility for flight research in advanced systems concepts. In *IEEE Computer, May 1989*.
119. Matsutani, M., Jang, J., Annaswamy, A., Crespo, L. G., Kenny, S. P. (2008). An adaptive control technology for safety of a GTM-like aircraft. In *NASA CR-2008-1, December 2008*.
120. Annaswamy, A., Jang, J., & Lavretsky, E. (2008). Stability margins for adaptive controllers in the presence of time-delay. In *AIAA Guidance, Navigation, and Control Conference, AIAA 2008-6659, August 2008*.
121. Li, D., Patel, V. V., Cao, C., Hovakimyan, N., & Wise, K. (2007). Optimization of the time-delay margin of $\mathcal{L}_1$ adaptive controller via the design of the underlying filter. In *AIAA Guidance, Navigation, and Control Conference, AIAA 2007-6646, August 2007*.

Chapter 2
Nonlinear Systems

Abstract A brief overview of nonlinear systems is presented in this chapter. Nonlinear systems are inherently more complex to study than linear systems. Nonlinear systems possess many complex behaviors that are not observed in linear systems. Multiple equilibrium points, limit cycle, finite escape time, and chaos are illustrative of some of the complex behaviors of nonlinear systems. Global stability of a nonlinear system over its entire solution domain is difficult to analyze. Linearization can provide information on the local stability of a region about an equilibrium point. The phase plane analysis of a nonlinear system is related to that of its linearized systems because the local behaviors of the nonlinear system can be approximated by the behaviors of its linearized systems in the vicinity of the equilibrium points. Because nonlinear systems can have multiple equilibrium points, one important fact to note is that the trajectories of a nonlinear system can exhibit unpredictable behaviors.

Nonlinear systems are abundant in nature. In fact, most real-world systems are inherently nonlinear. Linear systems in some regards are viewed as idealization of nonlinear systems in subspaces of nonlinear solutions. Nonlinear systems possess many complex behaviors that are not observed in linear systems. Multiple equilibrium points, limit cycle, finite escape time are illustrative of some of the complex behaviors of nonlinear systems. The learning objectives of this chapter are the following:

- To develop an understanding of equilibrium concepts and linearization; and
- To be able to assess local stability of equilibrium points.

■

Consider a typical control block diagram as shown in Fig. 2.1.

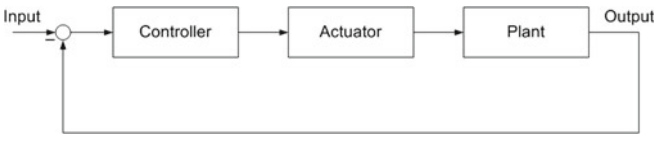

Fig. 2.1 Typical control block diagram

N.T. Nguyen, *Model-Reference Adaptive Control*, Advanced Textbooks
in Control and Signal Processing, https://doi.org/10.1007/978-3-319-56393-0_2

The objective of a controller is to enable the output of a system, called a plant, to track or follow a command input. A system generally can be described by a nonlinear plant

$$\dot{x} = f(x, u, t) \tag{2.1}$$

subject to an initial condition $x(t_0) = x_0$, where $x(t) = \left[x_1(t)\ x_2(t)\ \dots\ x_n(t) \right]^\top \in \mathbb{R}^n$ is called a state vector, $u(t) = \left[u_1(t)\ u_2(t)\ \dots\ u_m(t) \right]^\top \in \mathbb{R}^m$ is a control vector, $t \in \mathbb{R}^+$ is time, and $f() = \left[f_1()\ f_2()\ \dots\ f_n() \right]^\top \in \mathbb{R}^n$ is a nonlinear transition function.

The output, or response, of the system can generally be written as

$$y = h(x, u, t) \tag{2.2}$$

where $y(t) = \left[y_1(t)\ y_2(t)\ \dots\ y_l(t) \right]^\top \in \mathbb{R}^l$ is the system output and $h() = \left[h_1()\ h_2()\ \dots\ h_l() \right]^\top \in \mathbb{R}^l$ is a nonlinear output function.

Equations (2.1) and (2.2) together form the system state-space representation.

When $m = l = 1$, the system is said to be a single-input, single-output (SISO) system. When $m \neq 1$ and $l \neq 1$, the system is said to be a multiple-input, multiple-output (MIMO) system. The system can also be single-input, multiple-output (SIMO); or multiple-input, single-output (MISO).

When the system is explicitly dependent on time t as in Eqs. (2.1) and (2.2), the system is said to be non-autonomous or time-varying. When the explicit dependency on time is not present, then the system is said to be autonomous or time-invariant.

A special case of nonlinear systems is a linear affine-in-control form which is given by

$$\dot{x} = f(x, t) + g(x, t)\, u \tag{2.3}$$

$$y = h(x, t) \tag{2.4}$$

In contrast to nonlinear systems, a linear time-varying (LTV) state-space system is expressed by

$$\dot{x} = A(t)\, x + B(t)\, u \tag{2.5}$$

$$y = C(t)\, x + D(t)\, u \tag{2.6}$$

where the matrices $A(t)$, $B(t)$, $C(t)$, and $D(t)$ are functions of t.

When these matrices are constant matrices, then the following system is linear time-invariant (LTI):

$$\dot{x} = Ax + Bu \tag{2.7}$$

$$y = Cx + Du \tag{2.8}$$

LTI systems are much easier to analyze since there are a wealth of design and analysis tools for such systems. As a result, many control system designs are still based on a LTI representation.

The general solution for a LTI state-space system is given by

$$x = e^{A(t-t_0)}x_0 + \int_{t_0}^{t} e^{A(t-\tau)}Bu\,(\tau)\,d\tau \tag{2.9}$$

$$y = Ce^{A(t-t_0)}x_0 + C\int_{t_0}^{t} e^{A(t-\tau)}Bu\,(\tau)\,d\tau + Du\,(t) \tag{2.10}$$

where e^{At} is a matrix exponential function which is defined by the inverse Laplace transform

$$e^{At} = \mathscr{L}^{-1}\left[(sI - A)^{-1}\right] \tag{2.11}$$

Example 2.1:

- The following second-order spring-mass-damper system

$$m\ddot{x} + c\dot{x} + k\,(x)\,x = bu$$

  where m, c, and b are constant, $k\,(x)$ is a nonlinear spring function, and $u\,(x, \dot{x}) = f\,(x, \dot{x})$ is a nonlinear state feedback control is classified as an autonomous and nonlinear time-invariant system.
- The following spring-mass-damper system

$$m\ddot{x} + c\dot{x} + k\,(x)\,x = bu$$

  where $u\,(x, \dot{x}, t) = f\,(x, \dot{x}, t)$ is a nonlinear state feedback command-following control is classified as an non-autonomous and nonlinear time-varying system.
- The following spring-mass-damper system

$$m\ddot{x} + c\dot{x} + k\,(t)\,x = bu$$

  where $k\,(t)$ is a time-varying spring function is classified as a non-autonomous and nonlinear time-varying system if $u\,(x, \dot{x}, t)$ is a nonlinear state feedback command-following control or as a non-autonomous and linear time-varying system if $u\,(x, \dot{x}, t)$ is a linear state feedback command-following control.

■

In the block diagram in Fig. 2.1, the controller block represents a feedback control action such as a proportional-integral-derivative (PID) control. The output of the controller is a command to an actuator or servo system that actually controls the plant. A typical actuator system employed in many control systems is a servomotor that translates an actuator command signal into either a rotational or translational motion. The actuator system can be a source of nonlinearity due to such behaviors as

amplitude saturation and rate limiting when the actuator command exceeds certain limits. These nonlinear sources can make even a LTI control system to become nonlinear. Generally, actuator saturation should be avoided in order for a linear system to retain its linearity. Thus, actuators are sized appropriately to provide a bandwidth much larger than the control bandwidth of the system and the control gains are designed so as not to result in an actuator amplitude saturation or rate limiting. When properly designed, the actuator command will follow closely the actuator output. In an ideal case, the effect of the actuator system may be neglected during an initial design process.

Example 2.2: Consider a second-order plant

$$G(s) = \frac{X(s)}{U(s)} = \frac{b}{s^2 + 2\zeta\omega_n s + \omega_n^2}$$

whose actuator is subject to amplitude saturation and rate limiting described by

$$u(t) = \text{sat}(u_c(t)) = \begin{cases} u_{min} & u_c(t) < u_{min} \\ u_c(t) & u_{min} \le u_c(t) \le u_{max} \\ u_{max} & u_c(t) > u_{max} \end{cases}$$

$$u(t) = \text{rate}(u_c(t)) = \begin{cases} u(t - \Delta t) + \lambda_{min}\Delta t & \dot{u}_c(t) < \lambda_{min} \\ u_c(t) & \lambda_{min} \le \dot{u}_c(t) \le \lambda_{max} \\ u(t - \Delta t) + \lambda_{max}\Delta t & \dot{u}_c(t) >\le \lambda_{max} \end{cases}$$

where sat () is called a saturation function, rate () is called a rate limiter function, and $\dot{u}_c(t)$ is the actuator slew rate which is computed as

$$\dot{u}_c(t) = \frac{u_c(t) - u_c(t - \Delta t)}{\Delta t}$$

The saturation and rate limiter functions are nonlinear discontinuous functions since the input does not map linearly with the output when the amplitude or rate limit is exceeded.

The actuator command $u_c(t)$ is the output of the feedback controller. In this example, the goal is to enable $x(t)$ to track a sinusoidal input

$$r(t) = a \sin \omega t$$

The controller is designed to be a proportional-integral-derivative type

$$U_c(s) = \left(k_p + \frac{k_i}{s} + k_d s\right) E(s)$$

where $E(s) = R(s) - X(s)$.

Note that the system closed-loop transfer function for an ideal case with no actuator amplitude saturation is

$$\frac{X(s)}{R(s)} = \frac{bk_d s^2 + bk_p s + bk_i}{s^3 + (2\zeta\omega_n + bk_d)s^2 + \left(\omega_n^2 + bk_p\right)s + bk_i}$$

Even though the controller is linear, the response with the actuator saturation becomes quite nonlinear. Figure 2.2 shows the closed-loop response for $G(s) = \frac{5}{s^2+5s+6}, U(s) = \left(15 + \frac{8}{s} + 5s\right)E(s)$ with the amplitude limit at ± 1 for $r(t) = \sin t$.

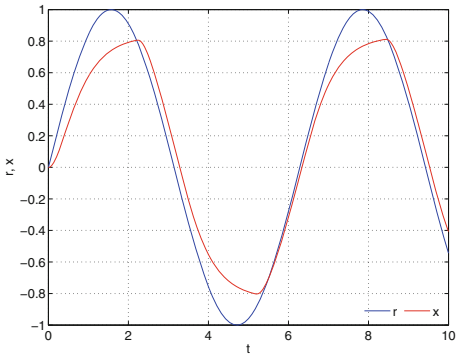

Fig. 2.2 Response due to amplitude saturation

2.1 Equilibrium and Linearization

All nonlinear autonomous systems possess a set of equilibrium points about which the systems exhibit certain stability properties. Denoting x^* as an equilibrium point, then for an autonomous system, the equilibrium points are the real roots of

$$f\left(x^*\right) = 0 \tag{2.12}$$

A system that is initially at an equilibrium point will remain there at all times since an equilibrium is a constant solution of an autonomous nonlinear system.

Unlike linear systems which can have only one equilibrium point, nonlinear systems can have multiple isolated equilibrium points. Under certain conditions, the behavior of a nonlinear system can be studied by linearization which can reveal some important local stability properties of the system at these equilibrium points. Linearization generally cannot predict the behavior of a nonlinear system far from an equilibrium point about which the linearization is performed.

Consider an autonomous system

$$\dot{x} = f(x) \tag{2.13}$$

The solution can be expressed as

$$x = x^* + \tilde{x} \tag{2.14}$$

where $\tilde{x}(t)$ is a small perturbation in the solution of $x(t)$ about the equilibrium x^*.

Then, Eq. (2.13) can be written as

$$\dot{x}^* + \dot{\tilde{x}} = f\left(x^* + \tilde{x}\right) \tag{2.15}$$

But, by the definition of an equilibrium point, $\dot{x}^* = 0$, and applying the Taylor series expansion yields the linearization of the nonlinear system (2.13) about the equilibrium point x^* as

$$\dot{\tilde{x}} = f\left(x^* + \tilde{x}\right) = f\left(x^*\right) + J\left(x^*\right)\tilde{x} + \cdots \approx J\left(x^*\right)\tilde{x} \tag{2.16}$$

where $J(x^*)$ is the Jacobian matrix of $f(x)$ evaluated at the equilibrium point x^* computed by

$$J\left(x^*\right) = \left.\frac{\partial f}{\partial x}\right|_{x=x^*} = \begin{bmatrix} \frac{\partial f_1}{\partial x_1} & \frac{\partial f_1}{\partial x_2} & \cdots & \frac{\partial f_1}{\partial x_n} \\ \frac{\partial f_2}{\partial x_1} & \frac{\partial f_2}{\partial x_2} & \cdots & \frac{\partial f_2}{\partial x_2} \\ \vdots & \vdots & \ddots & \vdots \\ \frac{\partial f_n}{\partial x_1} & \frac{\partial f_n}{\partial x_2} & \cdots & \frac{\partial f_n}{\partial x_n} \end{bmatrix}_{x=x^*} \tag{2.17}$$

Example 2.3 Consider a rotating pendulum without friction in Fig. 2.3. The equation of motion is given by

$$\ddot{\theta} + \frac{g}{l}\sin\theta - \omega^2 \sin\theta\cos\theta = 0$$

This can be cast in a state-space form by setting $x_1(t) = \theta(t)$ and $x_2(t) = \dot{\theta}(t)$ as

$$\begin{bmatrix} \dot{x}_1 \\ \dot{x}_2 \end{bmatrix} = \begin{bmatrix} x_2 \\ -\frac{g}{l}\sin x_1 + \omega^2 \sin x_1 \cos x_1 \end{bmatrix}$$

The equilibrium points can be found by setting $\dot{x}_1(t) = 0$ and $\dot{x}_2(t) = 0$. This gives the following solution:

$$x_1^* = \begin{cases} \cos^{-1}\left(\frac{g}{l\omega^2}\right) & , \omega \geq \sqrt{\frac{g}{l}} \\ 0,\ \pi & , \omega < \sqrt{\frac{g}{l}} \end{cases}$$

$$x_2^* = 0$$

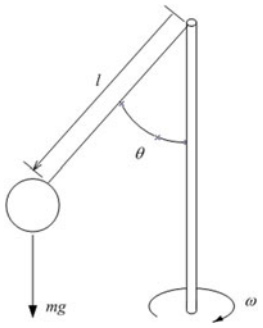

Fig. 2.3 Rotating pendulum

Physically, this means that one of the equilibrium points occurs when the angular speed ω exceeds a certain value and the pendulum will be suspended by an angle as the centrifugal force exerted on the pendulum is in balance with its weight. The other two equilibrium points occur when the angular speed ω is low enough and the pendulum is at either the bottom or the top in the vertical plane. Thus, this nonlinear system has three equilibrium points.

The equation of motion can be linearized by computing its Jacobian matrix as

$$J = \begin{bmatrix} 0 & 1 \\ -\frac{g}{l}\cos x_1 + \omega^2\left(\cos^2 x_1 - \sin^2 x_1\right) & 0 \end{bmatrix}$$

Evaluating the Jacobian matrix at the equilibrium points yields

$$J\left(\cos^{-1}\left(\frac{g}{l\omega^2}\right), 0\right) = \begin{bmatrix} 0 & 1 \\ \frac{g^2}{l^2\omega^2} - \omega^2 & 0 \end{bmatrix}$$

$$J\left(0, 0\right) = \begin{bmatrix} 0 & 1 \\ -\frac{g}{l} + \omega^2 & 0 \end{bmatrix}$$

$$J\left(\pi, 0\right) = \begin{bmatrix} 0 & 1 \\ \frac{g}{l} + \omega^2 & 0 \end{bmatrix}$$

The solutions of both the nonlinear and linearized equations of motion are in good agreement for $\omega < \sqrt{\frac{g}{l}}$ as shown in Fig. 2.4. At a higher value of $\theta(t)$, clearly the accuracy of the linearized solution tends to suffer as shown in Fig. 2.4. This is one of the drawbacks of the linearization in that the small perturbation assumption typically breaks down when the solution is not close enough to an equilibrium. The validity of a linearized solution therefore must be verified to ensure that the predicted linear behavior is a good approximation of the nonlinear behavior in the proximity to an equilibrium point.

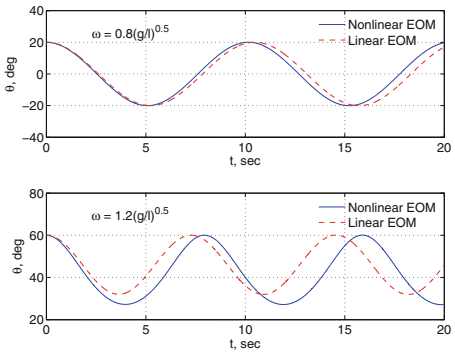

Fig. 2.4 Comparison between nonlinear and linear solutions, $\frac{g}{l} = 1$

2.2 Local Stability and Phase Plane Analysis

Global stability of a nonlinear system over its entire solution domain is difficult to analyze. Linearization can provide information on the local stability in a region about an equilibrium point. For a LTI system, there is only one equilibrium point which is the origin. For a linearized system, the origin corresponds to an equilibrium point of the nonlinear system about which the linearization is performed. Recall that a LTI system is absolutely stable if the eigenvalues of the transition matrix A all have negative real part. That is,

$$\Re\left(\lambda\left(A\right)\right) < 0 \tag{2.18}$$

A is then said to be a Hurwitz matrix. Notationally, it can also be written as $\lambda\left(A\right) \in \mathbb{C}^{-}$ where $\mathbb{C}^{-}$ is a space of complex numbers having negative real part.

Phase portraits are plots of trajectories of the solution which can be useful for studying the behaviors of second-order nonlinear systems. Phase portraits can also be used to study the behaviors of linearized systems from which local stability of the nonlinear systems can be learned. For a second-order LTI system, there are two

eigenvalues, denoted by λ_1 and λ_2. The trajectories in the vicinity of the equilibrium point can exhibit different characteristics depending on the values of λ_1 and λ_2.

1. Stable or unstable node occurs when both λ_1 and λ_2 are real and have the same sign. When $\lambda_1 < 0$ and $\lambda_2 < 0$, the node is a stable node and all trajectories converge to the node. When $\lambda_1 > 0$ and $\lambda_2 > 0$, the node is an unstable node and the trajectories diverge from the node. The behaviors of a stable node and an unstable node are illustrated in Fig. 2.5.

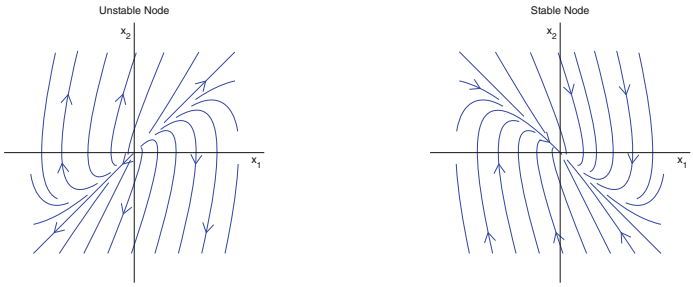

Fig. 2.5 Phase portrait of a node

2. Saddle point occurs when both λ_1 and λ_2 are real and have opposite signs. Because one of the eigenvalue corresponds to an unstable pole, half of the trajectories diverge from the center of a saddle point as shown in Fig. 2.6. The system is always on the verge of instability.

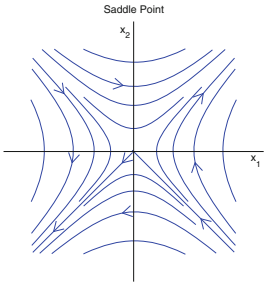

Fig. 2.6 Phase portrait of a saddle point

3. Stable or unstable focus occurs when both λ_1 and λ_2 are a complex conjugate pair. When $\mathrm{Re}(\lambda_1) < 0$ and $\mathrm{Re}(\lambda_2) < 0$, the focus is a stable focus and the trajectories spiral toward the focus as illustrated in Fig. 2.7. When $\mathrm{Re}(\lambda_1) > 0$ and $\mathrm{Re}(\lambda_2) > 0$, the focus is an unstable focus and the trajectories spiral outward from the focus as shown in Fig. 2.7.

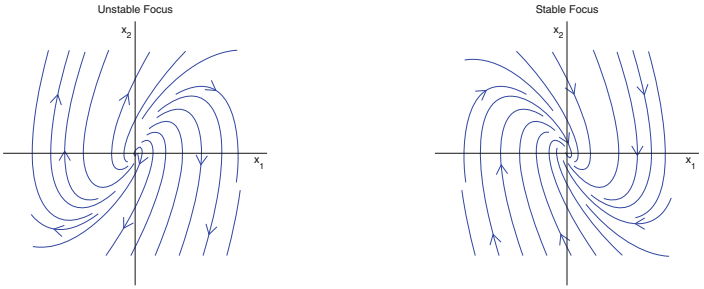

Fig. 2.7 Phase portrait of a focus

4. Center occurs when both λ_1 and λ_2 are purely imaginary. All trajectories encircle the center point at the origin with concentric-level curves as illustrated in Fig. 2.8.

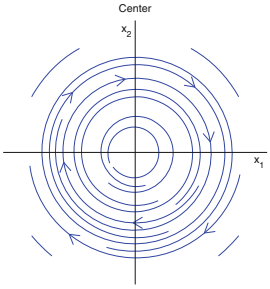

Fig. 2.8 Phase portrait of a center

The phase plane analysis of a nonlinear system is related to that of its linearized system because the local behaviors of the nonlinear system can be approximated by the behaviors of its linearized systems in the vicinity of the equilibrium points. Because a nonlinear system can have multiple equilibrium points, one important fact to note is that the trajectories of the nonlinear solution can exhibit unpredictable behaviors. For example, if the solution starts with an initial condition near a stable equilibrium point, it does not necessarily guarantee that the ensuing trajectories will converge to a stable node or focus if there exists an unstable equilibrium point in the solution set.

Example 2.4: From Example 2.3, the eigenvalues of the linearized systems are

$$\lambda_{1,2}\left[J\left(x_1^* = \cos^{-1}\left(\frac{g}{l\omega^2}\right)\right)\right] = \pm i\sqrt{\omega^2 - \frac{g^2}{l^2\omega^2}}$$

$$\lambda_{1,2}\left[J\left(x_1^* = 0\right)\right] = \pm i\sqrt{\frac{g}{l} - \omega^2}$$

$$\lambda_{1,2}\left[J\left(x_1^* = \pi\right)\right] = \pm\sqrt{\frac{g}{l} + \omega^2}$$

The first two equilibrium points are centers, and the last equilibrium point is a saddle point. The phase portrait is shown in Fig. 2.9.

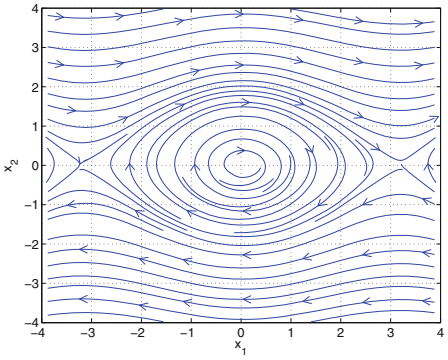

Fig. 2.9 Phase portrait of $\ddot{\theta} + \frac{g}{l}\sin\theta - \omega^2 \sin\theta\cos\theta = 0,\ \frac{g}{l} = 1,\ \omega = 0.8\sqrt{\frac{g}{l}}$

2.3 Other Nonlinear Behaviors

Nonlinear systems differ from linear systems in that they can exhibit many complex behaviors [1]. One feature which has been discussed is the existence of multiple isolated equilibrium points. There are many other complex behaviors that are unique to nonlinear systems, such as finite escape time, limit cycle, chaos.

1. Finite escape time: An unstable linear system becomes unbounded as time approaches to infinity. For nonlinear systems, an interesting phenomenon exists. It is possible for a nonlinear system to become unbounded in a finite interval of time. The solution then exhibits a finite escape time.

   Example 2.5: The nonlinear system

   $$\dot{x} = x^2$$

   subject to $x\,(0) = 1$ has a solution

   $$x\,(t) = -\frac{1}{t-1}$$

   which is defined only for $t \in [0, 1)$. The solution has a finite escape time at $t = 1$.

2. Limit cycle: For some nonlinear systems, a limit cycle is a periodic nonlinear solution represented by a closed trajectory in the phase plane such that all trajectories in its vicinity either converge to it or diverge from it. A limit cycle can be classified as stable, unstable, or neutrally stable depending on the behaviors of the trajectories of the solution in its vicinity. A stable limit cycle and a stable equilibrium point are the only two types of "regular" attractors.

   Example 2.6: The Van der Pol oscillator described by

$$\ddot{x} - \mu\left(1 - x^2\right)\dot{x} + x = 0$$

   has a stable limit cycle as shown in Fig. 2.10.

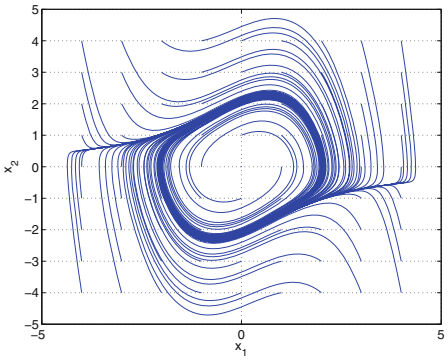

Fig. 2.10 Stable limit cycle of Van der Pol oscillator, $\mu = 0.5$

2.4 Summary

Nonlinear systems can have multiple isolated equilibrium points. Under certain conditions, the behavior of a nonlinear system can be studied by linearization which can reveal some important local stability properties of the nonlinear system at these equilibrium points. Linearization generally cannot predict the behavior of a nonlinear system far from an equilibrium point about which the linearization is performed. Nonlinear systems differ from linear systems in that they can exhibit many complex behaviors, such as finite escape time, limit cycle, chaos. Global stability of a nonlinear system over its entire solution domain is difficult to analyze. Linearization can provide information on the local stability in a region about an equilibrium point. The phase plane analysis of a nonlinear system is related to that of its linearized system because the local behaviors of the nonlinear system can be approximated by the behaviors of its linearized systems in the vicinity of the equilibrium points. Because a nonlinear system can have multiple equilibrium points, one important fact to note is that the trajectories of the nonlinear system can exhibit unpredictable behaviors.

2.5 Exercises

1. Consider the following PID control system with the actuator amplitude saturation and rate limiting:

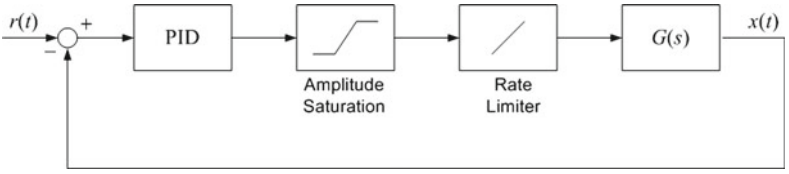

$$G(s) = \frac{5}{s^2 + 5s + 6}$$

with $k_p = 15$, $k_i = 8$, and $k_d = 5$ as the control gains. The actuator has both amplitude and rate limits between -1 and 1.

   a. Compute the characteristic roots of the ideal closed-loop system without consideration for actuator amplitude saturation and rate limiting.
   b. Construct a Simulink model for a sinusoidal input $r(t) = \sin t$. Plot the input, the ideal output without the actuator amplitude saturation and rate limiting, and the actual output for a simulation time $t = 10$ sec. Also plot the actuator command signal $u_c(t)$ and the control input signal to the plant $u(t)$.
   c. Comment on the effect of rate limiting.

2. Given

$$\ddot{\theta} + c\dot{\theta} + 2\sin\theta - 1 = 0$$

   a. Find all the equilibrium points of the system for $-\pi \leq \theta(t) \leq \pi$.
   b. Linearize the system and compute the eigenvalues about all the equilibrium points.
   c. Classify the types of the equilibrium points on a phase plane and plot the phase portrait of the nonlinear system.

3. Repeat Exercise 2 for

$$\begin{bmatrix} \dot{x}_1 \\ \dot{x}_2 \end{bmatrix} = \begin{bmatrix} -x_1 + x_1 x_2 \\ x_2 - x_1 x_2 \end{bmatrix}$$

4. Analytically determine the solution of the following nonlinear system:

$$\dot{x} = |x| x^2$$

with a general initial condition $x(0) = x_0$.

   a. Let $x_0 = 1$. Does the solution have a finite escape time? If so, determine it.
   b. Repeat part (a) with $x_0 = -1$.
   c. Comment on the effect of initial condition on the stability of the system.

Reference

1. Khalil, H. K. (2001). *Nonlinear systems*. Upper Saddle River: Prentice-Hall.

Chapter 3
Mathematical Preliminaries

Abstract This chapter presents some basic mathematical fundamentals for adaptive control theory. Vector and matrix norms are defined. The existence and uniqueness of a solution of a nonlinear differential equation are stated by the Cauchy theorem and the Lipschitz condition. Positive-valued functions are an important class of functions in adaptive control theory. Positive definiteness of a real-valued function is defined. The properties of a positive-definite matrix are given.

To be able to develop basic working knowledge of adaptive control, some mathematical fundamental concepts need to be understood. In this chapter, the learning objectives are to develop a basic understanding of:

- Norms as metric measures of vectors and matrices;
- Existence and uniqueness of ordinary differential equations in connection with the Lipschitz condition; and
- Positive-definite functions which are an important class of functions that are frequently used to establish stability of adaptive control.

3.1 Vector and Matrix Norms

3.1.1 Vector Norms

The state vector $x = \begin{bmatrix} x_1 & x_2 & \dots & x_n \end{bmatrix}^\top$ belongs to a set of real numbers in an n-dimensional Euclidean space $\mathbb{R}^n$. The Euclidean space is a metric space endowed with a notion of "distance" measure or norm. A real-valued quantity $\|x\|$ defined on $\mathbb{R}$ is said to be a norm of x if it satisfies the following conditions:

1. Positivity

$$\|x\| \geq 0 \, \forall x \in \mathbb{R}^n \tag{3.1}$$

N.T. Nguyen, *Model-Reference Adaptive Control*, Advanced Textbooks
in Control and Signal Processing, https://doi.org/10.1007/978-3-319-56393-0_3

2. Positive definiteness

$$\|x\| = 0 \tag{3.2}$$

if and only if $x = 0$.

3. Homogeneity

$$\|\alpha x\| = |\alpha| \, \|x\| \tag{3.3}$$

for any scalar α.

4. Triangle inequality

$$\|x + y\| \leq \|x\| + \|y\| \tag{3.4}$$

■

$\|x\|$ is said to be a semi-norm if it satisfies all the above conditions except the positive definiteness condition.

A p-norm of a vector $x \in \mathbb{C}^n$, where $\mathbb{C}^n$ is a complex number space that generalizes $\mathbb{R}^n$, is defined as

$$\|x\|_p = \left(\sum_{i=1}^{n} |x_i|^p \right)^{1/p} \tag{3.5}$$

for $p = 1, 2, \ldots, \infty$.

In special cases when $p = 1, 2, \infty$, the 1-, 2-, and infinity norms of x are defined as

$$\|x\|_1 = \sum_{i=1}^{n} |x_i| \tag{3.6}$$

$$\|x\|_2 = \sqrt{\sum_{i=1}^{n} |x_i|^2} \tag{3.7}$$

$$\|x\|_\infty = \max_{1 \leq i \leq n} |x_i| \tag{3.8}$$

The 2-norm is also called the Euclidean norm which is a "distance" measure of the vector x from the origin.

The inner product in the Euclidean space $\mathbb{R}^n$ is defined as

$$\langle x, y \rangle = \sum_{i=1}^{n} x_i y_i \tag{3.9}$$

In $\mathbb{R}^2$ and $\mathbb{R}^3$ spaces, the inner product is also known as the dot product. The inner product is also a measure in the Euclidean space since

$$\langle x, x \rangle = \|x\|_2^2 \tag{3.10}$$

A Euclidean space with a dot product is called an inner product space.

Let x and y be any two vectors, then the Cauchy-Schwartz inequality for the inner product is given by

$$\langle x, y\rangle \leq \|x\|_2 \, \|y\|_2 \tag{3.11}$$

Example 3.1 Verify that $\|x\|_2$, where $x \in \mathbb{R}^n$, satisfies the norm conditions.

Firstly, $\|x\|_2$ can be expressed as

$$\|x\|_2 = \sqrt{x_1^2 + x_2^2 + \cdots + x_n^2}$$

It is obvious that $\|x\|_2 \geq 0$ and $\|x\|_2 = 0$ if and only if $x_i = 0 \; \forall i = 1, 2, \ldots, n$. Thus, $\|x\|_2$ satisfies the positivity and positive definiteness conditions.

Since

$$\|\alpha x\|_2 = \sqrt{(\alpha x_1)^2 + (\alpha x_2)^2 + \cdots + (\alpha x_n)^2} = |\alpha| \sqrt{x_1^2 + x_2^2 + \cdots + x_n^2} = |\alpha| \, \|x\|_2$$

then $\|x\|_2$ satisfies the homogeneity condition.

Let $y \in \mathbb{R}^n$. Then,

$$\begin{aligned} \|x + y\|_2^2 &= (x_1 + y_1)^2 + (x_2 + y_2)^2 + \cdots + (x_n + y_n)^2 \\ &= x_1^2 + x_2^2 + \cdots + x_n^2 + 2x_1y_1 + 2x_2y_2 + \cdots + 2x_ny_n + y_1^2 + y_2^2 + \cdots + y_n^2 \\ &= \|x\|_2^2 + 2\,\langle x, y\rangle + \|y\|_2^2 \end{aligned}$$

Using the Cauchy-Schwartz inequality, one can write

$$\|x + y\|_2^2 \leq \|x\|_2^2 + 2\,\|x\|_2\,\|y\|_2 + \|y\|_2^2 = \left(\|x\|_2 + \|y\|_2\right)^2$$

Taking the square root of both sides yields the triangle inequality

$$\|x + y\|_2 \leq \|x\|_2 + \|y\|_2$$

Thus, $\|x\|_2$ satisfies all the norm conditions.

■

When $x\,(t)$ is a function of t, then the $\mathscr{L}_p$ norm is defined as

$$\|x\|_p = \left(\int_0^\infty \sum_{i=1}^{n} |x\,(t)|^p \, dt \right)^{1/p} \tag{3.12}$$

provided the integral exists, in which case $x \in \mathscr{L}_p$, the space with the $\mathscr{L}_p$ norm.

In particular, the $\mathscr{L}_1$, $\mathscr{L}_2$, and $\mathscr{L}_\infty$ norms are defined as

$$\|x\|_1 = \int_{t_0}^{\infty} \sum_{i=1}^{n} |x_i(t)|\, dt \tag{3.13}$$

$$\|x\|_2 = \sqrt{\int_{t_0}^{\infty} \sum_{i=1}^{n} |x_i(t)|^2\, dt} \tag{3.14}$$

$$\|x\|_\infty = \sup_{t \geq t_0} \max_{1 \leq i \leq n} |x_i(t)| \tag{3.15}$$

where the notation sup denotes the supremum over all t that yields the largest value of the argument.

Example 3.2 Let

$$x = \begin{bmatrix} 2e^{-t} \\ -e^{-2t} \end{bmatrix}$$

for all $t \geq 0$.

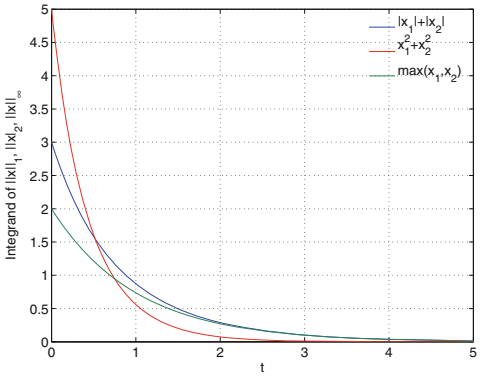

Fig. 3.1 Integrands of $\mathscr{L}_p$ norms

The integrands of the $\mathscr{L}_1$, $\mathscr{L}_2$, and $\mathscr{L}_\infty$ norms of $x(t)$ are shown in Fig. 3.1. The $\mathscr{L}_1$, $\mathscr{L}_2$, and $\mathscr{L}_\infty$ norms of $x(t)$ can be evaluated analytically as

$$\|x\|_1 = \int_0^{\infty} \left(2e^{-t} + e^{-2t}\right) dt = \frac{5}{2}$$

$$\|x\|_2 = \sqrt{\int_0^{\infty} \left(4e^{-2t} + e^{-4t}\right) dt} = \sqrt{\frac{9}{4}} = \frac{3}{2}$$

$$\|x\|_\infty = 2$$

Example 3.3 The function $x(t) = \sin t$ does not have a $\mathscr{L}_1$ or $\mathscr{L}_2$ norm because the integral of $\sin t$ for $t \in [0, \infty)$ does not exist. However, the $\mathscr{L}_\infty$ norm of $x(t)$ exists and is equal to 1. Thus, $x(t) \in \mathscr{L}_\infty$.

3.1.2 Matrix Norms

Let $A \in \mathbb{C}^m \times \mathbb{C}^n$ be an m-by n complex-valued matrix, then the induced p-norm of A is defined as

$$\|A\|_p = \sup_{x \neq 0} \frac{\|Ax\|_p}{\|x\|_p} \tag{3.16}$$

In special cases when $p = 1, 2, \infty$, then the 1-, 2-, and infinity norms of A are defined as

$$\|A\|_1 = \max_{1 \leq j \leq n} \sum_{i=1}^{m} |a_{ij}| \tag{3.17}$$

$$\|A\|_2 = \sqrt{\lambda_{max}(A^* A)} \tag{3.18}$$

$$\|A\|_\infty = \max_{1 \leq i \leq m} \sum_{j=1}^{n} |a_{ij}| \tag{3.19}$$

where a_{ij} is an element of the matrix A and A^* is the complex conjugate transpose of A. If $A \in \mathbb{R}^m \times \mathbb{R}^n$ is a real-valued matrix, then $A^* = A^\top$.

Another type of matrix norm is the Frobenius norm, which is not an induced norm and is defined as

$$\|A\|_F = \sqrt{\text{trace}(A^* A)} = \sqrt{\sum_{i=1}^{m} \sum_{j=1}^{n} |a_{ij}|^2} \tag{3.20}$$

where the trace operator is the sum of the diagonal elements of a square matrix, that is,

$$\text{trace}(A) = \sum_{i=1}^{n} a_{ii} \tag{3.21}$$

The matrix norm has the following properties:

$$\rho(A) \leq \|A\| \tag{3.22}$$

$$\|A + B\| \leq \|A\| + \|B\| \tag{3.23}$$

$$\|AB\| \leq \|A\| \, \|B\| \tag{3.24}$$

where A and B are any matrices of appropriate dimensions and ρ is the spectral radius operator of a square matrix which is defined as

$$\rho(A) = \max_{1 \leq i \leq n} |\lambda_i| \tag{3.25}$$

where λ_i is the ith eigenvalue of A.

Example 3.4 The norms of the following matrix A are to be computed:

$$A = \begin{bmatrix} 1+i & 0 \\ 2 & -1 \end{bmatrix}$$

The 1-norm of A is computed as

$$\|A\|_1 = \max_{1 \leq j \leq 2} \sum_{i=1}^{2} |a_{ij}| = \max(|1+i| + 2, |-1|) = \max\left(\sqrt{2} + 2, 1\right) = 3.4142$$

The 2-norm of A is computed as

$$A^* = \begin{bmatrix} 1-i & 2 \\ 0 & -1 \end{bmatrix}$$

$$A^*A = \begin{bmatrix} 1-i & 2 \\ 0 & -1 \end{bmatrix} \begin{bmatrix} 1+i & 0 \\ 2 & -1 \end{bmatrix} = \begin{bmatrix} 6 & -2 \\ -2 & 1 \end{bmatrix}$$

$$\lambda_{1,2}\left(A^*A\right) = 0.2984, \ 6.7016$$

$$\|A\|_2 = \sqrt{\lambda_{max}(A^*A)} = 2.5887$$

The infinity norm of A is computed as

$$\|A\|_\infty = \max_{1 \leq i \leq 2} \sum_{j=1}^{2} |a_{ij}| = \max(|1+i|, 2 + |-1|) = \max\left(\sqrt{2}, 3\right) = 3$$

The Frobenius norm of A is computed as

$$\|A\|_F = \sqrt{\text{trace}(A^*A)} = \sqrt{6+1} = 2.6458$$

The spectral radius of A is computed as

$$\lambda_{1,2}(A) = -1, 1+i$$

$$\rho(A) = \max(|-1|, |1+i|) = \sqrt{2} = 1.4142$$

Thus,

$$\rho(A) \leq \|A\|$$

3.2 Compact Set

A compact set is a mathematical representation of a region that contains a collection of mathematical objects. A compact set in a Euclidean space $\mathbb{R}^n$ is a closed and bounded set. In studying the Lyapunov stability theory, it is convenient to use the notion of a compact set to represent the collection of all the trajectories of a closed-loop adaptive control system.

Example 3.5 The set $\mathscr{S} \subset \mathbb{R}^2$ given by

$$\mathscr{S} = \left\{x \in \mathbb{R}^2 : |x_1| \leq a, |x_2| \leq b; a > 0, b > 0\right\}$$

is a compact set that represents a closed rectangular region in $\mathbb{R}^2$ as shown in Fig. 3.2.

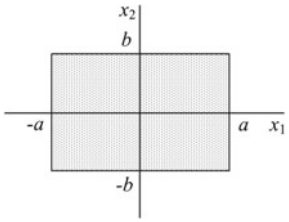

Fig. 3.2 A compact set

On the other hand, the complementary set $\mathscr{S}^c$ such that $\mathscr{S} \cup \mathscr{S}^c = \mathbb{R}^2$ (the union of $\mathscr{S}$ and $\mathscr{S}^c$ is $\mathbb{R}^2$)

$$\mathscr{S}^c = \left\{x \in \mathbb{R}^2 : |x_1| > a, |x_2| > b\right\}$$

is an open set and therefore is not a compact set.

3.3 Existence and Uniqueness

A nonlinear differential equation may or may not have a unique solution that is dependent continuously on an initial condition. Certain requirements are imposed on a nonlinear differential equation to ensure the existence of a unique solution. The existence and uniqueness are fundamental requirements for any nonlinear differential equations.

3.3.1 Cauchy Theorem

The existence of a solution of a nonlinear differential equation can be stated by the Cauchy theorem as follows:

Theorem 3.1 *Given*

$$\dot{x} = f(x, t) \tag{3.26}$$

with an initial condition $x(t_0) = x_0$, *if* $f(x, t)$ *is at least piecewise continuous in the closed region such that*

$$|t - t_0| \leq T, \ \|x - x_0\| \leq R \tag{3.27}$$

where $T > 0$ *and* $R > 0$ *are some positive constants, then there exists* $t_1 > t_0$ *such that at least one solution of Eq. (3.26) exists and is continuous over the time interval* $[t_0, t_1]$.

■

Geometrically, this simply means that continuity of $f(x, t)$ in a closed region that contains the initial condition ensures that there exists at least one continuous solution that lies therein. This is illustrated in Fig. 3.3. The gradient of a continuous solution of $x\left(t; t_0, x_0\right)$ starting from an initial condition $x(t_0) = x_0$ is the value of the function $f(x, t)$ at any point on the trajectory of $x(t)$. For the gradient to exist, $f(x, t)$ must be a continuous function.

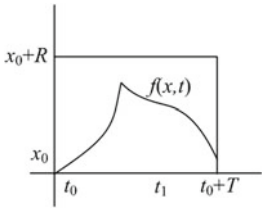

Fig. 3.3 Continuity of $f(x, t)$ in closed region

Example 3.6 Consider the differential equation

$$\dot{x} = \frac{1}{x - 1}$$

with $x\,(0) = 1$. It is obvious that $f\,(x)$ is discontinuous for $x = 1$ since $f\,(x)$ is defined for $x\,(t) > 1$ and $x\,(t) < 1$ for all t. So there is no solution for the equation with this initial condition. Now, suppose $x\,(0) = -1$. Then, $f\,(x)$ is defined in a region $x\,(t) < 1$ and $t \geq 0$ which includes $x_0 = -1$. Therefore, a solution exists for all $x\,(t) \leq -1$ and $t \geq 0$.

Note that the existence of a solution does not imply that the solution is unique. The requirement of uniqueness is imposed by the Lipschitz condition which is stated in the following theorem.

3.3.2 Global Lipschitz Condition

The uniqueness of a solution of a nonlinear differential equation can be stated by the following theorem:

Theorem 3.2 *If $f\,(x, t)$ is piecewise continuous in t and there exists a positive constant L such that*

$$\|f\,(x_2, t) - f\,(x_1, t)\| \leq L\,\|x_2 - x_1\| \tag{3.28}$$

for all $x_1, x_2 \in \mathbb{R}^n$ and $t \in [t_0, t_1]$, then Eq. (3.26) has a unique solution for all $t \in [t_0, t_1]$.

■

Inequality (3.28) is called the Lipschitz condition and the constant L is called a Lipschitz constant. When x_1 and x_2 are any two points in the Euclidean space $\mathbb{R}^n$, then $f\,(x, t)$ is said to be *globally* Lipschitz. Geometrically, the Lipschitz condition essentially imposes the continuity and boundedness of the partial derivative or the Jacobian of $f\,(x, t)$ with respect to $x\,(t)$ as illustrated in Fig. 3.4.

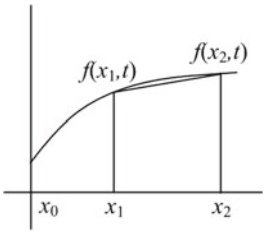

Fig. 3.4 Lipschitz condition

Example 3.7 The differential equation

$$\dot{x} = 3x^{\frac{2}{3}}$$

subject to $x\,(0) = 0$, not only has a solution $x\,(t) = t^3$ but also has a zero solution $x\,(t) = 0$. Thus, this equation does not have a unique solution.

The function $f\,(x) = 3x^{\frac{2}{3}}$ does not satisfy the global Lipschitz condition since the derivative of $f\,(x)$

$$f^{'}\,(x) = 2x^{-\frac{1}{3}}$$

is not bounded at $x = 0$.

Example 3.8

- The function $f\,(x) = x$ is globally Lipschitz since it has continuous and bounded derivative for all $x\,(t) \in \mathbb{R}$. The Lipschitz constant L is equal to 1.
- The function $f\,(x) = \sin x$ is globally Lipschitz since its derivative is continuous and bounded with a Lipschitz constant $L = 1$ for all $x\,(t) \in \mathbb{R}$.
- The function $f\,(x) = x^2$ is not globally Lipschitz since its derivative, $f^{'}\,(x) = 2x$, is unbounded for $x\,(t) \in \mathbb{R}$ as $x\,(t) \to \pm\infty$.

■

Note that the global Lipschitz condition is very restrictive since a function with this condition must have a bounded derivative for all values of $x\,(t) \in \mathbb{R}^n$ as $x\,(t) \to \pm\infty$. Many nonlinear physical models fail to satisfy this condition since physically there are usually upper and lower limits placed on variables of most if not all physical models. These limits thus does not require $x\,(t)$ to be in a domain that occupies the entire Euclidean space $\mathbb{R}^n$, but rather in a subset of it. This leads to a notion of local Lipschitz condition, which is less restrictive and can be easily satisfied by any nonlinear differential equations.

3.3.3 Local Lipschitz Condition

The uniqueness of a solution of a nonlinear differential equation in a finite neighborhood can be stated by the following theorem:

Theorem 3.3 *If $f\,(x, t)$ is piecewise continuous in t and there exists a positive constant L such that*

$$\|f\,(x_2, t) - f\,(x_1, t)\| \leq L\,\|x_2 - x_1\| \tag{3.29}$$

for some x_1 and x_2 in a finite neighborhood of x_0 and $t \in [t_0, t_1]$, then Eq. (3.26) has a unique solution in a finite time interval $t \in [t_0, t_0 + \delta]$, where $t_0 + \delta < t_1$.

■

The local Lipschitz condition now only imposes the continuity and boundedness of the partial derivative of $f(x, t)$ with respect to $x(t)$ over a finite neighborhood of x_0 as a subset of $\mathbb{R}^n$ instead of over all $x(t) \in \mathbb{R}^n$. Therefore, it is a less restrictive condition that can easily be met. In most cases, the local Lipschitz condition is a reasonable assumption for many continuous nonlinear functions.

Example 3.9 The differential equation

$$\dot{x} = 3x^{\frac{2}{3}}$$

subject to $x(0) = 1$ has a unique solution $x(t) = (t + 1)^3$ for a finite neighborhood of x_0, for example, $x(t) \in [1, 2]$. $f(x)$ satisfies the local Lipschitz condition since the derivative of $f(x)$ is now continuous and bounded for all $x(t) \in [1, 2]$.

Example 3.10 The function $f(x) = x^2$ is locally Lipschitz for any finite neighborhood of $x(t) \in [x_1, x_2]$, where x_1 and x_2 are finite-valued.

3.4 Positive Definite, Symmetric and Anti-Symmetric Matrices

3.4.1 Positive-Definite Matrix and Function

The Lyapunov stability theory for nonlinear systems often invokes a class of functions called positive-definite functions. One such function is a quadratic function

$$V(x) = x^\top P x \tag{3.30}$$

where $V(x) \in \mathbb{R}$ is a scalar function, $x \in \mathbb{R}^n$ is a vector, and $P \in \mathbb{R}^n \times \mathbb{R}^n$ is an n-by n matrix.

Definition 3.1 The quadratic scalar function $V(x)$ is said to be positive definite if $V(x) > 0$ or positive semi-definite if $V(x) \geq 0$ for all $x \neq 0$. Conversely, $V(x)$ is said to be negative definite if $V(x) < 0$ and negative semi-definite if $V(x) \leq 0$ for all $x \neq 0$.

Definition 3.2 The matrix P is said to be a positive-definite matrix, denoted as $P > 0$, if there exists a function $V(x)$ such that

$$V(x) = x^\top P x > 0 \tag{3.31}$$

Thus, $P > 0$ implies $V(x) > 0$.

■

A positive (negative) (semi)-definite matrix is defined the same way as a positive (negative) (semi-)definite function.

A positive-definite matrix P has the following properties:

- P is a symmetric matrix, that is,

$$P = P^{\top} \tag{3.32}$$

- All eigenvalues of P are real and positive, that is, $\lambda(P) > 0$.
- A scalar multiplication with a constant causes the product to have the same sign definiteness as the constant, that is, $\alpha P > 0$ if $\alpha > 0$ and $\alpha P < 0$ if $\alpha < 0$.
- Let A be any arbitrary matrix of appropriate dimension, then

$$A^{\top} P A > 0 \tag{3.33}$$

- Let Q be a positive-definite matrix of the same dimension as P, then

$$P + Q > 0 \tag{3.34}$$

- The quadratic function $V(x)$ is bounded from below and above by

$$\lambda_{min}(P) \|x\|_2^2 \leq V(x) \leq \lambda_{max}(P) \|x\|_2^2 \tag{3.35}$$

  which can be illustrated geometrically in Fig. 3.5, where $\lambda_{min}(.)$ and $\lambda_{max}(.)$ denote the minimum and maximum eigenvalues of a matrix, respectively.

The above properties apply for a negative definite matrix by reversing the inequality sign.

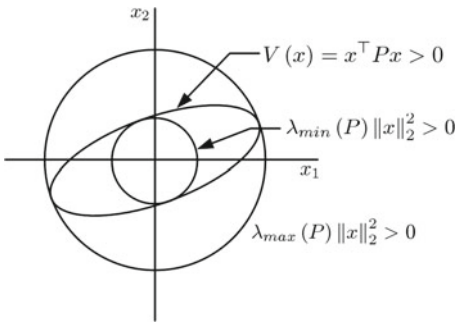

Fig. 3.5 Boundedness of positive-definite quadratic function

Example 3.11

- The identity matrix I is a positive-definite matrix.
- The matrix

$$P = \begin{bmatrix} 5 & 3 \\ 3 & 2 \end{bmatrix}$$

is positive definite since $\lambda_{1.2}(P) = 0.1459,\ 6.8541 > 0$.

- Let

$$A = \begin{bmatrix} 1 & -1 & 0 \\ 0 & 2 & 1 \end{bmatrix}$$

be an arbitrary matrix, then

$$A^\top P A = \begin{bmatrix} 1 & 2 \\ 2 & 5 \end{bmatrix} > 0$$

since $\lambda_{1,2}\left(A^\top P A\right) = 0.1716,\ 5.8284 > 0$.

- The quadratic function $V(x)$ is expressed as

$$V(x) = x^\top P x = 5x_1^2 + 6x_1x_2 + 2x_2^2$$

which, at a first glance, does not seem to be positive definite. By completing the square, it can be shown that $V(x) > 0$ as follows:

$$\begin{aligned} V(x) &= 5x_1^2 - \left(\frac{3}{\sqrt{2}}x_1\right)^2 + \left(\frac{3}{\sqrt{2}}x_1\right)^2 + 2\left(\frac{3}{\sqrt{2}}x_1\right)\left(\sqrt{2}x_2\right) + 2x_2^2 \\ &= \frac{1}{2}x_1^2 + \left(\frac{3}{\sqrt{2}}x_1 + \sqrt{2}x_2\right)^2 > 0 \end{aligned}$$

3.4.2 Anti-Symmetric Matrix

Definition 3.3 A matrix $Q \in \mathbb{R}^n \times \mathbb{R}^n$ is said to be an anti-symmetric (or skew-symmetric) matrix if

$$Q = -Q^\top \tag{3.36}$$

■

The elements of Q are then

$$q_{ij} = -q_{ji} \tag{3.37}$$

$$q_{ii} = 0 \tag{3.38}$$

An anti-symmetric matrix Q has the following properties:

- The eigenvalues of Q are purely imaginary if the matrix dimension n is even, and includes a zero if n is odd.
- $\det(Q) = 0$ or Q is singular if n is odd.
- Let A be any arbitrary matrix of appropriate dimension, then the product $A^\top QA$ is also an anti-symmetric matrix.
- Let $V(x)$ be a quadratic scalar function that is formed with Q. Then,

$$V(x) = x^\top Qx = 0 \tag{3.39}$$

Example 3.12 The matrix

$$Q = \begin{bmatrix} 0 & -4 & -1 \\ 4 & 0 & -1 \\ 1 & 1 & 0 \end{bmatrix}$$

is an anti-symmetric matrix. Its eigenvalues are $\lambda_{1,2,3}(Q) = 0, \pm 4.2426i$. Q is singular since one of its eigenvalues is zero or equivalently $\det(Q) = 0$.

The quadratic function given by

$$V(x) = x^\top Qx = 4x_1x_2 + x_1x_3 + x_2x_3 - 4x_1x_2 - x_1x_3 - x_2x_3$$

is identically zero. ■

Any arbitrary square matrix $A \in \mathbb{R}^n \times \mathbb{R}^n$ can be decomposed into a symmetric part and anti-symmetric part as follows:

$$A = M + N \tag{3.40}$$

where M is called the symmetric part of A and N is called the anti-symmetric part of A such that

$$M = \frac{1}{2}\left(A + A^\top\right) \tag{3.41}$$

$$N = \frac{1}{2}\left(A - A^\top\right) \tag{3.42}$$

If $V(x)$ is a quadratic function formed with A, then

$$V(x) = x^\top Ax = \frac{1}{2}x^\top\left(A + A^\top\right)x \tag{3.43}$$

3.5 Summary

Adaptive control theory requires a basic understanding of mathematics of matrix algebra. More advanced adaptive control theory requires a solid foundation in real analysis which is beyond the scope of this book. Various types of vector and matrix norms are defined. The existence and uniqueness of a solution of a nonlinear differential equation require the continuity condition and the Lipschitz condition. Positive-valued functions are an important class of functions in adaptive control theory. The positive definiteness of a real-valued function is defined. The properties of a positive-definite matrix are given.

3.6 Exercises

1. Verify that the 1-norm of $x \in \mathbb{R}^n$

$$\|x\|_1 = \sum_{i=1}^{n} |x_i|$$

   satisfies the norm conditions.
2. Compute analytically the 1-, 2-, infinity, and Frobenius norms of

$$A = \begin{bmatrix} 1 & 0 & -2 \\ 4 & 0 & 2 \\ -1 & 3 & 2 \end{bmatrix}$$

   and verify the answers with MATLAB using the function "norm."

   Note: MATLAB may be used to compute the eigenvalues.
3. Decompose A into its symmetric part P and anti-symmetric part Q. Write the quadratic function $V(x) = x^\top Px$. Is $V(x)$ positive (semi-)definite, negative (semi-)definite, or neither?
4. Given a set $\mathscr{C} \subset \mathbb{R}^2$

$$\mathscr{C} = \left\{x \in \mathbb{R}^2 : x_1^2 + 4x_2^2 - 1 < 0\right\}$$

   Is $\mathscr{C}$ a compact set? Write the set notation for the complementary set $\mathscr{C}^c$. Plot and illustrate the region in $\mathbb{R}^2$ that represents $\mathscr{C}$.
5. For each of the following equations, determine if $f(x)$ is locally Lipschitz at $x = x_0$ or globally Lipschitz:

a. $\dot{x} = \sqrt{x^2 + 1}, x_0 = 0.$
b. $\dot{x} = -x^3, x_0 = 1.$
c. $\dot{x} = \sqrt{x^3 + 1}, x_0 = 0.$

Chapter 4
Lyapunov Stability Theory

Abstract Stability of nonlinear systems are discussed in this chapter. Lyapunov stability, asymptotic stability, and exponential stability of an equilibrium point of a nonlinear system are defined. The Lyapunov's direct method is introduced as an indispensable tool for analyzing stability of nonlinear systems. The Barbashin–Krasovskii theorem provides a method for global stability analysis. The LaSalle's invariant set theorem provides a method for analyzing autonomous systems with invariant sets. Stability of non-autonomous systems involves the concepts of uniform stability, uniform boundedness, and uniform ultimate boundedness. The Barbalat's lemma is an important mathematical tool for analyzing asymptotic stability of adaptive control systems in connection with the concept of uniform continuity of a real-valued function.

Stability is an important consideration of any dynamical systems with feedback control. Stability for LTI systems can be analyzed by many well-established methods such as eigenvalue analysis, root locus, phase and gain margins, etc. For nonlinear systems, Lyapunov stability theory provides a powerful technique for stability analysis of such systems. The Lyapunov stability theory is central to the study of nonlinear adaptive control [1–4]. In this chapter, the learning objectives are to develop a basic understanding of:

N.T. Nguyen, *Model-Reference Adaptive Control*, Advanced Textbooks
in Control and Signal Processing, https://doi.org/10.1007/978-3-319-56393-0_4

- Various stability concepts for autonomous and non-autonomous systems, such as local stability, asymptotic stability, exponential stability, uniform stability, and uniform boundedness;
- Lyapunov's direct method and LaSalle's invariant set theorem for analyzing stability of nonlinear systems; and
- Uniform continuity concept and Barbalat's lemma for analyzing stability of non-autonomous systems.

4.1 Stability Concepts

Consider an autonomous system

$$\dot{x} = f(x) \tag{4.1}$$

with an initial condition $x(t_0) = x_0$, where $f(x)$ is locally Lipschitz in some subset $\mathscr{D}$ of $\mathbb{R}^n$ and the solution $x\left(t; t_{0,} x_0\right)$ exists and is unique in a region $B_R = \{x(t) \in \mathbb{R}^n : \|x\| < R\} \subset \mathscr{D}$ of an equilibrium point x^*. The region B_R can be thought of as a hypersphere in $\mathbb{R}^n$ with the origin at $x = x^*$. Colloquially, it is often referred to in the literature as a ball B_R. Since x^* is a constant vector, for convenience, the autonomous system can be transformed by shifting the equilibrium point to the origin at $x = 0$. Let $y(t) = x(t) - x^*$, then

$$\dot{y} = f\left(y + x^*\right) \triangleq g(y) \tag{4.2}$$

whose equilibrium is the origin $y^* = 0$.

Thus, for convenience, the equilibrium point for autonomous systems described by Eq. (4.1) is understood to be $x^* = 0$.

Example 4.1 The system

$$\begin{bmatrix} \dot{x}_1 \\ \dot{x}_2 \end{bmatrix} = \begin{bmatrix} -x_1 + x_1 x_2 \\ x_2 - x_1 x_2 \end{bmatrix}$$

has an equilibrium at $x_1^* = 1$ and $x_2^* = 1$.

The system can be transformed by letting $y_1(t) = x_1(t) - 1$ and $y_2(t) = x_2(t) - 1$ which yields

$$\begin{bmatrix} \dot{y}_1 \\ \dot{y}_2 \end{bmatrix} = \begin{bmatrix} -(y_1 + 1) + (y_1 + 1)(y_2 + 1) \\ (y_2 + 1) - (y_1 + 1)(y_2 + 1) \end{bmatrix} = \begin{bmatrix} y_1 y_2 + y_2 \\ -y_1 y_2 - y_1 \end{bmatrix}$$

4.1.1 Stability Definition

Definition 4.1 The equilibrium point $x^* = 0$ of a system starting at an initial condition $x(t_0) = x_0$ is said to be stable (in the sense of Lyapunov) if, for any $R > 0$, there exists some $r(R) > 0$ such that

$$\|x_0\| < r \Rightarrow \|x\| < R, \ \forall t \geq t_0 \tag{4.3}$$

Otherwise, the equilibrium point is unstable.

■

Stability concept essentially implies that, given a system with an initial condition close to the origin, the trajectory of the system can be kept arbitrarily close to it. Figure 4.1 illustrates the stability concept.

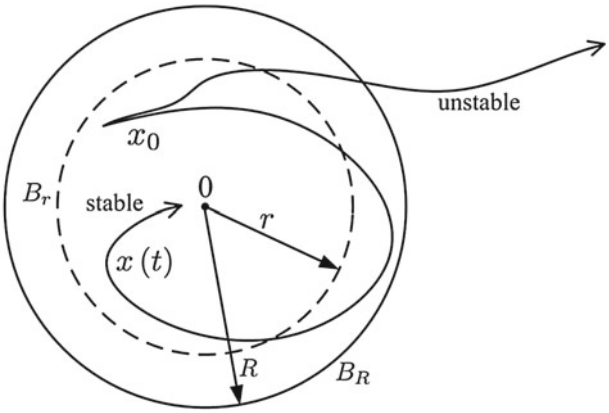

Fig. 4.1 Stability concept

Note that instability for linear systems means that the solution grows exponentially as $t \to \infty$ due to unstable poles in the right half plane, resulting in unbounded signals. For nonlinear systems, instability of an equilibrium does not always lead to unbounded signals. For example, the Van der Pol oscillator in Example 2.6 has a stable limit cycle that encloses an unstable equilibrium point at the origin. So, the equilibrium point in theory is unstable and the system cannot stay arbitrarily close to it. If we choose any arbitrary circle B_R to be completely inside the limit cycle, then no matter how close the initial condition is to the origin, the trajectory of the system will eventually escape the circle B_R as illustrated in Fig. 4.2. However, the trajectory tends to the limit cycle and remains there as $t \to \infty$.

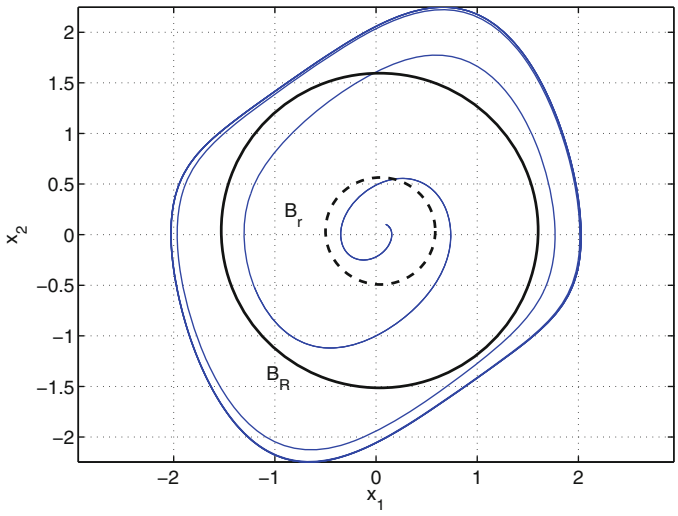

Fig. 4.2 Unstable origin of Van der Pol Oscillator

4.1.2 Asymptotic Stability

The stability concept in the Lyapunov sense does not explicitly imply that the trajectory of a nonlinear system will eventually converge to the origin. For example, an ideal spring-mass system without friction will display a sinusoidal motion forever if it is subject to a disturbance. So, the system is stable in the Lyapunov sense but does not converge to the origin. Asymptotic stability is a stronger stability concept than the Lyapunov stability concept and is defined as follows:

Definition 4.2 The equilibrium point $x^* = 0$ is said to be asymptotically stable if there exists some $r > 0$ such that

$$\|x_0\| < r \Rightarrow \lim_{t\to\infty} \|x\| = 0 \tag{4.4}$$

■

All trajectories starting within B_R will eventually converge to the origin. The origin is then said to be attractive. For a second-order system, both stable focus and stable node are attractive. The largest such region is called a region of attraction, defined as

$$\mathscr{R}_A = \left\{ x\left(t\right) \in \mathscr{D} : \lim_{t\to\infty} x\left(t\right) = 0 \right\} \tag{4.5}$$

It is noted that the asymptotic stability concept in the definition above is a local concept for any initial condition that lies within the ball B_R. If an equilibrium point of a system is asymptotically stable for all initial conditions $x_0 \in \mathbb{R}^n$, then the

equilibrium point is said to be asymptotically stable in the large. This notion is equivalent to global asymptotic stability.

Example 4.2 The equilibrium point of the system

$$\dot{x} = -x^2$$

with $x(0) = x_0 > 0$ is asymptotically stable since the solution

$$x(t) = \frac{x_0}{x_0 t + 1}$$

tends to zero as $t \to \infty$. The region of attraction is

$$\mathscr{R}_A = \left\{ x(t) \in \mathbb{R}^+ : x(t) = \frac{x_0}{x_0 t + 1}, x_0 > 0 \right\}$$

Note that the equilibrium point is unstable if $x_0 < 0$ and has a finite escape time at $t = -1/x_0$. So, the equilibrium is asymptotically stable for all $x(t) \in \mathbb{R}^+$ but not asymptotically stable in the large.

4.1.3 Exponential Stability

The rate of convergence of a solution of a nonlinear differential equation can be estimated by comparing its solution to an exponential decay function [2, 4]. This gives rise to a notion of exponential stability which is defined as follows:

Definition 4.3 The equilibrium point $x^* = 0$ is said to be exponentially stable if there exist two strictly positive constants α and β such that

$$\|x\| \leq \alpha \|x_0\| e^{-\beta(t-t_0)}, \ \forall x \in B_R, \ t \geq t_0 \tag{4.6}$$

■

This definition gives a local version of the exponential stability concept for some initial condition x_0 close to the origin. If the origin is exponentially stable for all initial conditions $x_0 \in \mathbb{R}^n$, then the equilibrium point is said to be exponentially stable in the large. The constant β is called the rate of convergence.

It is noted that exponential stability implies asymptotic stability, but the converse is not true.

Example 4.3 The differential equation

$$\dot{x} = -x\left(1 + \sin^2 x\right)$$

subject to $x(0) = 1$ is bounded from below and above by

$$-2|x| \leq |\dot{x}| \leq -|x|$$

if $x(t) > 0$.

The solution is bounded from below and above as shown in Fig. 4.3 by

$$e^{-2t} \leq |x(t)| \leq e^{-t}$$

Therefore, the equilibrium is exponentially stable and the rate of convergence is 1.

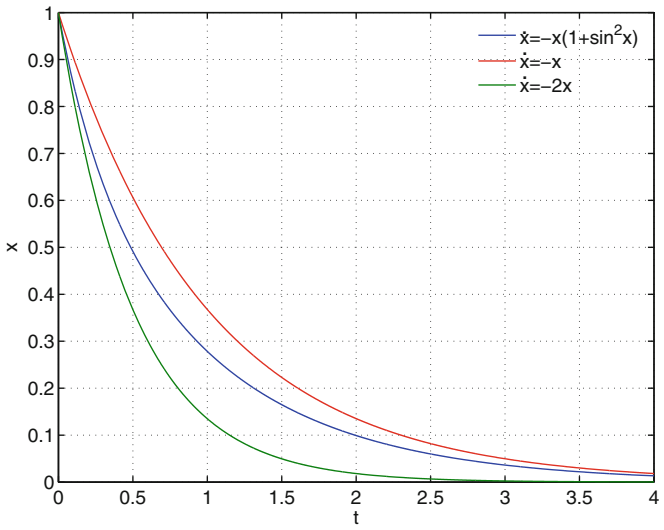

Fig. 4.3 Exponential stability

4.2 Lyapunov's Direct Method

4.2.1 Motivation

Consider a spring-mass-damper system with friction as shown in Fig. 4.4.

The equation of motion without external forces is described by

$$m\ddot{x} + c\dot{x} + kx = 0 \tag{4.7}$$

where m is the mass, $c > 0$ is the viscous friction coefficient, and k is the spring constant.

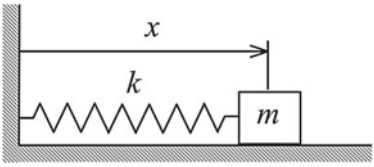

Fig. 4.4 Spring-mass system

The system in the state-space form is expressed as

$$\begin{bmatrix} \dot{x}_1 \\ \dot{x}_2 \end{bmatrix} = \begin{bmatrix} x_2 \\ -\frac{c}{m}x_2 - \frac{k}{m}x_1 \end{bmatrix} \tag{4.8}$$

where $x_1(t) = x(t)$ and $x_2(t) = \dot{x}(t)$. The system has an equilibrium point at $(0, 0)$, that is, it is at rest with zero displacement and velocity

The spring-mass-damper system possesses two types of energy: (1) kinetic energy and (2) potential energy. The kinetic energy of any moving point mass is given by

$$T = \frac{1}{2}mv^2 = \frac{1}{2}m\dot{x}^2 = \frac{1}{2}mx_2^2 \tag{4.9}$$

The potential energy for a spring is given by

$$U = \frac{1}{2}kx^2 = \frac{1}{2}kx_1^2 \tag{4.10}$$

The energy of the spring-mass-damper system is the sum of the kinetic energy and potential energy. Thus, the energy function of the system is defined as

$$E = T + U = \frac{1}{2}mx_2^2 + \frac{1}{2}kx_1^2 \tag{4.11}$$

Note that the energy function is a quadratic positive-definite function.

The friction force also does work on the mass. This type of work is called a non-conservative work which is usually due to a dissipative force, as opposed to a conservative work of which potential energy is one form. The work function is defined in general as

$$W = \oint F.dx \tag{4.12}$$

where F is a force acting on a mass that displaces it by an infinitesimal distance dx, and the integral is evaluated over a path that the mass traverses.

For a viscous friction force, the work done is evaluated as

$$W = \int c\dot{x}dx = \int c\dot{x}^2 dt = \int cx_2^2 dt \tag{4.13}$$

The total energy of the system is the sum of the energy and the work done. Thus,

$$E + W = \frac{1}{2}mx_2^2 + \frac{1}{2}kx_1^2 + \int cx_2^2 dt \tag{4.14}$$

According to the first law of thermodynamics, the total energy of a closed system is neither created or destroyed. In other words, the total energy is conserved and is equal to a constant. Thus,

$$E + W = \text{const} \tag{4.15}$$

or equivalently

$$\dot{E} + \dot{W} = 0 \tag{4.16}$$

This energy conservation law can be easily verified for the spring-mass-damper system as

$$\dot{E}+\dot{W} = mx_2\dot{x}_2+kx_1\dot{x}_1+\frac{d}{dt}\int cx_2^2 dt = mx_2\left(-\frac{c}{m}x_2 - \frac{k}{m}x_1\right)+kx_1x_2+cx_2^2 = 0 \tag{4.17}$$

The time derivative of the energy function is evaluated as

$$\dot{E} = mx_2\dot{x}_2 + kx_1\dot{x}_1 = mx_2\left(-\frac{c}{m}x_2 - \frac{k}{m}x_1\right) + kx_1x_2 = -cx_2^2 \leq 0 \tag{4.18}$$

for $c > 0$.

The reason $\dot{E}$ is only negative semi-definite is because $\dot{E}$ can be zero for any $x_1 \neq 0$.

Thus, for a dissipative system, the time derivative of the positive definite energy function is a negative semi-definite function. That is,

$$\dot{E} \leq 0 \tag{4.19}$$

The equilibrium point is then stable. Thus, stability of a dynamical system can be studied by examining the time derivative of the energy function. The Lyapunov stability theory is motivated by the concept of energy. In fact, the energy function is a Lyapunov function. Whereas the energy function is unique for a given physical system, a Lyapunov function can be any positive-definite function that satisfies the negative (semi-)definiteness of its time derivative.

Lyapunov's direct method is a powerful tool for assessing stability of an equilibrium of a nonlinear system directly without solving the system's dynamical equation.

The motivation of the method is based on the energy concept of a mechanical system. From the spring-mass-damper example, the following observations are made:

- The energy function is positive definite.
- The time rate of the energy function is negative semi-definite in which case the equilibrium is stable.

Aleksandr Mikhailovich Lyapunov (1857–1918) recognized that stability of a system can be proven without developing a true knowledge of the system energy using a class of positive-definite functions, known as Lyapunov functions, provided they can be found.

Definition 4.4 A function $V(x)$ is said to be a Lyapunov function if it satisfies the following conditions:

- $V(x)$ is positive definite; i.e.,

$$V(x) > 0 \tag{4.20}$$

  and has a continuous first partial derivative.
- $\dot{V}(x)$ is at least negative semi-definite; i.e.,

$$\dot{V}(x) = \frac{\partial V}{\partial x}\dot{x} = \frac{\partial V}{\partial x} f(x) \leq 0 \tag{4.21}$$

  or

$$\dot{V}(x) < 0 \tag{4.22}$$

■

Geometrically, a Lyapunov function may be illustrated by a bowl-shaped surface as shown in Fig. 4.5. The Lyapunov function is a level curve on the bowl starting

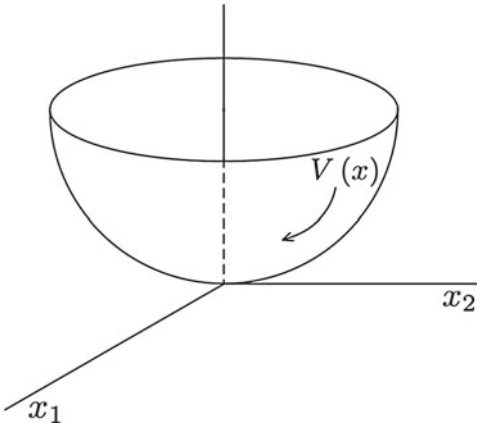

Fig. 4.5 Illustration of Lyapunov function

at the top and progressing downward toward the bottom of the bowl. The value of the Lyapunov function thus decreases toward zero at the bottom of the bowl which represents a stable equilibrium.

Example 4.4 For the spring-mass-damper system, the energy function is clearly a Lyapunov function. Suppose one chooses another Lyapunov candidate function

$$V(x) = x_1^2 + x_2^2 > 0$$

Then,

$$\dot{V}(x) = 2x_1\dot{x}_1 + 2x_2\dot{x}_2 = 2x_1x_2 + 2x_2\left(-\frac{c}{m}x_2 - \frac{k}{m}x_1\right) = 2x_1x_2\left(1 - \frac{k}{m}\right) - 2\frac{c}{m}x_2^2$$

Note that $\dot{V}(x)$ is not negative (semi-)definite because of the term with the product x_1x_2. So, this candidate function is not a Lyapunov function.

In many systems, finding a Lyapunov function is not trivial. Unfortunately, there is no straightforward way to obtain a Lyapunov function. Perhaps, the most obvious Lyapunov function for any system is the energy function, but it is not always easy to identify such a function for a nonlinear system unless one knows the physics of the system.

Example 4.5 Consider a pendulum with viscous friction whose motion is described by

$$ml^2\ddot{\theta} + c\dot{\theta} + mgl\sin\theta = 0$$

which is expressed in a state-space form as

$$\begin{bmatrix} \dot{x}_1 \\ \dot{x}_2 \end{bmatrix} = \begin{bmatrix} x_2 \\ -\frac{c}{ml^2}x_2 - \frac{g}{l}\sin x_1 \end{bmatrix}$$

with $x_1(t) = \theta(t)$ and $x_2(t) = \dot{\theta}(t)$.

It is not obvious what a Lyapunov candidate function would look like for this system. One can try

$$V(x) = x_1^2 + x_2^2$$

but that would not yield $\dot{V}(x) \leq 0$ since

$$\dot{V}(x) = 2x_1\dot{x}_1 + 2x_2\dot{x}_2 = 2x_1x_2 + 2x_2\left(-\frac{c}{ml^2}x_2 - \frac{g}{l}\sin x_1\right) \not\leq 0$$

The kinetic energy and potential energy for the pendulum are known to be

$$T = \frac{1}{2}ml^2x_2^2$$

$$U = mgl\,(1 - \cos x_1)$$

So, the energy function is

$$E = T + U = \frac{1}{2}ml^2x_2^2 + mgl\,(1 - \cos x_1) > 0$$

Using this as a Lyapunov function, then evaluating $\dot{V}\,(x)$ gives

$$\dot{V}\,(x) = ml^2x_2\dot{x}_2 + mgl\sin x_1\dot{x}_1 = ml^2x_2\left(-\frac{c}{ml^2}x_2 - \frac{g}{l}\sin x_1\right) + mgl\sin x_1x_2 = -cx_2^2 \leq 0$$

Thus, it is not surprising that the energy function can always be used for a Lyapunov function, provided such a function can be found.

■

In summary, it can be seen that the Lyapunov's direct method is a powerful technique for studying stability of an equilibrium point of a nonlinear system.

4.2.2 Lyapunov Theorem for Local Stability

Theorem 4.1 Let $x^* = 0$ be an equilibrium point and if there exists a Lyapunov function $V\,(x) > 0$ for all $x\,(t) \in B_R$ such that $\dot{V}\,(x) \leq 0$ for all $x\,(t) \in B_R$, then the equilibrium is locally stable in a Lyapunov sense. Moreover, if $\dot{V}\,(x) < 0$ for all $x\,(t) \in B_R$, then the equilibrium is locally asymptotically stable.

■

It is important to note that the Lyapunov's direct method only gives a sufficient condition for stability. Failure of a Lyapunov candidate function to satisfy the stability condition does not imply that the equilibrium is unstable. It simply means that a good Lyapunov candidate function may not have been identified. An exception to this rule is the energy function which provides both the necessary and sufficient conditions for stability.

Example 4.6 For the pendulum in Example 4.5, $\dot{V}\,(x)$ is negative semi-definite, so the equilibrium is locally stable.

Example 4.7 Consider the system

$$\begin{bmatrix}\dot{x}_1\\ \dot{x}_2\end{bmatrix} = \begin{bmatrix}x_1^3 + x_1x_2^2 - x_1\\ x_2^3 + x_1^2x_2 - x_2\end{bmatrix}$$

Choose a Lyapunov candidate function

$$V\,(x) = x_1^2 + x_2^2$$

Then, $\dot{V}(x)$ is evaluated as

$$\begin{aligned}\dot{V}(x) &= 2x_1\dot{x}_1 + 2x_2\dot{x}_2 = 2x_1\left(x_1^3 + x_1x_2^2 - x_1\right) + 2x_2\left(x_2^3 + x_1^2x_2 - x_2\right)\\ &= 2\left(x_1^2 + x_2^2\right)\left(x_1^2 + x_2^2 - 1\right)\end{aligned}$$

Observing $\dot{V}(x)$, one can conclude that $\dot{V}(x) < 0$ for all $x \in B_R$ where

$$B_R = \left\{x(t) \in \mathscr{D} \subset \mathbb{R}^2 : x_1^2 + x_2^2 < 1\right\}$$

The equilibrium is asymptotically stable. The region of attraction is B_R within which all the trajectories converge to the equilibrium.

Example 4.8 For the spring-mass-damper system, consider a Lyapunov candidate function

$$V(x) = x^\top Px > 0$$

where $x(t) = \left[x_1(t)\ x_2(t)\right]^\top$ and $P = P^\top > 0$ to be determined such that $\dot{V}(x) < 0$ for asymptotic stability.

Expressing $V(x)$ as

$$V(x) = \begin{bmatrix}x_1 & x_2\end{bmatrix}\begin{bmatrix}p_{11} & p_{12}\\ p_{12} & p_{22}\end{bmatrix}\begin{bmatrix}x_1\\ x_2\end{bmatrix} = p_{11}x_1^2 + 2p_{12}x_1x_2 + p_{22}x_2^2$$

where p_{ij} are elements of P, then evaluating $\dot{V}(x)$ yields

$$\begin{aligned}\dot{V}(x) &= 2p_{11}x_1\dot{x}_1 + 2p_{12}\left(x_1\dot{x}_2 + \dot{x}_1x_2\right) + 2p_{22}x_2\dot{x}_2\\ &= 2p_{11}x_1x_2 + 2p_{12}x_1\left(-\frac{c}{m}x_2 - \frac{k}{m}x_1\right) + 2p_{12}x_2^2 + 2p_{22}x_2\left(-\frac{c}{m}x_2 - \frac{k}{m}x_1\right)\\ &= -2p_{12}\frac{k}{m}x_1^2 + 2\left(p_{11} - p_{12}\frac{c}{m} - p_{22}\frac{k}{m}\right)x_1x_2 + 2\left(p_{12} - p_{22}\frac{c}{m}\right)x_2^2\end{aligned}$$

Since $\dot{V}(x) < 0$, one can choose

$$\dot{V}(x) = -2x_1^2 - 2x_2^2$$

Equating terms then yields

$$p_{12}\frac{k}{m} = 1 \Rightarrow p_{12} = \frac{m}{k}$$

$$p_{12} - p_{22}\frac{c}{m} = -1 \Rightarrow p_{22} = \frac{m}{c}(p_{12} + 1) = \frac{m}{c}\left(\frac{m}{k} + 1\right)$$

$$p_{11} - p_{12}\frac{c}{m} - p_{22}\frac{k}{m} = 0 \Rightarrow p_{11} = p_{12}\frac{c}{m} + p_{22}\frac{k}{m} = \frac{c}{k} + \frac{m}{c} + \frac{k}{c}$$

The matrix

$$P = \begin{bmatrix} \frac{c}{k} + \frac{m}{c} + \frac{k}{c} & \frac{m}{k} \\ \frac{m}{k} & \frac{m}{c}\left(\frac{m}{k} + 1\right) \end{bmatrix}$$

can be verified to be positive definite for $m > 0$, $c > 0$, and $k > 0$.

The system is then asymptotically stable. It is noted that since the system is linear, stability is always referred to in a global context.

Another approach to be considered is as follows:

The system can be expressed as

$$\dot{x} = Ax$$

where

$$A = \begin{bmatrix} 0 & 1 \\ -\frac{k}{m} & -\frac{c}{m} \end{bmatrix}$$

is a Hurwitz matrix with negative real part eigenvalues.

Proceeding to evaluate $\dot{V}(x)$ yields

$$\dot{V}(x) = \dot{x}^\top Px + x^\top P\dot{x}$$

which upon substitution yields

$$\dot{V}(x) = x^\top A^\top Px + x^\top PAx = x^\top \left(A^\top P + PA\right)x < 0$$

This inequality is satisfied if and only if

$$A^\top P + PA < 0$$

which is called a linear matrix inequality (LMI) that can be solved for P.

Alternatively, one can write the LMI as a linear matrix equation

$$A^\top P + PA = -Q$$

where $Q = Q^\top > 0$ is a positive-definite matrix. This equation is known as the algebraic Lyapunov equation.

Thus, setting $Q = 2I$, where I is an identity matrix, which in this case is a 2-by-2 matrix, then yields

$$\dot{V}(x) = -2x^\top x = -2x_1^2 - 2x_2^2$$

The matrix P is then solved from

$$A^\top P + PA = -2I$$

There are numerical methods that can be used to solve the Lyapunov equation. For a low matrix dimension less than 4, the equation can be solved analytically. For this example, one can set up

$$\begin{bmatrix} 0 & -\frac{k}{m} \\ 1 & -\frac{c}{m} \end{bmatrix} \begin{bmatrix} p_{11} & p_{12} \\ p_{12} & p_{22} \end{bmatrix} + \begin{bmatrix} p_{11} & p_{12} \\ p_{12} & p_{22} \end{bmatrix} \begin{bmatrix} 0 & 1 \\ -\frac{k}{m} & -\frac{c}{m} \end{bmatrix} = \begin{bmatrix} -2 & 0 \\ 0 & -2 \end{bmatrix}$$

then expand

$$\begin{bmatrix} -2p_{12}\frac{k}{m} & p_{11} - p_{12}\frac{c}{m} - p_{22}\frac{k}{m} \\ p_{11} - p_{12}\frac{c}{m} - p_{22}\frac{k}{m} & 2\left(p_{12} - p_{22}\frac{c}{m}\right) \end{bmatrix} = \begin{bmatrix} -2 & 0 \\ 0 & -2 \end{bmatrix}$$

and equate terms to solve for p_{ij}.

4.2.3 Lyapunov Theorem for Exponential Stability

Theorem 4.2 Let $x^* = 0$ be an equilibrium point and if there exists a Lyapunov function $V(x) > 0$ for all $x(t) \in B_R$ such that $\dot{V}(x) < 0$ for all $x(t) \in B_R$ and there also exist two positive constants η and β such that

$$V(x) \leq \eta \|x\|^2 \tag{4.23}$$

and

$$\dot{V}(x) \leq -\beta V(x) \tag{4.24}$$

then the equilibrium is locally exponentially stable.

Example 4.9 Consider

$$\dot{x} = -x\left(1 + \sin^2 x\right)$$

subject to $x(0) = 1$.

Choose a Lyapunov candidate function

$$V(x) = x^2 = \|x\|^2$$

So,

$$V(0) = x_0^2 = 1$$

$\dot{V}(x)$ is computed as

$$\dot{V}(x) = 2x\dot{x} = -2x^2\left(1 + \sin^2 x\right) \leq -2\|x\|^2 = -2V(x) < 0$$

Integrating $\dot{V}(x)$ yields

$$V(t) \leq V(0)\, e^{-2t}$$

or

$$x^2 \leq e^{-2t}$$

which is equivalent to

$$|x| \leq e^{-t}$$

4.2.4 Radially Unbounded Functions

Definition 4.5 A continuous, positive-valued function $\varphi(x) \in \mathbb{R}^+$ is said to belong to class $\mathscr{K}$; i.e., $\varphi(x) \in \mathscr{K}$, if

- $\varphi(0) = 0$
- $\varphi(x)$ is strictly increasing for all $x(t) \leq R$ or $x(t) < \infty$

Definition 4.6 A continuous, positive-valued function $\varphi(x) \in \mathbb{R}^+$ is said to belong to class $\mathscr{K}\mathscr{R}$; i.e., $\varphi(x) \in \mathscr{K}\mathscr{R}$, if

- $\varphi(0) = 0$
- $\varphi(x)$ is strictly increasing for all $x(t) < \infty$
- $\lim_{x\to\infty} \varphi(x) = \infty$

Definition 4.7 A continuous, positive-valued function $V(x) \in \mathbb{R}^+$ with $V(0) = 0$ is said to be a radially unbounded function if there exists a function $\varphi(\|x\|) \in \mathscr{K}\mathscr{R}$ such that $V(x) \geq \varphi(\|x\|)$ for all $x(t) \in \mathbb{R}^n$. Thus, $V(x)$ must be infinitely large when $\|x\|$ tends to infinity. That is,

$$V(x) \to \infty \text{ as } \|x\| \to \infty \tag{4.25}$$

4.2.5 Barbashin–Krasovskii Theorem for Global Asymptotic Stability

The asymptotic stability concept in the Lyapunov sense of an equilibrium point is a local concept such that there exists $V(x) > 0$ for all $x \in B_R$, where B_R is a finite region in $\mathscr{D} \subset \mathbb{R}^n$ for which the function $f(x)$ is locally Lipschitz, then $\dot{V}(x) < 0$. There exists a region of attraction $\mathscr{R}_A \subset \mathscr{D} \subset \mathbb{R}^n$ in which all trajectories will converge to the origin. On the other hand, asymptotic stability in the large is a global concept that requires the region of attraction to extend to the entire Euclidean space $\mathbb{R}^n$. As a result, $V(x) > 0$ must be defined for all $x \in \mathbb{R}^n$.

There is an additional requirement imposed on $V(x)$ for stability in the large. That is, $V(x)$ is required to be a radially unbounded function. The condition of the radial

unboundedness of $V(x)$ ensures that all trajectories in the large when $\|x\| \to \infty$ will be attracted to the origin. The global stability Lyapunov condition can be stated by the following Barbashin–Krasovskii theorem [2, 4]:

Theorem 4.3 The equilibrium point $x^* = 0$ is asymptotically stable in the large if there exists a radially unbounded Lyapunov function $V(x) > 0$ for all $x(t) \in \mathbb{R}^n$ such that $\dot{V}(x) < 0$ for all $x(t) \in \mathbb{R}^n$.

Example 4.10 Consider a scalar linear system

$$\dot{x} = -ax$$

where $a > 0$, whose equilibrium point at the origin is asymptotically stable in the large. Suppose a Lyapunov candidate function is chosen as

$$V_1(x) = \frac{x^2}{1+x^2} > 0$$

$V_1(x) \in \mathscr{K}$ but $V_1(x) \notin \mathscr{KR}$ since $V_1(0) = 0$ and $V_1(x)$ is strictly increasing for all $x(t) < \infty$, but $\lim_{x\to\infty} V_1(x) = 1$. This means that one cannot analyze global asymptotic stability of the origin of this system using this Lyapunov candidate function since

$$\dot{V}_1(x) = \frac{2x\dot{x}}{1+x^2} - \frac{2x^3\dot{x}}{\left(1+x^2\right)^2} = \frac{-2ax^2}{\left(1+x^2\right)^2} \to 0$$

as $\|x\| \to \infty$, which implies that the origin is not asymptotically stable as $\|x\| \to \infty$. Therefore, the origin is stable but not asymptotically stable in the large, which is a contradiction.

Now, suppose another Lyapunov candidate function is chosen as

$$V_2(x) = x^2 > 0$$

$V_2(x)$ is a radially unbounded function since there exists a function $\varphi(\|x\|) = \alpha x^2 \in \mathscr{KR}$, where $\alpha < 1$, such that $V_2(x) \geq \varphi(\|x\|)$ for all $x(t) < \infty$. Global asymptotic stability of the origin can be analyzed using this radially unbounded Lyapunov candidate function. Evaluating $\dot{V}_2(x)$ yields

$$\dot{V}_2(x) = 2x\dot{x} = -2ax^2 < 0$$

which implies that the origin is indeed asymptotically stable in the large.

4.2.6 LaSalle's Invariant Set Theorem

Asymptotic stability requires that $\dot{V}(x) < 0$. Yet, for the spring-mass-damper system, if the energy function is chosen as a Lyapunov function, then $\dot{V}(x) \leq 0$, even though the solution of the system is clearly asymptotic in the presence of a dissipative force due to the viscous friction. The LaSalle's invariant set theorem can resolve this apparent contradiction when an asymptotically stable equilibrium point of an autonomous system only satisfies the Lyapunov condition $\dot{V}(x) \leq 0$.

Definition 4.8 For an autonomous system, a set $\mathscr{M}$ is said to be invariant if every trajectory that starts from a point in $\mathscr{M}$ will remain in $\mathscr{M}$ for all future time [2, 4]. That is,

$$x(0) \in \mathscr{M} \Rightarrow x(t) \in \mathscr{M}, \ \forall t \geq t_0 \tag{4.26}$$

Example 4.11

- An equilibrium point is an invariant set because by definition $x(t) = x^*$ is a constant solution of an autonomous system so that

$$x(t) = x(t_0) = x^* \in \mathscr{M}, \ \forall t \geq t_0$$

- A region of attraction $\mathscr{R}_A$ is an invariant set since all trajectories in $\mathscr{R}_A$ will remain in $\mathscr{R}_A$ for all future time and converge to the origin as $t \to \infty$

$$\mathscr{R}_A = \left\{ x(t) \in \mathscr{M} : \lim_{t \to \infty} x(t) = 0 \right\}$$

- The limit cycle of the Van der Pol oscillator is an invariant set since any point on the limit cycle will remain on it for all future time.
- The entire Euclidean space $\mathbb{R}^n$ is a trivial invariant set since all trajectories must be in some subspace that belongs in $\mathbb{R}^n$.

■

The LaSalle's invariant set theorem is stated as follows:

Theorem 4.4 Given an autonomous system, let $V(x) > 0$ be a positive-definite function with a continuous first partial derivative such that $\dot{V}(x) \leq 0$ in some finite region $B_R \subset \mathscr{D}$. Let $\mathscr{R}$ be a set of all points where $\dot{V}(x) = 0$. Let $\mathscr{M}$ be the largest invariant set in $\mathscr{R}$. Then, every solution $x(t)$ starting in B_R approaches $\mathscr{M}$ as $t \to \infty$.

Example 4.12 Consider

$$\begin{bmatrix} \dot{x}_1 \\ \dot{x}_2 \end{bmatrix} = \begin{bmatrix} -x_1^3 - x_1 x_2^2 + x_1 \\ -x_2^3 - x_1^2 x_2 + x_2 \end{bmatrix}$$

Choose a Lyapunov candidate function

$$V(x) = x_1^2 + x_2^2$$

Then, $\dot{V}(x)$ is evaluated as

$$\begin{aligned}\dot{V}(x) &= 2x_1\left(-x_1^3 - x_1x_2^2 + x_1\right) + 2x_2\left(-x_2^3 - x_1^2x_2 + x_2\right)\\ &= -2x_1^2\left(x_1^2 + x_2^2 - 1\right) - 2x_2^2\left(x_1^2 + x_2^2 - 1\right)\\ &= -2\left(x_1^2 + x_2^2\right)\left(x_1^2 + x_2^2 - 1\right)\end{aligned}$$

$\dot{V}(x) < 0$ in a set $\mathscr{S}$ where

$$\mathscr{S} = \left\{x(t) \in B_R : x_1^2 + x_2^2 - 1 > 0\right\}$$

but $\dot{V}(x) \geq 0$ in the complementary set

$$\mathscr{S}^c = \left\{x(t) \in B_R : x_1^2 + x_2^2 - 1 \leq 0\right\}$$

which represents a circular region that includes the origin. Therefore, the origin is unstable.

Let $\mathscr{R}$ be a set of all points where $\dot{V}(x) = 0$. Then,

$$\mathscr{R} = \left\{x(t) \in B_R : g(x) = x_1^2 + x_2^2 - 1 = V(x) - 1 = 0\right\}$$

in fact represents a bounded solution $x(t)$ since all trajectories either inside or outside of $\mathscr{S}^c$ will move toward $\mathscr{R}$ and remain in $\mathscr{R}$ as illustrated in Fig. 4.6. Thus, $\mathscr{R}$ is an invariant set. One can also verify this by taking the time derivative of the function $g(x)$ that represents the trajectories in the set $\mathscr{R}$

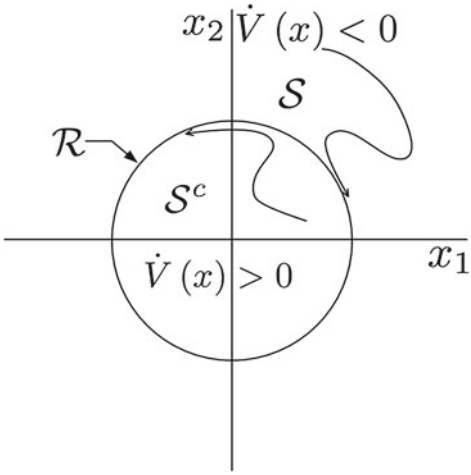

Fig. 4.6 Bounded solution set

$$\dot{g}(x) = \frac{d}{dt}(V-1) = \dot{V}(x) = 0,\ \forall x(t) \in \mathscr{R}$$

The Lyapunov function can be solved analytically by noting that

$$\dot{V} = -2V(V-1)$$

which leads to

$$\frac{dV}{V(V-1)} = -2dt$$

Using the partial fraction, this can be expressed as

$$\left(\frac{1}{V-1} - \frac{1}{V}\right) dV = -2dt$$

which yields the following general solution:

$$V(t) = \frac{V_0}{V_0 - (V_0 - 1)e^{-2t}}$$

As $t \to \infty$, $V(t)$ tends to a constant solution as shown in Fig. 4.7 with

$$\lim_{t\to\infty} V(t) = 1$$

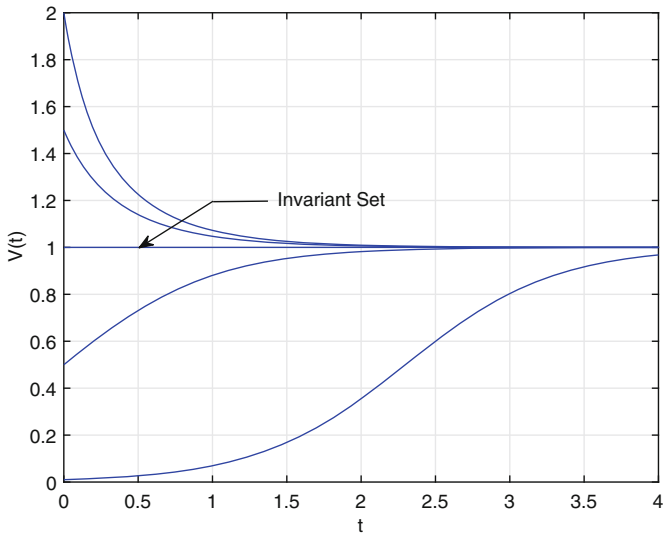

Fig. 4.7 Trajectories of Lyapunov function tending to an invariant set

which is in fact the set $\mathscr{R}$. Therefore, the set $\mathscr{R}$ is a bounding set of all possible solutions $x(t)$. Thus, $x(t) \in \mathscr{L}_\infty$; i.e., $x(t)$ is bounded.

Example 4.13 Consider the spring-mass-damper system. Choose the Lyapunov function to be the energy function

$$V(x) = \frac{1}{2}mx_2^2 + \frac{1}{2}kx_1^2$$

Then,

$$\dot{V}(x) = mx_2\dot{x}_2 + kx_1\dot{x}_1 = -cx_2^2 \leq 0$$

Since $\dot{V}(x)$ is negative semi-definite, then the origin is only stable in the Lyapunov sense, but not asymptotically stable as one would expect for a spring-mass-damper system with friction. Let $\mathscr{R}$ be a set of all points where $\dot{V}(x) = 0$. Then,

$$\mathscr{R} = \left\{x(t) \in \mathbb{R}^2 : \dot{V}(x) = 0 \Rightarrow x_2 = 0\right\}$$

is a collection of all points that lie on the x_1-axis. It follows that any point on this axis must satisfy

$$m\dot{x}_2 + kx_1 = 0$$

or

$$\dot{x}_2 = \ddot{x}_1 = -\frac{k}{m}x_1$$

If $x_1(t) \neq 0$, then $\ddot{x}_1(t) \neq 0$ with $\text{sgn}(\ddot{x}_1) = -\text{sgn}(x_1)$ in $\mathscr{R}$, where sgn () is the sign function which returns 1 if the argument is positive, 0 if the argument is zero, or -1 if the argument is negative. This means that a point on this axis cannot remain in $\mathscr{R}$ because the acceleration $\ddot{x}_1$ causes the point to move toward the origin, unless it is already at the origin.

Another way to find an invariant set is to evaluate the derivative of the function that describes $\mathscr{R}$ and set it equal to zero. Hence,

$$\dot{x}_2 = 0$$

which is satisfied if and only if $x_1(t) = 0$.

Thus, the invariant set $\mathscr{M} \subset \mathscr{R}$ is a set that contains only the origin. Then, according to the LaSalle's invariant set theorem, all trajectories will converge to the origin as $t \to \infty$. The origin then is asymptotically stable.

■

This example brings up an interesting observation that can be stated in the following corollary of the LaSalle's invariant set theorem:

Corollary 4.1 Let $V(x) > 0$ be a positive definite function with a continuous first partial derivative such that $\dot{V}(x) \leq 0$ in some finite region $B_R \subset \mathscr{D}$. Let $\mathscr{R} = \left\{x(t) \in B_R : \dot{V}(x) = 0\right\}$ and suppose that no solution can stay in $\mathscr{R}$ except the trivial

solution $x = 0$. Then, the origin is asymptotically stable. Moreover, if $V(x) > 0$ is a positive definite radially unbounded function and $\mathscr{R} = \left\{x(t) \in \mathbb{R}^n : \dot{V}(x) = 0\right\}$, then the origin is asymptotically stable in the large.

4.2.7 Differential Lyapunov Equation

The Lyapunov equation has a connection to the optimal control theory. In particular, the Lyapunov equation can be viewed as a special case of the Riccati equation for a Linear Quadratic Regulator (LQR) optimal control problem. Consider the following LTI system:

$$\dot{x} = Ax \tag{4.27}$$

subject to $x(t_0) = x_0$, where $x(t) \in \mathbb{R}^n$ and $A \in \mathbb{R}^n \times \mathbb{R}^n$.

It is of interest to find a condition that minimizes the following quadratic cost function:

$$\min J = \int_{t_0}^{t_f} x^\top Q x dt \tag{4.28}$$

where $Q > 0 \in \mathbb{R}^n \times \mathbb{R}^n$ is a positive definite matrix.

The solution can be established by the Pontryagin's maximum principle in the optimal control theory [5, 6]. The Hamiltonian function of this system is defined as

$$H = x^\top Q x + \lambda^\top (Ax + Bu) \tag{4.29}$$

where $\lambda(t) \in \mathbb{R}^n$ is called an adjoint or co-state vector.

The adjoint equation is given by

$$\dot{\lambda} = -\frac{\partial H^\top}{\partial x} = -Qx - A^\top \lambda \tag{4.30}$$

subject to the transversality (terminal time) condition

$$\lambda\left(t_f\right) = 0 \tag{4.31}$$

Choose a solution of $\lambda(t)$ in the form of

$$\lambda(t) = P(t)\, x \tag{4.32}$$

where $P(t) \in \mathbb{R}^n \times \mathbb{R}^n$ is a time-varying matrix.

Then, the adjoint equation is evaluated with the system dynamics as

$$\dot{P}x + PAx = -Qx - A^\top P x \tag{4.33}$$

By factoring out $x(t)$, the differential Lyapunov equation is obtained as

$$\dot{P} + PA + A^\top P + Q = 0 \tag{4.34}$$

subject to $P\left(t_f\right) = 0$.

Contrasting this with the differential Riccati equation

$$\dot{P} + PA + A^\top P - PBR^{-1}B^\top P + Q = 0 \tag{4.35}$$

the differential Lyapunov equation is a special case of the differential Riccati equation for $R \to \infty$.

Note that the differential Lyapunov equation is defined backward in time with the transversality condition given at the final time. By transforming into a time-to-go variable, $\tau = t_f - t$, then

$$\frac{dP}{d\tau} = PA + A^\top P + Q \tag{4.36}$$

subject to $P(0) = 0$ in the time-to-go coordinate.

If A is Hurwitz and let $t_f \to \infty$ which corresponds to an infinite time horizon solution, then the time-varying solution of the differential Lyapunov equation tends to a constant solution of the algebraic Lyapunov equation

$$PA + A^\top P + Q = 0 \tag{4.37}$$

The constant solution of P is given by

$$P = \lim_{\tau \to \infty} \int_0^\tau e^{A^\top \tau} Q e^{A\tau} d\tau \tag{4.38}$$

which is positive definite for $Q > 0$ and requires that A be Hurwitz since the solution must be a stable solution such that

$$\lim_{\tau \to \infty} e^{A\tau} = 0 \tag{4.39}$$

Example 4.14 Numerically compute P, given

$$A = \begin{bmatrix} 0 & 1 \\ -4 & -4 \end{bmatrix}, \; Q = \begin{bmatrix} 1 & 0 \\ 0 & 1 \end{bmatrix}$$

The differential Lyapunov equation in time-to-go can be solved using any numerical technique for solving differential equations such as the Euler or Runge–Kutta method. For example, the Euler method for solving the Lyapunov equation is as follows:

$$P_{i+1} = P_i + \Delta\tau \left(P_i A + A^\top P_i + Q\right)$$

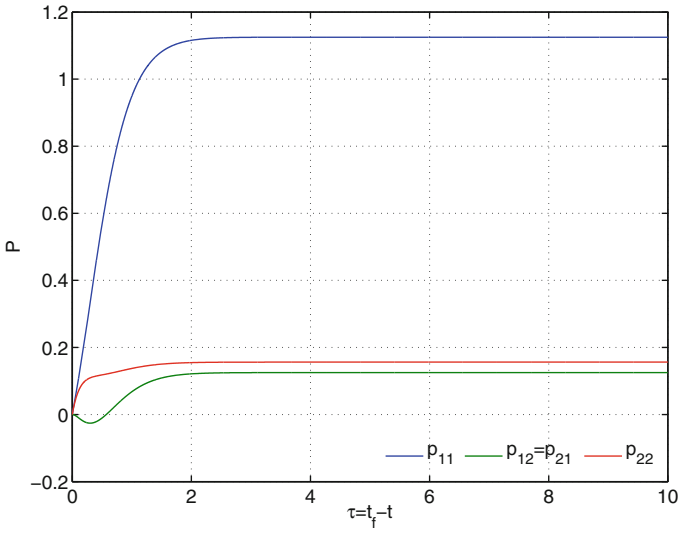

Fig. 4.8 Numerical solution of Lyapunov equation

where i denotes the value of $P(\tau)$ at a time $\tau_i = i\Delta\tau$.

The equation can be integrated until the solution converges to within a specified error. Figure 4.8 illustrates the solution convergence of the differential Lyapunov equation. The result is obtained as

$$P = \begin{bmatrix} 1.125 & 0.125 \\ 0.125 & 0.15625 \end{bmatrix}$$

4.3 Stability of Non-Autonomous Systems

Most of the concepts for Lyapunov stability for autonomous systems can be applied to non-autonomous systems with some additional considerations [2, 4].

Consider a non-autonomous system

$$\dot{x} = f(x, t) \tag{4.40}$$

subject to $x(t_0) = x_0$, where $f(x, t)$ is locally Lipschitz in $\mathscr{D} \times [0, \infty)$ and $\mathscr{D} \subset \mathbb{R}^n$.

The notion of the origin as an equilibrium point now takes on a different meaning in that the equilibrium point x^* must be time-invariant for all $t \geq t_0$ and satisfies

$$f(x^*, t) = 0 \tag{4.41}$$

Otherwise, the system does not have a "true" equilibrium point in the Lyapunov sense.

Example 4.15

- The system

$$\dot{x} = g(t)\, h(x)$$

has an equilibrium point x^* where

$$h\left(x^*\right) = 0$$

- The system

$$\dot{x} = g(t)\, h(x) + d(t)$$

does not have a true equilibrium point since $h(x)$ would have been a function of t to satisfy $\dot{x}(t) = 0$, which is a contradiction unless $g(t) = \alpha d(t)$ for some constant α.

4.3.1 Uniform Stability

The Lyapunov stability definition for a non-autonomous system is defined as follows:

Definition 4.9 The equilibrium point $x^* = 0$ is said to be stable (in the sense of Lyapunov) if, for any $R > 0$, there exists some $r(R, t_0) > 0$ such that

$$\|x_0\| < r \Rightarrow \|x\| < R,\ \forall t \geq t_0 \tag{4.42}$$

■

Note that the difference in this definition as compared to that for an autonomous system is the ball of radius r that encloses x_0 now may depend on the initial time t_0. Thus, the stability of the origin may also be dependent on the initial time.

The concept of uniform stability is an additional consideration for non-autonomous systems. Uniform stability implies that the radius $r = r(R)$ is not dependent on the initial time, and so are the stability properties of the equilibrium point. For autonomous systems, stability is independent of the initial time. This property is highly desirable since it eliminates the need for examining the effect of the initial time on the stability of a non-autonomous system.

Definition 4.10 Given a Lyapunov function $V(x, t)$ for a non-autonomous system that satisfies the following conditions:

$$V(0, t) = 0 \tag{4.43}$$

and

$$0 < V(x,t) \leq W(x) \tag{4.44}$$

where $W(x) > 0$ is a positive-definite function, then $V(x,t)$ is said to be a positive definite, decrescent function.

Example 4.16 The Lyapunov candidate function

$$V(x,t) = \left(1 + \sin^2 t\right)\left(x_1^2 + x_2^2\right)$$

is bounded from above by

$$0 < V(x,t) \leq 2\left(x_1^2 + x_2^2\right) = W(x)$$

Since $W(x) > 0$, then $V(x,t)$ is a positive definite, decrescent function. ■

The Lyapunov's direct method for a non-autonomous system is stated in the following theorem:

Theorem 4.5 If there exists a positive definite, decrescent Lyapunov function $V(x,t)$ for all $x(t) \in B_R$ and $t \geq 0$ such that

$$\dot{V}(x,t) = \frac{\partial V}{\partial x} f(x,t) + \frac{\partial V}{\partial t} \leq 0 \tag{4.45}$$

then the origin is said to be uniformly stable in the Lyapunov sense. Moreover, if $\dot{V}(x,t) < 0$, then the origin is said to be uniformly asymptotically stable, and additionally, if the region B_R is extended to the entire Euclidean space $\mathbb{R}^n$, then the origin is said to be uniformly asymptotically stable in the large.

4.3.2 Uniform Boundedness

When a non-autonomous system does not have an equilibrium point, stability of such a system is defined by the notion of boundedness [2, 4].

Definition 4.11 The solution of a non-autonomous system is said to be uniformly bounded if, for any $R > 0$, there exists some $r(R) > 0$ independent of the initial time t_0 such that

$$\|x_0\| < r \Rightarrow \|x\| \leq R, \ \forall t \geq t_0 \tag{4.46}$$

Moreover, the solution is said to be uniformly ultimately bounded if, for any $R > 0$, there exists some $r > 0$ independent of R and the initial time t_0 such that

$$\|x_0\| < r \Rightarrow \|x\| \leq R, \ \forall t \geq t_0 + T \tag{4.47}$$

where $T = T(r)$ is some time interval after the initial time t_0.

■

The uniform ultimate boundedness concept simply means that the solution may not be uniformly bounded initially according to Definition 4.11 but eventually becomes uniformly ultimately bounded after some time has passed. The constant R is called a bound if the solution is uniformly bounded or an ultimate bound if the solution is uniformly ultimately bounded.

The Lyapunov's direct method can be applied to a non-autonomous system according to the following theorem:

Theorem 4.6 Given a Lyapunov function $V(x,t)$ for all $\|x\| \geq R$ and $t \in [0,\infty)$, then the solution of the non-autonomous system (4.40) is said to be uniformly bounded if there exist functions $\varphi_1(\|x\|) \in \mathscr{K}\mathscr{R}$ and $\varphi_2(\|x\|) \in \mathscr{K}\mathscr{R}$ such that [2]

- $\varphi_1(\|x\|) \leq V(x,t) \leq \varphi_2(\|x\|)$
- $\dot{V}(x,t) \leq 0$

for all $\|x\| \geq R$ and $t \in [0,\infty)$. In addition, if there exists a function $\varphi_3(\|x\|) \in \mathscr{K}\mathscr{R}$ such that

- $\dot{V}(x,t) \leq -\varphi_3(\|x\|)$

for all $\|x\| \geq R$ and $t \in [0,\infty)$, then the solution is said to be uniformly ultimately bounded.

Example 4.17 Consider

$$\dot{x} = -x + 2\sin t$$

subject to $x(0) = x_0$.

The system does not have an equilibrium. The solution is

$$x = (x_0 + 1)e^{-t} + \sin t - \cos t$$

If $\|x_0\| < r$ and recognizing that $e^{-t} \leq 1$ and $|\sin t - \cos t| \leq \sqrt{2}$, then

$$\|x\| \leq \|x_0 + 1\| + \sqrt{2} < r + 1 + \sqrt{2} = R$$

Thus, one can choose $r(R) = R - 1 - \sqrt{2}$ according to Definition 4.11. So, the solution is uniformly bounded. Suppose $x_0 = 1$, then the bound is $R = 2 + \sqrt{2}$.

Moreover, as $t \to \infty$, then the solution tends to

$$x \to \sin t - \cos t$$

so that

$$\|x\| \leq \sqrt{2} = R$$

independent of r. The solution then is also uniformly ultimately bounded with an ultimate bound of $\sqrt{2}$ as shown in Fig. 4.9.

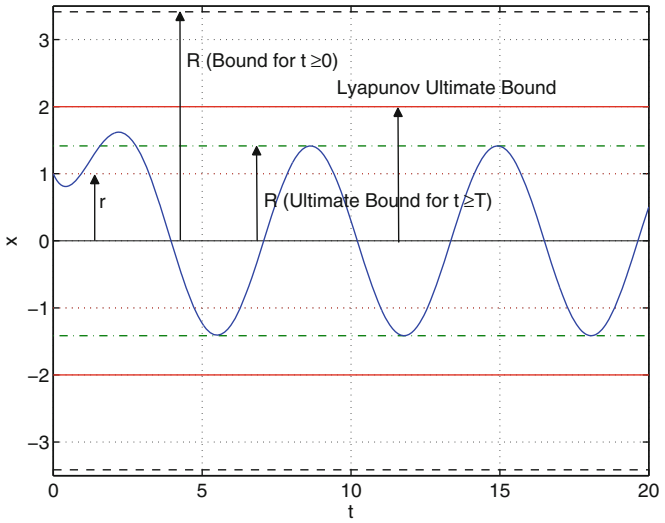

Fig. 4.9 Uniform ultimate boundedness

The Lyapunov's direct method is now applied to determine the uniform boundedness of a solution. Consider a Lyapunov candidate function for this system

$$V(x) = x^2 > 0$$

Note that one can always find $\varphi_1(\|x\|) \in \mathscr{K}\mathscr{R}$ and $\varphi_2(\|x\|) \in \mathscr{K}\mathscr{R}$ for this Lyapunov candidate function such that $\varphi_1(\|x\|) \leq V(x) \leq \varphi_2(\|x\|)$, for example, $\varphi_1(\|x\|) = ax^2$ with $a < 1$ and $\varphi_2(\|x\|) = bx^2$ with $b > 1$.

Then,

$$\dot{V}(x) = 2x\dot{x} = 2x(-x + 2\sin t) \leq -2x^2 + 4\|x\|$$

We see that

$$\dot{V}(x) \leq -2V(x) + 4\sqrt{V(x)}$$

Let $W(t) = \sqrt{V(t)} = \|x\|$. Then,

$$\dot{W} = \frac{\dot{V}}{2\sqrt{V}} = -\sqrt{V} + 2 \leq -W + 2$$

The solution of $W(t)$ is

$$W \leq (\|x_0\| - 2)\, e^{-t} + 2$$

Thus,

$$\lim_{t\to\infty} \|x\| = \lim_{t\to\infty} W \leq 2 = R$$

Choose

$$\varphi_3(\|x\|) = 2\|x\|^2 - 4\|x\|$$

Note that $\varphi_3(\|x\|) \in \mathscr{K}\mathscr{R}$ (verify!). Then, it follows that

$$\dot{V}(x) \leq -\varphi_3(\|x\|)$$

Then, $\dot{V}(x) \leq 0$ if $-2x^2 + 4\|x\| \leq 0$ or $\|x\| \geq 2$. Therefore, according to Theorem 4.6, the solution $x(t)$ is uniformly ultimately bounded with a Lyapunov ultimate bound of 2. It is noted that the Lyapunov ultimate bound is always more conservative or greater than or equal to the ultimate bound derived from the actual solution as illustrated in Fig. 4.9.

There is another way of showing that $x(t)$ is uniformly ultimately bounded. By completing the square, $\dot{V}(x)$ can also be expressed as

$$\dot{V}(x) \leq -2(\|x\| - 1)^2 + 2$$

Then, $\dot{V}(x) \leq 0$ if $-2(\|x\| - 1)^2 + 2 \leq 0$ or $\|x\| \geq 2$. Since $\dot{V}(x) \leq 0$ outside the compact set $\|x\| \leq 2$, but $\dot{V}(x) > 0$ inside it, therefore the solution $x(t)$ is uniformly ultimately bounded. Any trajectory that starts outside the compact set will reach the ultimate bound $\|x\| = 2$ because $\dot{V}(x) \leq 0$ outside the compact set. Any trajectory that starts inside the compact set will move away from the origin because $\dot{V}(x) > 0$ inside the compact set, but will eventually be attracted to the ultimate bound $\|x\| = 2$.

4.3.3 Barbalat's Lemma

The LaSalle's invariant set theorem can be used to show asymptotic stability of an equilibrium point for an autonomous system when $\dot{V}(x)$ is only negative semi-definite. This theorem cannot be used for non-autonomous systems. Therefore, it can be much more difficult to show asymptotic stability for a non-autonomous system than for an autonomous system. Barbalat's lemma is a mathematical tool that can be used to address this situation to some extent [4].

Firstly, the concept of uniform continuity needs to be introduced. A mathematical formal definition of uniform continuity of a function is given as follows:

Definition 4.12 The function $f(t) \in \mathbb{R}$ is uniformly continuous on a set $\mathscr{D}$ if, for any $\epsilon > 0$, there exists some $\delta(\epsilon) > 0$ such that

$$|t_2 - t_1| < \delta \Rightarrow |f(t_2) - f(t_1)| < \epsilon, \ \forall t_1, t_2 \tag{4.48}$$

■

The following statements are equivalent to the definition of uniform continuity:

- Suppose a function $f(t)$ is continuous on a closed finite interval $t \in [t_1, t_2]$. Then, $f(t)$ is uniformly continuous on $t \in [t_1, t_2]$.
- Suppose a function $f(t)$ is differentiable on a set $\mathscr{D}$, and there exists a constant $M > 0$ such that $\left|\dot{f}(t)\right| < M$ for all t. Then, $f(t)$ is uniformly continuous on $\mathscr{D}$.

In the simplest term, uniform continuity of a differentiable function $f(t)$ requires its derivative $\dot{f}(t)$ to exist and be bounded.

Example 4.18

- The function $f(t) = t^2$ for all $t \in [0, \infty)$ is continuous but is not uniformly continuous since $\dot{f}(t)$ is not bounded for all $t \in [0, \infty)$.
- The function $f(t) = t^2$ for $t \in [0, 1]$ is uniformly continuous since $f(t)$ is continuous for $t \in [0, 1]$.
- The function $f(t) = \sqrt{t}$ for all $t \in [0, \infty)$ does not have a bounded derivative $\dot{f}(t) = \frac{1}{2\sqrt{t}}$ for all $t \in [0, \infty)$, and since the interval is semi-open and infinite, one cannot readily conclude that $f(t)$ is not uniformly continuous on $t \in [0, \infty)$. However, this function is actually uniformly continuous on $t \in [0, \infty)$. To see this, we note that the interval can be divided into two subintervals $t \in [0, a]$ and $t \in [a, \infty)$ where $a > 0$. Then, $f(t)$ is uniformly continuous on $t \in [0, a]$ since $f(t)$ is continuous on $t \in [0, a]$, and furthermore $f(t)$ is also uniformly continuous on $t \in [a, \infty)$ since $\dot{f}(t) = \frac{1}{2\sqrt{t}}$ is bounded on $t \in [a, \infty)$. Therefore, in totality, $f(t)$ is uniformly continuous on $t \in [0, \infty)$.
- Consider a stable LTI system

$$\dot{x} = Ax + Bu$$

with $x(t_0) = x_0$ and a continuous bounded input $u(t)$. The system is exponentially stable with the solution

$$x = e^{-A(t-t_0)}x_0 + \int_{t_0}^{t} e^{A(t-\tau)}Bu(\tau)\,d\tau$$

Thus, $x(t)$ is a continuous bounded signal with a bounded derivative $\dot{x}(t)$ for all $t \in [0, \infty)$. Therefore, $x(t)$ is uniformly continuous. Any output signal

$$y = Cx + Bu$$

is also uniformly continuous if $u(t)$ has a bounded derivative. The system is then said to be bounded-input-bounded-output (BIBO) stable.

■

The Barbalat's lemma is now stated as follows:

Lemma 4.1 If the limit of a differentiable function $f(t)$ as $t \to \infty$ exists and is finite, and if $\dot{f}(t)$ is uniformly continuous, then $\lim_{t\to\infty} \dot{f}(t) = 0$.

Example 4.19

- The function $f(t) = e^{-t^2}$ has a finite limit as $t \to \infty$. To determine the uniform continuity of the first derivative $\dot{f}(t) = -2te^{-t^2}$, we need to determine whether or not the second derivative $\ddot{f}(t)$ is bounded for all $t \in [0, \infty)$. The second derivative $\ddot{f}(t) = -2e^{-t^2} + 4t^2e^{-t^2}$, in fact, is bounded because the exponential term e^{-t^2} decreases at a much faster rate than the power term t^2. Therefore, $\lim_{t\to\infty} \dot{f}(t) = 0$. In fact, one can verify $\lim_{t\to\infty} -2te^{-t^2} = 0$ using the L'Hospital rule.
- The function $f(t) = \frac{1}{t}\sin\left(t^2\right)$ which tends to zero as $t \to \infty$ but whose derivative $\dot{f}(t) = -\frac{1}{t^2}\sin\left(t^2\right) + 2\cos\left(t^2\right)$ does not have a limit as $t \to \infty$. Thus, it can be seen that even if the limit of a differentiable function $f(t)$ exists and is finite as $t \to \infty$, it does not necessarily imply that $\lim_{t\to\infty} \dot{f}(t) = 0$ since $\dot{f}(t)$ may not be uniformly continuous, that is, $\dot{f}(t)$ has a bounded derivative or equivalently $\ddot{f}(t)$ is bounded. Therefore, the function $f(t) = \frac{1}{t}\sin\left(t^2\right)$ does not satisfy the Barbalat's lemma.
- The function $f(t) = \sin(\ln t)$ whose derivative $\dot{f}(t) = \frac{1}{t}\cos(\ln t)$ tends to zero but $f(t)$ does not have a finite limit as $t \to \infty$. Thus, $\lim_{t\to\infty} \dot{f}(t) = 0$ does not necessarily imply that the limit of a differentiable function $f(t)$ exists and is finite. Therefore, the converse of the Barbalat's lemma is not true.

■

The Barbalat's lemma is now extended to the Lyapunov's direct method to examine the asymptotic stability of a non-autonomous system by the following Lyapunov-like lemma [4]:

Lemma 4.2 If a positive-definite function $V(x, t)$ has a finite limit as $t \to \infty$, and if $\dot{V}(x, t)$ is negative semi-definite and uniformly continuous for all $t \in [0, \infty)$, then $\dot{V}(x, t) \to 0$ as $t \to \infty$.

Example 4.20 Consider a simple adaptive control system

$$\dot{x} = -ax + b\left[u + \theta^* w(t)\right]$$

where $a > 0$, $w(t) \in \mathscr{L}_\infty$ is a bounded time-varying disturbance, and θ^* is an unknown constant parameter.

To cancel out the effect of the time-varying disturbance, an adaptive controller is designed as

$$u = -\theta(t)\, w(t)$$

where $\theta(t)$ is an adaptive parameter that estimates θ^*.

If $\theta(t) \to \theta^*$ as $t \to \infty$, then the adaptive controller perfectly cancels out the disturbance and the closed-loop system tends to an ideal reference model

$$\dot{x}_m = -ax_m$$

where $x_m(t)$ is the desired response of $x(t)$.

The adaptive parameter is computed as

$$\dot{\theta} = -bew\left(t\right)$$

where $e\left(t\right) = x_m\left(t\right) - x\left(t\right)$ is called a tracking error, described by the tracking error equation

$$\dot{e} = \dot{x}_m - \dot{x} = -ae + b\tilde{\theta}w\left(t\right)$$

where $\tilde{\theta}\left(t\right) = \theta\left(t\right) - \theta^*$ is the parameter estimation error.

The combined system is non-autonomous due to $w\left(t\right)$. Both the variables $e\left(t\right)$ and $\theta\left(t\right)$ are influenced by the tracking error equation $\dot{e}\left(t\right)$ and the adaptive law $\dot{\theta}\left(t\right)$. To show that the system is stable, choose the following Lyapunov candidate function that includes both the variables $e\left(t\right)$ and $\tilde{\theta}\left(t\right)$:

$$V\left(e, \theta\right) = e^2 + \tilde{\theta}^2$$

Then,

$$\dot{V}\left(e, \tilde{\theta}\right) = 2e\left[-ae + b\tilde{\theta}w\left(t\right)\right] + 2\tilde{\theta}\left[-bew\left(t\right)\right] = -2ae^2 \leq 0$$

Since $\dot{V}\left(e, \theta\right)$ is negative semi-definite, $e\left(t\right) \in \mathscr{L}_\infty$ and $\theta\left(t\right) \in \mathscr{L}_\infty$, i.e., they are bounded, but the LaSalle's invariant set theorem cannot be used to show that the tracking error $e\left(t\right)$ converges to zero. This is where the Barbalat's lemma comes in handy. Firstly, $V\left(e, \tilde{\theta}\right)$ must be shown to have a finite limit as $t \to \infty$. Since $\dot{V}\left(e, \tilde{\theta}\right) \leq 0$, then

$$\begin{aligned} V\left(e\left(t \to \infty\right), \tilde{\theta}\left(t \to \infty\right)\right) - V\left(e\left(t_0\right), \tilde{\theta}\left(t_0\right)\right) &= \int_{t_0}^{\infty} \dot{V}\left(e, \tilde{\theta}\right) dt \\ &= -2a\int_{t_0}^{\infty} e^2\left(t\right) dt = -2a\left\|e\right\|_2^2 \end{aligned}$$

$$\begin{aligned} V\left(e\left(t \to \infty\right), \tilde{\theta}\left(t \to \infty\right)\right) &= V\left(e\left(t_0\right), \tilde{\theta}\left(t_0\right)\right) - 2a\left\|e\right\|_2^2 \\ &= e^2\left(t_0\right) + \tilde{\theta}^2\left(t_0\right) - 2\left\|e\right\|_2^2 < \infty \end{aligned}$$

So, $V\left(e, \tilde{\theta}\right)$ has a finite limit as $t \to \infty$. Since $\left\|e\right\|_2$ exists, therefore $e\left(t\right) \in \mathscr{L}_2 \cap \mathscr{L}_\infty$.

Next, $\dot{V}\left(e, \tilde{\theta}\right)$ must be shown to be uniformly continuous. This can be done by examining the derivative of $\dot{V}\left(e, \tilde{\theta}\right)$ to see if it is bounded. $\ddot{V}\left(e, \tilde{\theta}\right)$ is computed as

$$\ddot{V}\left(e,\tilde{\theta}\right)=-4ae\left[-ae+b\tilde{\theta}w\left(t\right)\right]$$

Since $e\left(t\right)\in\mathscr{L}_2\cap\mathscr{L}_\infty$ and $\tilde{\theta}\left(t\right)\in\mathscr{L}_\infty$ by the virtue of $\dot{V}\left(e,\tilde{\theta}\right)\leq 0$, and $w\left(t\right)\in\mathscr{L}_\infty$ by assumption, then $\ddot{V}\left(e,\tilde{\theta}\right)\in\mathscr{L}_\infty$. Therefore, $\dot{V}\left(e,\tilde{\theta}\right)$ is uniformly continuous. It follows from the Barbalat's lemma that $\dot{V}\left(e,\tilde{\theta}\right)\to 0$ and hence $e\left(t\right)\to 0$ as $t\to\infty$. Note that one cannot conclude that the system is asymptotically stable since only $e\left(t\right)\to 0$ as $t\to\infty$, but $\tilde{\theta}\left(t\right)$ is only bounded.

4.4 Summary

The Lyapunov stability theory is the foundation of nonlinear systems and adaptive control theory. Various stability concepts for autonomous and non-autonomous systems are introduced. The Lyapunov's direct method is an indispensable tool for analyzing stability of nonlinear systems. Barbashin–Krasovskii theorem provides a method for global stability analysis. LaSalle's invariant set theorem provides another complementary tool for analyzing systems with invariant sets. Stability of non-autonomous systems involves the concepts of uniform stability, uniform boundedness, and uniform ultimate boundedness. Barbalat's lemma is an important mathematical tool for analyzing stability of adaptive control systems in connection with the concept of uniform continuity of a real-valued function.

4.5 Exercises

1. Given

$$\begin{bmatrix}\dot{x}_1\\ \dot{x}_2\end{bmatrix}=\begin{bmatrix}x_1\left(x_1^2+x_2^2-1\right)-x_2\\ x_1+x_2\left(x_1^2+x_2^2-1\right)\end{bmatrix}$$

   a. Determine all the equilibrium points of the system and linearize the system about the equilibrium points to classify the types of equilibrium points.
   b. Use the Lyapunov candidate function

$$V\left(x\right)=x_1^2+x_2^2$$

   to determine the types of Lyapunov stability of the equilibrium points and their corresponding regions of attraction, if any.

2. Given

$$\dot{x}=x\left(-1+\frac{1}{2}\sin x\right)$$

subject to $x\,(0) = 1$.

a. Determine the upper and lower bound solutions.
b. Use the Lyapunov candidate function

$$V\,(x) = x^2$$

to determine the type of Lyapunov stability and the upper bound of $V\,(x)$ as an explicit function of time.

3. Use the Lyapunov candidate function

$$V\,(x) = x_1^2 + x_2^2$$

to study stability of the origin of the system

$$\begin{bmatrix} \dot{x}_1 \\ \dot{x}_2 \end{bmatrix} = \begin{bmatrix} (x_2 - x_1)\left(x_1^2 + x_2^2\right) \\ (x_1 + x_2)\left(x_1^2 + x_2^2\right) \end{bmatrix}$$

4. Given

$$\dot{x} = Ax$$

a. Calculate analytically P that solves

$$A^\top P + PA = -2I$$

where

$$A = \begin{bmatrix} 0 & 1 \\ -4 & 4 \end{bmatrix}$$

and verify the result using the MATLAB function "lyap."
b. Determine if P is positive or negative (semi-)definite. What can be said about stability of the origin of this system.

5. Given

$$\begin{bmatrix} \dot{x}_1 \\ \dot{x}_2 \end{bmatrix} = \begin{bmatrix} x_1\left(1 - x_1^2 - x_2^2\right) + x_2 \\ -x_1 + x_2\left(1 - x_1^2 - x_2^2\right) \end{bmatrix}$$

a. Use the Lyapunov candidate function

$$V\,(x) = x_1^2 + x_2^2$$

to determine the type of Lyapunov stability of the origin.
b. Find an invariant set.
c. Solve for $V\,(t)$ as an explicit function of time and plot the trajectories of $V\,(t)$ for $V\,(0) = 0.01,\ 0.5,\ 1,\ 1.5,\ 2$.

6. Given

$$A = \begin{bmatrix} 0 & 1 & 0 \\ -1 & -1 & -2 \\ 1 & 0 & -1 \end{bmatrix}$$

Determine whether or not A is Hurwitz. If so, compute P using the Euler method to integrate the differential Lyapunov equation

$$\frac{dP}{d\tau} = PA + A^\top P + I$$

subject to $P(0) = 0$, where τ is time-to-go. Plot all six elements of P on the same plot and verify the result at the final time-to-go with the MATLAB function "lyap."

7. Use the Lyapunov's direct method to determine an ultimate bound of the solution $x(t)$ for the following equation:

$$\dot{x} = -x + \cos t \sin t$$

subject to $x(0) = 1$. Plot the solution $x(t)$ for $0 \leq t \leq 20$.

8. Given a non-autonomous system

$$\dot{x} = (-2 + \sin t)\, x - \cos t$$

   a. Show that the system is uniformly ultimately bounded by the Lyapunov theorem for non-autonomous systems. Also determine the ultimate bound of $\|x\|$.
   b. Plot the solution by numerically integrating the differential equation and show that it satisfies the ultimate bound.

9. Given

$$\dot{x} = -\left(1 + \sin^2 t\right) x + \cos t$$

   a. Use the Lyapunov candidate function

$$V(x) = x^2$$

   to determine the upper bound of $\dot{V}(x)$ as a function of $V(x)$.
   b. Let $W = \sqrt{V}$. Solve for the inequality $W(t)$ as an explicit function of time and determine the ultimate bound of the system.
   c. Show that the system is uniformly ultimately bounded.

10. For the following functions:

   a. $f(t) = \sin\left(e^{-t^2}\right)$
   b. $f(t) = e^{-\sin^2 t}$

Plot $f(t)$ for $t \in [0, 5]$. Determine whether or not the limit of $f(t)$ exists as $t \to \infty$ and $\dot{f}(t)$ is uniformly continuous. If so, use the Barbalat's lemma to show that $\dot{f}(t) \to 0$ as $t \to \infty$ and verify by taking the limit of $\dot{f}(t)$ as $t \to \infty$.

11. Consider the following adaptive control system:

$$\dot{e} = -e + \theta x$$

$$\dot{\theta} = -xe$$

where $e(t) = x_m(t) - x(t)$ is defined as the tracking error between a given explicit reference time signal $x_m(t)$ which is assumed to be bounded, i.e., $x_m(t) \in \mathscr{L}_\infty$, and the state variable $x(t)$. Show that the adaptive system is stable and that $e(t) \to 0$ as $t \to \infty$.

References

1. Åström, K. J. (2008). *and Wittenmark B*. Adaptive Control: Dover Publications Inc.
2. Khalil, H. K. (2001). *Nonlinear systems*. Upper Saddle River: Prentice-Hall.
3. Ioannu, P. A., & Sun, J. (1996). *Robust Adaptive Control*. Upper Saddle River: Prentice-Hall, Inc.
4. Slotine, J.-J., & Li, W. (1991). *Applied nonlinear control*. Upper Saddle River: Prentice-Hall, Inc.
5. Anderson, B., & Moore, J. (1971). *Linear optimal control*. Upper Saddle River: Prentice-Hall, Inc.
6. Bryson, A. E., & Ho, Y. C. (1979). *Applied optimal control: optimization, estimation, and control*. New Jersey: Wiley Inc.

Chapter 5
Model-Reference Adaptive Control

Abstract This chapter presents the fundamental theory of model-reference adaptive control. Various types of uncertainty are defined. The composition of a model-reference adaptive control system is presented. Adaptive control theory for first-order single-input single-output (SISO) systems, second-order SISO systems, and multiple-input multiple-output (MIMO) systems is presented. Both direct and indirect adaptive control methods are discussed. The direct adaptive control methods adjust the control gains online directly, whereas the indirect adaptive control methods estimate unknown system parameters for use in the update of the control gains. Asymptotic tracking is the fundamental property of model-reference adaptive control which guarantees that the tracking error tends to zero in the limit. On the other hand, adaptive parameters are only bounded in the model-reference adaptive control setting.

When designing a controller for a system, a control designer typically would like to know how the system behaves physically. This knowledge is usually captured in the form of a mathematical model. For many real-world applications, modeling of physical systems can never be perfect as systems may have parameter variations due to nonlinearity, parameter uncertainty due to modeling inaccuracy or imprecise measurements, uncertainty in exogenous disturbances coming from the operating environment, or other sources of uncertainty. The role of a modeling specialist is to reduce the system uncertainty as much as practicable. The control designer then uses a mathematical model of the system to design a controller which may incorporate performance measures and stability margins to account for any residual system uncertainty that cannot be completely accounted for.

In situations when the system uncertainty may become significant beyond a level of desired tolerance that can adversely affect the performance of a controller, adaptive control can play an important role in reducing the effects of the system uncertainty on the controller performance. Situations that may warrant the use of adaptive control could include unintended consequences of off-nominal modes of operation such as system failures or highly uncertain operating conditions, and complex system behaviors that can result in an increase in the complexity and hence cost of the modeling efforts. In this chapter, the learning objectives are as follows:

N.T. Nguyen, *Model-Reference Adaptive Control*, Advanced Textbooks
in Control and Signal Processing, https://doi.org/10.1007/978-3-319-56393-0_5

- To develop a basic understanding of system uncertainty and the composition of a typical model-reference adaptive control system and its functionality;
- To be able to apply various model-reference adaptive control techniques for direct and indirect adaptation for first-order, second-order, and MIMO systems;
- To be able to perform a Lyapunov stability proof of model-reference adaptive control using the Lyapunov's direct method and Barbalat's lemma; and
- To recognize that model-reference adaptive control achieves asymptotic tracking but only boundedness of adaptive parameters.

■

A typical model-reference adaptive control (MRAC) system block diagram is shown in Fig. 5.1.

There are generally two classes of adaptive control: (1) direct adaptive control and (2) indirect adaptive control [1, 2]. Adaptive control architectures that combine both types of adaptive control are also frequently used and are referred to as composite [2, 3], combined, or hybrid direct–indirect adaptive control [4]. A typical direct adaptive controller may be expressed as

$$u = k_x(t)\, x + k_r(t)\, r \tag{5.1}$$

where $k_x(t)$ and $k_r(t)$ are adjustable control gains. The mechanism to adjust these control gains is via an adaptive law. Thus, a direct adaptive control in effect adjusts a feedback control mechanism of a control system directly to cancel out any unwanted system uncertainty so that the performance of the control system can be regained in the presence of significant system uncertainty.

In contrast, an indirect adaptive controller achieves the same objective by adjusting the control gains in an indirect way, which may be expressed as

$$u = k_x(p(t))\, x + k_r(p(t))\, r \tag{5.2}$$

where $p(t)$ are system parameters that are estimated online to update the control gains.

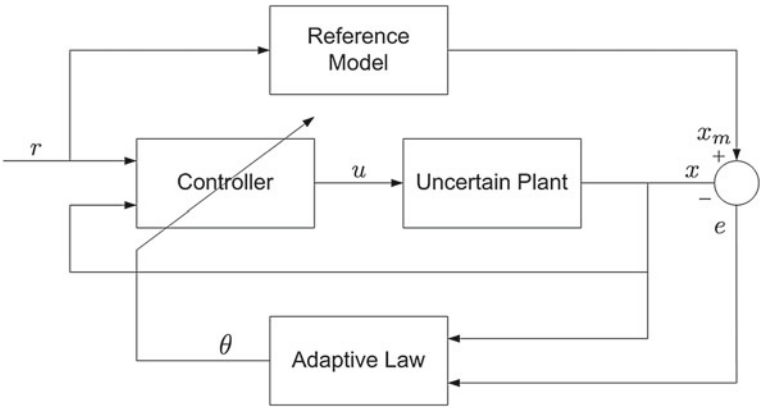

Fig. 5.1 A model-reference adaptive control system

Example 5.1 Consider a second-order LTI system

$$\ddot{x} + 2\zeta\omega_n\dot{x} + \omega_n^2 x = u$$

A controller is designed to enable the output $x(t)$ to track a constant command $r(t)$ and meet performance specifications for a closed-loop damping of ζ_m and a bandwidth frequency of ω_m. A PD (proportional-derivative) controller is designed as

$$u = k_p e + k_d \dot{e} + k_r r$$

where $e(t) = r(t) - x(t)$, to achieve the following closed-loop characteristic:

$$\ddot{x} + (2\zeta\omega_n + k_d)\dot{x} + \left(\omega_n^2 + k_p\right)x = (k_r + k_p)r$$

Choose

$$\omega_n^2 + k_p = \omega_m^2 \Rightarrow k_p = \omega_m^2 - \omega_n^2$$

$$2\zeta\omega_n + k_d = 2\zeta_m\omega_m \Rightarrow k_d = 2(\zeta_m\omega_m - \zeta\omega_n)$$

$$k_r = \omega_n^2$$

Then, the output $x(t)$ tracks the command $r(t)$ as $t \to \infty$.

Suppose the open-loop system natural frequency ω_n suddenly changes to a new value ω_n^* which may be unknown. The closed-loop system can now have a drastically different performance if the original control gains are used. To maintain the same performance specifications, the ideal control gains must be

$$k_p^* = \omega_m^2 - \omega_n^{*2} = k_p + \omega_n^2 - \omega_n^{*2}$$

$$k_d^* = 2\left(\zeta_m\omega_m - \zeta\omega_n^*\right) = k_d + 2\zeta\left(\omega_n - \omega_n^*\right)$$

$$k_r^* = \omega_n^{*2} = k_r - \omega_n^2 + \omega_n^{*2}$$

A direct adaptive controller seeks to adjust the original control gains k_p, k_d, and k_r toward the ideal control gains k_p^*, k_d^*, and k_r^*, respectively, directly without knowing the value of the uncertain parameter ω_n^*. On the other hand, an indirect adaptive controller seeks to adjust the control gains by estimating online the uncertain parameter ω_n^* and use the estimate of ω_n^* to re-compute the control gains as if the parameter estimate is the true value. This approach is often referred to as the Certainty Equivalence Principle.

5.1 Composition of a Model-Reference Adaptive Control System

5.1.1 Uncertain Plant

Adaptive control can deal with either linear or nonlinear plants with various types of uncertainty which can be structured uncertainty, unstructured uncertainty, or unmodeled dynamics.

1. Structured uncertainty is a source of uncertainty with uncertain parameters but known functional characteristics. It is also often referred to as parametric uncertainty.

Example 5.2 A linear spring-mass-damper system with an uncertain spring constant

$$m\ddot{x} + c\dot{x} + k^* x = u$$

where k^* is an uncertain parameter, is a system with structured or parametric uncertainty. The function $x\,(t)$ associated with k^* is a known characteristic that appears in the structured uncertainty.

2. Unstructured uncertainty is a source of uncertainty for which neither parameters or functional characteristics are certain.

Example 5.3 A spring-mass-damper system with an uncertain spring characteristic

$$m\ddot{x} + c\dot{x} + f^*\left(x, k^*\right) = u$$

where $f^*()$ is an uncertain function, is a system with unstructured uncertainty.

3. Unmodeled dynamics is a source of uncertainty that represents system internal or external dynamics that are not included in a plant model because they may be unmeasurable, unobservable, or assumed incorrectly to be negligible.

Example 5.4 The following linear spring-mass-damper system has unmodeled dynamics:

$$m\ddot{x} + c\dot{x} + k^* x = c_1 y + u$$

$$\dot{y} = c_2 x + c_3 y$$

where $y\,(t)$ is an internal system state that is not modeled, and c_i, $i = 1, 2, 3$ are parameters.

4. Matched uncertainty is a type of structured uncertainty that can be matched by the control input for a class of MIMO linear affine-in-control systems of the form

$$\dot{x} = f\,(x) + B\left[u + \Theta^{*\top}\Phi\,(x)\right] \tag{5.3}$$

where $x(t) \in \mathbb{R}^n$ is a state vector, $u(t) \in \mathbb{R}^m$ is a control vector, $B \in \mathbb{R}^n \times \mathbb{R}^m$ is a control input matrix, $\Theta^* \in \mathbb{R}^p \times \mathbb{R}^m$ is a matrix of uncertain parameters, and $\Phi(x) \in \mathbb{R}^p$ is a known bounded regressor function.
The quantity $\Theta^{*\top}\Phi(x)$ is called a parametric matched uncertainty since it appears in the range space of the control input matrix B. Recall from linear algebra that a range or column space of a matrix B consists of all possible products Bu. When a parametric uncertainty is matched, the control input can cancel out the uncertainty completely when the adaptation is perfect.

Example 5.5 The parametric uncertainty in the following LTI system:

$$\begin{bmatrix} \dot{x}_1 \\ \dot{x}_2 \end{bmatrix} = \begin{bmatrix} -1 & 1 \\ -1 & -2 \end{bmatrix} \begin{bmatrix} x_1 \\ x_2 \end{bmatrix} + \begin{bmatrix} 1 \\ 1 \end{bmatrix} \left(u + \begin{bmatrix} \delta_1 & \delta_2 \end{bmatrix} \begin{bmatrix} x_1 \\ x_2 \end{bmatrix} \right)$$

is a matched uncertainty where δ_1 and δ_2 are uncertain parameters.

5. Unmatched uncertainty is a type of uncertainty that cannot be matched by the control input for a class of MIMO linear affine-in-control systems of the form

$$\dot{x} = f(x) + Bu + \Theta^{*\top}\Phi(x) \tag{5.4}$$

A parametric uncertainty cannot be matched if the control input matrix $B \in \mathbb{R}^n \times \mathbb{R}^m$ is a non-square "tall" matrix, i.e., $n > m$, or if $B \in \mathbb{R}^n \times \mathbb{R}^n$ is a rank-deficient square matrix such that its inverse does not exist. In such a case, the control input cannot completely cancel out the uncertainty by adaptive control. Otherwise, the uncertainty may be cast as a matched uncertainty by the following pseudo-inverse transformation:

$$\dot{x} = f(x) + B\left[u + B^\top \left(BB^\top\right)^{-1} \Theta^{*\top}\Phi(x)\right] \tag{5.5}$$

where $B^\top \left(BB^\top\right)^{-1}$ is the right pseudo-inverse of a full-rank non-square "wide" matrix $B \in \mathbb{R}^n \times \mathbb{R}^m$ with $n < m$ and $\text{rank}(B) = n$, or where $B^\top \left(BB^\top\right)^{-1} = B^{-1}$ for a full-rank square matrix B.

Example 5.6 The parametric uncertainty in the following LTI system:

$$\begin{bmatrix} \dot{x}_1 \\ \dot{x}_2 \end{bmatrix} = \begin{bmatrix} -1 & 1 \\ -1 & -2 \end{bmatrix} \begin{bmatrix} x_1 \\ x_2 \end{bmatrix} + \begin{bmatrix} 1 \\ 1 \end{bmatrix} u + \begin{bmatrix} \delta_{11}x_1 + \delta_{12}x_2 \\ \delta_{21}x_1 + \delta_{22}x_2 \end{bmatrix}$$

is an unmatched uncertainty since B is a "tall" matrix. Intuitively, a tall matrix B implies the number of control inputs is less than the number state variables. Therefore, it would be difficult for the control inputs to cancel out the uncertainty in all the state variables.

Example 5.7 The parametric uncertainty in the following LTI system:

$$\begin{bmatrix} \dot{x}_1 \\ \dot{x}_2 \end{bmatrix} = \begin{bmatrix} -1 & 1 \\ -1 & -2 \end{bmatrix} \begin{bmatrix} x_1 \\ x_2 \end{bmatrix} + \begin{bmatrix} 1 & -1 & 2 \\ 1 & 2 & -1 \end{bmatrix} \begin{bmatrix} u_1 \\ u_2 \\ u_3 \end{bmatrix} + \begin{bmatrix} \delta_{11} & \delta_{12} \\ \delta_{21} & \delta_{22} \end{bmatrix} \begin{bmatrix} x_1 \\ x_2 \end{bmatrix}$$

is actually a matched uncertainty since B is a full-rank "wide" matrix whose pseudo-inverse exists

$$B^\top \left(BB^\top\right)^{-1} = \frac{1}{3} \begin{bmatrix} 1 & 1 \\ 0 & 1 \\ 1 & 0 \end{bmatrix}$$

So, the system can be cast as

$$\begin{bmatrix} \dot{x}_1 \\ \dot{x}_2 \end{bmatrix} = \begin{bmatrix} -1 & 1 \\ -1 & -2 \end{bmatrix} \begin{bmatrix} x_1 \\ x_2 \end{bmatrix} + \begin{bmatrix} 1 & -1 & 2 \\ 1 & 2 & -1 \end{bmatrix} \left(\begin{bmatrix} u_1 \\ u_2 \\ u_3 \end{bmatrix} + \frac{1}{3} \begin{bmatrix} \delta_{11} + \delta_{21} & \delta_{12} + \delta_{22} \\ \delta_{21} & \delta_{22} \\ \delta_{11} & \delta_{12} \end{bmatrix} \begin{bmatrix} x_1 \\ x_2 \end{bmatrix} \right)$$

6. Control input uncertainty is a type of uncertainty that exists in the control input matrix for a class of MIMO linear affine-in-control systems of the form

$$\dot{x} = f(x) + B\Lambda u \tag{5.6}$$

where Λ is a positive diagonal matrix whose diagonal elements represent the control input effectiveness uncertainty which can be in the amplitude or in the sign or both. When the uncertainty is in the amplitude, a control saturation can occur and may worsen the performance of a controller. When the uncertainty is in the sign, a control reversal can occur and potentially can cause instability.
An alternative form of a control input uncertainty is given by

$$\dot{x} = f(x) + (B + \Delta B)\, u \tag{5.7}$$

which is less common in adaptive control.

5.1.2 Reference Model

A reference model is used to specify a desired response of an adaptive control system to a command input. It is essentially a command shaping filter to achieve a desired command following. Since adaptive control is formulated as a command following or tracking control, the adaptation is operated on the tracking error between the reference model and the system output. A reference model must be designed properly for an adaptive control system to be able to follow. Typically, a reference model is formulated as a LTI model, but a nonlinear reference model can be used although a nonlinear design always brings up many complex issues. A LTI reference model

should capture all important performance specifications such as rise time and settling time, as well as robustness specifications such as phase and gain stability margins.

Example 5.8 For Example 5.1, the reference model for an adaptive control system could be selected to be a second-order system as

$$\ddot{x}_m + 2\zeta_m \omega_m \dot{x}_m + \omega_m^2 x_m = \omega_m^2 r$$

where $x_m(t)$ is a model-reference signal that only depends on the reference command input $r(t)$. ■

The tracking error is defined as

$$e = x_m - x \tag{5.8}$$

The objective of an adaptive control system is to adapt to system uncertainty so as to keep the tracking error as small as possible. In an ideal case when $e(t) \to 0$, then the system state follows the model-reference signal perfectly, i.e., $x(t) \to x_m(t)$.

5.1.3 Controller

A controller must be designed to provide overall system performance and stability for a nominal plant without uncertainty. Thus, it can be thought of as a baseline or nominal controller. The type of controllers is dictated by the objective of a control design. A controller can be linear or nonlinear but as always nonlinear controllers are much more difficult to design, analyze, and ultimately certify for operation in real systems. The controller can be a nominal controller augmented with an adaptive controller or a fully adaptive controller. The adaptive augmentation control design is more prevalent and generally should be more robust than a fully adaptive control design.

5.1.4 Adaptive Law

An adaptive law is a mathematical relationship that expresses explicitly how adaptive parameters should be adjusted to keep the tracking error as small as possible. An adaptive law can be either linear time-varying or nonlinear. In any case, stability of an adaptive control system usually must be analyzed using Lyapunov stability theory. Many different adaptive laws have been developed, and each has its own advantages as well as disadvantages. Ultimately, designing an adaptive control system comes down to a trade-off between performance and robustness. This trade-off can be made by a suitable selection of an adaptive law and a set of tuning parameters that are built into an adaptive law.

5.2 Direct MRAC for First-Order SISO Systems

Consider a first-order nonlinear SISO system

$$\dot{x} = ax + b\left[u + f\left(x\right)\right] \tag{5.9}$$

subject to $x\left(0\right) = x_0$, where $f\left(x\right)$ is a structured matched uncertainty that can be linearly parametrized as

$$f\left(x\right) = \sum_{i=1}^{p} \theta_i^* \phi_i\left(x\right) = \Theta^{*\top} \Phi\left(x\right) \tag{5.10}$$

where $\Theta^* = \left[\theta_1\ \theta_2\ \ldots\ \theta_p\right]^\top \in \mathbb{R}^p$ is an unknown constant vector, and $\Phi\left(x\right) = \left[\phi_1\left(x\right)\ \phi_2\left(x\right)\ \ldots\ \phi_p\left(x\right)\right]^\top \in \mathbb{R}^p$ is a vector of known bounded basis functions.

5.2.1 Case I: a and b Unknown but Sign of b Known

A reference model is specified as

$$\dot{x}_m = a_m x_m + b_m r \tag{5.11}$$

subject to $x_m\left(0\right) = x_{m_0}$, where $a_m < 0$ and $r\left(t\right) \in \mathscr{L}_\infty$ is a piecewise continuous bounded reference command signal, so that $x_m\left(t\right)$ is a uniformly bounded model-reference signal.

Firstly, define an ideal controller that perfectly cancels out the uncertainty and enables $x\left(t\right)$ to follow $x_m\left(t\right)$ as

$$u^* = k_x^* x + k_r^* r\left(t\right) - \Theta^{*\top} \Phi\left(x\right) \tag{5.12}$$

where the superscript $*$ denotes ideal constant values which are unknown.

Upon substituting into the plant model, we get the ideal closed-loop plant

$$\dot{x} = \left(a + bk^*\right) x + bk_r^* r \tag{5.13}$$

Comparing the ideal closed-loop plant to the reference model, the ideal gains k_x^* and k_r^* can be determined by the following model matching conditions:

$$a + bk_x^* = a_m \tag{5.14}$$

$$bk_r^* = b_m \tag{5.15}$$

It turns out that the solutions for k_x^* and k_r^* always exist since there are two independent equations with two unknowns.

The actual adaptive controller is an estimate of the ideal controller with a goal that in the limit the adaptive controller approaches the ideal controller. Let

$$u = k_x(t)\, x + k_r(t)\, r - \Theta^\top(t)\, \Phi(x) \tag{5.16}$$

be the adaptive controller, where $k_x(t)$, $k_r(t)$, and $\Theta(t)$ are the estimates of k_x^*, k_r^*, and Θ^*, respectively.

The adaptive controller is a direct adaptive controller since $k_x(t)$, $k_r(t)$, and $\Theta(t)$ are estimated directly without the knowledge of the unknown system parameters a, b, and Θ^*.

Now, define the estimation errors as

$$\tilde{k}_x(t) = k_x(t) - k_x^* \tag{5.17}$$

$$\tilde{k}_r(t) = k_r(t) - k_r^* \tag{5.18}$$

$$\tilde{\Theta}(t) = \Theta(t) - \Theta^* \tag{5.19}$$

Substituting these into the plant model gives

$$\dot{x} = \left(\underbrace{a + bk_x^*}_{a_m} + b\tilde{k}_x \right) x + \left(\underbrace{bk_r^*}_{b_m} + b\tilde{k}_r \right) r - b\tilde{\Theta}^\top \Phi(x) \tag{5.20}$$

Let $e(t) = x_m(t) - x(t)$ be the tracking error. Then, the closed-loop tracking error equation is established as

$$\dot{e} = \dot{x}_m - \dot{x} = a_m e - b\tilde{k}_x x - b\tilde{k}_r r + b\tilde{\Theta}^\top \Phi(x) \tag{5.21}$$

Note that the tracking error equation is non-autonomous due to $r(t)$.

Now, the task of defining the adaptive laws to adjust $k_x(t)$, $k_r(t)$, and $\Theta(t)$ is considered next. This can be accomplished by conducting a Lyapunov stability proof as follows:

Proof Choose a Lyapunov candidate function

$$V\left(e, \tilde{k}_x, \tilde{k}_r, \tilde{\Theta}\right) = e^2 + |b| \left(\frac{\tilde{k}_x^2}{\gamma_x} + \frac{\tilde{k}_r^2}{\gamma_r} + \tilde{\Theta}^\top \Gamma^{-1} \tilde{\Theta} \right) > 0 \tag{5.22}$$

where $\gamma_x > 0$ and $\gamma_r > 0$ are called the adaptation (or learning) rates for $k_x(t)$ and $k_r(t)$, and $\Gamma = \Gamma^\top > 0 \in \mathbb{R}^p \times \mathbb{R}^p$ is a positive-definite adaptation rate matrix for $\Theta(t)$.

$\dot{V}\left(e, \tilde{k}_x, \tilde{k}_r, \tilde{\Theta}\right)$ is evaluated as

$$\begin{aligned}\dot{V}\left(e, \tilde{k}_x, \tilde{k}_r, \tilde{\Theta}\right) &= 2e\dot{e} + |b|\left(\frac{2\tilde{k}_x\dot{\tilde{k}}_x}{\gamma_x} + \frac{2\tilde{k}_r\dot{\tilde{k}}_r}{\gamma_r} + 2\tilde{\Theta}^\top\Gamma^{-1}\dot{\tilde{\Theta}}\right)\\ &= 2a_m e^2 + 2\tilde{k}_x\left(-ebx + |b|\frac{\dot{\tilde{k}}_x}{\gamma_x}\right) + 2\tilde{k}_r\left(-ebr + |b|\frac{\dot{\tilde{k}}_r}{\gamma_r}\right)\\ &\quad + 2\tilde{\Theta}^\top\left[eb\Phi(x) + |b|\Gamma^{-1}\dot{\tilde{\Theta}}\right] \end{aligned} \tag{5.23}$$

Since $b = |b|\,\mathrm{sgn}b$, then $\dot{V}\left(e, \tilde{k}_x, \tilde{k}_r, \tilde{\Theta}\right) \leq 0$ if

$$-ex\mathrm{sgn}b + \frac{\dot{\tilde{k}}_x}{\gamma_x} = 0 \tag{5.24}$$

$$-er\mathrm{sgn}b + \frac{\dot{\tilde{k}}_r}{\gamma_r} = 0 \tag{5.25}$$

$$e\Phi(x)\,\mathrm{sgn}b + \Gamma^{-1}\dot{\tilde{\Theta}} = 0 \tag{5.26}$$

Because k_x^*, k_r^*, and Θ^* are constant, therefore from Eqs. (5.17)–(5.19) $\dot{\tilde{k}}_x = \dot{k}_x$, $\dot{\tilde{k}}_r = \dot{k}_r$, and $\dot{\tilde{\Theta}} = \dot{\Theta}$. Thus, the following adaptive laws are obtained:

$$\dot{k}_x = \gamma_x x e\mathrm{sgn}b \tag{5.27}$$

$$\dot{k}_r = \gamma_r r e\mathrm{sgn}b \tag{5.28}$$

$$\dot{\Theta} = -\Gamma\Phi(x)\,e\mathrm{sgn}b \tag{5.29}$$

Then,

$$\dot{V}\left(e, \tilde{k}_x, \tilde{k}_r, \tilde{\Theta}\right) = 2a_m e^2 \leq 0 \tag{5.30}$$

Since $\dot{V}\left(e, \tilde{k}_x, \tilde{k}_r, \tilde{\Theta}\right) \leq 0$, then $e(t), k_x(t), k_r(t)$, and $\Theta(t)$ are bounded. Then,

$$\lim_{t\to\infty} V\left(e, \tilde{k}_x, \tilde{k}_r, \tilde{\Theta}\right) = V\left(e_0, \tilde{k}_{x_0}, \tilde{k}_{r_0}, \tilde{\Theta}_0\right) + 2a_m \|e\|_2^2 \tag{5.31}$$

where $e(0) = e_0$, $\tilde{k}_x(0) = \tilde{k}_{x_0}$, $\tilde{k}_r(0) = \tilde{k}_{r_0}$, and $\tilde{\Theta}(0) = \tilde{\Theta}_0$.

So, $V\left(e, \tilde{k}_x, \tilde{k}_r, \tilde{\Theta}\right)$ has a finite limit as $t \to \infty$. Since $\|e\|_2$ exists, therefore $e(t) \in \mathscr{L}_2 \cap \mathscr{L}_\infty$, but $\|\dot{e}\| \in \mathscr{L}_\infty$.

$\dot{V}\left(e, \tilde{k}_x, \tilde{k}_r, \tilde{\Theta}\right)$ can be shown to be uniformly continuous by examining its derivative to see whether it is bounded. $\ddot{V}\left(e, \tilde{k}_x, \tilde{k}_r, \tilde{\Theta}\right)$ is computed as

$$\ddot{V}\left(e, \tilde{k}_x, \tilde{k}_r, \tilde{\Theta}\right) = 4a_m e\dot{e} = 4a_m e\left[a_m e - b\tilde{k}_x x - b\tilde{k}_r r + b\tilde{\Theta}^\top \Phi(x)\right] \tag{5.32}$$

Since $e(t), k_x(t), k_r(t)$, and $\Theta(t)$ are bounded by the virtue that $\dot{V}\left(e, \tilde{k}_x, \tilde{k}_r, \tilde{\Theta}\right) \leq 0$, $x(t)$ is bounded because $e(t)$ and $x_m(t)$ are bounded, $r(t)$ is a bounded reference command signal, and $\Phi(x)$ is bounded because $x(t)$ is bounded; therefore, $\ddot{V}\left(e, \tilde{k}_x, \tilde{k}_r, \tilde{\Theta}\right)$ is bounded. Thus, $\dot{V}\left(e, \tilde{k}_x, \tilde{k}_r, \tilde{\Theta}\right)$ is uniformly continuous. It follows from the Barbalat's lemma that $\dot{V}\left(e, \tilde{k}_x, \tilde{k}_r, \tilde{\Theta}\right) \to 0$, hence $e(t) \to 0$ as $t \to \infty$. The tracking error is asymptotically stable, but the whole adaptive control system is not asymptotically stable since $k_x(t)$, $k_r(t)$ and $\Theta(t)$ can only be shown to be bounded.

5.2.2 Case II: a and b Known

If a and b are known, then the gains k_x and k_r need not be estimated since they are known and can be found from the model matching conditions

$$k_x = \frac{a_m - a}{b} \tag{5.33}$$

$$k_r = \frac{b_m}{b} \tag{5.34}$$

Then, the adaptive controller is given by

$$u = k_x x + k_r r - \Theta^\top(t)\Phi(x) \tag{5.35}$$

where only $\Theta(t)$ needs to be adjusted.

The tracking error equation is then obtained as

$$\dot{e} = a_m e + b\tilde{\Theta}^\top \Phi(x) \tag{5.36}$$

The adaptive law can be found to be

$$\dot{\Theta} = -\Gamma\Phi(x)eb \tag{5.37}$$

Proof To show that the adaptive law is stable, choose a Lyapunov candidate function

$$V\left(e,\tilde{\Theta}\right)=e^2+\tilde{\Theta}^\top\Gamma^{-1}\tilde{\Theta}>0 \tag{5.38}$$

Then,

$$\dot{V}\left(e,\tilde{\Theta}\right)=2e\dot{e}+2\tilde{\Theta}^\top\Gamma^{-1}\dot{\tilde{\Theta}}=2a_me^2+2eb\tilde{\Theta}^\top\Phi\left(x\right)-2\tilde{\Theta}^\top eb\Phi\left(x\right)=2a_me^2\leq 0 \tag{5.39}$$

The Barbalat's lemma can be used to show that the tracking error is asymptotically stable, i.e., $e\left(t\right)\to 0$ as $t\to\infty$.

Example 5.9 Let $a=1$, $b=1$, $a_m=-1$, $b_m=1$, $r\left(t\right)=\sin t$, and $f\left(x\right)=\theta^*x\left(t\right)$, where θ^* is an unknown constant but for simulation purposes is taken to be $\theta^*=0.1$. Then, the control gains are computed as

$$k_x=\frac{a_m-a}{b}=-2$$

$$k_r=\frac{b_m}{b}=1$$

The adaptive controller is given by

$$u=-2x+r-\theta x$$

$$\dot{\theta}=-\gamma xeb$$

where $\gamma=1$ is chosen as the adaptation rate for $\theta\left(t\right)$.

Note that the controller is nonlinear even though the plant is linear. Figure 5.2 illustrates a block diagram of the adaptive controller.

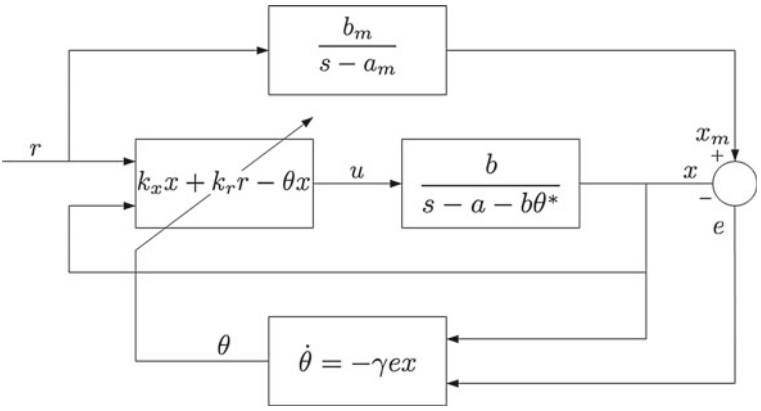

Fig. 5.2 Adaptive control block diagram

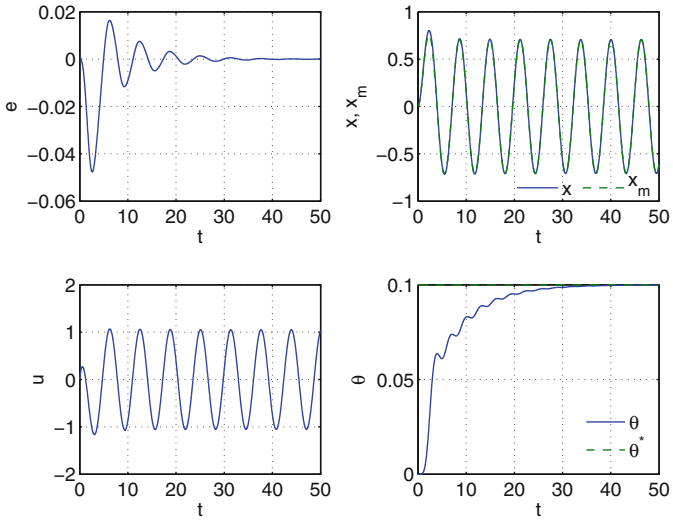

Fig. 5.3 Adaptive control system response

The results are shown in Fig. 5.3. It can be seen that $e(t) \to 0$ and $x(t) \to x_m(t)$ as $t \to \infty$. The estimate $\theta(t)$ also converges to the correct value of the uncertain parameter θ^*, although the convergence is quite gradual. The convergence rate can be increased by increasing the adaptation rate γ, but a large value of γ can lead to an increase in the sensitivity of the control system to noise and unmodeled dynamics that can lead to instability. In other words, a larger value of γ results in a better tracking performance but at the same time degrades the system robustness. In a practical design, the adaptation rate must be chosen carefully to maintain a sufficient robustness while achieving a desired level of performance.

5.3 Indirect MRAC for First-Order SISO Systems

Consider the system in Sect. 5.2.1 with a and b unknown, but sign of b is known. From the model matching conditions, if a and b can be estimated, then the gain k_x and k_r can be obtained. Therefore, the objective of indirect adaptive control is to estimate system parameters which are then used to update the control gains. Hence, indirect adaptive control is essentially a parameter identification method.

Let

$$k_x(t) = \frac{a_m - \hat{a}(t)}{\hat{b}(t)} \tag{5.40}$$

$$k_r(t) = \frac{b_m}{\hat{b}(t)} \tag{5.41}$$

Let $\tilde{a}(t) = \hat{a}(t) - a$ and $\tilde{b}(t) = \hat{b}(t) - b$ be the estimation errors. Now, the plant model is expressed as

$$\dot{x} = ax + \left(\hat{b} - \tilde{b}\right)\left[u + \Theta^{*^{\top}} \Phi(x)\right] \tag{5.42}$$

Then, substituting Eqs. (5.16), (5.40), and (5.41) into Eq. (5.42) yields

$$\begin{aligned}\dot{x} &= ax + \hat{b}\left[\frac{a_m - \hat{a}}{\hat{b}}x + \frac{b_m}{\hat{b}}r - \Theta^{\top}\Phi(x) + \Theta^{*^{\top}}\Phi(x)\right] \\ &\quad - \tilde{b}\left[\frac{a_m - \hat{a}}{\hat{b}}x + \frac{b_m}{\hat{b}}r - \Theta^{\top}\Phi(x) + \Theta^{*^{\top}}\Phi(x)\right] \\ &= (a_m - \tilde{a})x + b_m r - b\tilde{\Theta}^{\top}\Phi(x) - \tilde{b}\left(\frac{a_m - \hat{a}}{\hat{b}}x + \frac{b_m}{\hat{b}}r\right)\end{aligned} \tag{5.43}$$

Let

$$\bar{u} = k_x(t)x + k_r(t)r \tag{5.44}$$

Then, the tracking error equation is established as

$$\dot{e} = \dot{x}_m - \dot{x} = a_m e + \tilde{a}x + \tilde{b}\bar{u} + b\tilde{\Theta}^{\top}\Phi(x) \tag{5.45}$$

The Lyapunov's direct method is now used to find the adaptive laws as follows:

Proof Choose a Lyapunov candidate function

$$V\left(e, \tilde{a}, \tilde{b}, \tilde{\Theta}\right) = e^2 + \frac{\tilde{a}^2}{\gamma_a} + \frac{\tilde{b}^2}{\gamma_b} + |b|\tilde{\Theta}^{\top}\Gamma^{-1}\tilde{\Theta} > 0 \tag{5.46}$$

where $\gamma_a > 0$ and $\gamma_b > 0$ are the adaptation rates for $\hat{a}(t)$ and $\hat{b}(t)$, respectively.

Then, $\dot{V}\left(e, \tilde{a}, \tilde{b}, \tilde{\Theta}\right)$ is evaluated as

$$\begin{aligned}\dot{V}\left(e, \tilde{a}, \tilde{b}, \tilde{\Theta}\right) &= 2e\dot{e} + \frac{2\tilde{a}\dot{\tilde{a}}}{\gamma_a} + \frac{2\tilde{b}\dot{\tilde{b}}}{\gamma_b} + 2|b|\tilde{\Theta}^{\top}\Gamma^{-1}\dot{\tilde{\Theta}} \\ &= 2a_m e^2 + 2\tilde{a}\left(xe + \frac{\dot{\tilde{a}}}{\gamma_a}\right) + 2\tilde{b}\left(\bar{u}e + \frac{\dot{\tilde{b}}}{\gamma_b}\right) \\ &\quad + 2|b|\tilde{\Theta}^{\top}\left[\Phi(x)e\,\mathrm{sgn}b + \Gamma^{-1}\dot{\tilde{\Theta}}\right]\end{aligned} \tag{5.47}$$

Since a and b are constant, then $\dot{\tilde{a}} = \dot{\hat{a}}$ and $\dot{\tilde{b}} = \dot{\hat{b}}$. Thus, the adaptive laws are obtained as

$$\dot{\hat{a}} = -\gamma_a xe \tag{5.48}$$

$$\dot{\hat{b}} = -\gamma_b \bar{u} e \tag{5.49}$$

$$\dot{\Theta} = -\Gamma \Phi(x)\, e \operatorname{sgn} b \tag{5.50}$$

Then,

$$\dot{V}\left(e, \tilde{a}, \tilde{b}, \tilde{\Theta}\right) = 2a_m e^2 \leq 0 \tag{5.51}$$

Since $\dot{V}\left(e, \tilde{a}, \tilde{b}, \tilde{\Theta}\right) \leq 0$, then $e(t)$, $\hat{a}(t)$, $\hat{b}(t)$, and $\Theta(t)$ are bounded. Then,

$$\lim_{t\to\infty} V\left(e, \tilde{k}_x, \tilde{k}_r, \tilde{\Theta}\right) = V\left(e_0, \tilde{a}_0, \tilde{b}_0, \tilde{\Theta}_0\right) + 2a_m \|e\|_2^2 \tag{5.52}$$

where e_0 and $\tilde{\Theta}_0$ are defined previously, $\tilde{a}(0) = a_0$, and $\tilde{b}(0) = b_0$.

So, $V\left(e, \tilde{a}, \tilde{b}, \tilde{\Theta}\right)$ has a finite limit as $t \to \infty$. Since $\|e\|_2$ exists, therefore $e(t) \in \mathcal{L}_2 \cap \mathcal{L}_\infty$, but $\|\dot{e}\| \in \mathcal{L}_\infty$.

$\dot{V}\left(e, \tilde{a}, \tilde{b}, \tilde{\Theta}\right)$ can be shown to be uniformly continuous by examining its derivative to see whether it is bounded. $\ddot{V}\left(e, \tilde{a}, \tilde{b}, \tilde{\Theta}\right)$ is computed as

$$\ddot{V}\left(e, \tilde{a}, \tilde{b}, \tilde{\Theta}\right) = 4a_m e\dot{e} = 4a_m e\left[a_m e + \tilde{a}x + \tilde{b}\bar{u} + b\tilde{\Theta}^\top \Phi(x)\right] \tag{5.53}$$

Since $e(t)$, $\hat{a}(t)$, $\hat{b}(t)$, and $\Theta(t)$ are bounded by the virtue that $\dot{V}\left(e, \tilde{a}, \tilde{b}, \tilde{\Theta}\right) \leq 0$, $x(t)$ is bounded because $e(t)$ and $x_m(t)$ are bounded, $\bar{u}(t)$ is bounded because $x(t)$ is bounded and $r(t)$ is a bounded reference command signal, and $\Phi(x)$ is bounded because $x(t)$ is bounded; therefore, $\ddot{V}\left(e, \tilde{a}, \tilde{b}, \tilde{\Theta}\right)$ is bounded. Thus, $\dot{V}\left(e, \tilde{a}, \tilde{b}, \tilde{\Theta}\right)$ is uniformly continuous. It follows from the Barbalat's lemma that $\dot{V}\left(e, \tilde{a}, \tilde{b}, \tilde{\Theta}\right) \to 0$, hence $e(t) \to 0$ as $t \to \infty$. The tracking error is asymptotically stable.

■

It should be noted that the possibility of $\hat{b}(t) = 0$ does exist, and in such a case, the control gains will "blow up." Thus, indirect MRAC may not be as robust as direct MRAC. To prevent this from occurring, the adaptive law for $\hat{b}(t)$ must be modified so that the adaptation can take place in a closed subset of $\mathbb{R}$ that does not include $\hat{b}(t) = 0$. One technique for modification is the projection method which assumes a priori knowledge of b [2].

Suppose a lower bound on b is known, i.e., $0 < b_0 \leq |b|$, then the adaptive law can be modified by the projection method as

$$\dot{\hat{b}} = \begin{cases} -\gamma_b \bar{u} e & \text{if } \left|\hat{b}\right| > b_0 \text{ or if } \left|\hat{b}\right| = b_0 \text{ and } \frac{d\left|\hat{b}\right|}{dt} \geq 0 \\ 0 & \text{otherwise} \end{cases} \tag{5.54}$$

The projection method is essentially a constrained optimization which will be discussed in detail in Chap. 9. In the simplest term, the projection method allows the adaptation to take place in such a manner that an adaptive parameter will not violate its a priori bound. A simple explanation of the modified adaptive law is as follows:

Suppose one knows that b is bounded from below by b_0, i.e., $|b| \geq b_0$, then as long as $\left|\hat{b}\right| > b_0$, the unmodified adaptive law can be used normally. Now, suppose $\left|\hat{b}\right| = b_0$, there are two cases to consider: $\frac{d\left|\hat{b}\right|}{dt} < 0$ and $\frac{d\left|\hat{b}\right|}{dt} \geq 0$.

1. If $\frac{d\left|\hat{b}\right|}{dt} < 0$, then $\left|\hat{b}\right|$ is decreasing and $\left|\hat{b}\right| < b_0$ at some time $t + \Delta t$, which would violate the constraint $\left|\hat{b}\right| \geq b_0$. Therefore, to satisfy the constraint on b, $\frac{d\left|\hat{b}\right|}{dt} = 0$.
2. On the other hand, if $\frac{d\left|\hat{b}\right|}{dt} \geq 0$, then $\left|\hat{b}\right|$ is non-decreasing and $\left|\hat{b}\right| \geq b_0$, so that the unmodified adaptive law can be used normally.

The modified adaptive law thus guarantees that $\left|\hat{b}\right|$ will always be greater than or equal to b_0.

Proof Because of the modification, $\dot{V}\left(e, \tilde{a}, \tilde{b}, \tilde{\Theta}\right)$ will no longer be the same and is now dependent on the conditions on $\left|\hat{b}\right|$ and $\frac{d\left|\hat{b}\right|}{dt}$. Thus,

$$\begin{aligned}\dot{V}\left(e, \tilde{a}, \tilde{b}, \tilde{\Theta}\right) &= 2a_m e^2 + 2\tilde{b}\left(\bar{u}e + \frac{\dot{\tilde{b}}}{\gamma_b}\right) \\ &= \begin{cases} 2a_m e^2 \leq 0 & \text{if } \left|\hat{b}\right| \geq b_0 \text{ or if } \left|\hat{b}\right| = b_0 \text{ and } \frac{d\left|\hat{b}\right|}{dt} \geq 0 \\ a_m e^2 + 2\tilde{b}\bar{u}e & \text{if } \left|\hat{b}\right| = b_0 \text{ and } \frac{d\left|\hat{b}\right|}{dt} < 0 \end{cases} \end{aligned} \tag{5.55}$$

Consider the second case when $\left|\hat{b}\right| = b_0$ and $\frac{d\left|\hat{b}\right|}{dt} < 0$ for which the sign definiteness of $\dot{V}\left(e, \tilde{a}, \tilde{b}, \tilde{\Theta}\right)$ is still undefined. The condition $\frac{d\left|\hat{b}\right|}{dt} < 0$ gives

$$\frac{d\left|\hat{b}\right|}{dt} = \dot{\hat{b}}\text{sgn}b = -\gamma_b \bar{u}e\text{sgn}b < 0 \Rightarrow \bar{u}e\text{sgn}b > 0 \tag{5.56}$$

Since $\left|\hat{b}\right| = b_0$, then

$$2\tilde{b}\bar{u}e = 2\left(\hat{b} - b\right)\bar{u}e = 2\left[\left|\hat{b}\right|\text{sgn}b - |b|\,\text{sgn}b\right]\bar{u}e = 2\left(b_0 - |b|\right)\bar{u}e\text{sgn}b \tag{5.57}$$

Since $|b| \geq b_0$, which implies $|b| = b_0 + \delta > 0$ where $\delta \geq 0$, then $\bar{u}e\text{sgn}b > 0$ implies

$$2\tilde{b}\bar{u}e = 2\left(b_0 - b_0 - \delta\right)\bar{u}e\text{sgn}b = -2\delta\bar{u}e\text{sgn}b \leq 0 \tag{5.58}$$

Therefore,

$$\dot{V}\left(e, \tilde{a}, \tilde{b}, \tilde{\Theta}\right) = 2a_m e^2 + 2\tilde{b}\bar{u}e = 2a_m e^2 - 2\delta\bar{u}e\text{sgn}b \leq 2a_m e^2 \leq 0 \tag{5.59}$$

Using the usual Barbalat's lemma, one can conclude that $e(t) \to 0$ as $t \to \infty$.

5.4 Direct MRAC for Second-Order SISO Systems

Consider a second-order nonlinear SISO system

$$\ddot{y} + 2\zeta\omega_n\dot{y} + \omega_n^2 y = b\left[u + f(y, \dot{y})\right] \tag{5.60}$$

where ζ and ω_n are unknown and $f(y, \dot{y}) = \Theta^{*\top}\Phi(y, \dot{y})$ is defined in a manner similar to Eq. (5.10).

Let $x_1(t) = y(t)$, $x_2 = \dot{y}(t)$, and $x(t) = \left[x_1(t)\ x_2(t)\right]^\top \in \mathbb{R}^2$. The state-space form of the system is

$$\dot{x} = Ax + B\left[u + \Theta^*\Phi(x)\right] \tag{5.61}$$

where

$$A = \begin{bmatrix} 0 & 1 \\ -\omega_n^2 & -2\zeta\omega_n \end{bmatrix},\ B = \begin{bmatrix} 0 \\ b \end{bmatrix} \tag{5.62}$$

Let $x_{m_1}(t) = y_m(t)$, $x_{m_2} = \dot{y}_m(t)$, and $x_m(t) = \left[x_{m_1}(t)\ x_{m_2}(t)\right]^\top \in \mathbb{R}^2$. A reference model is given by

$$\dot{x}_m = A_m x_m + B_m r \tag{5.63}$$

where $r(t) \in \mathbb{R}$ is a bounded command signal, $A_m \in \mathbb{R}^2 \times \mathbb{R}^2$ is Hurwitz and known, and $B_m \in \mathbb{R}^2$ is also known.

5.4.1 Case I: A and B Unknown but Sign of b known

Firstly, the ideal controller is defined as

$$u^* = K_x^* x + k_r^* r - \Theta^{*\top}\Phi(x) \tag{5.64}$$

where $K_x^* \in \mathbb{R}^2$ and $k_r^* \in \mathbb{R}$ are constant but unknown ideal gains.

Comparing the ideal closed-loop plant to the reference model, the model matching conditions are

$$A + BK_x^* = A_m \tag{5.65}$$

$$Bk_r^* = B_m \tag{5.66}$$

Note that in general, one cannot always assume that K_x^* and k_r^* exist because A, A_m, B, and B_m may have different structures that do not allow the solutions for K_x^* and k_r^* to be determined. In most cases, if A and B are known, then K_x^* and k_r^* can be designed by any standard non-adaptive control techniques to stabilize the closed-loop system and enable it to follow a command. Then, A_m and B_m can be computed from A, B, K_x^*, and k_r^*.

Example 5.10 A second-order SISO system and a reference model are specified as

$$A = \begin{bmatrix} 0 & 1 \\ -1 & -1 \end{bmatrix},\ B = \begin{bmatrix} 0 \\ 1 \end{bmatrix},\ A_m = \begin{bmatrix} 0 & 1 \\ -16 & -2 \end{bmatrix},\ B_m = \begin{bmatrix} 0 \\ 2 \end{bmatrix}$$

Then, utilizing the pseudo-inverse, K_x^* and k_r^* can be solved as

$$K_x^* = \left(B^\top B\right)^{-1} B^\top (A_m - A) = \begin{bmatrix} 0 & 1 \end{bmatrix} \left(\begin{bmatrix} 0 & 1 \\ -16 & -2 \end{bmatrix} - \begin{bmatrix} 0 & 1 \\ -1 & -1 \end{bmatrix} \right) = \begin{bmatrix} -15 & -1 \end{bmatrix}$$

$$k_r^* = \left(B^\top B\right)^{-1} B^\top B_m = 2$$

Now, suppose

$$A_m = \begin{bmatrix} 1 & 1 \\ -16 & -2 \end{bmatrix}$$

Then, the solution of K_x^* is the same (verify!), but the model matching condition is not satisfied since

$$A + BK = \begin{bmatrix} 0 & 1 \\ -16 & -2 \end{bmatrix} \neq A_m$$

■

Thus, it is important to state an explicit assumption that there exist constant but unknown K_x^* and k_r^* such that the model matching conditions are satisfied. For a second-order SISO system, the model matching conditions are satisfied if A_m and B_m have the same structures as those of A and B, respectively.

A full-state feedback adaptive controller is designed as

$$u = K_x(t)\, x + k_r(t)\, r - \Theta^\top \Phi(x) \tag{5.67}$$

where $K_x(t) \in \mathbb{R}^2$ and $k_r(t) \in \mathbb{R}$.

Let $\tilde{K}_x(t) = K_x(t) - K_x^*$, $\tilde{k}_r(t) = k_r(t) - k_r^*$, and $\tilde{\Theta}(t) = \Theta(t) - \Theta^*$ be the estimation errors, then the closed-loop plant becomes

$$\dot{x} = \left(\underbrace{A + BK_x^*}_{A_m} + B\tilde{K}_x \right) x + \left(\underbrace{Bk_r^*}_{B_m} + B\tilde{k}_r \right) r - B\tilde{\Theta}^\top \Phi(x) \tag{5.68}$$

The closed-loop tracking error equation is now obtained as

$$\dot{e} = \dot{x}_m - \dot{x} = A_m e - B\tilde{K}_x x - B\tilde{k}_r r + B\tilde{\Theta}^\top \Phi(x) \tag{5.69}$$

where $e(t) = x_m(t) - x(t) \in \mathbb{R}^2$.

Proof To find the adaptive laws, choose a Lyapunov candidate function

$$V\left(e, \tilde{K}_x, \tilde{k}_r, \tilde{\Theta}\right) = e^\top P e + |b| \left(\tilde{K}_x \Gamma_x^{-1} \tilde{K}_x^\top + \frac{\tilde{k}_r^2}{\gamma_r} + \tilde{\Theta}^\top \Gamma_\Theta^{-1} \tilde{\Theta} \right) > 0 \tag{5.70}$$

where $\Gamma_x = \Gamma_x^\top > 0 \in \mathbb{R}^2 \times \mathbb{R}^2$ is a positive-definite adaptation rate matrix for $K_x(t)$ and $P = P^\top > 0 \in \mathbb{R}^2 \times \mathbb{R}^2$ that solves the following Lyapunov equation:

$$PA_m + A_m^\top P = -Q \tag{5.71}$$

where $Q = Q^\top > 0 \in \mathbb{R}^2 \times \mathbb{R}^2$.

Then, $\dot{V}\left(e, \tilde{K}_x, \tilde{k}_r, \tilde{\Theta}\right)$ is evaluated as

$$\dot{V}\left(e, \tilde{K}_x, \tilde{k}_r, \tilde{\Theta}\right) = \dot{e}^\top P e + e^\top P \dot{e} + |b| \left(2\tilde{K}_x \Gamma_x^{-1} \dot{\tilde{K}}_x^\top + \frac{2\tilde{k}_r \dot{\tilde{k}}_r}{\gamma_r} + 2\tilde{\Theta}^\top \Gamma_\Theta^{-1} \dot{\tilde{\Theta}} \right) \tag{5.72}$$

Substituting the tracking error equation yields

$$\begin{aligned} \dot{V}\left(e, \tilde{K}_x, \tilde{k}_r, \tilde{\Theta}\right) = {} & e^\top \left(PA_m + A_m^\top P \right) e + 2e^\top PB \left[-\tilde{K}_x x - \tilde{k}_r r + \tilde{\Theta}^\top \Phi(x) \right] \\ & + |b| \left(2\tilde{K}_x \Gamma_x^{-1} \dot{\tilde{K}}_x^\top + \frac{2\tilde{k}_r \dot{\tilde{k}}_r}{\gamma_r} + 2\tilde{\Theta}^\top \Gamma_\Theta^{-1} \dot{\tilde{\Theta}} \right) \end{aligned} \tag{5.73}$$

Let p_{ij}, $i = 1, 2$, $j = 1, 2$, be the elements of P and notice that

$$2e^\top PB = 2e^\top \bar{P} b \in \mathbb{R} \tag{5.74}$$

where $\bar{P} = \begin{bmatrix} p_{12} & p_{22} \end{bmatrix}^\top$.

Then, $\dot{V}\left(e, \tilde{K}_x, \tilde{k}_r, \tilde{\Theta}\right)$ can be expressed as

$$\dot{V}\left(e, \tilde{K}_x, \tilde{k}_r, \tilde{\Theta}\right) = -e^\top Qe + 2\,|b|\,\mathrm{sgn}\,(b)\left[-\tilde{K}_x x - \tilde{k}_r r + \tilde{\Theta}^\top \Phi\,(x)\right] e^\top \bar{P} + |b|\left(2\tilde{K}_x \Gamma_x^{-1}\dot{\tilde{K}}_x^\top + \frac{2\tilde{k}_r\dot{\tilde{k}}_r}{\gamma_r} + 2\tilde{\Theta}^\top \Gamma_\Theta^{-1}\dot{\tilde{\Theta}}\right) \tag{5.75}$$

or

$$\begin{aligned}\dot{V}\left(e, \tilde{K}_x, \tilde{k}_r, \tilde{\Theta}\right) = &-e^\top Qe + 2\,|b|\,\tilde{K}_x\left(-xe^\top \bar{P}\mathrm{sgn}b + \Gamma_x^{-1}\dot{\tilde{K}}_x^\top\right) \\ &+ 2\,|b|\,\tilde{k}_r\left(-re^\top \bar{P}\mathrm{sgn}b + \frac{\dot{\tilde{k}}_r}{\gamma_r}\right) \\ &+ 2\,|b|\,\tilde{\Theta}^\top\left[\Phi\,(x)\,e^\top \bar{P}\mathrm{sgn}b + \Gamma_\Theta^{-1}\dot{\tilde{\Theta}}\right]\end{aligned} \tag{5.76}$$

Thus, the following adaptive laws are obtained:

$$\dot{K}_x^\top = \Gamma_x x e^\top \bar{P}\mathrm{sgn}b \tag{5.77}$$

$$\dot{k}_r = \gamma_r r e^\top \bar{P}\mathrm{sgn}b \tag{5.78}$$

$$\dot{\Theta} = -\Gamma_\Theta \Phi\,(x)\,e^\top \bar{P}\mathrm{sgn}b \tag{5.79}$$

It follows that

$$\dot{V}\left(e, \tilde{K}_x, \tilde{k}_r, \tilde{\Theta}\right) = -e^\top Qe \le -\lambda_{min}\,(Q)\,\|e\|_2^2 \le 0 \tag{5.80}$$

Since $\dot{V}\left(e, \tilde{K}_x, \tilde{k}_r, \tilde{\Theta}\right) \le 0$, therefore $e\,(t)$, $K_x\,(t)$, $k_r\,(t)$, and $\Theta\,(t)$ are bounded. Then,

$$\lim_{t\to\infty} V\left(e, \tilde{K}_x, \tilde{k}_r, \tilde{\Theta}\right) = V\left(e_0, \tilde{K}_{x_0}, \tilde{k}_{r_0}, \tilde{\Theta}_0\right) - \lambda_{min}\,(Q)\,\|e\|_2^2 \tag{5.81}$$

So, $V\left(e, \tilde{K}_x, \tilde{k}_r, \tilde{\Theta}\right)$ has a finite limit as $t \to \infty$. Since $\|e\|_2$ exists, therefore $e\,(t) \in \mathscr{L}_2 \cap \mathscr{L}_\infty$, but $\|\dot{e}\| \in \mathscr{L}_\infty$.

$\dot{V}\left(e, \tilde{K}_x, \tilde{k}_r, \tilde{\Theta}\right)$ can be shown to be uniformly continuous by examining its derivative to see whether it is bounded, where

$$\begin{aligned}\ddot{V}\left(e, \tilde{K}_x, \tilde{k}_r, \tilde{\Theta}\right) = &-\dot{e}^\top Qe - e^\top Q\dot{e} = -e^\top\left(QA + A^\top Q\right)e \\ &- 2e^\top Q\left[A_m e - B\tilde{K}_x x - B\tilde{k}_r r + B\tilde{\Theta}^\top \Phi\,(x)\right]\end{aligned} \tag{5.82}$$

Since $e(t)$, $K_x(t)$, $k_r(t)$, and $\Theta(t)$ are bounded by the virtue of $\dot{V}\left(e, \tilde{K}_x, \tilde{k}_r, \tilde{\Theta}\right) \leq 0$, $x(t)$ is bounded because $e(t)$ and $x_m(t)$ are bounded, $r(t)$ is a bounded reference command signal, and $\Phi(x)$ is bounded because $x(t)$ is bounded, therefore $\ddot{V}\left(e, \tilde{K}_x, \tilde{k}_r, \tilde{\Theta}\right)$ is bounded. Thus, $\dot{V}\left(e, \tilde{K}_x, \tilde{k}_r, \tilde{\Theta}\right)$ is uniformly continuous. It follows from the Barbalat's lemma that $\dot{V}\left(e, \tilde{K}_x, \tilde{k}_r, \tilde{\Theta}\right) \to 0$, hence $e(t) \to 0$ as $t \to \infty$. Therefore, the tracking error is asymptotically stable.

Example 5.11 Design an adaptive controller for a second-order system

$$\ddot{y} + 2\zeta\omega_n\dot{y} + \omega_n^2 y = b\left[u + \Theta^{*\top}\Phi(y)\right]$$

where $\zeta > 0$, $\omega_n > 0$, $b > 0$, and $\Theta^{*\top} = \left[\theta_1^* \ \theta_2^*\right]$ are unknown, and

$$\Phi(y) = \begin{bmatrix} 1 \\ y^2 \end{bmatrix}$$

The reference model is given by

$$\ddot{y}_m + 2\zeta_m\omega_m\dot{y}_m + \omega_m^2 y_m = b_m r$$

where $\zeta_m = 0.5$, $\omega_m = 2$, $b_m = 4$, and $r(t) = \sin 2t$. For simulation purposes, the unknown parameters may be assumed to be $\zeta = -0.5$, $\omega_n = 1$, $b = 1$, and $\Theta^{*\top} = \left[0.5 \ -0.1\right]$.

Note that the open-loop plant is unstable with the eigenvalues $\lambda(A) = \frac{1\pm\sqrt{3}}{2}$ on the right half plane, and the ideal control gains K_x^* and k_r^* exist and are equal to

$$K_x^* = \left(B^\top B\right)^{-1} B^\top (A_m - A) = \left[-3 \ -3\right]$$

$$k_r^* = \frac{b_m}{b} = 4$$

Let $Q = I$, then the solution of the Lyapunov equation (5.71) is

$$P = \begin{bmatrix} \frac{3}{2} & \frac{1}{8} \\ \frac{1}{8} & \frac{5}{16} \end{bmatrix} \Rightarrow \bar{P} = \begin{bmatrix} \frac{1}{8} \\ \frac{5}{16} \end{bmatrix}$$

Let $\Gamma_x = \text{diag}\left(\gamma_{x_1}, \gamma_{x_2}\right)$ and $\Gamma_\Theta = \text{diag}\left(\gamma_{\theta_1}, \gamma_{\theta_2}\right)$. Then, the adaptive laws are

$$\begin{aligned} \dot{K}_x^\top &= \begin{bmatrix} \dot{k}_{x_1} \\ \dot{k}_{x_2} \end{bmatrix} = \Gamma_x x e^\top \bar{P} \underbrace{\text{sgn}(b)}_{1} = \begin{bmatrix} \gamma_{x_1} & 0 \\ 0 & \gamma_{x_2} \end{bmatrix} \begin{bmatrix} x_1 \\ x_2 \end{bmatrix} \begin{bmatrix} e_1 \ e_2 \end{bmatrix} \begin{bmatrix} \frac{1}{8} \\ \frac{5}{16} \end{bmatrix} \\ &= \left(\frac{1}{8}e_1 + \frac{5}{16}e_2\right) \begin{bmatrix} \gamma_{x_1} x_1 \\ \gamma_{x_2} x_2 \end{bmatrix} \end{aligned}$$

$$\dot{k}_r = \gamma_r r e^\top \bar{P} \text{sgn} b = \left(\frac{1}{8} e_1 + \frac{5}{16} e_2\right) \gamma_r r$$

$$\dot{\Theta} = \begin{bmatrix} \dot{\theta}_1 \\ \dot{\theta}_2 \end{bmatrix} = -\Gamma_\Theta \Phi(x) e^\top \bar{P} \text{sgn} b = -\begin{bmatrix} \gamma_{\theta_1} & 0 \\ 0 & \gamma_{\theta_2} \end{bmatrix} \begin{bmatrix} 1 \\ x_1^2 \end{bmatrix} \begin{bmatrix} e_1 & e_2 \end{bmatrix} \begin{bmatrix} \frac{1}{8} \\ \frac{5}{16} \end{bmatrix}$$
$$= -\left(\frac{1}{8} e_1 + \frac{5}{16} e_2\right) \begin{bmatrix} \gamma_{\theta_1} \\ \gamma_{\theta_2} x_1^2 \end{bmatrix}$$

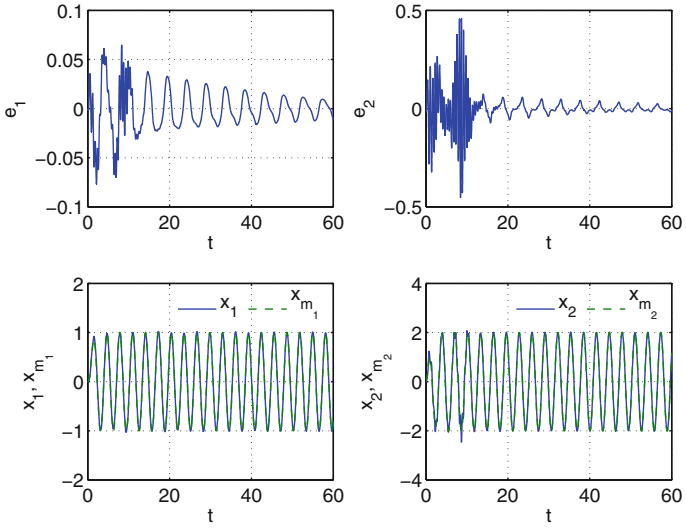

Fig. 5.4 Adaptive control system response

For simulations, all adaptation rates are chosen to be 100 and all initial conditions are set to zero. The results are shown in Figs. 5.4 and 5.5.

It is noted that the plant follows the reference model very well only after a short time, but the adaptive gains $K_x(t)$ and $k_r(t)$ and the adaptive parameter $\Theta(t)$ are converging much more slowly. When they converge, some of them do not converge to their true values, such as $k_{x_2}(t)$ and $k_r(t)$. This is one of the properties of MRAC whereby there is no assurance on the convergence of adaptive parameters to their true values.

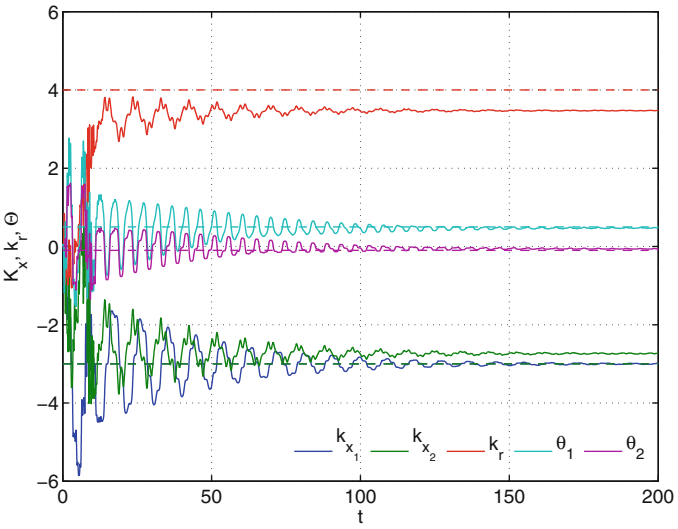

Fig. 5.5 Adaptive gains and adaptive parameters

5.4.2 Case II: A and B Known

If A and B are known, then it is assumed that there exist K_x and k_r that satisfy the model matching conditions

$$A + BK_x = A_m \tag{5.83}$$

$$Bk_r = B_m \tag{5.84}$$

For a second-order system, if A_m and B_m have the same structures as those of A and B, respectively, then K_x and k_r can be determined by using the pseudo-inverse method.

Let the adaptive controller be

$$u = K_x x + k_r r - \Theta^\top \Phi(x) \tag{5.85}$$

Then, the closed-loop plant is

$$\dot{x} = (A + BK_x)\, x + Bk_r r - B\tilde{\Theta}^\top \Phi(x) \tag{5.86}$$

and the tracking error equation is

$$\dot{e} = A_m e + B\tilde{\Theta}^\top \Phi(x) \tag{5.87}$$

Proof Choose a Lyapunov candidate function

$$V\left(e,\tilde{\Theta}\right)=e^{\top}Pe+\tilde{\Theta}^{\top}\Gamma^{-1}\tilde{\Theta}^{\top} \tag{5.88}$$

Then, $\dot{V}\left(e,\tilde{\Theta}\right)$ is evaluated as

$$\dot{V}\left(e,\tilde{\Theta}\right)=-e^{\top}Qe+2e^{\top}PB\tilde{\Theta}^{\top}\Phi\left(x\right)+2\tilde{\Theta}^{\top}\Gamma^{-1}\dot{\tilde{\Theta}} \tag{5.89}$$

Since $e^{\top}PB\in\mathbb{R}$ is a scalar value, then

$$\begin{aligned}\dot{V}\left(e,\tilde{\Theta}\right)&=-e^{\top}Qe+2\tilde{\Theta}^{\top}\Phi\left(x\right)e^{\top}PB+2\tilde{\Theta}^{\top}\Gamma^{-1}\dot{\tilde{\Theta}}\\&=-e^{\top}Qe+2\tilde{\Theta}^{\top}\left[\Phi\left(x\right)e^{\top}PB+\Gamma^{-1}\dot{\tilde{\Theta}}\right]\end{aligned} \tag{5.90}$$

Thus, the following adaptive law is obtained:

$$\dot{\Theta}=-\Gamma\Phi\left(x\right)e^{\top}PB \tag{5.91}$$

Then,

$$\dot{V}\left(e,\tilde{\Theta}\right)=-e^{\top}Qe\leq-\lambda_{min}\left(Q\right)\|e\|^{2} \tag{5.92}$$

Therefore, $e\left(t\right)$ and $\Theta\left(t\right)$ are bounded. Using the same argument with the Barbalat's lemma as in the previous sections, one can conclude that $\dot{V}\left(e,\tilde{\Theta}\right)$ is uniformly continuous so $\dot{V}\left(e,\tilde{\Theta}\right)\rightarrow 0$ as $t\rightarrow\infty$. Therefore, the tracking error is asymptotically stable with $e\left(t\right)\rightarrow 0$ as $t\rightarrow\infty$.

5.5 Indirect MRAC for Second-Order SISO Systems

Indirect MRAC for second-order systems is similar to that for first-order systems. Consider the second-order system in Sect. 5.4.1 with A and B unknown, but sign of b is known. Assuming that there exist K_x and k_r that satisfy the model matching conditions, and furthermore that A_m and B_m have the same structures as those of A and B, respectively, then A and B can be estimated. Let

$$A=\begin{bmatrix}0&1\\-\omega_n^2&-2\zeta\omega_n\end{bmatrix},\ B=\begin{bmatrix}0\\b\end{bmatrix},\ A_m=\begin{bmatrix}0&1\\-\omega_m^2&-2\zeta_m\omega_m\end{bmatrix},\ B=\begin{bmatrix}0\\b_m\end{bmatrix} \tag{5.93}$$

The model matching conditions are

$$\hat{A}(t) + \hat{B}(t) K_x(t) = A_m \tag{5.94}$$

$$\hat{B}(t) k_r(t) = B_m \tag{5.95}$$

from which $K_x(t)$ and $k_r(t)$ are determined by

$$\begin{aligned} K_x = \left(\hat{B}^\top \hat{B}\right)^{-1} \hat{B}^\top \left(A_m - \hat{A}\right) &= \frac{1}{\hat{b}^2} \left[0 \ \hat{b}\right] \begin{bmatrix} 0 & 0 \\ -\omega_m^2 + \hat{\omega}_n^2 & -2\zeta_m \omega_m + 2\hat{\zeta}\hat{\omega}_n \end{bmatrix} \\ &= \frac{1}{\hat{b}} \left[-\omega_m^2 + \hat{\omega}_n^2 \ -2\zeta_m \omega_m + 2\hat{\zeta}\hat{\omega}_n\right] \end{aligned} \tag{5.96}$$

$$k_r = \left(\hat{B}^\top \hat{B}\right)^{-1} \hat{B}^\top B_m = \frac{1}{\hat{b}^2} \left[0 \ \hat{b}\right] \begin{bmatrix} 0 \\ b_m \end{bmatrix} = \frac{b_m}{\hat{b}} \tag{5.97}$$

where $\hat{A}(t)$, $\hat{B}(t)$, $\hat{\omega}_n(t)$, and $\hat{\zeta}(t)$ are estimates of A, B, ω_n, and ζ, respectively.

Let $\tilde{A}(t) = \hat{A}(t) - A$ and $\tilde{B}(t) = \hat{B}(t) - B$ be the estimation errors. Now, the plant model is expressed as

$$\dot{x} = \left(\hat{A} - \tilde{A}\right) x + \left(\hat{B} - \tilde{B}\right) \left[u + \Theta^{*\top} \Phi(x)\right] \tag{5.98}$$

Then, substituting Eqs. (5.67), (5.96), and (5.97) into Eq. (5.98) yields

$$\begin{aligned} \dot{x} &= \left(\hat{A} - \tilde{A}\right) x + \hat{B} \left[K_x x + k_r r - \Theta^\top \Phi(x) + \Theta^{*\top} \Phi(x)\right] \\ &\quad - \tilde{B} \left[K_x x + k_r r - \Theta^\top \Phi(x) + \Theta^{*\top} \Phi(x)\right] \\ &= \left(\underbrace{\hat{A} + \hat{B} K_x}_{A_m} - \tilde{A}\right) x + \underbrace{\hat{B} k_r}_{B_m} r - B\tilde{\Theta}^\top \Phi(x) - \tilde{B}\left(K_x x + k_r r\right) \end{aligned} \tag{5.99}$$

Let

$$\bar{u} = K_x(t) x + k_r(t) r \tag{5.100}$$

Then, the tracking error equation is established as

$$\dot{e} = \dot{x}_m - \dot{x} = A_m e + \tilde{A} x + \tilde{B} \bar{u} + B\tilde{\Theta}^\top \Phi(x) \tag{5.101}$$

Proof Proceed as usual by choosing a Lyapunov candidate function

$$V\left(e, \tilde{A}, \tilde{B}, \tilde{\Theta}\right) = e^\top P e + \text{trace}\left(\tilde{A} \Gamma_A^{-1} \tilde{A}^\top\right) + \frac{\tilde{B}^\top \tilde{B}}{\gamma_b} + |b| \tilde{\Theta}^\top \Gamma_\Theta^{-1} \tilde{\Theta} \tag{5.102}$$

where $\Gamma_A = \Gamma_A^\top > 0 \in \mathbb{R}^2 \times \mathbb{R}^2$ is a positive-definite adaptation rate matrix for $\hat{A}(t)$.

Note that the matrix trace operator is used in the Lyapunov function to map a matrix product into a scalar quantity.

$\dot{V}\left(e, \tilde{A}, \tilde{B}, \tilde{\Theta}\right)$ is evaluated as

$$\dot{V}\left(e, \tilde{A}, \tilde{B}, \tilde{\Theta}\right) = -e^\top Q e + 2e^\top P\left[\tilde{A}x + \tilde{B}\bar{u} + B\tilde{\Theta}^\top \Phi(x)\right] + \text{trace}\left(2\tilde{A}\Gamma_A^{-1}\dot{\tilde{A}}^\top\right) + \frac{2\tilde{B}^\top \dot{\tilde{B}}}{\gamma_b} + 2|b|\,\tilde{\Theta}^\top \Gamma_\Theta^{-1}\dot{\tilde{\Theta}} \tag{5.103}$$

Now, consider the trace operator of a product of two vectors $C = \begin{bmatrix} c_1 & c_2 & \dots & c_n \end{bmatrix}^\top \in \mathbb{R}^n$ and $D = \begin{bmatrix} d_1 & d_2 & \dots & d_n \end{bmatrix}^\top \in \mathbb{R}^n$. Note that $C^\top D = D^\top C \in \mathbb{R}$ and $CD^\top \in \mathbb{R}^n \times \mathbb{R}^n$. Then, one of the identities of a trace operator is as follows:

$$\text{trace}\left(CD^\top\right) = C^\top D = D^\top C \tag{5.104}$$

This can be shown by evaluating both sides of the identity as

$$C^\top D = D^\top C = \sum_{i=1}^{n} c_i d_i \tag{5.105}$$

$$CD^\top = \left\{c_i d_j\right\},\ i, j = 1, 2, \dots, n \tag{5.106}$$

The trace operator is the sum of all the diagonal elements. Therefore,

$$\text{trace}\left(CD^\top\right) = \sum_{i=1}^{j} c_i d_i = C^\top D = D^\top C \tag{5.107}$$

Now, utilizing this trace identity, one can express

$$2\left(e^\top P\right)\left(\tilde{A}x\right) = \text{trace}\left(2\tilde{A}xe^\top P\right) \tag{5.108}$$

Also note that

$$2\left(e^\top P\right)\left(\tilde{B}\right) = 2\tilde{B}^\top Pe \tag{5.109}$$

and

$$2\left(e^\top PB\right)\left[\tilde{\Theta}^\top \Phi(x)\right] = 2\tilde{\Theta}^\top \Phi(x)\, e^\top PB = 2\tilde{\Theta}^\top \Phi(x)\, e^\top \bar{P}\,|b|\,\text{sgn}(b) \tag{5.110}$$

since the terms $e^\top PB$ and $e^\top P\tilde{B}$ are scalar quantities (verify!), where $\bar{P}$ is defined previously. Therefore,

$$\dot{V}\left(e,\tilde{A},\tilde{B},\tilde{\Theta}\right)=-e^{\top}Qe+\text{trace}\left[2\tilde{A}\left(xe^{\top}P+\Gamma_{A}^{-1}\dot{\tilde{A}}^{\top}\right)\right]\quad+2\tilde{B}^{\top}\left(Pe\bar{u}+\frac{\dot{\tilde{B}}}{\gamma_{b}}\right)$$
$$+2\left|b\right|\tilde{\Theta}^{\top}\left[\Phi\left(x\right)e^{\top}\bar{P}\text{sgn}b+\Gamma_{\Theta}^{-1}\dot{\tilde{\Theta}}\right] \tag{5.111}$$

The following adaptive laws are then obtained:

$$\dot{\hat{A}}^{\top}=-\Gamma_{A}xe^{\top}P \tag{5.112}$$

$$\dot{\hat{B}}=-\gamma_{b}Pe\bar{u} \tag{5.113}$$

$$\dot{\Theta}=-\Gamma_{\Theta}\Phi\left(x\right)e^{\top}\bar{P}\text{sgn}b \tag{5.114}$$

It follows that $e\left(t\right)$, $\tilde{A}\left(t\right)$, $\tilde{B}\left(t\right)$, and $\tilde{\Theta}\left(t\right)$ are bounded since

$$\dot{V}\left(e,\tilde{A},\tilde{B},\tilde{\Theta}\right)=-e^{\top}Qe\leq-\lambda_{min}\left(Q\right)\left\|e\right\|^{2} \tag{5.115}$$

$V\left(e,\tilde{A},\tilde{B},\tilde{\Theta}\right)$ has a finite limit as $t\rightarrow\infty$ since

$$V\left(t\rightarrow\infty\right)=V\left(t_{0}\right)-\int_{t_{0}}^{\infty}\lambda_{min}\left(Q\right)\left\|e\right\|^{2}dt<\infty \tag{5.116}$$

It can be shown that $\dot{V}\left(e,\tilde{A},\tilde{B},\tilde{\Theta}\right)$ is uniformly continuous because $\ddot{V}\left(e,\tilde{A},\tilde{B},\tilde{\Theta}\right)$ is bounded. Then, applying the Barbalat's lemma, one can conclude that the tracking error is asymptotically stable with $e\left(t\right)\rightarrow0$ as $t\rightarrow\infty$.

■

Let

$$\hat{\tilde{A}}=\left[\begin{array}{cc}0&1\end{array}\right]\hat{A}=\left[\begin{array}{cc}0&1\end{array}\right]\left[\begin{array}{cc}0&1\\-\hat{\omega}_{n}^{2}&-2\hat{\zeta}\hat{\omega}_{n}\end{array}\right]=\left[\begin{array}{cc}-\hat{\omega}_{n}^{2}&-2\hat{\zeta}\hat{\omega}_{n}\end{array}\right] \tag{5.117}$$

and since

$$\hat{b}=\left[\begin{array}{cc}0&1\end{array}\right]\hat{B}=\left[\begin{array}{cc}0&1\end{array}\right]\left[\begin{array}{c}0\\\hat{b}\end{array}\right] \tag{5.118}$$

then the adaptive laws can be expressed in terms of the estimates of the unknown quantities ω_{n} and ζ as

$$\dot{\hat{\tilde{A}}}^{\top}=-\Gamma_{A}xe^{\top}P\left[\begin{array}{c}0\\1\end{array}\right]=-\Gamma_{A}xe^{\top}\bar{P} \tag{5.119}$$

$$\dot{\hat{b}} = -\gamma_b \begin{bmatrix} 0 & 1 \end{bmatrix} P e \bar{u} = -\gamma_b \bar{P}^\top e \bar{u} = -\gamma_b \bar{u} e^\top \bar{P} \tag{5.120}$$

Let

$$\Gamma_A = \begin{bmatrix} \gamma_\omega & 0 \\ 0 & \gamma_\zeta \end{bmatrix} > 0 \tag{5.121}$$

Then,

$$\frac{d}{dt}\left(-\hat{\omega}_n^2\right) = -\gamma_\omega x_1 e^\top \bar{P} \tag{5.122}$$

or

$$\dot{\hat{\omega}}_n = \frac{\gamma_\omega x_1 e^\top \bar{P}}{2\hat{\omega}_n} \tag{5.123}$$

and

$$\frac{d}{dt}\left(-2\hat{\zeta}\hat{\omega}_n\right) = -2\hat{\omega}_n \dot{\hat{\zeta}} - 2\hat{\zeta}\dot{\hat{\omega}}_n = -\gamma_\zeta x_2 e^\top \bar{P} \tag{5.124}$$

or

$$\dot{\hat{\zeta}} = \frac{\left(\gamma_\zeta x_2 \hat{\omega}_n - \gamma_\omega x_1 \hat{\zeta}\right) e^\top \bar{P}}{2\hat{\omega}_n^2} \tag{5.125}$$

To prevent the possibility of $\hat{\omega}_n(t) = 0$ or $\hat{b}(t) = 0$ that will cause the adaptive laws to blow up, both the adaptive laws for estimating $\hat{\omega}_n(t)$ and $\hat{b}(t)$ need to be modified by the projection method according to

$$\dot{\hat{\omega}}_n = \begin{cases} \frac{\gamma_\omega x_1 e^\top \bar{P}}{2\hat{\omega}_n} & \text{if } \hat{\omega}_n > \omega_0 > 0 \text{ or if } \hat{\omega}_n = \omega_0 \text{ and } \dot{\hat{\omega}}_n \geq 0 \\ 0 & \text{otherwise} \end{cases} \tag{5.126}$$

$$\dot{\hat{b}} = \begin{cases} -\gamma_b \bar{u} e^\top \bar{P} & \text{if } \left|\hat{b}\right| > b_0 \text{ or if } \left|\hat{b}\right| = b_0 \text{ and } \frac{d\left|\hat{b}\right|}{dt} \geq 0 \\ 0 & \text{otherwise} \end{cases} \tag{5.127}$$

In the modified adaptive law for $\hat{\omega}_n(t)$, it is assumed that $\hat{\omega}_n(t)$ is always a positive quantity for a physically realizable system.

5.6 Direct MRAC for MIMO Systems

Consider a MIMO system with a matched uncertainty

$$\dot{x} = Ax + B\Lambda\left[u + f(x)\right] \tag{5.128}$$

where $x(t) \in \mathbb{R}^n$ is a state vector, $u(t) \in \mathbb{R}^m$ is a control vector, $A \in \mathbb{R}^n \times \mathbb{R}^n$ is a constant, known or unknown matrix, $B \in \mathbb{R}^n \times \mathbb{R}^m$ is a known matrix, $\Lambda = \Lambda^\top = \text{diag}(\lambda_1, \lambda_2, \ldots, \lambda_m) \in \mathbb{R}^m \times \mathbb{R}^m$ is a control input uncertainty and a diagonal matrix, and $f(x) \in \mathbb{R}^m$ is a matched uncertainty that can be linearly parametrized as

$$f(x) = \Theta^{*\top} \Phi(x) \tag{5.129}$$

where $\Theta^* \in \mathbb{R}^l \times \mathbb{R}^m$ is a constant, unknown matrix, and $\Phi(x) \in \mathbb{R}^l$ is a vector of known and bounded basis functions.

Furthermore, it is assumed that the pair $(A, B\Lambda)$ is controllable. Recall that the controllability condition ensures that the control input $u(t)$ has a sufficient access to the state space to stabilize all unstable modes of a plant. The controllability condition can be checked by the rank condition of the controllability matrix C, where

$$C = \left[B\Lambda \mid AB\Lambda \mid A^2 B\Lambda \mid \ldots \mid A^{n-1} B\Lambda \right] \tag{5.130}$$

The pair $(A, B\Lambda)$ is controllable if $\text{rank}(C) = n$.

The reference model is specified by

$$\dot{x}_m = A_m x_m + B_m r \tag{5.131}$$

where $x_m(t) \in \mathbb{R}^n$ is a reference state vector, $A_m \in \mathbb{R}^n \times \mathbb{R}^n$ is known and Hurwitz, $B_m \in \mathbb{R}^n \times \mathbb{R}^q$ is known, and $r(t) \in \mathbb{R}^q$ is a piecewise continuous and bounded command vector.

The objective is to design a full-state adaptive controller to allow $x(t)$ to follow $x_m(t)$.

5.6.1 Case I: A and Λ Unknown, but B and Sign of Λ Known

Firstly, it must be assumed that there exist ideal control gains K_x^* and K_r^* such that the following model matching conditions are satisfied:

$$A + B\Lambda K_x^* = A_m \tag{5.132}$$

$$B\Lambda K_r^* = B_m \tag{5.133}$$

If A_m and B_m have the same structures as those of A and $B\Lambda$, respectively, or if $B\Lambda$ is a square and invertible matrix, then there exist K_x^* and K_r^* that satisfy the model matching conditions.

Example 5.12 A MIMO system and a reference model are specified as

$$A = \begin{bmatrix} 1 & 1 \\ -1 & -1 \end{bmatrix}, \; B\Lambda = \begin{bmatrix} 1 & 1 \\ 0 & 1 \end{bmatrix}, \; A_m = \begin{bmatrix} 0 & 1 \\ -16 & -2 \end{bmatrix}, \; B_m = \begin{bmatrix} 2 & 0 \\ 0 & 1 \end{bmatrix}$$

Then,

$$K_x^* = (B\Lambda)^{-1}(A_m - A) = \begin{bmatrix} 14 & 1 \\ -15 & -1 \end{bmatrix}$$

$$K_r^* = (B\Lambda)^{-1} B_m = \begin{bmatrix} 2 & -1 \\ 0 & 1 \end{bmatrix}$$

■

Define an adaptive controller as

$$u = K_x(t)\,x + K_r(t)\,r - \Theta^\top \Phi(x) \tag{5.134}$$

where $K_x(t) \in \mathbb{R}^m \times \mathbb{R}^n$, $K_r(t) \in \mathbb{R}^m \times \mathbb{R}^q$, and $\Theta(t) \in \mathbb{R}^l \times \mathbb{R}^m$ are estimates of K_x^*, K_r^*, and Θ^*, respectively.

Let $\tilde{K}_x(t) = K_x(t) - K_x^*$, $\tilde{K}_r(t) = K_r(t) - K_r^*$, and $\tilde{\Theta}(t) = \Theta(t) - \Theta^*$ be the estimation errors. Then, the closed-loop plant model is expressed as

$$\dot{x} = \left(\underbrace{A + B\Lambda K_x^*}_{A_m} + B\Lambda \tilde{K}_x \right) x + \left(\underbrace{B\Lambda K_r^*}_{B_m} + B\Lambda \tilde{K}_r \right) r - B\Lambda \tilde{\Theta}^\top \Phi(x) \tag{5.135}$$

The closed-loop tracking error equation can now be formulated as

$$\dot{e} = \dot{x}_m - \dot{x} = A_m e - B\Lambda \tilde{K}_x x - B\Lambda \tilde{K}_r r + B\Lambda \tilde{\Theta}^\top \Phi(x) \tag{5.136}$$

Proof To derive the adaptive laws, choose the following Lyapunov candidate function:

$$V\left(e, \tilde{K}_x, \tilde{K}_r, \tilde{\Theta}\right) = e^\top P e + \text{trace}\left(|\Lambda|\,\tilde{K}_x \Gamma_x^{-1} \tilde{K}_x^\top\right) + \text{trace}\left(|\Lambda|\,\tilde{K}_r \Gamma_r^{-1} \tilde{K}_r^\top\right) + \text{trace}\left(|\Lambda|\,\tilde{\Theta}^\top \Gamma_\Theta^{-1} \tilde{\Theta}\right) \tag{5.137}$$

$\dot{V}\left(e, \tilde{K}_x, \tilde{K}_r, \tilde{\Theta}\right)$ is evaluated as

$$\begin{aligned} \dot{V}\left(e, \tilde{K}_x, \tilde{K}_r, \tilde{\Theta}\right) = {} & -e^\top Q e + 2e^\top P \left[-B\Lambda \tilde{K}_x x - B\Lambda \tilde{K}_r r + B\Lambda \tilde{\Theta}^\top \Phi(x) \right] \\ & + 2\text{trace}\left(|\Lambda|\,\tilde{K}_x \Gamma_x^{-1} \dot{\tilde{K}}_x^\top\right) \\ & + 2\text{trace}\left(|\Lambda|\,\tilde{K}_r \Gamma_r^{-1} \dot{\tilde{K}}_r^\top\right) + 2\text{trace}\left(|\Lambda|\,\tilde{\Theta}^\top \Gamma_\Theta^{-1} \dot{\tilde{\Theta}}\right) \end{aligned} \tag{5.138}$$

Utilizing the trace property $\text{trace}\left(CD^\top\right) = D^\top C$ and $\Lambda = \text{sgn}\Lambda\,|\Lambda|$ where $\text{sgn}\Lambda = \text{diag}(\text{sgn}\lambda_1, \text{sgn}\lambda_2, \ldots, \text{sgn}\lambda_m)$, then notice that

$$e^\top PB\Lambda\tilde{K}_x x = e^\top PB\text{sgn}\Lambda\,|\Lambda|\,\tilde{K}_x x = \text{trace}\left(|\Lambda|\,\tilde{K}_x x e^\top PB\text{sgn}\Lambda\right) \tag{5.139}$$

$$e^\top PB\Lambda\tilde{K}_r r = \text{trace}\left(|\Lambda|\,\tilde{K}_r r e^\top PB\text{sgn}\Lambda\right) \tag{5.140}$$

$$e^\top PB\Lambda\tilde{\Theta}^\top\Phi\,(x) = \text{trace}\left(|\Lambda|\,\tilde{\Theta}^\top\Phi\,(x)\,e^\top PB\text{sgn}\Lambda\right) \tag{5.141}$$

Then,

$$\begin{aligned}\dot{V}\left(e,\tilde{K}_x,\tilde{K}_r,\tilde{\Theta}\right) = -e^\top Qe &+ 2\text{trace}\left(|\Lambda|\,\tilde{K}_x\left[-xe^\top PB\text{sgn}\Lambda + \Gamma_x^{-1}\dot{\tilde{K}}_x^\top\right]\right)\\ &+ 2\text{trace}\left(|\Lambda|\,\tilde{K}_r\left[-re^\top PB\text{sgn}\Lambda + \Gamma_r^{-1}\dot{\tilde{K}}_r^\top\right]\right)\\ &+ 2\text{trace}\left(|\Lambda|\,\tilde{\Theta}^\top\left[\Phi\,(x)\,e^\top PB\text{sgn}\Lambda + \Gamma_\Theta^{-1}\dot{\tilde{\Theta}}\right]\right)\end{aligned} \tag{5.142}$$

Thus, the adaptive laws are obtained as

$$\dot{K}_x^\top = \Gamma_x xe^\top PB\text{sgn}\Lambda \tag{5.143}$$

$$\dot{K}_r^\top = \Gamma_r re^\top PB\text{sgn}\Lambda \tag{5.144}$$

$$\dot{\Theta} = -\Gamma_\Theta\Phi\,(x)\,e^\top PB\text{sgn}\Lambda \tag{5.145}$$

It follows that $e\,(t)$, $\tilde{K}_x\,(t)$, $\tilde{K}_r\,(t)$, and $\tilde{\Theta}\,(t)$ are bounded since

$$\dot{V}\left(e,\tilde{K}_x,\tilde{K}_r,\tilde{\Theta}\right) = -e^\top Qe \le -\lambda_{min}\,(Q)\,\|e\|^2 \le 0 \tag{5.146}$$

Using the usual argument with the Barbalat's lemma, the tracking error is asymptotically stable with $e\,(t) \to 0$ as $t \to \infty$.

Example 5.13 Let $x\,(t) = \left[x_1\,(t)\;x_2\,(t)\right]^\top$, $u\,(t) = \left[u_1\,(t)\;u_2\,(t)\right]^\top$, $\Phi\,(x) = \left[x_1^2\;x_2^2\right]^\top$, A is unknown, Λ is unknown but $\Lambda > 0$ so $s\text{gn}\Lambda = I$, and B is known and given by

$$B = \begin{bmatrix}1 & 1\\ 0 & 1\end{bmatrix}$$

A second-order reference model is specified by

$$\ddot{x}_{1m} + 2\zeta_m\omega_m\dot{x}_{1m} + \omega_m^2 x_{1m} = b_m r$$

where $\zeta_m = 0.5$, $\omega_m = 2$, $b_m = 4$, and $r\,(t) = \sin 2t$. For simulation purposes, the true A, Λ, and Θ^* matrices are

$$A = \begin{bmatrix} 1 & 1 \\ -1 & -1 \end{bmatrix},\ \Lambda = \begin{bmatrix} \frac{4}{5} & 0 \\ 0 & \frac{4}{5} \end{bmatrix}\ \Theta^* = \begin{bmatrix} 0.2 & 0 \\ 0 & -0.1 \end{bmatrix}$$

Since $B\Lambda$ is non-singular and invertible, K_x^* and K_r^* exist and are equal to

$$K_x^* = (B\Lambda)^{-1}(A_m - A) = \begin{bmatrix} \frac{4}{5} & \frac{4}{5} \\ 0 & \frac{4}{5} \end{bmatrix}^{-1} \left(\begin{bmatrix} 0 & 1 \\ -4 & -2 \end{bmatrix} - \begin{bmatrix} 1 & 1 \\ -1 & -1 \end{bmatrix} \right) = \begin{bmatrix} \frac{5}{2} & \frac{5}{4} \\ -\frac{15}{4} & -\frac{5}{4} \end{bmatrix}$$

$$K_r^* = (B\Lambda)^{-1} B_m = \begin{bmatrix} \frac{4}{5} & \frac{4}{5} \\ 0 & \frac{4}{5} \end{bmatrix}^{-1} \begin{bmatrix} 0 \\ 4 \end{bmatrix} = \begin{bmatrix} -5 \\ 5 \end{bmatrix}$$

Let $Q = I$, then the solution of the Lyapunov equation is

$$P = \begin{bmatrix} \frac{3}{2} & \frac{1}{8} \\ \frac{1}{8} & \frac{5}{16} \end{bmatrix}$$

Let $\Gamma_x = \text{diag}\left(\gamma_{x_1}, \gamma_{x_2}\right)$, $\Gamma_r = \gamma_r$, and $\Gamma_\Theta = \text{diag}\left(\gamma_{\theta_1}, \gamma_{\theta_2}\right)$. Then, the adaptive laws are

$$\begin{aligned} \dot{K}_x^\top &= \Gamma_x x e^\top P B \underbrace{\text{sgn}\Lambda}_{I} = \begin{bmatrix} \gamma_{x_1} & 0 \\ 0 & \gamma_{x_2} \end{bmatrix} \begin{bmatrix} x_1 \\ x_2 \end{bmatrix} \begin{bmatrix} e_1 & e_2 \end{bmatrix} \begin{bmatrix} \frac{3}{2} & \frac{13}{8} \\ \frac{1}{8} & \frac{7}{16} \end{bmatrix} \\ &= \begin{bmatrix} \gamma_{x_1} x_1 \left(\frac{3}{2} e_1 + \frac{1}{8} e_2\right) & \gamma_{x_1} x_1 \left(\frac{13}{8} e_1 + \frac{7}{16} e_2\right) \\ \gamma_{x_2} x_2 \left(\frac{3}{2} e_1 + \frac{1}{8} e_2\right) & \gamma_{x_2} x_2 \left(\frac{13}{8} e_1 + \frac{7}{16} e_2\right) \end{bmatrix} \end{aligned}$$

$$\dot{K}_r^\top = \Gamma_r r e^\top P B \text{sgn}\Lambda = \gamma_r r \begin{bmatrix} e_1 & e_2 \end{bmatrix} \begin{bmatrix} \frac{3}{2} & \frac{13}{8} \\ \frac{1}{8} & \frac{7}{16} \end{bmatrix} = \begin{bmatrix} \gamma_r r \left(\frac{3}{2} e_1 + \frac{1}{8} e_2\right) & \gamma_r r \left(\frac{13}{8} e_1 + \frac{7}{16} e_2\right) \end{bmatrix}$$

$$\begin{aligned} \dot{\Theta} &= -\Gamma_\Theta \Phi(x) e^\top P B \text{sgn}\Lambda = -\begin{bmatrix} \gamma_{\theta_1} & 0 \\ 0 & \gamma_{\theta_2} \end{bmatrix} \begin{bmatrix} x_1^2 \\ x_2^2 \end{bmatrix} \begin{bmatrix} e_1 & e_2 \end{bmatrix} \begin{bmatrix} \frac{3}{2} & \frac{13}{8} \\ \frac{1}{8} & \frac{7}{16} \end{bmatrix} \\ &= -\begin{bmatrix} \gamma_{\theta_1} x_1^2 \left(\frac{3}{2} e_1 + \frac{1}{8} e_2\right) & \gamma_{\theta_1} x_1^2 \left(\frac{13}{8} e_1 + \frac{7}{16} e_2\right) \\ \gamma_{\theta_2} x_2^2 \left(\frac{3}{2} e_1 + \frac{1}{8} e_2\right) & \gamma_{\theta_2} x_2^2 \left(\frac{13}{8} e_1 + \frac{7}{16} e_2\right) \end{bmatrix} \end{aligned}$$

For simulation, all adaptation rates are chosen to be 10 and all initial conditions are set to zero. The results are shown in Figs. 5.6, 5.7, 5.8, and 5.9.

It can be seen that the tracking error tends to zero so that $x(t)$ follows $x_m(t)$. Also note that $K_r(t)$ and some elements of $K_x(t)$ do not converge to their ideal values.

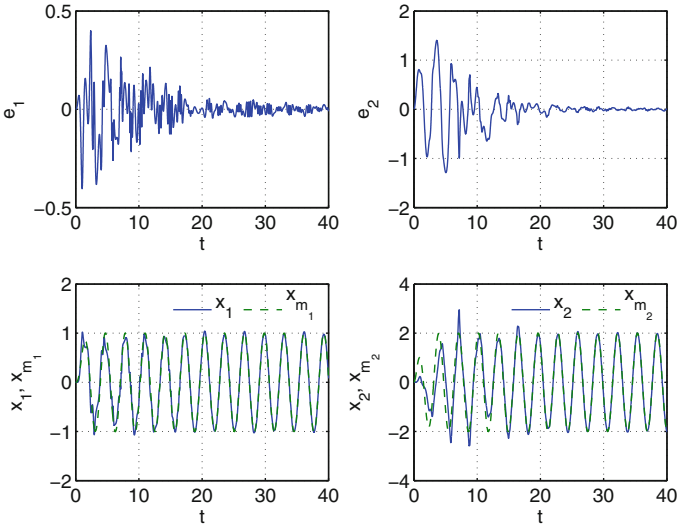

Fig. 5.6 Adaptive control system response

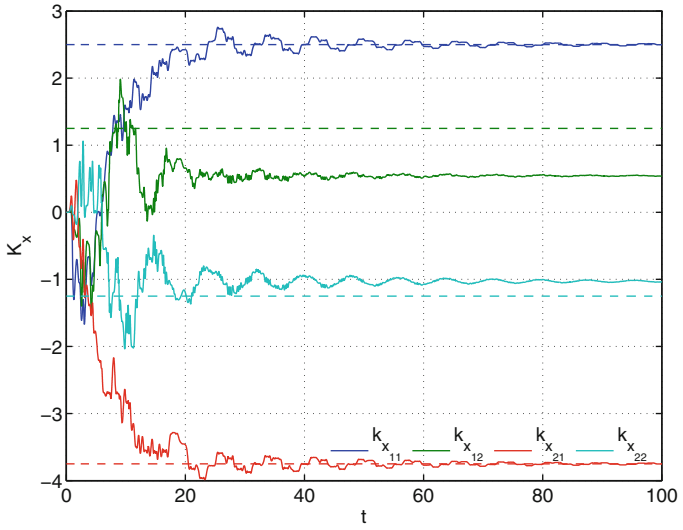

Fig. 5.7 Adaptive feedback gain K_x

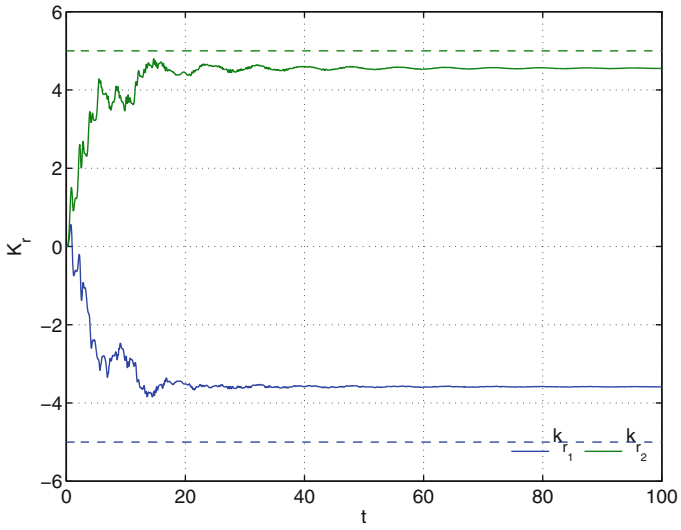

Fig. 5.8 Adaptive command gain K_r

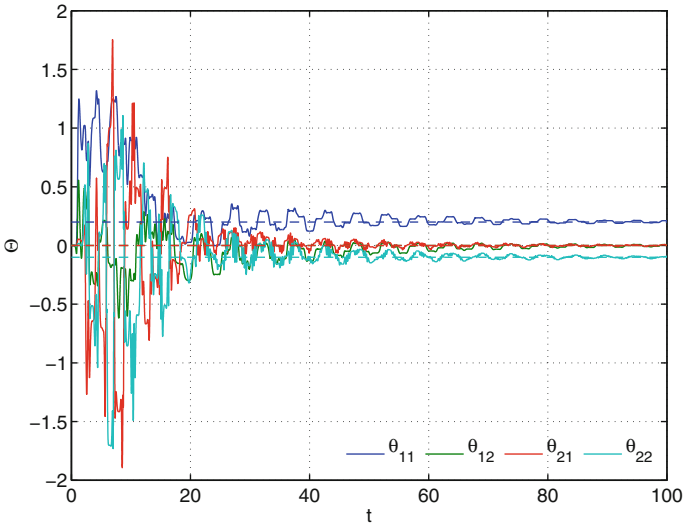

Fig. 5.9 Adaptive parameter Θ

5.6.2 Case II: A, B, $\Lambda = I$ Known

The plant model is given by

$$\dot{x} = Ax + B\left[u + \Theta^{*\top}\Phi(x)\right] \tag{5.147}$$

where both A and B are known.

Assuming that there exist K_x and K_r that satisfy the model matching conditions

$$A + BK_x = A_m \tag{5.148}$$

$$BK_r = B_m \tag{5.149}$$

then an adaptive controller is designed as

$$u = K_x x + K_r r - \Theta^{\top}(t)\Phi(x) \tag{5.150}$$

Let $\tilde{\Theta}(t) = \Theta(t) - \Theta^*$ be the estimation error, then the closed-loop plant model is

$$\dot{x} = \left(\underbrace{A + BK_x}_{A_m}\right)x + \underbrace{BK_r}_{B_m} r - B\tilde{\Theta}^{\top}\Phi(x) \tag{5.151}$$

The closed-loop tracking error equation is obtained as

$$\dot{e} = \dot{x}_m - \dot{x} = A_m e + B\tilde{\Theta}^{\top}\Phi(x) \tag{5.152}$$

Proof Choose a Lyapunov candidate function

$$V\left(e, \tilde{\Theta}\right) = e^{\top}Pe + \text{trace}\left(\tilde{\Theta}^{\top}\Gamma^{-1}\tilde{\Theta}\right) \tag{5.153}$$

Then,

$$\begin{aligned}\dot{V}\left(e, \tilde{\Theta}\right) &= -e^{\top}Qe + 2e^{\top}PB\tilde{\Theta}^{\top}\Phi(x) + 2\text{trace}\left(\tilde{\Theta}^{\top}\Gamma\dot{\tilde{\Theta}}\right) \\ &= -e^{\top}Qe + 2\text{trace}\left(\tilde{\Theta}^{\top}\left[\Phi(x)e^{\top}PB + \Gamma\dot{\tilde{\Theta}}\right]\right)\end{aligned} \tag{5.154}$$

The adaptive law is

$$\dot{\Theta} = -\Gamma\Phi(x)e^{\top}PB \tag{5.155}$$

Using the Barbalat's lemma, the tracking error can be shown to be asymptotically stable with $e(t) \to 0$ as $t \to \infty$.

5.7 Indirect MRAC for MIMO Systems

For the system in Sect. 5.6.1 with A and Λ unknown but B and sign of Λ known, assuming that $B\Lambda \in \mathbb{R}^n \times \mathbb{R}^m$ is invertible and $n \leq m$, then there exist K_x^* and K_r^* that satisfy the model matching conditions such that

$$K_x^* = (B\Lambda)^{-1}(A_m - A) \tag{5.156}$$

$$K_r^* = (B\Lambda)^{-1} B_m \tag{5.157}$$

If $\hat{A}(t)$ and $\hat{\Lambda}(t)$ are estimates of A and Λ, then the estimates of K_x^* and K_r^* are given by

$$K_x(t) = \left[B\hat{\Lambda}(t)\right]^{-1}\left[A_m - \hat{A}(t)\right] \tag{5.158}$$

$$K_r(t) = \left[B\hat{\Lambda}(t)\right]^{-1} B_m \tag{5.159}$$

Note that if $n < m$, then $\left[B\hat{\Lambda}(t)\right]^{-1}$ is defined by the right pseudo-inverse $\hat{\Lambda}^\top(t) B^\top \left[B\hat{\Lambda}(t)\hat{\Lambda}^\top(t) B^\top\right]^{-1}$.

Let the adaptive controller be

$$u = K_x(t)\, x + K_r(t)\, r - \Theta^\top(t)\, \Phi(x) \tag{5.160}$$

Let $\tilde{A}(t) = \hat{A}(t) - A$ and $\tilde{\Lambda}(t) = \hat{\Lambda}(t) - \Lambda$ be the estimation errors. Then, the closed-loop plant model is expressed as

$$\begin{aligned}\dot{x} &= Ax + B\left(\hat{\Lambda} - \tilde{\Lambda}\right)\left[K_x x + K_r r - \tilde{\Theta}^\top \Phi(x)\right] \\ &= \left(A + A_m - \hat{A}\right)x + B_m r - B\tilde{\Lambda}\left(K_x x + K_r r\right) - B\Lambda\tilde{\Theta}^\top\Phi(x)\end{aligned} \tag{5.161}$$

Let

$$\bar{u} = K_x x + K_r r \tag{5.162}$$

Then, the tracking error equation is obtained as

$$\dot{e} = \dot{x}_m - \dot{x} = A_m e + \tilde{A}x + B\tilde{\Lambda}\bar{u} + B\Lambda\tilde{\Theta}^\top\Phi(x) \tag{5.163}$$

Proof Choose a Lyapunov candidate function

$$V\left(e, \tilde{A}, \tilde{B}, \tilde{\Theta}\right) = e^\top P e + \text{trace}\left(\tilde{A}\Gamma_A^{-1}\tilde{A}^\top\right) + \text{trace}\left(\tilde{A}\Gamma_\Lambda^{-1}\tilde{A}^\top\right) + \text{trace}\left(|\Lambda|\,\tilde{\Theta}^\top\Gamma_\Theta^{-1}\tilde{\Theta}\right) \tag{5.164}$$

Then,

$$\dot{V}\left(e,\tilde{A},\tilde{B},\tilde{\Theta}\right)=-e^{\top}Qe+2e^{\top}P\left[\tilde{A}x+B\tilde{\Lambda}\bar{u}+B\Lambda\tilde{\Theta}^{\top}\Phi\left(x\right)\right]$$
$$+2\text{trace}\left(\tilde{A}\Gamma_{A}^{-1}\dot{\tilde{A}}^{\top}\right)+2\text{trace}\left(\tilde{\Lambda}\Gamma_{\Lambda}^{-1}\dot{\tilde{\Lambda}}^{\top}\right)+2\text{trace}\left(\left|\Lambda\right|\tilde{\Theta}^{\top}\Gamma_{\Theta}^{-1}\dot{\tilde{\Theta}}\right)\quad(5.165)$$

Utilizing the following relationships:

$$e^{\top}P\tilde{A}x=\text{trace}\left(\tilde{A}xe^{\top}P\right)\quad(5.166)$$

$$e^{\top}PB\tilde{\Lambda}\bar{u}=\text{trace}\left(\tilde{\Lambda}\bar{u}e^{\top}PB\right)\quad(5.167)$$

$$e^{\top}PB\Lambda\tilde{\Theta}^{\top}\Phi\left(x\right)=e^{\top}PB\text{sgn}\left(\Lambda\right)\left|\Lambda\right|\tilde{\Theta}^{\top}\Phi\left(x\right)=\text{trace}\left(\left|\Lambda\right|\tilde{\Theta}^{\top}\Phi\left(x\right)e^{\top}PB\text{sgn}\left(\Lambda\right)\right)\quad(5.168)$$

we obtain

$$\dot{V}\left(e,\tilde{A},\tilde{B},\tilde{\Theta}\right)=-e^{\top}Qe+2\text{trace}\left(\tilde{A}\left[xe^{\top}P+\Gamma_{A}^{-1}\dot{\tilde{A}}^{\top}\right]\right)$$
$$+2\text{trace}\left(\tilde{\Lambda}\left[\bar{u}e^{\top}PB+\Gamma_{\Lambda}^{-1}\dot{\tilde{\Lambda}}^{\top}\right]\right)$$
$$+2\text{trace}\left(\left|\Lambda\right|\tilde{\Theta}^{\top}\left[\Phi\left(x\right)e^{\top}PB\text{sgn}\left(\Lambda\right)+\Gamma_{\Theta}^{-1}\dot{\tilde{\Theta}}\right]\right)\quad(5.169)$$

from which the adaptive laws are obtained as

$$\dot{\tilde{A}}^{\top}=-\Gamma_{A}xe^{\top}P\quad(5.170)$$

$$\dot{\tilde{\Lambda}}^{\top}=-\Gamma_{\Lambda}\bar{u}e^{\top}PB\quad(5.171)$$

$$\dot{\tilde{\Theta}}=-\Gamma_{\Theta}\Phi\left(x\right)e^{\top}PB\text{sgn}\Lambda\quad(5.172)$$

Since $\dot{V}\left(e,\tilde{A},\tilde{B},\tilde{\Theta}\right)\leq-\lambda_{min}\left(Q\right)\left\|e\right\|^{2}\leq0$ and $\ddot{V}\left(e,\tilde{A},\tilde{B},\tilde{\Theta}\right)\in\mathscr{L}_{\infty}$, then $\dot{V}\left(e,\tilde{A},\tilde{B},\tilde{\Theta}\right)$ is uniformly continuous. In addition, $V\left(t\rightarrow\infty\right)\leq V\left(t_{0}\right)$. Therefore, according to the Barbalat's lemma, the tracking error is asymptotically stable with $e\left(t\right)\rightarrow0$ as $t\rightarrow\infty$.

■

Because $\hat{\Lambda}\left(t\right)$ is involved in a matrix inversion operation, $\hat{\Lambda}\left(t\right)$ cannot be singular assuming B is non-singular. Therefore, the adaptive law for $\hat{\Lambda}\left(t\right)$ needs to be modified by the projection method if a priori knowledge of the bounds on the elements of Λ is available. Suppose the diagonal elements are bounded by $\lambda_{i_0}\leq\left|\hat{\lambda}_{ii}\right|\leq1$, and the non-diagonal elements are bounded to be close to zero such that $\left|\hat{\lambda}_{ij}\right|\leq\epsilon,\ i\neq j$. Then, the modified adaptive law for the diagonal elements can be expressed as

$$\dot{\hat{\lambda}}_{ii} = \begin{cases} -\left(\Gamma_\Lambda \bar{u} e^\top P B\right)_{ii} & \text{if } 1 \geq \left|\hat{\lambda}_{ii}\right| \geq \lambda_{i_0}, \text{ or if } \left|\hat{\lambda}_{ii}\right| = \lambda_{i_0} \text{ and } \frac{d\left|\hat{\lambda}_{ii}\right|}{dt} \geq 0, \text{ or if } \left|\hat{\lambda}_{ii}\right| = 1 \text{ and } \frac{d\left|\hat{\lambda}_{ii}\right|}{dt} \leq 0 \\ 0 & \text{otherwise} \end{cases} \tag{5.173}$$

and the modified adaptive law for the non-diagonal elements can be expressed as

$$\dot{\hat{\lambda}}_{ij} = \begin{cases} -\left(\Gamma_\Lambda \bar{u} e^\top P B\right)_{ji} & \text{if } \left|\hat{\lambda}_{ij}\right| \leq \epsilon, \text{ or if } \left|\hat{\lambda}_{ij}\right| = \epsilon \text{ and } \frac{d\left|\hat{\lambda}_{ij}\right|}{dt} \leq 0 \\ 0 & \text{otherwise} \end{cases} \tag{5.174}$$

5.8 Summary

In situations when the system uncertainty may become significant beyond a level of desired tolerance that can adversely affect the performance of a controller, adaptive control can play an important role in reducing the effects of the system uncertainty on the controller performance. Situations that may warrant the use of adaptive control could include unintended consequences of off-nominal modes of operation such as system failures or highly uncertain operating conditions, and complex system behaviors that can result in an increase in the complexity and hence cost of the modeling efforts.

There are generally two classes of adaptive control: (1) direct adaptive control and (2) indirect adaptive control. Adaptive control architectures that combine both types of adaptive control are also frequently used and are referred to as composite, combined, or hybrid direct–indirect adaptive control. Adaptive control can deal with either linear or nonlinear plants with various types of uncertainty which can be structured uncertainty, unstructured uncertainty, or unmodeled dynamics. Matched uncertainty is a type of structured uncertainty that can be matched by the control input for a class of MIMO linear affine-in-control systems. Adaptive control systems can be designed to provide cancellation of a matched uncertainty. When an uncertainty cannot be matched, it is called an unmatched uncertainty. Adaptive control systems can be designed to accommodate unmatched uncertainty, but cannot cancel the unmatched uncertainty in general. Control input uncertainty is a type of uncertainty that exists in the control input matrix for a class of MIMO linear affine-in-control systems. Control input uncertainty can be in the amplitude or in the sign or both. When the control input uncertainty is in the amplitude, a control saturation can occur and may worsen the performance of a controller. When the input uncertainty is in the sign, a control reversal can occur and potentially can cause instability. Control input uncertainty in general presents more challenges to adaptive control designers.

A reference model is used to specify a desired response of an adaptive control system to a command input. It is essentially a command shaping filter to achieve a desired command following. Since adaptive control is formulated as a command following or tracking control, the adaptation is operated on the tracking error between the reference model and the system output. A reference model must be designed properly for an adaptive control system to be able to follow.

Various direct and indirect model-reference adaptive control techniques for first-order and second-order SISO systems and MIMO systems are presented. MRAC can be shown to achieve asymptotic tracking, but it does not guarantee that adaptive parameters converge to their true values. The Lyapunov stability theory shows that adaptive parameter estimation errors are only bounded but not asymptotic.

5.9 Exercises

1. Consider a first-order nonlinear SISO system with a matched uncertainty

$$\dot{x} = ax + b\left[u + \theta^* \phi(x)\right]$$

where a is unknown, but b is known, θ^* is unknown, and $\phi(x) = x^2$.
A reference model is specified by

$$\dot{x}_m = a_m x_m + b_m r$$

where $a_m < 0$ and b_m are known, and $r(t)$ is a bounded command signal.

   a. Design and implement in Simulink a direct adaptive controller that enables the plant output $x(t)$ to track the reference model signal $x_m(t)$, given $b = 2$, $a_m = -1$, $b_m = 1$, and $r(t) = \sin t$. For adaptation rates, use $\gamma_x = 1$ and $\gamma = 1$. For simulation purposes, assume $a = 1$ and $\theta^* = 0.2$ for the unknown parameters. Plot $e(t)$, $x(t)$, $x_m(t)$, $u(t)$, and $\theta(t)$ for $t \in [0, 50]$.
   b. Show by the Lyapunov stability analysis that the tracking error is asymptotically stable, i.e., $e(t) \to 0$ as $t \to \infty$.
   c. Repeat part (a) for $r(t) = 1(t)$ where $1(t)$ is the unit step function. Plot the same sets of data as in part (a). Comment on the convergence of $k_x(t)$ and $\theta(t)$ to the ideal values k_x^* and θ^*.

2. Consider the following first-order plant

$$\dot{x} = ax + b\left[u + \theta^* \phi(x)\right]$$

where a , $b > 0$, θ^* is unknown, and $\phi(x) = x^2$. Design an indirect adaptive controller in Simulink by estimating a, b, and θ^* so that the plant follows a reference model

$$\dot{x}_m = a_m x_m + b_m r$$

where $a_m = -1$, $b_m = 1$, and $r(t) = \sin t$. For simulation purposes, use $a = 1$, $b = 1$, $\theta^* = 0.1$, $x(0) = x_m(0) = 1$, $\hat{a}(0) = 0$, $\hat{b}(0) = 1.5$, $\gamma_a = \gamma_b = \gamma_\theta = 1$. Also assume that a lower bound of b is $b_0 = 0.5$. Plot the time histories of $e(t)$, $x(t)$ vs. $x_m(t)$, $\hat{a}(t)$, $\hat{b}(t)$, and $\hat{\theta}(t)$ for $t \in [0, 50]$

3. Derive direct MRAC laws for a second-order SISO system

$$\ddot{y} + 2\zeta\omega_n\dot{y} + \omega_n^2 y = b\left[u + \Theta^{*\top}\Phi\left(y\right)\right]$$

where ζ and ω_n are unknown, but b is known. Show by applying the Barbalat's lemma that the tracking error is asymptotically stable.
Design a direct adaptive controller for a second-order system using the following information: $b = 1$, $\zeta_m = 0.5$, $\omega_m = 2$, $b_m = 4$, $r\left(t\right) = \sin 2t$, and

$$\Phi\left(y\right) = \begin{bmatrix} 1 \\ y^2 \end{bmatrix}$$

For simulation purposes, the unknown parameters may be assumed to be $\zeta = -0.5$, $\omega_n = 1$, and $\Theta^{*\top} = \begin{bmatrix} 0.5 & -0.1 \end{bmatrix}$, and all initial conditions are assumed to be zero. Use $\Gamma_x = \Gamma_\Theta = 100I$. Plot the time histories of $e\left(t\right)$, $x\left(t\right)$ vs. $x_m\left(t\right)$, $K_x\left(t\right)$, and $\Theta\left(t\right)$ for $t \in [0, 100]$.

4. For Exercise 3, suppose b is unknown, but $b > 0$ is known. Design an indirect adaptive controller in Simulink. For simulation purposes, all initial conditions are assumed to be zero, except for $\hat{\omega}_n(0) = 0.8$ and $\hat{b}\left(0\right) = 0.6$. For simplicity, use the unmodified adaptive laws for $\hat{\omega}_n\left(t\right)$ and $\hat{b}\left(t\right)$. Use $\gamma_\omega = \gamma_\zeta = \gamma_b = 10$ and $\Gamma_\Theta = 10I$. Plot the time histories of $e\left(t\right)$, $x\left(t\right)$ vs. $x_m\left(t\right)$, $\hat{\omega}_n\left(t\right)$, $\hat{\zeta}\left(t\right)$, $\hat{b}\left(t\right)$, and $\Theta\left(t\right)$ for $t \in [0, 100]$.

5. Thus far, we have considered adaptive control with a matched uncertainty as a function of x. In physical systems, an external disturbance is generally a function of t. Adaptive control can be used for disturbance rejection if the disturbance structure is known. Suppose the matched uncertainty is a function of t, then all the adaptive laws can still be used by just replacing $\Phi\left(x\right)$ by $\Phi\left(t\right)$, assuming $\Phi\left(t\right)$ is known and bounded.
Consider the following first-order plant:

$$\dot{x} = ax + b\left[u + \theta^*\phi\left(t\right)\right]$$

where a , b, and θ^* are unknown, but $b > 0$ is known, and $\phi\left(t\right) = \sin 2t - \cos 4t$. Design an indirect adaptive controller in Simulink by estimating a, b, and θ^* so that the plant follows a reference model

$$\dot{x}_m = a_m x_m + b_m r$$

where $a_m = -1$, $b_m = 1$, and $r\left(t\right) = \sin t$. For simulation purposes, use $a = 1$, $b = 1$, $\theta^* = 0.1$, $x\left(0\right) = x_m\left(0\right) = 1$, $\hat{a}\left(0\right) = 0$, $\hat{b}\left(0\right) = 1.5$, $\gamma_a = \gamma_b = \gamma_\theta = 1$. Also assume that a lower bound of b is $b_0 = 0.5$. Plot the time histories of $e\left(t\right)$, $x\left(t\right)$ vs. $x_m\left(t\right)$, $\hat{a}\left(t\right)$, $\hat{b}\left(t\right)$, and $\hat{\theta}\left(t\right)$ for $t \in [0, 50]$.

6. Derive direct MRAC laws for a MIMO system

$$\dot{x} = Ax + B\left[u + \Theta^{*\top}\Phi(x)\right]$$

where A is unknown, but B is known. Show by applying the Barbalat's lemma that the tracking error is asymptotically stable.
Given $x(t) = \left[x_1(t)\ x_2(t)\right]^\top$, $u(t) = \left[u_1(t)\ u_2(t)\right]^\top$, $\Phi(x) = \left[x_1^2\ x_2^2\right]^\top$, and

$$B = \begin{bmatrix} 1 & 1 \\ 0 & 1 \end{bmatrix}$$

design a direct adaptive controller in Simulink for the MIMO system to follow a second-order SISO system specified by

$$\dot{x}_m = A_m x + B_m r$$

where $r(t) = \sin 2t$ and

$$A_m = \begin{bmatrix} 0 & 1 \\ -4 & -2 \end{bmatrix},\ B_m = \begin{bmatrix} 0 \\ 4 \end{bmatrix}$$

For simulation purposes, the unknown parameters may be assumed to be

$$A = \begin{bmatrix} 1 & 1 \\ -1 & -1 \end{bmatrix},\ \Theta^* = \begin{bmatrix} 0.2 & 0 \\ 0 & -0.1 \end{bmatrix}$$

and all initial conditions are assumed to be zero. Use $\Gamma_x = \Gamma_\Theta = 10I$. Plot the time histories of $e(t)$, $x(t)$ vs. $x_m(t)$, $K_x(t)$, and $\Theta(t)$ for $t \in [0, 100]$.

References

1. Åström, K. J., & Wittenmark, B. (2008). *Adaptive control*. New York: Dover Publications Inc.
2. Ioannu, P. A., & Sun, J. (1996). *Robust adaptive control*. Upper Saddle River: Prentice-Hall Inc.
3. Lavretsky, E. (2009). Combined/composite model reference adaptive control. *IEEE Transactions on Automatic Control*, *54*(11), 2692–2697.
4. Ishihara, A., Al-Ali, K., Kulkarni, N., & Nguyen, N. (2009). Modeling Error Driven Robot Control, AIAA Infotech@Aerospace Conference, AIAA-2009-1974.

Chapter 6
Least-Squares Parameter Identification

Abstract This chapter presents the fundamental theory of least-squares parameter identification. Least-squares methods are central to function approximation theory and data regression analysis. Least-squares methods can also be used in adaptive control as indirect adaptive control methods to estimate unknown system parameters to provide the information for adjusting the control gains. The batch least-squares method is often used for data regression analysis. Least-squares gradient and recursive least-squares methods are well-suited for on-line time series analysis and adaptive control. The concept of persistent excitation is introduced as a fundamental requirement for exponential parameter convergence of least-squares methods. Indirect least-squares adaptive control theory is introduced. The adaptation signal is based on the plant modeling error in contrast to the tracking error for model-reference adaptive control. An important notion to recognize is that the plant modeling error is the source of the tracking error and not vice versa. The combined least-squares model-reference adaptive control uses both the plant modeling error and tracking error for adaptation. As a result, the adaptation mechanism is highly effective. Both the least-squares gradient and recursive least-squares methods can also be used separately in adaptive control without combining with model-reference adaptive control. A fundamental difference with the least-squares adaptive control methods from model-reference adaptive control is that a parameter convergence to true system parameters is guaranteed in the presence of a persistently exciting input signal.

Indirect model-reference adaptive control is one technique for identifying uncertain parameters of a dynamical system. A more common method for parameter identification is the well-known least-squares method [1–3]. The least-squares approach to function approximation and parameter identification is derived from the minimization of the approximation error between a process and a model of the process. Parameter convergence is usually obtained if the so-called persistent excitation condition is met. The well-known recursive least-squares method is fundamental to many system identification techniques.

N.T. Nguyen, *Model-Reference Adaptive Control*, Advanced Textbooks
in Control and Signal Processing, https://doi.org/10.1007/978-3-319-56393-0_6

Least-squares methods can be used in adaptive control whereby the plant's unknown parameters are estimated by least-squares methods to provide the information to adjust the control gains. Many least-squares adaptive control methods can be found in the literature [4–8]. Artificial neural network-based adaptive control using least-squares methods is also common in the literature [7, 9]. Chebyshev orthogonal polynomials have been used as basis functions for least-squares adaptive control [10]. Hybrid adaptive control is a method that combines a direct model-reference adaptive control to reduce the tracking error with an indirect recursive least-squares parameter estimation to reduce the plant modeling error simultaneously [11]. Concurrent learning adaptive control is a least-squares modification to adaptive control problems whereby the uncertainty can be linearly parameterized, and the modified weight training law uses an estimate of the ideal weights formed on-line by solving a least-squares problem using recorded and current data concurrently [5].

In this chapter, the learning objectives are:

- To develop an understanding of least-squares parameter estimation and the notion of persistent excitation for parameter convergence;
- To be able to apply least-squares methods for parameter estimation; and
- To recognize and be able to use least-squares methods as indirect adaptive control techniques.

6.1 Least-Squares Regression

Suppose the input–output transfer function of a system is given by a set of measurement data $y(t) \in \mathbb{R}^n$ as a function of some independent variable $x(t) \in \mathbb{R}^p$, expressed as data pairs (x_i, y_i), $i = 1, 2, \ldots, N$. Furthermore, suppose the transfer function between $x(t)$ and $y(t)$ can be linearly parameterized as

$$y = \Theta^{*\top} \Phi(x) \tag{6.1}$$

where $\Theta^* \in \mathbb{R}^m \times \mathbb{R}^n$ is a matrix of constant but unknown coefficients and $\Phi(x) \in \mathbb{R}^m$ is a bounded regressor (or basis function) vector and is assumed to be known.

Let $\hat{y}$ be an estimate of y such that

$$\hat{y} = \Theta^{\top} \Phi(x) \tag{6.2}$$

where Θ is the estimate of Θ^*.

Formulate an approximation error ϵ as

$$\epsilon = \hat{y} - y = \Theta^{\top} \Phi(x) - y \tag{6.3}$$

Consider the following cost function:

$$J(\Theta) = \frac{1}{2}\sum_{i=1}^{N} \epsilon_i^\top \epsilon_i \tag{6.4}$$

When $J(\Theta)$ is minimized, the approximation error is also minimized. Then, $\hat{y}$ approximates y in a least-squares sense. Thus, the parameter identification problem is posed as a minimization problem.

The necessary condition is given by

$$\frac{\partial J^\top}{\partial \Theta^\top} = \nabla J_\Theta(\Theta) = \sum_{i=1}^{N} \frac{\partial \epsilon_i}{\partial \Theta^\top} \epsilon_i^\top = \sum_{i=1}^{N} \Phi(x_i)\left[\Phi^\top(x_i)\Theta - y_i^\top\right] = 0 \tag{6.5}$$

where $\nabla J_\Theta(\Theta)$ is called the gradient of $J(\Theta)$ with respect to Θ.

Thus, Θ can be found by solving the following least-squares regression equation:

$$\Theta = A^{-1}B \tag{6.6}$$

where

$$A = \sum_{i=1}^{N} \Phi(x_i)\Phi^\top(x_i) \tag{6.7}$$

$$B = \sum_{i=1}^{N} \Phi(x_i) y_i^\top \tag{6.8}$$

and A is a non-singular matrix if there are sufficient unique data.

Example 6.1 Suppose $y(t) \in \mathbb{R}$ is a scalar variable which can be approximated as a p-th degree polynomial in terms of $x(t) \in \mathbb{R}$ as

$$y = \theta_0 + \theta_1 x + \cdots + \theta_p x^p = \sum_{j=0}^{p} \theta_j x^j = \Theta^\top \Phi(x)$$

where $\Theta^\top = \left[\theta_0\ \theta_1\ \ldots\ \theta_p\right]$ and $\Phi(x) = \left[1\ x\ \ldots\ x^p\right]^\top$.

The least-squares regression equation is expressed as

$$A\Theta = B$$

where

$$A = \sum_{i=1}^{N} \Phi(x_i)\,\Phi^{\top}(x_i) = \sum_{i=1}^{N} \begin{bmatrix} 1 \\ x_i \\ \vdots \\ x_i^p \end{bmatrix} \begin{bmatrix} 1 & x_i & \cdots & x_i^p \end{bmatrix}$$

$$= \begin{bmatrix} \sum_{i=1}^{N} 1 & \sum_{i=1}^{N} x_i & \cdots & \sum_{i=1}^{N} x_i^p \\ \sum_{i=1}^{N} x_i & \sum_{i=1}^{N} x_i^2 & \cdots & \sum_{i=1}^{N} x_i^{p+1} \\ \vdots & \vdots & \ddots & \vdots \\ \sum_{i=1}^{N} x_i^p & \sum_{i=1}^{N} x_i^{p+1} & \cdots & \sum_{i=1}^{N} x_i^{2p} \end{bmatrix} = \left\{ \sum_{i=1}^{N} x_i^{j+k} \right\}_{jk}$$

$$B = \sum_{i=1}^{N} \Phi(x_i)\, y_i^{\top} = \sum_{i=1}^{N} \begin{bmatrix} 1 \\ x_i \\ \vdots \\ x_i^p \end{bmatrix} y_i = \begin{bmatrix} \sum_{i=1}^{N} y_i \\ \sum_{i=1}^{N} x_i y_i \\ \vdots \\ \sum_{i=1}^{N} x_i^p y_i \end{bmatrix} = \left\{ \sum_{i=1}^{N} x_i^j y_i \right\}_j$$

This least-squares regression method is in fact a polynomial curve-fitting technique. For example, let $p = 2$, then the quadratic curve-fitting coefficients can be found by

$$\Theta = A^{-1} B$$

where

$$A = \begin{bmatrix} N & \sum_{i=1}^{N} x_i & \sum_{i=1}^{N} x_i^2 \\ \sum_{i=1}^{N} x_i & \sum_{i=1}^{N} x_i^2 & \sum_{i=1}^{N} x_i^3 \\ \sum_{i=1}^{N} x_i^2 & \sum_{i=1}^{N} x_i^3 & \sum_{i=1}^{N} x_i^4 \end{bmatrix}, \quad B = \begin{bmatrix} \sum_{i=1}^{N} y_i \\ \sum_{i=1}^{N} x_i y_i \\ \sum_{i=1}^{N} x_i^2 y_i \end{bmatrix}$$

When all available data are used in the least-squares regression method, it is sometimes called a batch least-squares method. This is usually when there are sufficient data over a given time interval and the estimates of the unknown coefficients are not needed immediately at each time step.

6.2 Convex Optimization and Least-Squares Gradient Method

When the estimates of the unknown coefficients are needed at each time step, Θ can be estimated recursively using each pair of data (x_i, y_i) at each time step.

Consider the following cost function:

$$J(\Theta) = \frac{1}{2} \epsilon^{\top} \epsilon \tag{6.9}$$

The gradient of the cost function with respect to Θ is given by

$$\frac{\partial J^{\top}}{\partial \Theta^{\top}} = \nabla J_{\Theta}(\Theta) = \left(\frac{\partial \epsilon}{\partial \Theta^{\top}}\right)\epsilon^{\top} = \Phi(x)\,\epsilon^{\top} \tag{6.10}$$

To determine a least-squares estimation based on a given data pair at each time step, the concept of convex optimization is now introduced.

Definition 6.1 A subset $\mathscr{S}$ is said to be convex if there exist x, y in $\mathscr{S}$ and a constant $\alpha \in [0, 1]$ such that $\alpha x + (1-\alpha)\, y$ is also in $\mathscr{S}$. A function $f(x)$ is said to be convex in a convex set $\mathscr{S}$ if, for every x, y in $\mathscr{S}$, then

$$f(\alpha x + (1-\alpha)\, y) \leq \alpha f(x) + (1-\alpha)\, f(y) \tag{6.11}$$

■

Note that $J(\Theta)$ is convex since

$$\begin{aligned}
&\frac{1}{2}\left[\alpha\epsilon + (1-\alpha)\,\epsilon_1\right]^{\top}\left[\alpha\epsilon + (1-\alpha)\,\epsilon_1\right] \\
&\quad = \frac{1}{2}\alpha^2\epsilon^{\top}\epsilon + \alpha(1-\alpha)\,\epsilon^{\top}\epsilon_1 + \frac{1}{2}(1-\alpha)^2\,\epsilon_1^{\top}\epsilon_1 \\
&\quad = \frac{1}{2}\alpha^2\left(\epsilon^{\top}\epsilon - 2\epsilon^{\top}\epsilon_1\right) + \alpha\epsilon^{\top}\epsilon_1 + \frac{1}{2}(1-\alpha)^2\,\epsilon_1^{\top}\epsilon_1
\end{aligned} \tag{6.12}$$

But, $\alpha^2 \leq \alpha$ and $(1-\alpha)^2 \leq 1-\alpha$ for all $\alpha \in [0, 1]$. So,

$$\frac{1}{2}\alpha\left(\epsilon^{\top}\epsilon - 2\epsilon^{\top}\epsilon_1\right) + \alpha\epsilon^{\top}\epsilon_1 + \frac{1}{2}(1-\alpha)\,\epsilon_1^{\top}\epsilon_1 \leq \alpha\frac{1}{2}\epsilon^{\top}\epsilon + (1-\alpha)\,\frac{1}{2}\epsilon_1^{\top}\epsilon_1 \tag{6.13}$$

If $f(x) \in \mathscr{C}^1$, i.e., $f(x)$ is differentiable at least once, then

$$f(y) \geq f(x) + (\nabla f(x))^{\top}(y - x) \tag{6.14}$$

If $f(x) \in \mathscr{C}^2$, then $f(x)$ is convex if $\nabla^2 f(x) \geq 0$ where $\nabla^2 f(x)$ is called the Hessian of $f(x)$.

Now, consider the minimization of $J(\Theta)$. Θ^* is said to be a global minimum of $J(\Theta)$ if

$$J\left(\Theta^*\right) \leq J(\Theta) \tag{6.15}$$

This implies that $\nabla J_{\Theta}(\Theta^*) = 0$ and $\nabla^2 J_{\Theta}(\Theta^*) \geq 0$ since $J(\Theta)$ is twice-differentiable with respect to Θ.

Utilizing the Taylor series expansion, one writes

$$\nabla J_{\Theta}\left(\Theta^*\right) = \nabla J_{\Theta}\left(\Theta^* + \Delta\Theta\right) + \nabla^2 J_{\Theta}\left(\Theta^* + \Delta\Theta\right)\Delta\Theta + \underbrace{\mathscr{O}\left(\Delta\Theta^{\top}\Delta\Theta\right)}_{\approx 0} \tag{6.16}$$

Since $\nabla J_\Theta(\Theta^*) = 0$, $\nabla J_\Theta(\Theta^* + \Delta\Theta) = \nabla J_\Theta(\Theta)$, and $\nabla^2 J_\Theta(\Theta^* + \Delta\Theta) = \nabla^2 J_\Theta(\Theta)$, then

$$\Delta\Theta = -\left[\nabla^2 J_\Theta(\Theta)\right]^{-1} \nabla J_\Theta(\Theta) \tag{6.17}$$

Equation (6.17) can be written in a discrete-time form as

$$\Theta_{i+1} = \Theta_i - \left[\nabla^2 J_\Theta(\Theta_i)\right]^{-1} \nabla J_\Theta(\Theta_i) \tag{6.18}$$

This is known as a second-order gradient or Newton's method for convex optimization. It is noted that the inverse of the Hessian matrix is generally numerically intensive. So, a first-order approximation can be made by recognizing that $\nabla^2 J_\Theta^{-1}(\Theta) \approx \nabla^2 J_\Theta^{-1}(\Theta^*) = \varepsilon \geq 0$, where ε is a small positive parameter, when Θ is in the neighborhood of Θ^*. This approximation leads to the well-known steepest descent or first-order gradient method for convex optimization given by

$$\Theta_{i+1} = \Theta_i - \varepsilon \nabla J_\Theta(\Theta_i) \tag{6.19}$$

Now, dividing both sides by Δt and taking the limit as $\Delta t \to 0$ yield

$$\dot{\Theta} = -\Gamma \nabla J_\Theta(\Theta) \tag{6.20}$$

where $\Gamma = \Gamma^\top > 0 \in \mathbb{R}^m \times \mathbb{R}^m$ is a positive-definite adaptation rate matrix which effectively replaces $\frac{\varepsilon}{\Delta t}$. This is the continuous-time version of the gradient method.

Returning to the minimization of $J(\Theta)$ for estimating Θ^*, the differential form of the least-squares estimation of $\Theta(t)$ can be expressed using the gradient method as

$$\dot{\Theta} = -\Gamma \nabla J_\Theta(\Theta) = -\Gamma \Phi(x) \epsilon^\top \tag{6.21}$$

Notice the resemblance of this least-squares gradient method to a model-reference adaptive law, where the approximation error $\epsilon(t)$ replaces the tracking error $e(t)$.

Example 6.2 For Example 6.1, the least-squares gradient method is expressed as

$$\dot{\Theta} = \begin{bmatrix} \dot{\theta}_0 \\ \dot{\theta}_1 \\ \vdots \\ \dot{\theta}_p \end{bmatrix} = -\Gamma \left(\begin{bmatrix} 1 & x & \cdots & x^p \\ x & x^2 & \cdots & x^{p+1} \\ \vdots & \vdots & \ddots & \vdots \\ x^p & x^{p+1} & \cdots & x^{2p} \end{bmatrix} \begin{bmatrix} \theta_0 \\ \theta_1 \\ \vdots \\ \theta_p \end{bmatrix} - \begin{bmatrix} y \\ xy \\ \vdots \\ x^p y \end{bmatrix} \right)$$

6.3 Persistent Excitation and Parameter Convergence

Let $\tilde{\Theta}(t) = \Theta(t) - \Theta^*$ be the estimation error, then

$$\epsilon = \Theta^\top \Phi(x)\, \Theta - y = \tilde{\Theta}^\top \Phi(x) \tag{6.22}$$

The least-squares gradient method can be written as

$$\dot{\tilde{\Theta}} = \dot{\Theta} = -\Gamma \Phi(x) \Phi^{\top}(x) \tilde{\Theta} \tag{6.23}$$

Proof Choose a Lyapunov candidate function

$$V\left(\tilde{\Theta}\right) = \text{trace}\left(\tilde{\Theta}^{\top} \Gamma^{-1} \tilde{\Theta}\right) \tag{6.24}$$

Then,

$$\begin{aligned} \dot{V}\left(\tilde{\Theta}\right) &= 2\text{trace}\left(\tilde{\Theta}^{\top} \Gamma^{-1} \dot{\tilde{\Theta}}\right) = -2\text{trace}\left(\tilde{\Theta}^{\top} \Phi(x) \Phi^{\top}(x) \tilde{\Theta}\right) \\ &= -2\Phi^{\top}(x) \tilde{\Theta} \tilde{\Theta}^{\top} \Phi(x) = -2\epsilon^{\top} \epsilon = -2\|\epsilon\|^2 \leq 0 \end{aligned} \tag{6.25}$$

Note that $\dot{V}\left(\tilde{\Theta}\right)$ can only be negative semi-definite because $\dot{V}\left(\tilde{\Theta}\right)$ can be zero when $\Phi(x) = 0$ independent of $\tilde{\Theta}(t)$. One can establish that $V\left(\tilde{\Theta}\right)$ has a finite limit as $t \to \infty$ since

$$V(t \to \infty) = V(t_0) - 2\int_{t_0}^{\infty} \|\epsilon\|^2 dt < \infty \tag{6.26}$$

which implies

$$2\int_{t_0}^{\infty} \|\epsilon\|^2 dt = V(t_0) - V(t \to \infty) < \infty \tag{6.27}$$

Therefore, $\epsilon(t) \in \mathscr{L}_2 \cap \mathscr{L}_{\infty}$. Moreover, since $\Phi(x) \in \mathscr{L}_{\infty}$ as a result of $\epsilon(t) \in \mathscr{L}_2 \cap \mathscr{L}_{\infty}$, then $\tilde{\Theta}(t) \in \mathscr{L}_{\infty}$, but there is no assurance that $\tilde{\Theta}(t) \to 0$ as $t \to \infty$ which implies a parameter convergence.

One cannot conclude that $\dot{V}\left(\tilde{\Theta}\right)$ is uniformly continuous since

$$\ddot{V}\left(\tilde{\Theta}\right) = -4\epsilon^{\top} \dot{\epsilon} = -4\epsilon^{\top}\left[\dot{\tilde{\Theta}}^{\top} \Phi(x) + \tilde{\Theta}^{\top} \dot{\Phi}(x)\right] \tag{6.28}$$

is not necessarily bounded because there is no other condition placed on $\Phi(x)$ except $\Phi(x) \in \mathscr{L}_{\infty}$. For $\dot{V}\left(\tilde{\Theta}\right)$ to be uniformly continuous, an additional condition $\dot{\Phi}(x) \in \mathscr{L}_{\infty}$ is required. Then, using the Barbalat's lemma, one can conclude that $\dot{V}\left(\tilde{\Theta}\right) \to 0$ or $\epsilon(t) \to 0$ which also implies that $\dot{\Theta}(t) \to 0$ as $t \to \infty$. Note that, from Eq. (6.23), $\dot{\Theta}(t) \to 0$ does not necessarily imply that $\tilde{\Theta}(t) \to 0$ since $\Phi(x)$ can also tend to zero instead of $\tilde{\Theta}(t)$.

So, up to this point, one can only show that the approximation error $\epsilon(t)$ can tend to zero if $\dot{\Phi}(x) \in \mathscr{L}_{\infty}$, but the estimation error $\tilde{\Theta}(t)$ does not necessarily tend to zero since $\Phi(x)$ can be a zero signal at some time interval. To examine the issue of

the parameter convergence, Eq. (6.23) can be solved as

$$\tilde{\Theta}(t) = \exp\left[-\Gamma \int_{t_0}^{t} \Phi(x)\, \Phi^{\top}(x)\, d\tau\right] \tilde{\Theta}_0 \tag{6.29}$$

where $\tilde{\Theta}_0 = \tilde{\Theta}(t_0)$.

Note that $x(t)$ is an independent variable as a function of t. Then, for $\tilde{\Theta}(t)$ to be exponentially stable which implies an exponential parameter convergence, the following condition is required:

$$\int_{t}^{t+T} \Phi(x)\, \Phi^{\top}(x)\, d\tau \geq \alpha_0 I \tag{6.30}$$

for all $t \geq t_0$ and some $\alpha_0 > 0$.

This condition is called the persistent excitation (PE) condition which essentially requires an input signal to be persistently exciting (PE), that is, a signal that does not go to zero after some finite time when a parameter convergence has not been established [1]. Another interpretation of the persistent excitation condition is that, for parameters to converge exponentially, an input signal must be sufficiently rich to excite all system modes associated with the parameters to be identified. It should be noted that while the persistent excitation is needed for a parameter convergence, in practice, input signals that are persistently exciting can lead to unwanted consequences such as exciting unknown or unmodeled dynamics that can have deleterious effects on stability of a dynamical system.

Another observation to be made is that if $x(t)$ is a state variable of a closed-loop system, one cannot assume that the persistent excitation condition can easily be satisfied. This can be explained as follows:

Suppose a parameter identification is used for adaptive control, then the closed-loop stability usually implies a parameter convergence to the ideal values of the unknown parameters. However, the parameter convergence requires the persistent excitation condition which depends on $x(t)$ which in turn depends on the parameter convergence. This is a circular argument. Therefore, it is difficult to assert the PE condition when $\Phi(x)$ depends on a feedback action. However, if $x(t)$ is an independent variable, then the persistent excitation condition can be verified. In practice, a control system can have a persistent excitation if a command signal is PE. This is a fundamental process of system identification.

Suppose the persistent excitation condition is satisfied, then the estimation error is given by

$$\left|\left|\tilde{\Theta}\right|\right| \leq \left|\left|\tilde{\Theta}_0\right|\right| e^{-\gamma alph_0}, \forall t \in [t_1, t_1 + T], t_1 > t_0 \tag{6.31}$$

where $\gamma = \lambda_{min}(\Gamma)$ is the smallest eigenvalue of Γ. Thus, $\tilde{\Theta}(t)$ is exponentially stable with $\tilde{\Theta}(t) \to 0$ as $t \to \infty$. Hence, the parameter convergence is established. It follows that the approximation error is also asymptotically stable (but not necessarily exponentially stable because of $\Phi(x)$) with $\epsilon(t) \to 0$ as $t \to \infty$.

Since $\left\|\Phi^{\top}(x)\,\Phi(x)\right\| \geq \left\|\Phi(x)\,\Phi^{\top}(x)\right\|$, it implies

$$\alpha_0 I \leq \int_t^{t+T} \Phi(x)\Phi^{\top}(x)\,d\tau \leq \int_t^{t+T} \Phi^{\top}(x)\,\Phi(x)d\tau I = \beta_0 I \tag{6.32}$$

Then, if the persistent excitation condition is satisfied, $\dot{V}\left(\tilde{\Theta}\right)$ is expressed as

$$\dot{V}\left(\tilde{\Theta}\right) \leq -\frac{2\alpha_0 V\left(\tilde{\Theta}\right)}{\lambda_{max}\left(\Gamma^{-1}\right)} \tag{6.33}$$

Thus, the least-squares gradient method is exponentially stable with the rate of convergence of $\frac{\alpha_0}{\lambda_{max}\left(\Gamma^{-1}\right)}$.

Example 6.3 Consider a scalar estimation error equation

$$\dot{\tilde{\theta}} = -\gamma\phi^2(t)\,\tilde{\theta}$$

subject to $\tilde{\theta}(0) = 1$, where

$$\phi(t) = \frac{1}{1+t}$$

which is bounded. Then,

$$\tilde{\theta}(t) = \exp\left[-\gamma\int_0^t \frac{d\tau}{(1+\tau)^2}\right] = \exp\left[\gamma\left(\frac{1}{1+t} - 1\right)\right] = \exp\left(\frac{-\gamma t}{1+t}\right)$$

$$\dot{\tilde{\theta}}(t) = -\frac{\gamma}{(1+t)^2}\exp\left(\frac{-\gamma t}{1+t}\right)$$

As $t \to \infty$, $\dot{\tilde{\theta}}(t) \to 0$ but $\tilde{\theta}(t) \to e^{-\gamma} \neq 0$. Thus, $\phi(t)$ is not PE and does not guarantee a parameter convergence. The only way to ensure that $\tilde{\theta}(t) \to 0$ is for $\gamma \to \infty$.

Consider another signal with zero value in some time interval such as

$$\phi(t) = \begin{cases} 1 & 0 \leq t \leq 1 \\ 0 & t > 1 \end{cases}$$

Then,

$$\tilde{\theta}(t) = \begin{cases} e^{-\gamma t} & 0 \leq t \leq 1 \\ e^{-\gamma} & t > 1 \end{cases}$$

which leads to the same conclusion that $\phi(t)$ is not PE.

Example 6.4 Consider $\Phi(t) = \left[1 \ \sin t\right]^\top$. Then,

$$\Phi(t)\Phi^\top(t) = \begin{bmatrix} 1 & \sin t \\ \sin t & \sin^2 t \end{bmatrix}$$

Notice that $\Phi(t)\Phi^\top(t)$ is singular at any instant of time t. The PE condition is evaluated as

$$\begin{aligned}\int_t^{t+T} \Phi(\tau)\Phi^\top(\tau)\,d\tau &= \int_t^{t+T} \begin{bmatrix} 1 & \sin\tau \\ \sin\tau & \sin^2\tau \end{bmatrix} d\tau = \begin{bmatrix} \tau & -\cos\tau \\ -\cos\tau & \frac{\tau}{2} - \frac{1}{4}\sin 2\tau \end{bmatrix}_t^{t+T} \\ &= \begin{bmatrix} T & \cos(t) - \cos(t+T) \\ \cos(t) - \cos(t+T) & \frac{T}{2} - \frac{1}{4}\sin 2(t+T) + \frac{1}{4}\sin 2t \end{bmatrix}\end{aligned}$$

Now, T must be chosen such that the PE condition is satisfied. Let $T = 2\pi$ which is the period of the signal. Then, $\Phi(t)$ is PE since

$$\begin{aligned}\int_t^{t+T} \Phi(\tau)\Phi^\top(\tau)\,d\tau &= \begin{bmatrix} 2\pi & \cos(t) - \cos(t+2\pi) \\ \cos(t) - \cos(t+2\pi) & 1 - \frac{1}{4}\sin 2(t+2\pi) + \frac{1}{4}\sin 2t \end{bmatrix} \\ &= \begin{bmatrix} 2\pi & 0 \\ 0 & \pi \end{bmatrix} = \pi \begin{bmatrix} 2 & 0 \\ 0 & 1 \end{bmatrix} \geq \pi \begin{bmatrix} 1 & 0 \\ 0 & 1 \end{bmatrix}\end{aligned}$$

Thus, $\alpha_0 = \pi$. The estimation error is exponentially stable and a parameter convergence is guaranteed since

$$\left|\left|\tilde{\Theta}\right|\right| \leq \left|\left|\tilde{\Theta}_0\right|\right| e^{-\pi\gamma t}, \ \forall t \in [t_1, t_1 + 2\pi], \ t_1 > t_0$$

6.4 Recursive Least-Squares

Consider the following cost function:

$$J(\Theta) = \frac{1}{2}\int_{t_0}^{t} \epsilon^\top \epsilon\, d\tau \tag{6.34}$$

which is the continuous-time version of the cost function in Sect. 6.1.

The necessary condition is

$$\nabla J_\Theta(\Theta) = \frac{\partial J^\top}{\partial \Theta^\top} = \int_{t_0}^{t} \Phi(x)\left[\Phi^\top(x)\Theta - y^\top\right] d\tau = 0 \tag{6.35}$$

from which $\Theta(t)$ is obtained as

$$\Theta = \left[\int_{t_0}^{t} \Phi(x)\,\Phi^{\top}(x)\,d\tau\right]^{-1} \int_{t_0}^{t} \Phi(x)\,y^{\top} d\tau \tag{6.36}$$

assuming the inverse of $\int_{t_0}^{t} \Phi(x)\,\Phi^{\top}(x)\,d\tau$ exists. Note that the matrix $\Phi(x)\,\Phi^{\top}(x)$ is always singular and is not invertible. However, if the PE condition is satisfied, then $\int_{t_0}^{t} \Phi(x)\,\Phi^{\top}(x)\,d\tau$ is invertible.

Introducing a matrix $R(t) = R^{\top}(t) > 0 \in \mathbb{R}^m \times \mathbb{R}^m$ where

$$R = \left[\int_{t_0}^{t} \Phi(x)\,\Phi^{\top}(x)\,d\tau\right]^{-1} \tag{6.37}$$

then

$$R^{-1}\Theta = \int_{t_0}^{t} \Phi(x)\,y^{\top} d\tau \tag{6.38}$$

Upon differentiation, this yields

$$R^{-1}\dot{\Theta} + \frac{dR^{-1}}{dt}\Theta = \Phi(x)\,y^{\top} \tag{6.39}$$

From Eq. (6.37), we obtain

$$\frac{dR^{-1}}{dt} = \Phi(x)\,\Phi^{\top}(x) \tag{6.40}$$

Therefore,

$$\dot{\Theta} = -R\Phi(x)\left[\Phi^{\top}(x)\,\Theta - y^{\top}\right] = -R\Phi(x)\,\epsilon^{\top} \tag{6.41}$$

Now, since $R(t)\,R^{-1}(t) = I$, then

$$\dot{R}R^{-1} + R\frac{dR^{-1}}{dt} = 0 \tag{6.42}$$

Thus,

$$\dot{R} = -R\Phi(x)\,\Phi^{\top}(x)\,R \tag{6.43}$$

Both Eqs. (6.41) and (6.43) constitute the well-known recursive least-squares (RLS) parameter identification method. The time-varying matrix $R(t)$ is called the covariance matrix, and the RLS formula is similar to the Kalman filter where Eq. (6.43) is a differential Riccati equation for a zero-order plant model. Comparing Eqs. (6.21)–(6.41), $R(t)$ plays the role of Γ as a time-varying adaptation rate matrix and Eq. (6.43) is effectively an adaptive law for the time-varying adaptation rate matrix.

Let $\tilde{\Theta}(t) = \Theta(t) - \Theta^*$ be the estimation error. Since $\epsilon(t) = \tilde{\Theta}^\top(t)\Phi(x)$, then

$$\dot{\tilde{\Theta}} = -R\Phi(x)\Phi^\top(x)\tilde{\Theta} \tag{6.44}$$

Proof Choose a Lyapunov candidate function

$$V\left(\tilde{\Theta}\right) = \text{trace}\left(\tilde{\Theta}^\top R^{-1}\tilde{\Theta}\right) \tag{6.45}$$

Then,

$$\begin{aligned}\dot{V}\left(\tilde{\Theta}\right) &= \text{trace}\left(2\tilde{\Theta}^\top R^{-1}\dot{\tilde{\Theta}} + \tilde{\Theta}^\top \frac{dR^{-1}}{dt}\tilde{\Theta}\right)\\ &= \text{trace}\left(-2\tilde{\Theta}^\top\Phi(x)\Phi^\top(x)\tilde{\Theta} + \tilde{\Theta}^\top\Phi(x)\Phi^\top(x)\tilde{\Theta}\right)\\ &= -\text{trace}\left(\tilde{\Theta}^\top\Phi(x)\Phi^\top(x)\tilde{\Theta}\right) = -\epsilon^\top\epsilon = -\|\epsilon\|^2 \le 0\end{aligned} \tag{6.46}$$

One can establish that $V\left(\tilde{\Theta}\right)$ has a finite limit as $t \to \infty$ since

$$V(t \to \infty) = V(t_0) - \int_{t_0}^{\infty} \|\epsilon\|^2 dt < \infty \tag{6.47}$$

Therefore, $\epsilon(t) \in \mathscr{L}_2 \cap \mathscr{L}_\infty$. Since $\Phi(x) \in \mathscr{L}_\infty$ because $\epsilon(t) \in \mathscr{L}_2 \cap \mathscr{L}_\infty$, then $\tilde{\Theta}(t) \in \mathscr{L}_\infty$, but there is no guarantee that $\tilde{\Theta}(t) \to 0$ as $t \to \infty$ which implies a parameter convergence, unless $\Phi(x)$ is PE.

Note that $\dot{V}\left(\tilde{\Theta}\right)$ is not necessarily uniformly continuous since this would require that $\ddot{V}\left(\tilde{\Theta}\right)$ is bounded. Evaluating $\ddot{V}\left(\tilde{\Theta}\right)$ as

$$\begin{aligned}\ddot{V}\left(\tilde{\Theta}\right) &= -2\epsilon^\top\dot{\epsilon} = -2\epsilon^\top\left[\dot{\tilde{\Theta}}^\top\Phi(x) + \tilde{\Theta}^\top\dot{\Phi}(x)\right]\\ &= -2\epsilon^\top\left[-\tilde{\Theta}^\top\Phi(x)\Phi^\top(x)R\Phi(x) + \tilde{\Theta}^\top\dot{\Phi}(x)\right]\\ &= -2\epsilon^\top\left[-\tilde{\Theta}^\top\Phi(x)\Phi^\top(x)\left[\int_{t_0}^{t}\Phi(x)\Phi^\top(x)\,d\tau\right]^{-1}\Phi(x) + \tilde{\Theta}^\top\dot{\Phi}(x)\right]\end{aligned} \tag{6.48}$$

Therefore, $\ddot{V}\left(\tilde{\Theta}\right)$ is bounded if the following conditions are met:

- $\dot{\Phi}(x) \in \mathscr{L}_\infty$.
- $\left[\int_{t_0}^{t}\Phi(x)\Phi^\top(x)\,d\tau\right]^{-1}$ is invertible which implies $\Phi(x)$ is PE.

If these conditions are satisfied, then using the Barbalat's lemma, it can be shown that $\epsilon(t) \to 0$ as $t \to \infty$. In addition, $\tilde{\Theta}(t) \to 0$ as $t \to \infty$ and the parameter convergence is achieved. ■

Note that there are various versions of the RLS method. One popular version is the RLS method with normalization where the adaptive law for $R(t)$ is modified as follows:

$$\dot{R} = -\frac{R\Phi(x)\Phi^{\top}(x)R}{1+n^2} \tag{6.49}$$

where $1+n^2(x) = 1+\Phi^{\top}(x)R\Phi(x)$ is called a normalization factor.

The time derivative of the Lyapunov candidate function for the RLS method with normalization is

$$\begin{aligned}\dot{V}\left(\tilde{\Theta}\right) &= \text{trace}\left(-2\tilde{\Theta}^{\top}\Phi(x)\Phi^{\top}(x)\tilde{\Theta} + \frac{\tilde{\Theta}^{\top}\Phi(x)\Phi^{\top}(x)\tilde{\Theta}}{1+n^2}\right) \\ &= -\text{trace}\left(\tilde{\Theta}^{\top}\Phi(x)\Phi^{\top}(x)\tilde{\Theta}\left(\frac{1+2n^2}{1+n^2}\right)\right) \\ &= -\epsilon^{\top}\epsilon\left(\frac{1+2n^2}{1+n^2}\right) = -\|\epsilon\|^2\left(\frac{1+2n^2}{1+n^2}\right) \leq 0\end{aligned} \tag{6.50}$$

Note that $\dot{V}\left(\tilde{\Theta}\right)$ is more negative with than without normalization. Therefore, the effect of normalization is to make the adaptive law for $R(t)$ more stable, but the parameter convergence is slower.

Another popular version is the RLS method with a forgetting factor and normalization, which is given without derivation by

$$\dot{R} = \beta R - \frac{R\Phi(x)\Phi^{\top}(x)R}{1+n^2} \tag{6.51}$$

where $0 \leq \beta \leq 1$ is called a forgetting factor.

6.5 Indirect Adaptive Control with Least-Squares Parameter Identification

Consider the following MIMO system with a matched uncertainty in Sect. 5.7 with $A \in \mathbb{R}^n \times \mathbb{R}^n$ unknown, but $B \in \mathbb{R}^n \times \mathbb{R}^m$ known with $n \leq m$ [4]:

$$\dot{x} = Ax + B\left[u + \Theta^{*\top}\Phi(x)\right] \tag{6.52}$$

where $\Theta^* \in \mathbb{R}^l \times \mathbb{R}^m$ and $\Phi(x) \in \mathbb{R}^l$ is a bounded regressor (or basis function) vector and is assumed to be known.

The objective is to design an indirect adaptive controller with least-squares parameter identification that follows a reference model

$$\dot{x}_m = A_m x_m + B_m r \tag{6.53}$$

where $A_m \in \mathbb{R}^n \times \mathbb{R}^n$ is Hurwitz $B_m \in \mathbb{R}^n \times \mathbb{R}^q$, and $r(t) \in \mathbb{R}^q \in \mathscr{L}_\infty$ is a piecewise continuous and bounded reference command signal.

Note that if $n < m$, then B^{-1} is defined by the right pseudo-inverse $B^\top \left(BB^\top\right)^{-1}$. Assuming B is invertible, then there exist K_x^* and K_r^* that satisfy the model matching conditions. If $\hat{A}(t)$ is an estimate of A, then the estimate of K_x^* is given by

$$K_x(t) = B^{-1}\left[A_m - \hat{A}(t)\right] \tag{6.54}$$

Let the adaptive controller be

$$u = K_x(t)\, x + K_r r - \Theta^\top(t)\, \Phi(x) \tag{6.55}$$

where $K_r = B^{-1} B_m$ is known.

Then, the closed-loop plant model is given by

$$\dot{x} = \left(A + A_m - \hat{A}\right) x + B_m r + B\left(\Theta^{*\top} - \Theta^\top\right) \Phi(x) \tag{6.56}$$

where

$$\bar{u} = K_x x + K_r r \tag{6.57}$$

If $\hat{A}(t) \to A$ and $\Theta(t) \to \Theta^*$, then $\dot{x}(t)$ converges to

$$\dot{x}_d = A_m x + B_m r = \hat{A} x + B\bar{u} \tag{6.58}$$

which follows the reference model if $x(t) \to x_m(t)$.

Now, define the plant modeling error as the difference between $\dot{x}_d(t)$ and $\dot{x}(t)$. Then,

$$\epsilon = \dot{x}_d - \dot{x} = \hat{A}x + B\bar{u} - \dot{x} = \left(\hat{A} - A\right) x + B\left(\Theta^\top - \Theta^{*\top}\right) \Phi(x) = \tilde{A}x + B\tilde{\Theta}^\top \Phi(x) \tag{6.59}$$

Then, the tracking error equation is expressed in terms of the plant modeling error as

$$\dot{e} = \dot{x}_m - \dot{x} = \dot{x}_m - \dot{x}_d + \dot{x}_d - \dot{x} = A_m e + \epsilon \tag{6.60}$$

Thus, we see that the plant modeling error $\epsilon(t)$ between the true plant and the actual plant actually is what really affects the tracking error $e(t)$. So, if we can minimize the plant modeling error, then the tracking error will also be minimized.

Let $\tilde{\Omega}^{\top}(t) = \left[\tilde{A}(t)\ B\tilde{\Theta}^{\top}(t)\right] \in \mathbb{R}^n \times \mathbb{R}^{n+l}$ and $\Psi(x) = \left[x^{\top}\ \Phi^{\top}(x)\right]^{\top} \in \mathbb{R}^{n+1}$ where $\tilde{A}(t) = \hat{A}(t) - A$ and $\tilde{\Theta}(t) = \Theta(t) - \Theta^*$. Then, the plant modeling error is expressed as

$$\epsilon = \tilde{\Omega}^{\top}\Psi(x) \tag{6.61}$$

The tracking error equation is also expressed as

$$\dot{e} = A_m e + \tilde{\Omega}^{\top}\Psi(x) \tag{6.62}$$

Consider the following cost function:

$$J\left(\tilde{\Omega}\right) = \frac{1}{2}\epsilon^{\top}\epsilon \tag{6.63}$$

Then, the least-squares gradient adaptive law is given by

$$\dot{\Omega} = -\Gamma\frac{\partial J^{\top}}{\partial\tilde{\Omega}^{\top}} = -\Gamma\Psi(x)\,\epsilon^{\top} \tag{6.64}$$

For the standard RLS adaptive law, the constant adaptation rate matrix Γ is replaced by the covariance matrix $R(t)$ as follows:

$$\dot{\Omega} = -R\Psi(x)\,\epsilon^{\top} \tag{6.65}$$

$$\dot{R} = -R\Psi(x)\,\Psi^{\top}(x)\,R \tag{6.66}$$

We now combine the least-squares gradient adaptive law with the MRAC adaptive law to obtain the following adaptive law which we call combined least-squares gradient MRAC adaptive law:

$$\dot{\Omega} = -\Gamma\Psi(x)\left(\epsilon^{\top} + e^{\top}P\right) \tag{6.67}$$

To compute $\hat{A}(t)$, and $\Theta(t)$ from $\Omega(t)$, it is noted that

$$\Omega = \begin{bmatrix}\Omega_1\\ \Omega_2\end{bmatrix} = \begin{bmatrix}\hat{A}^{\top}\\ \Theta B^{\top}\end{bmatrix} \Rightarrow \begin{bmatrix}\hat{A}^{\top}\\ \Theta\end{bmatrix} = \begin{bmatrix}\Omega_1\\ \Omega_2 B^{-\top}\end{bmatrix} \tag{6.68}$$

Proof To prove stability of the combined RLS MRAC adaptive laws, we choose a Lyapunov candidate function

$$V\left(e,\tilde{\Omega}\right)=e^{\top}Pe+\text{trace}\left(\tilde{\Omega}^{\top}R^{-1}\tilde{\Omega}\right) \tag{6.69}$$

Then, $\dot{V}\left(e,\tilde{\Omega}\right)$ is evaluated as

$$\begin{aligned}\dot{V}\left(e,\tilde{\Omega}\right)&=-e^{\top}Qe+2e^{\top}P\epsilon+\text{trace}\left(-2\tilde{\Omega}^{\top}\Psi\left(x\right)\left(\epsilon^{\top}+e^{\top}P\right)+\tilde{\Omega}^{\top}\frac{dR^{-1}}{dt}\tilde{\Omega}\right)\\&=-e^{\top}Qe+2e^{\top}P\epsilon-2\left(\epsilon^{\top}+e^{\top}P\right)\epsilon+\underbrace{\Psi^{\top}\left(x\right)\tilde{\Omega}}_{\epsilon^{\top}}\underbrace{\tilde{\Omega}^{\top}\Psi\left(x\right)}_{\epsilon}\\&=-e^{\top}Qe-\epsilon^{\top}\epsilon\leq-\lambda_{min}\left(Q\right)\left\|e\right\|^{2}-\left\|\epsilon\right\|^{2}\end{aligned} \tag{6.70}$$

Note that $\dot{V}\left(e,\tilde{\Omega}\right)\leq 0$ as opposed to $\dot{V}\left(e,\tilde{\Omega}\right)<0$ because the condition of $\Psi\left(x\right)$ on which $\epsilon\left(t\right)$ depends on has not been imposed. Therefore, $e\left(t\right)\in\mathscr{L}_2\cap\mathscr{L}_\infty$, $\epsilon\left(t\right)\in\mathscr{L}_2\cap\mathscr{L}_\infty$, $\dot{e}\left(t\right)\in\mathscr{L}_\infty$, and $\tilde{\Omega}\in\mathscr{L}_\infty$. Applying the Barbalat's lemma, we evaluate $\ddot{V}\left(e,\tilde{\Omega}\right)$ as

$$\begin{aligned}\ddot{V}\left(e,\tilde{\Omega}\right)&=-2e^{\top}Q\left(A_me+\epsilon\right)-\epsilon^{\top}\left[\dot{\tilde{\Omega}}^{\top}\Psi\left(x\right)+\tilde{\Omega}^{\top}\dot{\Psi}\left(x\right)\right]\\&=-2e^{\top}Q\left(A_me+\epsilon\right)-\epsilon^{\top}\left[-\left(Pe+\epsilon\right)\Psi^{\top}\left(x\right)R\Psi\left(x\right)+\tilde{\Omega}^{\top}\dot{\Psi}\left(x\right)\right]\end{aligned} \tag{6.71}$$

But, by definition

$$R=\left[\int_{t_0}^{t}\Psi\left(x\right)\Psi^{\top}\left(x\right)d\tau\right]^{-1} \tag{6.72}$$

If $\dot{\Psi}\left(x\right)\in\mathscr{L}_\infty$ and if $\Psi\left(x\right)$ satisfies the PE condition, then $\ddot{V}\left(e,\tilde{\Omega}\right)\in\mathscr{L}_\infty$. Therefore, $\dot{V}\left(e,\tilde{\Omega}\right)$ is uniformly continuous. It follows that $e\left(t\right)\to 0$, $\epsilon\left(t\right)\to 0$, and $\tilde{\Omega}\left(t\right)\to 0$ as $t\to\infty$. Since $\tilde{\Omega}\left(t\right)$ tends to zero exponentially because of the PE condition, $e\left(t\right)$ also tends to zero exponentially. Thus, the system achieves exponential stability.

Proof If $\Psi\left(x\right)$ satisfies the PE condition, then we have

$$\dot{V}\left(e,\tilde{\Omega}\right)\leq-\lambda_{min}\left(Q\right)\left\|e\right\|^{2}-\alpha_0\left\|\tilde{\Omega}\right\|^{2} \tag{6.73}$$

Choose Q and β_0 from Eq. (6.32) such that $\lambda_{min}\left(Q\right)=\frac{\alpha_0\lambda_{max}\left(P\right)}{\beta_0}$. Then,

$$\dot{V}\left(e,\tilde{\Omega}\right) \leq -\frac{\alpha_0 \lambda_{max}(P)}{\beta_0}\|e\|^2 - \alpha_0\left\|\tilde{\Omega}\right\|^2 \leq -\frac{\alpha_0 V\left(e,\tilde{\Omega}\right)}{\beta_0} \tag{6.74}$$

Thus, the system is exponentially stable with the convergence rate of $\frac{\alpha_0}{2\beta_0}$.

■

Note that for the combined least-squares gradient MRAC adaptive laws, it can be shown that

$$\dot{V}\left(e,\tilde{\Omega}\right) = -e^\top Qe - 2\epsilon^\top\epsilon \leq -\lambda_{min}(Q)\|e\|^2 - 2\|\epsilon\|^2 \tag{6.75}$$

$\ddot{V}\left(e,\tilde{\Omega}\right)$ is evaluated as

$$\ddot{V}\left(e,\tilde{\Omega}\right) = -2e^\top Q\left(A_m e + \epsilon\right) - 2\epsilon^\top\left[-\left(Pe+\epsilon\right)\Psi^\top(x)\,\Gamma\Psi(x) + \tilde{\Omega}^\top\dot{\Psi}(x)\right] \tag{6.76}$$

If $\dot{\Psi}(x) \in \mathscr{L}_\infty$, then $\ddot{V}\left(e,\tilde{\Omega}\right)$ is bounded. Therefore, $\dot{V}\left(e,\tilde{\Omega}\right)$ is uniformly continuous. It follows that $e(t) \to 0$ and $\epsilon(t) \to 0$ as $t \to \infty$. The rate of convergence of $\epsilon(t)$ is twice as large as that of the combined RLS MRAC adaptive laws. In addition, if $\Psi(x)$ satisfies the PE condition, then the exponential parameter convergence is achieved.

Example 6.5 Consider a first-order system with a matched uncertainty

$$\dot{x} = ax + b\left(u + \theta^* x^2\right)$$

where a and θ^* are unknown, but $b = 2$. For simulation purposes, $a = 1$ and $\theta^* = 0.2$.

The reference model is given by

$$\dot{x}_m = a_m x_m + b_m r$$

where $a_m = -1$, $b_m = 1$, and $r(t) = \sin t$.

The combined RLS MRAC is computed as

$$\dot{\Omega} = \begin{bmatrix} \dot{\hat{a}} \\ b\dot{\theta} \end{bmatrix} = -\begin{bmatrix} r_{11} & r_{12} \\ r_{12} & r_{22} \end{bmatrix}\begin{bmatrix} x(\epsilon+e) \\ x^2(\epsilon+e) \end{bmatrix}$$

$$\dot{R} = \begin{bmatrix} \dot{r}_{11} & \dot{r}_{12} \\ \dot{r}_{12} & \dot{r}_{22} \end{bmatrix} = -\begin{bmatrix} r_{11} & r_{12} \\ r_{12} & r_{22} \end{bmatrix}\begin{bmatrix} x^2 & x^3 \\ x^3 & x^4 \end{bmatrix}\begin{bmatrix} r_{11} & r_{12} \\ r_{12} & r_{22} \end{bmatrix}$$

with the initial conditions $\Omega(0) = 0$ and $R(0) = 10I$, where

$$\epsilon = \hat{a}x + b\bar{u} - \dot{x}$$

$$\bar{u} = k_x(t)\,x + k_r r = \frac{a_m - \hat{a}}{b}x + \frac{b_m}{b}r$$

Simulation results are shown in Figs. 6.1 and 6.2.

It can be seen that $\hat{a}(t)$ and $\theta(t)$ tends to their true values, and the tracking error $e(t)$ also tends to zero. The covariance matrix $R(t)$ which acts as time-varying adaptation rate matrix Γ converges to zero as $t \to \infty$.

For comparison, the combined least-squares gradient MRAC method is used

$$\dot{\Omega} = \begin{bmatrix} \dot{\hat{a}} \\ b\dot{\theta} \end{bmatrix} = -\begin{bmatrix} \gamma_{11} & 0 \\ 0 & \gamma_{22} \end{bmatrix} \begin{bmatrix} x(\epsilon + e) \\ x^2(\epsilon + e) \end{bmatrix}$$

where $\gamma_a = \gamma_\theta = 10$.

The simulation results are shown in Fig. 6.3.

The tracking error tends to zero asymptotically much faster than the combined RLS MRAC method. The combined least-squares gradient MRAC method generally provides a much better parameter convergence than the combined RLS MRAC method. ■

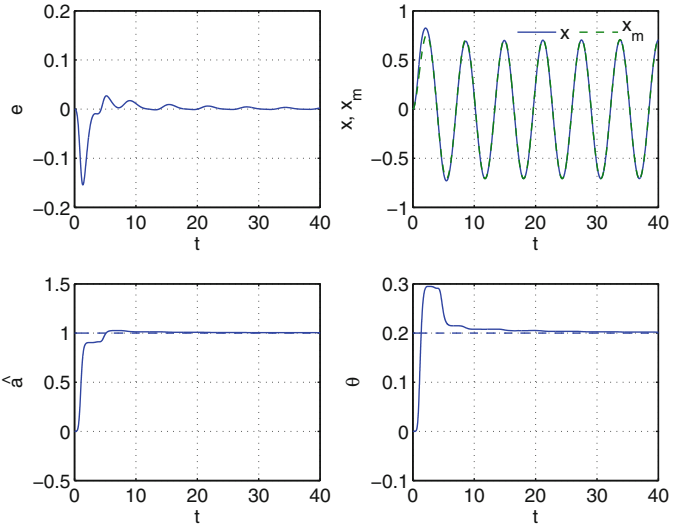

Fig. 6.1 Combined RLS MRAC

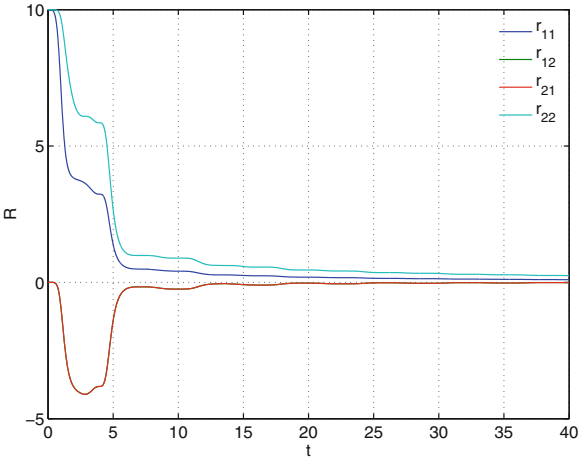

Fig. 6.2 Covariance matrix R

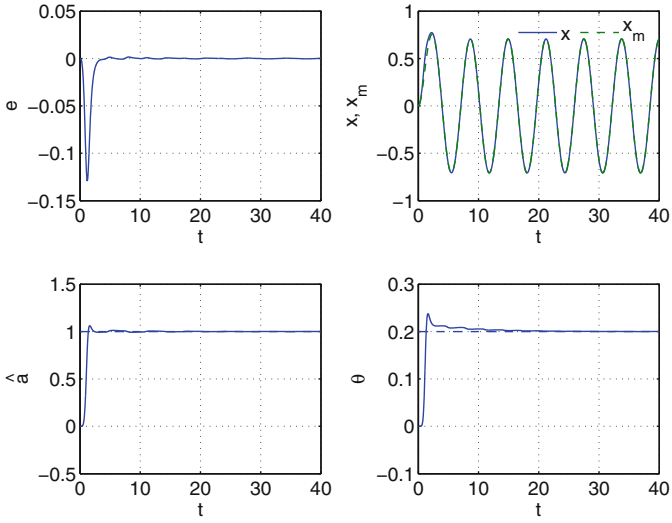

Fig. 6.3 Combined least-squares gradient MRAC

While the combined least-squares MRAC method can provide an exponential parameter convergence, we should note that the pure least-squares method can also be used for adaptive control without combining with MRAC. Both Eqs. (6.64) and (6.65) are pure least-squares adaptive laws without MRAC. Let us examine the behavior of pure RLS adaptive control from Eqs. (6.65) and (6.66).

Proof Choose a Lyapunov candidate function

$$V\left(e,\tilde{\Omega}\right)=e^{\top}Pe+\mu\,\text{trace}\left(\tilde{\Omega}^{\top}R^{-1}\tilde{\Omega}\right) \tag{6.77}$$

with $\mu>0$.
$\dot{V}\left(e,\tilde{\Omega}\right)$ is evaluated as

$$\begin{aligned}\dot{V}\left(e,\tilde{\Omega}\right)&=-e^{\top}Qe+2e^{\top}P\epsilon+\mu\text{trace}\left(-2\tilde{\Omega}^{\top}\Psi\left(x\right)\epsilon^{\top}+\tilde{\Omega}^{\top}\Psi\left(x\right)\Psi^{\top}\left(x\right)\tilde{\Omega}\right)\\&=-e^{\top}Qe+2e^{\top}P\epsilon-\mu\epsilon^{\top}\epsilon\leq-\lambda_{min}\left(Q\right)\|e\|^{2}\\&\quad+2\lambda_{max}\left(P\right)\|e\|\,\|\epsilon\|-\mu\,\|\epsilon\|^{2}\end{aligned} \tag{6.78}$$

$\dot{V}\left(e,\tilde{\Omega}\right)$ is now not negative semi-definite unconditionally. We note that

$$-\frac{\lambda_{max}^{2}\left(P\right)}{\delta^{2}}\|e\|^{2}+2\lambda_{max}\left(P\right)\|e\|\,\|\epsilon\|-\delta^{2}\|\epsilon\|^{2}=-\left[\frac{\lambda_{max}\left(P\right)}{\delta}\|e\|-\delta\|\epsilon\|\right]^{2}\leq0 \tag{6.79}$$

Therefore, $\dot{V}\left(e,\tilde{\Omega}\right)$ can be expressed as

$$\dot{V}\left(e,\tilde{\Omega}\right)\leq-\left[\lambda_{min}\left(Q\right)-\frac{\lambda_{max}^{2}\left(P\right)}{\delta^{2}}\right]\|e\|^{2}-\left(\mu-\delta^{2}\right)\|\epsilon\|^{2} \tag{6.80}$$

Then, $\dot{V}\left(e,\tilde{\Omega}\right)\leq0$ if $\frac{\lambda_{max}(P)}{\sqrt{\lambda_{min}(Q)}}<\delta<\sqrt{\mu}$. Furthermore, if $\Psi\left(x\right)$ satisfies the PE condition, then from Eq. (6.32) we have

$$\dot{V}\left(e,\tilde{\Omega}\right)\leq-\left[\lambda_{min}\left(Q\right)-\frac{\lambda_{max}^{2}\left(P\right)}{\delta^{2}}\right]\|e\|^{2}-\alpha_{0}\left(\mu-\delta^{2}\right)\left\|\tilde{\Omega}\right\|^{2} \tag{6.81}$$

Choose Q and β_0 from Eq. (6.32) such that $\lambda_{min}\left(Q\right)-\frac{\lambda_{max}^{2}(P)}{\delta^{2}}=\frac{\alpha_{0}\left(\mu-\delta^{2}\right)\lambda_{max}(P)}{\mu\beta_{0}}$. Then,

$$\dot{V}\left(e,\tilde{\Omega}\right)\leq-\frac{\alpha_{0}\left(\mu-\delta^{2}\right)\lambda_{max}\left(P\right)}{\mu\beta_{0}}\|e\|^{2}-\alpha_{0}\left(\mu-\delta^{2}\right)\left\|\tilde{\Omega}\right\|^{2}\leq-\frac{\alpha_{0}\left(\mu-\delta^{2}\right)V\left(e,\tilde{\Omega}\right)}{\mu\beta_{0}} \tag{6.82}$$

Thus, the system is exponentially stable with the convergence rate of $\frac{\alpha_{0}\left(\mu-\delta^{2}\right)}{2\mu\beta_{0}}$. ■

From Sect. 6.3, for the least-squares gradient method, if $\dot{\Psi}\left(x\right)\in\mathscr{L}_{\infty}$, then the plant modeling error is asymptotically stable with $\epsilon\left(t\right)\rightarrow0$ as $t\rightarrow\infty$. This implies that the tracking error is also asymptotically stable with $e\left(t\right)\rightarrow0$ as $t\rightarrow\infty$.

However, for the RLS method, asymptotic tracking additionally requires the PE condition, but it is important to recognize that the PE condition cannot be verified in a closed-loop system. So, if the PE condition is not satisfied, then the plant modeling error is only bounded for the RLS method. This implies that the tracking error is only bounded but is not asymptotically stable.

Example 6.6 Consider Example 6.5

$$\dot{x} = ax + b\left(u + \theta^* x^2\right)$$

where a and θ^* are unknown, but $b = 2$. For simulation purposes, $a = 1$ and $\theta^* = 0.2$.

Let $r(t) = \sin \frac{\pi}{10} t$ for $t \in [0, 5]$ and $r(t) = 1$ for $t \in [5, 40]$.
The RLS adaptive control method is implemented as

$$\dot{\Omega} = \begin{bmatrix} \dot{\hat{a}} \\ b\dot{\theta} \end{bmatrix} = -\begin{bmatrix} r_{11} & r_{12} \\ r_{12} & r_{22} \end{bmatrix} \begin{bmatrix} x\epsilon \\ x^2\epsilon \end{bmatrix}$$

with $R(0) = I$.

The simulation results are shown in Fig. 6.4.

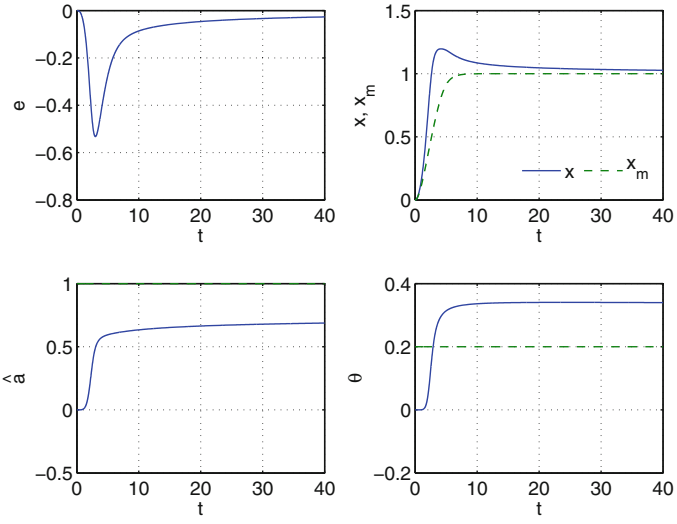

Fig. 6.4 RLS adaptive control

For comparison, the least-squares gradient adaptive control method is also implemented as

$$\dot{\Omega} = \begin{bmatrix} \dot{\hat{a}} \\ b\dot{\theta} \end{bmatrix} = -\begin{bmatrix} \gamma_{11} & 0 \\ 0 & \gamma_{22} \end{bmatrix} \begin{bmatrix} x\epsilon \\ x^2\epsilon \end{bmatrix}$$

with $\Gamma = I$.

The simulation results are shown in Fig. 6.5. It can be seen that the least-squares gradient adaptive control achieves asymptotic tracking with $e(t) \to 0$ as $t \to \infty$. Both the RLS and least-squares gradient adaptive control do not achieve a parameter convergence with this reference command signal.

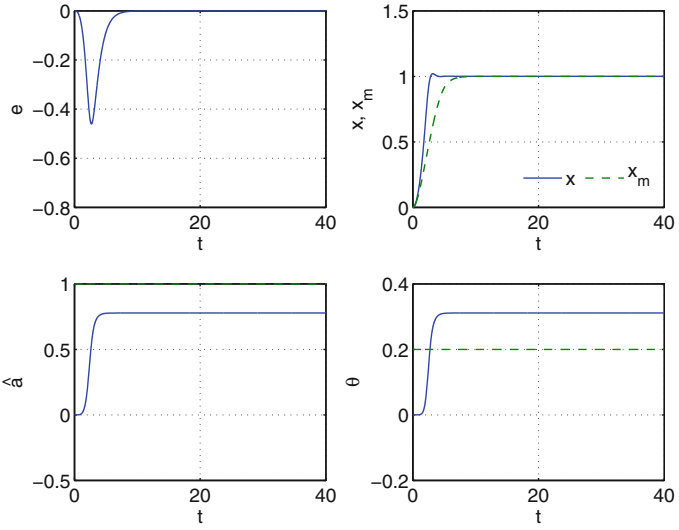

Fig. 6.5 Least-squares gradient adaptive control

6.6 Estimation of Time Derivative Signals

In least-squares adaptive control, the signal $\dot{x}(t)$ is required in the computation of the plant modeling error. In many applications, this signal may not be available. Therefore, in these situations, the signal $\dot{x}(t)$ needs to be estimated. One method of estimating $\dot{x}(t)$ is to use a backward finite-difference method as

$$\hat{\dot{x}}(t) = \frac{x(t) - x(t - \Delta t)}{\Delta t} \tag{6.83}$$

to estimate $\dot{x}(t)$ at a current time step using the current and past state information.

The disadvantage of numerical differentiation is the introduction of noise into the signal.

Another approach is to sample data sufficiently and then use them to construct an at least C^1 smooth time function using a cubic or B-spline method over a finite time interval. This curve is then differentiated at the spline knots to find the estimated time derivative values. This derivative estimate would tend to result in lower noise than the backward finite-difference method [11]. In either case, the derivative computation will introduce a noise source. Least-squares methods are generally robust to noise,

especially if the noise source is a normal Gaussian distribution. Therefore, least-squares adaptive control should be generally more effective than model-reference adaptive control in the presence of noisy measurements. A possibility to suppress noise source is to use a low-pass filter to smooth out the reconstructed signal from numerical differentiation, but the use of a low-pass filter will also introduce a phase delay into the signal which can have a stability implication.

An alternative approach of estimating the signal $\dot{x}(t)$ without numerical differentiation is via a model prediction method. Consider a predictor model of the plant in Eq. (9.341) as follows [4]:

$$\dot{\hat{x}} = A_m \hat{x} + \left(\hat{A} - A_m\right) x + B\left[u + \Theta^\top \Phi(x)\right] \tag{6.84}$$

If $\hat{A}(t) \to A$ and $\Theta(t) \to \Theta^*$, then $\dot{\hat{x}}(t) \to \dot{x}(t)$. Thus, $\dot{\hat{x}}(t)$ is in fact an estimate of $\dot{x}(t)$. The estimate $\dot{\hat{x}}(t)$ only depends on the information of the current state, the control, and the adaptive parameters. The predictor model thus can be used to provide the estimate of the signal $\dot{x}(t)$ without differentiation.

As the adaptation proceeds, the predictor model should converge to the plant model with $\hat{x}(t) \to x(t) + e_p(t)$ as $t \to \infty$, where $e_p(t) = \hat{x}(t) - x(t)$ is the predictor error whose dynamics are described by

$$\dot{e}_p = \dot{\hat{x}} - \dot{x} = A_m e_p + \tilde{A} x + B\tilde{\Theta}^\top \Phi(x) \tag{6.85}$$

Therefore, as $\hat{A}(t) \to A$ and $\Theta(t) \to \Theta^*$, $e_p(t) \to 0$ and $\dot{\hat{x}}(t) \to \dot{x}(t)$.

The plant modeling error based on the predictor model is established by

$$\epsilon_p = \dot{x}_d - \dot{\hat{x}} = \dot{x}_d - \dot{x} - \dot{e}_p = \epsilon - \dot{e}_p \tag{6.86}$$

If the predictor error converges to zero, i.e., $e_p(t) \to 0$, then $\epsilon_p(t) \to \epsilon(t)$. Therefore, the signal $\epsilon_p(t)$ could be used in least-squares adaptive control in lieu of the signal $\epsilon(t)$.

6.7 Summary

Least-squares parameter identification is central to function approximation theory and data regression analysis. Least-squares methods for function approximation and parameter identification are derived from the minimization of the approximation error between a process and a model of the process. Least-squares methods can be used in adaptive control whereby the plant's unknown parameters are estimated by least-squares methods to provide the information to adjust the control gains. Various least-squares techniques are presented, including batch least-squares, least-squares gradient for real-time update, and recursive least-squares.

Parameter convergence in least-squares real-time update laws depends on a condition called persistent excitation (PE). This condition essentially requires an input signal to be persistently exciting (PE), that is, a signal that does not go to zero after some finite time when a parameter convergence has not been established. For parameter identification to converge exponentially, an input signal must be sufficiently rich to excite all system modes associated with the parameters to be identified. While the persistent excitation condition is needed for a parameter convergence, in practice, input signals that are persistently exciting can lead to unwanted consequences such as exciting unknown or unmodeled dynamics that can have deleterious effects on stability of a dynamical system. In general, the persistent excitation condition for closed-loop systems is not easily verified.

Least-squares indirect adaptive control methods are discussed to show how least-squares methods can be used in adaptive control settings. Whereas in MRAC, the tracking error is used to drive the adaptation, least-squares adaptive control provides an adaptation mechanism based on the plant modeling error. The combined least-squares MRAC uses both the tracking error and plant modeling error for the adaptation. Both the least-squares gradient and recursive least-squares adaptive control can achieve exponential tracking and parameter convergence if the persistent excitation condition is satisfied. In general, the plant modeling error requires the time derivative signals of the state information. In some applications, these signals may not be available from measurements. The model prediction method could afford an advantage in that the estimated time derivative signals do not require numerical differentiation which could introduce noise.

6.8 Exercises

1. A process is represented by a set of data (t, x, y) given in the MATLAB file "Process_Data.mat" where the output $y(t)$ can be approximated by a $fourth-th$ degree polynomial in terms of $x(t)$ with end point conditions $y = 0$ and $\frac{dy}{dx} = 0$ at $x = 0$. Determine numerically the matrix A and vector B and solve for the coefficients $\theta_i, i = 2, 3, 4$. Compare the result with the MATLAB function "polyfit."
2. Write MATLAB code to solve Exercise 6.1 using the least-squares gradient method with $\Theta(0) = 0$ and $\Gamma = 10$. Plot $\theta_i(t)$ versus t. Compare the result with that in Exercise 6.1. Note that the Euler method for the least-squares gradient method is expressed as

$$\Theta_{i+1} = \Theta_i - \Delta t \Gamma \Phi(x_i) \left[\Phi^\top(x_i)\Theta_i - y_i\right]$$

3. Determine if the following functions are persistently exciting (PE), and if so, determine T and α.

a. $\phi(t) = e^{-t}$. (Hint: find limit of $\tilde{\theta}(t)$ as $t \to \infty$)
b. $\Phi(t) = \begin{bmatrix} \cos \pi t \\ \sin \pi t \end{bmatrix}$

4. Consider a first-order system with a matched uncertainty

$$\dot{x} = ax + b\left[u + \theta^* \phi(t)\right]$$

where a and θ^* are unknown, but $b = 2$, and $\phi(t) = \sin t$. For simulation purposes, use $a = 1$ and $\theta^* = 0.2$. The reference model is given by

$$\dot{x}_m = a_m x_m + b_m r$$

where $a_m = -1$, $b_m = 1$, and $r(t) = \sin t$.
Implement in Simulink an indirect adaptive control using the recursive least-squares method with normalization. All initial conditions are zero. Use $R(0) = 10$. Plot $e(t)$, $x(t)$ versus $x_m(t)$, $\hat{a}(t)$, and $\theta(t)$, for $t \in [0, 40]$.

References

1. Ioannu, P. A., & Sun, J. (1996). *Robust adaptive control*. Upper Saddle River: Prentice-Hall Inc.
2. Slotine, J.-J., & Li, W. (1991). *Applied nonlinear control*. Upper Saddle River: Prentice-Hall Inc.
3. Bobal, V. (2005). *Digital self-tuning controllers: algorithms, implementation, and applications*. London: Springer.
4. Nguyen, N. (2013). Least-squares model reference adaptive control with chebyshev orthogonal polynomial approximation. *AIAA Journal of Aerospace Information Systems*, *10*(6), 268–286.
5. Chowdhary, G., & Johnson, E. (2011). Theory and flight-test validation of a concurrent-learning adaptive controller. *AIAA Journal of Guidance, Control, and Dynamics*, *34*(2), 592–607.
6. Chowdhary, G., Yucelen, T., & Nguyen, N. (2013). Concurrent learning adaptive control of the aeroelastic generic transport model. In *AIAA Infotech@Aerospace Conference, AIAA-2013-5135*.
7. Guo, L. (1996). Self-convergence of weighted least-squares with applications to stochastic adaptive control. *IEEE Transactions on Automatic Control*, *41*(1), 79–89.
8. Lai, T., & Wei, C.-Z. (1986). Extended least squares and their applications to adaptive control and prediction in linear systems. *IEEE Transactions on Automatic Control*, *31*(10), 898–906.
9. Suykens, J., Vandewalle, J., & deMoor, B. (1996). *Artificial neural networks for modeling and control of non-linear systems*. Dordrecht: Kluwer Academic Publisher.
10. Zou, A., Kumar, K., & Hou, Z. (2010). Attitude control of spacecraft using chebyshev neural networks. *IEEE Transactions on Neural Networks*, *21*(9), 1457–1471.
11. Nguyen, N., Krishnakumar, K., Kaneshige, J., & Nespeca, P. (2008). Flight dynamics modeling and hybrid adaptive control of damaged asymmetric aircraft. *AIAA Journal of Guidance, Control, and Dynamics*, *31*(3), 751–764.

Chapter 7
Function Approximation and Adaptive Control with Unstructured Uncertainty

Abstract This chapter presents the fundamental theories of least-squares function approximation and least-squares adaptive control of systems with unstructured uncertainty. The function approximation theory based on polynomials, in particular the Chebyshev orthogonal polynomials, and neural networks is presented. The Chebyshev orthogonal polynomials are generally considered to be optimal for function approximation of real-valued functions. The Chebyshev polynomial function approximation is therefore more accurate than function approximation with regular polynomials. The neural network function approximation theory for a two-layer neural network is presented for two types of activation functions: sigmoidal function and radial basis function. Model-reference adaptive control of systems with unstructured uncertainty is developed in connection with the function approximation theory. Least-squares direct adaptive control methods with polynomial approximation and neural network approximation are presented. Because the least-squares methods can guarantee the parameter convergence, the least-squares adaptive control methods are shown to achieve uniform ultimate boundedness of control signals in the presence of unstructured uncertainty. The standard model-reference adaptive control can be used for systems with unstructured uncertainty using polynomial or neural network approximation. Unlike the least-squares adaptive control methods, boundedness of tracking error is guaranteed but boundedness of adaptive parameters cannot be mathematically guaranteed. This can lead to robustness issues with model-reference adaptive control, such as the well-known parameter drift problem. In general, least-squares adaptive control achieves better performance and robustness than model-reference adaptive control.

In many physical applications, there is no clear certainty about the structure between the input and output of a process. In systems with unstructured uncertainty, the mapping between the input and output is usually not known. Modeling systems with unstructured uncertainty require function approximation. Polynomial regression and neural networks are common methods for function approximation. Adaptive control of systems with unstructured uncertainty can be addressed with least-squares function approximation.

N.T. Nguyen, *Model-Reference Adaptive Control*, Advanced Textbooks in Control and Signal Processing, https://doi.org/10.1007/978-3-319-56393-0_7

In this chapter, the learning objectives are:

- To develop an understanding of function approximation using orthogonal polynomials such as Chebyshev polynomials and neural networks using sigmoidal and radial basis functions;
- To be able to apply least-squares methods for single-hidden layer neural network function approximation;
- To develop a working knowledge of using various least-squares direct and indirect adaptive control techniques for systems with unstructured uncertainty; and
- To recognize that the standard model-reference adaptive control is not robust for systems with unstructured uncertainty due to the possibility of unbounded adaptive parameters.

7.1 Polynomial Approximation by Least-Squares

Let $y(t) \in \mathbb{R}^n$ be the output of a process, expressed as

$$y = f(x) \tag{7.1}$$

where $x(t) \in \mathbb{R}^p$ is the input and $f(x) \in \mathbb{R}^n$ is an unknown function but assumed to be bounded function.

Any sufficiently smooth function $f(x) \in C^q$ can be expanded as a Taylor series about some $x = \bar{x}$

$$f(x) = f(\bar{x}) + \sum_{i=1}^{p} \frac{\partial f(\bar{x})}{\partial x_i}(x_i - \bar{x}_i) + \frac{1}{2}\sum_{i=1}^{p}\sum_{j=1}^{p} \frac{\partial f(\bar{x})}{\partial x_i x_j}(x_i - \bar{x}_i)(x_j - \bar{x}_j) + \cdots \tag{7.2}$$

$f(x)$ can be represented as

$$f(x) = \Theta^{*\top} \Phi(x) - \varepsilon^*(x) \tag{7.3}$$

where $\Theta^* \in \mathbb{R}^l \times \mathbb{R}^n$ is a matrix of constant but unknown coefficients, $\Phi(x) \in \mathbb{R}^l$ is a vector of regressors in terms of monomials of x

$$\Phi(x) = \left[1 \; x_1 \; x_2 \; \ldots \; x_p \; x_1^2 \; x_1 x_2 \; \ldots \; x_p^2 \; \ldots \; x_1^q \; x_1 x_2^{q-1} \; \ldots \; x_p^q\right] \tag{7.4}$$

and $\varepsilon^*(x)$ is a function approximation error which depends on x.

$f(x)$ is approximated by

$$\hat{y} = \Theta^\top \Phi(x) \tag{7.5}$$

where $\Theta(t) \in \mathbb{R}^l \times \mathbb{R}^n$ is the estimate of Θ^*.

Then, $\hat{y}(t) \to f(x)$ as $q \to \infty$. This means that any sufficiently smooth function can be approximated by a polynomial of q-th degree. Then, the function approximation error could be made sufficiently small on a compact domain of $x(t)$ such that $\sup_{x \in \mathscr{D}} \|\varepsilon^*(x)\| \leq \varepsilon_0^*$ for all $x(t) \in \mathscr{D} \subset \mathbb{R}^p$.

Another type of polynomials that can be used for function approximation is a class of orthogonal polynomials which form a true basis that spans a Hilbert inner product space with the following inner product definition:

$$\int_a^b w(x)\, p_i(x)\, p_j(x)\, dx = \delta_{ij} \tag{7.6}$$

where $\delta_{ij} = 1$ if $i = j$ and $\delta_{ij} = 0$ if $i \neq j$.

There are many orthogonal polynomial classes. The Chebyshev polynomials are one such polynomial class that is frequently used in function approximation. In particular, the first few Chebyshev polynomials of the first kind are shown as follows:

$$\begin{gathered} T_0(x) = 1 \\ T_1(x) = x \\ T_2(x) = 2x^2 - 1 \\ T_3(x) = 4x^3 - 3x \\ T_4(x) = 8x^4 - 8x^2 + 1 \\ \vdots \\ T_{n+1}(x) = 2xT_n(x) - T_{n-1}(x) \end{gathered} \tag{7.7}$$

One advantage of orthogonal polynomials over regular polynomials is that lower-degree orthogonal polynomials can provide a good function approximation with minimal loss of accuracy as compared to higher-degree regular polynomials [1, 2]. Thus, it is economical in function approximation to use the Chebyshev polynomials.

The coefficient vector Θ can be computed using various least-squares methods such as the batch least-squares, least-squares gradient method, or RLS method. Note that since $\Theta^\top \Phi(x)$ is an approximation of an unknown function $f(x)$, the approximation error will not be asymptotic regardless whether or not $\Phi(x)$ is PE.

Example 7.1 Approximate

$$y = \sin x + \cos 2x + e^{-x^2}$$

over a compact domain $x(t) \in [-1, 1]$, where $x(t) = \sin 10t$, with a 4^{th}-degree Chebyshev polynomial using the least-squares gradient method with $\Gamma_\Theta = 2I$ and $\Theta(0) = 0$.

The approximation results are shown in Fig. 7.1 for 1000 s which shows an excellent parameter convergence after only less than 100 s. The root mean square error is 3.8×10^{-4}.

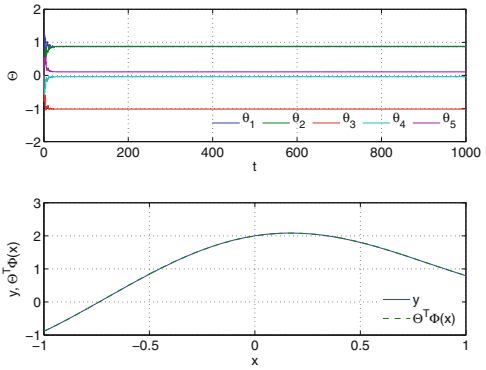

Fig. 7.1 Chebyshev polynomial approximation

7.2 Neural Network Approximation

Neural network is a concept pioneered in the 1960s in the artificial intelligence fields as an attempt to represent a simple model of how a human brain neuron connectivity works. Neural networks have been used in many applications such as classifiers, pattern recognition, function approximation, and adaptive control [1, 3–12]. The terminology "intelligent control" has been used loosely to describe adaptive control with neural networks. A neural network is a network of connectivity of neurons that form various layers of neurons to describe a complex input–output mapping. Figure 7.2 is a two-layer neural network that performs input–output mapping. A neural network with connectivity progressing from inputs to an output is called a feedforward neural network. A neural network with a closed-loop connectivity between some elements of the neural network is called a recurrent neural network.

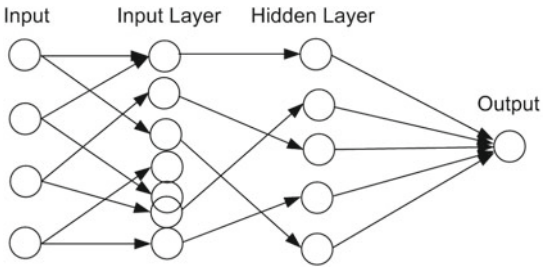

Fig. 7.2 Feedforward neural network

Feedforward neural networks have been shown to be capable of approximating a large class of nonlinear functions on a compact domain to within any specified accuracy. That is,

$$f(x) = \hat{f}(x) - \varepsilon^*(x) \tag{7.8}$$

such that $\sup_{x \in \mathscr{D}} \|\varepsilon^*(x)\| \leq \varepsilon_0$ for all $x \in \mathscr{D} \subset \mathbb{R}^n$.

Each neuron in a layer has two main components: a weighted summing junction and an activation function, which can be linear or, most commonly, nonlinear. Figure 7.3 illustrates a neuron with a set of inputs passing through an activation function to form a set of outputs.

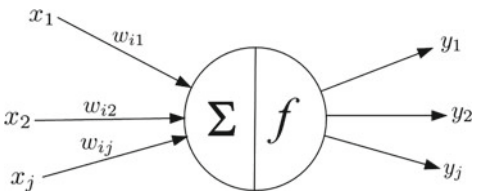

Fig. 7.3 Neuron and activation function

If $x(t) \in \mathbb{R}^p$ is an input to a neuron and $y(t) \in \mathbb{R}^n$ is an output of a neuron, then a neuron performs the following computation:

$$y = f\left(W^\top x + b\right) \tag{7.9}$$

where W is called a weight matrix and b is a constant vector called a bias vector.

Example 7.2 A second-degree polynomial regression can be represented by a neural network as follows:

The inputs are x^2, x, and 1, and the output is y as shown in Fig. 7.4. The activation function is linear, that is,

$$y = W^\top \Phi(x) = w_2 x^2 + w_1 x + w_0$$

where $\Phi(x)$ is the input function. ■

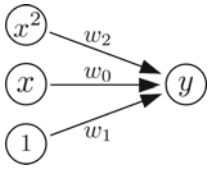

Fig. 7.4 Polynomial neural network representation

The most common activation functions are sigmoidal and radial basis functions (RBF) since these functions possess a universal approximation property, which

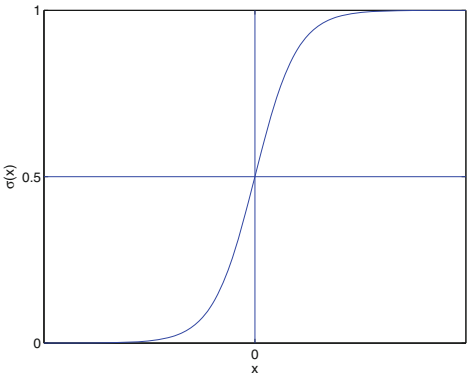

Fig. 7.5 Sigmoidal function

implies that any nonlinear function can be approximated by these functions. Note that a polynomial in some sense can be viewed as a universal approximator since any sufficiently smooth function can be represented by a Taylor series.

A sigmoidal function or also called a logistic function as shown in Fig. 7.5 is described by

$$\sigma(x) = \frac{1}{1 + e^{-ax}} \tag{7.10}$$

An unknown function can be approximated by a sigmoidal neural network as

$$\hat{y} = \hat{f}(x) = V^\top \sigma\left(W_x^\top x + W_0\right) + V_0 = \Theta^\top \Phi\left(W^\top \bar{x}\right) \tag{7.11}$$

where $V \in \mathbb{R}^m \times \mathbb{R}^n$ and $W_x \in \mathbb{R}^n \times \mathbb{R}^m$ are weight matrices, $W_0 \in \mathbb{R}^m$ and $V_0 \in \mathbb{R}^n$ are bias vectors, $\Theta^\top = \left[V_0 \; V^\top\right] \in \mathbb{R}^n \times \mathbb{R}^{m+1}$, $W^\top = \left[W_0 \; W_x^\top\right] \in \mathbb{R}^m \times \mathbb{R}^{n+1}$, $\bar{x} = \left[1 \; x^\top\right]^\top \in \mathbb{R}^{n+1}$, $\Phi\left(W^\top \bar{x}\right) = \left[1 \; \sigma^\top\left(W^\top \bar{x}\right)\right]^\top \in \mathbb{R}^{m+1}$, and $\sigma\left(W^\top \bar{x}\right) = \left[\sigma\left(W_1^\top \bar{x}\right) \; \sigma\left(W_2^\top \bar{x}\right) \ldots \sigma\left(W_m^\top \bar{x}\right)\right]^\top \in \mathbb{R}^m$, where $W_j \in \mathbb{R}^{n+1}$, $j = 1, \ldots, m$ are column vectors of W.

A radial basis function (RBF), more commonly known as a Gaussian normal distribution or "bell-shaped" curve as shown in Fig. 7.6, is given by

$$\psi(x) = e^{-ax^2} \tag{7.12}$$

An unknown function can be approximated by an RBF neural network as

$$\hat{y} = \hat{f}(x) = V^\top \psi\left(W_x^\top x + W_0\right) + V_0 = \Theta^\top \Phi\left(W^\top \bar{x}\right) \tag{7.13}$$

As with a linear regression, the coefficients of a neural network can be estimated from the input–output data. The process of estimation is called "training" or "teaching" a neural network. This is essentially a least-squares estimation. A "pre-trained"

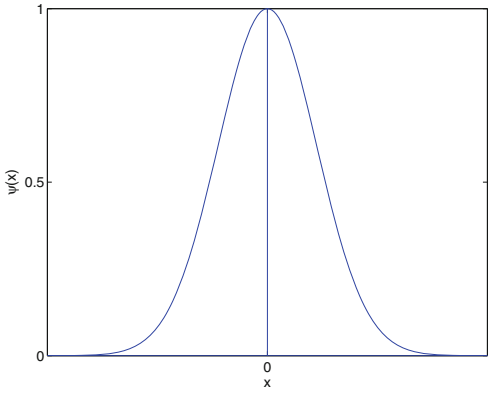

Fig. 7.6 Radial basis function

or "off-line" neural network is one whose coefficients are estimated a priori from data or model information. An "on-line learning" neural network is one whose coefficients are recursively estimated usually from a gradient method such as "back propagation" in real time.

Consider a sigmoidal neural network approximation. The gradient method can be applied to derive least-squares learning laws for a neural network to minimize the following cost function:

$$J = \frac{1}{2}\varepsilon^\top \varepsilon = \frac{1}{2}\left[\Theta^\top \Phi\left(W^\top \bar{x}\right) - y\right]^\top \left[\Theta^\top \Phi\left(W^\top \bar{x}\right) - y\right] \tag{7.14}$$

Taking the partial derivatives of J with respect to the weight matrices and bias vectors yields

$$\nabla J_\Theta = \frac{\partial J^\top}{\partial \Theta^\top} = \frac{\partial \varepsilon}{\partial \Theta^\top}\varepsilon^\top = \Phi\left(W^\top \bar{x}\right)\varepsilon^\top \tag{7.15}$$

$$\nabla J_W = \frac{\partial J}{\partial W} = \frac{\partial\left(W^\top \bar{x}\right)}{\partial W^\top}\varepsilon^\top \frac{\partial \varepsilon}{\partial\left(W^\top \bar{x}\right)} = \bar{x}\varepsilon^\top V^\top \sigma'\left(W^\top \bar{x}\right) \tag{7.16}$$

where $\sigma'\left(W^\top \bar{x}\right) = \text{diag}\left(\sigma'\left(W_1^\top \bar{x}\right), \sigma'\left(W_2^\top \bar{x}\right), \ldots, \sigma'\left(W_m^\top \bar{x}\right)\right)$ is a diagonal matrix with

$$\sigma'(x) = \frac{ae^{-ax}}{(1+e^{-ax})^2} \tag{7.17}$$

Then, the least-squares gradient learning laws for the neural network are given by

$$\dot{\Theta} = -\Gamma_\Theta \Phi\left(W^\top \bar{x}\right)\varepsilon^\top \tag{7.18}$$

$$\dot{W} = -\Gamma_W \bar{x}\varepsilon^\top V^\top \sigma'\left(W^\top \bar{x}\right) \tag{7.19}$$

Example 7.3 Consider Example 7.1. Approximate

$$y = \sin x + \cos 2x + e^{-x^2}$$

over a compact domain $x\,(t) \in [-1, 1]$, where $x\,(t) = \sin 10t$.

$y\,(t)$ is approximated by the following sigmoidal neural network:

$$\hat{y} = v_0 + v_1\sigma\left(w_{0_1} + w_1 x\right) + v_2\sigma\left(w_{0_2} + w_2 x\right) + v_3\sigma\left(w_{0_3} + w_3 x\right)$$

$$\Theta = \begin{bmatrix} v_0 \\ v_1 \\ v_2 \\ v_3 \end{bmatrix},\ V = \begin{bmatrix} v_1 \\ v_2 \\ v_3 \end{bmatrix},\ W = \begin{bmatrix} w_{0_1} & w_{0_2} & w_{0_3} \\ w_1 & w_2 & w_3 \end{bmatrix}$$

$$\bar{x} = \begin{bmatrix} 1 \\ x \end{bmatrix},\ \Phi\left(W^\top x\right) = \begin{bmatrix} 1 \\ \sigma\left(w_{0_1} + w_1 x\right) \\ \sigma\left(w_{0_2} + w_2 x\right) \\ \sigma\left(w_{0_3} + w_3 x\right) \end{bmatrix},$$

$$\sigma'\left(W^\top \bar{x}\right) = \begin{bmatrix} \sigma'\left(w_{0_1} + w_1 x\right) & 0 & 0 \\ 0 & \sigma'\left(w_{0_2} + w_2 x\right) & 0 \\ 0 & 0 & \sigma'\left(w_{0_3} + w_3 x\right) \end{bmatrix}$$

Note that the initial conditions of $\Theta\,(t)$ and $W\,(t)$ are usually set by a random number generator. Otherwise, if they are zero, then $V\,(t)$ and $W\,(t)$ will have identical elements, that is, $v_1 = v_2 = v_3$, $w_{0_1} = w_{0_2} = w_{0_3}$, and $w_1 = w_2 = w_3$. For this example, let $\Gamma_\Theta = \Gamma_W = 10I$. The neural network approximation is shown in Fig. 7.7.

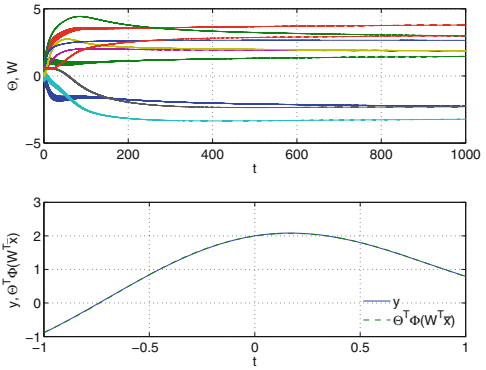

Fig. 7.7 Sigmoidal neural net approximation

Note that the neural network approximation converges much more slowly than the Chebyshev polynomial approximation in Example 7.1. Some of the neural network weights are still converging even after 1000 s. The root mean square error is 6.9×10^{-4} which is about twice that for the Chebyshev polynomial approximation. The neural network has ten weighting coefficients while the Chebyshev polynomial has only five coefficients.

7.3 Adaptive Control with Unstructured Uncertainty

Consider the following system with a matched unstructured uncertainty:

$$\dot{x} = Ax + B\left[u + f\left(x\right)\right] \tag{7.20}$$

where $x\left(t\right) \in \mathbb{R}^n$ is a state vector, $u\left(t\right) \in \mathbb{R}^m$ is a control vector, $A \in \mathbb{R}^n \times \mathbb{R}^n$ is a constant, but unknown matrix, $B \in \mathbb{R}^n \times \mathbb{R}^m$ with $n \leq m$ is a known matrix such that (A, B) is controllable, and $f\left(x\right) \in \mathbb{R}^m$ is a matched unstructured uncertainty.

The unknown function $f\left(x\right)$ can be approximated by a polynomial or any function that can be expressed as

$$f\left(x\right) = \Theta^{*\top} \Phi\left(x\right) - \varepsilon^*\left(x\right) \tag{7.21}$$

where $\Theta^* \in \mathbb{R}^l \times \mathbb{R}^m$ is an unknown constant ideal weight matrix, $\Phi\left(x\right) \in \mathbb{R}^l$ is a vector of orthogonal basis functions, and $\varepsilon^*\left(x\right) \in \mathbb{R}^m$ is the function approximation error.

Alternatively, the unknown function $f\left(x\right)$ can also be approximated by a neural network

$$f\left(x\right) = \Theta^{*\top} \Phi\left(W^{*\top} \bar{x}\right) - \varepsilon^*\left(x\right) \tag{7.22}$$

where $\Theta^* \in \mathbb{R}^{l+1} \times \mathbb{R}^m$ and $W^* \in \mathbb{R}^{n+1} \times \mathbb{R}^l$ are unknown constant ideal weight matrices, $\bar{x} = \left[1 \; x^\top\right]^\top \in \mathbb{R}^{n+1}$, $\Phi\left(W^{*\top} \bar{x}\right) = \left[1 \; \sigma^\top\left(W^\top \bar{x}\right)\right]^\top \in \mathbb{R}^{l+1}$.

$\varepsilon^*\left(x\right)$ can be made sufficiently small in a compact domain of $x\left(t\right)$ such that $\sup_{x \in \mathscr{D}} \left\|\varepsilon^*\left(x\right)\right\| \leq \varepsilon_0^*$ for all $x\left(t\right) \in \mathscr{D} \subset \mathbb{R}^n$ by a suitable selection of $\Phi\left(x\right)$ or $\Phi\left(W^{*\top} \bar{x}\right)$.

The objective is to design a full-state feedback in order for $x\left(t\right)$ to follow a reference model described by

$$\dot{x}_m = A_m x_m + B_m r \tag{7.23}$$

where $x_m\left(t\right) \in \mathbb{R}^n$ is a reference state vector, $A_m \in \mathbb{R}^n \times \mathbb{R}^n$ is known and Hurwitz, $B_m \in \mathbb{R}^n \times \mathbb{R}^q$ is known, and $r\left(t\right) \in \mathbb{R}^q \in \mathscr{L}_\infty$ is a piecewise continuous and bounded reference command vector.

7.3.1 Recursive Least-Squares Direct Adaptive Control with Matrix Inversion

We assume that there exist ideal control gains K_x^* and K_r^* that satisfy the model matching conditions

$$A + BK_x^* = A_m \tag{7.24}$$

$$BK_r^* = B_m \tag{7.25}$$

Let the adaptive controller be

$$u = K_x(t)x + K_r r - \Theta^\top \Phi(x) \tag{7.26}$$

where $K_r = K_r^*$ is known.

Let $\hat{A}(t)$ be an estimate of A, then

$$\hat{A}(t) = A_m - BK_x(t) \tag{7.27}$$

The closed-loop plant is expressed as

$$\dot{x} = \left(A_m - BK_x^*\right)x + B\left[K_x x + K_r r - \Theta^\top \Phi(x) + \Theta^{*\top}\Phi(x) - \varepsilon^*(x)\right] \tag{7.28}$$

Let $\tilde{K}_x(t) = K_x(t) - K_x^*$ and $\tilde{\Theta}(t) = \Theta(t) - \Theta^*$ be the estimation errors, then

$$\dot{x} = \left(A_m + B\tilde{K}_x\right)x + B_m r - B\tilde{\Theta}^\top \Phi(x) - B\varepsilon^* \tag{7.29}$$

Define a desired plant model as

$$\dot{x}_d = A_m x + B_m r \tag{7.30}$$

Then, formulate the plant modeling error as

$$\varepsilon = \dot{x}_d - \dot{x} = \hat{A}x + B\bar{u} - \dot{x} = -B\tilde{K}_x x + B\tilde{\Theta}^\top \Phi(x) + B\varepsilon^* \tag{7.31}$$

Let $\tilde{\Omega}^\top(t) = \left[-B\tilde{K}_x(t)\ B\tilde{\Theta}^\top(t)\right] \in \mathbb{R}^n \times \mathbb{R}^{n+l}$, and $\Psi(x) = \left[x^\top\ \Phi^\top(x)\right]^\top \in \mathbb{R}^{n+l}$. Then, the plant modeling error can be expressed as

$$\varepsilon = \tilde{\Omega}^\top \Psi(x) + B\varepsilon^* \tag{7.32}$$

The tracking error equation can be expressed in terms of the plant modeling error as

$$\dot{e} = \dot{x}_m - \dot{x} = \dot{x}_m - \dot{x}_d + \dot{x}_d - \dot{x} = A_m e + \varepsilon \tag{7.33}$$

The pure RLS adaptive laws are

$$\dot{\Omega} = -R\Psi(x)\,\varepsilon^{\top} \tag{7.34}$$

$$\dot{R} = -R\Psi(x)\,\Psi^{\top}(x)\,R \tag{7.35}$$

$K_x(t)$ and $\Theta(t)$ can be computed from $\Omega(t)$ as

$$\Omega = \begin{bmatrix} \Omega_1 \\ \Omega_2 \end{bmatrix} = \begin{bmatrix} -K_x^{\top} B^{\top} \\ \Theta B^{\top} \end{bmatrix} \Rightarrow \begin{bmatrix} K_x^{\top} \\ \Theta \end{bmatrix} = \begin{bmatrix} -\Omega_1 B^{-\top} \\ \Omega_2 B^{-\top} \end{bmatrix} \tag{7.36}$$

Note that $K_x(t)$ and $\Theta(t)$ require the matrix inverse B^{-1}. This sometimes can cause some issues which will be discussed later.

The estimation error equation for the RLS adaptive law is obtained as

$$\dot{\tilde{\Omega}} = -R\Psi(x)\left[\Psi^{\top}(x)\,\tilde{\Omega} + \varepsilon^{*\top} B^{\top}\right] \tag{7.37}$$

The RLS adaptive laws can be shown to result in a parameter convergence.

Proof Choose a Lyapunov candidate function

$$V\left(\tilde{\Omega}\right) = \text{trace}\left(\tilde{\Omega}^{\top} R^{-1} \tilde{\Omega}\right) \tag{7.38}$$

Then, $\dot{V}\left(\tilde{\Omega}\right)$ is evaluated as

$$\begin{aligned} \dot{V}\left(\tilde{\Omega}\right) &= \text{trace}\left(-2\underbrace{\tilde{\Omega}^{\top}\Psi(x)}_{\varepsilon - B\varepsilon^*}\varepsilon^{\top} + \underbrace{\tilde{\Omega}^{\top}\Psi(x)}_{\varepsilon - B\varepsilon^*}\underbrace{\Psi^{\top}(x)\,\tilde{\Omega}}_{\varepsilon^{\top} - \varepsilon^{*\top}B^{\top}}\right) \\ &= -2\varepsilon^{\top}\left(\varepsilon - B\varepsilon^*\right) + \left(\varepsilon^{\top} - \varepsilon^{*\top}B^{\top}\right)\left(\varepsilon - B\varepsilon^*\right) \\ &= -\varepsilon^{\top}\varepsilon + \varepsilon^{*\top}B^{\top}B\varepsilon^* \le -\|\varepsilon\|^2 + \|B\|^2\varepsilon_0^{*2} \\ &\le -\|\Psi(x)\|^2\left\|\tilde{\Omega}\right\|^2 + 2\|\Psi(x)\|\left\|\tilde{\Omega}\right\|\|B\|\,\varepsilon_0^* \end{aligned} \tag{7.39}$$

We see that $\dot{V}\left(\tilde{\Omega}\right) \le 0$ if $\|\varepsilon\| \ge \|B\|\,\varepsilon_0^*$ and $\left\|\tilde{\Omega}\right\| \ge \frac{2\|B\|\varepsilon_0^*}{\Psi_0}$ where $\Psi_0 = \|\Psi(x)\|$. Therefore, $\varepsilon(t) \in \mathscr{L}_\infty$, $\tilde{\Omega}(t) \in \mathscr{L}_\infty$, and $\Psi(x) \in \mathscr{L}_\infty$. We evaluate $\ddot{V}\left(\tilde{\Omega}\right)$ as

$$\begin{aligned}\ddot{V}\left(\tilde{\Omega}\right) &= -2\varepsilon^{\top}\dot{\varepsilon} = -2\varepsilon^{\top}\left[\dot{\tilde{\Omega}}^{\top}\Psi\left(x\right) + \tilde{\Omega}^{\top}\dot{\Psi}\left(x\right)\right] \\ &= -2\varepsilon^{\top}\left[-\varepsilon\Psi^{\top}\left(x\right)R\Psi\left(x\right) + \tilde{\Omega}^{\top}\dot{\Psi}\left(x\right)\right] \\ &= -2\varepsilon^{\top}\left[-\varepsilon\Psi^{\top}\left(x\right)\underbrace{\left[\int_{t_0}^{t}\Psi\left(x\right)\Psi^{\top}\left(x\right)d\tau\right]^{-1}}_{R}\Psi\left(x\right) + \tilde{\Omega}^{\top}\dot{\Psi}\left(x\right)\right]\end{aligned} \tag{7.40}$$

$\ddot{V}\left(\tilde{\Omega}\right)$ is bounded if $\Psi\left(x\right)$ satisfies the PE condition and $\dot{\Psi}\left(x\right) \in \mathscr{L}_{\infty}$. Applying the Barbalat's lemma, we conclude that $\|\varepsilon\| \rightarrow \|B\|\varepsilon_0^*$ and $\left\|\tilde{\Omega}\right\| \rightarrow \frac{2\|B\|\varepsilon_0^*}{\Psi_0}$ as $t \rightarrow \infty$. ■

The tracking error can now be shown to be uniformly ultimate bounded.

Proof Choose a Lyapunov candidate function

$$V\left(e, \tilde{\Omega}\right) = e^{\top}Pe + \mu\text{trace}\left(\tilde{\Omega}^{\top}R^{-1}\tilde{\Omega}\right) \tag{7.41}$$

with $\mu > 0$.
$\dot{V}\left(e, \tilde{\Omega}\right)$ is evaluated as

$$\begin{aligned}\dot{V}\left(e, \tilde{\Omega}\right) &= -e^{\top}Qe + 2e^{\top}P\varepsilon - \mu\varepsilon^{\top}\varepsilon + \mu\varepsilon^{*\top}B^{\top}B\varepsilon^{*} \\ &\leq -\lambda_{min}\left(Q\right)\|e\|^2 + 2\lambda_{max}\left(P\right)\|e\|\,\|\varepsilon\| - \mu\left[\left[\|\varepsilon\|\right]\right]^2 + \mu\|B\|^2\varepsilon_0^{*2}\end{aligned} \tag{7.42}$$

Using the inequality

$$2\lambda_{max}\left(P\right)\|e\|\,\|\varepsilon\| \leq \frac{\lambda_{max}^2(P)}{\delta^2}\|e\|^2 + \delta^2\|\varepsilon\|^2 \tag{7.43}$$

then $\dot{V}\left(e, \tilde{\Omega}\right)$ can be expressed as

$$\dot{V}\left(e, \tilde{\Omega}\right) \leq -\left[\lambda_{min}\left(Q\right) - \frac{\lambda_{max}^2\left(P\right)}{\delta^2}\right]\|e\|^2 - (\mu - \delta^2)\|\Psi(x)\|^2\|\tilde{\Omega}\|^2 + \mu\|B\|^2\varepsilon_0^{*2} \tag{7.44}$$

Thus, $\dot{V}\left(e, \tilde{\Omega}\right) \leq 0$ if $\frac{\lambda_{max}(P)}{\sqrt{\lambda_{min}(Q)}} < \delta < \sqrt{\mu}$ and is further bounded by

$$\dot{V}(e, \tilde{\Omega}) \leq -\left[\lambda_{min}(Q) - \frac{\lambda_{max}^2(P)}{\delta^2}\right]\|e\|^2 + \mu\|B\|^2\varepsilon_0^{*2} \tag{7.45}$$

Then, the largest lower bound of $\|e\|$ is obtained by letting $\dot{V}(e, \tilde{\Omega}) \leq 0$ as

$$\|e\| \geq \frac{\sqrt{\mu}\,\|B\|\,\varepsilon_0^*}{\sqrt{\lambda_{min}(Q) - \frac{\lambda_{max}^2(P)}{\delta^2}}} = p \tag{7.46}$$

Similarly, $\dot{V}\left(e, \tilde{\Omega}\right)$ is also bounded by

$$\dot{V}\left(e, \tilde{\Omega}\right) \leq -(\mu - \delta^2)\|\Psi(x)\|^2\|\tilde{\Omega}\|^2 + \mu\|B\|^2\varepsilon_0^{*2} \tag{7.47}$$

Then, the largest lower bound of $\left\|\tilde{\Omega}\right\|$ is obtained as

$$\left\|\tilde{\Omega}\right\| \geq \frac{\sqrt{\mu}\|B\|\varepsilon_0^*}{\Psi_0\sqrt{\mu - \delta^2}} = \alpha \tag{7.48}$$

Let $\mathscr{D}$ be a subset that contains all trajectories of $e(t)$ and $\tilde{\Omega}(t)$. Let $\mathscr{R}_\alpha \subset \mathscr{D}$ and $\mathscr{R}_\beta \subset \mathscr{D}$ be two subsets in $\mathscr{D}$ defined by the lower bounds and upper bounds of $\|e\|$ and $\left\|\tilde{\Omega}\right\|$, respectively, where

$$\mathscr{R}_\alpha = \left\{e(t) \in \mathbb{R}^n, \tilde{\Omega}(t) \in \mathbb{R}^{n+l} \times \mathbb{R}^n : \|e\| \leq p, \left\|\tilde{\Omega}\right\| \leq \alpha\right\} \tag{7.49}$$

$$\mathscr{R}_\beta = \left\{e(t) \in \mathbb{R}^n, \tilde{\Omega}(t) \in \mathbb{R}^{n+l} \times \mathbb{R}^n : \|e\| \leq \rho, \left\|\tilde{\Omega}\right\| \leq \beta\right\} \tag{7.50}$$

where ρ and β are the upper bounds of $\|e\|$ and $\left\|\tilde{\Omega}\right\|$, respectively.

Then, we see that $\dot{V}\left(e, \tilde{\Omega}\right) \leq 0$ for all $e(t) \in \mathscr{D} - \mathscr{R}_\alpha$, that is, a region outside $\mathscr{R}_\alpha$. Let $\mathscr{S}_\alpha$ be the smallest subset that encloses $\mathscr{R}_\alpha$ such that $\mathscr{R}_\alpha \subseteq \mathscr{S}_\alpha$. That is, $\mathscr{S}_\alpha$ is a hypersphere that circumscribes $\mathscr{R}_\alpha$ which is given by

$$\mathscr{S}_\alpha = \left\{e(t) \in \mathbb{R}^n, \tilde{\Omega}(t) \in \mathbb{R}^{n+l} \times \mathbb{R}^n : V\left(e, \tilde{\Omega}\right) \leq \lambda_{max}(P)\,p^2 + \mu\lambda_{max}\left(R^{-1}\right)\alpha^2\right\} \tag{7.51}$$

where $\lambda_{max}(R^{-1})$ is the largest eigenvalue of $R^{-1}(t)$ for all t.

Let $\mathscr{S}_\beta$ be the largest subset inside $\mathscr{R}_\beta$ that encloses $\mathscr{S}_\alpha$ such that $\mathscr{S}_\beta \subseteq \mathscr{R}_\beta$. That is, $\mathscr{S}_\beta$ is an inscribed hypersphere in $\mathscr{R}_\beta$ which is given by

$$\mathscr{S}_\beta = \left\{e(t) \in \mathbb{R}^n, \tilde{\Omega}(t) \in \mathbb{R}^{n+l} \times \mathbb{R}^n : V\left(e, \tilde{\Omega}\right) \leq \lambda_{min}(P)\,\rho^2 + \mu\lambda_{min}\left(R^{-1}\right)\beta^2\right\} \tag{7.52}$$

where $\lambda_{min}(R^{-1})$ is the smallest eigenvalue of $R^{-1}(t)$ for all t.

We see that $\mathscr{S}_\alpha \subseteq \mathscr{S}_\beta$. Then, the ultimate bound of $\|e\|$ can be found by setting $\mathscr{S}_\alpha = \mathscr{S}_\beta$ [13]. Thus,

$$\lambda_{min}(P)\rho^2 + \mu\lambda_{min}\left(R^{-1}\right)\beta^2 = \lambda_{max}(P)p^2 + \mu\lambda_{max}\left(R^{-1}\right)\alpha^2 \tag{7.53}$$

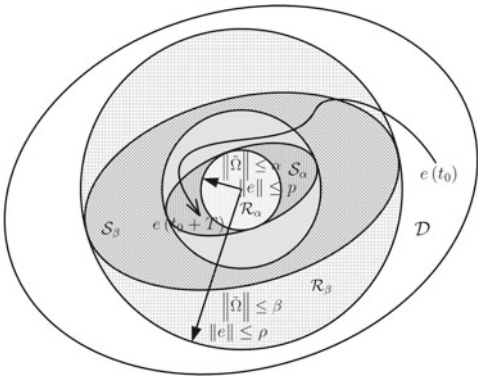

Fig. 7.8 Bounding sets for uniform ultimate boundedness

Since $\|e\| \le \rho$ and $\left\|\tilde{\Omega}\right\| \le \beta$ in $\mathscr{S}_\beta$, it follows that [13]

$$\lambda_{min}(P)\|e\|^2 \le \lambda_{max}(P)p^2 + \mu\lambda_{max}\left(R^{-1}\right)\alpha^2 \tag{7.54}$$

$$\mu\lambda_{min}\left(R^{-1}\right)\left\|\tilde{\Omega}\right\|^2 \le \lambda_{max}(P)p^2 + \mu\lambda_{max}\left(R^{-1}\right)\alpha^2 \tag{7.55}$$

Then, the ultimate bounds of $\|e\|$ and $\left\|\tilde{\Omega}\right\|$ are obtained as

$$\|e\| \le \sqrt{\frac{\lambda_{max}(P)p^2 + \mu\lambda_{max}\left(R^{-1}\right)\alpha^2}{\lambda_{min}(P)}} = \rho \tag{7.56}$$

$$\left\|\tilde{\Omega}\right\| \le \sqrt{\frac{\lambda_{max}(P)p^2 + \mu\lambda_{max}\left(R^{-1}\right)\alpha^2}{\mu\lambda_{min}\left(R^{-1}\right)}} = \beta \tag{7.57}$$

The bounding sets for uniform ultimate boundedness are illustrated in Fig. 7.8.

7.3.2 Modified Recursive Least-Squares Direct Adaptive Control without Matrix Inversion

In the RLS adaptive laws, the matrix inverse B^{-1} is used to compute the adaptive parameters $K(t)$ and $\Theta(t)$. This sometimes can cause issues when B^{-1} is small

or when $B \in \mathbb{R}^n \times \mathbb{R}^m$ with $n > m$. The RLS adaptive control can be modified to eliminate the need for thes matrix inversion of the B matrix in the case of $B \in \mathbb{R}^n \times \mathbb{R}^m$ with $n > m$.

Let $\tilde{\Omega}^\top (t) = \left[-\tilde{K}_x (t) \ \tilde{\Theta}^\top (t) \right] \in \mathbb{R}^m \times \mathbb{R}^{n+1}$ and $\Psi (x) = \left[x^\top \ \Phi^\top (x) \right]^\top \in \mathbb{R}^{n+l}$. Then, the plant modeling error can be expressed as

$$\varepsilon = B\tilde{\Omega}^\top \Psi (x) + B\varepsilon^* \tag{7.58}$$

The modified RLS adaptive laws are

$$\dot{\Omega} = -R\Psi (x) \varepsilon^\top B \tag{7.59}$$

$$\dot{R} = -\eta R\Psi (x) \Psi^\top (x) R \tag{7.60}$$

where $\eta > 0$ is an adjustment factor.

$K_x (t)$ and $\Theta (t)$ can be computed from $\Omega (t)$ as

$$\Omega = \begin{bmatrix} \Omega_1 \\ \Omega_2 \end{bmatrix} = \begin{bmatrix} -K_x^\top \\ \Theta \end{bmatrix} \Rightarrow \begin{bmatrix} K_x^\top \\ \Theta \end{bmatrix} = \begin{bmatrix} -\Omega_1 \\ \Omega_2 \end{bmatrix} \tag{7.61}$$

Note that $K_x (t)$ and $\Theta (t)$ no longer require the matrix inverse B^{-1}.

The estimation error equation for the modified RLS adaptive law is obtained as

$$\dot{\tilde{\Omega}} = -R\Psi (x) \left[\Psi^\top (x) \tilde{\Omega} + \varepsilon^{*\top} \right] B^\top B \tag{7.62}$$

The tracking error equation can be expressed in terms of the plant modeling error as

$$\dot{e} = \dot{x}_m - \dot{x} = \dot{x}_m - \dot{x}_d + \dot{x}_d - \dot{x} = A_m e + \varepsilon = A_m e + B\tilde{\Omega}^\top \Psi (x) + B\varepsilon^* \tag{7.63}$$

The RLS adaptive laws can be shown to result in a parameter convergence if $\eta < 2\lambda_{min} \left(B^\top B \right)$ as follows:

Proof Choose a Lyapunov candidate function

$$V \left(\tilde{\Omega} \right) = \text{trace} \left(\tilde{\Omega}^\top R^{-1} \tilde{\Omega} \right) \tag{7.64}$$

Then, $\dot{V} \left(\tilde{\Omega} \right)$ is evaluated as

$$\begin{aligned}\dot{V}\left(\tilde{\Omega}\right) &= \text{trace}\left(-2\tilde{\Omega}^{\top}\Psi\left(x\right)\varepsilon^{\top}B + \eta\tilde{\Omega}^{\top}\Psi\left(x\right)\Psi^{\top}\left(x\right)\tilde{\Omega}\right)\\ &= -2\varepsilon^{\top}B\tilde{\Omega}^{\top}\Psi\left(x\right) + \eta\Psi^{\top}\left(x\right)\tilde{\Omega}\tilde{\Omega}^{\top}\Psi\left(x\right)\\ &= -2\varepsilon^{\top}\varepsilon + 2\varepsilon^{\top}B\varepsilon^{*} + \eta\Psi^{\top}\left(x\right)\tilde{\Omega}\tilde{\Omega}^{\top}\Psi\left(x\right)\\ &\leq -2\left\|\varepsilon\right\|^{2} + 2\left\|B\right\|\left\|\varepsilon\right\|\varepsilon_{0}^{*} + \eta\left\|\Psi\left(x\right)\right\|^{2}\left\|\tilde{\Omega}\right\|^{2}\\ &\leq -\left[2\lambda_{min}\left(B^{\top}B\right) - \eta\right]\left\|\Psi\left(x\right)\right\|^{2}\left\|\tilde{\Omega}\right\|^{2} + 2\lambda_{max}\left(B^{\top}B\right)\left\|\Psi\left(x\right)\right\|\left\|\tilde{\Omega}\right\|\varepsilon_{0}^{*}\end{aligned} \tag{7.65}$$

Thus, $\dot{V}\left(\tilde{\Omega}\right) \leq 0$ if $\eta < 2\lambda_{min}\left(B^{\top}B\right)$ and $\left\|\tilde{\Omega}\right\| \geq \frac{c_1\varepsilon_0^*}{\Psi_0}$ where $c_1 = \frac{2\lambda_{max}\left(B^{\top}B\right)}{2\lambda_{min}\left(B^{\top}B\right)-\eta}$. We note that

$$\lambda_{min}\left(B^{\top}B\right)\left\|\Psi\left(x\right)\right\|^{2}\left\|\tilde{\Omega}\right\|^{2} \leq \left\|\varepsilon\right\|^{2} + 2\left\|B\right\|\left\|\varepsilon\right\|\varepsilon_{0}^{*} + \lambda_{max}\left(B^{\top}B\right)\varepsilon_{0}^{*2} \tag{7.66}$$

Therefore, $\dot{V}\left(\tilde{\Omega}\right)$ is also expressed in terms of $\left\|\varepsilon\right\|$ as

$$\begin{aligned}\dot{V}\left(\tilde{\Omega}\right) \leq &-\left[2 - \frac{\eta}{\lambda_{min}\left(B^{\top}B\right)}\right]\left\|\varepsilon\right\|^{2} + 2\left[1 + \frac{\eta}{\lambda_{min}\left(B^{\top}B\right)}\right]\left\|B\right\|\left\|\varepsilon\right\|\varepsilon_{0}^{*}\\ &+ \frac{\eta\lambda_{max}(B^{\top}B)}{\lambda_{min}(B^{\top}B)}\varepsilon_{0}^{*2} \leq 0\end{aligned} \tag{7.67}$$

which yields $\left\|\varepsilon\right\| \geq c_2\left\|B\right\|\varepsilon_0^*$ where $c_2 = \frac{\lambda_{min}\left(B^{\top}B\right)+\eta}{2\lambda_{min}\left(B^{\top}B\right)-\eta}\left[1 + \sqrt{1 + \frac{\eta\left[2\lambda_{min}\left(B^{\top}B\right)-\eta\right]}{\left[\lambda_{min}\left(B^{\top}B\right)+\eta\right]^{2}}}\right]$.

Therefore, $\varepsilon\left(t\right) \in \mathscr{L}_{\infty}$, $\tilde{\Omega}\left(t\right) \in \mathscr{L}_{\infty}$, and $\Psi\left(x\right) \in \mathscr{L}_{\infty}$. We evaluate $\ddot{V}\left(\tilde{\Omega}\right)$ as

$$\begin{aligned}\ddot{V}\left(\tilde{\Omega}\right) = &-2\left[\Psi^{\top}\left(x\right)\tilde{\Omega}\left(2B^{\top}B - \eta I\right) + \varepsilon^{*\top}B^{\top}B\right]\\ &\times\left[-B^{\top}\varepsilon\Psi^{\top}\left(x\right)\underbrace{\left[\int_{t_0}^{t}\Psi\left(x\right)\Psi^{\top}\left(x\right)d\tau\right]^{-1}}_{R}\Psi\left(x\right) + \tilde{\Omega}^{\top}\dot{\Psi}\left(x\right)\right]\end{aligned} \tag{7.68}$$

$\ddot{V}\left(\tilde{\Omega}\right)$ is bounded if $\Psi\left(x\right)$ satisfies the PE condition and $\dot{\Psi}\left(x\right) \in \mathscr{L}_{\infty}$. Applying the Barbalat's lemma, we conclude that $\left\|\varepsilon\right\| \to c_2\left\|B\right\|\varepsilon_0^*$ and $\left\|\tilde{\Omega}\right\| \to \frac{c_1\|B\|\varepsilon_0^*}{\Psi_0}$ as $t \to \infty$. ■

The tracking error can now be shown to be uniformly ultimately bounded.

Proof Choose a Lyapunov candidate function

$$V\left(e, \tilde{\Omega}\right) = e^{\top}Pe + \mu\,\text{trace}\left(\tilde{\Omega}^{\top}R^{-1}\tilde{\Omega}\right) \tag{7.69}$$

with $\mu > 0$.

$\dot{V}\left(e, \tilde{\Omega}\right)$ is evaluated as

$$\begin{aligned}\dot{V}\left(e, \tilde{\Omega}\right) &= -e^{\top} Qe + 2e^{\top} PB\tilde{\Omega}^{\top}\Psi\left(x\right) + 2e^{\top} PB\varepsilon^{*} \\ &\quad - 2\mu\varepsilon^{\top}\varepsilon + 2\mu\varepsilon^{\top} B\varepsilon^{*} + \mu\eta\Psi^{\top}\left(x\right)\tilde{\Omega}\tilde{\Omega}^{\top}\Psi\left(x\right) \\ &\quad \leq -\lambda_{min}\left(Q\right)\|e\|^{2} + 2\|PB\|\|e\|\|\Psi\left(x\right)\|\left\|\tilde{\Omega}\right\| + 2\|PB\|\|e\|\varepsilon_{0}^{*} \\ &\quad - \mu\left[2\lambda_{min}\left(B^{\top}B\right) - \eta\right]\|\Psi\left(x\right)\|^{2}\left\|\tilde{\Omega}\right\|^{2} \\ &\quad + 2\mu\lambda_{max}\left(B^{\top}B\right)\|\Psi\left(x\right)\|\left\|\tilde{\Omega}\right\|\varepsilon_{0}^{*} \end{aligned} \tag{7.70}$$

Using the inequality

$$2\|PB\|\|e\|\|\Psi\left(x\right)\|\left\|\tilde{\Omega}\right\| \leq \frac{\|PB\|^{2}}{\delta^{2}}\|e\|^{2} + \delta^{2}\|\Psi(x)\|^{2}\|\tilde{\Omega}\|^{2} \tag{7.71}$$

$\dot{V}\left(e, \tilde{\Omega}\right)$ is expressed as

$$\begin{aligned}\dot{V}\left(e, \tilde{\Omega}\right) &\leq -\left(\lambda_{min}(Q) - \frac{\|PB\|^{2}}{\delta^{2}}\right)\|e\|^{2} + 2\|PB\|\|e\|\varepsilon_{0}* \\ &\quad - \left\{\mu\left[2\lambda_{min}\left(B^{\top}B\right) - \eta\right] - \delta^{2}\right\}\|\Psi(x)\|^{2}\left\|\tilde{\Omega}\right\|^{2} \\ &\quad + 2\mu\lambda_{max}\left(B^{\top}B\right)\|\Psi(x)\|\left\|\tilde{\Omega}\right\|\varepsilon_{0}^{*} \end{aligned} \tag{7.72}$$

Thus, $\dot{V}\left(e, \tilde{\Omega}\right) \leq 0$ if $\frac{\|PB\|}{\sqrt{\lambda_{min}(Q)}} < \delta < \sqrt{\mu[2\lambda_{min}(B^{\top}B) - \eta]}$. Upon completing the square, we obtain

$$\dot{V}\left(e, \tilde{\Omega}\right) \leq -c_{1}\left(\|e\| - c_{2}\right)^{2} + c_{1}c_{2}^{2} - c_{3}\left(\|\Psi(x)\|^{2}\left\|\tilde{\Omega}\right\| - c_{4}\right)^{2} + c_{3}c_{4}^{2} \tag{7.73}$$

where $c_{1} = \lambda_{min}\left(Q\right) - \frac{\|PB\|^{2}}{\delta^{2}}$, $c_{2} = \frac{\|PB\|\varepsilon_{0}^{*}}{c_{1}}$, $c_{3} = \mu\left[2\lambda_{min}(B^{\top}B) - \eta\right] - \delta^{2}$, and $c_{4} = \frac{\mu\lambda_{max}(B^{\top}B)\varepsilon_{0}^{*}}{c_{3}}$.

Then, the largest lower bound of $\|e\|$ is obtained from

$$\dot{V}(e, \tilde{\Omega}) \leq -c_{1}(\|e\| - c_{2})^{2} + c_{1}c_{2}^{2} + c_{3}c_{4}^{2} \leq 0 \tag{7.74}$$

which yeilds

$$\|e\| \geq c_{2} + \sqrt{c_{2}^{2} + \frac{c_{3}c_{4}^{2}}{c_{1}}} = p \tag{7.75}$$

Similarly, the largest lower bound of $\left\|\tilde{\Omega}\right\|$ is obtained from

$$\dot{V}\left(e,\tilde{\Omega}\right) \leq -c_3\left(\|\Psi(x)\|^2\left\|\tilde{\Omega}\right\| - c_4\right)^2 + c_1c_2^2 + c_3c_4^2 \leq 0 \tag{7.76}$$

which yields

$$\left\|\tilde{\Omega}\right\| \geq \frac{c_4 + \sqrt{\frac{c_1c_2^2}{c_3} + c_4^2}}{\Psi_0} = \alpha \tag{7.77}$$

Thus, $\dot{V}\left(e,\tilde{\Omega}\right) \leq 0$ outside a compact set defined by $\mathscr{R}_\alpha = \left\{e\,(t) \in \mathbb{R}^n, \tilde{\Omega}\,(t) \in \mathbb{R}^{n+l} \times \mathbb{R}^n : \|e\| \leq p, \left\|\tilde{\Omega}\right\| \leq \alpha\right\}$. Therefore, the tracking error is uniformly ultimately bounded with the ultimate bound

$$\|e\| \leq \sqrt{\frac{\lambda_{max}(P)p^2 + \mu\lambda_{max}(R^{-1})\alpha^2}{\lambda_{min}(P)}} = \rho \tag{7.78}$$

■

Note that since $n > m$, then η can be made independent of the B matrix by scaling the modified RLS adaptive laws by the left pseudo-inverse as

$$\dot{\Omega} = -R\Psi\,(x)\,\varepsilon^\top B\left(B^\top B\right)^{-1} \tag{7.79}$$

Then, the estimation error equation for the scaled RLS adaptive law becomes

$$\dot{\tilde{\Omega}} = -R\Psi\,(x)\left[\Psi^\top\,(x)\,\tilde{\Omega} + \varepsilon\right] \tag{7.80}$$

A similar Lyapunov stability analysis can be performed to show that $0 \leq \eta < 2$, which is independent of B for the scaled RLS adaptive laws.

7.3.3 Least-Squares Gradient Direct Adaptive Control

Least-squares gradient adaptive laws can be designed to not require the use of the matrix inverse B^{-1}. The modified least-squares gradient adaptive laws are given by

$$\dot{K}_x^\top = \Gamma_x x\varepsilon^\top B \tag{7.81}$$

$$\dot{\Theta} = -\Gamma_\Theta\Phi\,(x)\,\varepsilon^\top B \tag{7.82}$$

Note the resemblance of least-squares gradient adaptive laws to MRAC, where the plant modeling error $\varepsilon(t)$ replaces the tracking error $e(t)$. The tracking error equation can be expressed in terms of the plant modeling error as

$$\dot{e} = A_m e + \varepsilon = A_m e - B\tilde{K}_x x + B\tilde{\Theta}^\top \Phi(x) + B\varepsilon^* \tag{7.83}$$

The parameter convergence and uniform ultimate boundedness can be established by the following proof:

Proof Choose a Lyapunov candidate function

$$V\left(\tilde{K}_x, \tilde{\Theta}\right) = \text{trace}\left(\tilde{K}_x \Gamma_x^{-1} \tilde{K}^\top\right) + \text{trace}\left(\tilde{\Theta}^\top \Gamma_\Theta^{-1} \tilde{\Theta}\right) \tag{7.84}$$

Then, $\dot{V}\left(\tilde{K}_x, \tilde{\Theta}\right)$ is evaluated as

$$\begin{aligned}\dot{V}\left(\tilde{K}_x, \tilde{\Theta}\right) &= \text{trace}\left(2\tilde{K}_x x\varepsilon^\top B\right) + \text{trace}\left(-2\tilde{\Theta}^\top \Phi(x)\varepsilon^\top B\right) \\ &= -2\varepsilon^\top\left[-B\tilde{K}_x x + B\tilde{\Theta}^\top \Phi(x)\right] \\ &= -2\varepsilon^\top\varepsilon + 2\varepsilon^\top B\varepsilon^* \le -2\|\varepsilon\|^2 + 2\|B\|\|\varepsilon\|\varepsilon_0^*\end{aligned} \tag{7.85}$$

We see that $\dot{V}\left(\tilde{K}_x, \tilde{\Theta}\right) \le 0$ if $\|\varepsilon\| \ge \|B\|\varepsilon_0^*$. If $\dot{\Psi}(x) \in \mathscr{L}_\infty$, then $\|\varepsilon\| \to \|B\|\varepsilon_0^*$ as $t \to \infty$.

For the tracking error, we use the Lyapunov candidate function

$$V\left(e, \tilde{K}_x, \tilde{\Theta}\right) = e^\top P e + \mu\,\text{trace}\left(\tilde{K}_x \Gamma_x^{-1} \tilde{K}^\top\right) + \mu\,\text{trace}\left(\tilde{\Theta}^\top \Gamma_\Theta^{-1} \tilde{\Theta}\right) \tag{7.86}$$

with $\mu > 0$.

Then, $\dot{V}\left(e, \tilde{K}_x, \tilde{\Theta}\right)$ is evaluated as

$$\begin{aligned}\dot{V}\left(e, \tilde{K}_x, \tilde{\Theta}\right) &= -e^\top Q e + 2e^\top P\varepsilon + \mu\,\text{trace}\left(2\tilde{K}_x x\varepsilon^\top B\right) + \mu\,\text{trace}\left(-2\tilde{\Theta}^\top \Phi(x)\varepsilon^\top B\right) \\ &= -e^\top Q e + 2e^\top P\varepsilon - 2\mu\varepsilon^\top\varepsilon + 2\mu\varepsilon^\top B\varepsilon^* \\ &\le -\lambda_{min}(Q)\|e\|^2 + 2\lambda_{max}(P)\|e\|\|\varepsilon\| - 2\mu\|\varepsilon\|^2 + 2\mu\|B\|\|\varepsilon\|\varepsilon_0^*\end{aligned} \tag{7.87}$$

Using the inequality

$$2\lambda_{max}(P)\|e\|\|\varepsilon\| \le \frac{\lambda_{max}^2(P)}{\delta^2}\|e\|^2 + \delta^2\|\varepsilon\|^2 \tag{7.88}$$

and completing the square, we obtain

$$\dot{V}\left(e, \tilde{K}_x, \tilde{\Theta}\right) \leq -\left[\lambda_{min}(Q) - \frac{\lambda_{max}^2(P)}{\delta^2}\right]\|e\|^2 - (2\mu - \delta^2)\left[\|\varepsilon\| - \frac{\mu\|B\|\varepsilon_0^*}{2\mu - \delta^2}\right]^2 + \frac{\mu^2\|B\|^2\varepsilon_0^{*2}}{(2\mu - \delta^2)} \tag{7.89}$$

Then, $\dot{V}\left(e, \tilde{K}_x, \tilde{\Theta}\right) \leq 0$ if $\frac{\lambda_{max}(P)}{\sqrt{\lambda_{min}(Q)}} < \delta < \sqrt{2\mu}$. The largest lower bounds of $\|e\|$ and $\|\varepsilon\|$ and then obtained as

$$\|e\| \geq \frac{\mu\,\|B\|\,\varepsilon_0^*}{\sqrt{(2\mu - \delta^2)\left[\lambda_{min}(Q) - \frac{\lambda_{max}^2(P)}{\delta^2}\right]}} = p \tag{7.90}$$

$$\|\varepsilon\| \geq \frac{2\mu\|B\|\varepsilon_0^*}{2\mu - \delta^2} = \alpha \tag{7.91}$$

Since $\dot{V}\left(e, \tilde{K}_x, \tilde{\Theta}\right) \leq 0$ outside a compact set, the closed-loop adaptive system is uniformly ultimately bounded.

Example 7.4 Consider a first-order system with unstructured uncertainty

$$\dot{x} = ax + b\,[u + f\,(x)]$$

where a and $f\,(x)$ are unknown, but $b = 1$. For simulation purposes, $a = 1$ and $f\,(x) = 0.2\left(\sin 2x + \cos 4x + e^{-x^2}\right)$.

The reference model is given by

$$\dot{x}_m = a_m x_m + b_m r$$

where $a_m = -1$, $b_m = 1$, and $r\,(t) = \sin t$.

Since $f\,(x)$ is unknown, a polynomial of q-degree is used to approximate $f\,(x)$ as

$$f\,(x) = a_0 + a_1 x + \cdots + a_q x^q - \varepsilon^*\,(x) = \Theta^{*\top}\Phi\,(x) - \varepsilon^*\,(x)$$

where a_i, $i = 0, 1, \ldots, q$ are constant unknown coefficients.

The adaptive controller is designed as

$$u = k_x\,(t)\,x + k_r r - \Theta^\top\,(t)\,\Phi\,(x)$$

where $k_x\,(t)$ and $\Theta\,(t)$ are computed by the least-squares gradient adaptive law as

$$\dot{\Omega} = \begin{bmatrix} \dot{k}_x \\ \dot{\Theta} \end{bmatrix} = -\Gamma \begin{bmatrix} -x\varepsilon b \\ \Phi\,(x)\,\varepsilon b \end{bmatrix}$$

with $\Omega(0) = 0$ and $\Gamma = I$, where

$$\varepsilon = \hat{a}x + b\bar{u} - \dot{x}$$

$$\hat{a} = a_m - bk_x$$

$$\bar{u} = k_x x + k_r r$$

The tracking error for $q = 1, 2, 3, 4$ is shown in Figs. 7.9 and 7.10. Note that the tracking error improves for $q \geq 2$. Even the tracking error improves, the function $f(x)$ does not seem to be well approximated as shown in Fig. 7.11. This is also due to $k_x(t)$ and $\Theta(t)$ not quite converging.

Now, suppose the Chebyshev orthogonal polynomials are used instead. Then,

$$f(x) = a_0 + a_1 T_1(x) + \cdots + a_q T_q(x) - \varepsilon^*(x) = \Theta^{*\top} \Phi(x) - \varepsilon^*(x)$$

The simulation results are as shown in Fig. 7.12. For $q = 1$, the result is the same as that for the regular polynomial. However, it can be seen that the tracking error significantly reduces for $q = 2$ with the Chebyshev polynomial and is even smaller than that for $q = 4$ with the regular polynomial. For $q = 4$, the Chebyshev polynomial approximation results in a very small tracking error. The parameter convergence of the Chebyshev polynomial coefficients is excellent for $q = 4$ as shown in Fig. 7.13. The unknown function is very well approximated by a fourth-degree Chebyshev polynomial as shown in Fig. 7.14.

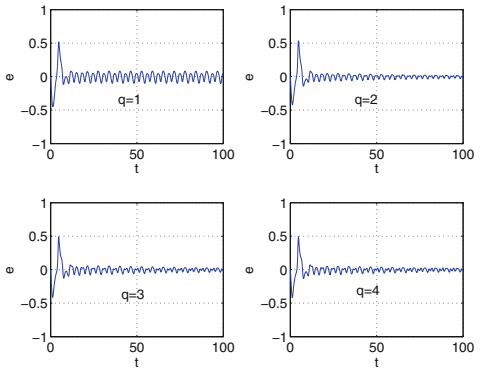

Fig. 7.9 Tracking error with regular q-th degree polynomial approximation

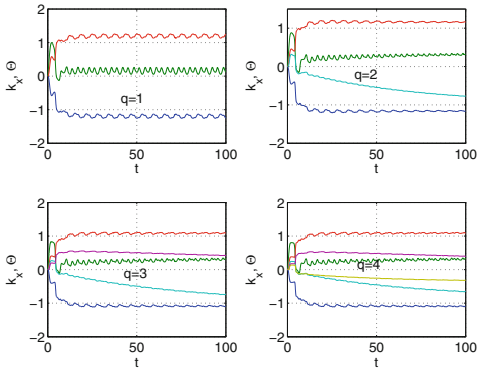

Fig. 7.10 k_x and Θ with regular q-th degree polynomial approximation

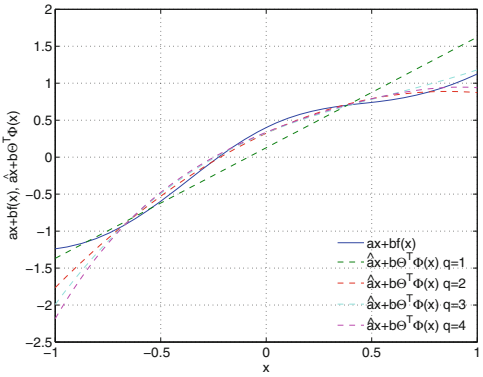

Fig. 7.11 Function approximation at $t = 100$ with regular q-th degree polynomial

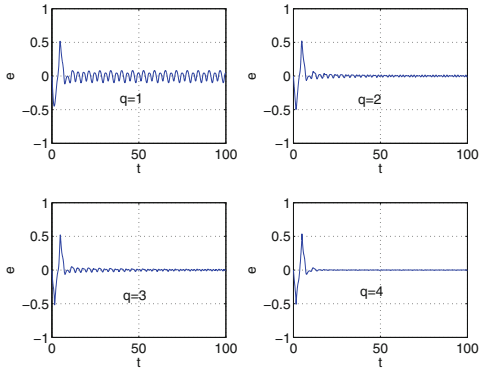

Fig. 7.12 Tracking error with Chebyshev q-th degree polynomial approximation

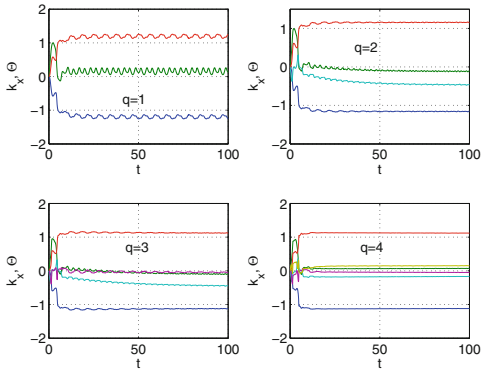

Fig. 7.13 k_x and Θ with Chebyshev q-th degree polynomial approximation

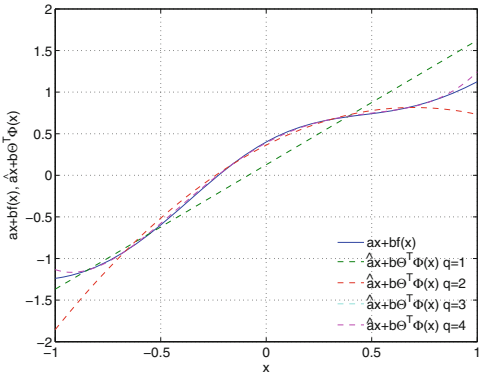

Fig. 7.14 Function approximation at $t = 100$ with Chebyshev q-th degree polynomial

7.3.4 Least-Squares Gradient Direct Adaptive Control with Neural Network Approximation

If $f(x)$ is approximated by a neural network, then the adaptive controller is expressed as

$$u = K_x(t)\,x + K_r r - \Theta^{\top}\Phi\left(W^{\top}\bar{x}\right) \tag{7.92}$$

Then, the plant modeling error is expressed as

$$\varepsilon = \dot{x}_d - \dot{x} = \hat{A}x + B\bar{u} - \dot{x} = -B\tilde{K}_x x + B\Theta^{\top}\Phi\left(W^{\top}\bar{x}\right) - B\Theta^{*\top}\Phi\left(W^{*\top}\bar{x}\right) + B\varepsilon^{*} \tag{7.93}$$

Utilizing the Taylor series expansion, this can be written as

$$\varepsilon = -B\tilde{K}_x x + B\Theta^\top \Phi\left(W^\top \bar{x}\right) - B\left(\Theta^\top - \tilde{\Theta}^\top\right) \times \left[\Phi\left(W^\top \bar{x}\right) + \Phi'\left(W^\top \bar{x}\right)\left(W^{*\top}\bar{x} - W^\top \bar{x}\right) + \cdots\right] + B\varepsilon^* \tag{7.94}$$

Combining the higher-order terms with the neural network approximation error $\varepsilon^*(x)$, then

$$\varepsilon = -B\tilde{K}_x x + B\tilde{\Theta}^\top \Phi\left(W^\top \bar{x}\right) + B\Theta^\top \Phi'\left(W^\top \bar{x}\right)\tilde{W}^\top \bar{x} + B\delta \tag{7.95}$$

where $\delta(x)$ is the combined approximation error due to the Taylor series truncation and the neural network approximation.

This becomes

$$\varepsilon = -B\tilde{K}_x x + B\tilde{\Theta}^\top \Phi\left(W^\top \bar{x}\right) + BV^\top \sigma'\left(W^\top \bar{x}\right)\tilde{W}^\top \bar{x} + B\delta \tag{7.96}$$

The least-squares gradient adaptive laws for $K_x(t)$, $\Theta(t)$, and $W(t)$ are then given by

$$\dot{K}_x^\top = \Gamma_x x \varepsilon^\top B \tag{7.97}$$

$$\dot{\Theta} = -\Gamma_\Theta \Phi\left(W^\top \bar{x}\right)\varepsilon^\top B \tag{7.98}$$

$$\dot{W} = -\Gamma_W \bar{x}\varepsilon^\top B V^\top \sigma'\left(W^\top \bar{x}\right) \tag{7.99}$$

We will examine the parameter convergence and uniform ultimate boundedness with the general least-squares gradient adaptive laws by performing the following proof:

Proof We choose a Lyapunov candidate function

$$V\left(\tilde{K}_x, \tilde{\Theta}, \tilde{W}\right) = \text{trace}\left(\tilde{K}\Gamma_x^{-1}\tilde{K}^\top\right) + \text{trace}\left(\tilde{\Theta}^\top \Gamma_\Theta^{-1}\tilde{\Theta}\right) + \text{trace}\left(\tilde{W}^\top \Gamma_W^{-1}\tilde{W}\right) \tag{7.100}$$

Then,

$$\begin{aligned}
\dot{V}\left(\tilde{K}_x, \tilde{\Theta}, \tilde{W}\right) &= 2\text{trace}\left(\tilde{K}_x x\varepsilon^\top B\right) + 2\text{trace}\left(-\tilde{\Theta}^\top \Phi\left(W^\top \bar{x}\right)\varepsilon^\top B\right) \\
&\quad + 2\text{trace}\left(-\tilde{W}^\top \bar{x}\varepsilon^\top B V^\top \sigma'\left(W^\top \bar{x}\right)\right) \\
&= 2\varepsilon^\top B\tilde{K}_x x - 2\varepsilon^\top B\tilde{\Theta}^\top \Phi\left(W^\top \bar{x}\right) - 2\varepsilon^\top BV^\top \sigma'\left(W^\top \bar{x}\right)\tilde{W}^\top \bar{x} \\
&= -2\varepsilon^\top \left[\underbrace{-B\tilde{K}_x x + B\tilde{\Theta}^\top \Phi\left(W^\top \bar{x}\right) + BV^\top \sigma'\left(W^\top \bar{x}\right)\tilde{W}^\top \bar{x}}_{\varepsilon - B\delta}\right] \\
&= -2\varepsilon^\top \varepsilon + 2\varepsilon^\top B\delta \leq -2\|\varepsilon\|^2 + 2\|B\|\|\varepsilon\|\delta_0
\end{aligned} \tag{7.101}$$

where $\sup_{x\in\mathscr{D}} \|\delta(x)\| \leq \delta_0$.

We see that $\dot{V}\left(\tilde{K}_x, \tilde{\Theta}, \tilde{W}\right) \leq 0$ if $\|\varepsilon\| \geq \|B\| \delta_0$. Therefore, $\varepsilon(t) \in \mathscr{L}_\infty$, $\tilde{K}_x(t) \in \mathscr{L}_\infty$, $\tilde{\Theta}(t) \in \mathscr{L}_\infty$, $\tilde{W}(t) \in \mathscr{L}_\infty$, $x(t) \in \mathscr{L}_\infty$, and $\Phi\left(W^\top \bar{x}\right) \in \mathscr{L}_\infty$. If $\dot{x}(t) \in \mathscr{L}_\infty$ and $\dot{\Phi}\left(W^\top \bar{x}\right) \in \mathscr{L}_\infty$, then using the Barbalat's lemma, we can show that $\|\varepsilon\| \to \|B\| \delta_0$ as $t \to \infty$. Note that we do not need to show for least-squares gradient adaptive laws that the PE condition must be satisfied in order for $\dot{V}\left(\tilde{K}_x, \tilde{\Theta}, \tilde{W}\right) \to 0$ as $t \to \infty$, but for exponential parameter convergence the PE condition is still required.

The tracking error behavior is now examined next. Choose a Lyapunov candidate function

$$V\left(e, \tilde{K}_x, \tilde{\Theta}, \tilde{W}\right) = e^\top P e + \mu \text{trace}\left(\tilde{K}_x \Gamma_x^{-1} \tilde{K}_x^\top\right) + \mu \text{trace}\left(\tilde{\Theta}^\top \Gamma_\Theta^{-1} \tilde{\Theta}\right) + \mu \text{trace}\left(\tilde{W}^\top \Gamma_W^{-1} \tilde{W}\right) \tag{7.102}$$

Then,

$$\begin{aligned} \dot{V}\left(e, \tilde{K}_x, \tilde{\Theta}, \tilde{W}\right) &= -e^\top Q e + 2e^\top P \varepsilon - 2\mu \varepsilon^\top \varepsilon + 2\mu \varepsilon^\top B \delta \\ &\leq -\lambda_{min}(Q) \|e\|^2 + 2\lambda_{max}(P) \|e\| \|\varepsilon\| - 2\mu \|\varepsilon\|^2 \\ &\quad + 2\mu \|B\| \|\varepsilon\| \delta_0 \end{aligned} \tag{7.103}$$

Using the results in Sect. 7.3.3, $\dot{V}\left(e, \tilde{K}_x, \tilde{\Theta}, \tilde{W}\right) \leq 0$ outside a compact set defined by the following lower bounds of $\|e\|$ and $\|\varepsilon\|$:

$$\|e\| \geq \frac{\mu \|B\| \delta_0}{\sqrt{(2\mu - \delta^2)\left[\lambda_{min}(Q) - \frac{\lambda_{max}^2(P)}{\delta^2}\right]}} = p \tag{7.104}$$

$$\|\varepsilon\| \geq \frac{2\mu \|B\| \delta_0}{2\mu - \delta^2} = \alpha \tag{7.105}$$

Therefore, the closed-loop adaptive system is uniformly ultimately bounded.

7.3.5 MRAC with Neural Network Approximation

By now, it can be seen that there are at least two approaches to adaptive control. One approach is based on the Lyapunov method which is the basis for MRAC and another approach is based on the least-squares adaptive control. The underlying principle of both the MRAC and the least-squares adaptive control is to reduce system uncertainty

by either parameter identification of parametric structured uncertainty or function approximation of unstructured uncertainty.

Consider the previous system with a matched unstructured uncertainty

$$\dot{x} = Ax + B\left[u + f\left(x\right)\right] \tag{7.106}$$

where the unknown function $f\left(x\right)$ is approximated by a linearly parametrized function

$$f\left(x\right) = \Theta^{*\top}\Phi\left(x\right) - \varepsilon^{*}\left(x\right) \tag{7.107}$$

Then, it can be shown that all the adaptive laws developed in Sects. 5.6 and 5.7 could be used to estimate Θ^{*} with some caveats as explained later. For example, if A and B are known, then Eq. (5.155) from Sect. 5.6.2 can be used to update $\Theta\left(t\right)$ as

$$\dot{\Theta} = -\Gamma\Phi\left(x\right)e^{\top}PB \tag{7.108}$$

Since A and B are known, assuming there exist constant control gain matrices K_x and K_r that satisfy the model matching conditions

$$A + BK_x = A_m \tag{7.109}$$

$$BK_r = B_m \tag{7.110}$$

then the adaptive controller is given by

$$u = K_x x + K_r r - \Theta^{\top}\left(t\right)\Phi\left(x\right) \tag{7.111}$$

where $\Theta\left(t\right) \in \mathbb{R}^{l} \times \mathbb{R}^{m}$ is the estimate of Θ^{*}.

The closed-loop plant model becomes

$$\dot{x} = \left(\underbrace{A + BK_x}_{A_m}\right)x + \underbrace{BK_r}_{B_m}r + B\left[-\Theta^{\top}\Phi\left(x\right) + \Theta^{*\top}\Phi\left(x\right) - \varepsilon^{*}\left(x\right)\right] \tag{7.112}$$

Let $\tilde{\Theta}\left(t\right) = \Theta\left(t\right) - \Theta^{*}$. The tracking error equation is obtained as

$$\dot{e} = \dot{x}_m - \dot{x} = A_m e + B\tilde{\Theta}^{\top}\Phi\left(x\right) + B\varepsilon^{*} \tag{7.113}$$

Proof Choose a Lyapunov candidate function

$$V\left(e, \tilde{\Theta}\right) = e^{\top}Pe + \text{trace}\left(\tilde{\Theta}^{\top}\Gamma^{-1}\tilde{\Theta}\right) \tag{7.114}$$

Then,

$$\begin{aligned}\dot{V}\left(e,\tilde{\Theta}\right) &= -e^{\top}Qe + 2e^{\top}P\left[B\tilde{\Theta}^{\top}\Phi\left(x\right) + B\varepsilon^{*}\right] - 2\text{trace}\left(\tilde{\Theta}^{\top}\Phi\left(x\right)e^{\top}PB\right)\\ &= -e^{\top}Qe + 2e^{\top}PB\left[\tilde{\Theta}^{\top}\Phi\left(x\right) + B\varepsilon^{*}\right] - 2e^{\top}PB\tilde{\Theta}^{\top}\Phi\left(x\right)\\ &= -e^{\top}Qe + 2e^{\top}PB\varepsilon^{*} \leq -\lambda_{min}\left(Q\right)\|e\|^{2} + 2\|PB\|\|e\|\varepsilon_{0}^{*} \end{aligned} \tag{7.115}$$

Thus, $\dot{V}\left(e,\tilde{\Theta}\right) \leq 0$ if

$$-\lambda_{min}\left(Q\right)\|e\|^{2} + 2\|PB\|\|e\|\varepsilon_{0}^{*} \leq 0 \Rightarrow \|e\| \geq \frac{2\|PB\|\varepsilon_{0}^{*}}{\lambda_{min}\left(Q\right)} = p \tag{7.116}$$

■

At a first glance, it may be tempted to conclude that the tracking error is uniformly ultimately bounded, but this conclusion would be incorrect since the tracking error is only bounded. The reason for the least-squares adaptive laws to result in a uniformly ultimately bounded tracking error is that any least-squares method guarantees that the approximation error is at least bounded. This implies that the parameter estimation error $\tilde{\Theta}\left(t\right)$ is also bounded. In addition, if the uncertainty is structured and the basis function is PE, then the parameter estimation error tends to zero, which implies a parameter convergence. If both the tracking error and parameter estimation error can be shown to be bounded, then the system is uniformly ultimately bounded.

For MRAC, the condition for $\dot{V}\left(e,\tilde{\Theta}\right) \leq 0$ in Eq. (7.116) does not say anything about the parameter estimation error $\tilde{\Theta}\left(t\right)$. Let

$$B_{r} = \left\{e\left(t\right) \in \mathbb{R}^{n} : \|e\| \leq p\right\} \tag{7.117}$$

Since B_r does not contain any information on $\tilde{\Theta}\left(t\right)$, B_r is an open set with $\tilde{\Theta}\left(t\right)$ free to grow inside B_r as illustrated in Fig. 7.15. A trajectory of $\left(e\left(t\right),\tilde{\Theta}\left(t\right)\right)$ may go outside of B_r, but $\dot{V}\left(e,\tilde{\Theta}\right) \leq 0$ is outside of B_r, so the trajectory will go back

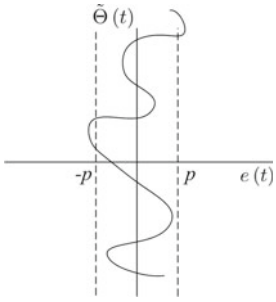

Fig. 7.15 Trajectory of MRAC with unstructured uncertainty

toward B_r. However, if $\tilde{\Theta}(t)$ grows too large inside B_r, the small approximation error assumption may be violated. Consequently, the boundary of B_r may also grow and therefore $e(t)$ can also grow. The possibility of a parameter drift that can lead to a point where the system becomes unstable may exist when an adaptive law does not provide a mathematically guaranteed bound on adaptive parameters. As a result, the standard MRAC as developed in Chap. 5 for systems with unstructured uncertainty is non-robust. Instability due to a parameter drift when adaptive parameters are not bounded is a well-known issue with adaptive control. In this regard, least-squares adaptive control offers an advantage over the standard MRAC since the adaptive parameters are bounded. Robust modification of MRAC is another way to address this issue. In summary, it is generally not a good practice to use the standard MRAC for systems with unstructured uncertainty.

Example 7.5 Consider Example 7.4. The MRAC laws are given by

$$\dot{k}_x = \gamma_x x e b$$

$$\dot{\Theta} = -\Gamma_\Theta \Phi(x) e b$$

where $e(t) = x_m(t) - x(t)$, $\gamma_x = 1$, and $\Gamma_\Theta = I$.

Let $\Phi(x)$ be a vector of the basis Chebyshev polynomials up to $T_4(x)$. The simulation results are shown in Figs. 7.16, 7.17, and 7.18.

Comparing to Figs. 7.12, 7.13, and 7.14, the tracking error is not as good with the MRAC laws as with the least-squares gradient adaptive laws. The parameters $k_x(t)$ and $\Theta(t)$ are more oscillatory and do not converge. For some reason, the second-degree Chebyshev polynomial produces the best tracking for the MRAC laws. The function approximation by the MRAC laws is poorer than that by the least-squares gradient method. This is not surprising since MRAC is not intended to be a parameter identification method. Its sole purpose is to reduce the tracking error. ■

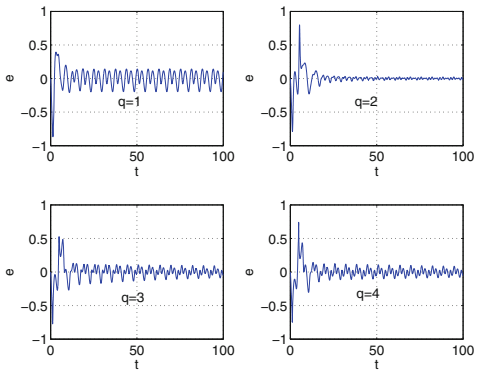

Fig. 7.16 Direct MRAC with Chebyshev fourth-degree polynomial

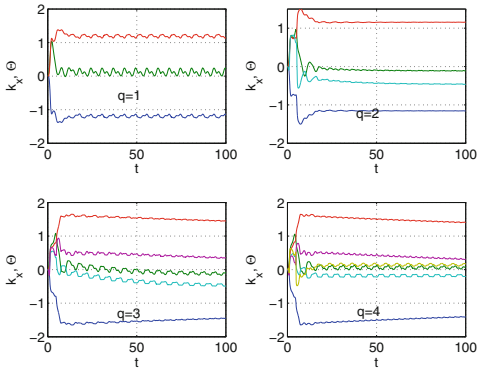

Fig. 7.17 k_x and Θ with Chebyshev q-th degree polynomial approximation

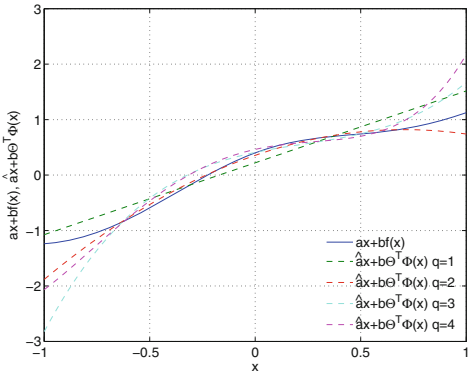

Fig. 7.18 Function approximation at $t = 100$ with Chebyshev q-th degree polynomial

Now, consider neural network MRAC when $f(x)$ is approximated by a neural network. The adaptive controller is then modified as

$$u = K_x x + K_r r - \Theta^\top \Phi\left(W^\top \bar{x}\right) \tag{7.118}$$

The tracking error equation is obtained as

$$\dot{e} = A_m e + B\tilde{\Theta}^\top \Phi\left(W^\top \bar{x}\right) + BV^\top \sigma'\left(W^\top \bar{x}\right)\tilde{W}^\top \bar{x} + B\delta \tag{7.119}$$

Proof Choose a Lyapunov candidate function

$$V\left(e, \tilde{\Theta}, \tilde{W}\right) = e^\top Pe + \text{trace}\left(\tilde{\Theta}^\top \Gamma_\Theta^{-1}\tilde{\Theta}\right) + \text{trace}\left(\tilde{W}^\top \Gamma_W^{-1}\tilde{W}\right) \tag{7.120}$$

Differentiating $V\left(e, \tilde{\Theta}, \tilde{W}\right)$ yields

$$\dot{V}\left(e, \tilde{\Theta}, \tilde{W}\right) = -e^{\top} Q e + 2e^{\top} P\left[B\tilde{\Theta}^{\top}\Phi\left(W^{\top}\bar{x}\right) + BV^{\top}\sigma'\left(W^{\top}\bar{x}\right)\tilde{W}^{\top}\bar{x} + B\delta\right] + 2\text{trace}\left(\tilde{\Theta}^{\top}\Gamma_{\Theta}^{-1}\dot{\tilde{\Theta}}\right) + 2\text{trace}\left(\tilde{W}^{\top}\Gamma_{W}^{-1}\dot{\tilde{W}}\right) \tag{7.121}$$

Note that

$$e^{\top} PB\tilde{\Theta}^{\top}\Phi\left(W^{\top}\bar{x}\right) = \text{trace}\left(\tilde{\Theta}^{\top}\Phi\left(W^{\top}\bar{x}\right)e^{\top} PB\right) \tag{7.122}$$

$$e^{\top} PBV^{\top}\sigma'\left(W^{\top}\bar{x}\right)\tilde{W}^{\top}\bar{x} = \text{trace}\left(\tilde{W}^{\top}\bar{x}e^{\top} PBV^{\top}\sigma'\left(W^{\top}\bar{x}\right)\right) \tag{7.123}$$

Hence,

$$\dot{V}\left(e, \tilde{\Theta}, \tilde{W}\right) = -e^{\top} Q e + 2e^{\top} PB\delta + 2\text{trace}\left(\tilde{\Theta}^{\top}\left[\Phi\left(W^{\top}\bar{x}\right)e^{\top} PB + \Gamma_{\Theta}^{-1}\dot{\tilde{\Theta}}\right]\right) + 2\text{trace}\left(\tilde{W}^{\top}\left[\bar{x}e^{\top} PBV^{\top}\sigma'\left(W^{\top}\bar{x}\right) + \Gamma_{W}^{-1}\dot{\tilde{W}}\right]\right) \tag{7.124}$$

Setting the trace terms to zero yields the neural network adaptive laws

$$\dot{\Theta} = -\Gamma_{\Theta}\Phi\left(W^{\top}\bar{x}\right)e^{\top} PB \tag{7.125}$$

$$\dot{W} = -\Gamma_{W}\bar{x}e^{\top} PBV^{\top}\sigma'\left(W^{\top}\bar{x}\right) \tag{7.126}$$

Then,

$$\dot{V}\left(e, \tilde{\Theta}, \tilde{W}\right) = -e^{\top} Q e + 2e^{\top} PB\bar{\varepsilon} \leq -\lambda_{min}(Q)\|e\| + 2\|PB\|\|e\|\delta_0 \tag{7.127}$$

Therefore, $\dot{V}\left(e, \tilde{\Theta}, \tilde{W}\right) \leq 0$ if

$$\|e\| \geq \frac{2\|PB\|\delta_0}{\lambda_{min}(Q)} = p \tag{7.128}$$

As discussed previously, stability of the tracking error cannot be guaranteed due to the potential for a parameter drift. However, since the neural network activation function is a bounded function; therefore, in comparison with other types of function approximation, neural network MRAC tends to be more robust than the standard MRAC.

Example 7.6 Consider Example 7.4. $f(x)$ is to be approximated by a neural network. The MRAC neural network adaptive laws are given by

$$\dot{k}_x = \gamma_x xeb$$

$$\dot{\Theta} = -\Gamma_{\Theta} \Phi \left(W^{\top} \bar{x} \right) eb$$

$$\dot{W} = -\Gamma_{W} \bar{x} eb V^{\top} \sigma' \left(W^{\top} \bar{x} \right)$$

where $\Theta(t) \in \mathbb{R}^5$, $W(t) \in \mathbb{R}^2 \times \mathbb{R}^4$ and $\Gamma_{\Theta} = \Gamma_W = 10I$. The initial conditions are given by

$$\Theta(0) = \begin{bmatrix} -0.2 \\ -0.1 \\ 0 \\ 0.1 \\ -0.2 \end{bmatrix}, \; W(0) = \begin{bmatrix} 0 & 0.1 & 0.2 & 0.3 \\ -0.3 & -0.2 & -0.1 & 0 \end{bmatrix}$$

The neural network topology is shown in Fig. 7.19. The simulation results are shown in Fig. 7.20.

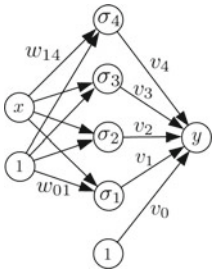

Fig. 7.19 Neural network topology

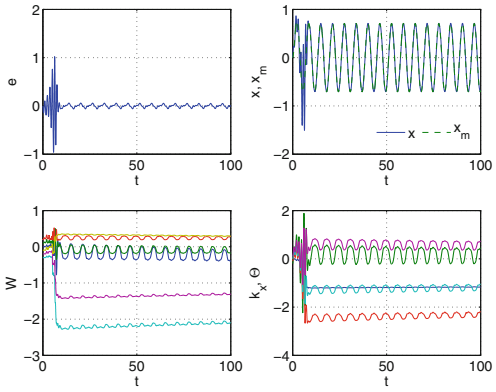

Fig. 7.20 Neural net adaptive control system response

The neural network adaptive control appears to reduce the tracking error a bit better than the direct MRAC with Chebyshev polynomial approximation. However, there is a large transient at the beginning. This is probably due to the initial conditions of $\Theta(t)$ and $W(t)$ being chosen arbitrarily, and the poor initial approximation that causes the tracking error to grow before the learning becomes effective in reducing the tracking error. The neural network adaptive control does not seem to perform as well as the least-squares gradient method with the Chebyshev polynomials. ■

In the context of least-squares adaptive control, the plant modeling error $\varepsilon(t)$ represents a modeling error between the true plant and the desired plant. Modeling errors in dynamical systems usually arise from the presence of system uncertainty. In model-reference adaptive control, the tracking error $e(t)$ is exclusively used as a control signal to drive the adaptation so as to cancel out undesired effects of system uncertainty on closed-loop systems. Philosophically, the tracking error is a manifestation of the plant modeling error which in turn is a direct consequence of the system uncertainty. Thus, the tracking error is a result of the plant modeling error, but not vice versa. One can separate control and system identification as two related dynamical actions. A control action is generally designed to reduce the tracking error to ensure that a closed-loop system follows a reference model as closely as possible. The objective of adaptive control is not so much to estimate the uncertainty itself but rather to achieve a desired reference model, regardless whether or not a parameter convergence is achieved. Example 7.5 clearly demonstrates that model-reference adaptive control does a rather poor job on parameter estimation even with the Chebyshev polynomials.

On the other hand, a system identification action uses the plant modeling error to estimate the uncertainty directly by least-squares estimation methods. The goal of a system identification is first and foremost to achieve a parameter convergence. The system identification action can achieve a better parameter convergence than MRAC. System identification is usually performed in an open-loop process without directly influencing a control action. Both the system identification and control can also be combined together to provide a very effective adaptation strategy. Using parameter estimates, least-squares adaptive control can be formulated to cancel out effects of system uncertainty by feeding back the parameter estimates into an adaptive control law. In so doing, least-squares adaptive control achieves bounded tracking and bounded adaptive parameters, whereas MRAC can only achieve bounded tracking.

7.4 Summary

In many physical applications, there is no clear certainty about the structure between the input and output of a process. In systems with unstructured uncertainty, the mapping between the input and output is usually not known. Polynomial approximation by least-squares methods is a well-known regression method. Regular polynomials are frequently used in least-squares data regression. Other types of polynomials can

also be used. One class of polynomials that can offer better function approximation over the regular polynomials is orthogonal polynomials. Orthogonal polynomials form true basis functions that span the Euclidean space. In particular, the Chebyshev orthogonal polynomials are generally considered to be optimal that can accurately approximate real-valued functions with the smallest degree for the same accuracy as a regular polynomial approximation.

Neural networks have been used in many applications such as classifiers, pattern recognition, function approximation, and adaptive control. A neural network is a nonlinear function approximation that models a complex input–output nonlinear mapping. Two basic types of neural networks are discussed: sigmoidal or logistic functions and radial basis functions. Various adaptive control methods for unstructured uncertainty are presented. Both least-squares and model-reference adaptive control with polynomial and neural network function approximation are shown to be able to handle adaptive control systems with unstructured uncertainty. Least-squares adaptive control, in general, exhibits better performance and robustness than MRAC. Robustness of least-squares adaptive control is achieved through the natural parameter identification process which ensures parameter boundedness, whereas MRAC cannot guarantee boundedness of adaptive parameters. This leads to robustness issues, such as a parameter drift.

7.5 Exercises

1. Approximate
$$y = 0.1 \sin 0.4x + \cos^2 2x$$
where $x(t) = \sin t$ for $t \in [0, 60]$, by a fourth-degree Chebyshev polynomial using the least-squares gradient method with $\Gamma = 100I$ and $\Delta t = 0.001$. Initialize $\Theta(t)$ with zero. Plot $\Theta(t)$ versus t. Plot $y(t)$ and $\hat{y}(t)$ versus $x(t)$ on the same plot. Compute the root mean square error between $y(t)$ and $\hat{y}(t)$.
2. Implement a sigmoidal neural network
$$\hat{y} = \hat{f}(x) = V^\top \sigma\left(W_x^\top x + W_0\right) + V_0 = \Theta^\top \Phi\left(W^\top \bar{x}\right)$$
where
$$\sigma(x) = \frac{1}{1 + e^{-x}}$$
to approximate $y(t)$ in Exercise 7.1 with $\Theta(t) \in \mathbb{R}^5$, $W(t) \in \mathbb{R}^2 \times \mathbb{R}^4$ and $\Gamma_\Theta = \Gamma_W = 100I$ and $\Delta t = 0.001$. The initial conditions $\Theta(0)$ and $W(0)$ are to be generated by a random number generator. Plot $\Theta(t)$ and $W(t)$ versus t. Plot $y(t)$ and $\hat{y}(t)$ versus $x(t)$ on the same plot. Compute the root mean square error between $y(t)$ and $\hat{y}(t)$.
3. Consider a first-order system with a matched unstructured uncertainty

$$\dot{x} = ax + b\left[u + f\left(x\right)\right]$$

where a and $f\left(x\right)$ are unknown, but $b = 2$. For simulation purposes, $a = 1$ and $f\left(x\right) = 0.1\sin 0.4x + \cos^2 2x$.
The reference model is given by

$$\dot{x}_m = a_m x_m + b_m r$$

where $a_m = -1$, $b_m = 1$, and $r\left(t\right) = \sin t$.
Implement in Simulink a direct adaptive control using a least-squares gradient method to approximate $f\left(x\right)$ by a 4^{th}-degree Chebyshev polynomial. All initial conditions are zero. Use $\Gamma = 0.2I$. Plot $e\left(t\right), x\left(t\right)$ versus $x_m\left(t\right), k_x\left(t\right)$, and $\Theta\left(t\right)$ for $t \in [0, 60]$.

References

1. Lee, T., & Jeng, J. (1998). The chebyshev-polynomials-based unified model neural networks for function approximation. *IEEE Transactions on Systems, Man, and Cybernetics, Part B: Cybernetics*, *28*(6), 925–935.
2. Mason, J., & Handscomb, D. (2002). *Chebyshev polynomials*. Boca Raton: Chapman and Hall/CRC.
3. Cybenko, G. (1989). Approximation by superpositions of a sigmoidal function. *Mathematics of Control Signals Systems*, *2*, 303–314.
4. Suykens, J., Vandewalle, J., & deMoor, B. (1996). *Artificial neural networks for modeling and control of non-linear systems*. Dordrecht: Kluwer Academic Publisher.
5. Wang, X., Huang, Y., & Nguyen, N. (2010). Robustness quantification of recurrent neural network using unscented transform. *Elsevier Journal of Neural Computing*, *74*(1–3).
6. Calise, A. J., & Rysdyk, R. T. (1998). Nonlinear adaptive flight control using neural networks. *IEEE Control System Magazine*, *18*(6), 1425.
7. Ishihara, A., Ben-Menahem, S., & Nguyen, N. (2009). Protection ellipsoids for stability analysis of feedforward neural-net controllers. In *International Joint Conference on Neural Networks*.
8. Johnson, E. N., Calise, A. J., El-Shirbiny, H. A., & Rysdyk, R. T. (2000). Feedback linearization with neural network augmentation applied to X-33 attitude control. *AIAA Guidance, Navigation, and Control Conference, AIAA-2000-4157*.
9. Kim, B. S., & Calise, A. J. (1997). Nonlinear flight control using neural networks. *Journal of Guidance, Control, and Dynamics*, *20*(1), 26–33.
10. Lam, Q., Nguyen, N., & Oppenheimer, M. (2012). Intelligent adaptive flight control using optimal control modification and neural network as control augmentation layer and robustness enhancer. In *AIAA Infotech@Aerospace Conference, AIAA-2012-2519*.
11. Lewis, F. W., Jagannathan, S., & Yesildirak, A. (1998). *Neural network control of robot manipulators and non-linear systems*. Boca Raton: CRC.
12. Zou, A., Kumar, K., & Hou, Z. (2010). Attitude control of spacecraft using chebyshev neural networks. *IEEE Transactions on Neural Networks*, *21*(9), 1457–1471.
13. Khalil, H. K. (2001). *Nonlinear systems*. Upper Saddle River: Prentice-Hall.

Chapter 8
Robustness Issues with Adaptive Control

Abstract This chapter discusses limitations and weaknesses of model-reference adaptive control. Parameter drift is the result of the lack of a mathematical guarantee of boundedness of adaptive parameters. Systems with bounded external disturbances under feedback control actions using model-reference adaptive control can experience a signal growth of a control gain or an adaptive parameter even though both the state and control signals remain bounded. This signal growth associated with the parameter drift can cause instability of adaptive systems. Model-reference adaptive control for non-minimum phase systems presents a major challenge. Non-minimum phase systems have unstable zeros in the right half plane. Such systems cannot tolerate large control gain signals. Model-reference adaptive control attempts to seek the ideal property of asymptotic tracking. In so doing, an unstable pole-zero cancelation occurs that leads to instability. For non-minimum phase systems, adaptive control designers generally have to be aware of the limiting values of adaptive parameters in order to prevent instability. Time-delay systems are another source of challenge for model-reference adaptive control. Many real systems have latency which results in a time delay at the control input. Time delay is caused by a variety of sources such as communication bus latency, computational latency, transport delay, etc. Time-delay systems are a special class of non-minimum phase systems. Model-reference adaptive control of time-delay systems is sensitive to the amplitude of the time delay. As the time delay increases, robustness of model-reference adaptive control decreases. As a consequence, instability can occur. Model-reference adaptive control is generally sensitive to unmodeled dynamics. In a control system design, high-order dynamics of internal states of the system sometimes are neglected in the control design. The neglected internal dynamics, or unmodeled dynamics, can result in loss of robustness of adaptive control systems. The mechanism of instability for a first-order SISO system with a second-order unmodeled actuator dynamics is presented. The instability mechanism can be due to the frequency of a reference command signal or an initial condition of an adaptive parameter that coincides with the zero phase margin condition. Fast adaptation is referred to the use of a large adaptation rate to achieve the improved tracking performance. An analogy of an integral control action of a linear time-invariant system is presented. As the integral control gain increases, the cross-over frequency of the closed-loop system increases. As a consequence, the phase margin or time-delay margin of the system decreases. Fast adaptation

N.T. Nguyen, *Model-Reference Adaptive Control*, Advanced Textbooks
in Control and Signal Processing, https://doi.org/10.1007/978-3-319-56393-0_8

of model-reference adaptive control is analogous to the integral control of a linear control system whereby the adaptation rate plays the equivalent role as the integral control gain. As the adaptation rate increases, the time-delay margin of an adaptive control system decreases. In the limit, the time-delay margin tends to zero as the adaptation rate tends to infinity. Thus, the adaptation rate has a strong influence on the closed-loop stability of an adaptive control system.

Model-reference adaptive control (MRAC) can be used in an adaptive control system to track a reference command signal by estimating directly the control gains or indirectly the adaptive parameters so as to cancel out the unwanted effect of the system uncertainty. Asymptotic tracking can be achieved if the uncertainty is structured. However, with unstructured uncertainty, MRAC is generally non-robust since the bounds on the adaptive parameters cannot be established by the Lyapunov stability analysis. Consequently, a parameter drift can result that can cause an adaptive control algorithm to blow up [1]. As the complexity of a plant increases, robustness of MRAC becomes increasingly difficult to ascertain. In practical applications, the knowledge of a real plant can never be established precisely. Thus, a model of a physical plant often cannot fully capture all the effects due to unmodeled dynamics, unstructured uncertainty, and exogenous disturbances that may exist in a real plant. All these effects can produce closed-loop dynamics that can lead to instability when MRAC is used in an adaptive controller [2]. Some of the causes of robustness issues with adaptive control are discussed in this chapter.

The learning objectives of this chapter are:

- To understand robustness issues with the parameter drift due to unbounded adaptive parameters in the presence of exogenous disturbances and unstructured uncertainty;
- To develop an understanding of and to know how to deal with the non-minimum phase behaviors due to unstable zeros that cause instability of closed-loop adaptive systems resulting from an unstable pole-zero cancellation;
- To be able to recognize and to deal with time-delay systems which can cause instability of closed-loop adaptive systems when adaptive parameters are permitted to be unconstrained;
- To understand robustness issues with unmodeled dynamics due to complex behaviors of systems which impose design constraints that adaptive control fails to account for; and
- To be familiar with the concept of fast adaptation which results in loss of robustness as the time-delay margin of a closed-loop adaptive system tends to zero.

8.1 Parameter Drift

Parameter drift is a consequence when the bound on an adaptive parameter cannot be established by the Lyapunov stability analysis. Consider a MIMO system with an unknown bounded disturbance

$$\dot{x} = Ax + Bu + w \tag{8.1}$$

where $x(t) \in \mathbb{R}^n$ is a state vector, $u(t) \in \mathbb{R}^m$ is a control vector, $A \in \mathbb{R}^n \times \mathbb{R}^n$ is a constant but unknown matrix, $B \in \mathbb{R}^n \times \mathbb{R}^m$ is a known matrix such that (A, B) is controllable, and $w(t) \in \mathbb{R}^n$ is an unknown bounded exogenous disturbance.

An adaptive controller is designed to achieve tracking of a reference model

$$\dot{x}_m = A_m + B_m r \tag{8.2}$$

where $x_m(t) \in \mathbb{R}^n$ is a reference state vector, $A_m \in \mathbb{R}^n \times \mathbb{R}^n$ is known and Hurwitz, $B_m \in \mathbb{R}^n \times \mathbb{R}^q$ is known, and $r(t) \in \mathbb{R}^q$ is a piecewise continuous and bounded reference command vector.

The ideal feedback gain K_x^* and feedforward gain K_r can be determined from the model matching conditions as

$$A + BK_x^* = A_m \tag{8.3}$$

$$BK_r = B_m \tag{8.4}$$

Suppose the disturbance is not accounted for, then one can design an adaptive controller as

$$u = K_x(t)\, x + K_r r \tag{8.5}$$

The feedback gain $K_x(t)$ is computed by the following MRAC law:

$$\dot{K}_x^\top = \Gamma_x x e^\top P B \tag{8.6}$$

where $e(t) = x_m(t) - x(t)$ is the tracking error, $\Gamma_x = \Gamma_x^\top > 0 \in \mathbb{R}^n \times \mathbb{R}^n$ is an adaptation rate matrix, and $P = P^\top > 0 \in \mathbb{R}^n \times \mathbb{R}^n$ solves the Lyapunov equation

$$PA_m + A_m^\top P = -Q \tag{8.7}$$

where $Q = Q^\top > 0 \in \mathbb{R}^n \times \mathbb{R}^n$ is a positive-definite matrix.

The closed-loop plant is expressed as

$$\dot{x} = (A + BK_x)\, x + BK_r r + w \tag{8.8}$$

Let $\tilde{K}_x(t) = K_x(t) - K_x^*$. Then, the tracking error equation is obtained as

$$\dot{e} = A_m e - B\tilde{K}_x x - w \tag{8.9}$$

Stability of the adaptive system is analyzed by the Lyapunov's direct method.

Proof Choose a Lyapunov candidate function

$$V\left(e, \tilde{K}_x\right) = e^\top Pe + \text{trace}\left(\tilde{K}_x \Gamma_x^{-1} \tilde{K}_x^\top\right) \tag{8.10}$$

Then,

$$\dot{V}\left(e, \tilde{K}_x\right) = -e^\top Qe - 2e^\top Pw \leq -\lambda_{min}(Q)\|e\|^2 + 2\lambda_{max}(P)\|e\| w_0 \tag{8.11}$$

where $w_0 = \max \|w\|_\infty$.

Therefore, $\dot{V}\left(e, \tilde{K}_x\right) \leq 0$ if

$$\|e\| \geq \frac{2\lambda_{max}(P) w_0}{\lambda_{min}(Q)} = p \tag{8.12}$$

However, the Lyapunov stability analysis provides no information on the bound of $\tilde{K}_x(t)$. Therefore, $\tilde{K}_x(t)$ can potentially become unbounded in certain situations. ■

To further illustrate this point, consider a first-order SISO system

$$\dot{x} = ax + bu + w \tag{8.13}$$

where a is unknown and b is known.

An adaptive controller is designed to regulate $x(t)$ to follow a zero reference model whereby $x_m(t) = 0$ for all t as

$$u = k_x(t) x \tag{8.14}$$

Then, the adaptive law for $k_x(t)$ is given by

$$\dot{k}_x = -\gamma_x x^2 b \tag{8.15}$$

It can be shown that it is possible for a bounded response of $x(t)$ to exist that would result in an unbounded signal $k_x(t)$.

Example 8.1 Consider the following solution:

$$x = (1+t)^n$$

which is bounded for $n \leq 0$.

Then,

$$k_x - k_x(0) = -\gamma_x b \int_0^t (1+\tau)^{2n} d\tau = -\gamma_x b \frac{(1+t)^{2n+1} - 1}{2n+1}$$

For $k_x(t)$ to be bounded, we require $2n+1<0$ or $n<-\frac{1}{2}$.
The control signal is computed as

$$u=-\left[\gamma_x b\frac{(1+t)^{2n+1}-1}{2n+1}-k_x(0)\right](1+t)^n$$

The disturbance $w(t)$ that results in this particular solution of $x(t)$ can be found by

$$w=\dot{x}-ax-bu=n(1+t)^{n-1}-a(1+t)^n+b\left[\gamma_x b\frac{(1+t)^{2n+1}-1}{2n+1}-k_x(0)\right](1+t)^n$$

Both the control signal and the disturbance are bounded if $3n+1\leq 0$ or $n\leq-\frac{1}{3}$ and $n\neq-\frac{1}{2}$. Thus, the system is completely bounded if $n<-\frac{1}{2}$. However, if $-\frac{1}{2}<n\leq-\frac{1}{3}$, then $x(t)$, $u(t)$, and $w(t)$ are bounded, but $k_x(t)$ becomes unbounded as $t\to\infty$. The boundedness of the adaptive system is illustrated in Table 8.1.

The response of the closed-loop system with $a=1$, $b=1$, $n=-\frac{5}{12}$, $\gamma_x=10$, $x(0)=1$, and $k_x(0)=0$ is shown in Fig. 8.1.

This example demonstrates that it is possible to have bounded disturbances or control signals but yet unbounded adaptive parameters.

■

One explanation of the parameter drift can be given as follows:

For a sufficiently large disturbance, the adaptive controller attempts to generate a high-gain control in order to reduce the effect of the disturbance. In the limit, the steady-state solution of $x(t)$ is obtained as

$$x^*=-\frac{w}{a+k_x^*} \tag{8.16}$$

As $w(t)$ is sufficiently large, $k_x(t)$ tends to a large negative value in order to keep $x(t)$ close to zero. This high-gain control can cause $k_x(t)$ to become unbounded. In the limit as $x(t)\to 0$ to achieve the ideal asymptotic tracking property of MRAC, $k_x(t)\to\infty$. While Example 8.1 shows that $x(t)$ can remain bounded even though $k_x(t)$ is unbounded, in practice, a high-gain control with a large value of $k_x(t)$ can be

Table 8.1 Boundedness of example adaptive system

	$x(t)$	$u(t)$	$w(t)$	$k_x(t)$
$n>0$	$\notin\mathcal{L}_\infty$	$\notin\mathcal{L}_\infty$	$\notin\mathcal{L}_\infty$	$\notin\mathcal{L}_\infty$
$-\frac{1}{3}<n\leq 0$	$\in\mathcal{L}_\infty$	$\notin\mathcal{L}_\infty$	$\notin\mathcal{L}_\infty$	$\notin\mathcal{L}_\infty$
$-\frac{1}{2}<n\leq-\frac{1}{3}$	$\in\mathcal{L}_\infty$	$\in\mathcal{L}_\infty$	$\in\mathcal{L}_\infty$	$\notin\mathcal{L}_\infty$
$n=-\frac{1}{2}$	$\in\mathcal{L}_\infty$	$\notin\mathcal{L}_\infty$	$\notin\mathcal{L}_\infty$	$\notin\mathcal{L}_\infty$
$n<-\frac{1}{2}$	$\in\mathcal{L}_\infty$	$\in\mathcal{L}_\infty$	$\in\mathcal{L}_\infty$	$\in\mathcal{L}_\infty$

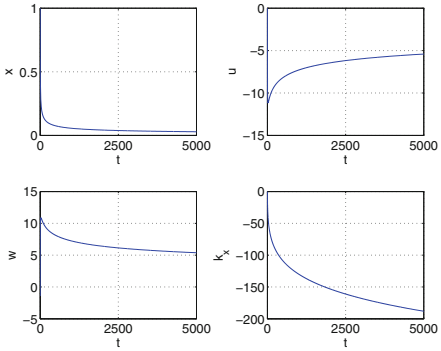

Fig. 8.1 Effect of parameter drift for $n = -\frac{5}{12}$ and $\gamma_x = 10$

problematic since real plants can include other closed-loop behaviors that can lead to instability when $k_x(t)$ becomes large. Thus, a parameter drift can lead to instability in practical applications.

8.2 Non-minimum Phase Systems

A transfer function of a SISO system is called minimum phase if all of its poles and zeros are in the left half plane. If any of the zeros lie in the right half plane, then the system is called non-minimum phase. A non-minimum phase system is more difficult to control since the existence of the unstable zeros can limit the values of stable feedback gains. Increasing feedback gains beyond certain limits will cause the closed-loop poles to become unstable.

Example 8.2 The system

$$\frac{y(s)}{u(s)} = \frac{s+1}{(s+2)(s+3)}$$

$$y = x$$

is minimum phase. For a feedback with $u(s) = k_x x(s) + k_r r(s)$, the closed-loop transfer function

$$\frac{y(s)}{r(s)} \triangleq G(s) = \frac{k_r}{s^2 + (5-k_x)s + 6 - k_x}$$

has stable closed-loop poles for all values of $k_x \in (-\infty, 5)$.

On the other hand, the system

$$\frac{x(s)}{u(s)} = \frac{s-1}{(s+2)(s+3)}$$

is non-minimum phase. The closed-loop transfer function

$$G(s) = \frac{k_r}{s^2 + (5-k_x)s + 6 + k_x}$$

has an unstable closed-loop pole at $s = 1$ when $k_x \to -\infty$. The zero cross-over value of k_x when the pole becomes unstable occurs at $k_x = -6$.

■

If the system exhibits a non-minimum phase behavior, then the adaptation can result in instability due to MRAC attempting to perform an unstable pole-zero cancellation in order to achieve asymptotic tracking.

Example 8.3 Consider the system

$$\dot{x} = ax + bu - 2z + w$$

$$\dot{z} = -z + u$$

$$y = x$$

where $a < 0$ is unknown and $w(t)$ is a disturbance.

The system is non-minimum phase with a transfer function

$$\frac{x(s)}{u(s)} = \frac{s-1}{(s-a)(s+1)}$$

If the same adaptive controller is used for the same disturbance in Example 8.1 with $n = -1$, then the disturbance $w(t)$ is bounded and the response of the closed-loop system in Example 8.1 is completely bounded. However, this is no longer the case for the non-minimum phase system in this example. Let $a = -1, b = 1, \gamma_x = 1$, $x(0) = 1$, and $k_x(0)$. The closed-loop system is unstable as shown in Fig. 8.2.

In fact, the closed-loop system is unstable even when the disturbance is zero and $\gamma_x = 10$ as shown in Fig. 8.3.

Now, suppose the plan is minimum phase with

$$\dot{x} = ax + u + 2z + w$$

$$\dot{z} = -z + u$$

$$y = x$$

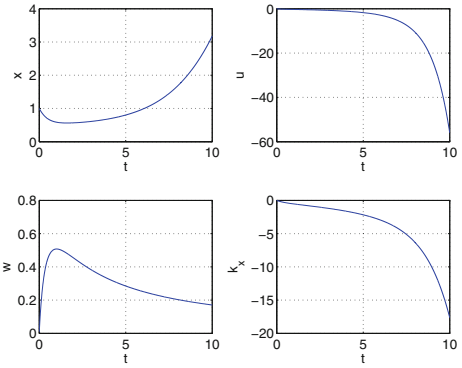

Fig. 8.2 Response of non-minimum phase system with disturbance, $\gamma_x = 1$

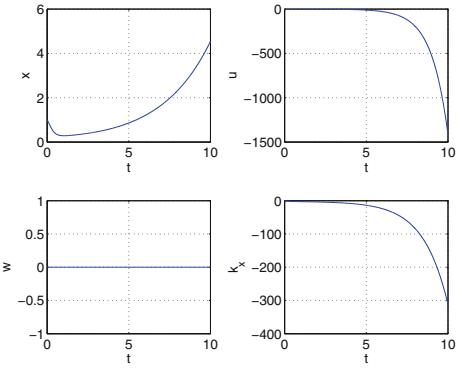

Fig. 8.3 Response of non-minimum phase system with zero disturbance, $\gamma_x = 10$

The closed-loop system now is stable with the same adaptive controller as shown in Fig. 8.4.

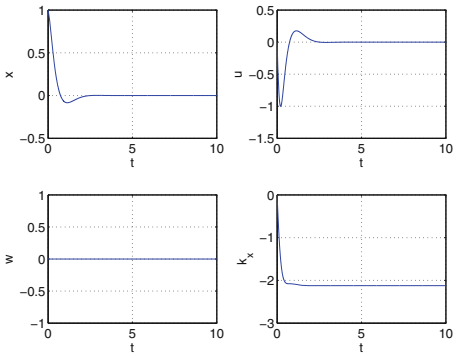

Fig. 8.4 Response of minimum phase system with zero disturbance, $\gamma_x = 10$

8.3 Time-Delay Systems

Many real systems have latency which results in a time delay at the control input. Time delay is caused by a variety of sources such as communication bus latency, computational latency, transport delay, etc. Time-delay systems are a special class of non-minimum phase systems which exhibit some similar behaviors with respect to adaptive control. Model-reference adaptive control of time-delay systems is challenging as no well-established theory is available. Instability can result when an adaptive parameter exceeds a certain limit.

Consider a time-delay MIMO system with a matched uncertainty

$$\dot{x} = Ax + B\left[u\left(t - t_d\right) + \Theta^{*\top}\Phi\left(x\right)\right] \tag{8.17}$$

where t_d is a known time delay.

If A and B are known, then an adaptive controller can be designed for the delay-free system as

$$u = K_x x + K_r r - \Theta^{\top}\Phi\left(x\right) \tag{8.18}$$

$$\dot{\Theta} = -\Gamma\Phi\left(x\right)e^{\top}PB \tag{8.19}$$

When a time delay is present, there exists an upper limit on the value of the adaptation rate matrix Γ that ensures stable adaptation. Thus, the adaptation rate can no longer be chosen arbitrary but rather by a careful consideration of the effect of the time delay present in the system. Unfortunately, no well-established theory currently exists that would enable a systematic design of adaptive control for time-delay systems. As a result, the design is relied upon extensive Monte-Carlo simulations to ensure that a proper adaptation rate is selected.

Consider a time-delay SISO system

$$\dot{x} = ax + bu\left(t - t_d\right) \tag{8.20}$$

where $x\left(t\right) \in \mathbb{R}$, $u\left(t\right) \in \mathbb{R}$, and $b > 0$.

The open-loop transfer function

$$\frac{x\left(s\right)}{u\left(s\right)} = \frac{be^{-t_d s}}{s - a} \tag{8.21}$$

is non-minimum phase since there exists a multiplicity of zeros in the right half plane due to the term $e^{-t_d s}$.

The system has a feedback control

$$u = k_x x \tag{8.22}$$

with a closed-loop pole $s = a + bk_x < 0$.

The feedback gain k_x is designed to be robust in the presence of the time delay to ensure stability of the closed-loop system.

The closed-loop transfer function

$$G(s) = \frac{k_r}{s - a - bk_x e^{-t_d s}} \tag{8.23}$$

is not absolutely stable but conditionally stable for $k_{x_{min}} < k_x < -\frac{a}{b}$.

The system pole can be computed by letting $s = \sigma + j\omega$. Then,

$$\sigma + j\omega - a - bk_x e^{-t_d \sigma} e^{-j\omega t_d} = 0 \tag{8.24}$$

The zero cross-over value of k_x is established by setting $\sigma = 0$. Using the Euler's formula

$$e^{-j\omega t_d} = \cos \omega t_d - j \sin \omega t_d, \tag{8.25}$$

the real part and imaginary parts are equated to zero so that the following equations are obtained:

$$-a - bk_x \cos \omega t_d = 0 \tag{8.26}$$

$$\omega + bk_x \sin \omega t_d = 0 \tag{8.27}$$

The solutions of these equations yield the $j\omega$-axis cross-over frequency from which $k_{x_{min}}$ can be determined as

$$\omega = \sqrt{b^2 k_{x_{min}}^2 - a^2} \tag{8.28}$$

$$a + bk_{x_{min}} \cos\left(\sqrt{b^2 k_{x_{min}}^2 - a^2} t_d\right) = 0 \tag{8.29}$$

Thus, the closed-loop system is stable for all values of $k_{x_{min}} < k_x < -\frac{a}{b}$.

Suppose the constant a is unknown and the adaptive controller in Eqs. (8.14) and (8.15) is used to regulate $x(t)$ to zero. Without the time delay, the adaptation rate can be arbitrarily chosen. However, in the presence of the time delay, there exists an upper limit on γ_x that ensures stability of the closed-loop system. Thus, the closed-loop adaptive system is stable if $\gamma_x \leq \gamma_{x_{max}}$ such that

$$k_x = k_x(0) - \int_0^t \gamma_{x_{max}} x^2 b d\tau > k_{x_{min}} \tag{8.30}$$

Example 8.4 Suppose $a = -1$, $b = 1$, and $t_d = 0.5$ s. The minimum feedback gain is computed to be $k_{x_{min}} = -3.8069$. The response of the closed-loop adaptive system is shown in Fig. 8.5 for a time step $\Delta t = 0.001$. For $\gamma_x = 7$ and $k_x(0) = 0$, $k_x(t) \to -3.5081 > k_{x_{min}}$ as $t \to \infty$. Thus, the closed-loop system is stable. For $\gamma_x = 7.6$, $k_x(t)$ becomes unbounded and the closed-loop system is unstable. Therefore, the maximum adaptation rate $\gamma_{x_{max}}$ is some value between 7 and 7.6.

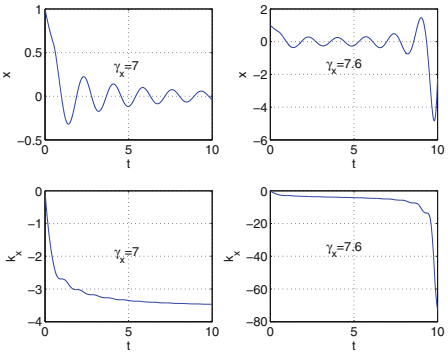

Fig. 8.5 Response of time-delay system

8.4 Unmodeled Dynamics

Non-minimum phase systems are a special class of systems with unmodeled dynamics. Unmodeled dynamics are dynamics that actually exist in a plant but are not accounted for in a control design. This is a very common situation since most control designs are based on mathematical models of some real plants that most likely do not fully capture all the complex physics. In some cases, the neglected dynamics do not present problems in a design, but in other cases, controllers that are designed based on slightly inaccurate mathematical models can lead to catastrophic consequences. Therefore, it is a good practice to include stability margins in any control design to account for effects of unmodeled dynamics. Traditional gain and phase margins are well-established design criteria for linear control design for SISO systems. For adaptive control, there is no such equivalent stability margin nor is there any well-established theory for analysis of stability margins of adaptive systems.

Consider the system

$$\dot{x} = Ax + Bu + \Delta(x, z, u) \tag{8.31}$$

$$\dot{z} = f(x, z, u) \tag{8.32}$$

$$y = x \tag{8.33}$$

where $z(t)$ is an internal state vector which may be unmeasurable or unobservable, $\Delta(x, z, u)$ is the plant model error that is unknown and not accounted for, $\dot{z}(t)$ is the unmodeled dynamics, and $y(t)$ is the plant output vector which is equal to the measurable state vector $x(t)$.

If model-reference adaptive control is used in a control design by assuming $\Delta(x, z, u) = 0$, then it is clear that such a control design is non-robust as demonstrated by instability phenomena of MRAC for non-minimum phase systems.

Research in robust adaptive control was motivated by instability phenomena of adaptive control. In fact, instability of adaptive control in the early 1960s which contributed to the crash of one of the NASA X-15 hypersonic vehicles caused a great deal of concern about the viability of adaptive control. Rohrs et al. investigated various instability mechanisms of adaptive control in the 1980s [2]. The Rohrs counterexample exposes the weakness of MRAC in its inability to provide robustness in the presence of unmodeled dynamics.

To illustrate the lack of robustness to unmodeled dynamics associated with MRAC, consider the following first-order SISO system with a second-order SISO actuator plant:

$$\dot{x} = ax + bu \tag{8.34}$$

$$\ddot{u} + 2\zeta\omega_n\dot{u} + \omega_n^2 u = \omega_n^2 u_c \tag{8.35}$$

where $a < 0$, $b > 0$, $\zeta > 0$, $\omega > 0$, and $u_c(t)$ is the actuator command.

Suppose we want to design an adaptive controller to track a first-order reference model

$$\dot{x}_m = a_m x_m + b_m r \tag{8.36}$$

where $a_m < 0$.

Without knowing or ignoring the actuator dynamics, the adaptive controller is designed to be of the form

$$u_c = k_y(t)\, y + k_r(t)\, r \tag{8.37}$$

where $k_x(t)$ and $k_r(t)$ are adjusted by the following MRAC adaptive laws:

$$\dot{k}_y = \gamma_x y e \tag{8.38}$$

$$\dot{k}_r = \gamma_r r e \tag{8.39}$$

where $e(t) = y_m(t) - y(t)$.

Let us now consider a non-adaptive control design with k_y and k_r constant. The open-loop transfer function of the plant with actuator dynamics is expressed as

$$\frac{y(s)}{u_c(s)} = \frac{b\omega_n^2}{(s-a)\left(s^2 + 2\zeta\omega_n s + \omega_n^2\right)} \tag{8.40}$$

We introduce a time delay at the input $u_c(t)$. Then, the closed-loop transfer function is obtained as

$$G(s) = \frac{b\omega_n^2 k_r e^{-\omega t_d}}{(s-a)\left(s^2 + 2\zeta\omega_n s + \omega_n^2\right) - b\omega_n^2 k_y e^{-\omega t_d}} \tag{8.41}$$

Let $s = j\omega$. Then, the characteristic equation of the closed-loop transfer function is computed as

$$-j\omega^3-(2\zeta\omega_n - a)\,\omega^2+\left(\omega_n^2 - 2a\zeta\omega_n\right)\,j\omega-a\omega_n^2-b\omega_n^2k_y\,(\cos\omega t_d - j\sin\omega t_d) = 0 \tag{8.42}$$

Separating the real part and imaginary part leads to the following equations:

$$-(2\zeta\omega_n - a)\,\omega^2 - a\omega_n^2 - b\omega_n^2k_y\cos\omega t_d = 0 \tag{8.43}$$

$$-\omega^3 + \left(\omega_n^2 - 2a\zeta\omega_n\right)\omega + b\omega_n^2k_y\sin\omega t_d = 0 \tag{8.44}$$

The phase margin of the closed-loop plant is then obtained as

$$\phi = \omega t_d = \sin^{-1}\left[\frac{\omega^3 - \left(\omega_n^2 - 2a\zeta\omega_n\right)\omega}{b\omega_n^2k_y}\right] \tag{8.45}$$

or alternatively as

$$\phi = \omega t_d = \tan^{-1}\left[\frac{\omega^3 - \left(\omega_n^2 - 2a\zeta\omega_n\right)\omega}{-(2\zeta\omega_n - a)\,\omega^2 - a\omega_n^2}\right] \tag{8.46}$$

The system has zero phase margin if

$$\omega \triangleq \omega_0 = \sqrt{\omega_n^2 - 2a\zeta\omega_n} \tag{8.47}$$

The feedback gain k_y affects the cross-over frequency of the closed-loop system according to the following equation:

$$\omega^6 + \left(a^2 + 4\zeta^2\omega_n^2 - 2\omega_n^2\right)\omega^4 + \left(\omega_n^2 + 4a^2\zeta^2 - 2a^2\right)\omega_n^2\omega^2 + \left(a^2 - b^2k_y^2\right)\omega_n^4 = 0 \tag{8.48}$$

We now return to the adaptive control design. Suppose the reference command signal is specified as

$$r = r_0\sin\omega_0 t \tag{8.49}$$

Since the reference command signal provides frequency input that matches the cross-over frequency at zero phase margin, the closed-loop adaptive system will be unstable.

Example 8.5 Let $a = -1$, $b = 1$, $a_m = -2$, $b_m = 2$, $\omega_n = 5$ rad/s, and $\zeta = 0.5$. Then the cross-over frequency at zero phase margin is computed to be $\omega_0 = \sqrt{30}$ rad/s. The reference command signal is then specified as

$$r = \sin\sqrt{30}t$$

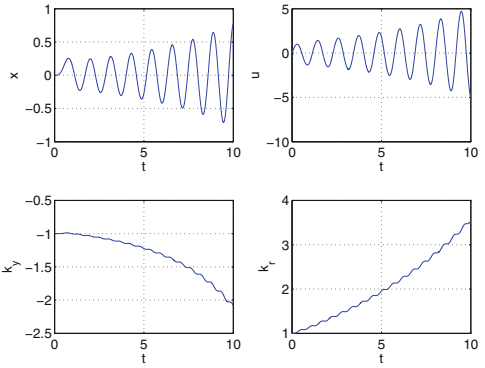

Fig. 8.6 Instability of MRAC due to unmodeled dynamics with reference command at zero phase margin cross-over frequency $r = \sin\sqrt{30}t$, $k_y(0) = -1$

We choose $\gamma_x = 1$, $\gamma_r = 1$, and the initial conditions $k_y(0) = -1$ and $k_r(0) = 1$. The closed-loop adaptive system is indeed unstable as shown in Fig. 8.6. This illustrates the lack of robustness of MRAC to unmodeled dynamics.

Suppose we change the frequency of the reference command signal to 3 rad/s. The adaptive system is now stable with $k_y(t) \to -3.5763$ and $k_r(t) \to 1.2982$ as shown in Fig. 8.7.

The closed-loop stability of an adaptive system also depends on the initialization of the adaptive feedback gain $k_y(t)$. To illustrate this, we compute the feedback gain corresponding to the cross-over frequency at zero phase margin $\omega_0 = \sqrt{30}$. This results in $k_{y_0} = -\frac{31}{5} = -6.2$. For the reference command signal $r(t) = \sin 3t$ which results in a stable closed-loop adaptive system as shown in Fig. 8.7, suppose we initialize the adaptive law with $k_y(0) = -6.2$. The closed-loop system is now on the verge of instability as shown in Fig. 8.8.

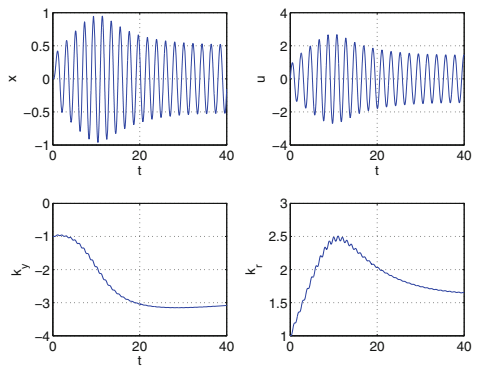

Fig. 8.7 Stable response with reference command $r = \sin 3t$, $k_y(0) = -1$

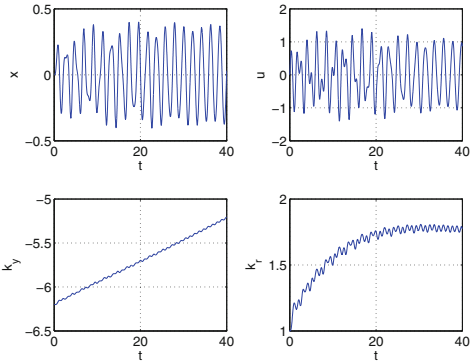

Fig. 8.8 Incipient instability of MRAC due to unmodeled dynamics with reference command $r = \sin 3t$, $k_y(0) = -6.2$ at zero phase margin

Example 8.6 The Rorhs counterexample is defined with the following parameters: $a = -1$, $b = 2$, $a_m = -3$, $b_m = 3$, $\omega = \sqrt{229}$, and $\zeta = \frac{30}{2\sqrt{229}}$ [2].

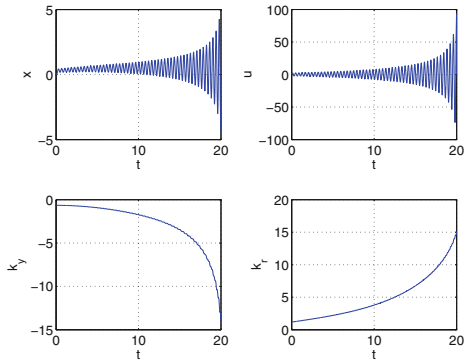

Fig. 8.9 Instability of MRAC by Rohrs counterexample

The adaptive laws are initialized with $k_y(0) = -0.65$ and $k_r(0) = 1.14$. The adaptation rates are chosen to be $\gamma_x = 1$ and $\gamma_r = 1$. The zero phase-margin frequency is computed to be $\omega_0 = \sqrt{259} = 16.1$ rad/s. The reference command is given by

$$r = 0.3 + 1.85 \sin 16.1t$$

As a result, instability occurs as shown in Fig. 8.9.

■

Typically, actuator dynamics must be sufficiently faster than the plant dynamics in order to maintain enough stability margins for a controller. This usually means that the actuator frequency bandwidth ω_n must be greater than the control frequency

bandwidth ω, that is, $\omega_n \gg \omega$. Then, the closed-loop transfer function in Eq. (8.41) may be approximated by

$$G(s) = \frac{bk_r e^{-\omega t_d}}{s - a - bk_y e^{-\omega t_d}} \tag{8.50}$$

This results in the following cross-over frequency and phase margin:

$$\omega = \sqrt{b^2 k_y^2 - a^2} \tag{8.51}$$

$$\phi = \omega t_d = \sin^{-1}\left(-\frac{\omega}{bk_y}\right) \tag{8.52}$$

for $|bk_y| > |a|$. As $k_y \to -\infty, \phi \to \frac{\pi}{2}$. The closed-loop system is therefore robustly stable in the presence of high gain.

8.5 Fast Adaptation

Model-reference adaptive control is designed to achieve asymptotic tracking for systems with matched structured uncertainty. In practice, asymptotic tracking is a highly demanding requirement that can be difficult to meet. For systems with unknown disturbances and unstructured uncertainty which are more frequently encountered in practice, only bounded tracking could be achieved with MRAC, but there is no guarantee of boundedness of adaptive parameters. As the adaptation rate increases, the tracking error reduces and the tracking performance is improved. This is usually referred to as fast adaptation. However, as seen previously, for systems with non-minimum phase behaviors, time delay, and unmodeled dynamics, increasing adaptation rate beyond a certain limit can result in instability. Robustness of MRAC, in general, requires a small adaptation rate. Therefore, tracking performance and robustness are often viewed as two directly competing requirements in adaptive control. This viewpoint is also valid for any linear control design.

Consider a first-order SISO system

$$\dot{x} = ax + bu \tag{8.53}$$

A linear proportional-integral (PI) controller is designed to enable the plant output $x(t)$ to track a reference signal $x_m(t)$ as

$$u = k_x x + k_i \int_0^t (x - x_m)\, d\tau \tag{8.54}$$

The closed-loop plant is expressed as

$$\dot{x} = \left(a + bk_p\right) x + bk_i \int_0^t (x - x_m)\, d\tau \tag{8.55}$$

Differentiating yields

$$\ddot{x} - \left(a + bk_p\right) \dot{x} - bk_i x = -bk_i x_m \tag{8.56}$$

The closed-loop plant is stable with $a + bk_p < 0$ and $k_i < 0$. As $k_i \to \infty$, $x(t) \to x_m(t)$. Thus, increasing the integral gain improves the tracking performance.

The frequency of the closed-loop system is $\omega_n^2 = -bk_i$. Thus, as $k_i \to \infty$ and $\omega_n \to \infty$, the closed-loop response becomes highly oscillatory. It is of interest to find out what happens to the stability margins of the closed-loop system as $k_i \to \infty$.

Suppose the input is delayed by an amount t_d so that the closed-loop plant is given by

$$x = -\frac{bk_i x_m e^{-t_d s}}{s^2 - as - bk_p s e^{-t_d s} - bk_i e^{-t_d s}} \tag{8.57}$$

The stability of the closed-loop plant can be analyzed by setting $s = j\omega$ which yields

$$-\omega^2 - aj\omega - \left(bk_p j\omega + bk_i\right)(\cos \omega t_d - j \sin \omega t_d) = 0 \tag{8.58}$$

Equating the real and imaginary parts to zero results in the following equations:

$$-\omega^2 - bk_p \omega \sin \omega t_d - bk_i \cos \omega t_d = 0 \tag{8.59}$$

$$-a\omega - bk_p \omega \cos \omega t_d + bk_i \sin \omega t_d = 0 \tag{8.60}$$

These equations can be recast as

$$b^2 k_p^2 \omega^2 \sin^2 \omega t_d + b^2 k_p k_i \omega \sin 2\omega t_d + b^2 k_i^2 \cos^2 \omega t_d = \omega^4 \tag{8.61}$$

$$b^2 k_p^2 \omega^2 \cos^2 \omega t_d - b^2 k_p k_i \omega \sin 2\omega t_d + b^2 k_i^2 \sin^2 \omega t_d = a^2 \omega^2 \tag{8.62}$$

Adding the two equations together yields

$$\omega^4 + \left(a^2 - b^2 k_p^2\right) \omega^2 - b^2 k_i^2 = 0 \tag{8.63}$$

The cross-over frequency is then computed as

$$\omega = \sqrt{\frac{b^2 k_p^2 - a^2}{2} \left[1 + \sqrt{1 + \frac{4b^2 k_i^2}{\left(b^2 k_p^2 - a^2\right)^2}}\right]} \tag{8.64}$$

Multiplying Eq. (8.59) by bk_i and Eq. (8.60) by $bk_p \omega$ and then adding the resulting equations together yield

$$\left(abk_p + bk_i\right)\omega^2 + \left(b^2k_p^2\omega^2 + b^2k_i^2\right)\cos\omega t_d = 0 \tag{8.65}$$

The closed-loop plant is then stable for all $t \leq t_d$ where t_d is called a time-delay margin which is computed as

$$t_d = \frac{1}{\omega}\cos^{-1}\left[-\frac{\left(abk_p + bk_i\right)\omega^2}{b^2k_p^2\omega^2 + b^2k_i^2}\right] \tag{8.66}$$

Now, consider a limiting case when $\omega_n^2 = -bk_i \to \infty$. Then,

$$\omega \to \omega_n \to \infty \tag{8.67}$$

$$t_d \to \frac{1}{\omega}\cos^{-1}\frac{\omega_n^4}{\omega_n^4} \to 0 \tag{8.68}$$

The phase margin of the closed-loop plant is computed to be

$$\phi = \omega t_d \to 0 \tag{8.69}$$

Thus, as the integral gain increases, the closed-loop response becomes more oscillatory and the time-delay margin and phase margin of the closed-loop plant decrease. In the limit, these margins tend to zero as $k_i \to \infty$. On the other hand, the tracking performance is improved with increasing the integral gain. Clearly, the two requirements cannot be simultaneously met. Thus, a control design typically strives for a balance between these two competing requirements by a judicious choice of k_i.

Suppose the plant becomes uncertain with a being an unknown parameter. A reference model is specified by

$$\dot{x}_m = a_m x_m + b_m r \tag{8.70}$$

where $r\,(t)$ is a constant signal.

Then, an adaptive controller is designed as

$$u = k_x\,(t)\,x + k_r r \tag{8.71}$$

$$\dot{k}_x = \gamma_x x\,(x_m - x)\,b \tag{8.72}$$

where $k_r = \frac{b_m}{b}$.

Differentiating the closed-loop plant yields

$$\ddot{x} - [a + bk_x\,(t)]\,\dot{x} + b^2\gamma_x x^3 = b^2\gamma_x x^2 x_m \tag{8.73}$$

Contrasting Eq. (8.73) with Eq. (8.56), one can conclude that the effect of adaptive control is very similar to that of the linear integral control. In fact, let

$$k_i(x) = -\gamma_x x^2 b \tag{8.74}$$

Then, the closed-loop plant can be expressed as

$$\ddot{x} - [a + bk_x(t)]\dot{x} - bk_i(x)x = -bk_i(x)x_m \tag{8.75}$$

Differentiating the adaptive controller yields

$$\dot{u} = k_i(x)(x - x_m) + k_x(t)\dot{x} + k_r\dot{r} \tag{8.76}$$

Then, integrating yields

$$u = \int_0^t k_x(t)\dot{x}d\tau + \int_0^t k_i(x)(x - x_m)d\tau + k_r r \tag{8.77}$$

Therefore, adaptive control in some way can be viewed as a nonlinear integral control. This leads to an observation that as γ_x increases, the closed-loop response becomes more oscillatory and the time-delay margin of the closed-loop plant decreases. In the limit, as $\gamma_x \to \infty$, the time-delay margin tends to zero. Robustness of MRAC therefore decreases as the adaptation rate increases.

Example 8.7 Let $a = 1$, $b = 1$, and $x_m(t) = 1$. To track a reference command, a linear PI controller is designed with $k_p = -2$ and $k_i = -500$. The cross-over frequency and time-delay margin are computed to be $\omega = 22.3942$ rad/s and $t_d = 0.0020$ s. Thus, the closed-loop system is stable for any time delay up to 0.0020 s. The cross-over frequency ω and time-delay margin t_d as a function of the integral gain k_i are shown in Fig. 8.10. As can be seen, the cross-over frequency increases and the time-delay margin decreases as the magnitude of the integral gain k_i increases. Therefore, high frequency integral gain should be avoided in any design.

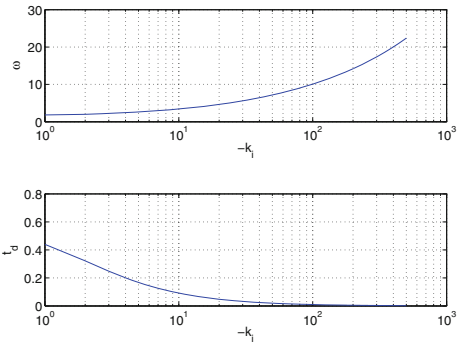

Fig. 8.10 Cross-over frequency and time-delay margin as function of integral gain

Suppose an adaptive controller is used instead. Let $a_m = -1$, $b_m = 1$, and $r(t) = 1$. Choose a large value of γ_x, say, $\gamma_x = 500$ to achieve fast adaptation. With the initial conditions $x(0) = 0$ and $k_x(0) = 0$, the responses of the closed-loop adaptive system and linear system are shown in Fig. 8.11. Note that the responses exhibit high frequency oscillations as indicated by the analysis. As $x(t) \to x_m(t) = 1$, then $k_i(x) \to \approx -\gamma_x x_m^2(t) b \approx -500$. Thus, the adaptation rate $\gamma_x = 500$ is effectively equivalent to the integral gain $k_i = -500$. Therefore, the closed-loop adaptive system may tend to exhibit similar behaviors as the closed-loop linear system. In fact, if a time delay $t_d = 0.0020\,\text{s}$ is introduced at the input, both systems become unstable and have similar responses as shown in Fig. 8.12.

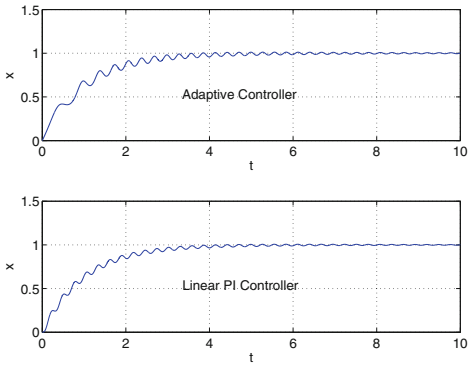

Fig. 8.11 Responses of adaptive systems and linear systems with fast adaptation

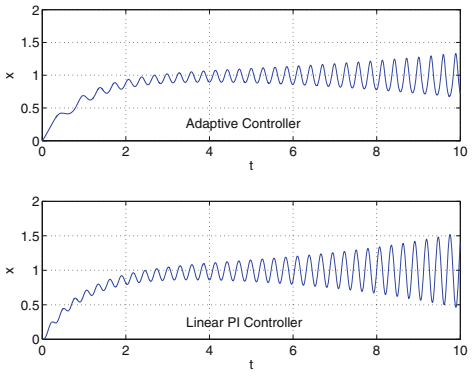

Fig. 8.12 Responses of adaptive systems and linear systems with fast adaptation and time delay

8.6 Summary

Model-reference adaptive control is designed to achieve asymptotic tracking. This ideal property of MRAC is a benefit but also a problem. MRAC is generally non-robust since the bound on an adaptive parameter cannot be established by the Lyapunov stability analysis. A parameter drift can result that can cause an adaptive control algorithm to blow up. As the complexity of a plant increases, robustness of MRAC becomes increasingly difficult to ascertain. In practical applications, the knowledge of a real plant can never be established precisely. Thus, a model of a physical plant often cannot fully capture all the effects due to unmodeled dynamics, unstructured uncertainty, and exogenous disturbances that may exist in a real plant. All these effects can produce closed-loop dynamics that can lead to instability when MRAC is used in an adaptive controller.

Examples of the lack of robustness of MRAC to the parameter drift, time delay, non-minimum phase plants, unmodeled dynamics, and fast adaptation are illustrated. For a sufficiently large disturbance, MRAC attempts to seek the ideal asymptotic tracking property. In theory, to reject the disturbance, MRAC generates a high-gain control in order to reduce the effect of the disturbance. This high-gain control can cause adaptive parameters to become unbounded. A parameter drift can lead to instability in practical situations.

Non-minimum phase systems are more difficult to control since the existence of the unstable zeros imposes limiting values on stable feedback gains. MRAC always seeks the ideal asymptotic tracking property by attempting to perform an unstable pole-zero cancellation, which leads to instability in non-minimum phase systems. For non-minimum phase systems, adaptive control designers generally have to be aware of the limiting values of adaptive parameters in order to prevent potential instability.

Many real systems have latency which results in a time delay at the control input. Time delay is caused by a variety of sources such as communication bus latency, computational latency, transport delay, etc. Time-delay systems are a special class of non-minimum phase systems. Instability can result when an adaptive parameter exceeds a certain limit. Without the time delay, the adaptation rate in MRAC can be arbitrarily chosen. However, in the presence of the time delay, there exists an upper limit on the adaptation rate that can ensure the closed-loop stability of an adaptive system. Thus, the closed-loop adaptive system is stable if the adaptation rate is kept below this limit.

Unmodeled dynamics are dynamics that actually exist in a plant but are not accounted for in a control design. This is a very common situation since most control designs are based on mathematical models of some real plants that most likely do not fully capture all the complex physics. In some cases, the neglected dynamics do not present problems in a design, but in other cases, controllers that are designed based on slightly inaccurate mathematical models can lead to catastrophic consequences. MRAC is known to be non-robust to unmodeled dynamics. When a reference command signal contains a frequency close to a zero phase margin due to unmodeled

dynamics, instability can occur. Initialization of adaptive parameters can also affect the closed-loop stability if the initial condition coincides with a near zero phase margin.

Fast adaptation refers to the notion that a large adaptation rate can be used to achieve fast reference model following. In the limit, as the adaptation rate increases to a theoretically infinite value, robustness of MRAC as measured by the time-delay margin tends to zero. As with the case with non-minimum phase, time delay, and unmodeled dynamics, MRAC can cause instability when a large adaptation rate is used for fast adaptation.

8.7 Exercises

1. Consider a first-order SISO system

$$\dot{x} = ax + bu + w$$

where $w(t)$ is a bounded disturbance and $u(t)$ is an adaptive controller defined as

$$u = k_x x$$

$$\dot{k}_x = -\gamma_x x^2 b$$

Suppose the solution of $x(t)$ is given by

$$x = t(1+t)^p$$

   a. Analyze parameter drift behaviors of the closed-loop system by finding all values of p that result in unbounded feedback gain $k_x(t)$ and all values of p that result in a completely bounded system.
   b. Implement the adaptive controller in Simulink using the following information: $a = 1$, $b = 1$, $\gamma_x = 1$, $x(0) = 0$, and $k_x(0) = 0$ with a time step $\Delta t = 0.001$ s for two different values of p: one for unbounded $k_x(t)$ and the other for all bounded signals. Plot the time histories of $x(t)$, $u(t)$, $w(t)$, and $k_x(t)$ for each of the values of p for $t \in [0, 20]$ s.

2. Consider a time delay second-order SISO system

$$\ddot{y} - \dot{y} + y = u(t - t_d)$$

where t_d is an unknown time delay.
The unstable open-loop plant is stabilized with a linear derivative controller

$$u = k_d^* \dot{y}$$

where $k_d^* = -7$.

a. Calculate analytically the cross-over frequency ω and the time-delay margin t_d that corresponds to neutral stability of the closed-loop system.
b. Now, suppose an adaptive controller is designed to follow the delay-free closed-loop system with the linear derivative controller as the reference model

$$\ddot{y}_m + 6\dot{y}_m + y_m = 0$$

Let $x(t) = \begin{bmatrix} y(t) & \dot{y}(t) \end{bmatrix}^\top \in \mathbb{R}^2$, then the open-loop plant is designed with an adaptive derivative controller

$$u = K_x x$$

$$\dot{K}_x^\top = -\Gamma_x x x^\top P B$$

where $K_x(t) = \begin{bmatrix} 0 & k_d(t) \end{bmatrix}$ and $\Gamma_x = \text{diag}(0, \gamma_x)$ and γ_x is an adaptation rate.
Implement the adaptive controller in Simulink using the following information: $Q = I$, $y(0) = 1$, $\dot{y}(0) = 0$, and $K_x(0) = 0$ with a time step $\Delta t = 0.001$ s. Determine $\gamma_{x_{max}}$ that causes the closed-loop system to be on the verge of instability by trial-and-error to within 0.1 accuracy. Calculate $k_{d_{min}}$ that corresponds to $\gamma_{x_{max}}$. Plot the time histories of $x(t)$, $u(t)$, and $k_d(t)$ for $t \in [0, 10]$ s.

3. For the Rohrs' counterexample, stability of the closed-loop system is affected by the frequency of the reference command signal $r(t)$. Write the closed-loop transfer function from $r(t)$ to $y(t)$. Then, compute the cross-over frequency ω for the reference command signal

$$r = 0.3 + 1.85 \sin \omega t$$

to give a 60° phase margin. Also compute the ideal feedback gain k_y^* corresponding to this phase margin. Implement in Simulink the Rohrs' counterexample using the same initial conditions $k_y(0)$ and $k_r(0)$ with $\gamma_y = \gamma_r = 1$ and $\Delta t = 0.001$ s. Plot the time histories of $y(t)$, $u(t)$, $k_y(t)$, and $k_r(t)$ for $t \in [0, 60]$ s.

References

1. Ioannu, P. A., & Sun, J. (1996). *Robust adaptive control*. Upper Saddle River: Prentice-Hall, Inc.
2. Rohrs, C. E., Valavani, L., Athans, M., & Stein, G. (1985). Robustness of continuous-time adaptive control algorithms in the presence of unmodeled dynamics. *IEEE Transactions on Automatic Control*, *AC-30*(9) 881–889.

Chapter 9
Robust Adaptive Control

Abstract This chapter presents several techniques for improved robustness of model-reference adaptive control. These techniques, called robust modification, achieve increased robustness through two general principles: (1) limiting adaptive parameters and (2) adding damping mechanisms in the adaptive laws to bound adaptive parameters. The dead-zone method and the projection method are two common robust modification schemes based on the principle of limiting adaptive parameters. The dead-zone method prevents the adaptation when the tracking error norm falls below a certain threshold. This method prevents adaptive systems from adapting to noise which can lead to a parameter drift. The projection method is widely used in practical adaptive control applications. The method requires the knowledge of a priority bounds on system parameters. Once the bounds are given, a convex set is established. The projection method then permits the normal adaptation mechanism of model-reference adaptive control as long as the adaptive parameters remain inside the convex set. If the adaptive parameters reach the boundary of the convex set, the projection method changes the adaptation mechanism to bring the adaptive parameters back into the set. The σ modification and e modification are two well-known robust modification techniques based on the principle of adding damping mechanisms to bound adaptive parameters. These two methods are discussed, and the Lyapunov stability proofs are provided. The optimal control modification and the adaptive loop recovery modification are two recent robust modification methods that also add damping mechanisms to model-reference adaptive control. The optimal control modification is developed from the optimal control theory. The principle of the optimal control modification is to explicitly seek a bounded tracking as opposed to the asymptotic tracking with model-reference adaptive control. The bounded tracking is formulated as a minimization of the tracking error norm bounded from an unknown lower bound. A trade-off between bounded tracking and stability robustness can therefore be achieved. The damping term in the optimal control modification is related to the persistent excitation condition. The optimal control modification exhibits a linear asymptotic property under fast adaptation. For linear uncertain systems, the optimal control modification causes the closed-loop systems to tend to linear systems in the limit. This property can be leveraged for the design and analysis of adaptive control systems using many existing well-known linear control techniques. The adaptive loop recovery modification is designed to minimize the

N.T. Nguyen, *Model-Reference Adaptive Control*, Advanced Textbooks
in Control and Signal Processing, https://doi.org/10.1007/978-3-319-56393-0_9

nonlinearity in a closed-loop plant so that the stability margin of a linear reference model could be preserved. This results in a damping term proportional to the square of the derivative of the input function. As the damping term increases, in theory the nonlinearity of a closed-loop system decreases so that the closed-loop plant can follow a linear reference model which possesses all the required stability margin properties. The $\mathscr{L}_1$ adaptive control has gained a lot of attention in the recent years due to its ability to achieve robustness with fast adaptation for a given a priori bound on the uncertainty. The underlying principle of the $\mathscr{L}_1$ adaptive control is the use of fast adaptation for improved transient or tracking performance coupled with a low-pass filter to suppress high-frequency responses for improved robustness. As a result, the $\mathscr{L}_1$ adaptive control can be designed to achieve stability margins under fast adaptation for a given a priori bound on the uncertainty. The basic working concept of the $\mathscr{L}_1$ adaptive control is presented. The bi-objective optimal control modification is an extension of the optimal control modification designed to achieved improved performance and robustness of systems with input uncertainty. The adaptation mechanism relies on two sources of errors: the normal tracking error and the predictor error. A predictor model of a plant is constructed to estimate the open-loop response of the plant. The predictor error is formed as the difference between the plant and the predictor model. This error signal is then added to the optimal control modification adaptive law to enable the input uncertainty to be estimated. Model-reference adaptive control of singularly perturbed systems is presented to address slow actuator dynamics. The singular perturbation method is used to decouple the slow and fast dynamics of a plant and its actuator. The asymptotic outer solution of the singularly perturbed system is then used in the design of model-reference adaptive control. This modification effectively modifies an adaptive control signal to account for slow actuator dynamics by scaling the adaptive law to achieve tracking. Adaptive control of linear uncertain systems using the linear asymptotic property of the optimal control modification method is presented for non-strictly positive real (SPR) systems and non-minimum phase systems. The non-SPR plant is modeled as a first-order SISO system with a second-order unmodeled actuator dynamics. The plant has relative degree 3 while the first-order reference model is SPR with relative degree 1. By invoking the linear asymptotic property, the optimal control modification can be designed to guarantee a specified phase margin of the asymptotic linear closed-loop system. For non-minimum phase systems, the standard model-reference adaptive control is known to be unstable due to the unstable pole-zero cancellation as a result of the ideal property of asymptotic tracking. The optimal control modification is applied as an output feedback adaptive control design that prevents the unstable pole-zero cancellation by achieving bounded tracking. The resulting output feedback adaptive control design, while preventing instability, can produce poor tracking performance. A Luenberger observer state feedback adaptive control method is developed to improve the tracking performance. The standard model-reference adaptive control still suffers the same issue with the lack of robustness if the non-minimum phase plant is required to track a minimum phase reference model. On the other hand, the opti-

mal control modification can produce good tracking performance for both minimum phase and non-minimum phase reference models.

Research in robust adaptive control was motivated by instability phenomena of adaptive control. In fact, instability of adaptive control in the early 1960s which contributed to the crash of one of the NASA X-15 hypersonic vehicles caused a great deal of concern about the viability of adaptive control. Rohrs et al. investigated instability mechanisms of adaptive control due to unmodeled dynamics in the 1980s [1]. As a result, various robust modification schemes had since been developed to ensure boundedness of adaptive parameters. The σ modification and the e modification are two well-known robust modification methods [2, 4]. Other techniques such as the dead-zone method and the projection method are also used to improve robustness of adaptive control algorithms [5]. In recent years, there have been numerous new advanced robust adaptive control methods developed, such as the adaptive loop recovery [6], composite model-reference adaptive control [7], $\mathscr{L}_1$ adaptive control [8], optimal control modification [9], derivative-free adaptive control [10], and many others. The reader is referred to Chap. 1 for a more extensive list of these recent adaptive control methods. The principle of robust modification is based on two central themes: (1) limiting adaptive parameters and (2) adding damping mechanisms to model-reference adaptive control. The robustness issues with the parameter drift, non-minimum phase behaviors, time delay, unmodeled dynamics, and fast adaptation are largely ameliorated with these robust modification schemes, but are not entirely eliminated if the nature of the uncertainty is not completely known.

In this chapter, a variety of robust adaptive control methods will be covered. The learning objectives of this chapter are:

- To develop an understanding and to know how to apply common techniques for enhancing robustness in model-reference adaptive control, namely the dead-zone method, the projection method, σ modification, and e modification;
- To be able to understand and apply new modern robust adaptive control techniques, namely the optimal control modification, the bi-objective optimal control modification, the adaptive loop recovery, and the $\mathscr{L}_1$ adaptive control;
- To develop an understanding of the linear asymptotic property of the optimal control modification that can be used to estimate the time-delay margin of a closed-loop adaptive system;
- To understand and to know how to apply time-varying adaptation rate techniques of normalization and covariance adjustment to improve robustness;
- To recognize robustness issues with slow actuators and to be able to apply the singular perturbation method for systems with slow actuator dynamics; and
- To be able to address systems with unmodeled dynamics and non-minimum phase plants with relative degree 1 by applying the linear asymptotic property of the optimal control modification.

9.1 Dead-Zone Method

Parameter drift can occur when noise is present in a signal. If the signal-to-noise ratio is sufficiently small, adaptive control would attempt to reduce noise instead of the tracking error. As a result, adaptive parameters would continue to be integrated, thereby leading to a parameter drift. Thus, the dead-zone method can be used to stop the adaptation process when the tracking error is reduced below a certain level [5].

The dead-zone method for the adaptive law in Eq. (8.19) is stated as

$$\dot{\Theta} = \begin{cases} -\Gamma \Phi(x) e^{\top} PB & \|e\| > e_0 \\ 0 & \|e\| \leq e_0 \end{cases} \tag{9.1}$$

where e_0 is an adaptation threshold to be selected.

Assuming that e_0 is properly chosen, then the dead-zone method will improve robustness of MRAC since the adaptive parameters will be "frozen" when the adaptation process ceases. The adaptive parameters can be shown to be bounded by the Lyapunov stability analysis as follows:

Proof When $\|e\| > e_0$, the adaptation process is active. The usual result of the Lyapunov stability analysis was given in Sect. 8.1 with a bounded tracking error. When $\|e\| \leq e_0$, the adaptation is shut off to prevent the potential parameter drift as $e(t) \to 0$. Then, the following Lyapunov candidate function is used:

$$V(e) = e^{\top} Pe \tag{9.2}$$

The tracking error equation is given by

$$\dot{e} = A_m e + B\tilde{\Theta}^{\top} \Phi(x) - w \tag{9.3}$$

where $w(t)$ is the noise disturbance.

Then,

$$\dot{V}(e) = -e^{\top} Qe + 2e^{\top} PB\tilde{\Theta}^{\top} \Phi(x) - 2e^{\top} Pw \tag{9.4}$$

$\dot{V}(e) \leq 0$ requires

$$2e^{\top} PB\tilde{\Theta}^{\top} \Phi(x) \leq e^{\top} Qe + 2e^{\top} Pw \tag{9.5}$$

or

$$\left\|\tilde{\Theta}\right\| \leq \frac{\lambda_{max}(Q)\|e\| + 2\lambda_{max}(P) w_0}{2\|PB\|\|\Phi(x)\|} \leq \frac{\lambda_{max}(Q) e_0 + 2\lambda_{max}(P) w_0}{2\|PB\|\Phi_0} \tag{9.6}$$

Since $\|e\| \leq e_0$, it implies that $\|\Phi(x)\| \leq \Phi_0$ is bounded. Thus, $\left\|\tilde{\Theta}\right\|$ is also bounded from above. The adaptive law with the dead-zone method therefore is robust and can prevent a parameter drift.

■

The difficulty with the dead-zone method usually lies with the selection of e_0 which is generally by trial-and-error. If the threshold is set too large, then the adaptation process may be prematurely terminated by the dead-zone method. On the other hand, if it is set too low, then the integral action of the adaptive law can lead to a parameter drift.

Example 9.1 For Example 8.1 with $k_x(t)$ unbounded for $n = -\frac{5}{12}$, using the dead-zone method with $|x| > 0.2$, the value of $k_x(t)$ is limited to -54.2195. Since $w(t) \to 0$ as $t \to \infty$, $x(t)$ will also tend to zero with the dead-zone method. However, it tends to zero at a slower rate than that with MRAC. The response of the closed-loop system with the dead-zone method is compared to that with MRAC as shown in Fig. 9.1. A time delay is injected at the input. The closed-loop system can tolerate up to $t_d = 0.0235\,\text{s}$ with MRAC and $t_d = 0.0285\,\text{s}$ with the dead-zone method. This indicates that the dead-zone method is more robust than MRAC.

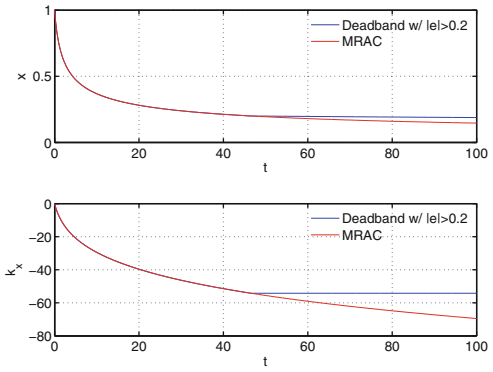

Fig. 9.1 MRAC with dead-zone method

9.2 Projection Method

The projection method is used to limit adaptive parameters based on a priori knowledge of the uncertainty. This may be a contradiction since uncertainty is usually not known a priori. However, an adaptive controller can be designed under a certain assumption of the uncertainty. As long as the uncertainty does not violate the assumption, then the projection method is guaranteed to provide robustness.

To motivate the concept, consider a convex optimization problem

$$\min \; J(\Theta) = f(\Theta) \tag{9.7}$$

where $\Theta(t) \in \mathbb{R}^n$ and $f(\Theta) \in \mathbb{R}$ is a convex function, i.e.,

$$f(\alpha x + (1-\alpha) y) \leq \alpha f(x) + (1-\alpha) f(y) \tag{9.8}$$

for some $\alpha \in [0, 1]$, subject to an equality constraint

$$g(\Theta) = 0 \tag{9.9}$$

where $g(\Theta) \in \mathbb{R}$ is a convex function.

This is a constrained optimization problem. We can solve this problem by using the Lagrange multiplier method. Introducing a Lagrange multiplier $\lambda(t)$, also called an adjoint variable, then the augmented cost function is expressed as

$$J(\Theta) = f(\Theta) + \lambda g(\Theta) \tag{9.10}$$

The second term is the augmented term which does not change the cost function since $g(\Theta) = 0$.

The necessary condition of optimality is obtained as

$$\nabla J_\Theta(\Theta) = \frac{\partial J}{\partial \Theta} = 0 \tag{9.11}$$

This yields

$$\nabla f_\Theta(\Theta) + \lambda \nabla g_\Theta(\Theta) = 0 \tag{9.12}$$

where $\nabla f_\Theta(\Theta) \in \mathbb{R}^n$ and $\nabla g_\Theta(\Theta) \in \mathbb{R}^n$.

Pre-multiplying Eq. (9.12) by $\nabla^\top g_\Theta(\Theta)$ yields

$$\nabla^\top g_\Theta(\Theta) \nabla f_\Theta(\Theta) + \lambda \nabla^\top g_\Theta(\Theta) \nabla g_\Theta(\Theta) = 0 \tag{9.13}$$

Using the pseudo-inverse, $\lambda(t)$ is obtained as

$$\lambda = -\frac{\nabla^\top g_\Theta(\Theta) \nabla f_\Theta(\Theta)}{\nabla^\top g_\Theta(\Theta) \nabla g_\Theta(\Theta)} \tag{9.14}$$

Thus, the adjoint variable $\lambda(t)$ is negative of the projection of the vector $\nabla J_\Theta(\Theta)$ onto the vector $\nabla g_\Theta(\Theta)$.

Now, the gradient update law for $\Theta(t)$ is given by

$$\dot{\Theta} = -\Gamma \nabla J_\Theta(\Theta) = -\Gamma \left[\nabla f_\Theta(\Theta) + \lambda \nabla g_\Theta(\Theta)\right] \tag{9.15}$$

Substituting $\lambda(t)$ into the gradient update law results in

$$\dot{\Theta} = -\Gamma\left[\nabla f_{\Theta}(\Theta) - \frac{\nabla g_{\Theta}(\Theta)\nabla^{\top} g_{\Theta}(\Theta)\nabla f_{\Theta}(\Theta)}{\nabla^{\top} g_{\Theta}(\Theta)\nabla g_{\Theta}(\Theta)}\right] \tag{9.16}$$

The update law can also be expressed by a projection operator as

$$\dot{\Theta} = \text{Pro}(\Theta, -\Gamma\nabla J_{\Theta}(\Theta)) = -\Gamma\left[I - \frac{\nabla g_{\Theta}(\Theta)\nabla^{\top} g_{\Theta}(\Theta)}{\nabla^{\top} g_{\Theta}(\Theta)\nabla g_{\Theta}(\Theta)}\right]\nabla J_{\Theta}(\Theta) \tag{9.17}$$

The projection thus restricts of the optimal solution to only permissible values of $\Theta(t)$ that lie on the constraint set $g(\Theta) = 0$.

For example, consider the following constraint:

$$g(\Theta) = \left(\Theta - \Theta^*\right)^{\top}\left(\Theta - \Theta^*\right) - R^2 = 0 \tag{9.18}$$

which is a circle with the center at $\Theta(t) = \Theta^*$ and the radius R.

$g(\Theta)$ can be verified to be a convex function. Then,

$$\nabla g_{\Theta}(\Theta) = 2\left(\Theta - \Theta^*\right) \tag{9.19}$$

The least-squares gradient adaptive law with this constraint is given by

$$\dot{\Theta} = -\Gamma\left[I - \frac{(\Theta - \Theta^*)(\Theta - \Theta^*)^{\top}}{R^2}\right]\Phi(x)\varepsilon^{\top} \tag{9.20}$$

A more common situation in adaptive control typically involves an inequality constraint defined by a convex set

$$\mathcal{S} = \left\{\Theta(t) \in \mathbb{R}^n : g(\Theta) \leq 0\right\} \tag{9.21}$$

The optimization solution is then restricted to all permissible values of $\Theta(t)$ inside the compact set $\mathcal{S}$. If the initial values of $\Theta(t)$ is inside $\mathcal{S}$, then there are two situations to consider:

1. If $\Theta(t)$ remains inside $\mathcal{S}$ where $g(\Theta) < 0$, then the optimization is unconstrained and the standard gradient update law is used.
2. If $\Theta(t)$ is on the boundary of $\mathcal{S}$ where $g(\Theta) = 0$, then two situations can occur. If $\Theta(t)$ proceeds in a direction toward $\mathcal{S}$, then the standard gradient update law for the unconstrained optimization is used. The direction toward $\mathcal{S}$ is such that ∇g_{Θ} points toward $\mathcal{S}$ and generally is in the opposite direction to that of $-\nabla J_{\Theta}$. This implies the dot product between ∇g_{Θ} and $-\nabla J_{\Theta}$ is negative, or $-\nabla^{\top} J_{\Theta}\nabla g_{\Theta} \leq 0$. If $\Theta(t)$ moves away from $\mathcal{S}$ in a direction such that $-\nabla^{\top} J_{\Theta}\nabla g_{\Theta} > 0$, then the projection method is used to bring $\Theta(t)$ back onto a tangent plane of $\mathcal{S}$. $\Theta(t)$ would then proceed in the direction on the boundary of $\mathcal{S}$.

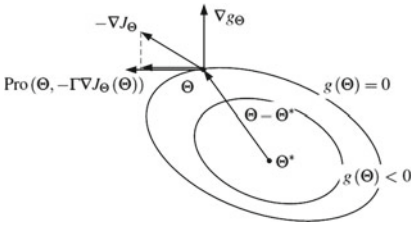

Fig. 9.2 Projection method

From Fig. 9.2, when $\Theta(t)$ moves away from $\mathscr{S}$, it follows that

$$\left(\Theta-\Theta^*\right)^\top \nabla g_\Theta(\Theta) > 0 \tag{9.22}$$

The projection method is then stated as [5]

$$\dot{\Theta} = \mathrm{Pro}(\Theta, -\Gamma\nabla J_\Theta(\Theta)) = \begin{cases} -\Gamma\nabla J_\Theta(\Theta) & \text{if } g(\Theta)<0 \text{ or if } g(\Theta)=0 \\ & \text{and } -\nabla^\top J_\Theta \nabla g_\Theta(\Theta) \le 0 \\ -\Gamma\left[I-\dfrac{\nabla g_\Theta(\Theta)\nabla^\top g_\Theta(\Theta)}{\nabla^\top g_\Theta(\Theta)\nabla g_\Theta(\Theta)}\right]\nabla J_\Theta(\Theta) & \text{if } g(\Theta)\ge 0 \\ & \text{and } -\nabla^\top J_\Theta(\Theta)\nabla g_\Theta(\Theta) > 0 \end{cases} \tag{9.23}$$

Using the projection method for MRAC, the adaptive law is expressed as

$$\dot{\Theta} = \mathrm{Pro}\left(\Theta, -\Gamma\Phi(x)e^\top PB\right) = \begin{cases} -\Gamma\Phi(x)e^\top PB & \text{if } g(\Theta)<0 \text{ or if } g(\Theta)=0 \\ & \text{and } -\left[\Phi(x)e^\top PB\right]^\top \nabla g_\Theta(\Theta)\le 0 \\ -\Gamma\left[I-\dfrac{\nabla g_\Theta(\Theta)\nabla^\top g_\Theta(\Theta)}{\nabla^\top g_\Theta(\Theta)\nabla g_\Theta(\Theta)}\right]\Phi(x)e^\top PB & \text{if } g(\Theta)\ge 0 \\ & \text{and } -\left[\Phi(x)e^\top PB\right]^\top \nabla g_\Theta(\Theta) > 0 \end{cases} \tag{9.24}$$

The projection method can be shown to achieve uniform ultimate boundedness by the Lyapunov stability analysis as follows:

Proof When $g(\Theta)<0$ or $g(\Theta)=0$ and $\Theta(t)$ moves toward $\mathscr{S}$, then the usual result of the Lyapunov analysis in Sect. 8.1 is obtained. When $g(\Theta)\ge 0$ and $\Theta(t)$ moves away from $\mathscr{S}$, then the projection method is used.

Choose a Lyapunov candidate function

$$V\left(e,\tilde{\Theta}\right) = e^\top Pe + \tilde{\Theta}^\top\Gamma^{-1}\tilde{\Theta} \tag{9.25}$$

Then,

$$\dot{V}\left(e,\tilde{\Theta}\right)=-e^{\top}Qe-2e^{\top}Pw+2\tilde{\Theta}^{\top}\frac{\nabla g_{\Theta}\left(\Theta\right)\nabla^{\top}g_{\Theta}\left(\Theta\right)}{\nabla^{\top}g_{\Theta}\left(\Theta\right)\nabla g_{\Theta}\left(\Theta\right)}\Phi\left(x\right)e^{\top}PB \quad (9.26)$$

The direction of $\Theta\left(t\right)$ away from $\mathscr{S}$ is defined by $-\left[\Phi\left(x\right)e^{\top}PB\right]^{\top}\nabla g_{\Theta}\left(\Theta\right)>0$. Then, let $\nabla^{\top}g_{\Theta}\left(\Theta\right)\Phi\left(x\right)e^{\top}PB=-c_0<0$ where $c_0>0$. It follows from Eq. (9.22) that

$$\dot{V}\left(e,\tilde{\Theta}\right)\leq-\lambda_{min}\left(Q\right)\left\|e\right\|^2+2\lambda_{max}\left(P\right)\left\|e\right\|w_0-\frac{2c_0\tilde{\Theta}^{\top}\nabla g_{\Theta}\left(\Theta\right)}{\nabla^{\top}g_{\Theta}\left(\Theta\right)\nabla g_{\Theta}\left(\Theta\right)} \quad (9.27)$$

Suppose $g\left(\Theta\right)$ is defined by Eq. (9.18). Then,

$$2\tilde{\Theta}^{\top}\nabla g_{\Theta}\left(\Theta\right)=4\tilde{\Theta}^{\top}\tilde{\Theta}=4R^2=\nabla^{\top}g_{\Theta}\left(\Theta\right)\nabla g_{\Theta}\left(\Theta\right) \quad (9.28)$$

So,

$$\begin{aligned}\dot{V}\left(e,\tilde{\Theta}\right)&\leq-\lambda_{min}\left(Q\right)\left\|e\right\|^2+2\lambda_{max}\left(P\right)\left\|e\right\|w_0-2c_0\\&\leq-\lambda_{min}\left(Q\right)\left\|e\right\|^2+2\lambda_{max}\left(P\right)\left\|e\right\|w_0\end{aligned} \quad (9.29)$$

Thus, $\dot{V}\left(e,\tilde{\Theta}\right)\leq 0$ if

$$\left\|e\right\|\geq\frac{2\lambda_{max}\left(P\right)w_0}{\lambda_{min}\left(Q\right)}=p \quad (9.30)$$

Since $g\left(\Theta\right)\geq 0$, then $\left\|\tilde{\Theta}\right\|$ is bounded from below by $\left\|\tilde{\Theta}\right\|\geq R$. We want the trajectory of $\tilde{\Theta}\left(t\right)$ to return to the set $\mathscr{S}$. Thus, $\dot{V}\left(e,\tilde{\Theta}\right)\geq 0$ inside a compact set

$$\mathscr{S}=\left\{\left(\left\|e\right\|,\left\|\tilde{\Theta}\right\|\right):\left\|e\right\|\leq p\text{ and }\left\|\tilde{\Theta}\right\|\leq R\right\} \quad (9.31)$$

but $\dot{V}\left(e,\tilde{\Theta}\right)\leq 0$ outside $\mathscr{S}$ to ensure that both $e\left(t\right)$ and $\tilde{\Theta}\left(t\right)$ are uniformly ultimately bounded.

The ultimate bounds can be found from the following inequalities:

$$\begin{aligned}\lambda_{min}\left(P\right)\left\|e\right\|^2&\leq\lambda_{min}\left(P\right)\left\|e\right\|^2+\lambda_{min}\left(\Gamma^{-1}\right)\left\|\tilde{\Theta}\right\|^2\\&\leq V\left(e,\tilde{\Theta}\right)\leq\lambda_{max}\left(P\right)p^2+\lambda_{max}\left(\Gamma^{-1}\right)R^2\end{aligned} \quad (9.32)$$

$$\lambda_{min}\left(\Gamma^{-1}\right)\left\|\tilde{\Theta}\right\|^2 \leq \lambda_{min}(P)\|e\|^2 + \lambda_{min}\left(\Gamma^{-1}\right)\left\|\tilde{\Theta}\right\|^2 \leq V\left(e,\tilde{\Theta}\right)$$
$$\leq \lambda_{max}(P)\,p^2 + \lambda_{max}\left(\Gamma^{-1}\right)R^2 \tag{9.33}$$

Thus,

$$p \leq \|e\| \leq \sqrt{\frac{\lambda_{max}(P)\,p^2 + \lambda_{max}\left(\Gamma^{-1}\right)R^2}{\lambda_{min}(P)}} = \rho \tag{9.34}$$

$$R \leq \left\|\tilde{\Theta}\right\| \leq \sqrt{\frac{\lambda_{max}(P)\,p^2 + \lambda_{max}\left(\Gamma^{-1}\right)R^2}{\lambda_{min}\left(\Gamma^{-1}\right)}} = \beta \tag{9.35}$$

■

Therefore, the projection method improves robustness of MRAC by constraining the adaptive parameters to remain within a convex set. The boundedness of the adaptive parameters causes an increase in the ultimate bound of the tracking error. Since $g(\Theta)$ is a scalar function that constrains the adaptive parameters, the challenge is to obtain such a function. For example, the convex function $g(\Theta)$ in Eq. (9.18) can also be expressed as

$$g(\Theta) = \sum_{i=1}^{n}\left(\theta_i - \theta_i^*\right)^2 - R^2 \leq 0 \tag{9.36}$$

Then,

$$\theta_{i_{min}} = \theta_i^* - R \leq \theta_i \leq \theta_i^* + R = \theta_{i_{max}} \tag{9.37}$$

The problem is that the range of θ_i which is equal to $\theta_{i_{max}} - \theta_{i_{min}}$ is determined by a single parameter R when in practice each θ_i could have a different range. For example, if a priori bounds on the adaptive parameters can be determined such that

$$\theta_{i_{min}} = \theta_i^* - r_i \leq \theta_i \leq \theta_i^* + r_i = \theta_{i_{max}} \tag{9.38}$$

Then, R is determined as

$$R = \min_{i=1}^{n}(r_i) \tag{9.39}$$

This would then result in an over-constrained convex set wherein one or more adaptive parameters will be over-constrained. Thus, a convex scalar function may not be sufficiently flexible for handling more than one adaptive parameter. In such situations, a convex vector function could be used.

Suppose a convex vector function is defined as

$$g(\Theta) = [g_i(\theta_i)] = \begin{bmatrix} (\theta_1 - \theta_1^*)^2 - r_1^2 \\ \vdots \\ (\theta_m - \theta_m^*)^2 - r_m^2 \end{bmatrix} \tag{9.40}$$

where $m \leq n$.

The augmented cost function is expressed as

$$J(\Theta) = f(\Theta) + g^\top(\Theta)\lambda = f(\Theta) + \sum_{i=1}^{m} \lambda_i g_i(\theta_i) \tag{9.41}$$

where $\lambda(t) \in \mathbb{R}^m$.

Then,

$$\nabla f_\Theta(\Theta) + \nabla^\top g(\Theta)\lambda = 0 \tag{9.42}$$

$\lambda(t)$ can be solved by the pseudo-inverse as

$$\lambda = -\left[\nabla g_\Theta(\Theta)\nabla^\top g_\Theta(\Theta)\right]^{-1}\nabla g(\Theta)\nabla f_\Theta(\Theta) \tag{9.43}$$

The projection operator then becomes

$$\begin{aligned} \dot{\Theta} &= \text{Pro}(\Theta, -\Gamma\nabla J_\Theta(\Theta)) \\ &= -\Gamma\left\{I - \nabla^\top g(\Theta)\left[\nabla g_\Theta(\Theta)\nabla^\top g_\Theta(\Theta)\right]^{-1}\nabla g(\Theta)\right\}\nabla J_\Theta(\Theta) \end{aligned} \tag{9.44}$$

if $g_i(\theta_i) \geq 0$ and $-\left[\nabla^\top J_\Theta(\Theta)\nabla^\top g_\Theta(\Theta)\right]_i > 0, i = 1, \ldots, m$.

For the special case when $m = n$, then

$$\lambda = -\nabla^{-\top} g(\Theta)\nabla f_\Theta(\Theta) \tag{9.45}$$

The projection operator turns out to be equal to zero since

$$\dot{\Theta} = \text{Pro}(\Theta, -\Gamma\nabla J_\Theta(\Theta)) = -\Gamma\left\{I - \nabla^\top g(\Theta)\nabla^{-\top} g(\Theta)\right\}\nabla J_\Theta(\Theta) = 0 \tag{9.46}$$

if $g_i(\theta_i) \geq 0$ and $-\left[\nabla^\top J_\Theta(\Theta)\nabla^\top g_\Theta(\Theta)\right]_i > 0, i = 1, \ldots, m$.

This leads to a more intuitive projection method for MRAC which can be stated in a column-wise format as

$$\dot{\theta}_i = \begin{cases} -\left[\Gamma\Phi(x)e^\top PB\right]_i & \text{if } (\theta_i - \theta_i^*)^2 < r_i^2 \text{ or if } (\theta_i - \theta_i^*)^2 = r_i^2 \\ & \text{and } -\left[\Phi(x)e^\top PB\right]_i^\top (\theta_i - \theta_i^*) \leq 0 \\ 0 & \text{otherwise} \end{cases} \tag{9.47}$$

The same projection method can be used when $\Theta(t)$ is a matrix for each element $\theta_{ij}(t)$.

The challenge with the projection method is to be able to determine θ_i^* and r_i^* a priori. Since technically θ_i^* is an unknown ideal parameter, the projection method has the same shortcoming as the dead-zone method in that a priori knowledge of the uncertainty must be established. This illustrates an important point that robustness can never be attained for any adaptive control design if the uncertainty is completely unknown. Thus, with some knowledge on the bounds of the adaptive parameters, the projection method can be used as an effective robust modification to MRAC.

Example 9.2 For Example 8.4, the largest negative feedback gain that the system can tolerate is $k_{x_{min}} = -3.8069$. If a priori knowledge of this limiting feedback gain is known, then the projection method can be used to enforce the constraint on $k_x(t)$ during the adaptation process. Suppose this constraint is specified as

$$\left|k_x - k_x^*\right| \leq r$$

where $k_x^* = 0$ and $r = 3$.

Using an adaptation rate $\gamma_x = 7.6$, which, in Example 8.4, would result in instability, the closed-loop system is now stable with $k_x(t) \to -3$ when the adaptation is shut off as shown in Fig. 9.3.

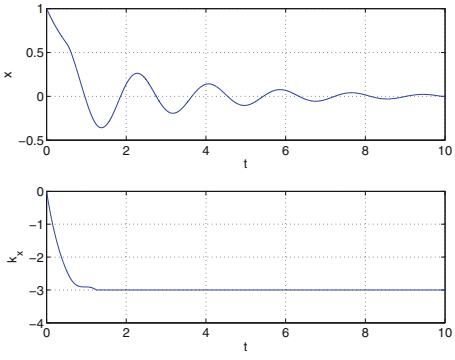

Fig. 9.3 MRAC with projection method

9.3 σ Modification

Rohrs' investigation of robustness of adaptive control in the presence of unmodeled dynamics exhibits the various instability mechanisms of model-reference adaptive

control [1]. Since then, researchers began to examine ways to modify the standard MRAC to improve robustness. A number of modifications were developed in the 1980s, among which the σ modification is perhaps the simplest modification method that demonstrates the potential for improved robustness. The σ modification method was developed by Ioannu and Kokotovic [2]. It is widely used in adaptive control practice due to its simplicity.

Consider a MIMO system with a parametric matched uncertainty and an unknown bounded disturbance

$$\dot{x} = Ax + B\left[u + \Theta^{*\top}\Phi\left(x\right)\right] + w \tag{9.48}$$

where $x\left(t\right) \in \mathbb{R}^n$ is a state vector, $u\left(t\right) \in \mathbb{R}^m$ is a control vector, $A \in \mathbb{R}^n \times \mathbb{R}^n$ is known, $B \in \mathbb{R}^n \times \mathbb{R}^m$ is also known such that $\left(A, B\right)$ is controllable, $\Theta^* \in \mathbb{R}^p \times \mathbb{R}^m$ is the unknown parameter, $\Phi\left(x\right) \in \mathbb{R}^p$ is a known, bounded function, and $w\left(t\right) \in \mathbb{R}^n$ is an unknown bounded disturbance.

The reference model is given by

$$\dot{x}_m = A_m x_m + B_m r \tag{9.49}$$

where $A_m \in \mathbb{R}^n \times \mathbb{R}^n$ is known and Hurwitz, $B_m \in \mathbb{R}^n \times \mathbb{R}^r$ is known, and $r\left(t\right) \in \mathbb{R}^r$ is a bounded reference command signal.

We assume that K_x and K_r can be determined from the model matching conditions

$$A + BK_x = A_m \tag{9.50}$$

$$BK_r = B_m \tag{9.51}$$

Then, the adaptive controller is designed as

$$u = K_x x + K_r r - \Theta^{\top}\Phi\left(x\right) \tag{9.52}$$

The σ modification to the adaptive law that estimates $\Theta\left(t\right)$ is described by

$$\dot{\Theta} = -\Gamma\left[\Phi\left(x\right)e^{\top}PB + \sigma\Theta\right] \tag{9.53}$$

where $\sigma > 0$ is the modification parameter.

The modification term effectively introduces a constant damping into the adaptive law, thereby providing a mechanism to bound the adaptive parameters. The σ modification is quite effective and yet simple to implement. It is frequently used in adaptive control to ensure robustness. By bounding the adaptive parameters, the ideal asymptotic tracking property of MRAC is no longer preserved with the σ modification.

The σ modification can be shown to be stable by the Lyapunov's direct method as follows:

Proof Choose a Lyapunov candidate function

$$V\left(e,\tilde{\Theta}\right)=e^{\top}Pe+\text{trace}\left(\tilde{\Theta}^{\top}\Gamma^{-1}\tilde{\Theta}\right) \tag{9.54}$$

The tracking error equation is obtained as

$$\dot{e}=A_m e+B\tilde{\Theta}^{\top}\Phi\left(x\right)-w \tag{9.55}$$

Evaluating $\dot{V}\left(e,\tilde{\Theta}\right)$ yields

$$\dot{V}\left(e,\tilde{\Theta}\right)=-e^{\top}Qe+2e^{\top}PB\tilde{\Theta}^{\top}\Phi\left(x\right)-2e^{\top}Pw+\text{trace}\left(-2\tilde{\Theta}^{\top}\left[\Phi\left(x\right)e^{\top}PB+\sigma\Theta\right]\right) \tag{9.56}$$

This can be simplified as

$$\begin{aligned}\dot{V}\left(e,\tilde{\Theta}\right)&=-e^{\top}Qe-2e^{\top}Pw-2\sigma\,\text{trace}\left(\tilde{\Theta}^{\top}\Theta\right)\\&=-e^{\top}Qe-2e^{\top}Pw-2\sigma\,\text{trace}\left(\tilde{\Theta}^{\top}\tilde{\Theta}+\tilde{\Theta}^{\top}\Theta^{*}\right)\end{aligned} \tag{9.57}$$

Therefore, $\dot{V}\left(e,\tilde{\Theta}\right)$ is bounded by

$$\dot{V}\left(e,\tilde{\Theta}\right)\leq-\lambda_{min}\left(Q\right)\|e\|^{2}+2\|e\|\lambda_{max}\left(P\right)w_0-2\sigma\left\|\tilde{\Theta}\right\|^{2}+2\sigma\left\|\tilde{\Theta}\right\|\Theta_0 \tag{9.58}$$

where $w_0=\max\|w\|_{\infty}$ and $\Theta_0=\|\Theta^{*}\|$.

To show that the solution is bounded, we need to show that $\dot{V}\left(e,\tilde{\Theta}\right)>0$ inside a compact set but $\dot{V}\left(e,\tilde{\Theta}\right)\leq 0$ outside it. To that end, completing the square yields

$$\begin{aligned}\dot{V}\left(e,\tilde{\Theta}\right)\leq&-\lambda_{min}\left(Q\right)\left[\|e\|-\frac{\lambda_{max}\left(P\right)w_0}{\lambda_{min}\left(Q\right)}\right]^{2}\\&+\frac{\lambda_{max}^{2}\left(P\right)w_0^{2}}{\lambda_{min}\left(Q\right)}-2\sigma\left(\left\|\tilde{\Theta}\right\|-\frac{\Theta_0}{2}\right)^{2}+\frac{\sigma\Theta_0^{2}}{2}\end{aligned} \tag{9.59}$$

Thus, $\dot{V}\left(e, \tilde{\Theta}\right) \leq 0$ if

$$\|e\| \geq \frac{\lambda_{max}(P) w_0}{\lambda_{min}(Q)} + \sqrt{\frac{\lambda_{max}^2(P) w_0^2}{\lambda_{min}^2(Q)} + \frac{\sigma \Theta_0^2}{2\lambda_{min}(Q)}} = p \tag{9.60}$$

or

$$\left\|\tilde{\Theta}\right\| \geq \frac{\Theta_0}{2} + \sqrt{\frac{\lambda_{max}^2(P) w_0^2}{2\sigma\lambda_{min}(Q)} + \frac{\Theta_0^2}{4}} = \alpha \tag{9.61}$$

$\dot{V}\left(e, \tilde{\Theta}\right) \leq 0$ outside a compact set $\mathscr{S}$ defined by

$$\mathscr{S} = \left\{ \left(\|e\|, \left\|\tilde{\Theta}\right\|\right) : \lambda_{min}(Q) \left[\|e\| - \frac{\lambda_{max}(P) w_0}{\lambda_{min}(Q)}\right]^2 + 2\sigma \left(\left\|\tilde{\Theta}\right\|^2 - \frac{\Theta_0}{2}\right)^2 \leq \frac{\lambda_{max}^2(P) w_0^2}{\lambda_{min}(Q)} + \frac{\sigma \Theta_0^2}{2} \right\} \tag{9.62}$$

Therefore, the solution is uniformly ultimately bounded with the ultimate bounds determined by

$$p \leq \|e\| \leq \sqrt{\frac{\lambda_{max}(P) p^2 + \lambda_{max}\left(\Gamma^{-1}\right)\alpha^2}{\lambda_{min}(P)}} = \rho \tag{9.63}$$

$$\alpha \leq \left\|\tilde{\Theta}\right\| \leq \sqrt{\frac{\lambda_{max}(P) p^2 + \lambda_{max}\left(\Gamma^{-1}\right)\alpha^2}{\lambda_{min}\left(\Gamma^{-1}\right)}} = \beta \tag{9.64}$$

■

We see that the ultimate bound for the tracking error increases due to the σ modification term. This is a consequence of the trade-off between the tracking performance and robustness. Another interesting observation is that, if $\sigma = 0$, then the standard MRAC is recovered and $\left\|\tilde{\Theta}\right\|$ is unbounded if w_0 is not zero. This is consistent with the parameter drift behavior in the standard MRAC.

If the adaptive controller is a regulator type and the disturbance is zero, then the closed-loop system is autonomous and is expressed as

$$\dot{x} = A_m x - B\left(\Theta - \Theta^*\right)\Phi(x) \tag{9.65}$$

$$\dot{\Theta} = -\Gamma\left[-\Phi(x) x^\top P B + \sigma\Theta\right] \tag{9.66}$$

Let $\Gamma \to \infty$, then the equilibrium of this system is determined as

$$\bar{x} = A_m^{-1} B \left[\frac{1}{\sigma} \Phi(\bar{x}) \bar{x}^\top P B - \Theta^* \right] \Phi(\bar{x}) \tag{9.67}$$

$$\bar{\Theta} = \frac{1}{\sigma} \Phi(\bar{x}) \bar{x}^\top P B \tag{9.68}$$

The equilibrium adaptive parameter $\bar{\Theta}$ thus is inversely proportional to the modification parameter σ. The equilibrium state $\bar{x}$ is also inversely proportional to σ. As the value of the modification parameter σ increases, the tracking error becomes larger. The reduced tracking performance of the σ modification offers better robustness to unmodeled dynamics in return. Because the adaptive parameter is proven to be bounded, the parameter drift issue is eliminated.

Example 9.3 Consider the parameter drift example in Example 8.1. Let

$$x = (1+t)^n$$

The σ modification adaptive law is given by

$$\dot{k}_x = -\gamma_x \left(x^2 b + \sigma k_x \right)$$

which could also be expressed as

$$\frac{d}{dt} \left(e^{\gamma_x \sigma t} k_x \right) = -e^{\gamma_x \sigma t} \gamma_x x^2 b$$

The solution of this equation is

$$e^{\gamma_x \sigma t} k_x - k_x(0) = -\gamma_x b \left[\frac{e^{\gamma_x \sigma t} (1+t)^{2n} - 1}{\gamma_x \sigma} - \frac{2n e^{\gamma_x \sigma t} (1+t)^{2n-1} - 2n}{\gamma_x^2 \sigma^2} + \frac{2n(2n-1) e^{\gamma_x \sigma t} (1+t)^{2n-2} - 2n(2n-1)}{\gamma_x^3 \sigma^3} - \cdots \right]$$

which yields

$$k_x = e^{-\gamma_x \sigma t} \left[k_x(0) - \gamma_x b \left(-\frac{1}{\gamma_x \sigma} + \frac{2n}{\gamma_x^2 \sigma^2} - \frac{2n(2n-1)}{\gamma_x^3 \sigma^3} + \cdots \right) \right] - \gamma_x b \left[\frac{(1+t)^{2n}}{\gamma_x \sigma} - \frac{2n(1+t)^{2n-1}}{\gamma_x^2 \sigma^2} + \frac{2n(2n-1)(1+t)^{2n-2}}{\gamma_x^3 \sigma^3} - \cdots \right]$$

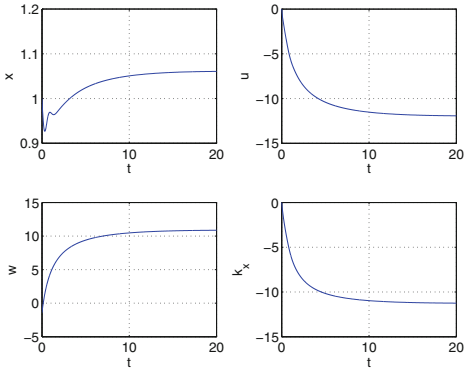

Fig. 9.4 σ modification

Note that not only $x\,(t)$ is bounded for all $n < 0$, but $k_x\,(t)$ is also bounded. Thus, the σ modification has eliminated the parameter drift issue.

The response of the closed-loop plant for the same disturbance in this example with $n = -\frac{5}{12}$, $x\,(0) = 1$, $k_x\,(0) = 0$, $\gamma_x = 10$, and $\sigma = 0.1$ is shown in Fig. 9.4. Note that with MRAC, $k_x\,(t)$ is unbounded but now becomes bounded with the σ modification.

■

Consider a MIMO system

$$\dot{x} = Ax + Bu \tag{9.69}$$

where A is unknown.

The plant is designed with the following adaptive controller:

$$u = K_x\,(t)\,x + K_r r \tag{9.70}$$

to follow the reference model in Eq. (9.49).

The σ modification adaptive law for $K_x\,(t)$ is given by

$$\dot{K}_x^\top = \Gamma_x \left(xe^\top PB - \sigma K_x^\top\right) \tag{9.71}$$

Differentiating the closed-loop plant gives

$$\ddot{x} = A\dot{x} + B\dot{K}_x x + BK_x\dot{x} + BK_r\dot{r} \tag{9.72}$$

Then,

$$\ddot{x} - (A + BK_x)\,\dot{x} - B\left(B^\top Pex^\top + \sigma K_x\right)\Gamma_x x = BK_r\dot{r} \tag{9.73}$$

The second term on the left-hand side acts as a damping term due to the proportional control action. The third term is effectively a nonlinear integral control. Without

the σ modification term, as Γ_x increases, robustness of the closed-loop plant is reduced. In the limit as $\Gamma_x \to \infty$, the time-delay margin of the closed-loop plant goes to zero. In the presence of the σ modification term, the integral control action tends to zero as $\Gamma_x \to \infty$, thereby improving robustness of the adaptive controller.

Consider the SISO plant in Sect. 8.5, the σ modification adaptive law for $k_x(t)$ is

$$\dot{k}_x = \gamma_x (xeb - \sigma k_x) \tag{9.74}$$

The closed-loop plant is then expressed as

$$\ddot{x} - (a + bk_x)\dot{x} - b\gamma_x (xeb - \sigma k_x) x = bk_r \dot{r} \tag{9.75}$$

The third term in the left-hand side is the nonlinear integral control

$$k_i(x) = \gamma_x (xeb - \sigma k_x) = \dot{k}_x \tag{9.76}$$

Thus, the σ modification changes the ideal integral control action of the adaptive controller.

Suppose $\gamma_x \to \infty$ and $r(t)$ is a constant reference command signal, then $k_x(t)$ tends to an equilibrium

$$\bar{k}_x \to \frac{\bar{x}\bar{e}b}{\sigma} \tag{9.77}$$

This effectively reduces the integral gain k_i to zero. Then, the closed-loop system tends to

$$\dot{x} = \left(a + \frac{\bar{x}\bar{e}b^2}{\sigma}\right) x + bk_r r \tag{9.78}$$

The cross-over frequency and time-delay margin are obtained as

$$\omega = \sqrt{\frac{\bar{x}^2\bar{e}^2b^4}{\sigma^2} - a^2} \tag{9.79}$$

$$t_d = \frac{1}{\omega}\cos^{-1}\left(-\frac{\sigma a}{\bar{x}\bar{e}b^2}\right) \tag{9.80}$$

It can be seen that as $\gamma_x \to \infty$, the time-delay margin of the closed-loop system remains finite. In contrast, for MRAC, the time-delay margin goes to zero as $\gamma_x \to \infty$. In fact, by setting $\sigma = 0$ for MRAC, we see that $\omega \to \infty$ and $t_d \to 0$. Since the time-delay margin is a measure of robustness, the σ modification clearly is more robust than the standard MRAC.

The equilibrium state is determined by letting $\gamma_x \to \infty$ in the adaptive law for $k_x(t)$ so that

$$\bar{x}^2 - \bar{x}_m\bar{x} + \frac{\sigma\bar{k}_x}{b} = 0 \tag{9.81}$$

which yields

$$\bar{x} = \frac{\bar{x}_m}{2}\left(1 + \sqrt{1 - \frac{4\sigma \bar{k}_x}{b\bar{x}_m^2}}\right) \tag{9.82}$$

The σ modification therefore causes $x(t)$ to not follow $x_m(t)$. So, the ideal property of asymptotic tracking of MRAC is not preserved. This is a trade-off with improved robustness.

The equilibrium value of $k_x(t)$ can be determined from the state equation

$$\dot{x} = (a + bk_x)x + bk_r r \tag{9.83}$$

where $r(t)$ is a constant reference command signal.

This results in

$$\bar{k}_x = -\frac{k_r r}{\bar{x}} - \frac{a}{b} \tag{9.84}$$

Since the reference model is given by

$$\dot{x}_m = a_m x_m + b_m r \tag{9.85}$$

therefore $a + bk_x^* = a_m$ and $bk_r = b_m$ by the model matching conditions. Then, the equilibrium reference state is related to the constant reference command signal according to

$$r = -\frac{a_m \bar{x}_m}{b_m} \tag{9.86}$$

Substituting into the equilibrium value of $k_x(t)$ gives

$$\bar{k}_x = \frac{a_m \bar{x}_m}{b\bar{x}} - \frac{a}{b} \tag{9.87}$$

If $\bar{x} \to \bar{x}_m$, then ideally $\bar{k}_x \to k_x^*$. With the σ modification, the adaptive parameter does not tend to its ideal value because the tracking is not asymptotic.

Using the equilibrium value of $k_x(t)$, the equilibrium state can be determined explicitly as a function of the equilibrium reference state $\bar{x}_m$ from the following equation:

$$b^2\bar{x}^3 - b^2\bar{x}_m\bar{x}^2 - \sigma a\bar{x} + \sigma a_m \bar{x}_m = 0 \tag{9.88}$$

Because the tracking is not asymptotic and the adaptive parameter does not tend to its ideal value, a switching modification to the σ modification has been proposed by Ioannu [3]. The switching σ modification turns on the σ modification when the adaptive parameter exceeds a certain threshold and switches off when the adaptive parameter falls below the threshold. When the σ modification is switched off, the adaptive law will attempt to restore its ideal property of asymptotic tracking. In practice, the switching can cause transients and high-frequency oscillations that could present a problem in itself.

The switching σ modification is stated as

$$\sigma = \begin{cases} \sigma_0 & \|\Theta\| \geq \Theta_0 \\ 0 & \|\Theta\| < \Theta_0 \end{cases} \tag{9.89}$$

As with the dead-zone method, the selection of the adaptive parameter threshold is usually not guided by systematic design approaches, but rather by trial-and-error.

Example 9.4 Consider Example 8.7. Keeping everything the same but using a value of $\sigma = 0.1$, the responses of the closed-loop system with and without a time delay of 0.0020 s are shown in Fig. 9.5. Note that the two responses are very similar, whereas the response with the standard MRAC with a time delay of 0.0020 s shows that the closed-loop system is unstable. All high-frequency oscillations are no longer present.

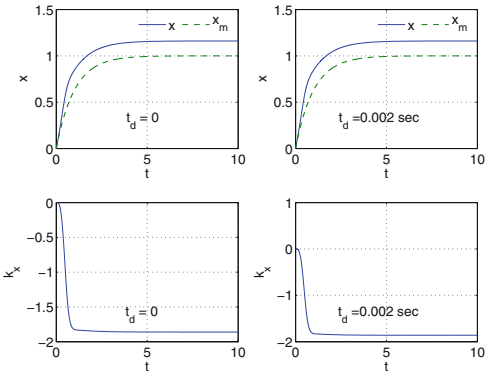

Fig. 9.5 Responses due to σ modification with and without time delay

The ideal feedback gain is computed to be $k_x^* = -2$. The equilibrium state is then computed from

$$\bar{x}^3 - \bar{x}^2 - 0.1\bar{x} - 0.1 = 0$$

which yields $\bar{x} = 1.1604$.

The equilibrium value of $k_x(t)$ is computed to be –1.8617. The simulation gives the same results as the analytical solutions. The time delay that the system can tolerate is 0.145 s estimated from the simulation.

9.4 *e* Modification

The *e* modification is another popular robust modification adaptive law. Developed by Narendra and Annaswammy [4], it is supposed to have overcome a limitation with the σ modification in that it can achieve asymptotic tracking under some conditions while improving robustness.

The e modification adaptive law is stated as

$$\dot{\Theta} = -\Gamma \left[\Phi(x) e^{\top} PB + \mu \left\| e^{\top} PB \right\| \Theta \right] \tag{9.90}$$

where $\mu > 0$ is the modification parameter.

The goal of the e modification is to reduce the damping term proportionally to the norm of the tracking error. As the tracking error tends to zero in the ideal case with MRAC, the damping term is also reduced to zero, thereby restoring the ideal asymptotic tracking property of MRAC. However, the stability analysis shows that the e modification only achieves bounded tracking. The ideal property of MRAC can no longer be preserved in all cases. So, asymptotic tracking cannot be achieved in general with increased robustness. This is a trade-off between performance and robustness that typically exists in all control designs.

The stability proof is given as follows:

Proof Choose the usual Lyapunov candidate function

$$V\left(e, \tilde{\Theta}\right) = e^{\top} Pe + \text{trace}\left(\tilde{\Theta}^{\top} \Gamma^{-1} \tilde{\Theta}\right) \tag{9.91}$$

Evaluating $\dot{V}\left(e, \tilde{\Theta}\right)$ yields

$$\begin{aligned} \dot{V}\left(e, \tilde{\Theta}\right) = & -e^{\top} Qe + 2e^{\top} PB\tilde{\Theta}^{\top} \Phi(x) - 2e^{\top} Pw \\ & + \text{trace}\left(-2\tilde{\Theta}^{\top} \left[\Phi(x) e^{\top} PB + \mu \left\| e^{\top} PB \right\| \Theta \right] \right) \end{aligned} \tag{9.92}$$

This can be simplified as

$$\dot{V}\left(e, \tilde{\Theta}\right) = -e^{\top} Qe - 2e^{\top} Pw - 2\mu \left\| e^{\top} PB \right\| \text{trace}\left(\tilde{\Theta}^{\top} \tilde{\Theta} + \tilde{\Theta}^{\top} \Theta^{*}\right) \tag{9.93}$$

$\dot{V}\left(e, \tilde{\Theta}\right)$ is bounded by

$$\begin{aligned} \dot{V}\left(e, \tilde{\Theta}\right) \leq & -\lambda_{min}(Q) \|e\|^2 + 2\|e\| \lambda_{max}(P) w_0 - 2\mu \|e\| \|PB\| \left\| \tilde{\Theta} \right\|^2 \\ & + 2\mu \|e\| \|PB\| \left\| \tilde{\Theta} \right\| \Theta_0 \end{aligned} \tag{9.94}$$

where $w_0 = \max \|w\|_{\infty}$ and $\Theta_0 = \|\Theta^*\|$.

To find the largest lower bound of $\|e\|$, we want to maximize the bound on $\dot{V}\left(e, \tilde{\Theta}\right)$. Taking the partial derivative of $\dot{V}\left(e, \tilde{\Theta}\right)$ with respect to $\left\| \tilde{\Theta} \right\|$ and setting it equal to zero yield

$$-4\mu \|e\| \|PB\| \left\| \tilde{\Theta} \right\| + 2\mu \|e\| \|PB\| \Theta_0 = 0 \tag{9.95}$$

Solving for $\left\|\tilde{\Theta}\right\|$ that maximizes $\dot{V}\left(e, \tilde{\Theta}\right)$ gives

$$\left\|\tilde{\Theta}\right\| = \frac{\Theta_0}{2} \tag{9.96}$$

Then,

$$\dot{V}\left(e, \tilde{\Theta}\right) \leq -\lambda_{min}(Q)\|e\|^2 + 2\|e\|\lambda_{max}(P)w_0 + \frac{\mu\|e\|\|PB\|\Theta_0^2}{2} \tag{9.97}$$

$\dot{V}\left(e, \tilde{\Theta}\right) \leq 0$ if

$$\|e\| \geq \frac{4\lambda_{max}(P)w_0 + \mu\|PB\|\Theta_0^2}{2\lambda_{min}(Q)} = p \tag{9.98}$$

Also, note that $\dot{V}\left(e, \tilde{\Theta}\right)$ is bounded by

$$\dot{V}\left(e, \tilde{\Theta}\right) \leq 2\|e\|\lambda_{max}(P)w_0 - 2\mu\|e\|\|PB\|\left\|\tilde{\Theta}\right\|^2 + 2\mu\|e\|\|PB\|\left\|\tilde{\Theta}\right\|\Theta_0 \tag{9.99}$$

Then, $\dot{V}\left(e, \tilde{\Theta}\right) \leq 0$ if

$$\left\|\tilde{\Theta}\right\| \geq \frac{\Theta_0}{2} + \sqrt{\frac{\Theta_0^2}{4} + \frac{\lambda_{max}(P)w_0}{\mu\|PB\|}} = \alpha \tag{9.100}$$

Therefore, $\dot{V}\left(e, \tilde{\Theta}\right) \leq 0$ outside a compact set $\mathscr{S}$ defined by

$$\mathscr{S} = \left\{\left(\|e\|, \left\|\tilde{\Theta}\right\|\right) : \|e\| \leq p \text{ and } \left\|\tilde{\Theta}\right\| \leq \alpha\right\} \tag{9.101}$$

Therefore, both $\|e\|$ and $\left\|\tilde{\Theta}\right\|$ are uniformly ultimate bounded with the ultimate bounds determined from Eqs. (9.63) and (9.64). Thus, the e modification results in bounded tracking. As can be seen, the duality of tracking performance and robustness cannot usually be simultaneously met.

Example 9.5 Consider the parameter drift example in Example 8.1. The response of the closed-loop plant for the same disturbance in this example with $p = -\frac{5}{12}$, $x(0) = 1, k_x(0) = 0, \gamma_x = 10$, and $\mu = 0.1$ is shown in Fig. 9.6. The e modification produces all bounded signals of the closed-loop system.

■

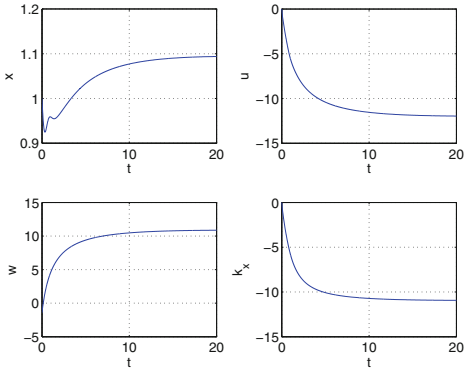

Fig. 9.6 *e* modification

Consider the SISO plant in Sect. 8.5, the *e* modification adaptive law for $k_x(t)$ is

$$\dot{k}_x = \gamma_x (xeb - \mu |eb| k_x) \tag{9.102}$$

The closed-loop plant is expressed as

$$\ddot{x} - (a + bk_x)\dot{x} - b\gamma_x (xeb - \mu |eb| k_x) x = bk_r \dot{r} \tag{9.103}$$

The nonlinear integral control with a nonlinear integral gain is obtained as

$$k_i(x) = \gamma_x (xeb - \mu |eb| k_x) = \dot{k}_x \tag{9.104}$$

As $\gamma_x \to \infty$, the equilibrium state can be determined by

$$b\bar{x}^2 - b\bar{x}\bar{x}_m + \mu |\bar{e}b| \bar{k}_x = 0 \tag{9.105}$$

where $\bar{x}_m$ is the equilibrium reference state for a constant reference command signal $r(t)$.

Then,

$$\bar{x}^2 - \left(\bar{x}_m \pm \mu \bar{k}_x\right) \bar{x} \pm \mu \bar{k}_x \bar{x}_m = 0 \tag{9.106}$$

which yields

$$\bar{x} = \frac{\bar{x}_m \pm \mu \bar{k}_x}{2} \left[1 + \sqrt{1 \mp \frac{4\mu \bar{k}_x \bar{x}_m}{\left(\bar{x}_m \pm \mu \bar{k}_x\right)^2}} \right] \tag{9.107}$$

where the upper sign is for $eb > 0$ and the lower sign is for $eb < 0$.

Using the equilibrium value of $k_x(t)$, the equilibrium state can be determined explicitly as a function of the equilibrium reference state $\bar{x}_m$ from the following

equation:

$$b\bar{x}^3 + (-b\bar{x}_m \pm \mu a)\,\bar{x}^2 \mp \mu\,(a + a_m)\,\bar{x}_m\bar{x} \pm \mu a_m\bar{x}_m^2 = 0 \tag{9.108}$$

This equation leads to an interesting observation. Since there are multiple roots, only one of these roots is a valid solution. One possible solution is $\bar{x} = \bar{x}_m$, which corresponds to asymptotic tracking. The other solution could be one of the other roots, depending on the nature of the equilibrium. The closed-loop system is linearized as

$$\dot{\tilde{x}} = \left(a + b\bar{k}_x\right)\tilde{x} + b\bar{x}\tilde{k} \tag{9.109}$$

$$\dot{\tilde{k}}_x = \gamma_x b\left(\bar{x}_m - 2\bar{x} \pm \mu\bar{k}_x\right)\tilde{x} \mp \gamma_x b\mu\,(\bar{x}_m - \bar{x})\,\tilde{k}_x \tag{9.110}$$

Then, the Jacobian is obtained as

$$J\left(\bar{x}, \bar{k}_x\right) = \begin{bmatrix} a + b\bar{k}_x & b\bar{x} \\ \gamma_x b\left(\bar{x}_m - 2\bar{x} \pm \mu\bar{k}_x\right) & \mp\gamma_x b\mu\,(\bar{x}_m - \bar{x}) \end{bmatrix} \tag{9.111}$$

The solution converges to a stable equilibrium which can be evaluated by examining of the eigenvalues of the Jacobian matrix.

Example 9.6 Consider Example 8.7 with $a = 1, b = 1$, and $a_m = -1$, the responses of the closed-loop system with a constant reference command signal $r\,(t) = 1$ for $\mu = 0.2$ and $\mu = 0.8$ are shown in Fig. 9.7.

For $\mu = 0.2$, the solution of $x\,(t)$ tends to the equilibrium reference state $\bar{x}_m = 1$, and $k_x\,(t)$ tends to its the equilibrium value at $k_x^* = -2$. The roots of the polynomial of $\bar{x}$ for $\mu = 0.2$ assuming $eb < 0$

$$\bar{x}^3 - 1.2\bar{x}^2 + 0.2 = 0$$

are 1, 0.5583, and -0.3583. The eigenvalues of the Jacobian are $(-0.5000 \pm 17.3133i)$, $(-4.3332, 46.7162)$, and $(4.6460, 133.9710)$ for the respective roots. Therefore, the equilibrium state is $\bar{x} = 1$ since it is the only stable equilibrium. The tracking is therefore asymptotic as shown in Fig. 9.7.

For $\mu = 0.8$, $x\,(t) \to \bar{x} = 1.3798$, and $k_x\,(t) \to \bar{k}_x = -1.7247$. The roots of the polynomial of $\bar{x}$ for $\mu = 0.8$ assuming $eb < 0$

$$\bar{x}^3 - 1.8\bar{x}^2 + 0.8 = 0$$

are 1.3798, 1, and -0.5798. The eigenvalues of the Jacobian are $(-2.4781, -150.1650)$, $(-0.5000 \pm 17.3133i)$, and $(2.4523, 631.1908)$ for the respective roots. The first equilibrium is a stable node and the second equilibrium is a stable focus. The stable node is more attractive because all trajectories converge exponentially faster to the first equilibrium than to the second equilibrium. Therefore, the equilibrium state is $\bar{x} = 1.3798$. The tracking is no longer asymptotic as shown in

Fig. 9.7. The equilibrium value of $k_x(t)$ is computed to be –1.7247 which agrees with the simulation result.

Now, consider a time-varying reference command signal $r(t) = \sin 2t - \cos 4t$. The responses of the closed-loop system $\mu = 0.2$ and $\mu = 0.8$ are shown in Fig. 9.8. The tracking error is no longer asymptotic as can be seen. The closed-loop system is non-autonomous, so it does not have a true equilibrium. As μ increases, the tracking performance is degraded, while robustness increases. For small values of μ, it appears that asymptotic tracking is almost achieved.

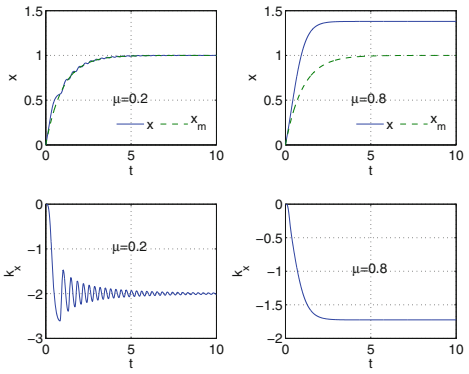

Fig. 9.7 *e* modification for constant reference command signal

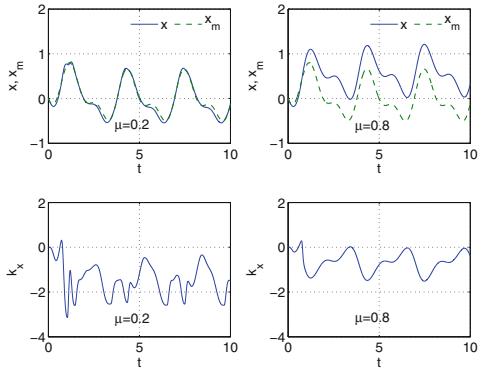

Fig. 9.8 *e* modification for time-varying reference command signal

9.5 Optimal Control Modification

Robust adaptive control achieves robustness by compromising the ideal asymptotic tracking property of MRAC. Almost all robust modifications in adaptive control result in bounded tracking. Recognizing this important requirement of robust adaptive control, the optimal control modification is a robust modification in adaptive control that addresses adaptive control in the context of optimal control. More specifically, the optimal control modification is designed as an optimal control solution to minimize the tracking error norm bounded away from the origin by an unknown lower bound. By not allowing the tracking error to tend to the origin asymptotically, increased robustness can be achieved. This method was developed by Nguyen in 2008 [9, 11]. The method has been subjected to various rigorous validation tests including pilot-in-loop flight simulation experiments [12, 13] and flight tests on NASA F/A-18A aircraft [14–17].

The optimal control modification is formulated from the optimal control theory as an adaptive optimal control method. The optimal control modification adaptive law is given by

$$\dot{\Theta} = -\Gamma \Phi (x) \left[e^{\top} P - \nu \Phi^{\top} (x) \Theta B^{\top} P A_m^{-1} \right] B \tag{9.112}$$

where $\nu > 0$ is the modification parameter.

To motivate the development of the method, we will review some basic principles in optimal control theory.

9.5.1 Optimal Control

In optimal control, we are interested in finding an extremal function that maximizes or minimizes an integral [19]

$$J = \int_{t_0}^{t_f} L (x, u) \, dt \tag{9.113}$$

where $x (t) \in \mathbb{R}^n$ is a state vector, and $u (t) \in \mathbb{R}^p$ is a control vector.

This is a functional extremization or optimization. The optimization finds a function that maximizes or minimizes the integral J, which is most commonly referred to as a cost functional or simply cost function. The integrand L () is called an objective function. The state vector $x (t)$ and the control vector $u (t)$ belong to a dynamical process described by

$$\dot{x} = f (x, u) \tag{9.114}$$

The solution of the optimization must satisfy the state equation (9.114). Therefore, the state equation imposes a dynamical constraint on the optimization. Thus, the optimization is referred to as a constrained optimization. A standard problem definition in optimal control can usually be stated as follows:

Find an optimal control $u^*(t)$ that minimizes the cost function

$$\min J = \int_{t_0}^{t_f} L(x,u)\,dt \tag{9.115}$$

subject to Eq. (9.114).

From calculus, the Lagrange multiplier method is used to minimize a function with constraints. The cost function is augmented by a Lagrange multiplier as

$$J = \int_{t_0}^{t_f} \left\{ L(x,u) + \underbrace{\lambda^\top [f(x,u) - \dot{x}]}_{\mathbf{0}} \right\} dt \tag{9.116}$$

where $\lambda(t) \in \mathbb{R}^n$ is the Lagrange multiplier and is often called an adjoint or co-state vector.

Note that the augmented term is zero, so in effect the cost function does not change. We define a Hamiltonian function as

$$H(x,u) = L(x,u) + \lambda^\top f(x,u) \tag{9.117}$$

The standard tool in optimal control is calculus of variations. The cost function is perturbed by a small variation δx in the state vector and variation δu in the control vector. These variations result in the cost function being perturbed by a small variation such that

$$J + \delta J = \int_{t_0}^{t_f} \left[H(x + \delta x, u + \delta u) - \lambda^\top (\dot{x} + \delta \dot{x}) \right] dt \tag{9.118}$$

Equation (9.118) can be evaluated as

$$J + \delta J = \int_{t_0}^{t_f} \left[H(x,u) + \frac{\partial H}{\partial x}\delta x + \frac{\partial H}{\partial u}\delta u - \lambda^\top \dot{x} - \lambda^\top \delta \dot{x} \right] dt \tag{9.119}$$

Consider the term $\lambda^\top \delta \dot{x}$. Integrating by parts yields

$$\int_{t_0}^{t_f} \lambda^\top \delta \dot{x} dt = \lambda^\top (t_f)\,\delta x (t_f) - \lambda^\top (t_0)\,\delta x (t_0) - \int_{t_0}^{t_f} \dot{\lambda}^\top \delta x dt \tag{9.120}$$

Then,

$$J + \delta J = \underbrace{\int_{t_0}^{t_f} \left[H(x,u) - \lambda^\top \dot{x} \right] dt}_{J}$$

$$+\int_{t_0}^{t_f}\left[\frac{\partial H}{\partial x}\delta x+\frac{\partial H}{\partial u}\delta u+\dot{\lambda}^{\top}\delta x\right]dt-\lambda^{\top}\left(t_f\right)\delta x\left(t_f\right)+\lambda^{\top}\left(t_0\right)\delta x\left(t_0\right) \tag{9.121}$$

The variation in the cost function then becomes

$$\delta J=\int_{t_0}^{t_f}\left[\left(\frac{\partial H}{\partial x}\delta x+\dot{\lambda}^{\top}\right)\delta x+\frac{\partial H}{\partial u}\delta u\right]dt-\lambda^{\top}\left(t_f\right)\delta x\left(t_f\right)+\lambda^{\top}\left(t_0\right)\delta x\left(t_0\right) \tag{9.122}$$

J is rendered minimum when its variation is zero, i.e., $\delta J=0$, which results in the adjoint equation

$$\dot{\lambda}=-\frac{\partial H}{\partial x}^{\top}=-\nabla H_x^{\top} \tag{9.123}$$

and the necessary condition of optimality

$$\frac{\partial H}{\partial u}^{\top}=\nabla H_u^{\top}=0 \tag{9.124}$$

Since the initial condition $x\left(t_0\right)=x_0$ is specified for the initial value problem, then there is no variation in $x\left(t\right)$ at $t=t_0$, i.e., $\delta x\left(t_0\right)=0$. At the final time $t=t_f$, $x\left(t_f\right)$ is generally unknown, and so $\delta x\left(t_f\right)\neq 0$. Therefore, the optimality enforces a transversality condition

$$\lambda\left(t_f\right)=0 \tag{9.125}$$

which is the final time condition for the adjoint equation.

The optimization is described by a two-point boundary value problem

$$\begin{cases}\dot{x}=f\left(x,u^*\right) & x\left(t_0\right)=x_0\\ \dot{\lambda}=-\nabla H_x^{\top}\left(x,u^*,\lambda\right) & \lambda\left(t_f\right)=0\end{cases} \tag{9.126}$$

with the optimal control $u^*\left(t\right)$ obtained from the optimality condition (9.124) when there is no constraint on $u\left(t\right)$, or more generally from the celebrated Pontryagin's minimum principle

$$u^*\left(t\right)=\arg\min_{u\in\mathscr{U}}H\left(x,u\right) \tag{9.127}$$

which states that the optimal control $u^*\left(t\right)$ which belongs to an admissible set of control $\mathscr{U}$ is one that minimizes $H\left(x,u\right)$.

The Pontryagin's maximum principle can deal with constraints on the control such as $u_{min}\leq u\left(t\right)\leq u_{max}$. So, in determining an optimal control, we must also evaluate the Hamiltonian with the bounding values of $u\left(t\right)$ if $u\left(t\right)$ is constrained.

Example 9.7 Consider an ordinary function minimization with $H\left(u\right)=-u^2+u$ and $-1\leq u\leq 1$. Then,

$$\nabla H_u = -2u + 1 = 0 \Rightarrow u = \frac{1}{2}$$

If u is unconstrained, then the answer is $u^* = \frac{1}{2}$. However, u is constrained to be between -1 and 1. So, we need to evaluate $H(u)$ at $u = \frac{1}{2}$ as well as at the two bounding values $u = \pm 1$. Then, $H\left(\frac{1}{2}\right) = \frac{1}{4}$, $H(-1) = -2$, and $H(1) = 0$. So, the optimal value of u that minimizes $H(u)$ is

$$u^* = \arg \min_{u \in \left(-1, \frac{1}{3}, 1\right)} H(u) = -1$$

■

The two-point boundary value problem is so-called because half of the boundary conditions are at the initial time $t = t_0$ and the other half are at the final time $t = t_f$. The solution method is generally quite complicated and usually must be solved by numerical methods such as the shooting method. For a general optimization problem, the gradient method has a certain appeal in that the system equations are solved exactly at each iteration, with the control variable $u^*(t)$ being perturbed from one iteration to the next to "home in" on the optimal solution. The solution method usually starts with an initial guess of the control. This then allows the state vector to be computed by integrating the state equation forward in time using the specified initial conditions. Once the state vector is computed, the adjoint equation is integrated backward in time using the final time transversality conditions. The control is then updated for the next iteration. The whole solution process is iterated until a convergence on the control is obtained. A schematic of the gradient optimization is shown in Fig. 9.9. The gradient method is given by

$$u_{i+1} = u_i - \varepsilon \nabla H_u^\top \tag{9.128}$$

where $\varepsilon = \varepsilon^\top > 0$ is a positive-definite control-gradient weighting matrix and i is the iteration index.

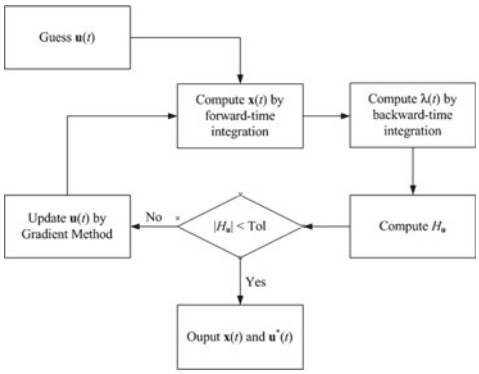

Fig. 9.9 Schematic diagram of gradient method

This update is also called the steepest descent method. Visualizing a bowl-shaped Hamiltonian function H, the gradient ∇H_u defines the magnitude and direction of the local slope of the Hamiltonian function as illustrated in Fig. 9.10. Perturbing the control by some function of ∇H_u moves the control toward the bottom of the bowl. A proper selection of the step size is critical for a rapid convergence to the minimizing control. If ε is too small, the convergence may require a large number of iterations. On the other hand, if ε is too large, the convergence may not occur at all. Therefore, the effectiveness of a gradient method is predicated upon a judicious choice of the weighting matrix ε. If the weighting matrix ε is the inverse of the Hessian matrix $\nabla^2 H_u$ of the Hamiltonian function, then the gradient method is known as the second-order gradient or Newton–Raphson method.

$$u_{i+1} = u_i - \left(\nabla^2 H_u\right)^{-1} \nabla H_u^\top \tag{9.129}$$

The continuous time version of the steepest descend method is the gradient search method

$$\dot{u} = -\Gamma \nabla H_u^\top \tag{9.130}$$

where $\Gamma = \Gamma^\top > 0$ is the adaptation rate matrix.

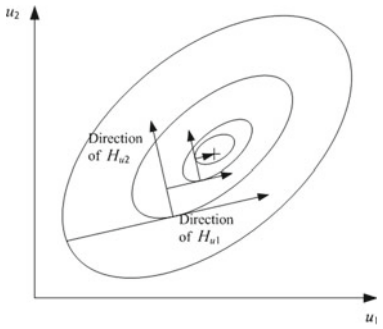

Fig. 9.10 Steepest descent approach to a minimum Hamiltonian function

Now, consider a Linear Quadratic Regulator (LOR) optimal control design for a MIMO system

$$\dot{x} = A_p x + B_p u \tag{9.131}$$

$$y = Cx \tag{9.132}$$

where $x(t) \in \mathbb{R}^n$, $u(t) \in \mathbb{R}^p$, and $y(t) \in \mathbb{R}^m$, with $m \leq p \leq n$

The objective is to design an optimal control that enables the state vector $y(t)$ to track a command $r(t)$. To design a tracking controller for a step command where $r(t)$ is a constant signal, we introduce an integral error state

$$e = \int_0^t (y - r)\, d\tau \tag{9.133}$$

Then,

$$\dot{e} = y - r = Cx - r \tag{9.134}$$

If the controller is a stabilizing controller, then as $t \to \infty$, $e(t) \to 0$, and so $y(t) \to r(t)$.

The integral error state is then augmented to the plant model as

$$\underbrace{\begin{bmatrix} \dot{e} \\ \dot{x} \end{bmatrix}}_{\dot{z}} = \underbrace{\begin{bmatrix} 0 & C \\ 0 & A_p \end{bmatrix}}_{A} \underbrace{\begin{bmatrix} e \\ x \end{bmatrix}}_{z} + \underbrace{\begin{bmatrix} 0 \\ B_p \end{bmatrix}}_{B} u - \underbrace{\begin{bmatrix} I \\ 0 \end{bmatrix}}_{D} r \tag{9.135}$$

Let $z(t) = \left[e^\top(t)\ x^\top(t) \right]^\top$, then the augmented plant is expressed as

$$\dot{z} = Az + Bu - Dr \tag{9.136}$$

We design an optimal control that minimizes the following linear quadratic cost function:

$$J = \lim_{t \to \infty} \frac{1}{2} \int_0^{t_f} \left(z^\top Q z + u^\top R u \right) dt \tag{9.137}$$

Applying the optimal control method, the Hamiltonian function is defined as

$$H(z, u) = \frac{1}{2} z^\top Q z + \frac{1}{2} u^\top R u + \lambda^\top (Az + Bu - Dr) \tag{9.138}$$

The adjoint equation and the necessary condition of optimality are obtained as

$$\dot{\lambda} = -\nabla H_z^\top = -Qz - A^\top \lambda \tag{9.139}$$

subject to the transversality condition $\lambda\left(t_f\right) = 0$, and

$$\nabla H_u^\top = Ru + B^\top \lambda = 0 \Rightarrow u^* = -R^{-1} B^\top \lambda \tag{9.140}$$

The optimal control problem can be solved by the "sweep" method [18] which assumes an adjoint solution of $\lambda(t)$ of the form

$$\lambda = Wz + Vr \tag{9.141}$$

Then, substituting the assumed solution of $\lambda(t)$ into the adjoint equation with the optimal control $u^*(t)$, we get

$$\dot{W}z + W\left[\underbrace{Az - BR^{-1}B^{\top}\left(Wz + Vr\right) - Dr}_{\dot{z}}\right] + \dot{V}r = -Qz - A^{\top}\left(Wz + Vr\right) \tag{9.142}$$

Separating terms by $z\left(t\right)$ and $r\left(t\right)$ yields the following equations:

$$\dot{W} + WA + A^{\top}W - WBR^{-1}B^{\top}W + Q = 0 \tag{9.143}$$

$$\dot{V} + A^{\top}V - WBR^{-1}B^{\top}V - WD = 0 \tag{9.144}$$

subject to the transversality conditions $W\left(t_f\right) = V\left(t_f\right) = 0$.

Equation (9.143) is the celebrated differential Riccati equation in optimal control. Since $t_f \to \infty$, this is called an infinite-time horizon control problem. Equations (9.143) and (9.144) have the following algebraic solutions:

$$WA + A^{\top}W - WBR^{-1}B^{\top}W + Q = 0 \tag{9.145}$$

$$V = \left(A^{\top} - WBR^{-1}B^{\top}\right)^{-1}WD \tag{9.146}$$

The optimal control is then obtained as

$$u = K_z z + K_r r \tag{9.147}$$

where the optimal control gains K_x and K_r are given by

$$K_z = -R^{-1}B^{\top}W \tag{9.148}$$

$$K_r = -R^{-1}B^{\top}\left(A^{\top} - WBR^{-1}B^{\top}\right)^{-1}WD \tag{9.149}$$

The closed-loop plant becomes

$$\dot{z} = A_m z + B_m r \tag{9.150}$$

where

$$A_m = A - BR^{-1}B^{\top}W \tag{9.151}$$

$$B_m = -BR^{-1}B^{\top}\left(A^{\top} - WBR^{-1}B^{\top}\right)^{-1}WD - D \tag{9.152}$$

9.5.2 Derivation of Optimal Control Modification

Given the MIMO system in Sect. 9.3, the optimal control modification seeks to minimize the $\mathscr{L}_2$ norm of the tracking error bounded away from the origin with a cost

function [9]

$$J = \lim_{t_f \to \infty} \frac{1}{2} \int_0^{t_f} (e - \Delta)^\top Q (e - \Delta) \, dt \tag{9.153}$$

where $\Delta(t)$ represents an unknown lower bound of the tracking error, subject to tracking error dynamics described by

$$\dot{e} = A_m e + B\tilde{\Theta}^\top \Phi(x) - w \tag{9.154}$$

The cost function J is convex and represents the weighted norm square measured from a point on the trajectory of $e(t)$ to the normal surface of a hypersphere $B_\Delta = \{e(t) \in \mathbb{R}^n : \|e\| \leq \|\Delta\|\} \subset \mathscr{D} \subset \mathbb{R}^n$ as illustrated in Fig. 9.11. The cost function is designed to provide robustness by not seeking the ideal property of asymptotic tracking of MRAC whereby $e(t) \to 0$ as $t \to \infty$, but rather a bounded tracking whereby the tracking error tends to some lower bound $\Delta(t)$ away from the origin. By not requiring asymptotic tracking, the adaptation therefore can be made more robust. Thus, the tracking performance can be traded with robustness by a suitable design of the optimal control modification adaptive law.

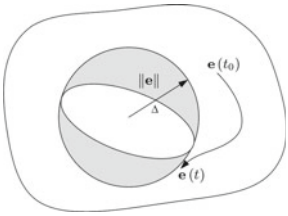

Fig. 9.11 Tracking error bound

Using the optimal control framework, we define the Hamiltonian function as

$$H\left(e, \tilde{\Theta}\right) = \frac{1}{2}(e - \Delta)^\top Q (e - \Delta) + \lambda^\top \left[A_m e + B\tilde{\Theta}^\top \Phi(x) - w\right] \tag{9.155}$$

where $\lambda(t) \in \mathbb{R}^n$ is an adjoint vector.

Then, the adjoint equation is found by

$$\dot{\lambda} = -\nabla H_e^\top = -Q(e - \Delta) - A_m^\top \lambda \tag{9.156}$$

with the transversality condition $\lambda\left(t_f \to \infty\right) = 0$ since $e(0)$ is known.

Treating $\tilde{\Theta}(t)$ as a control variable, the necessary condition is obtained as

$$\nabla H_{\tilde{\Theta}}^\top = \Phi(x) \lambda^\top B \tag{9.157}$$

The optimal control modification adaptive law is then expressed by the gradient update law as

$$\dot{\hat{\Theta}} = -\Gamma \nabla H_{\hat{\Theta}}^{\top} = -\Gamma \Phi(x) \lambda^{\top} B \tag{9.158}$$

Note that the adaptive law is dependent upon the adjoint vector which is governed by the adjoint equation. To eliminate $\lambda(t)$, we use the "sweep" method by assuming the following adjoint solution:

$$\lambda = Pe + S\Theta^{\top} \Phi(x) \tag{9.159}$$

Substituting $\lambda(t)$ in the adjoint equation yields

$$\begin{aligned} &\dot{P}e + P\left[A_m e + B\left(\Theta - \Theta^*\right)^{\top} \Phi(x) - w\right] + \dot{S}\Theta^{\top} \Phi(x) + S\frac{d\left[\Theta^{\top} \Phi(x)\right]}{dt} \\ &\quad = -Q(e - \Delta) - A_m^{\top}\left[Pe + S\Theta^{\top} \Phi(x)\right] \end{aligned} \tag{9.160}$$

Separating the equation that contains $e(t)$, $\Theta^{\top}(t) \Phi(x)$, and the remaining terms result in

$$\dot{P} + PA_m + A_m^{\top} P + Q = 0 \tag{9.161}$$

$$\dot{S} + A_m^{\top} S + PB = 0 \tag{9.162}$$

$$Q\Delta + PB\Theta^{*\top} \Phi(x) + Pw - S\frac{d\left[\Theta^{\top} \Phi(x)\right]}{dt} = 0 \tag{9.163}$$

subject to the transversality conditions $P\left(t_f \to \infty\right) = 0$ and $S\left(t_f \to \infty\right) = 0$.

Equation (9.161) is the differential Lyapunov equation. Equation (9.163) shows that the unknown lower bound $\Delta(t)$ of the tracking error is a function of the parametric uncertainty Θ^* and the unknown disturbance $w(t)$. Thus, as long as the uncertainty and disturbance exist, the lower bound will be finite, thereby causing the tracking error to be bounded away from the origin as opposed to tending to the origin asymptotically as required by MRAC. Robustness thereby is achieved.

For the infinite-time horizon optimal control problem as $t \to \infty$, the solutions to both Eqs. (9.161) and (9.162) tend to their constant solutions at $t = 0$ which are given by

$$PA_m + A_m^{\top} P + Q = 0 \tag{9.164}$$

$$A_m^{\top} S + PB = 0 \tag{9.165}$$

Equation (9.164) is the familiar Lyapunov equation in adaptive control (see Sect. 4.2.7), where now the weighting matrix Q is clearly shown to be connected to the cost function of minimizing the tracking error. The solution to Eq. (9.165) is also given by

$$S = -A_m^{-\top} PB \tag{9.166}$$

The adjoint solution is then obtained as

$$\lambda = Pe - A_m^{-\top} PB\Theta^\top \Phi(x) \tag{9.167}$$

Substituting the adjoint solution into the gradient update law in Eq. (9.158) yields the "ideal" optimal control modification adaptive law

$$\dot{\Theta} = -\Gamma \Phi(x) \left[e^\top P - \Phi^\top(x) \Theta B^\top P A_m^{-1} \right] B \tag{9.168}$$

The first term in the adaptive law is the familiar MRAC. The second term is the damping term of the optimal control modification. So, this analysis is able to show the connection between adaptive control and optimal control.

In any design, the ability to adjust a controller to obtain a desired tracking performance and robustness is important. Therefore, suboptimal solutions may provide a more flexible, yet practical approach to a control design by allowing a trade-off between the optimality and other design considerations. Thus, to enable the optimal control modification adaptive law to be sufficiently flexible for a control design, a modification parameter $\nu > 0$ is introduced as a gain to allow for the adjustment of the optimal control modification term. The role of the modification parameter ν is important. If the tracking performance is more desired in a control design than robustness, then ν could be selected to be a small value. In the limit when $\nu = 0$, the standard MRAC is recovered and asymptotic tracking performance is achieved but at the expense of robustness. On the other hand, if robustness is a priority in a design, then a larger value of ν should be chosen.

Thus, the solution of S is modified as

$$S = -\nu A_m^{-\top} PB \tag{9.169}$$

This results in the final form of the optimal control modification

$$\dot{\Theta} = -\Gamma \Phi(x) \left[e^\top P - \nu \Phi^\top(x) \Theta B^\top P A_m^{-1} \right] B \tag{9.170}$$

The bound on $\Delta(t)$ as $t_f \to \infty$ can be estimated by

$$\|\Delta\| \leq \frac{1}{\lambda_{min}(Q)} \left\{ \|PB\| \left\| \Theta^{*\top} \Phi(x) \right\| + \lambda_{max}(P) w_0 + \nu \left\| A_m^{-\top} PB \right\| \left\| \frac{d\left[\Theta^\top \Phi(x)\right]}{dt} \right\| \right\} \tag{9.171}$$

Since the optimal control modification provides a damping mechanism to MRAC, the modification term must be negative definite with respect to Θ. Examining the modification term $\Gamma \nu \Phi(x) \Phi^\top(x) \Theta B^\top P A_m^{-1} B$, the product $\Phi(x) \Phi^\top(x)$ is a positive semi-definite null matrix, and $\Gamma \nu > 0$. Therefore, $B^\top P A_m^{-1} B$ is required to be negative definite.

Any square real matrix C can be decomposed into a symmetric part M and anti-symmetric part N

$$C = M + N \tag{9.172}$$

where

$$M = M^\top = \frac{1}{2}\left(C + C^\top\right) \tag{9.173}$$

$$N = -N^\top = \frac{1}{2}\left(C - C^\top\right) \tag{9.174}$$

Consider the quadratic scalar function $x^\top Cx$ for any arbitrary $x(t) \in \mathbb{R}^n$.

$$x^\top Cx = x^\top Mx + x^\top Nx \tag{9.175}$$

Recall that for any anti-symmetric matrix N, $x^\top Nx = 0$. Therefore,

$$x^\top Cx = x^\top Mx \tag{9.176}$$

This expression is useful for determining the sign definiteness of a matrix. It follows that, if the symmetric part M is positive (negative) definite, then C is also positive (negative) definite. Utilizing this property, the symmetric part of PA_m^{-1} is negative definite since

$$M = \frac{1}{2}\left(PA_m^{-1} + A_m^{-\top}P\right) = -\frac{1}{2}A_m^{-\top}QA_m^{-1} < 0 \tag{9.177}$$

Therefore, $x^\top B^\top PA_m^{-1}Bx = -\frac{1}{2}x^\top B^\top A_m^{-\top}QA_m^{-1}Bx < 0$. Thus, the optimal control modification term is negative definite with respect to $\Theta(t)$.

Consider a SISO system in Sect. 8.1. The optimal control modification adaptive law is given by

$$\dot{k}_x = -\gamma_x\left(x^2 b - \nu x^2 a_m^{-1} b^2 k_x\right) \tag{9.178}$$

Since $a_m < 0$, the modification term is negative with respect to $k_x(t)$. The feedback gain $k_x(t)$ can be computed as

$$\frac{\dot{k}_x}{1 - \nu a_m^{-1} b k_x} = -\gamma x^2 b \tag{9.179}$$

The standard MRAC is

$$\dot{k}_x^* = -\gamma x^2 b \tag{9.180}$$

where k_x^* denotes the ideal feedback gain obtained from MRAC.

Therefore,

$$\frac{\dot{k}_x}{1 - \nu a_m^{-1} b k_x} = \dot{k}_x^* \tag{9.181}$$

This equation can easily be solved. The solution is

$$-\frac{1}{\nu a_m^{-1} b} \ln \frac{1-\nu a_m^{-1} b k_x}{1-\nu a_m^{-1} b k_x(0)} = k_x^* - k_x^*(0) \tag{9.182}$$

This yields

$$k_x = \frac{1}{\nu a_m^{-1} b} - \frac{1-\nu a_m^{-1} b k_x(0)}{\nu a_m^{-1} b} \exp\left\{-\nu a_m^{-1} b\left[k_x^* - k_x(0)\right]\right\} \tag{9.183}$$

In the case of the parameter drift, $k_x^*(t) \to -\infty$ for $b > 0$ with the standard MRAC, therefore $-\nu a_m^{-1} b k_x^*(t) \to -\infty$. This implies that $k_x(t)$ is bounded with the optimal control modification.

The optimal control modification exhibits some nice properties that make it easy to analyze. Since $k_x(t)$ is bounded, the equilibrium value of $k_x(t)$ can be analytically obtained by letting $\gamma_x \to \infty$ which yields

$$\bar{k}_x = \frac{1}{\nu a_m^{-1} b} \tag{9.184}$$

The equilibrium value of $k_x(t)$ can also be obtained from the solution of $k_x(t)$ as $k_x^*(t) \to -\infty$ which yields the same result.

The equilibrium value of $k_x(t)$ thus is inversely proportional to the optimal control modification parameter ν.

$k_x(t)$ can then be expressed as

$$k_x = \bar{k}_x - \bar{k}_x \left[1 - \frac{k_x(0)}{\bar{k}_x}\right] \exp\left[-\frac{k_x^* - k_x(0)}{\bar{k}_x}\right] \tag{9.185}$$

The closed-loop plant with $k_x(t) \to \bar{k}_x$ is

$$\dot{x} = \left(a + \frac{a_m}{\nu}\right) x + w \tag{9.186}$$

The closed-loop plant is stable if

$$a + \frac{a_m}{\nu} < 0 \Rightarrow \nu < -\frac{a_m}{a} \tag{9.187}$$

This yields two cases

$$\nu \begin{cases} < -\frac{a_m}{a} & a > 0 \\ > 0 & a < 0 \end{cases} \tag{9.188}$$

The first case is when the open-loop plant is stable, i.e., $a < 0$. Then, the optimal control modification parameter ν can take on any positive value. Thus, if the plant

is open-loop stable, then the optimal control modification is guaranteed to be stable for all values of $\nu > 0$.

The second case is when the open-loop plant is unstable, i.e., $a > 0$, then there exists an upper limit of the modification parameter ν as indicated in Eq. (9.188). This implies that the modification parameter ν has to be chosen based on a priori knowledge of a. This is perhaps counterintuitive since the problem statement indicates that a is unknown which implies that the upper limit of ν is also unknown. However, this is consistent with the robust control framework. Robust stability generally requires a priori knowledge of the upper bound of the uncertainty. With a complete lack of knowledge of the uncertainty, it is difficult to ensure robustness of any control systems. Therefore, the optimal control modification can be designed to guarantee the closed-loop stability for a given specification of the open-loop plant uncertainty.

Example 9.8 Consider the parameter drift example in Example 8.1, $k_x^*(t)$ is given by

$$k_x^* - k_x^*(0) = -\gamma_x b \frac{(1+t)^{2n+1} - 1}{2n+1}$$

$k_x^*(t) \to -\infty$ if $n > -\frac{1}{2}$.

With the optimal control modification, $k_x(t)$ is obtained as

$$k_x = \frac{1}{\nu a_m^{-1} b} - \frac{1 - \nu a_m^{-1} b k_x(0)}{\nu a_m^{-1} b} \exp\left[\gamma_x \nu a_m^{-1} b^2 \frac{(1+t)^{2n+1} - 1}{2n+1}\right]$$

Therefore, $k_x(t)$ is bounded for all n if the modification parameter ν is selected such that $a + \frac{a_m}{\nu} < 0$. Then, the optimal control modification has eliminated the parameter drift issue.

Let $a = 1$, $b = 1$, and $a_m = -1$. Then, $\nu = 0.1$ is chosen to satisfy the limiting condition which dictates that $\nu < 1$ for the closed-loop stability. The response of the closed-loop plant for the same disturbance in this example with $n = -\frac{5}{12}$, $x(0) = 1$, $k_x(0) = 0$, and $\gamma_x = 10$ is shown in Fig. 9.12. The equilibrium value is calculated to be $\bar{k}_x = -10$ which agrees exactly with the simulation result.

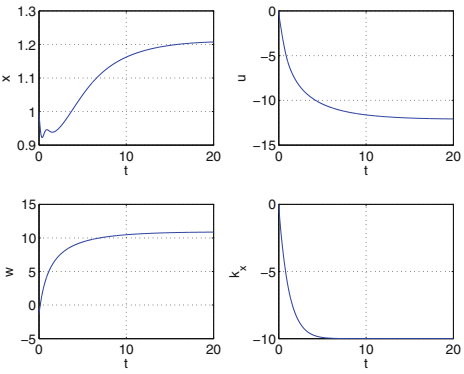

Fig. 9.12 Optimal control modification

9.5.3 Lyapunov Stability Analysis

The optimal control modification can be shown to achieve stable and bounded tracking by the Lyapunov's direct method as follows:

Proof Choose a Lyapunov candidate function

$$V\left(e,\tilde{\Theta}\right)=e^{\top}Pe+\text{trace}\left(\tilde{\Theta}^{\top}\Gamma^{-1}\tilde{\Theta}\right) \tag{9.189}$$

Differentiating $V\left(e,\tilde{\Theta}\right)$ yields

$$\begin{aligned}\dot{V}\left(e,\tilde{\Theta}\right)&=-e^{\top}Qe+2e^{\top}PB\tilde{\Theta}^{\top}\Phi\left(x\right)-2e^{\top}Pw\\&\quad-2\text{trace}\left(\tilde{\Theta}^{\top}\Phi\left(x\right)\left[e^{\top}P-\nu\Phi^{\top}\left(x\right)\Theta B^{\top}PA_m^{-1}\right]B\right)\\&=-e^{\top}Qe-2e^{\top}Pw+2\nu\Phi^{\top}\left(x\right)\Theta B^{\top}PA_m^{-1}B\tilde{\Theta}^{\top}\Phi\left(x\right)\end{aligned} \tag{9.190}$$

Then,

$$\begin{aligned}\dot{V}\left(e,\tilde{\Theta}\right)&=-e^{\top}Qe-2e^{\top}Pw+2\nu\Phi^{\top}\left(x\right)\tilde{\Theta}B^{\top}PA_m^{-1}B\tilde{\Theta}^{\top}\Phi\left(x\right)\\&\quad+2\nu\Phi^{\top}\left(x\right)\Theta^{*}B^{\top}PA_m^{-1}B\tilde{\Theta}^{\top}\Phi\left(x\right)\end{aligned} \tag{9.191}$$

But, $B^{\top}PA_m^{-1}B<0$. So,

$$2\nu\Phi^{\top}\left(x\right)\tilde{\Theta}B^{\top}PA_m^{-1}B\tilde{\Theta}^{\top}\Phi\left(x\right)=-\nu\Phi^{\top}\left(x\right)\tilde{\Theta}B^{\top}A_m^{-\top}QA_m^{-1}B\tilde{\Theta}^{\top}\Phi\left(x\right) \tag{9.192}$$

Then, $\dot{V}\left(e,\tilde{\Theta}\right)$ is bounded by

$$\begin{aligned}\dot{V}\left(e,\tilde{\Theta}\right)&\leq-\lambda_{min}\left(Q\right)\left\|e\right\|^2+2\lambda_{max}\left(P\right)\left\|e\right\|w_0\\&\quad-\nu\lambda_{min}\left(B^{\top}A_m^{-\top}QA_m^{-1}B\right)\left\|\Phi\left(x\right)\right\|^2\left\|\tilde{\Theta}\right\|^2\\&\quad+2\nu\left\|B^{\top}PA_m^{-1}B\right\|\left\|\Phi\left(x\right)\right\|^2\left\|\tilde{\Theta}\right\|\Theta_0\end{aligned} \tag{9.193}$$

Let $c_1=\lambda_{min}\left(Q\right)$, $c_2=\frac{\lambda_{max}(P)w_0}{c_1}$, $c_3=\lambda_{min}\left(B^{\top}A_m^{-\top}QA_m^{-1}B\right)$, and $c_4=\frac{\left\|B^{\top}PA_m^{-1}B\right\|\Theta_0}{c_3}$. Then, upon completing the square, we get

$$\dot{V}\left(e,\tilde{\Theta}\right)\leq-c_1\left(\left\|e\right\|-c_2\right)^2+c_1c_2^2-\nu c_3\left\|\Phi\left(x\right)\right\|^2\left(\left\|\tilde{\Theta}\right\|-c_4\right)^2+\nu c_3c_4^2\left\|\Phi\left(x\right)\right\|^2 \tag{9.194}$$

$\dot{V}\left(e,\tilde{\Theta}\right)\leq0$ implies

$$\|e\| \geq c_2 + \sqrt{c_2^2 + \frac{\nu c_3 c_4^2 \|\Phi(x)\|^2}{c_1}} = p \tag{9.195}$$

$$\left\|\tilde{\Theta}\right\| \geq c_4 + \sqrt{c_4^2 + \frac{c_1 c_2^2}{\nu c_3 \|\Phi(x)\|^2}} = \alpha \tag{9.196}$$

Note that the lower bounds p and α are dependent on $\|\Phi(x)\|$. Therefore, to prove boundedness, we also need to show that $\|\Phi(x)\|$ is bounded. If $\Phi(x)$ is a bounded function such as $\sin x$, sigmoidal or radial basis functions, then $\|\Phi(x)\| \leq \Phi_0$ and the solution is uniformly ultimately bounded. The ultimate bounds can be established as

$$\|e\| \leq \rho = \sqrt{\frac{\lambda_{max}(P) p^2 + \lambda_{max}\left(\Gamma^{-1}\right)\alpha^2}{\lambda_{min}(P)}} \tag{9.197}$$

$$\left\|\tilde{\Theta}\right\| \leq \beta = \sqrt{\frac{\lambda_{max}(P) p^2 + \lambda_{max}\left(\Gamma^{-1}\right)\alpha^2}{\lambda_{min}\left(\Gamma^{-1}\right)}} \tag{9.198}$$

Otherwise, we consider the following cases:

1. The closed-loop plant with the nominal controller and no disturbance is stable. That is, $\Theta(t) = 0$ and $w(t) = 0$. This is the same as stating that the uncertainty is non-destabilizing. The tracking error equation becomes

$$\dot{e} = A_m e - B\Theta^{*\top}\Phi(x) \tag{9.199}$$

Choose a Lyapunov candidate function

$$V(e) = e^\top P e \tag{9.200}$$

Then,

$$\dot{V}(e) = -e^\top Q e - 2e^\top P B \Theta^{*\top}\Phi(x) \leq -\lambda_{min}(Q)\|e\|^2 + 2\|e\|\|PB\|\Theta_0\|\Phi(x)\| \tag{9.201}$$

Since the plant is stable, $\dot{V}(e) \leq 0$ which implies $\|\Phi(x)\|$ is bounded by

$$\|\Phi(x)\| \leq \frac{\lambda_{min}(Q)\|e\|}{2\|PB\|\Theta_0} \tag{9.202}$$

Substituting Eq. (9.202) into Eq. (9.194) yields

$$\dot{V}\left(e,\tilde{\Theta}\right) \leq -c_1\left(\|e\| - c_2\right)^2 + c_1 c_2^2 - \nu c_3 \frac{\lambda_{min}^2\left(Q\right)\|e\|^2}{4\|PB\|^2 \Theta_0^2}\left(\left\|\tilde{\Theta}\right\| - c_4\right)^2 + \nu c_3 c_4^2 \frac{\lambda_{min}^2\left(Q\right)\|e\|^2}{4\|PB\|^2 \Theta_0^2} \tag{9.203}$$

$\dot{V}\left(e\right) \leq 0$ requires the coefficient of $\|e\|^2$ to be negative. Therefore, there exists a maximum value ν_{max} for which $\nu < \nu_{max}$ where

$$\nu_{max} = \frac{4\lambda_{min}\left(B^\top A_m^{-\top} Q A_m^{-1} B\right)\|PB\|^2}{\lambda_{min}\left(Q\right)\left\|B^\top P A_m^{-1} B\right\|^2} \tag{9.204}$$

Note that ν_{max} is not dependent on the bound of the parametric uncertainty Θ_0. $\dot{V}\left(e,\tilde{\Theta}\right)$ then becomes

$$\dot{V}\left(e,\tilde{\Theta}\right) \leq -c_1\left(1 - \frac{\nu}{\nu_{max}}\right)\|e\|^2 + 2c_1 c_2\|e\| - \nu c_3 \frac{\lambda_{min}^2\left(Q\right)\|e\|^2}{4\|PB\|^2 \Theta_0^2}\left(\left\|\tilde{\Theta}\right\| - c_4\right)^2 \tag{9.205}$$

Upon completing the square, we get

$$\dot{V}\left(e,\tilde{\Theta}\right) \leq -c_1\left(1 - \frac{\nu}{\nu_{max}}\right)\left(\|e\| - \frac{c_2}{1 - \frac{\nu}{\nu_{max}}}\right)^2 + \frac{c_1 c_2^2}{1 - \frac{\nu}{\nu_{max}}} - \frac{\nu c_3 \lambda_{min}^2\left(Q\right)\|e\|^2}{4\|PB\|^2 \Theta_0^2}\left(\left\|\tilde{\Theta}\right\| - c_4\right)^2 \tag{9.206}$$

The lower bound of $\|e\|$ for which $\dot{V}\left(e,\tilde{\Theta}\right) \leq 0$ is determined from

$$-c_1\left(1 - \frac{\nu}{\nu_{max}}\right)\|e\|^2 + 2c_1 c_2\|e\| \leq 0 \tag{9.207}$$

which yields

$$\|e\| \geq \frac{2c_2}{1 - \frac{\nu}{\nu_{max}}} = p \tag{9.208}$$

The lower bound of $\left\|\tilde{\Theta}\right\|$ is determined by setting $\|e\| = \frac{c_2}{1 - \frac{\nu}{\nu_{max}}}$ that renders

$$\dot{V}\left(\tilde{\Theta}\right) \leq \frac{c_1 c_2^2}{1 - \frac{\nu}{\nu_{max}}} - \frac{\nu c_3 \lambda_{min}^2\left(Q\right) c_2^2}{4\left(1 - \frac{\nu}{\nu_{max}}\right)^2 \|PB\|^2 \Theta_0^2}\left(\left\|\tilde{\Theta}\right\| - c_4\right)^2 \tag{9.209}$$

Therefore, $\dot{V}\left(\tilde{\Theta}\right) \leq 0$ implies

$$\left\|\tilde{\Theta}\right\| \geq c_4 + \sqrt{\frac{4c_1\left(1-\frac{\nu}{\nu_{max}}\right)\|PB\|^2\Theta_0^2}{\nu c_3 \lambda_{min}^2(Q)}} = \alpha \tag{9.210}$$

Then, the closed-loop system is uniformly ultimately bounded with the ultimate bounds given by Eqs. (9.197) and (9.198).

2. The closed-loop plant with the nominal controller has no stability guarantee. The uncertainty can be destabilizing. If $\nu = 0$, then from Eqs. (9.195) and (9.196), we see that $\|e\|$ is bounded but $\left\|\tilde{\Theta}\right\|$ is unbounded. This illustrates the parameter drift behavior of MRAC. On the other hand, if $\nu \to \infty$, then $\left\|\tilde{\Theta}\right\|$ is bounded, but $\|e\|$ can be unbounded. Thus, there exists a maximum value ν_{max} such that $\nu < \nu_{max}$ which corresponds to the largest value of $\|\Phi(x)\| \leq \Phi_0$ that renders the largest ultimate bound of $\|e\|$. From Eq. (9.194), the largest ultimate bound of $\|e\|$ is determined from

$$\dot{V}\left(e, \tilde{\Theta}\right) \leq -c_1(\|e\| - c_2)^2 + c_1c_2^2 + \nu c_3 c_4^2 \|\Phi(x)\|^2 \tag{9.211}$$

But,

$$-e^\top Qe = -(x_m - x)^\top Q(x_m - x) = -x^\top Qx + 2x_m Qx - x_m^\top Qx_m \tag{9.212}$$

Therefore,

$$-c_1\|e\|^2 \leq -c_1\|x\|^2 + 2c_5\|x\|\|x_m\| - c_1\|x_m\|^2 \tag{9.213}$$

where $c_5 = \lambda_{max}(Q)$.
Let

$$\begin{aligned}\varphi(\|x\|, \|x_m\|, Q, \nu, w_0, \Theta_0) = -c_1\|x\|^2 + 2(c_1c_2 + c_5\|x_m\|)\|x\| \\ + 2c_1c_2\|x_m\| - c_1\|x_m\|^2 + \nu c_3c_4^2\|\Phi(x)\|^2\end{aligned} \tag{9.214}$$

where $\varphi()$ is the largest upper bound of $\dot{V}\left(e, \tilde{\Theta}\right)$ such that $\dot{V}\left(e, \tilde{\Theta}\right) \leq \varphi(\|x\|, \|x_m\|, Q, \nu, w_0, \Theta_0)$.
Then, for any $\nu < \nu_{max}$, $\|x\|$ can be determined by

$$\|x\| = \varphi^{-1}(\|x_m\|, Q, \nu, w_0, \Theta_0) \tag{9.215}$$

where $\varphi^{-1}()$ is an inverse function of $\varphi()$.
It follows that $\|\Phi(x)\|$ is bounded such that

$$\|\Phi(x)\| = \left\|\Phi\left(\varphi^{-1}\left(\|x_m\|, Q, \nu, w_0, \Theta_0\right)\right)\right\| = \Phi_0 \tag{9.216}$$

Then, the closed-loop system is uniformly ultimately bounded with

$$c_2 + \sqrt{c_2^2 + \frac{\nu c_3 c_4^2 \Phi_0^2}{c_1}} = p \leq \|e\| \leq \rho = \sqrt{\frac{\lambda_{max}(P) r^2 + \lambda_{max}\left(\Gamma^{-1}\right)\alpha^2}{\lambda_{min}(P)}} \tag{9.217}$$

$$c_4 + \sqrt{c_4^2 + \frac{c_1 c_2^2}{\nu c_3 \Phi_0^2}} = \alpha \leq \left\|\tilde{\Theta}\right\| \leq \beta = \sqrt{\frac{\lambda_{max}(P) r^2 + \lambda_{max}\left(\Gamma^{-1}\right)\alpha^2}{\lambda_{min}\left(\Gamma^{-1}\right)}} \tag{9.218}$$

for any $0 < \nu < \nu_{max}$.
Consider a special case when $\Phi(x)$ belongs to a class of regressor functions such that $\|\Phi(x)\| \leq \|x\|$. This class of regressor functions also includes $\Phi(x) = x$. Then, from Eq. (9.214), $\dot{V}\left(e, \tilde{\Theta}\right)$ is bounded by

$$\begin{aligned}\varphi\left(\|x\|, \|x_m\|, Q, \nu, w_0, \Theta_0\right) = &-\left(c_1 - \nu c_3 c_4^2\right)\|x\|^2 + 2\left(c_1 c_2 + c_5\|x_m\|\right)\|x\| \\ &+ 2c_1 c_2\|x_m\| - c_1\|x_m\|^2\end{aligned} \tag{9.219}$$

$\|x\|$ is obtained from

$$\begin{aligned}\|x\| &= \varphi^{-1}\left(\|x_m\|, Q, \nu, w_0, \Theta_0\right) \\ &= \frac{c_2 + c_5\|x_m\| + \sqrt{\left(c_1 c_2 + c_5\|x_m\|\right)^2 + 4\left(c_1 + \nu c_3 c_4^2\right)\left(2c_1 c_2\|x_m\| - c_1\|x_m\|^2\right)}}{c_1 - \nu c_3 c_4^2}\end{aligned} \tag{9.220}$$

for any $0 < \nu < \nu_{max}$ such that $c_1 - \nu c_3 c_4^2 > 0$ which yields

$$\nu_{max} = \frac{c_1}{c_3 c_4^2} = \frac{\lambda_{min}(Q)\lambda_{min}\left(B^\top A_m^{-\top} Q A_m^{-1} B\right)}{\left\|B^\top P A_m^{-1} B\right\|^2 \Theta_0^2} \tag{9.221}$$

Note that ν_{max} is now dependent on the upper bound of the parametric uncertainty Θ_0 and is a conservative estimate since the negative definite term with $||\tilde{\Theta}||^2$ in Eq. (9.194) is neglected. As the bound of the uncertainty increases, ν_{max} must be reduced to ensure the stability of the closed-loop system. Thus, the stability of the optimal control modification depends on the bound of the uncertainty. The adaptive law is guaranteed to be stable if a priori knowledge of the bound of the uncertainty exists.

■

In contrast to the σ modification and e modification which do not impose a limit on the modification parameters σ and μ, respectively, it may seem that the optimal

control modification adaptive law is more restrictive. However, the lack of a well-defined limit on the modification parameter can sometimes be a source of stability issues. Numerical simulations using the Rohrs counterexample have shown that both the σ modification and e modification as well as the optimal control modification all exhibit limiting values on the modification parameters σ, μ, and ν, respectively.

Is should be noted that the limiting value ν_{max} derived from the Lyapunov analysis, in general, is a conservative estimate of the true limiting value ν_{max}. Consider the following first-order SISO system with an adaptive regulator controller using the optimal control modification:

$$\dot{x} = ax + b\left(u + \theta^* x\right) \tag{9.222}$$

$$u = k_x x - \theta\left(t\right) x \tag{9.223}$$

$$\dot{\theta} = -\gamma\left(-x^2 b - \nu x^2 a_m^{-1} b^2 \theta\right) \tag{9.224}$$

with a and b known, and $a_m < 0$.

The closed-loop system is

$$\dot{x} = \left(a_m - b\theta + b\theta^*\right) x \tag{9.225}$$

Note that the adaptive law implicitly uses $p = 1$ where p is the solution of the scalar Lyapunov equation

$$2pa_m = -q \tag{9.226}$$

By letting $\gamma \to \infty$, the equilibrium value of $\theta\left(t\right)$ is found to be

$$\bar{\theta} = -\frac{1}{\nu a_m^{-1} b} \tag{9.227}$$

Using the equilibrium value $\bar{\theta}$, the closed-loop system becomes

$$\dot{x} = \left(a_m + \frac{a_m}{\nu} + b\theta^*\right) x \tag{9.228}$$

If the uncertainty is stabilizing, then $b\theta^* < 0$. Then, the closed-loop system is stable for any $\nu > 0$. Yet, using Eq. (9.204) from the Lyapunov analysis, ν should be limited by

$$\nu_{max} = \frac{4b^2 a_m^{-2} b^2}{b^4 a_m^{-2}} = 4 \tag{9.229}$$

If the uncertainty is destabilizing but the closed-loop plant with the nominal (non-adaptive) controller $u\left(t\right) = k_x x\left(t\right)$ is stable, then $0 < b\theta^* < -a_m$. Then, the closed-loop system is still stable for any $\nu > 0$. Yet, using Eq. (9.221), ν should be limited by

$$\nu_{max} = \frac{4a_m^2 b^2 a_m^{-2}}{b^4 a_m^{-2} \theta^{*2}} = \left(\frac{2a_m}{b\theta^*}\right)^2 \tag{9.230}$$

Finally, if the uncertainty is destabilizing and the closed-loop plant with the nominal controller is unstable, then $b\theta^* > -a_m$. The closed-loop plant is stable if

$$a_m + \frac{a_m}{\nu} + b\theta^* < 0 \tag{9.231}$$

Then, ν is limited by

$$\nu_{max} = -\frac{a_m}{a_m + b\theta^*} \tag{9.232}$$

Combining with the Lyapunov expression, ν_{max} is expressed as

$$\nu_{max} = \min\left[\left(\frac{2a_m}{b\theta^*}\right)^2, -\frac{a_m}{a_m + b\theta^*}\right] \tag{9.233}$$

Let $b\theta^* = -\alpha a_m$ where $\alpha > 1$, then $\left(\frac{2a_m}{b\theta^*}\right)^2 \to \left(\frac{2}{\alpha}\right)^2$ and $-\frac{a_m}{a_m + b\theta^*} \to \frac{1}{\alpha - 1}$. Since $\left(\frac{2}{\alpha}\right)^2 < \frac{1}{\alpha - 1}$ for all $\alpha > 1$, therefore the most conservative value of ν_{max} is established by the Lyapunov analysis which is equal to

$$\nu_{max} = \frac{4}{\alpha^2} \tag{9.234}$$

On the other hand, the least conservative value of ν_{max} is the true value of ν_{max} which is equal to

$$\nu_{max} = \frac{1}{\alpha - 1} \tag{9.235}$$

While the optimal control modification is defined according to Eq. (9.170), there are other variances of the optimal control modification. These variances are:

$$\dot{\Theta} = -\Gamma \Phi(x)\left[e^\top P + \nu \Phi^\top(x)\Theta B^\top A_m^{-\top} Q A_m^{-1}\right] B \tag{9.236}$$

$$\dot{\Theta} = -\Gamma \Phi(x)\left[e^\top P + \nu \Phi^\top(x)\Theta B^\top R\right] B \tag{9.237}$$

$$\dot{\Theta} = -\Gamma \Phi(x)\left[e^\top P B + \nu \Phi^\top(x)\Theta R\right] \tag{9.238}$$

$$\dot{\Theta} = -\Gamma \Phi(x)\left[e^\top P B + \nu \Phi^\top(x)\Theta\right] \tag{9.239}$$

where $R = R^\top > 0$ is a positive-definite matrix.

9.5.4 Linear Asymptotic Property

Consider a linear uncertain MIMO system

$$\dot{x} = Ax + B\left(u + \Theta^{*^{\top}} x\right) \tag{9.240}$$

The plant is designed with the following adaptive controller:

$$u = K_x x + K_r r - \Theta^{\top}(t)\, x \tag{9.241}$$

to follow a reference model

$$\dot{x}_m = A_m x_m + B_m r \tag{9.242}$$

where $A_m = A + BK_x$ and $B_m = BK_r$.

The optimal control modification adaptive law for $\Theta(t)$ is given by

$$\dot{\Theta} = -\Gamma\left(xe^{\top} PB - \nu x x^{\top} \Theta B^{\top} P A_m^{-1} B\right) \tag{9.243}$$

It has been shown that MRAC is non-robust with fast adaptation. The time-delay margin of MRAC tends to zero as the adaptation rate tends to infinity. The optimal control modification exhibits a linear asymptotic property as $\Gamma \to \infty$ since the equilibrium value $\Theta(t)$ is independent of $x(t)$ if $x_m(t) = 0$, as has been shown for simple SISO systems [20, 21]. The equilibrium value of $\Theta^{\top}(t)\, x(t)$ is given by

$$\bar{\Theta}^{\top} x = \frac{1}{\nu}\left(B^{\top} A_m^{-\top} PB\right)^{-1} B^{\top} Pe \tag{9.244}$$

Then, the closed-loop system tends to the following asymptotic linear system as $\Gamma \to \infty$ in the limit:

$$\begin{aligned}\dot{x} = &\left[A_m + \frac{1}{\nu} B\left(B^{\top} A_m^{-\top} PB\right)^{-1} B^{\top} P + B\Theta^{*^{\top}}\right] x \\ &- \frac{1}{\nu} B\left(B^{\top} A_m^{-\top} PB\right)^{-1} B^{\top} P x_m + B_m r\end{aligned} \tag{9.245}$$

This system is stable for all $\nu > 0$ if $A_m + B\Theta^{*^{\top}}$ is Hurwitz and stable for $\nu < \nu_{max}$ if $A_m + B\Theta^{*^{\top}}$ is an unstable matrix.

Consider a special case when $\nu = 1$ corresponding to the optimal control solution of the adaptive law and B is a square invertible matrix, then

$$A_m + B\left(B^\top A_m^{-\top} P B\right)^{-1} B^\top P = P^{-1} P A_m + B B^{-1} P^{-1} A_m^\top B^{-\top} B^\top P$$
$$= P^{-1}\left(P A_m + A_m^\top P\right) = -P^{-1} Q \tag{9.246}$$

The tracking error equation tends to in the limit

$$\dot{e} = -\left(P^{-1} Q - B\Theta^{*^\top}\right) e - B\Theta^{*^\top} x_m \tag{9.247}$$

Since $P > 0$ and $Q > 0$, $-P^{-1} Q < 0$. The closed-loop poles of the ideal system with $\Theta^* = 0$ are all negative real. Therefore, the closed-loop system has the best stability margin. The ideal system is exponentially stable with no high-frequency oscillations. By choosing Q appropriately, the closed-loop system is guaranteed to be stable if $-P^{-1} Q + B\Theta^{*^\top}$ is Hurwitz.

The linear asymptotic property of the optimal control modification is quite useful since it can be used for stability analysis using many available linear analysis tools. Another advantage that comes with the linear asymptotic property is the scaled input–output behavior of the closed-loop system. That is, if $r(t)$ is scaled by a multiplier c, then $x(t)$ is scaled by the same amount. To see this, we express the asymptotic closed-loop system as a transfer function

$$sx = \left[A_m + \frac{1}{\nu} B\left(B^\top A_m^{-\top} P B\right)^{-1} B^\top P + B\Theta^{*^\top}\right] x$$
$$- \frac{1}{\nu} B\left(B^\top A_m^{-\top} P B\right)^{-1} B^\top P x_m + B_m r \tag{9.248}$$

From the reference model, we get

$$s x_m = A_m x_m + B_m r \Rightarrow x_m = (sI - A_m)^{-1} B_m r \tag{9.249}$$

Therefore,

$$x = \left[sI - A_m - \frac{1}{\nu} B\left(B^\top A_m^{-\top} P B\right)^{-1} B^\top P - B\Theta^{*^\top}\right]^{-1}$$
$$\times \left[-\frac{1}{\nu} B\left(B^\top A_m^{-\top} P B\right)^{-1} B^\top P (sI - A_m)^{-1} + I\right] B_m r \tag{9.250}$$

If $x(t) = x_0(t)$ is the response due to $r(t) = r_0(t)$ and if $r(t)$ is scaled by a constant multiplier c, i.e., $r(t) = c r_0(t)$, then it follows that $x(t)$ is also scaled by the same multiplier c, i.e., $x(t) = c x_0(t)$. The scale input–output behavior makes the optimal control modification more predictable than the standard MRAC which does not possess this linear asymptotic property.

If $r(t)$ is a constant signal, then the equilibrium value of $x(t)$ can be found by setting $s = 0$ as $t \to \infty$. Then,

$$\bar{x} = -\left[A_m + \frac{1}{\nu} B \left(B^\top A_m^{-\top} P B\right)^{-1} B^\top P + B\Theta^{*\top}\right]^{-1} \times \left[\frac{1}{\nu} B \left(B^\top A_m^{-\top} P B\right)^{-1} B^\top P A_m^{-1} + I\right] B_m r \tag{9.251}$$

If $\nu = 0$, then the ideal property of asymptotic tracking of MRAC is recovered since

$$\begin{aligned}\bar{x} &= -\lim_{\nu \to 0}\left[A_m + \frac{1}{\nu} B \left(B^\top A_m^{-\top} P B\right)^{-1} B^\top P + B\Theta^{*\top}\right]^{-1} \\ &\quad \times \left[\frac{1}{\nu} B \left(B^\top A_m^{-\top} P B\right)^{-1} B^\top P A_m^{-1} + I\right] B_m r \\ &= -\lim_{\nu \to 0}\left[\frac{1}{\nu} B \left(B^\top A_m^{-\top} P B\right)^{-1} B^\top P\right]^{-1} \frac{1}{\nu} B \left(B^\top A_m^{-\top} P B\right)^{-1} B^\top P A_m^{-1} B_m r \\ &= -A_m^{-1} B_m r = \bar{x}_m \end{aligned} \tag{9.252}$$

The equilibrium value of the tracking error is given by

$$\bar{e} = \bar{x}_m - \bar{x} = \left\{-A_m^{-1} + \left[A_m + \frac{1}{\nu} B \left(B^\top A_m^{-\top} P B\right)^{-1} B^\top P + B\Theta^{*\top}\right]^{-1} \times \left[\frac{1}{\nu} B \left(B^\top A_m^{-\top} P B\right)^{-1} B^\top P A_m^{-1} + I\right]\right\} B_m r \tag{9.253}$$

The largest norm of $\bar{e}(t)$ can be interpreted as a steady-state error when $\Gamma \to \infty$ which is given by

$$\|\bar{e}\| = \left\| -A_m^{-1} B_m + \left[A_m + \frac{1}{\nu} B \left(B^\top A_m^{-\top} P B\right)^{-1} B^\top P + B\Theta^{*\top}\right]^{-1} \times \left[\frac{1}{\nu} B \left(B^\top A_m^{-\top} P B\right)^{-1} B^\top P A_m^{-1} + I\right] B_m \right\| \|r\| \tag{9.254}$$

The linear asymptotic property also affords another advantage in that the stability margins of the system in the limit can be computed.

Consider a first-order time-delay SISO system with an optimal control modification adaptive controller

$$\dot{x} = ax + b\left[u(t - t_d) + \theta^* x\right] \tag{9.255}$$

$$u = k_x x + k_r r - \theta(t) x \tag{9.256}$$

$$\dot{\theta} = -\gamma \left(xeb - \nu x^2 a_m^{-1} b^2 \theta \right) \tag{9.257}$$

with a and b known and $a_m = a + bk_x < 0$.

For fast adaptation with $\gamma \to \infty$ and a constant command signal $r(t)$, the equilibrium value of $\theta(t) x(t)$ is

$$\bar{\theta} x = \frac{x_m - x}{\nu a_m^{-1} b} \tag{9.258}$$

Then, the closed-loop plant tends to in the limit

$$\dot{x} = \left(a + b\theta^*\right) x + \left(bk_x + \frac{a_m}{\nu}\right) x(t - t_d) - \frac{a_m}{\nu} x_m(t - t_d) + bk_r r(t - t_d) \tag{9.259}$$

To simplify the analysis, let $r(t) = 1$ and $x_m(t) = 1$. Then, the characteristic equation with $s = j\omega$ is

$$j\omega - \left(a + b\theta^*\right) - \left(bk_x + \frac{a_m}{\nu}\right) (\cos \omega t_d - j \sin \omega t_d) = 0 \tag{9.260}$$

which results in the following equations:

$$-\left(a + b\theta^*\right) - \left(bk_x + \frac{a_m}{\nu}\right) \cos \omega t_d = 0 \tag{9.261}$$

$$\omega + \left(bk_x + \frac{a_m}{\nu}\right) \sin \omega t_d = 0 \tag{9.262}$$

Then, the cross-over frequency and time-delay margin are computed as

$$\omega = \sqrt{\left(bk_x + \frac{a_m}{\nu}\right)^2 - (a + b\theta^*)^2} \tag{9.263}$$

$$t_d = \frac{1}{\omega} \cos^{-1} \left(-\frac{a + b\theta^*}{bk_x + \frac{a_m}{\nu}} \right) \tag{9.264}$$

If $\nu = 0$, then the optimal control modification reverts to the standard MRAC. Then, the time-delay margin tends to zero precisely as follows:

$$\omega = \lim_{\nu \to 0} \sqrt{\left(bk_x + \frac{a_m}{\nu}\right)^2 - (a + b\theta^*)^2} \to \infty \tag{9.265}$$

$$t_d = \lim_{\nu \to 0} \frac{1}{\omega} \cos^{-1} \left(-\frac{a + b\theta^*}{bk_x + \frac{a_m}{\nu}} \right) = 0 \tag{9.266}$$

This is the expected result for MRAC. For any $0 < \nu < \nu_{max}$, the optimal control modification yields a non-zero time-delay margin with fast adaptation. This is a robustness property of any robust adaptive control with the ability to provide sufficient stability margins under fast adaptation. For a given time delay t_d and a priori knowledge of θ^*, the modification parameter ν thus can be computed to guarantee stability of the closed-loop system.

Example 9.9 Let $a = 1$, $a_m = -1$, $b = b_m = 1$, $\theta^* = 0.2$, and $r(t) = 1$. This is the same example as Example 8.7 which has a time-delay margin of 0.0020 s for $\gamma_x = 500$. The open-loop system is unstable. So, the limiting value of ν is computed as

$$\nu_{max} = \left(\frac{2a_m}{b\theta^*}\right)^2 = 1$$

Choose $\nu = 0.1 < 1$. The time-delay margin for the closed-loop system with the optimal control modification is calculated as

$$\omega = \sqrt{\frac{1}{\nu^2} - 1} = 9.9499 \text{ rad/s}$$

$$t_d = \frac{1}{\sqrt{\frac{1}{\nu^2} - 1}} \cos^{-1} \nu = 0.1478 \text{ sec}$$

Since the time-delay margin t_d decreases with increasing the adaptation rate γ, therefore, for finite γ, the time-delay margin estimated with $\gamma \to \infty$ is the lowest estimate of the time-delay margin for any finite $\gamma < \infty$. In other words, the estimated time-delay margin $t_d = 0.1478$ s using the linear asymptotic property provides a lower bound on the time-delay margin. The actual time-delay margin for any arbitrary adaptation rate γ should be greater than this value in theory. We see that, for even a small value of ν, a significant increase in the time-delay margin can be achieved as compared to the time-delay margin of 0.0020 s for the standard MRAC with $\gamma_x = 500$. In the limit as $\nu \to 0$, $t_d \to 0$ corresponding to the standard MRAC as $\gamma_x \to \infty$.

The steady-state error is estimated to be

$$\bar{e} = \left[-a_m^{-1} + \left(a_m + \frac{a_m}{\nu} + b\theta^*\right)^{-1} \left(\frac{1}{\nu} + 1\right)\right] b_m r = -0.0185$$

The equilibrium value of $\theta(t)$ is computed to be

$$\bar{\theta} = \frac{\bar{e}}{\nu a_m^{-1} b \bar{x}} = \frac{\bar{e}}{\nu a_m^{-1} b (\bar{x}_m - \bar{e})} = 0.1818$$

We choose $\gamma = 100$ and $\theta(0) = 0$. The results of the simulation with the optimal control modification are shown in Fig. 9.13. The closed-loop system is completely stable. The tracking error $e(t)$and the adaptive parameter $\theta(t)$ converge to –0.0185 and 0.1818, respectively, at 10 s. Thus, the simulation results agree exactly with the equilibrium values of $\bar{e}$ and $\bar{\theta}$.

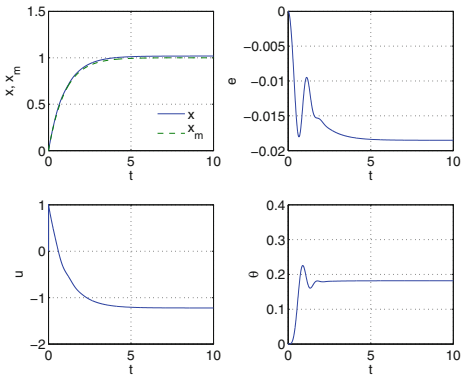

Fig. 9.13 Optimal control modification with $\gamma = 100$

When a time delay equal to 0.1477 s is injected at the input, the closed-loop system is on the verge of instability as shown in Fig. 9.14. In fact, for $\gamma = 1000$ using a time step $\Delta t = 0.0001$, the closed-loop system becomes unstable at 0.1478 s as predicted. Thus, the numerical evidence of the time-delay margin is in agreement with the analytical prediction.

To illustrate the linear asymptotic property, we consider the asymptotic linear system in the limit as follows:

$$\dot{x} = ax + b\theta^* x - b\frac{x_m - x}{va_m^{-1}b}$$

Figure 9.15 shows the closed-loop response with the optimal control modification for $r(t) = 1 + \sin 2t + \cos 4t$. The closed-loop response follows the asymptotic linear system almost perfectly as both responses are on top of each other.

To illustrate the scaled input–output linear behavior of the optimal control modification, the reference command signal $r(t) = 1 + \sin 2t + \cos 4t$ is doubled so that the new command is $r_1(t) = 2 + 2\sin 2t + 2\cos 4t$. Let $x_1(t)$ be the closed-loop response to $r_1(t)$. Then, the response of $x_1(t)$ is twice that of $x(t)$ as shown in Fig. 9.16.

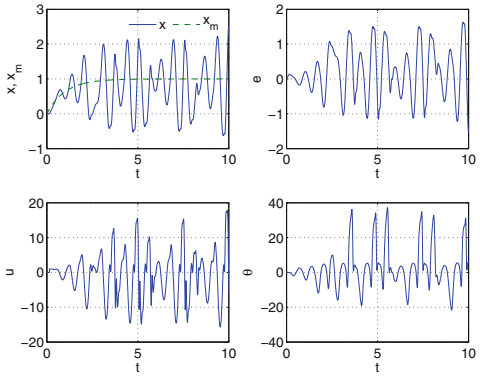

Fig. 9.14 Optimal control modification with $\gamma = 1000$ for $t_d = 0.1477\,\mathrm{s}$

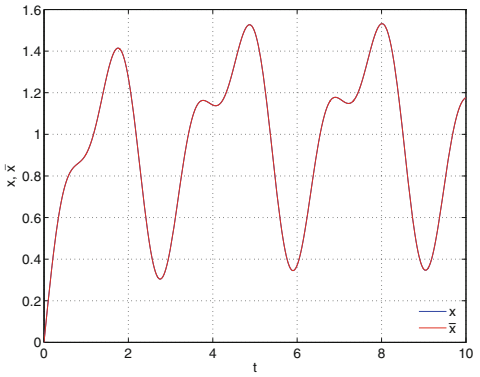

Fig. 9.15 Scaled input–output property of adaptive control

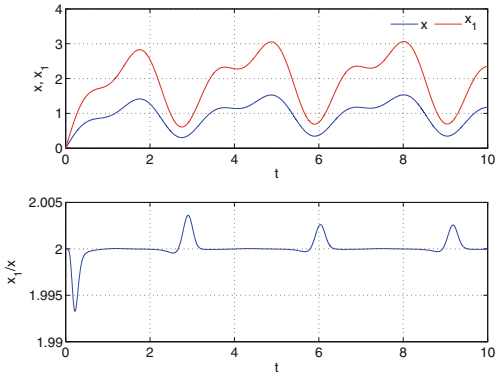

Fig. 9.16 Scaled input–output property of adaptive control

9.6 Adaptive Loop Recovery Modification

Adaptive loop recovery modification is another recent robust modification adaptive law developed by Calise and Yucelen in 2009 [6]. The adaptive loop recovery modification is intended to achieve asymptotic tracking while preserving the stability margin of the reference model to the degree possible even under uncertainty. The modification is given by

$$\dot{\Theta} = -\Gamma \left[\Phi (x) e^{\top} P B + \eta \Phi_x (x) \Phi_x^{\top} (x) \Theta \right] \tag{9.267}$$

where $\eta > 0$ is a modification parameter and $\Phi_x (x) = \frac{d\Phi(x)}{dx}$.

The adaptive loop recovery modification is based on the idea of seeking an adaptive law that minimizes the nonlinearity in a closed-loop plant so that the stability margin of a linear reference model could be preserved. Consider the tracking error equation with no disturbance

$$\dot{e} = A_m e + B \tilde{\Theta}^{\top} \Phi (x) \tag{9.268}$$

The tracking error equation can be linearized as

$$\Delta \dot{e} = A_m \Delta e + B \Delta \tilde{\Theta}^{\top} \Phi (\bar{x}) + B \tilde{\Theta}^{\top} \Phi_x (\bar{x}) (x - \bar{x}) \tag{9.269}$$

where $\bar{x}$ is the equilibrium state.

If $\Delta \tilde{\Theta} (t) = 0$ and $\tilde{\Theta}^{\top} (t) \Phi_x (\bar{x}) = 0$, then

$$\Delta \dot{e} = A_m \Delta e \tag{9.270}$$

Then, the closed-loop plant follows the reference model exactly and the stability of the reference model is preserved.

This leads to a hypothesis that if the quantity $\Theta^{\top} (t) \Phi_x (x)$ is minimized, asymptotic tracking is achieved, and the stability margin of the reference model is preserved. This can be established by minimizing the following cost function:

$$J = \frac{1}{2} \Phi_x^{\top} (x) \Theta \Theta^{\top} \Phi_x (x) \tag{9.271}$$

as an unconstrained optimization.

The gradient of the cost function is computed as

$$\nabla J_{\Theta} = \Phi_x (x) \Phi_x^{\top} (x) \Theta \tag{9.272}$$

The gradient update law then is expressed as

$$\dot{\Theta} = -\Gamma \nabla J_{\Theta} = -\Gamma \Phi_x (x) \Phi_x^{\top} (x) \Theta \tag{9.273}$$

Adding the standard MRAC to the update law results in the adaptive loop recovery modification.

The original stability proof is based on a singular perturbation approach [6, 22]. The reader is referred to the original work [6, 22] for the formal proof. It can be shown that the stability proof of the optimal control modification can also be applied to the adaptive loop recovery modification since both adaptive laws have their damping terms proportional to some positive-definite function of $x(t)$. The alternate proof is as follows:

Proof Choose a Lyapunov candidate function

$$V\left(e,\tilde{\Theta}\right)=e^{\top}Pe+\text{trace}\left(\tilde{\Theta}^{\top}\Gamma^{-1}\tilde{\Theta}\right) \tag{9.274}$$

$\dot{V}\left(e,\tilde{\Theta}\right)$ is evaluated as

$$\begin{aligned}\dot{V}\left(e,\tilde{\Theta}\right)&=-e^{\top}Qe+2e^{\top}PB\tilde{\Theta}^{\top}\Phi(x)-2e^{\top}Pw\\&\quad-2\text{trace}\left(\tilde{\Theta}^{\top}\left[\Phi(x)e^{\top}PB+\eta\Phi_x(x)\Phi_x^{\top}(x)\Theta\right]\right)\\&=-e^{\top}Qe-2e^{\top}Pw-2\eta\Phi_x^{\top}(x)\Theta\tilde{\Theta}^{\top}\Phi_x(x)\end{aligned} \tag{9.275}$$

Then, $\dot{V}\left(e,\tilde{\Theta}\right)$ is bounded by

$$\begin{aligned}\dot{V}\left(e,\tilde{\Theta}\right)&\leq-\lambda_{min}(Q)\|e\|^2+2\lambda_{max}(P)\|e\|w_0-2\eta\|\Phi_x(x)\|^2\left\|\tilde{\Theta}\right\|^2\\&\quad+2\eta\|\Phi_x(x)\|^2\left\|\tilde{\Theta}\right\|\Theta_0\end{aligned} \tag{9.276}$$

Let $c_1=\lambda_{min}(Q)$ and $c_2=\dfrac{\lambda_{max}(P)w_0}{c_1}$. Upon completing the square, we get

$$\dot{V}\left(e,\tilde{\Theta}\right)\leq-c_1(\|e\|-c_2)^2+c_1c_2^2-2\eta\|\Phi_x(x)\|^2\left(\left\|\tilde{\Theta}\right\|-\frac{\Theta_0}{2}\right)^2+\frac{\eta}{2}\|\Phi_x(x)\|^2\Theta_0^2 \tag{9.277}$$

Then, $\dot{V}\left(e,\tilde{\Theta}\right)\leq 0$ implies

$$\|e\|\geq c_2+\sqrt{c_2^2+\frac{\eta\|\Phi_x(x)\|^2\Theta_0^2}{2c_1}}=p \tag{9.278}$$

$$\left\|\tilde{\Theta}\right\|\geq\frac{\Theta_0}{2}+\sqrt{\frac{\Theta_0^2}{4}+\frac{c_1c_2^2}{2\eta\|\Phi_x(x)\|^2}}=\alpha \tag{9.279}$$

Note that the lower bounds p and α are dependent on $\|\Phi_x(x)\|$. Therefore, to prove boundedness, we need to show that $\|\Phi_x(x)\|$ is bounded.

There exists a maximum value η_{max} such that $\eta < \eta_{max}$ for which $\dot{V}\left(e, \tilde{\Theta}\right) \leq 0$. Let

$$\varphi(\|x\|, \|x_m\|, Q, \eta, w_0, \Theta_0) = -c_1\|x\|^2 + 2(c_1c_2 + c_3\|x_m\|)\|x\| + 2c_1c_2\|x_m\| - c_1\|x_m\|^2 + \frac{\eta}{2}\|\Phi_x(x)\|^2\Theta_0^2 \tag{9.280}$$

where $c_3 = \lambda_{max}(Q) > 0$.

Then, $\|\Phi_x(x)\|$ is bounded by

$$\|\Phi_x(x)\| = \left\|\Phi_x\left(\varphi^{-1}(\|x_m\|_\infty, Q, \nu, w_0, \Theta_0)\right)\right\| = \Phi_{x_0} \tag{9.281}$$

It follows that the closed-loop system is also uniformly ultimately bounded for any $0 < \eta < \eta_{max}$.

Consider a special case when $\Phi(x)$ belongs to a class of regressor functions such that $\|\Phi(x)\| \leq \|x\|^2$ or $\|\Phi_x(x)\| \leq 2\|x\|$. Then, it can be shown that the adaptive loop recovery modification is stable and bounded for any $0 \leq \eta < \eta_{max}$ with a conservative estimate of η_{max} given by

$$\eta_{max} = \frac{\lambda_{min}(Q)}{2\Theta_0^2} \tag{9.282}$$

Consider another special case when $\Phi(x)$ belong to a class of regressor functions such that $\|\Phi(x)\| \leq \|x\|$ or $\|\Phi_x(x)\| \leq 1$. Then, the adaptive loop recovery modification is unconditionally stable.

■

Since the possibility of $\Phi_x(x)$ being unbounded exists, the adaptive loop recovery modification only works for any $\Phi(x)$ such that $\Phi_x(x)$ is bounded. For example, if $\Phi(x) = x^p$, then the adaptive law is valid only for $p \geq 1$. If $p = 1$, then $\Phi_x(x) = 1$, and the adaptive loop recovery modification becomes the σ modification.

Example 9.10 Consider a first-order SISO plant

$$\dot{x} = ax + b\left[u + \theta^*\phi(x)\right]$$

with an adaptive controller

$$u = k_x x + k_r r - \theta(t)\phi(x)$$

Suppose $\phi(x) = x^2$. Then, the adaptive loop recovery modification is expressed as

$$\dot{\theta} = -\gamma \left(x^2 eb + 4\eta x^2 \theta \right)$$

Consider the fast adaptation condition when $\gamma \to \infty$, then the asymptotic behavior of the adaptive loop recovery modification is given by

$$\bar{\theta} x^2 = -\frac{(x_m - x)\, bx^2}{4\eta}$$

$$\bar{u} = k_x x + k_r r + \frac{(x_m - x)\, bx^2}{4\eta}$$

The closed-loop plant then becomes as $\gamma \to \infty$

$$\dot{x} = a_m x + b_m r + b \left[\frac{(x_m - x)\, bx^2}{4\eta} + \theta^* x^2 \right]$$

Let $r(t)$ be a constant command signal. Then, the equilibrium value of $x(t)$ can be determined from

$$-a_m b^2 \bar{x}^3 + \left(4\eta b a_m \theta^* - b^2 b_m r \right) \bar{x}^2 + 4\eta a_m^2 \bar{x} + 4\eta a_m b_m r = 0$$

For example, let $r(t) = 1$, $a = 1$, $b = 1$, $\theta^* = 0.5$, $a_m = -2$, $b_m = 2$, and $\eta = 0.1$. Then, $\bar{x} = 1.1223$ and $\bar{\theta} = 0.3058$. The closed-loop response of the adaptive loop recovery modification with $k_x = -3$, $k_r = 2$, and $\gamma = 1$ is shown in Fig. 9.17. The simulation results of $\bar{x}$ and $\bar{\theta}$ agree exactly with the analytical values.

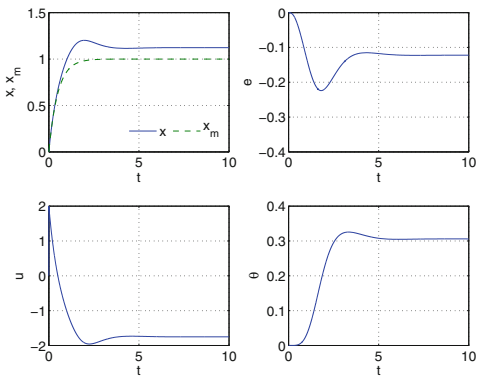

Fig. 9.17 Closed-loop response with adaptive loop recovery modification

■

Consider a special case when the asymptotic behavior of the adaptive loop recovery modification results in a linear controller for a certain function $\phi(x)$. The adaptive law is expressed in general as

$$\dot{\theta} = -\gamma \left[\phi(x) eb + \eta \phi_x^2(x) \theta \right] \tag{9.283}$$

For the linear asymptotic property to exist,

$$\phi_x^2(x) = c^2 \phi^2(x) \tag{9.284}$$

where $c > 0$, as $\gamma \to \infty$.

This results in the differential equation

$$\frac{d\phi}{\phi} = c dx \tag{9.285}$$

which has the following bounded solution:

$$\phi(x) = e^{-cx} \tag{9.286}$$

Then, the adaptive loop recovery modification and the optimal control modification have the same linear asymptotic property if $\eta c^2 = -\nu b^2 a_m^{-1}$. Note that even though the adaptive controller tends to a linear controller asymptotically, the closed-loop plant is still nonlinear since $\phi(x)$ is nonlinear.

Example 9.11 Consider a time-delay first-order SISO system

$$\dot{x} = ax + b \left[u(t - t_d) + \theta^* e^{-x} \right]$$

The adaptive controller with the adaptive loop recovery modification is given by

$$u = k_x x + k_r r - \theta(t) e^{-x}$$

$$\dot{\theta} = -\gamma \left(e^{-x} eb + \eta e^{-2x} \theta \right)$$

where $a + bk_x = a_m$ and $bk_r = b_m$.

Since $\phi(x) = e^{-x}$, the adaptive loop recovery modification is the same as the optimal control modification. The linear asymptotic adaptive controller is obtained by noticing that $\theta(t) \phi(x) \to -\dfrac{eb}{\eta}$ in the limit as $\gamma \to \infty$ so that

$$u \to k_x x + k_r r + \frac{eb}{\eta}$$

Even though the adaptive controller is linear in the limit, the closed-loop plant is nonlinear due to the nonlinear uncertainty since

$$\dot{x} = ax + b\left[\left(k_x - \frac{b}{\eta}\right)x\left(t - t_d\right) + k_r r\left(t - t_d\right) + \frac{b}{\eta}x_m\left(t - t_d\right) + \theta^* e^{-x}\right]$$

Let $a = 1$, $b = 1$, $\theta^* = 2$, $t_d = 0.1$, $a_m = -1$, $b_m = 1$, $r(t) = 1$, $\eta = 0.1$, and $\gamma = 10$. The response is shown in Fig. 9.18.

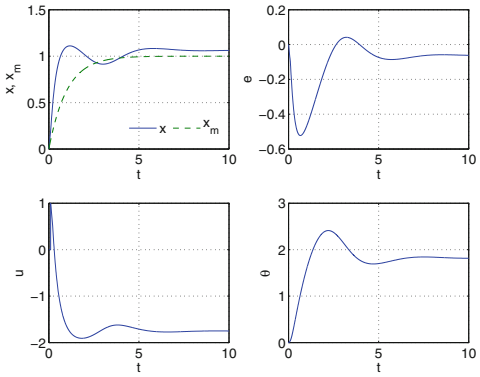

Fig. 9.18 Closed-loop response with adaptive loop recovery modification with $t_d = 0.1$ s

■

It is instructive at this point to summarize the four robust modification schemes for model-reference adaptive control that add damping mechanisms to the adaptation process, namely the σ modification, the e modification, the optimal control modification, and the adaptive loop recovery modification. Table 9.1 shows the four modification adaptive laws. Each of these modification adaptive laws has its own relative merit to one another, but all in general will improve robustness of model-reference adaptive control in their own way by providing a damping mechanism to bound adaptive parameters from the possibility of a parameter drift for systems with exogenous disturbances, non-minimum phase behaviors, time delay, and unmodeled dynamics.

Table 9.1 Four robust modification adaptive laws

σ modification	$\dot{\Theta} = -\Gamma\left[\Phi(x)e^{\top}PB + \sigma\Theta\right]$
e modification	$\dot{\Theta} = -\Gamma\left[\Phi(x)e^{\top}PB + \mu\left\|e^{\top}PB\right\|\Theta\right]$
Optimal control modification	$\dot{\Theta} = -\Gamma\left[\Phi(x)e^{\top}PB - \nu\Phi(x)\Phi^{\top}(x)\Theta B^{\top}PA_m^{-1}B\right]$
Adaptive loop recovery modification	$\dot{\Theta} = -\Gamma\left[\Phi(x)e^{\top}PB + \eta\Phi_x(x)\Phi_x^{\top}(x)\Theta\right]$

9.7 $\mathscr{L}_1$ Adaptive Control

The $\mathscr{L}_1$ adaptive control has gained a considerable attention in recent years due to its ability to achieve robustness with fast adaptation for a given a priori bound on the uncertainty. The $\mathscr{L}_1$ adaptive control was developed by Hovakimyan and Cao in 2006 [8, 23, 24]. Since then, it has been widely used in adaptive control practice. The underlying principle of the $\mathscr{L}_1$ adaptive control is the use of fast adaptation for improved transient or tracking performance coupled with a low-pass filter to suppress high-frequency responses for improved robustness. As a result, the $\mathscr{L}_1$ adaptive control can be designed to achieve stability margins under fast adaptation for a given a priori bound on the uncertainty. Theoretical proofs of guaranteed robustness bounds, stability margins, and tracking performance in transient and steady-state responses for the $\mathscr{L}_1$ adaptive control are well-established [8].

Consider the following linear SISO uncertain system with a matched uncertainty:

$$\dot{x} = A_m x + B\left[u + \Theta^{*\top}(t)(t)\, x + d(t)\right] \tag{9.287}$$

$$y = Hx \tag{9.288}$$

subject to $x(0) = x_0$, where $x(t) \in \mathbb{R}^n$ is a state vector, $u(t) \in \mathbb{R}$ is a control input, $y(t) \in \mathbb{R}$ is a plant output, $A_m \in \mathbb{R}^n \times \mathbb{R}^n$ is a known Hurwitz matrix, $B \in \mathbb{R}^n$ is a known column vector, $H \in \mathbb{R}^n$ is a known row vector, $\Theta^*(t) \in \mathbb{R}^n$ is unknown time-varying state uncertainty, and $d(t) \in \mathbb{R}$ is a matched bounded time-varying disturbance.

We assume that $\Theta^*(t) \in \mathscr{S}_{\Theta^*}$ and $d(t) \in \mathscr{S}_d$ where $\mathscr{S}_{\Theta^*}$ and $\mathscr{S}_{\mathbf{d}}$ are known compact sets defined a priori. Since $\Theta^*(t)$ is time-varying, we also require $\left\|\dot{\Theta}^*\right\| \leq \Delta$. Further, we assume that the disturbance and its derivatives are bounded with $|d| \leq d_0$ and $\left|\dot{d}\right| \leq \delta$. Without loss of generality, the following known constraint sets can be used to bound the adaptive parameters:

$$\mathscr{S}_{\Theta^*} = \left\{ \Theta^*(t) \in \mathbb{R}^n : g\left(\Theta^*\right) = \begin{bmatrix} \left(\theta_1^* - \frac{\theta_{1_{max}}^* + \theta_{1_{min}}^*}{2}\right)^2 - \left(\frac{\theta_{1_{max}}^* - \theta_{1_{min}}^*}{2}\right)^2 \\ \vdots \\ \left(\theta_n^* - \frac{\theta_{n_{max}}^* + \theta_{n_{min}}^*}{2}\right)^2 - \left(\frac{\theta_{n_{max}}^* - \theta_{n_{min}}^*}{2}\right)^2 \end{bmatrix} \leq 0 \right\} \tag{9.289}$$

$$\mathscr{S}_d = \left\{ d(t) \in \mathbb{R} : g_d(d) = \left(d - \frac{d_{max} + d_{min}}{2}\right) - \left(\frac{d_{max} - d_{min}}{2}\right)^2 \leq 0 \right\} \tag{9.290}$$

A state-predictor model is defined as

$$\dot{\hat{x}} = A_m \hat{x} + B\left[u + \Theta^{\top}(t)\, x + \hat{d}(t)\right] \tag{9.291}$$

with the initial condition $\hat{x}(0) = x_0$, where $\hat{x}(t)$, $\Theta(t)$ and $\hat{d}(t)$ are estimates of $x(t)$, $\Theta^*(t)$, and $d(t)$, respectively.

We define the state-predictor error as $e_p(t) = \hat{x}(t) - x(t)$. Then, the estimates of $\Theta^*(t)$, and $d(t)$ are computed from the following adaptive laws with the projection method:

$$\dot{\Theta} = \text{Pro}\left(\Theta, -\Gamma x e_p^\top PB\right) = \begin{cases} -\Gamma x e_p^\top PB & \text{if } g(\Theta) < 0 \text{ or if } g(\Theta) = 0 \\ & \text{and } -\left(x e_p^\top PB\right)^\top \nabla g_\Theta(\Theta) \le 0 \\ 0 & \text{otherwise} \end{cases} \tag{9.292}$$

$$\dot{\hat{d}} = \text{Pro}\left(\hat{d}, -\gamma_d e_p^\top PB\right) = \begin{cases} -\gamma_d e_p^\top PB & \text{if } g_d\left(\hat{d}\right) < 0 \text{ or if } g_d\left(\hat{d}\right) = 0 \\ & \text{and } -e_p^\top PB \nabla g_d\left(\hat{d}\right) \le 0 \\ 0 & \text{otherwise} \end{cases} \tag{9.293}$$

with the initial conditions $\Theta(0) = \Theta_0$ and $\hat{d}(0) = \hat{d}_0$.

The adaptive laws can be shown to be stable as follows:

Proof The predictor error equation is established as

$$\dot{e}_p = \dot{\hat{x}} - \dot{x} = A_m e_p + B\left(\tilde{\Theta}^\top x + \tilde{d}\right) \tag{9.294}$$

where $\tilde{\Theta}(t) = \Theta(t) - \Theta^*(t)$ and $\tilde{d}(t) = \hat{d}(t) - d(t)$.

Choose a Lyapunov candidate function

$$V\left(e_p, \tilde{\Theta}, \tilde{d}\right) = e_p^\top P e_p + \tilde{\Theta}^\top \Gamma^{-1} \tilde{\Theta} + \frac{\tilde{d}^2}{\gamma_d} \tag{9.295}$$

The projection method guarantees that $\Theta(t)$ and $\hat{d}(t)$ stay inside their constraint sets. Then, $\dot{V}\left(e_p, \tilde{\Theta}, \tilde{d}\right)$ is evaluated as

$$\begin{aligned} \dot{V}\left(e_p, \tilde{\Theta}, \tilde{d}\right) &= -e_p^\top Q e_p - 2\tilde{\Theta}^\top \Gamma^{-1} \dot{\Theta}^* - \frac{2\tilde{d}\dot{d}}{\gamma_d} \\ &\le -\lambda_{min}(Q) \left\|e_p\right\|^2 + 2\lambda_{max}\left(\Gamma^{-1}\right) \left\|\tilde{\Theta}\right\| \Delta + \frac{2\left\|\tilde{d}\right\| \delta}{\gamma_d} \end{aligned} \tag{9.296}$$

$\tilde{\Theta}(t)$ and $\tilde{d}(t)$ are constrained by

$$\theta_{i_{min}} - \theta_i^* \le \tilde{\theta}_i \le \theta_{i_{max}} - \theta_i^* \tag{9.297}$$

$$d_{min} - d \le \tilde{d} \le d_{max} - d \tag{9.298}$$

This implies

$$\left|\tilde{\theta}_i\right| \leq \max\left(\left|\theta_{i_{min}} - \theta_i^*\right|, \left|\theta_{i_{max}} - \theta_i^*\right|\right) \leq \max\left(\left|\theta_{i_{min}}\right|, \left|\theta_{i_{max}}\right|\right) + \max\left|\theta_i^*\right| \quad (9.299)$$

$$\left|\tilde{d}\right| \leq \max\left(\left|d_{min} - d\right|, \left|d_{max} - d\right|\right) \leq \max\left(\left|d_{min}\right|, \left|d_{max}\right|\right) + \max|d| = \tilde{d}_0 \quad (9.300)$$

Let $\tilde{\Theta}_0 = \max\left(\max\left(\left|\theta_{i_{min}}\right|, \left|\theta_{i_{max}}\right|\right) + \max\left|\theta_i^*\right|\right)$. Then,

$$\dot{V}\left(e_p, \tilde{\Theta}, \tilde{d}\right) \leq -\lambda_{min}(Q)\left\|e_p\right\|^2 + 2\lambda_{max}\left(\Gamma^{-1}\right)\tilde{\Theta}_0\Delta + 2\gamma_d^{-1}\tilde{d}_0\delta \quad (9.301)$$

$\dot{V}\left(e_p, \tilde{\Theta}, \tilde{d}\right) \leq 0$ implies

$$\left\|e_p\right\| \geq \frac{2\lambda_{max}\left(\Gamma^{-1}\right)\tilde{\Theta}_0\Delta + 2\gamma_d^{-1}\tilde{d}_0\delta}{\lambda_{min}(Q)} = p \quad (9.302)$$

There exists an upper bound of $\left\|e_p\right\|$ along with the upper bounds of $\left\|\tilde{\Theta}\right\|$ and $\left\|\tilde{d}\right\|$ that establish a compact set outside which $\dot{V}\left(e_p, \tilde{\Theta}, \tilde{d}\right) \leq 0$. Therefore, all signals are bounded.

■

The $\mathscr{L}_1$ adaptive controller is defined as

$$u(s) = -kD(s)w(s) \quad (9.303)$$

where $k > 0$ is a feedback gain, $D(s)$ is a proper transfer function and $w(s)$ is the Laplace transform of

$$w(t) = u(t) + \Theta^\top(t)x + \hat{d}(t) - k_r r(t) \quad (9.304)$$

where the command feedforward gain k_r is given by

$$k_r = -\frac{1}{HA_m^{-1}B} \quad (9.305)$$

The ideal controller is given by

$$u^*(t) = -\Theta^{*\top}(t)x(t) - d(t) + k_r r(t) \quad (9.306)$$

The ideal closed-loop plant then becomes

$$\dot{x} = A_m x + Bk_r r \quad (9.307)$$

The $\mathscr{L}_1$ reference controller is then given by the filtered version of the ideal controller

$$u_m(s) = C(s)\, u^*(s) \tag{9.308}$$

where $C(s)$ is a low-pass filter which can be obtained as

$$C(s) = \frac{kD(s)}{1 + kD(s)} \tag{9.309}$$

We require $C(0) = 1$. Thus, $D(s)$ can be any suitable transfer function that satisfies $\lim_{s\to 0} \frac{1}{D(s)} = 0$.

The design of the $\mathscr{L}_1$ adaptive control then essentially comes down to the design of the feedback gain k and the transfer function $D(s)$ which defines the low-pass filter $C(s)$.

The closed-loop reference system formed by the $\mathscr{L}_1$ reference controller is then obtained as

$$sx(s) = A_m x(s) + B\left[C(s)\, u^*(s) + k_r r(s) - u^*(s)\right] \tag{9.310}$$

Let the largest bound of Θ^* be defined using the $\mathscr{L}_1$ norm definition as

$$L = \left\|\Theta^*\right\|_1 = \max \sum_{i=1}^{n} \left|\theta_i^*\right| \tag{9.311}$$

Then, for the closed-loop reference system to be stable, the $\mathscr{L}_1$ norm of the system transfer function $G(s)$ must satisfy the following condition:

$$\|G(s)\| = \left\|(sI - A_m)^{-1} B\left[1 - C(s)\right]\right\|_1 L < 1 \tag{9.312}$$

This condition is the stability condition on the unit circle for discrete-time which is equivalent to the Hurwitz stability condition of the matrix $A_m + B\left[1 - C(s)\right]\Theta^{*\top}$ for continuous time.

The choices of k and $D(s)$ can greatly influence the performance and stability of the $\mathscr{L}_1$ adaptive control. For example, consider the following transfer function:

$$D(s) = \frac{1}{s} \tag{9.313}$$

which satisfies the ideal closed-loop transfer function

$$C(0) = \left.\frac{k}{s+k}\right|_{s=0} = 1 \tag{9.314}$$

Then, the $\mathscr{L}_1$ adaptive controller is given by

$$u = -\frac{k}{s} w(s) \tag{9.315}$$

or, in the time domain,

$$\dot{u} = -ku - k\left[\Theta^{\top}(t)\, x + \hat{d}(t) - k_r r\right] \tag{9.316}$$

Consider the case when Θ^* and d are constant. Then, the closed-loop reference system becomes

$$\begin{bmatrix} \dot{x} \\ \dot{u} \end{bmatrix} = \begin{bmatrix} A_m + B\Theta^{*\top} & B \\ -k\Theta^{*\top} & -k \end{bmatrix} \begin{bmatrix} x \\ u \end{bmatrix} + \begin{bmatrix} Bd \\ -k(d - k_r r) \end{bmatrix} \tag{9.317}$$

The stability condition requires

$$A_c = \begin{bmatrix} A_m + B\Theta^{*\top} & B \\ -k\Theta^{*\top} & -k \end{bmatrix} \tag{9.318}$$

to be Hurwitz by a suitable selection of the feedback gain $k > 0$.

Consider a first-order SISO plant as

$$\dot{x} = a_m x + b\left(u + \theta^* x + d\right) \tag{9.319}$$

where θ^* and d are unknown constants with given known bounds.

The predictor model is

$$\dot{\hat{x}} = a_m \hat{x} + b\left(u + \theta x + \hat{d}\right) \tag{9.320}$$

Choose $D(s) = \dfrac{1}{s}$. Then, the $\mathscr{L}_1$ adaptive controller is defined as

$$u = -\frac{k}{s} w(s) \tag{9.321}$$

$$\dot{\theta} = \text{Pro}\left(\theta, -\gamma x e_p b\right) \tag{9.322}$$

$$\dot{\hat{d}} = \text{Pro}\left(\hat{d}, -\gamma_d e_p b\right) \tag{9.323}$$

Then, the closed-loop plant matrix is

$$A_c = \begin{bmatrix} a_m + b\theta^* & b \\ -k\theta^* & -k \end{bmatrix} \tag{9.324}$$

The closed-loop characteristic equation is then obtained as

$$\det(sI - A_c) = \begin{vmatrix} s - a_m - b\theta^* & -b \\ k\theta^* & s + k \end{vmatrix} = s^2 + \left(k - a_m - b\theta^*\right) s - ka_m = 0 \tag{9.325}$$

Comparing the characteristic equation to that of a second-order system

$$s^2 + 2\zeta\omega_n s + \omega_n^2 = 0 \tag{9.326}$$

then

$$\omega_n^2 = -ka_m \tag{9.327}$$

$$2\zeta\omega_n = k - a_m - b\theta^* \tag{9.328}$$

For a specified damping ratio ζ, k can be computed from

$$k^2 - 2k\left(a_m + b\theta^* - 2\zeta^2 a_m\right) + \left(a_m + b\theta^*\right)^2 = 0 \tag{9.329}$$

which yields

$$k = a_m + b\theta^* - 2\zeta^2 a_m + 2\zeta\sqrt{a_m\left[-\left(a_m + b\theta^*\right) + \zeta^2 a_m\right]} \tag{9.330}$$

Consider two cases:

1. The open-loop plant with uncertainty is stable with $a_m + b\theta^* < 0$. Then, $k \geq -\left(a_m + b\theta^*\right) > 0$ if
$$\zeta \geq \sqrt{\frac{a_m + b\theta^*}{a_m}} \tag{9.331}$$

2. The open-loop plant with uncertainty is unstable with $a_m + b\theta^* > 0$. Then, the closed-loop poles are computed as
$$s = -\frac{k - a_m - b\theta^*}{2}\left[1 \pm \sqrt{1 + \frac{4ka_m}{\left(k - a_m - b\theta^*\right)^2}}\right] \tag{9.332}$$
which lie in the left half plane if $k > a_m + b\theta^*$.

Example 9.12 Consider the parameter drift example in Example 8.1. Let $a_m = -1$, $b = 1$, $\theta^* = 2$, and $d(t) = \dfrac{w(t)}{b}$ with $p = -\dfrac{5}{12}$.

Choose $D(s) = \dfrac{1}{s}$. Since $a_m + b\theta^* = 1 > 0$, we choose $k = 2 > 1$. Then, the $\mathscr{L}_1$ adaptive regulator controller is specified by

$$\dot{u} = -2u - 2\left(\theta x + \hat{d}\right)$$

$$\dot{\theta} = \text{Pro}\left(\theta, -\gamma x e_p b\right) = \begin{cases} -\gamma x e_p b & \text{if } \theta_{min} < \theta < \theta_{max} \text{ or if } \theta = \theta_{min} \\ & \text{and } \dot{\theta} \geq 0 \text{ or if } \theta = \theta_{max} \text{ and } \dot{\theta} \leq 0 \\ 0 & \text{otherwise} \end{cases}$$

$$\dot{\hat{d}} = \text{Pro}\left(\hat{d}, -\gamma_d e_p b\right) = \begin{cases} -\gamma_d e_p b & \text{if } d_{min} \leq \hat{d} \leq d_{max} \text{ or if } \hat{d} = d_{min} \\ & \text{and } \dot{\hat{d}} \geq 0 \text{ or if } \hat{d} = d_{max} \text{ and } \dot{\hat{d}} \leq 0 \\ 0 & \text{otherwise} \end{cases}$$

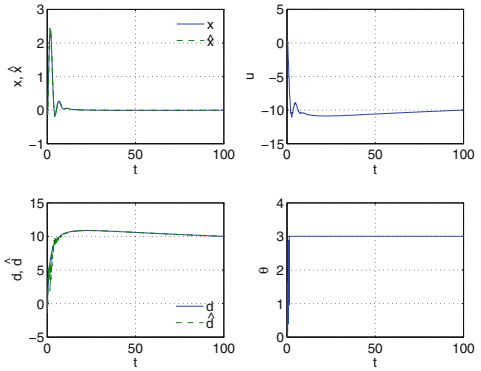

Fig. 9.19 Closed-loop response with $\mathscr{L}_1$ adaptive control, $\theta \to \theta_{max}$

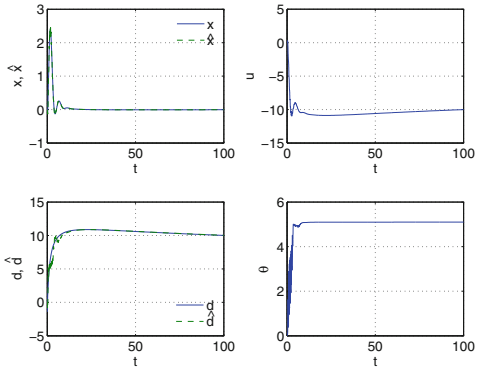

Fig. 9.20 Closed-loop response with $\mathscr{L}_1$ adaptive control, $\theta \to \bar{\theta} < \theta_{max}$

We choose $\theta_{min} = 0$, $\theta_{max} = 3$, $d_{min} = -2$, and $d_{max} = 11$. To ensure fast adaptation, γ and γ_d must be chosen to be large values. The time step must be chosen sufficiently small if γ and γ_d are large. Choose $\Delta t = 0.001$ and $\gamma = \gamma_d = 100$. The initial conditions are $x(0) = 0$, $\hat{x}(0) = 0$, $\theta(0) = 0$, and $\hat{d}(0) = 0$. The response of the closed-loop system with the $\mathscr{L}_1$ adaptive controller is shown in Fig. 9.19. Notice that $\theta(t) \to \theta_{max}$ because the upper bound of $\theta(t)$ is set too small. Nonetheless, $x(t) \to \varepsilon$ as $t \to \infty$ and $\hat{d}(t) \to d(t) + \delta$.

Suppose the upper bound is increased to $\theta_{max} = 10$. Then, the response with the new upper bound of $\theta(t)$ is shown in Fig. 9.20. The response shows that $\theta(t) \to \bar{\theta} = 5.1011 < \theta_{max}$. Note that $\theta(t)$ does not tend to θ^*.

9.8 Normalization

Fast adaptation can lead to loss of robustness of MRAC. Fast adaptation is usually associated with the use of a large adaptation rate. However, this is not the only effect of fast adaptation. When the amplitude of the regressor function $\Phi(x)$ is large, the effect is equivalent. Normalization is a technique that can be used to achieve more robust adaptation for large amplitude inputs [5]. The objective of the normalization is to reduce the effect of fast adaptation based on the amplitude of the regressor function. Normalized adaptation can achieve a significant increase in the time-delay margin of a closed-loop adaptive system. The normalized MRAC is given by

$$\dot{\Theta} = -\frac{\Gamma \Phi(x) e^{\top} PB}{1 + \Phi^{\top}(x) R \Phi(x)} \tag{9.333}$$

where $R = R^{\top} > 0$ is a positive-definite weighting matrix.

To prevent the parameter drift, the projection method can be used to bound adaptive parameters. Thus, the normalized MRAC with the projection method is described by

$$\dot{\Theta} = \text{Pro}\left(\Theta, -\frac{\Gamma \Phi(x) e^{\top} PB}{1 + \Phi^{\top}(x) R \Phi(x)}\right) \tag{9.334}$$

where $\Theta(t)$ is constrained to stay within a constraint set such that $\left\|\tilde{\Theta}\right\| \leq \tilde{\Theta}_0$.

The quantity $1 + \Phi^{\top}(x) R \Phi(x)$ is called the normalization factor. If the amplitude of the regressor function $\Phi(x)$ is large when the closed-loop system exhibits poor robustness, the normalization effectively reduces the adaptation process to improve robustness. The stability proof of the normalized optimal control modification is provided as follows:

Proof Choose a Lyapunov candidate function

$$V\left(e, \tilde{\Theta}\right) = e^{\top} Pe + \text{trace}\left(\tilde{\Theta}^{\top} \Gamma^{-1} \tilde{\Theta}\right) \tag{9.335}$$

There are two cases to consider.

1. Consider the case when $g(\Theta) < 0$ or $g(\Theta) = 0$ and $-\left[\Phi(x) e^{\top} PB\right]^{\top} \nabla g_{\Theta}(\Theta) \leq 0$. Then, evaluating $\dot{V}\left(e, \tilde{\Theta}\right)$ yields

$$\begin{aligned}\dot{V}\left(e, \tilde{\Theta}\right) &= -e^{\top} Qe - 2e^{\top} Pw + \frac{2e^{\top} PB\tilde{\Theta}^{\top} \Phi(x) \Phi^{\top}(x) R\Phi(x)}{1 + \Phi^{\top}(x) R\Phi(x)} \\ &\leq -\lambda_{min}(Q) \|e\|^2 + 2\|e\| \lambda_{max}(P) w_0 \\ &\quad + \frac{2e^{\top} PB\tilde{\Theta}^{\top} \Phi(x) \lambda_{max}(R) \|\Phi(x)\|^2}{m^2(\|x\|)}\end{aligned} \tag{9.336}$$

where $m^2(\|x\|) = 1 + \lambda_{min}(R) \|\Phi(x)\|^2$.
Suppose $g(\Theta) = (\Theta - \Theta^*)^{\top} (\Theta - \Theta^*) - \beta^2 \leq 0$. Then, $\nabla g_{\Theta}(\Theta) = 2\tilde{\Theta}$. So,

$$-\left[\Phi(x) e^{\top} PB\right]^{\top} \nabla g_{\Theta}(\Theta) = -2e^{\top} PB\tilde{\Theta}^{\top} \Phi(x) = -c_0 \leq 0 \tag{9.337}$$

where $c_0 > 0$.
Therefore,

$$\dot{V}\left(e, \tilde{\Theta}\right) \leq -\lambda_{min}(Q) \|e\|^2 + 2\|e\| \lambda_{max}(P) w_0 + \frac{c_0 \lambda_{max}(R) \|\Phi(x)\|^2}{m^2(\|x\|)} \tag{9.338}$$

Note that $\frac{\|\Phi(x)\|^2}{m^2(\|x\|)} \leq \frac{1}{\lambda_{min}(R)}$. Then, it follows that $\dot{V}\left(e, \tilde{\Theta}\right) \leq 0$ if

$$-c_1 \|e\|^2 + 2c_1 c_2 \|e\| + \frac{c_0 \lambda_{max}(R)}{\lambda_{min}(R)} \leq 0 \tag{9.339}$$

or

$$\|e\| \geq c_2 + \sqrt{c_2 + \frac{c_0 \lambda_{max}(R)}{c_1 \lambda_{min}(R)}} = p \tag{9.340}$$

where $c_1 = \lambda_{min}(Q)$ and $c_2 = \frac{\lambda_{max}(P) w_0}{\lambda_{min}(Q)}$.
Since $g(\Theta) \leq 0$, then $\left\|\tilde{\Theta}\right\|$ has an upper bound where $\left\|\tilde{\Theta}\right\| \leq \beta$. Then, the closed-loop system is uniformly ultimately bounded with the following ultimate bound:

$$p \leq \|e\| \leq \sqrt{\frac{\lambda_{max}(P) p^2 + \lambda_{max}\left(\Gamma^{-1}\right) \alpha^2}{\lambda_{min}(P)}} = \rho \tag{9.341}$$

$$\alpha \leq \left\|\tilde{\Theta}\right\| \leq \sqrt{\frac{\lambda_{max}(P) p^2 + \lambda_{max}\left(\Gamma^{-1}\right) \alpha^2}{\lambda_{min}(P)}} = \beta \tag{9.342}$$

2. Consider the case when $g(\Theta) \geq 0$ and $-\left[\Phi(x) e^{\top} PB\right]^{\top} \nabla g_{\Theta}(\Theta) > 0$. Then,

$$\dot{V}\left(e, \tilde{\Theta}\right) = -e^{\top} Qe - 2e^{\top} Pw + 2\tilde{\Theta}^{\top} \frac{\nabla g_{\Theta}(\Theta) \nabla^{\top} g_{\Theta}(\Theta)}{\nabla^{\top} g_{\Theta}(\Theta) \nabla g_{\Theta}(\Theta)} \frac{\Phi(x) e^{\top} PB\Phi^{\top}(x) R\Phi(x)}{1 + \Phi^{\top}(x) R\Phi(x)} \tag{9.343}$$

For the same $g(\Theta)$, $2e^{\top} PB\tilde{\Theta}^{\top}\Phi(x) = -c_0 < 0$ where $c_0 > 0$. Then,

$$\frac{\nabla g_{\Theta}(\Theta) \nabla^{\top} g_{\Theta}}{\nabla^{\top} g_{\Theta}(\Theta) \nabla g_{\Theta}(\Theta)} = \frac{\tilde{\Theta}\tilde{\Theta}^{\top}}{\tilde{\Theta}^{\top}\tilde{\Theta}} \tag{9.344}$$

Therefore,

$$\begin{aligned} \dot{V}\left(e, \tilde{\Theta}\right) &\leq -\lambda_{min}(Q) \|e\|^2 + 2\|e\| \lambda_{max}(P) w_0 - \frac{c_0 \lambda_{min}(R) \|\Phi(x)\|^2}{n^2(\|x\|)} \\ &\leq -\lambda_{min}(Q) \|e\|^2 + 2\|e\| \lambda_{max}(P) w_0 \end{aligned} \tag{9.345}$$

where $n^2(\|x\|) = 1 + \lambda_{max}(R) \|\Phi(x)\|^2$.
Thus, $\dot{V}\left(e, \tilde{\Theta}\right) \leq 0$ if

$$\|e\| \geq \frac{2\lambda_{max}(P) w_0}{\lambda_{min}(Q)} = p \tag{9.346}$$

Since $g(\Theta) \geq 0$, then $\left\|\tilde{\Theta}\right\|$ is bounded from below such that $\left\|\tilde{\Theta}\right\| \geq \alpha$. Therefore, the closed-loop system is uniformly ultimately bounded.

■

Note that the normalization technique will result in poorer tracking as $\lambda_{max}(R)$ increases, but at the same time improve robustness in the presence of large amplitude inputs or fast adaptation.

For the normalized MRAC without the projection method, if a disturbance does not exist, the tracking error is asymptotic, but in the presence of a disturbance, the Lyapunov stability proof does not guarantee boundedness of the adaptive parameters. Therefore, the normalized MRAC without the projection method is not robust to the parameter drift.

In lieu of the projection method, the normalization technique can be used in conjunction with any one of the robust modification schemes such as the σ modification, e modification, and optimal control modification. For example, the normalized σ modification is given by

$$\dot{\Theta} = -\frac{\Gamma\left(\Phi(x) e^{\top} PB + \sigma\Theta\right)}{1 + \Phi^{\top}(x) R\Phi(x)} \tag{9.347}$$

Since there is no projection, R and σ have to be chosen such that the closed-loop system is stable. This can be determined from the Lyapunov stability analysis as follows:

Proof Choose the usual Lyapunov candidate function

$$V\left(e,\tilde{\Theta}\right)=e^{\top}Pe+\text{trace}\left(\tilde{\Theta}^{\top}\Gamma^{-1}\tilde{\Theta}\right) \tag{9.348}$$

Then, evaluating $\dot{V}\left(e,\tilde{\Theta}\right)$ and recognizing that $\frac{\|\Phi(x)\|^2}{m^2(\|x\|)}\leq\frac{1}{\lambda_{min}(R)}$ yield

$$\begin{aligned}\dot{V}\left(e,\tilde{\Theta}\right)&=-e^{\top}Qe+2e^{\top}PB\tilde{\Theta}^{\top}\Phi(x)-2e^{\top}Pw\\&\quad-\text{trace}\left(\frac{2\tilde{\Theta}^{\top}\left(\Phi(x)e^{\top}PB+\sigma\Theta\right)}{1+\Phi^{\top}(x)R\Phi(x)}\right)\\&\leq-\lambda_{min}(Q)\|e\|^2+2\|e\|\lambda_{max}(P)w_0\\&\quad+\frac{2\lambda_{max}(R)\|e\|\|PB\|\left\|\tilde{\Theta}\right\|\|\Phi(x)\|}{\lambda_{min}(R)}-\frac{2\sigma\left\|\tilde{\Theta}\right\|^2}{n^2(\|x\|)}+\frac{2\sigma\left\|\tilde{\Theta}\right\|\Theta_0}{m^2(\|x\|)}\end{aligned} \tag{9.349}$$

Utilizing the inequality $2\|a\|\|b\|\leq\|a\|^2+\|b\|^2$, $\dot{V}\left(e,\tilde{\Theta}\right)$ is bounded by

$$\begin{aligned}\dot{V}\left(e,\tilde{\Theta}\right)&\leq-c_1(\|e\|-c_2)^2+c_1c_2^2+\frac{\lambda_{max}(R)\|PB\|\left\|\tilde{\Theta}\right\|^2\|\Phi(x)\|^2}{\lambda_{min}(R)}\\&\quad-c_3\left(\left\|\tilde{\Theta}\right\|-c_4\right)^2+c_3c_4^2\end{aligned} \tag{9.350}$$

where $c_1=\lambda_{min}(Q)-\frac{\lambda_{max}(R)\|PB\|}{\lambda_{min}(R)}$, $c_2=\frac{\lambda_{max}(P)w_0}{c_1}$, $c_3=\frac{2\sigma}{n^2(\|x\|)}$, and $c_4=\frac{n^2(\|x\|)\Theta_0}{2m^2(\|x\|)}$.

$\dot{V}\left(e,\tilde{\Theta}\right)$ can be made larger by setting $\left\|\tilde{\Theta}\right\|=c_4$. Recognizing that $\frac{n^2(\|x\|)}{m^2(\|x\|)}\leq\frac{\lambda_{max}(R)}{\lambda_{min}(R)}$ and $\frac{n^2(\|x\|)}{m^4(\|x\|)}\leq1$, then

$$\dot{V}\left(e,\tilde{\Theta}\right)\leq-c_1(\|e\|-c_2)^2+c_1c_2^2+\frac{\lambda_{max}^3(R)\|PB\|\Theta_0^2\|\Phi(x)\|^2}{4\lambda_{min}^3(R)}+\frac{\sigma\Theta_0^2}{2} \tag{9.351}$$

Therefore, R and σ are chosen such that the following inequality is satisfied:

$$\begin{aligned}\varphi(\|x\|,\|x_m\|,Q,R,w_0,\Theta_0)&=-c_1\|x\|^2+2(c_1c_2+c_5\|x_m\|)\|x\|\\&\quad+2c_1c_2\|x_m\|-c_1\|x_m\|^2+c_6\|\Phi(x)\|^2+c_7\leq0\end{aligned} \tag{9.352}$$

where $c_5 = \lambda_{max}(Q) - \dfrac{\lambda_{max}(R)\|PB\|}{\lambda_{min}(R)}$, $c_6 = \dfrac{\lambda_{max}^3(R)\|PB\|\Theta_0^2}{4\lambda_{min}^3(R)}$, and $c_7 = \dfrac{\sigma\Theta_0^2}{2}$.

■

The use of the normalization in conjunction with a robust modification scheme can significantly improve robustness to the parameter drift, time delay, and unmodeled dynamics [16, 25].

Consider a first-order SISO system with an adaptive controller using the normalized MRAC without the projection method

$$\dot{x} = ax + bu \tag{9.353}$$

$$u = k_x(t)x + k_r r \tag{9.354}$$

$$\dot{k}_x = \frac{\gamma_x x(x_m - x)b}{1 + Rx^2} \tag{9.355}$$

where $r(t)$ is a constant reference command signal.

Differentiating the closed-loop plant gives

$$\ddot{x} - [a + bk_x(t)]\dot{x} + b\frac{\gamma_x x^2 b}{1 + Rx^2}x = b\frac{\gamma_x x^2 x_m b}{1 + Rx^2} \tag{9.356}$$

The effect of the normalized MRAC is to reduce the nonlinear integral control action of MRAC. The effective nonlinear integral gain of the normalized MRAC is given by

$$k_i(x) = \frac{\gamma_x x^2 b}{1 + Rx^2} \tag{9.357}$$

Then, the closed-loop plant is expressed as

$$\ddot{x} - [a + bk_x(t)]\dot{x} + bk_i(x)x = bk_i(x)x_m \tag{9.358}$$

Note that $k_i(x)$ is a bounded function where

$$0 < k_i(x) \leq \frac{\gamma_x b}{R} \tag{9.359}$$

Thus, the maximum closed-loop frequency is independent of $x(t)$. So, any large amplitude input will not affect the nonlinear integral control action. Nonetheless, $k_i(x)$ can still tend to a large value with γ_x.

Example 9.13 Consider the following first-order SISO system:

$$\dot{x} = ax + b\left(u + \theta^* x^2\right)$$

where $a = 1$ and $b = 1$ are known, and $\theta^* = 2$ is unknown.

An adaptive controller is designed as

$$u = k_x x + k_r r - \theta(t) x^2$$

using the normalized MRAC without the projection method

$$\dot{\theta} = -\frac{\gamma x^2 eb}{1 + Rx^4}$$

The reference model is given by

$$\dot{x}_m = a_m x_m + b_m r$$

where $a_m = -1$, $b_m = 1$, and $r(t) = 1$.

Choose $\gamma = 1000$, $R = 100$, and $x(0) = 1$. The closed-loop responses with the standard MRAC and normalized MRAC are shown in Fig. 9.21. The response with the standard MRAC exhibits high-frequency oscillations due to the use a large adaptation rate. On the other hand, the normalized MRAC effectively eliminates the effect of fast adaptation. Both the tracking error and parameter estimation error converge to zero since there is no disturbance.

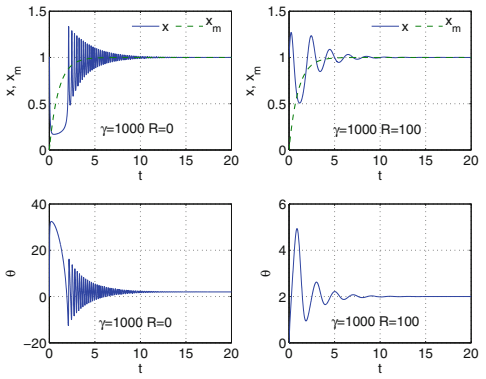

Fig. 9.21 Closed-loop responses with standard MRAC and normalized MRAC

Example 9.14 Consider Example 8.1

$$\dot{x} = ax + bu + w$$

where

$$w = p(1+t)^{p-1} - a(1+t)^p + b\left[\gamma_x b \frac{(1+t)^{2p+1} - 1}{2p+1} - k_x(0)\right](1+t)^p$$

and an adaptive regulator controller

$$u = k_x(t)\, x$$

where $k_x(t)$ is computed by the normalized MRAC without the projection method

$$\dot{k}_x = -\frac{\gamma_x x^2 b}{1 + Rx^2}$$

Let $a = 1$, $b = 1$, $n = -\frac{5}{12}$, $\gamma_x = 10$, and $R = 1$. The closed-loop response with the normalized MRAC is shown in Fig. 9.22. Notice that the response exhibits a parameter drift as $k_x(t) \to -\infty$. Thus, the normalized MRAC without the projection method is not robust to the parameter drift.

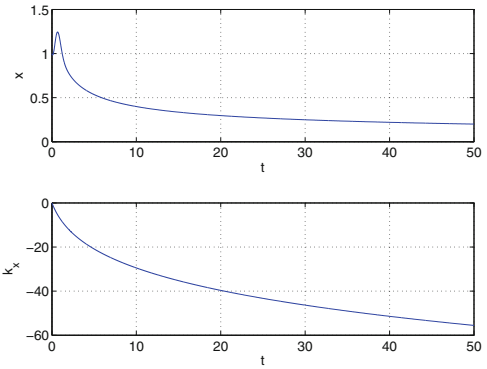

Fig. 9.22 Parameter drift with normalized MRAC

9.9 Covariance Adjustment of Adaptation Rate

Fast adaptation is needed to reduce the tracking error rapidly when a large uncertainty is present in a system. However, in most situations, when the adaptation process has achieved sufficiently a desired level of tracking performance, fast adaptation is usually no longer needed. Maintaining fast adaptation even when after the adaptation has achieved its objective can result in persistent learning. At best, persistent learning would do nothing to further improve the tracking performance once the adaptation has achieved its objective. At worst, persistent learning reduces robustness of an adaptive controller which is not highly desired. Therefore, the adaptation rate can be reduced by a covariance adjustment method. The adjustment allows for an arbitrarily large initial adaptation rate to be used to enable fast adaptation. The covariance adjustment then adjusts the adaptation rate toward a lower value to achieve improved robustness

as the adaptation proceeds. By reducing the adaptation rate, improved robustness can be achieved with the covariance adjustment, while the tracking performance during the initial adaptation is retained [5, 16, 25].

The standard MRAC with the covariance adjustment of the adaptation rate is described by

$$\dot{\Theta} = -\Gamma(t)\,\Phi(x)\,e^{\top}PB \tag{9.360}$$

$$\dot{\Gamma} = -\eta\Gamma\Phi(x)\,\Phi^{\top}(x)\,\Gamma \tag{9.361}$$

where $\eta > 0$ is an adjustment parameter.

The adjustment method is the same as the update law for the covariance matrix $R(t)$ in the recursive least-squares method.

Note that there are other variances of the covariance adjustment method. The covariance adjustment with a forgetting factor is given by

$$\dot{\Gamma} = \beta\Gamma - \eta\Gamma\Phi(x)\,\Phi^{\top}(x)\,\Gamma \tag{9.362}$$

where $\beta > 0$ is a forgetting factor.

The covariance adjustment with the normalization is given by

$$\dot{\Gamma} = \frac{\beta\Gamma - \eta\Gamma\Phi(x)\,\Phi^{\top}(x)\,\Gamma}{1 + \Phi^{\top}(x)\,R\Phi(x)} \tag{9.363}$$

The projection method can be used to bound the adaptive parameter. Thus, the MRAC with the projection method and covariance adjustment of the adaptation rate is described by

$$\dot{\Theta} = \mathrm{Pro}\left(\Theta, -\Gamma(t)\,\Phi(x)\,e^{\top}PB\right) \tag{9.364}$$

The stability proof of the covariance adjustment of the adaptation rate is as follows:

Proof Choose a Lyapunov candidate function

$$V\left(e, \tilde{\Theta}\right) = e^{\top}Pe + \mathrm{trace}\left(\tilde{\Theta}^{\top}\Gamma^{-1}\tilde{\Theta}\right) \tag{9.365}$$

Consider the case when $g(\Theta) < 0$ or $g(\Theta) = 0$ and $-\left[\Phi(x)\,e^{\top}PB\right]^{\top}\nabla g_{\Theta}(\Theta) \leq 0$. $\dot{V}\left(e, \tilde{\Theta}\right)$ is evaluated as

$$\dot{V}\left(e, \tilde{\Theta}\right) = -e^{\top}Qe - 2e^{\top}Pw + \mathrm{trace}\left(\tilde{\Theta}^{\top}\frac{d\Gamma^{-1}}{dt}\tilde{\Theta}\right) \tag{9.366}$$

But,

$$\Gamma\Gamma^{-1} = I \tag{9.367}$$

Then,

$$\dot{\Gamma}\Gamma^{-1} + \Gamma\frac{d\Gamma^{-1}}{dt} = 0 \tag{9.368}$$

So,

$$\frac{d\Gamma^{-1}}{dt} = -\Gamma^{-1}\dot{\Gamma}\Gamma^{-1} = \eta\Phi(x)\Phi^{\top}(x) \tag{9.369}$$

Therefore,

$$\dot{V}\left(e,\tilde{\Theta}\right) = -e^{\top}Qe - 2e^{\top}Pw + \eta\Phi^{\top}(x)\tilde{\Theta}\tilde{\Theta}^{\top}\Phi(x) \leq -\lambda_{min}(Q)\|e\|^2 + 2\|e\|\lambda_{max}(P)w_0 + \eta\left\|\tilde{\Theta}\right\|^2\|\Phi(x)\|^2 \tag{9.370}$$

Since $\left\|\tilde{\Theta}\right\| \leq \beta$ where β is the a priori bound from the projection method, then the parameter η is chosen to ensure that $\dot{V}\left(e,\tilde{\Theta}\right) \leq 0$ or equivalently the following inequality is satisfied:

$$\varphi\left(\|x\|,\|x_m\|,Q,\eta,w_0,\left\|\tilde{\Theta}\right\|\right) = -c_1\|x\|^2 + 2\left(c_1c_2 + c_5\|x_m\|\right)\|x\| + 2c_1c_2\|x_m\| - c_1\|x_m\|^2 + \eta\beta^2\|\Phi(x)\|^2 \leq 0 \tag{9.371}$$

■

Note that if a disturbance does not exist, then the tracking error converges asymptotically to zero, but the adaptive parameter is bounded. In the presence of a disturbance, a parameter drift can still exist even though the adaptation rate is continuously adjusted toward zero. In theory, the adaptive parameter would stop drifting when $\Gamma(t) \to 0$ as $t \to \infty$. In practice, the adaptive parameter can reach a sufficiently large value that can cause robustness issues. Therefore, the covariance adjustment method needs to be used in conjunction with the projection method or any robust modification schemes to prevent a parameter drift.

When used in conjunction with a robust modification scheme, the covariance adjustment method can further improve robustness. For example, the optimal control modification with the covariance adjustment is described by [25]

$$\dot{\Theta} = -\Gamma(t)\Phi(x)\left[e^{\top}P - \nu\Phi^{\top}(x)\Theta B^{\top}PA_m^{-1}\right]B \tag{9.372}$$

$$\dot{\Gamma} = -\eta\Gamma\Phi(x)\Phi^{\top}(x)\Gamma \tag{9.373}$$

Then, $\dot{V}\left(e,\tilde{\Theta}\right)$ is given by

$$\dot{V}\left(e,\tilde{\Theta}\right) \leq -c_1\left(\|e\| - c_2\right)^2 + c_1c_2^2 - \nu c_3\|\Phi(x)\|^2\left(\left\|\tilde{\Theta}\right\| - c_4\right)^2 + \nu c_3c_4^2\|\Phi(x)\|^2 \tag{9.374}$$

where c_1, c_2, c_4 are defined in Sect. 9.5, $c_3 = \lambda_{min}\left(B^\top A_m^{-\top} Q A_m^{-1} B\right)\left(1 - \frac{\eta}{\eta_{max}}\right)$, and $0 \leq \eta < \eta_{max}$ with $\eta_{max} = \nu\lambda_{min}\left(B^\top A_m^{-\top} Q A_m^{-1} B\right)$.

Thus, $\dot{V}\left(e, \tilde{\Theta}\right) \leq 0$ outside a compact set. Therefore, the closed-loop adaptive system is completely bounded.

Consider a first-order SISO system with an adaptive controller with the covariance adjustment of the adaptation rate

$$\dot{x} = ax + bu \tag{9.375}$$

$$u = k_x(t)\, x + k_r r \tag{9.376}$$

$$\dot{k}_x = \gamma_x x e b \tag{9.377}$$

$$\dot{\gamma}_x = -\eta\gamma_x^2 x^2 \tag{9.378}$$

The adaptation rate can be integrated as

$$-\frac{d\gamma_x}{\gamma_x^2} = \eta x^2 dt \Rightarrow \frac{1}{\gamma_x} - \frac{1}{\gamma_x(0)} = \eta\int_0^t x^2(\tau)\, d\tau \tag{9.379}$$

This yields

$$\gamma_x = \frac{\gamma_x(0)}{1 + \gamma_x(0)\,\eta\int_0^t x^2(\tau)\, d\tau} \tag{9.380}$$

Then, the adaptive law becomes

$$\dot{k}_x = \frac{\gamma_x(0)\, x e b}{1 + \gamma_x(0)\,\eta\int_0^t x^2(\tau)\, d\tau} \tag{9.381}$$

which is effectively a normalized adaptive law with an integral square normalization factor.

Let $r(t)$ be a constant reference command signal. Differentiating the closed-loop plant gives

$$\ddot{x} - [a + bk_x(t)]\,\dot{x} + bk_i(x)\, x = bk_i(x)\, x_m \tag{9.382}$$

where $k_i(x)$ is the nonlinear integral gain

$$k_i(x) = \frac{\gamma_x(0)\, x^2 b}{1 + \gamma_x(0)\,\eta\int_0^t x^2(\tau)\, d\tau} \tag{9.383}$$

As $t \to \infty$, $k_i(x) \to 0$ because $\int_0^t x^2(\tau)\, d\tau \to \infty$ since $r(t)$ is a constant command signal for which $x(t) \notin \mathcal{L}_2$. Therefore, the effect of fast adaptation is entirely eliminated.

The effect of the covariance adjustment of the adaptation rate is to gradually shut down the adaptation process. A problem associated with the covariance adjustment is that, once the adaptation rate is reduced to a value near zero, the adaptation process has to be restarted manually if a new uncertainty becomes present, whereas the adaptation rate with any other adaptive control methods will be finite and the adaptation process can be made to always remain active. It is possible to design a resetting adaptation process using the covariance adjustment. The adaptation process can be reset with a new initial value of the adaptation rate whenever a threshold criterion is satisfied. For example, a covariance adjustment resetting algorithm could be expressed as

$$\dot{\Gamma} = \begin{cases} \dot{\Gamma} \text{ with } \Gamma(t_e) = \Gamma_e & t \geq t_e \text{ when } \|e(t)\| > e_0 \text{ at } t = t_e \\ \dot{\Gamma} \text{ with } \Gamma(0) = \Gamma_0 & \text{otherwise} \end{cases} \tag{9.384}$$

The threshold should be chosen judiciously so that the trigger would occur appropriately to prevent false triggering. Also, when a switching action occurs with a large change in the value of the initial condition of $\Gamma(t)$, to prevent transient behaviors, a filter can be used to phase in the new initial condition of $\Gamma(t)$. For example, if a first-order filter is used, then

$$\dot{\Gamma} = -\lambda(\Gamma - \Gamma_e) \tag{9.385}$$

for $t \in [t_e, t_e + \Delta t]$, where $\lambda > 0$, $\Gamma(t_e) = \Gamma(t)$ at $t = t_e$ is computed from the previous covariance adjustment, and Γ_e is the new reset initial condition of $\Gamma(t)$.

Example 9.15 Consider the same first-order SISO system in Example 9.13

$$\dot{x} = ax + b\left(u + \theta^* x^2\right)$$

The MRAC adaptive law with the covariance adjustment without the projection method is given by

$$\dot{\theta} = -\gamma x^2 eb$$

$$\dot{\gamma} = -\eta \gamma^2 x^4$$

Let $\gamma(0) = 1000$ and $\eta = 0.1$. The response of the closed-loop system is shown in Fig. 9.23. Comparing to Fig. 9.21, the response with the covariance adjustment is free of high-frequency oscillations. Both the tracking error and adaptive parameter estimation error tend to zero asymptotically. The value of the adaptation rate at $t = 20\,\text{s}$ is $\gamma(t) = 0.6146$ which is substantially less than the initial value of $\gamma(0) = 1000$.

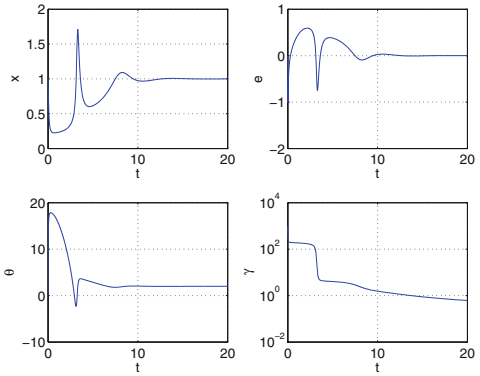

Fig. 9.23 Closed-loop response with covariance adjustment of adaptation rate

Example 9.16 Consider the same parameter drift example in Example 9.14 with the covariance adjustment without the projection method

$$\dot{k}_x = -\gamma_x x^2 b$$

$$\dot{\gamma}_x = -\eta \gamma_x^2 x^2$$

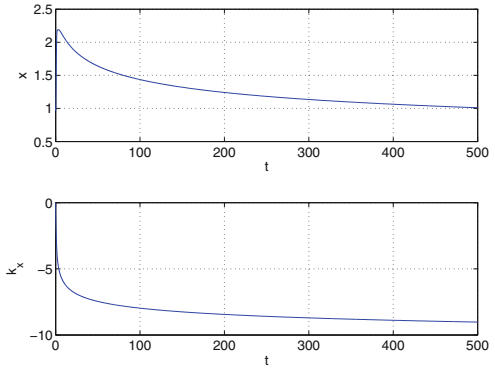

Fig. 9.24 Parameter drift with MRAC with covariance adjustment

Let $\gamma_x(0) = 10$ and $\eta = 1$. The response is shown in Fig. 9.24. Note that even though the value of $k_x(t)$ appears to reach a steady-state value, in fact, $k_x(t)$ is just drifting very slowly because the adaptation rate is very small and never reaches zero in a finite time.

9.10 Optimal Control Modification for Systems with Control Input Uncertainty

In certain situations, the control effectiveness of a control system may be impaired due to failures. When an uncertainty exists in the control input, the system can undergo significant changes in its closed-loop characteristics that can compromise stability and performance of the control system. The control signal must be modified accordingly to produce achievable dynamics in the presence of the reduced control effectiveness.

Consider a linear plant with a control input uncertainty and a matched uncertainty

$$\dot{x} = Ax + B\Lambda\left(u + \Omega^{*^{\top}} x\right) \tag{9.386}$$

where $x(t) \in \mathbb{R}^n$ is a state vector, $u(t) \in \mathbb{R}^m$ is a control vector, $A \in \mathbb{R}^n \times \mathbb{R}^n$ and $B \in \mathbb{R}^n \times \mathbb{R}^m$ are constant and known matrices such that the pair (A, B) is controllable, $\Lambda \in \mathbb{R}^m \times \mathbb{R}^m$ is an unknown control effectiveness diagonal matrix, and $\Omega^* \in \mathbb{R}^{n\times m}$ is an unknown constant matrix.

Let $\Delta A = B\Lambda\Omega^{*\top}$ and $\Delta B = B(\Lambda - I)$. Then, the plant can also be expressed as

$$\dot{x} = (A + \Delta A)x + (B + \Delta B)u \tag{9.387}$$

A nominal fixed gain controller is designed to stabilize the plant with no uncertainty and enable it to track a reference command $r(t)$

$$\bar{u} = K_x x + K_r r \tag{9.388}$$

where $r(t) \in \mathbb{R}^q \in \mathscr{L}_\infty$ is a piecewise continuous and bounded reference command vector.

The closed-loop nominal plant without uncertainty is obtained as

$$\dot{x} = A_m x + B_m r \tag{9.389}$$

where $A_m = A + BK_x \in \mathbb{R}^n \times \mathbb{R}^n$ is Hurwitz and $B_m = BK_r \in \mathbb{R}^n \times \mathbb{R}^q$ is a matrix with $q \leq n$.

This closed-loop nominal plant is then used to specify a reference model

$$\dot{x}_m = A_m x_m + B_m r \tag{9.390}$$

where $x_m(t) \in \mathbb{R}^n$ is a reference state vector.

The objective is to design a full-state feedback adaptive augmentation controller to enable $x(t)$ to follow $x_m(t)$ in the presence of uncertainty due to ΔA and ΔB with the following controller:

$$u = \bar{u} + \Delta K_x x + \Delta K_r r - \Omega^{\top} x \tag{9.391}$$

For convenience. $u(t)$ can be expressed as

$$u = \bar{u} - \Theta^{\top} \Phi(x, r) \tag{9.392}$$

where $\Theta^{\top}(t) = \left[-\Delta K_x(t) + \Omega^{\top}(t) \; -\Delta K_r(t) \right] \in \mathbb{R}^m \times \mathbb{R}^{n+q}$ and $\Phi(x, r) = \left[x^{\top} \; r^{\top} \right]^{\top} \in \mathbb{R}^{n+q}$.

It is assumed that there exist constant and unknown matrices ΔK_x^* and ΔK_r^* such that the following model matching conditions are satisfied:

$$A + B\Lambda \left(K_x + \Delta K_x^* \right) = A_m \tag{9.393}$$

$$B\Lambda \left(K_r + \Delta K_r^* \right) = B_m \tag{9.394}$$

Let $\tilde{\Lambda}(t) = \hat{\Lambda}(t) - \Lambda$, $\Delta \tilde{K}_x(t) = \Delta K_x(t) - \Delta K_x^*$, $\Delta \tilde{K}_r(t) = \Delta K_r(t) - \Delta K_r^*$, $\tilde{\Omega}(t) = \Omega(t) - \Omega^*$, and $\tilde{\Theta}(t) = \Theta(t) - \Theta^*$ be the estimation errors. Then, the closed-loop plant becomes

$$\dot{x} = A_m x + B_m r - B\hat{\Lambda}\tilde{\Theta}^{\top} \Phi(x, r) + B\tilde{\Lambda}\tilde{\Theta}^{\top} \Phi(x, r) \tag{9.395}$$

Defining the tracking error as $e(t) = x_m(t) - x(t)$, then the tracking error equation becomes

$$\dot{e} = A_m e + B\hat{\Lambda}\tilde{\Theta}^{\top} \Phi(x, r) + B\varepsilon \tag{9.396}$$

where

$$\varepsilon = -\tilde{\Lambda}\tilde{\Theta}^{\top} \Phi(x, r) \tag{9.397}$$

If the sign of Λ is known, then the standard MRAC law for adjusting $\Theta(t)$ is given by

$$\dot{\Theta} = -\Gamma_{\Theta} \Phi(x, r) e^{\top} P B \operatorname{sgn} \Lambda \tag{9.398}$$

This MRAC law, while providing asymptotic tracking, does not provide robustness to potential unmodeled dynamics. The optimal control modification adaptive law can be used to provide robust adaptation as [21]

$$\dot{\Theta} = -\Gamma_{\Theta} \Phi(x, r) \left[e^{\top} P - \nu \Phi^{\top}(x, r) \Theta \hat{\Lambda}^{\top} B^{\top} P A_m^{-1} \right] B\hat{\Lambda} \tag{9.399}$$

It is noted that the adaptive law depends on the estimate of Λ which needs to be computed. Toward this end, a predictor model of the plant is defined as

$$\dot{\hat{x}} = A_m \hat{x} + (A - A_m) x + B\hat{\Lambda} \left(u + \Omega^{\top} x \right) \tag{9.400}$$

Define the predictor error as $e_p(t) = \hat{x}(t) - x(t)$, then

$$\dot{e}_p = A_m e_p + B\hat{\Lambda}\tilde{\Omega}^\top x + B\tilde{\Lambda}\left(u + \Omega^\top x\right) + B\varepsilon_p \tag{9.401}$$

where

$$\varepsilon_p = -\tilde{\Lambda}\tilde{\Omega}^\top x \tag{9.402}$$

Then, Λ can be estimated by the following adaptive laws:

$$\dot{\Omega} = -\Gamma_\Omega x\left(e_p^\top P - \nu x^\top \Omega \hat{\Lambda}^\top B^\top P A_m^{-1}\right) B\hat{\Lambda} \tag{9.403}$$

$$\dot{\hat{\Lambda}}^\top = -\Gamma_\Lambda\left(u + \Omega^\top x\right)\left[e_p^\top P - \nu\left(u^\top + x^\top\Omega\right)\hat{\Lambda}^\top B^\top P A_m^{-1}\right] B \tag{9.404}$$

The Lyapunov stability proof is provided as follows:

Proof Choose a Lyapunov candidate function

$$\begin{aligned} V\left(e, e_p\tilde{\Theta}, \tilde{\Omega}, \tilde{\Lambda}\right) = {} & e^\top P e + e_p^\top P e_p + \text{trace}\left(\tilde{\Theta}^\top \Gamma_\Theta^{-1}\tilde{\Theta}\right) \\ & + \text{trace}\left(\tilde{\Omega}^\top \Gamma_\Omega^{-1}\tilde{\Omega}\right) + \text{trace}\left(\tilde{\Lambda}\Gamma_\Lambda^{-1}\tilde{\Lambda}^\top\right) \end{aligned} \tag{9.405}$$

Evaluating $\dot{V}\left(e, e_p, \tilde{\Theta}, \tilde{\Omega}, \tilde{\Lambda}\right)$ yields

$$\begin{aligned} \dot{V}\left(e, e_p\tilde{\Theta}, \tilde{\Omega}, \tilde{\Lambda}\right) = {} & -e^\top Q e - e_p^\top Q e_p + 2e^\top P B\varepsilon + 2e_p^\top P B\varepsilon_p \\ & + 2\nu\text{trace}\left(\tilde{\Theta}^\top \Phi\left(x, r\right)\Phi^\top\left(x, r\right)\Theta\hat{\Lambda}^\top B^\top P A_m^{-1} B\hat{\Lambda}\right) \\ & + 2\nu\text{trace}\left(\tilde{\Omega}^\top x x^\top \Omega\hat{\Lambda}^\top B^\top P A_m^{-1} B\hat{\Lambda}\right) \\ & + 2\nu\text{trace}\left(\tilde{\Lambda}\left(u + \Omega^\top x\right)\left(u^\top + x^\top\Omega\right)\hat{\Lambda}^\top B^\top P A_m^{-1} B\right) \end{aligned} \tag{9.406}$$

Let $\bar{B} = \left[\begin{array}{ccc} B & B & B \end{array}\right] \in \mathbb{R}^n \times \mathbb{R}^{3m}, \Pi\left(t\right) = \left[\begin{array}{ccc} \Theta\left(t\right)\hat{\Lambda}^\top\left(t\right) & 0 & 0 \\ 0 & \Omega\left(t\right)\hat{\Lambda}^\top\left(t\right) & 0 \\ 0 & 0 & \hat{\Lambda}^\top\left(t\right) \end{array}\right] \in \mathbb{R}^{2n+m+q} \times \mathbb{R}^{3m}, \Psi\left(x, r\right) = \left[\begin{array}{cccc} \Phi^\top\left(x, r\right) & x^\top & u^\top + x^\top\Omega \end{array}\right]^\top \in \mathbb{R}^{2n+m+q}$, then

$$\begin{aligned} & \text{trace}\left(\tilde{\Pi}^\top\Psi\left(x, r\right)\Psi^\top\left(x, r\right)\Pi\bar{B}^\top P A_m^1\bar{B}\right) \\ & \quad = \text{trace}\left(\tilde{\Theta}^\top\Phi\left(x, r\right)\Phi^\top\left(x, r\right)\Theta\hat{\Lambda}^\top B^\top P A_m^{-1} B\hat{\Lambda}\right) \\ & \qquad + \text{trace}\left(\tilde{\Omega}^\top x x^\top\Omega\hat{\Lambda}^\top B^\top P A_m^{-1} B\hat{\Lambda}\right) \\ & \qquad + \text{trace}\left(\tilde{\Lambda}\left(u + \Omega^\top x\right)\left(u^\top + x^\top\Omega\right)\hat{\Lambda}^\top B^\top P A_m^{-1} B\right) \end{aligned} \tag{9.407}$$

$\dot{V}\left(e, e_p, \tilde{\Theta}, \tilde{\Omega}, \tilde{\Lambda}\right)$ can be expressed as

$$\begin{aligned}\dot{V}\left(e, e_p \tilde{\Pi}\right) = & -e^\top Q e - e_p^\top Q e_p + 2e^\top P B \varepsilon + 2e_p^\top P B \varepsilon_p \\ & - \nu \Psi^\top (x, r)\, \tilde{\Pi} \bar{B}^\top A_m^{-\top} Q A_m^{-1} \bar{B} \tilde{\Pi}^\top \Psi (x, r) \\ & + 2\nu \Psi^\top (x, r)\, \Pi^* \bar{B}^\top P A_m^{-1} \bar{B} \tilde{\Pi}^\top \Psi (x, r)\end{aligned} \tag{9.408}$$

Then, $\dot{V}\left(e, e_p \tilde{\Pi}\right)$ is bounded by

$$\begin{aligned}\dot{V}\left(e, e_p \tilde{\Pi}\right) \leq & -\lambda_{min}(Q)\left(\|e\|^2 + \left\|e_p\right\|^2\right) + 2\|PB\|\left(\|e\|\varepsilon_0 + \left\|e_p\right\|\varepsilon_{p_0}\right) \\ & - \nu \lambda_{min}\left(\bar{B}^\top A_m^{-\top} Q A_m^{-1} \bar{B}\right) \|\Psi (x, r)\|^2 \left\|\tilde{\Pi}\right\|^2 \\ & + 2\nu \left\|\bar{B}^\top P A_m^{-1} \bar{B}\right\| \|\Psi (x, r)\|^2 \left\|\tilde{\Pi}\right\| \Pi_0\end{aligned} \tag{9.409}$$

where $\sup_{\forall x \in \mathscr{D}} \|\varepsilon (x)\| \leq \varepsilon_0$, $\sup_{\forall x \in \mathscr{D}} \left\|\varepsilon_p (x)\right\| \leq \varepsilon_{p_0}$, and $\Pi_0 = \|\Pi^*\|$.

Let $c_1 = \lambda_{min}(Q), c_2 = \dfrac{\|PB\|\varepsilon_0}{\lambda_{min}(Q)}, c_3 = \dfrac{\|PB\|\varepsilon_{p_0}}{\lambda_{min}(Q)}, c_4 = \lambda_{min}\left(\bar{B}^\top A_m^{-\top} Q A_m^{-1} \bar{B}\right)$ $\|\Psi (x, r)\|^2$, and $c_5 = \dfrac{\left\|\bar{B}^\top P A_m^{-1} \bar{B}\right\| \Pi_0}{\lambda_{min}\left(\bar{B}^\top A_m^{-\top} Q A_m^{-1} \bar{B}\right)}$. Then,

$$\begin{aligned}\dot{V}\left(e, e_p \tilde{\Pi}\right) \leq & -c_1 (\|e\| - c_2)^2 + c_1 c_2^2 - c_1 \left(\left\|e_p\right\| - c_3\right)^2 \\ & + c_1 c_3^2 - \nu c_4 \left(\left\|\tilde{\Pi}\right\| - c_5\right)^2 + \nu c_4 c_5^2\end{aligned} \tag{9.410}$$

Thus, $\dot{V}\left(e, e_p, \tilde{\Pi}\right) \leq 0$ outside a compact set $\mathscr{S}$ defined by

$$\begin{aligned}\mathscr{S} = \Big\{ & \left(e(t), e_p(t), \tilde{\Pi}(t)\right) : c_1 (\|e\| - c_2)^2 + c_1 \left(\left\|e_p\right\| - c_3\right)^2 \\ & + \nu c_4 \left(\left\|\tilde{\Pi}\right\| - c_5\right)^2 \leq c_1 c_2^2 + c_1 c_3^2 + \nu c_4 c_5^2 \Big\}\end{aligned} \tag{9.411}$$

This implies

$$\|e\| \geq c_2 + \sqrt{c_2^2 + c_3^2 + \frac{\nu c_4 c_5^2}{c_1}} = p \tag{9.412}$$

$$\left\|e_p\right\| \geq c_3 + \sqrt{c_2^2 + c_3^2 + \frac{\nu c_4 c_5^2}{c_1}} = q \tag{9.413}$$

$$\left\|\tilde{\Pi}\right\| \geq c_5 + \sqrt{c_5^2 + \frac{c_1 c_2^2 + c_1 c_3^2}{\nu c_4}} = \alpha \tag{9.414}$$

There exists Ψ_0 such that $\|\Psi(x,r)\| \leq \Psi_0$ for any $0 < \nu < \nu_{max}$ that satisfies the following inequalities:

$$\begin{aligned}\varphi(\|x\|, \|x_m\|, Q, \nu, \varepsilon_0, \Pi_0) = &-c_1\|x\|^2 + 2(c_1 c_2 + \lambda_{max}(Q)\|x_m\|)\|x\| \\ &+ 2c_1 c_2\|x_m\| - c_1\|x_m\|^2 + c_1 c_3^2 \\ &+ \nu c_4(\|\Psi(x,r)\|)c_5^2 \leq 0\end{aligned} \tag{9.415}$$

$$\begin{aligned}\phi\left(\left\|x_p\right\|, \|x_m\|, Q, \nu, \varepsilon_{p_0}, \Pi_0\right) = &-c_1\left\|x_p\right\|^2 + 2(c_1 c_3 + \lambda_{max}(Q)\|x\|)\left\|x_p\right\| \\ &+ 2c_1 c_3\|x\| - c_1\|x\|^2 + c_1 c_2^2 \\ &+ \nu c_4(\|\Psi(x,r)\|)c_5^2 \leq 0\end{aligned} \tag{9.416}$$

Then, the lower bounds which are dependent on $\|\Psi(x,r)\|$ also exist. Since $\dot{V}\left(e, e_p, \tilde{\Pi}\right) \leq 0$ outside the compact set $\mathscr{S}$, $V\left(e, e_p, \tilde{\Pi}\right) \leq V_0$, where V_0 is the smallest upper bound of $V\left(e, e_p, \tilde{\Pi}\right)$ which is given by

$$V_0 = \lambda_{max}(P)\left(p^2 + q^2\right) + \left[\lambda_{max}\left(\Gamma_{\Theta}^{-1}\right) + \lambda_{max}\left(\Gamma_{\Omega}^{-1}\right) + \lambda_{max}\left(\Gamma_{\Lambda}^{-1}\right)\right]\alpha^2 \tag{9.417}$$

Then,

$$\lambda_{min}(P)\|e\|^2 \leq V\left(e, e_p, \tilde{\Pi}\right) \leq V_0 \tag{9.418}$$

$$\lambda_{min}(P)\left\|e_p\right\|^2 \leq V\left(e, e_p, \tilde{\Pi}\right) \leq V_0 \tag{9.419}$$

Therefore, the closed-loop system is uniformly ultimately bounded with the following ultimate bounds:

$$\|e\| \leq \sqrt{\frac{V_0}{\lambda_{min}(P)}} \tag{9.420}$$

$$\left\|e_p\right\| \leq \sqrt{\frac{V_0}{\lambda_{min}(P)}} \tag{9.421}$$

9.11 Bi-Objective Optimal Control Modification for Systems with Control Input Uncertainty

Consider the following MIMO system with a control input uncertainty and a matched uncertainty:

$$\dot{x} = Ax + B\Lambda\left[u + \Theta^{*\top}\Phi\left(x\right)\right] + w \tag{9.422}$$

where $x\left(t\right) \in \mathbb{R}^n$ is a state vector, $u\left(t\right) \in \mathbb{R}^m$ is a control vector, $A \in \mathbb{R}^n \times \mathbb{R}^n$ is known, $B \in \mathbb{R}^n \times \mathbb{R}^m$ is also known such that (A, B) is controllable, $\Lambda = \Lambda^\top > 0 \in \mathbb{R}^m \times \mathbb{R}^m$ is a constant unknown diagonal matrix which represents a control input uncertainty, $\Theta^* \in \mathbb{R}^p \times \mathbb{R}^m$ is the unknown parameter, $\Phi\left(x\right) \in \mathbb{R}^p$ is a known regressor function, and $w\left(t\right) \in \mathbb{R}^n$ is a bounded exogenous disturbance with a bounded time derivative, i.e., $\sup \|w\| \leq w_0$ and $\sup \|\dot{w}\| \leq \delta_0$.

The closed-loop plant is designed to follow a reference model specified as

$$\dot{x}_m = A_m x_m + B_m r \tag{9.423}$$

where $x_m\left(t\right) \in \mathbb{R}^n$ is a reference state vector, $A_m \in \mathbb{R}^n \times \mathbb{R}^n$ is Hurwitz, and $B_m \in \mathbb{R}^n \times \mathbb{R}^q$ is a matrix associated with a piecewise continuous and bounded reference command vector $r\left(t\right) \in \mathbb{R}^q$.

In the presence of both the control input uncertainty and matched uncertainty due to Λ and Θ^*, an adaptive controller is designed as

$$u = K_x\left(t\right)x + K_r\left(t\right)r - \Theta^\top\left(t\right)\Phi\left(x\right) \tag{9.424}$$

where $K_x\left(t\right) \in \mathbb{R}^m \times \mathbb{R}^n$ is an adaptive feedback gain, $K_r\left(t\right) \in \mathbb{R}^m \times \mathbb{R}^q$ is an adaptive command feedforward gain, and $\Theta\left(t\right) \in \mathbb{R}^p \times \mathbb{R}^m$ is the estimate of Θ^*.

We assume that there exist constant and unknown matrices K_x^* and K_r^* such that the following model matching conditions are satisfied:

$$A + B\Lambda K_x^* = A_m \tag{9.425}$$

$$B\Lambda K_r^* = B_m \tag{9.426}$$

If Λ is unknown but sign of Λ is known, then the standard MRAC adaptive laws are given by

$$\dot{K}_x^\top = \Gamma_x x e^\top P B \mathrm{sgn}\Lambda \tag{9.427}$$

$$\dot{K}_r^\top = \Gamma_r r e^\top P B \mathrm{sgn}\Lambda \tag{9.428}$$

$$\dot{\Theta} = -\Gamma_\Theta \Phi\left(x\right) e^\top P B \mathrm{sgn}\Lambda \tag{9.429}$$

However, the standard MRAC is non-robust. To improve robustness, the adaptive laws should include any one of the robust modification schemes or the projection method. For example, the σ modification adaptive laws are given by

$$\dot{K}_x^\top = \Gamma_x \left(x e^\top P B \text{sgn} \Lambda - \sigma K_x^\top \right) \tag{9.430}$$

$$\dot{K}_r^\top = \Gamma_r \left(r e^\top P B \text{sgn} \Lambda - \sigma K_r^\top \right) \tag{9.431}$$

$$\dot{\Theta} = -\Gamma_\Theta \left[\Phi (x) e^\top P B \text{sgn} \Lambda + \sigma \Theta \right] \tag{9.432}$$

If Λ is completely unknown, then we need to consider other approaches such as the method in Sect. 9.10. We now introduce a new optimal control modification method that uses two types of errors for the adaptation: tracking error and predictor error. We call this bi-objective optimal control modification adaptive law [26–29]. Model-reference adaptive control that uses both the tracking error and the predictor error or the plant modeling error is also called composite adaptive control [30]. Other works that have also used this type of adaptation include hybrid adaptive control [31] and composite model-reference adaptive control [7].

Let $\tilde{\Lambda}(t) = \hat{\Lambda}(t) - \Lambda$, $\tilde{K}_x(t) = K_x(t) - K_x^*$, $\tilde{K}_r(t) = K_r(t) - K_r^*$, and $\tilde{\Theta}(t) = \Theta(t) - \Theta^*$ be the estimation errors. Then, the closed-loop plant becomes

$$\dot{x} = A_m x + B_m r + B \left(\hat{\Lambda} - \tilde{\Lambda} \right) \left[\tilde{K}_x x + \tilde{K}_r r - \tilde{\Theta}^\top \Phi (x) \right] + w \tag{9.433}$$

The tracking error equation is obtained as

$$\dot{e} = A_m e + B \hat{\Lambda} \left[-\tilde{K}_x x - \tilde{K}_r r + \tilde{\Theta}^\top \Phi (x) \right] - w + B \varepsilon \tag{9.434}$$

where $\varepsilon(t) \in \mathbb{R}^m$ is the residual estimation error of the plant model

$$\varepsilon = \tilde{\Lambda} \left[\tilde{K}_x x + \tilde{K}_r r - \tilde{\Theta}^\top \Phi (x) \right] \tag{9.435}$$

such that $\sup \|\varepsilon\| \leq \varepsilon_0$.

Consider a predictor model of the plant as

$$\dot{\hat{x}} = A_m \hat{x} + (A - A_m) x + B \hat{\Lambda} \left[u + \Theta^\top \Phi (x) \right] + \hat{w} \tag{9.436}$$

where $\hat{w}(t)$ is the estimate of the disturbance $w(t)$.

We define the predictor error as $e_p(t) = \hat{x}(t) - x(t)$, then

$$\dot{e}_p = A_m e_p + B \tilde{\Lambda} \left[u + \Theta^\top \Phi (x) \right] + B \hat{\Lambda} \tilde{\Theta}^\top \Phi (x) + \tilde{w} + B \varepsilon_p \tag{9.437}$$

where $\tilde{w}(t) = \hat{w}(t) - w(t)$ is the disturbance estimation error, and $\varepsilon_p(t) \in \mathbb{R}^m$ is the residual estimation error of the predictor model

$$\varepsilon_p = -\tilde{\Lambda}\tilde{\Theta}^\top \Phi(x) \tag{9.438}$$

such that $\sup \|\varepsilon_p\| \leq \varepsilon_{p_0}$.

Proposition The following bi-objective optimal control modification adaptive laws can be used to compute $K_x(t)$, $K_r(t)$, and $\Theta(t)$:

$$\dot{K}_x^\top = \Gamma_x x \left(e^\top P + \nu u^\top \hat{\Lambda}^\top B^\top P A_m^{-1}\right) B\hat{\Lambda} \tag{9.439}$$

$$\dot{K}_r^\top = \Gamma_r r \left(e^\top P + \nu u^\top \hat{\Lambda}^\top B^\top P A_m^{-1}\right) B\hat{\Lambda} \tag{9.440}$$

$$\begin{aligned}\dot{\Theta} = -\Gamma_\Theta \Phi(x) \Big(&e^\top P + \nu u^\top \hat{\Lambda}^\top B^\top P A_m^{-1} + e_p^\top W \\ &- \eta \left\{\left[u + 2\Theta^\top \Phi(x)\right]^\top \hat{\Lambda}^\top B^\top + \hat{w}^\top\right\} W A_m^{-1}\Big) B\hat{\Lambda}\end{aligned} \tag{9.441}$$

$$\dot{\hat{\Lambda}}^\top = -\Gamma_\Lambda \left[u + \Theta^\top \Phi(x)\right] \left(e_p^\top W - \eta \left\{\left[u + 2\Theta^\top \Phi(x)\right]^\top \hat{\Lambda}^\top B^\top + \hat{w}^\top\right\} W A_m^{-1}\right) B \tag{9.442}$$

$$\dot{\hat{w}}^\top = -\gamma_w \left(e_p^\top W - \eta \left\{\left[u + 2\Theta^\top \Phi(x)\right]^\top \hat{\Lambda}^\top B^\top + \hat{w}^\top\right\} W A_m^{-1}\right) \tag{9.443}$$

where $\Gamma_x = \Gamma_x^\top > 0 \in \mathbb{R}^n \times \mathbb{R}^n$, $\Gamma_r = \Gamma_r^\top > 0 \in \mathbb{R}^q \times \mathbb{R}^q$, $\Gamma_\Theta = \Gamma_\Theta^\top > 0 \in \mathbb{R}^p \times \mathbb{R}^p$, $\Gamma_\Lambda = \Gamma_\Lambda^\top > 0 \in \mathbb{R}^m \times \mathbb{R}^m$, and $\gamma_w > 0$ are adaptation rate matrices; $\nu > 0 \in \mathbb{R}$ and $\eta > 0 \in \mathbb{R}$ are the optimal control modification parameters; and $P = P^\top > 0 \in \mathbb{R}^n \times \mathbb{R}^n$ and $W = W^\top > 0 \in \mathbb{R}^n \times \mathbb{R}^n$ are the solutions of the following Lyapunov equations:

$$PA_m + A_m^\top P = -Q \tag{9.444}$$

$$WA_m + A_m^\top W = -R \tag{9.445}$$

where $Q = Q^\top > 0 \in \mathbb{R}^n \times \mathbb{R}^n$ and $R = R^\top > 0 \in \mathbb{R}^n \times \mathbb{R}^n$ are positive-definite weighting matrices.

The bi-objective optimal control modification adaptive laws are considered to be the generalization of the optimal control modification adaptive laws developed in Sect. 9.10.

The optimal control modification adaptive laws are called bi-objective because they use both the tracking error and the predictor error for adaptation and are derived from the following infinite-time horizon cost functions:

$$J_1 = \lim_{t_f \to \infty} \frac{1}{2} \int_0^{t_f} (e - \Delta_1)^\top Q (e - \Delta_1)\, dt \tag{9.446}$$

$$J_2 = \lim_{t_f \to \infty} \frac{1}{2} \int_0^{t_f} \left(e_p - \Delta_2\right)^\top R \left(e_p - \Delta_2\right) dt \tag{9.447}$$

subject to Eqs. (9.434) and (9.437), where $\Delta_1(t)$ and $\Delta_2(t)$ represent the unknown lower bounds of the tracking error and the predictor error, respectively.

The cost functions J_1 and J_2 are combined into the following bi-objective cost function:

$$J = J_1 + J_2 \tag{9.448}$$

The bi-objective cost function J combines both the objectives of minimization of the tracking error and the predictor error bounded away from the origin. Geometrically, it represents the sum of the weighted norm squares measured from the trajectories of $e(t)$ and $e_p(t)$ to the normal surface of a hypersphere $B_\Delta = \left\{e(t) \in \mathbb{R}^n, e_p(t) \in \mathbb{R}^n : (e - \Delta_1)^\top Q (e - \Delta_1) + \left(e_p - \Delta_2\right)^\top R \left(e_p - \Delta_2\right) \leq \Delta^2\right\} \subset \mathscr{D} \subset \mathbb{R}^n$. The bi-objective cost function is designed to provide stability robustness by not seeking asymptotic tracking which results in $e(t) \to 0$ and $e_p(t) \to 0$ as $t_f \to \infty$, but rather bounded tracking which results in the errors tending to some lower bounds. By not requiring asymptotic tracking, the adaptation can be made more robust. Therefore, the tracking performance can be traded with stability robustness by a suitable selection of the modification parameters ν and η. Increasing the tracking performance by reducing ν and or η will decrease stability robustness of the adaptive laws to unmodeled dynamics, and vice versa.

The adaptive laws are derived from the Pontryagin's minimum principle as follows:

Proof Using the optimal control framework, the Hamiltonian of the cost function is defined as

$$\begin{aligned} H = {} & \frac{1}{2} (e - \Delta_1)^\top Q (e - \Delta_1) + \frac{1}{2} \left(e_p - \Delta_2\right)^\top R \left(e_p - \Delta_2\right) \\ & + \lambda^\top \left\{A_m e + B \hat{\Lambda} \left[-\tilde{K}_x x - \tilde{K}_r r + \tilde{\Theta}^\top \Phi(x)\right] - w + B\varepsilon\right\} \\ & + \mu^\top \left\{A_m e_p + B \tilde{\Lambda} \left[u + \Theta^\top \Phi(x)\right] + B \hat{\Lambda} \tilde{\Theta}^\top \Phi(x) + \hat{w} - w + B\varepsilon_p\right\} \end{aligned} \tag{9.449}$$

where $\lambda(t) \in \mathbb{R}^n$ and $\mu(t) \in \mathbb{R}^n$ are adjoint variables.

The adjoint equations can be obtained from the necessary conditions of optimality as

$$\dot{\lambda} = -\nabla H_e^\top = -Q (e - \Delta_1) - A_m^\top \lambda \tag{9.450}$$

$$\dot{\mu} = -\nabla H_{e_p}^\top = -R \left(e_p - \Delta_2\right) - A_m^\top \mu \tag{9.451}$$

subject to the transversality conditions $\lambda\left(t_f \to \infty\right) = 0$ and $\mu\left(t_f \to \infty\right) = 0$ since both $e\,(0)$ and $e_p\,(0)$ are given.

Treating $\tilde{K}_x\,(t)$, $\tilde{K}_r\,(t)$, $\tilde{\Theta}\,(t)$, $\tilde{\Lambda}\,(t)$, and $\hat{w}\,(t)$ as control variables, then the optimal control solutions are obtained by the following gradient-based adaptive laws:

$$\dot{K}_x^\top = \dot{\tilde{K}}_x^\top = -\Gamma_x \nabla H_{\tilde{K}_x} = \Gamma_x x \lambda^\top B \hat{\Lambda} \tag{9.452}$$

$$\dot{K}_r^\top = \dot{\tilde{K}}_r^\top = -\Gamma_r \nabla H_{\tilde{K}_r} = \Gamma_r r \lambda^\top B \hat{\Lambda} \tag{9.453}$$

$$\dot{\Theta} = \dot{\tilde{\Theta}} = -\Gamma_\Theta \nabla H_{\tilde{\Theta}}^\top = -\Gamma_\Theta \Phi\,(x)\left(\lambda^\top + \mu^\top\right) B \hat{\Lambda} \tag{9.454}$$

$$\dot{\hat{\Lambda}}^\top = \dot{\tilde{\Lambda}}^\top = -\Gamma_\Lambda \nabla H_{\tilde{\Lambda}} = -\Gamma_\Lambda \left[u + \Theta^\top \Phi\,(x)\right] \mu^\top B \tag{9.455}$$

$$\dot{\hat{w}}^\top = -\gamma_w \nabla H_{\hat{w}} = -\gamma_w \mu^\top \tag{9.456}$$

The closed-form solutions can be obtained by eliminating the adjoint variables $\lambda\,(t)$ and $\mu\,(t)$ using the "sweep" method with the following assumed solutions of the adjoint equations:

$$\lambda = Pe + S\hat{\Lambda}\left[-K_x x - K_r r + \Theta^\top \Phi\,(x)\right] \tag{9.457}$$

$$\mu = We_p + T\hat{\Lambda}\left[u + 2\Theta^\top \Phi\,(x)\right] + V\hat{w} \tag{9.458}$$

Substituting the adjoint solutions back into the adjoint equations yields

$$\begin{aligned}
&\dot{P}e + PA_m e + PB\hat{\Lambda}\left[-K_x x - K_r r + \Theta^\top \Phi\,(x)\right] \\
&\quad - PB\hat{\Lambda}\left[-K_x^* x - K_r^* r + \Theta^{*\top} \Phi\,(x)\right] - Pw + PB\varepsilon \\
&\quad + \dot{S}\hat{\Lambda}\left[-K_x x - K_r r + \Theta^\top \Phi\,(x)\right] \\
&\quad + S\frac{d\left\{\hat{\Lambda}\left[-K_x x - K_r r + \Theta^\top \Phi\,(x)\right]\right\}}{dt} \\
&\quad = -Q\,(e - \Delta_1) - A_m^\top Pe - A_m^\top S\hat{\Lambda}\left[-K_x x - K_r r + \Theta^\top \Phi\,(x)\right]
\end{aligned} \tag{9.459}$$

$$\begin{aligned}
&\dot{W}e_p + WA_m e_p + WB\hat{\Lambda}\left[u + \Theta^\top \Phi\,(x)\right] - WB\Lambda\left[u + \Theta^\top \Phi\,(x)\right] + WB\hat{\Lambda}\Theta^\top \Phi\,(x) \\
&\quad - WB\hat{\Lambda}\Theta^{*\top} \Phi\,(x) + W\hat{w} - Ww + WB\varepsilon_p \\
&\quad + \dot{T}\hat{\Lambda}\left[u + 2\Theta^\top \Phi\,(x)\right] + T\frac{d\left\{\hat{\Lambda}\left[u + 2\Theta^\top \Phi\,(x)\right]\right\}}{dt} + \dot{V}\hat{w} \\
&\quad + V\dot{\hat{w}} = -R\left(e_p - \Delta_2\right) - A_m^\top We_p - A_m^\top T\hat{\Lambda}\left[u + 2\Theta^\top \Phi\,(x)\right] - A_m^\top V\hat{w}
\end{aligned} \tag{9.460}$$

Equating terms yields the following equations:

$$\dot{P} + PA_m + A_m^\top P + Q = 0 \tag{9.461}$$

$$\dot{S} + A_m^\top S + PB = 0 \tag{9.462}$$

$$\begin{aligned} &Q\Delta_1 + PB\hat{\Lambda}\left[-K_x^* x - K_r^* r + \Theta^{*\top}\Phi(x)\right] + Pw \\ &\quad - PB\varepsilon - S\frac{d\left\{\hat{\Lambda}\left[-K_x x - K_r r + \Theta^\top \Phi(x)\right]\right\}}{dt} = 0 \end{aligned} \tag{9.463}$$

$$\dot{W} + WA_m + A_m^\top W + R = 0 \tag{9.464}$$

$$\dot{T} + A_m^\top T + WB = 0 \tag{9.465}$$

$$\dot{V} + A_m^\top V + W = 0 \tag{9.466}$$

$$\begin{aligned} &R\Delta_2 + WB\Lambda\left[u + \Theta^\top \Phi(x)\right] + WB\hat{\Lambda}\Theta^{*\top}\Phi(x) + Ww - WB\varepsilon_p \\ &\quad - T\frac{d\left\{\hat{\Lambda}\left[u + 2\Theta^\top \Phi(x)\right]\right\}}{dt} - V\dot{\hat{w}} = 0 \end{aligned} \tag{9.467}$$

subject to the transversality conditions $P\left(t_f \to \infty\right) = 0$, $S\left(t_f \to \infty\right) = 0$, $W\left(t_f \to \infty\right) = 0$, $T\left(t_f \to \infty\right) = 0$, and $V\left(t_f \to \infty\right) = 0$.

The infinite-time horizon solutions of $P(t)$ and $W(t)$ as $t_f \to \infty$ tend to their equilibrium solutions at $t = 0$ and are given by the algebraic Lyapunov equations

$$PA_m + A_m^\top P + Q = 0 \tag{9.468}$$

$$WA_m + A_m^\top W + R = 0 \tag{9.469}$$

The solutions of $S(t)$, $T(t)$, and $V(t)$ also tend to their equilibrium solutions

$$A_m^\top S + PB = 0 \tag{9.470}$$

$$A_m^\top T + WB = 0 \tag{9.471}$$

$$A_m^\top V + W = 0 \tag{9.472}$$

As with any control design, performance and robustness are often considered as two competing design requirements. Increasing robustness tends to require a compromise in performance and vice versa. Thus, to enable the bi-objective optimal control modification adaptive laws to be sufficiently flexible for a control design, the

modification parameters $\nu > 0$ and $\eta > 0$ are introduced as design free parameters to allow for the adjustment of the bi-objective optimal control modification terms in the adaptive laws.

Thus, the solutions of $S(t)$, $T(t)$, and $V(t)$ are given by

$$S = -\nu A_m^{-\top} PB \tag{9.473}$$

$$T = -\eta A_m^{-\top} WB \tag{9.474}$$

$$V = -\eta A_m^{-\top} W \tag{9.475}$$

Using the expression of $u(t)$, the adjoint solutions are then obtained as

$$\lambda = Pe + \nu A_m^{-\top} PB\hat{\Lambda} u \tag{9.476}$$

$$\mu = We_p - \eta A_m^{-\top} WB\hat{\Lambda}\left[u + 2\Theta^{\top}\Phi(x)\right] - \eta A_m^{-\top} W\hat{w} \tag{9.477}$$

Substituting the adjoint solutions into the gradient-based adaptive laws yields the bi-objective optimal control modification adaptive laws in Eqs. (9.452)–(9.456).

■

We note that $K_x(t)$ and $K_r(t)$ are adapted based on the tracking error, $\hat{\Lambda}(t)$ and $\hat{w}(t)$ are adapted based on the predictor error, and $\Theta(t)$ is adapted based on both the tracking error and the predictor error.

The bounds on $\Delta_1(t)$ and $\Delta_2(t)$ as $t_f \to \infty$ can be estimated by

$$\begin{aligned}\|\Delta_1\| \leq \frac{1}{\lambda_{min}(Q)}\Bigg[&\|PB\hat{\Lambda}\|\left\|-K_x^* x - K_r^* r + \Theta^{*\top}\Phi(x)\right\| + \lambda_{max}(P) w_0 + \|PB\|\varepsilon_0 \\ &+ \nu\left\|A_m^{-\top} PB\right\|\left\|\frac{d\left\{\hat{\Lambda}\left[-K_x x - K_r r + \Theta^{\top}\Phi(x)\right]\right\}}{dt}\right\|\Bigg]\end{aligned} \tag{9.478}$$

$$\begin{aligned}\|\Delta_2\| \leq \frac{1}{\lambda_{min}(R)}\Bigg[&\|WB\Lambda\|\left\|u + \Theta^{\top}\Phi(x)\right\| + \|WB\hat{\Lambda}\|\left\|\Theta^{*\top}\Phi(x)\right\| + \lambda_{max}(W) w_0 \\ &+ \|WB\|\varepsilon_{p_0} + \eta\left\|A_m^{-\top} WB\right\|\left\|\frac{d\left\{\hat{\Lambda}\left[u + 2\Theta^{\top}\Phi(x)\right]\right\}}{dt}\right\| + \eta\left\|A_m^{-\top} W\right\|\|\dot{\hat{w}}\|\Bigg]\end{aligned} \tag{9.479}$$

which are dependent upon the modification parameters, control effectiveness uncertainty, matched uncertainty, and residual tracking error and predictor error.

Note that if $R = Q$ and $\eta = \nu$, then the bi-objective optimal control modification adaptive laws for $\Theta(t)$, $\hat{\Lambda}(t)$, and $\hat{w}(t)$ become

$$\dot{\Theta} = -\Gamma_\Theta \Phi(x) \left[\left(e^\top + e_p^\top \right) P - \nu \left\{ 2\Phi^\top(x)\, \Theta \hat{\Lambda}^\top B^\top + \hat{w}^\top \right\} P A_m^{-1} \right] B \hat{\Lambda} \tag{9.480}$$

$$\dot{\hat{\Lambda}}^\top = -\Gamma_\Lambda \left[u + \Theta^\top \Phi(x) \right] \left(e_p^\top P - \nu \left\{ \left[u + 2\Theta^\top \Phi(x) \right]^\top \hat{\Lambda}^\top B^\top + \hat{w}^\top \right\} P A_m^{-1} \right) B \tag{9.481}$$

$$\dot{\hat{w}}^\top = -\gamma_w \left(e_p^\top P - \nu \left\{ \left[u + 2\Theta^\top \Phi(x) \right]^\top \hat{\Lambda}^\top B^\top + \hat{w}^\top \right\} P A_m^{-1} \right) \tag{9.482}$$

The bi-objective optimal control modification adaptive laws can be shown to be stable as follows:

Proof Choose a Lyapunov candidate function

$$\begin{aligned} V\left(e, e_p, \tilde{K}_x, \tilde{K}_r, \tilde{\Theta}, \tilde{\Lambda}, \tilde{w}\right) = {} & e^\top P e + e_p^\top W e_p + \operatorname{trace}\left(\tilde{K}_x \Gamma_x^{-1} \tilde{K}_x^\top \right) \\ & + \operatorname{trace}\left(\tilde{K}_r \Gamma_r^{-1} \tilde{K}_r^\top \right) + \operatorname{trace}\left(\tilde{\Theta}^\top \Gamma_\Theta^{-1} \tilde{\Theta} \right) \\ & + \operatorname{trace}\left(\tilde{\Lambda} \Gamma_\Lambda^{-1} \tilde{\Lambda}^\top \right) + \tilde{w}^\top \gamma_w^{-1} \tilde{w} \end{aligned} \tag{9.483}$$

Evaluating $\dot{V}\left(e, e_p, \tilde{K}_x, \tilde{K}_r, \tilde{\Theta}, \tilde{\Lambda}, \tilde{w}\right)$ yields

$$\begin{aligned} \dot{V}\left(e, e_p, \tilde{K}_x, \tilde{K}_r, \tilde{\Theta}, \tilde{\Lambda}, \tilde{w}\right) = {} & -e^\top Q e + 2e^\top P B \hat{\Lambda} \left[-\tilde{K}_x x - \tilde{K}_r r + \tilde{\Theta}^\top \Phi(x) \right] \\ & - 2e^\top P w + 2e^\top P B \varepsilon \\ & - e_p^\top R e_p + 2e_p^\top W B \left\{ \tilde{\Lambda} \left[u + \Theta^\top \Phi(x) \right] + \hat{\Lambda} \tilde{\Theta}^\top \Phi(x) \right\} \\ & + 2e_p^\top W \tilde{w} + 2e_p^\top W B \varepsilon_p \\ & + 2\operatorname{trace}\left(\tilde{K}_x x \left(e^\top P + \nu u^\top \hat{\Lambda}^\top B^\top P A_m^{-1} \right) B \hat{\Lambda} \right) \\ & + 2\operatorname{trace}\left(\tilde{K}_r r \left(e^\top P + \nu u^\top \hat{\Lambda}^\top B^\top P A_m^{-1} \right) B \hat{\Lambda} \right) \\ & - 2\operatorname{trace}\left(\tilde{\Theta}^\top \Phi(x) \left(e^\top P + \nu u^\top \hat{\Lambda}^\top B^\top P A_m^{-1} + e_p^\top W \right. \right. \\ & \left. \left. - \eta \left\{ \left[u + 2\Theta^\top \Phi(x) \right]^\top \hat{\Lambda}^\top B^\top + \hat{w}^\top \right\} W A_m^{-1} \right) B \hat{\Lambda} \right) \\ & - 2\operatorname{trace}\left(\tilde{\Lambda} \left[u + \Theta^\top \Phi(x) \right] \right. \\ & \left. \left(e_p^\top W - \eta \left\{ \left[u + 2\Theta^\top \Phi(x) \right]^\top \hat{\Lambda}^\top B^\top + \hat{w}^\top \right\} W A_m^{-1} \right) B \right) \\ & - 2e_p^\top W \tilde{w} + 2 \left(\eta \left\{ \left[u + 2\Theta^\top \Phi(x) \right]^\top \hat{\Lambda}^\top B^\top + \hat{w}^\top \right\} W A_m^{-1} \right) \tilde{w} \\ & - 2\dot{w}^\top \gamma_w^{-1} \tilde{w} \end{aligned} \tag{9.484}$$

$\dot{V}\left(e, e_p, \tilde{K}_x, \tilde{K}_r, \tilde{\Theta}, \tilde{\Lambda}, \tilde{w}\right)$ can be further simplified as

$$\begin{aligned}\dot{V}\left(e, e_p, \tilde{K}_x, \tilde{K}_r, \tilde{\Theta}, \tilde{\Lambda}, \tilde{w}\right) = & -e^\top Qe - 2e^\top Pw + 2e^\top PB\varepsilon - e_p^\top Re_p + 2e_p^\top WB\varepsilon_p - 2\dot{w}^\top \gamma_w^{-1}\tilde{w} \\ & + 2\nu u^\top \hat{\Lambda}^\top B^\top PA_m^{-1}B\hat{\Lambda}\tilde{u} \\ & + 2\eta \text{trace}\left(\tilde{\Theta}^\top \Phi(x)\left\{\left[u + 2\Theta^\top \Phi(x)\right]^\top \hat{\Lambda}^\top B^\top + \hat{w}^\top\right\} WA_m^{-1}B\hat{\Lambda}\right) \\ & + 2\eta \text{trace}\left(\tilde{\Lambda}\left[u + \Theta^\top \Phi(x)\right]\right. \\ & \left.\left\{\left[u + 2\Theta^\top \Phi(x)\right]^\top \hat{\Lambda}^\top B^\top + \hat{w}^\top\right\} WA_m^{-1}B\right) \\ & + 2\eta \text{trace}\left(\tilde{w}\left\{\left[u + 2\Theta^\top \Phi(x)\right]^\top \hat{\Lambda}^\top B^\top + \hat{w}^\top\right\} WA_m^{-1}\right) \end{aligned} \tag{9.485}$$

where $\tilde{u}(t) = \tilde{K}_x(t)x(t) + \tilde{K}_r(t)r(t) - \tilde{\Theta}^\top(t)\Phi(x)$.

Let $\bar{B} = \begin{bmatrix} B & B & I \end{bmatrix} \in \mathbb{R}^n \times \mathbb{R}^{2m+n}$, $\Omega(t) = \begin{bmatrix} \Theta(t)\hat{\Lambda}^\top(t) & 0 & 0 \\ 0 & \hat{\Lambda}^\top(t) & 0 \\ 0 & 0 & \hat{w}^\top(t) \end{bmatrix} \in \mathbb{R}^{p+m+1} \times \mathbb{R}^{2m+n}$, $\Psi(x, r) = \begin{bmatrix} \Phi(x) \\ u + \Theta^\top \Phi(x) \\ 1 \end{bmatrix} \in \mathbb{R}^{p+m+1}$. Then,

$$\begin{aligned} & \text{trace}\left(\tilde{\Omega}^\top \Psi(x, r)\Psi^\top(x, r)\Omega\bar{B}^\top WA_m^{-1}\bar{B}\right) \\ & = \text{trace}\left(\tilde{\Theta}^\top \Phi(x)\left\{\left[u + 2\Theta^\top \Phi(x)\right]^\top \hat{\Lambda}^\top B^\top + \hat{w}^\top\right\} WA_m^{-1}B\hat{\Lambda}\right) \\ & \quad \times \text{trace}\left(\tilde{\Lambda}\left[u + \Theta^\top \Phi(x)\right]\left\{\left[u + 2\Theta^\top \Phi(x)\right]^\top \hat{\Lambda}^\top B^\top + \hat{w}^\top\right\} WA_m^{-1}B\right) \\ & \quad + \text{trace}\left(\tilde{w}\left\{\left[u + 2\Theta^\top \Phi(x)\right]^\top \hat{\Lambda}^\top B^\top + \hat{w}^\top\right\} WA_m^{-1}\right) \end{aligned} \tag{9.486}$$

where $\tilde{\Omega}(t) = \Omega(t) - \Omega^*$ and $\Omega^*(t) = \begin{bmatrix} \Theta^* & 0 & 0 \\ 0 & \Lambda^\top & 0 \\ 0 & 0 & w^\top(t) \end{bmatrix} \in \mathbb{R}^{p+m+1} \times \mathbb{R}^{2m+n}$.

Thus,

$$\begin{aligned}\dot{V}\left(e, e_p, \tilde{u}, \tilde{\Omega}\right) = & -e^\top Qe - 2e^\top Pw + 2e^\top PB\varepsilon - e_p^\top Re_p + 2e_p^\top WB\varepsilon_p - 2\dot{w}^\top \gamma_w^{-1}\tilde{w} \\ & + 2\nu u^\top \hat{\Lambda}^\top B^\top PA_m^{-1}B\hat{\Lambda}\tilde{u} + 2\eta\Psi^\top(x, r)\Omega\bar{B}^\top WA_m^{-1}\bar{B}\tilde{\Omega}^\top \Psi(x, r) \end{aligned} \tag{9.487}$$

Note that $B^\top PA_m^{-1}B^\top$ and $\bar{B}^\top WA_m^{-1}\bar{B}$ are both negative definite matrices, therefore

$$\begin{aligned}\dot{V}\left(e,e_p,\tilde{\Omega},\tilde{u}\right)=&-e^\top Qe-2e^\top Pw+2e^\top PB\varepsilon-e_p^\top Re_p+2e_p^\top WB\varepsilon_p-2\dot{w}^\top\gamma_w^{-1}\tilde{w}\\&-\nu\tilde{u}^\top\hat{\Lambda}^\top B^\top A_m^{-\top}QA_m^{-1}B\hat{\Lambda}\tilde{u}+2\nu u^{*\top}\hat{\Lambda}^\top B^\top PA_m^{-1}B\hat{\Lambda}\tilde{u}\\&-\eta\Psi^\top(x,r)\,\tilde{\Omega}\bar{B}^\top A_m^{-\top}RA_m^{-1}\bar{B}\tilde{\Omega}^\top\Psi(x,r)\\&+2\eta\Psi^\top(x,r)\,\Omega^*\bar{B}^\top WA_m^{-1}\bar{B}\tilde{\Omega}^\top\Psi(x,r)\end{aligned}\tag{9.488}$$

Let $K(t)=\left[\begin{array}{ccc}K_x(t) & K_r(t) & -\Theta^\top(t)\end{array}\right]\in\mathbb{R}^m\times\mathbb{R}^{n+q+p}$ and $z(x,r)=\left[\begin{array}{c}x\\ r\\ \Phi(x)\end{array}\right]$ $\in\mathbb{R}^{n+q+p}$. Then, $\dot{V}\left(e,e_p,\tilde{\Omega},\tilde{u}\right)$ is bounded by

$$\begin{aligned}\dot{V}\left(e,e_p,\tilde{K},\tilde{\Omega}\right)\leq&-\lambda_{min}(Q)\|e\|^2+2\|e\|\lambda_{max}(P)w_0+2\|e\|\|PB\|\varepsilon_0\\&-\lambda_{min}(R)\left\|e_p\right\|^2+2\left\|e_p\right\|\|WB\|\varepsilon_{p_0}\\&+2\gamma_w^{-1}\left\|\tilde{\Omega}\right\|\delta_0-\nu\lambda_{min}\left(B^\top A_m^{-\top}QA_m^{-1}B\right)\|z(x,r)\|^2\left\|\hat{\Lambda}\right\|^2\left\|\tilde{K}\right\|^2\\&+2\nu\|z(x,r)\|^2\left\|B^\top PA_m^{-1}B\right\|\left\|\hat{\Lambda}\right\|^2\left\|\tilde{K}\right\|K_0\\&-\eta\lambda_{min}\left(\bar{B}^\top A_m^{-\top}RA_m^{-1}\bar{B}\right)\|\Psi(x,r)\|^2\left\|\tilde{\Omega}\right\|^2\\&+2\eta\left\|\bar{B}^\top WA_m^{-1}\bar{B}\right\|\|\Psi(x,r)\|^2\left\|\tilde{\Omega}\right\|\Omega_0\end{aligned}\tag{9.489}$$

where $K_0=\|K^*\|$ and $\Omega_0=\sup\|\Omega^*\|$.

Let $c_1=\lambda_{min}(Q)$, $c_2=\frac{\lambda_{max}(P)w_0+\|PB\|\varepsilon_0}{\lambda_{min}(Q)}$, $c_3=\lambda_{min}(R)$, $c_4=\frac{\|WB\|\varepsilon_{p_0}}{\lambda_{min}(R)}$, $c_5=\lambda_{min}\left(B^\top A_m^{-\top}QA_m^{-1}B\right)\|z(x,r)\|^2$, $c_6=\frac{\left\|B^\top PA_m^{-1}B\right\|K_0}{\lambda_{min}\left(B^\top A_m^{-\top}QA_m^{-1}B\right)}$, $c_7=\lambda_{min}$ $\left(\bar{B}^\top A_m^{-\top}RA_m^{-1}\bar{B}\right)\|\Psi(x,r)\|^2$, and $c_8=\frac{\left\|\bar{B}^\top WA_m^{-1}\bar{B}\right\|\Omega_0}{\lambda_{min}\left(\bar{B}^\top A_m^{-\top}RA_m^{-1}\bar{B}\right)}+\frac{\gamma_w^{-1}\delta_0}{\eta c_7\left\|\bar{B}\right\|^2}$. Then,

$$\begin{aligned}\dot{V}\left(e,e_p,\tilde{K},\tilde{\Omega}\right)\leq&-c_1(\|e\|-c_2)^2+c_1c_2^2-c_3\left(\left\|e_p\right\|-c_4\right)^2+c_3c_4^2\\&-\nu c_5\left\|\hat{\Lambda}\right\|^2\left(\left\|\tilde{K}\right\|-c_6\right)^2+\nu c_5c_6^2\left\|\hat{\Lambda}\right\|^2\\&-\eta c_7\left(\left\|\tilde{\Omega}\right\|-c_8\right)^2+\eta c_7c_8^2\end{aligned}\tag{9.490}$$

Note that $\left\|\tilde{\Lambda}\right\|\leq\left\|\tilde{\Omega}\right\|$. Then,

$$\left\|\hat{\Lambda}\right\|^2=\left\|\Lambda+\tilde{\Lambda}\right\|^2\leq\left(\|\Lambda\|+\left\|\tilde{\Omega}\right\|\right)^2\tag{9.491}$$

Let $\left\|\tilde{\Omega}\right\|=c_8$. Then, $\dot{V}\left(e,e_p,\tilde{K},\tilde{\Omega}\right)$ is bounded by

$$\dot{V}\left(e, e_p, \tilde{K}, \tilde{\Omega}\right) \leq -c_1 \left(\|e\| - c_2\right)^2 + c_1 c_2^2 - c_3 \left(\left\|e_p\right\| - c_4\right)^2 + c_3 c_4^2 - \nu c_5 \Lambda_0^2 \left(\left\|\tilde{K}\right\| - c_6\right)^2 + \nu c_5 c_6^2 \Lambda_0^2 + \eta c_7 c_8^2 \quad (9.492)$$

where $\Lambda_0 = \left(\|\Lambda\| + c_8\right)^2$.

Thus, $\dot{V}\left(e, e_p, \tilde{K}, \tilde{\Omega}\right) \leq 0$ outside a compact set $\mathscr{S}$ defined as

$$\mathscr{S} = \left\{ \left(e\left(t\right), e_p\left(t\right), \tilde{K}\left(t\right), \tilde{\Omega}\left(t\right)\right) : c_1 \left(\|e\| - c_2\right)^2 + c_3 \left(\left\|e_p\right\| - c_4\right)^2 + \nu c_5 \Lambda_0^2 \left(\left\|\tilde{K}\right\| - c_6\right)^2 + \eta c_7 \left(\left\|\tilde{\Omega}\right\| - c_8\right)^2 \leq c_1 c_2^2 + c_3 c_4^2 + \nu c_5 c_6^2 \Lambda_0^2 + \eta c_7 c_8^2 \right\} \quad (9.493)$$

This implies

$$\|e\| \geq c_2 + \sqrt{c_2^2 + \frac{c_3 c_4^2 + \nu c_5 c_6^2 \Lambda_0^2 + \eta c_7 c_8^2}{c_1}} = p \quad (9.494)$$

$$\left\|e_p\right\| \geq c_4 + \sqrt{c_4^2 + \frac{c_1 c_2^2 + \nu c_5 c_6^2 \Lambda_0^2 + \eta c_7 c_8^2}{c_3}} = q \quad (9.495)$$

$$\left\|\tilde{K}\right\| \geq c_6 + \sqrt{c_6^2 + \frac{c_1 c_2^2 + c_3 c_4^2 + \eta c_7 c_8^2}{\nu c_5 \Lambda_0^2}} = \alpha \quad (9.496)$$

$$\left\|\tilde{\Omega}\right\| \geq c_8 + \sqrt{c_8^2 + \frac{c_1 c_2^2 + c_3 c_4^2 + \nu c_5 c_6^2 \Lambda_0^2}{\eta c_7}} = \beta \quad (9.497)$$

There exist z_0 and Ψ_0 such that $\|z\left(x, r\right)\| \leq z_0$ and $\|\Psi\left(x, r\right)\| \leq \Psi_0$ for any $0 < \nu < \nu_{max}$ and $0 < \eta < \eta_{max}$ that satisfy the following inequalities:

$$\begin{aligned} \varphi\left(\|x\|, \|x_m\|, Q, \nu, w_0, \varepsilon_0, \Lambda_0, K_0\right) = & -c_1 \|x\|^2 + 2\left(c_1 c_2 + \lambda_{max}\left(Q\right)\|x_m\|\right)\|x\| \\ & + 2 c_1 c_2 \|x_m\| - c_1 \|x_m\|^2 \\ & + c_3 c_4^2 + \nu c_5 \left(\|z\left(x, r\right)\|\right) c_6^2 \Lambda_0^2 \\ & + \eta c_7 \left(\|\Psi\left(x, r\right)\|\right) c_8^2 \leq 0 \end{aligned} \quad (9.498)$$

$$\begin{aligned}\phi\left(\left\|x_p\right\|, \left\|x_m\right\|, R, \eta, \dot{w}_0, \varepsilon_{p0}, B_0, \Omega_0\right) = & -c_3\left\|x_p\right\|^2 + 2\left(c_3c_4 + \lambda_{max}(R)\left\|x\right\|\right)\left\|x_p\right\| \\ & + 2c_3c_4\left\|x\right\| - c_3\left\|x\right\|^2 \\ & + c_1c_2^2 + \nu c_5\left(\left\|z(x,r)\right\|\right)c_6^2\Lambda_0^2 \\ & + \eta c_7\left(\left\|\Psi(x,r)\right\|\right)c_8^2 \leq 0 \end{aligned} \tag{9.499}$$

Then, the lower bounds which are dependent on $\|z(x,r)\|$ and $\|\Psi(x,r)\|$ also exist. Since $\dot{V}\left(e, e_p, \tilde{K}, \tilde{\Omega}\right) \leq 0$ outside the compact set $\mathscr{S}$, $\lim_{t\to\infty} V\left(e, e_p, \tilde{K}, \tilde{\Omega}\right) \leq V_0$, where V_0 is the smallest upper bound of $V\left(e, e_p, \tilde{K}, \tilde{\Omega}\right)$ which is given by

$$\begin{aligned} V_0 = & \lambda_{max}(P)\,p^2 + \lambda_{max}(W)\,q^2 + \lambda_{max}\left(\Gamma_x^{-1}\right)\alpha^2 \\ & + \lambda_{max}\left(\Gamma_r^{-1}\right)\alpha^2 + \lambda_{max}\left(\Gamma_\Theta^{-1}\right)\left(\alpha^2 + \beta^2\right) \\ & + \lambda_{max}\left(\Gamma_\Lambda^{-1}\right)\beta^2 + \gamma_w^{-1}\beta^2 \end{aligned} \tag{9.500}$$

Then,

$$\lambda_{min}(P)\left\|e\right\|^2 \leq V\left(e, e_p, \tilde{K}, \tilde{\Omega}\right) \leq V_0 \tag{9.501}$$

$$\lambda_{min}(W)\left\|e_p\right\|^2 \leq V\left(e, e_p, \tilde{K}, \tilde{\Omega}\right) \leq V_0 \tag{9.502}$$

Therefore, the closed-loop system is uniformly ultimately bounded with the following ultimate bounds:

$$\left\|e\right\| \leq \sqrt{\frac{V_0}{\lambda_{min}(P)}} \tag{9.503}$$

$$\left\|e_p\right\| \leq \sqrt{\frac{V_0}{\lambda_{min}(W)}} \tag{9.504}$$

Example 9.17 Consider a first-order SISO plant

$$\dot{x} = ax + b\lambda\left[u(t - t_d) + \theta^* x^2\right] + w$$

where $a = 1$ and $b = 1$ are known, $\lambda = -1$ and $\theta^* = 0.2$ are unknown, $t_d = 0.1\,\mathrm{s}$ is a known time delay, and $w(t) = 0.01(\sin t + \cos 2t)$.

The reference model is given by

$$\dot{x}_m = a_m x_m + b_m r$$

where $a_m = -2$, $b_m = 2$, and $r(t) = \sin t$.

The nominal control input effectiveness is equal to unity. So, $\lambda = -1$ represents a full control reversal which is generally challenging to any control systems.

The baseline nominal control gains are $\bar{k}_x = \frac{a_m - a}{b} = -3$ and $k_r = \frac{b_m}{b} = 2$. With the full control reversal, the ideal unknown control gains are $k_x^* = -\bar{k}_x = 3$ and $k_r^* = -\bar{k}_r = -2$.

The adaptive controller is designed as

$$u = k_x(t)\, x + k_r r(t) - \theta(t)\, x^2$$

using the bi-objective optimal control modification method with the following predictor model:

$$\dot{\hat{x}} = a_m \hat{x} + (a - a_m)\, x + b\hat{\lambda}\left[u(t - t_d) + \theta x^2\right] + \hat{w}$$

The bi-objective optimal control adaptive laws are

$$\dot{k}_x = \gamma_x x \left(e + \nu u \hat{\lambda} b a_m^{-1}\right) b\hat{\lambda}$$

$$\dot{k}_r = \gamma_r r \left(e + \nu u \hat{\lambda} b a_m^{-1}\right) b\hat{\lambda}$$

$$\dot{\theta} = -\gamma_\theta x^2 \left\{e + \nu u \hat{\lambda} b a_m^{-1} + e_p - \eta\left[\left(u + 2\theta x^2\right)\hat{\lambda} b + \hat{w}\right] a_m^{-1}\right\} b\hat{\lambda}$$

$$\dot{\hat{\lambda}} = -\gamma_\lambda \left(u + \theta x^2\right)\left\{e_p - \eta\left[\left(u + 2\theta x^2\right)\hat{\lambda} b + \hat{w}\right] a_m^{-1}\right\} b$$

$$\dot{\hat{w}} = -\gamma_w \left\{e_p - \eta\left[\left(u + 2\theta x^2\right)\hat{\lambda} b + \hat{w}\right] a_m^{-1}\right\}$$

The initial conditions are $k_x(0) = \bar{k}_x$, $k_r(0) = \bar{k}_r$, $\theta(0) = 0$, $\hat{\lambda}(0) = 1$, $\hat{w}(0) = 0$. The adaptive gains are chosen to be $\gamma_x = \gamma_r = \gamma_\theta = \gamma_\lambda = \gamma_w = 10$, and the modification parameters are chosen to be $\nu = 0.1$ and $\eta = 0.01$.

The closed-loop response with $r(t) = \sin t$ for $t \in [0, 60]$ is shown in Fig. 9.25. It can be seen that $x(t)$ eventually tracks $x_m(t)$, but the two signals are initially 180^o out of phase due to the control reversal. The signal $\hat{x}(t)$ approximates $x(t)$ very well after 10 s. Overall, the bi-objective optimal control modification method demonstrates a good tracking performance.

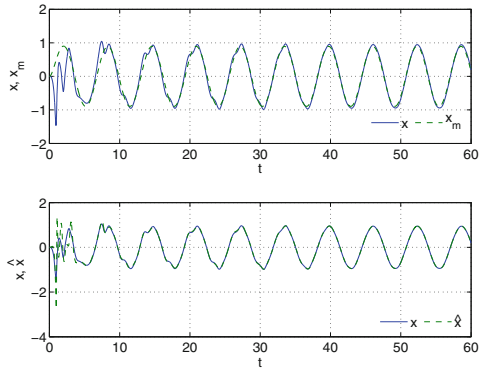

Fig. 9.25 Closed-loop response with bi-objective optimal control modification

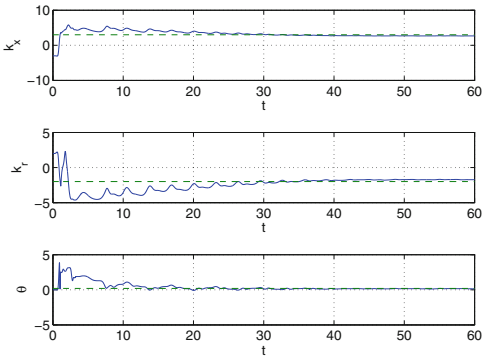

Fig. 9.26 Adaptive parameter convergence of bi-objective optimal control modification

The adaptive parameters $k_x(t)$, $k_r(t)$, and $\theta(t)$ are shown in Fig. 9.26. These adaptive parameters show a parameter convergence to their corresponding ideal values. The parameter convergence is also facilitated by having a persistently exciting reference command signal $r(t) = \sin t$.

The estimates of the control input effectiveness $\hat{\lambda}(t)$ and disturbance $\hat{w}(t)$ are shown in Fig. 9.27. It can be seen that $\hat{\lambda}(t)$ converges nicely to the ideal value of -1. Because of the parameter convergence of $\hat{\lambda}(t)$, the bi-objective optimal control modification adaptive laws remain stable in light of the sign reversal of the control input effectiveness. Without accurate estimation of $\hat{\lambda}(t)$, it will be a challenge for any adaptive control method to be able to maintain stability. It is also noted that this parameter convergence is achieved even with a time delay of 0.1 s. The bi-objective optimal control modification remains stable up to a time delay of 0.108 s.

For comparison, we redesign the adaptive controller with the optimal control modification with the predictor model according to Sect. 9.10. The optimal control modification adaptive laws are

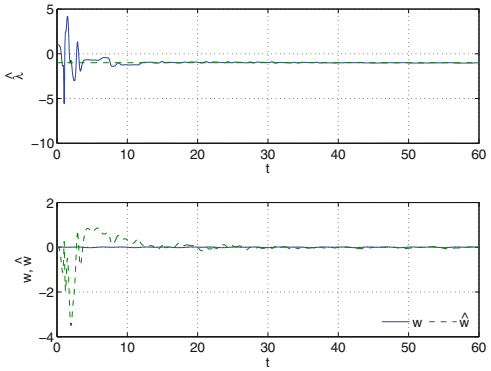

Fig. 9.27 Estimation of control input effectiveness and disturbance with bi-objective optimal control modification

$$\dot{k}_x = \gamma_x x \left(e + \nu x k_x \hat{\lambda} b a_m^{-1} \right) b \hat{\lambda}$$

$$\dot{k}_r = \gamma_r r \left(e + \nu r k_r \hat{\lambda} b a_m^{-1} \right) b \hat{\lambda}$$

$$\dot{\theta} = -\gamma_\theta x^2 \left(e_p - \eta x^2 \theta \hat{\lambda} b a_m^{-1} \right) b \hat{\lambda}$$

$$\dot{\hat{\lambda}} = -\gamma_\lambda \left(u + \theta x^2 \right) \left[e_p - \eta \left(u + \theta x^2 \right) \hat{\lambda} b a_m^{-1} \right] b$$

$$\dot{\hat{w}} = -\gamma_w \left(e_p - \eta \hat{w} a_m^{-1} \right)$$

Keeping the same initial conditions, it can be seen that the optimal control modification performs worse than the bi-objective optimal control modification as shown in Figs. 9.28, 9.29 and 9.30. Even though the predictor model does an excellent job of estimating $x(t)$, the tracking performance is much worse than that with the bi-objective optimal control modification. The adaptive parameters also suffers from a poor parameter convergence with the optimal control modification as shown in Figs. 9.29 and 9.30.

By setting $\nu = 0$ and $\eta = 0$, one can recover the standard MRAC adaptive laws with the predictor model. Comparing robustness of the three controllers, the optimal control modification has the largest time-delay margin of 0.116 s, whereas the standard MRAC has the smallest time-delay margin of 0.082 s.

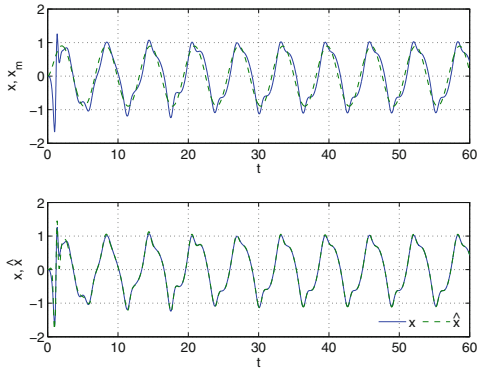

Fig. 9.28 Closed-loop response with optimal control modification

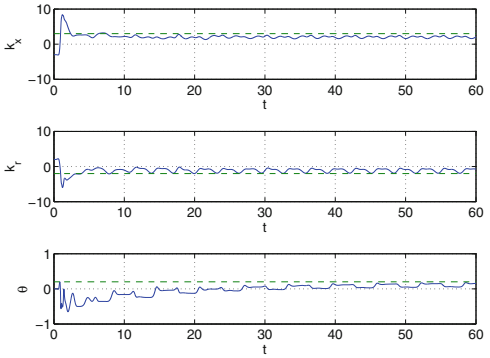

Fig. 9.29 Adaptive parameter convergence of optimal control modification

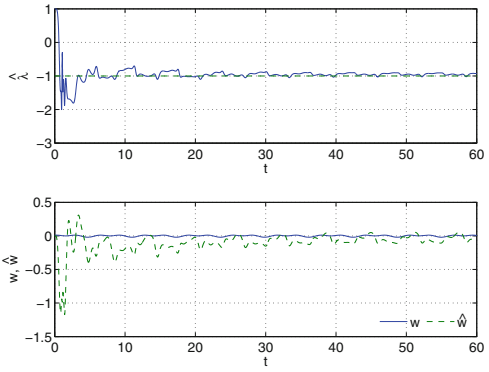

Fig. 9.30 Estimation of control input effectiveness and disturbance with optimal control modification

9.12 Adaptive Control for Singularly Perturbed Systems with First-Order Slow Actuator Dynamics

When there exists a timescale separation between a fast plant and a slow actuator which prevents the plant from following a reference model, a singular perturbation approach can be used to separate the time scale between the plant and actuator and then modify the adaptive law to account for the slow actuator in the singularly perturbed system [32]. The singular perturbation approach transforms the original system into a reduced-order system in slow time. A model matching condition is applied to the reduced-order system and the reference model in the transformed slow time coordinate that results in changes in the actuator command to accommodate the slow actuator dynamics. The resulting control signal can then track the reference model better than if the actuator command is not modified.

Consider a linear plant as

$$\dot{x} = Ax + B\left(u + \Theta^{*\top} x\right) \tag{9.505}$$

where $x(t) \in \mathbb{R}^n$ is a state vector, $u(t) \in \mathbb{R}^n$ is a control vector, $A \in \mathbb{R}^n \times \mathbb{R}^n$ and $B \in \mathbb{R}^{n\times m}$ with $m \geq n$ are known matrices such that the pair (A, B) is controllable and furthermore A is Hurwitz, and $\Theta^* \in \mathbb{R}^m \times \mathbb{R}^n$ is an unknown constant matrix.

The controller $u(t)$ is subject to slow first-order actuator dynamics

$$\dot{u} = \varepsilon G(u - u_c) \tag{9.506}$$

where $u_c(t) \in \mathbb{R}^m$ is an actuator command vector, ε is a positive constant, and $G \in \mathbb{R}^{m\times m}$ is a known Hurwitz matrix.

The objective is to design the controller $u(t)$ that enables the plant to follow a reference model

$$\dot{x}_m = A_m x_m + B_m r \tag{9.507}$$

where $A_m \in \mathbb{R}^n \times \mathbb{R}^n$ is Hurwitz and known, $B_m \in \mathbb{R}^n \times \mathbb{R}^q$ is also known, and $r(t) \in \mathbb{R}^q \in \mathscr{L}_\infty$ is a bounded command vector.

If the actuator dynamics are sufficiently fast relative to the reference model dynamics, that is, $\varepsilon \|G\| \gg \|A_m\|$, then the effect of actuator dynamics may be negligible. This is generally the case for most applications whereby the actuator dynamics typically are several times faster than the plant dynamics to be controlled. The robustness issues with unmodeled actuator dynamics can then be avoided. Then, we design a controller $u(t)$ to follow an actuator command as

$$u_c = K_x^* x + K_r^* r - u_{ad} \tag{9.508}$$

where $K_x^* \in \mathbb{R}^m \times \mathbb{R}^n$ and $K_r^* \in \mathbb{R}^m \times \mathbb{R}^q$ are known nominal gain matrices, and $u_{ad}(t) \in \mathbb{R}^m$ is an adaptive signal.

The control gain matrices K_x^* and K_r^* can be chosen to satisfy the model matching conditions $A + BK_x^* = A_m$ and $BK_r^* = B_m$, and the adaptive signal $u_{ad}(t)$ is chosen to be

$$u_{ad} = \Theta^\top \Phi(x) \tag{9.509}$$

where $\Theta(t)$ is an estimate of Θ^*.

Defining the tracking error as $e(t) = x_m(t) - x(t)$, then the tracking error equation becomes

$$\dot{e} = A_m e + B\tilde{\Theta}^\top x \tag{9.510}$$

where $\tilde{\Theta}(t) = \Theta(t) - \Theta^*$ is the estimation error.

In the case of slow actuator dynamics when $\varepsilon \ll 1$ is a small parameter and $\varepsilon \|G\| \ll \|A\|$, then $x(t)$ has "fast" dynamics and $u(t)$ has "slow" dynamics. This will lead to robustness issues. To decouple the fast state $x(t)$ and slow state $u(t)$, we perform a timescale separation by applying the singular perturbation method. Toward that end, we consider a slow time transformation

$$\tau = \varepsilon t \tag{9.511}$$

where τ is a slow time variable.

Then, the plant and actuator models are transformed into a singularly perturbed system as

$$\varepsilon \frac{dx}{d\tau} = Ax + B\left(u + \Theta^{*\top} x\right) \tag{9.512}$$

$$\frac{du}{d\tau} = G(u - u_c) \tag{9.513}$$

The Tikhonov's theorem can be used to approximate the solution of the singularly perturbed system with the solution of a "reduced-order" system by setting $\varepsilon = 0$ [33]. Then, $x(u, \varepsilon)$ is on a fast manifold. The fast dynamics result in $x(u, \varepsilon)$ tending to its asymptotic solution in near zero time as $\varepsilon \to 0$. Thus, the reduced-order system is given by

$$\varepsilon \frac{dx_0}{d\tau} = Ax_0 + B\left[u_0 + \Theta^{*\top} x_0\right] = 0 \tag{9.514}$$

$$\frac{du_0}{d\tau} = G(u_0 - u_c) \tag{9.515}$$

where $x_0(\tau)$ and $u_0(\tau)$ are the "outer" solution of the singularly perturbed system.

The term "outer" is in connection with the concept of "inner" or "boundary layer" and "outer" solutions which have the origin in the boundary layer theory due to Prandtl. The "inner" or "boundary layer" solution for this system is obtained from

$$\dot{x}_i = Ax_i + B\left[u_i + \Theta^{*\top} x_i\right] \tag{9.516}$$

$$\dot{u}_i = \varepsilon G\left(u_i - u_c\right) = 0 \tag{9.517}$$

The solution is then expressed as

$$x\left(t\right) = x_0\left(t\right) + x_i\left(t\right) - x_{MAE}\left(t\right) \tag{9.518}$$

where $x_{MAE}\left(t\right)$ is a correction term by a matched asymptotic expansion method applied to both the inner and outer solutions [34]. The outer solution is in fact the asymptotic solution of the original system as $t \to \infty$.

The solution of $x_0\left(\tau\right)$ is obtained as

$$x_0 = -\left(A + B\Theta^{*\top}\right)^{-1} Bu_0 \tag{9.519}$$

Differentiating Eq. (9.519) with respect to the slow time variable and then substituting the actuator model into the result yield

$$\frac{dx_0}{d\tau} = -\left(A + B\Theta^{*\top}\right)^{-1} BG\left(u_0 - u_c\right) \tag{9.520}$$

From Eq. (9.514), we have

$$u_0 = -\bar{B}^{-1}Ax_0 - \Theta^{*\top}x_0 \tag{9.521}$$

where $\bar{B}^{-1} = B^{\top}\left(BB^{\top}\right)^{-1}$ is the right pseudo-inverse of B.

Hence, we obtain the following reduced-order plant model constrained by the slow actuator dynamics:

$$\frac{dx_0}{d\tau} = \left(A + B\Theta^{*\top}\right)^{-1} BG\left(\bar{B}^{-1}Ax_0 + \Theta^{*\top}x_0 + u_c\right) \tag{9.522}$$

Using the matrix inversion lemma, we obtain

$$\left(A + B\Theta^{*\top}\right)^{-1} = A^{-1} - A^{-1}B\left(I + \Theta^{*\top}A^{-1}B\right)^{-1}\Theta^{*\top}A^{-1} \tag{9.523}$$

Let $\Psi^{*\top} = A^{-1}B\left(I + \Theta^{*\top}A^{-1}B\right)^{-1}\Theta^{*\top}A^{-1}$. Then,

$$\begin{aligned}\frac{dx_0}{d\tau} = {} & A^{-1}BG\bar{B}^{-1}Ax_0 + \left[-\Psi^{*\top}BG\bar{B}^{-1}A + \left(A^{-1} - \Psi^{*\top}\right)BG\Theta^{*\top}\right]x_0 \\ & + \left(A^{-1} - \Psi^{*\top}\right)BGu_c\end{aligned} \tag{9.524}$$

We will consider the asymptotic solution of the singularly perturbed system. In effect, the inner solution is neglected so that $x\left(t\right) = x_0\left(t\right)$. The reduced-order model is expressed as

$$\frac{dx}{d\tau} = A_s x + B_s \Lambda \left(u_c + \Theta_s^{*\top} x \right) \tag{9.525}$$

where $A_s = A^{-1} B G \bar{B}^{-1} A$, $B_s = A^{-1} B G$, $B_s \Lambda = \left(A^{-1} - \Psi^{*\top} \right) B G$, and $B_s \Lambda \Theta_s^{*\top} = -\Psi^{*\top} B G \bar{B}^{-1} A + \left(A^{-1} - \Psi^{*\top} \right) B G \Theta^{*\top}$.

If A_s is Hurwitz and $\Theta_s^* = 0$, then the Tikhonov's theorem guarantees that the reduced solution with $\varepsilon > 0$ converges to the solution of the original system as $\varepsilon \to 0$ [33].

Because of the slow actuator dynamics, the time scale of the response of the plant cannot exceed that of the actuator. Thus, if the reference model is faster than the actuator model, the tracking error cannot be guaranteed to be small even with adaptive control due to the model mismatch. A possible solution is to revise the reference model to match the actuator-constrained plant model, or alternatively to redesign the actuator command to reduce the tracking error.

In slow time, the reference model is expressed as

$$\frac{dx_m}{d\tau} = \frac{1}{\varepsilon} \left(A_m x_m + B_m r \right) \tag{9.526}$$

We make the following choice for the actuator command signal:

$$u_c = K_x x + K_r r - u_{ad} \tag{9.527}$$

where K_x and K_r are nominal control gains for the normal plant without the slow actuator dynamics and $u_{ad}(t)$ is of the form

$$u_{ad} = \Delta K_x(t)\, x + \Delta K_r(t)\, r - \Theta_s^\top(t)\, x = -\Omega^\top(t)\, \Phi(x, r) \tag{9.528}$$

where $\Omega^\top(t) = \left[\Theta_s^\top(t) - \Delta K_x(t) - \Delta K_r(t) \right]$ and $\Phi(x, r) = \left[x^\top \; r^\top \right]^\top$.

We assume that there exist ideal control gain matrices ΔK_x^* and ΔK_r^* that satisfy the following model matching conditions:

$$\frac{1}{\varepsilon} A_m = A_s + B_s \Lambda \left(K_x + \Delta K_x^* \right) \tag{9.529}$$

$$\frac{1}{\varepsilon} B_m = B_s \Lambda \left(K_r + \Delta K_r^* \right) \tag{9.530}$$

Then, the closed-loop system becomes

$$\frac{dx}{d\tau} = \frac{1}{\varepsilon} \left(A_m x_m + B_m r \right) - B_s \Lambda \tilde{\Omega}^\top \Phi(x, r) \tag{9.531}$$

where $\tilde{\Omega}_s(t) = \Omega_s(t) - \Omega_s^*$.

The tracking error equation in slow time is obtained as

$$\frac{de}{d\tau} = \frac{dx_m}{d\tau} - \frac{dx}{d\tau} = \frac{1}{\varepsilon}\left[A_m e + \varepsilon B_s \Lambda \tilde{\Omega}^\top \Phi\left(x, r\right)\right] \tag{9.532}$$

Since A_m is Hurwitz and if $\tilde{\Omega}\left(t\right)$ is bounded, then the Tikhonov's theorem guarantees that the reduced solution with $\varepsilon > 0$ converges to the solution of the original system as $\varepsilon \to 0$.

Transforming into the real time, the tracking error equation becomes

$$\dot{e} = A_m e + \varepsilon B_s \Lambda \tilde{\Omega}^\top \Phi\left(x, r\right) \tag{9.533}$$

If Λ is a diagonal matrix of known sign, then the optimal control modification adaptive law in real time is given by

$$\dot{\Omega} = -\varepsilon \Gamma \Phi\left(x, r\right)\left[e^\top P \mathrm{sgn}\Lambda - \varepsilon \nu \Phi^\top\left(x, r\right)\Omega B_s^\top P A_m^{-1}\right] B_s \tag{9.534}$$

However, this assumption is not always guaranteed since Λ can be of mixed sign. The bi-objective optimal control modification adaptive law can be used to estimate Λ using the following predictor model:

$$\dot{\hat{x}} = A_m \hat{x} + \left(\varepsilon A_s - A_m\right) x + \varepsilon B_s \hat{\Lambda}\left(u_c + \Theta_s^\top x\right) \tag{9.535}$$

Then, the bi-objective optimal control modification adaptive laws are expressed as

$$\begin{aligned}\dot{\Omega} = -\varepsilon \Gamma_\Omega \Phi\left(x, r\right)\Big\{&e^\top P + \varepsilon \nu u^\top \hat{\Lambda}^\top B^\top P A_m^{-1} + e_p^\top W \\ &-\varepsilon \eta\left[u + 2\Theta_s^\top \Phi\left(x\right)\right]^\top \hat{\Lambda}^\top B_s^\top W A_m^{-1}\Big\} B_s \hat{\Lambda}\end{aligned} \tag{9.536}$$

$$\dot{\Theta}_s = -\varepsilon \Gamma_{\Theta_s} x\left\{e_p^\top W - \varepsilon \eta\left[u + 2\Theta_s^\top \Phi\left(x\right)\right]^\top \hat{\Lambda}^\top B_s^\top W A_m^{-1}\right\} B_s \hat{\Lambda} \tag{9.537}$$

$$\dot{\hat{\Lambda}}^\top = -\varepsilon \Gamma_\Lambda\left[u + \Theta_s^\top \Phi\left(x\right)\right]\left\{e_p^\top W - \varepsilon \eta\left[u + 2\Theta_s^\top \Phi\left(x\right)\right]^\top \hat{\Lambda}^\top B_s^\top W A_m^{-1}\right\} B_s \tag{9.538}$$

where $e_p\left(t\right) = \hat{x}\left(t\right) - x\left(t\right)$.

Example 9.18 Consider the following simple scalar system:

$$\dot{x} = ax + bu + \theta^* x + w\left(t\right)$$

with slow first-order actuator dynamics

$$\dot{u} = \varepsilon g\left(u - u_c\right)$$

where $a < 0$, $g < 0$, $\varepsilon > 0$, $|\varepsilon g| < |a|$, and $w\left(t\right)$ is a disturbance signal.

The reference model is

$$\dot{x}_m = a_m x_m + b_m r$$

where $a_m < 0$.

The actuator command for the slow actuator dynamics is designed as

$$u_c = k_x x + k_r r - \Omega^\top \Phi(x, r)$$

where $k_x = \frac{a_m - a}{b}$, $k_r = \frac{b_m}{b}$, and $\Phi(x, r) = \begin{bmatrix} x & r \end{bmatrix}^\top$.

Note that, if the actuator dynamics are fast, then the actuator command is

$$u_c = k_x x + k_r r - \theta x$$

The optimal control modification adaptive law for the slow actuator dynamics is

$$\dot{\Omega} = -\varepsilon \Gamma \Phi(x, r) \left[e \operatorname{sgn}\lambda - \varepsilon \nu \Phi^\top(x, r) \Omega b_s a_m^{-1} \right] b_s$$

where $b_s = \frac{bg}{a}$ and $\lambda = \frac{a}{a + b\theta^*}$, and for the fast actuator dynamics is

$$\dot{\theta} = -\Gamma x \left(e - \nu x \theta b a_m^{-1} \right) b$$

If a and g are nominally of the same order of magnitude, then we note that, for the slow actuator dynamics, the effective adaptive gain is reduced by ε for a similar performance as that for the fast actuator dynamics.

For the numerical example, we let $a = -1$, $b = 1$, $\theta^* = 0.1$, $g = -1$, $\varepsilon = 0.1$, $a_m = -5$, $b_m = 1$, $r(t) = \sin t$, and $w(t) = 0.05 \sin 10t$. The responses due to the standard MRAC adaptive law and optimal control modification adaptive law with the singular perturbation approach are shown in Fig. 9.31. The response for the standard MRAC exhibits more initial transients than that for the optimal control modification using the same adaptive gain.

Figure 9.32 is the plot of the control input and actuator command with the singular perturbation approach. As can be seen, the actuator command signal is quite large relative to the control input. This is due to the fact that the actuator dynamics are slow so a large actuator command does not translate into the same control input in a finite time. The effectiveness of the optimal control modification is demonstrated by the reduced amplitude of oscillations in the control input significantly over that due to the standard MRAC.

Figure 9.33 shows the responses due to the unmodified actuator command for the fast actuator dynamics. As can be seen, the control input is insufficient to allow the plant to follow the reference model even with adaptive control.

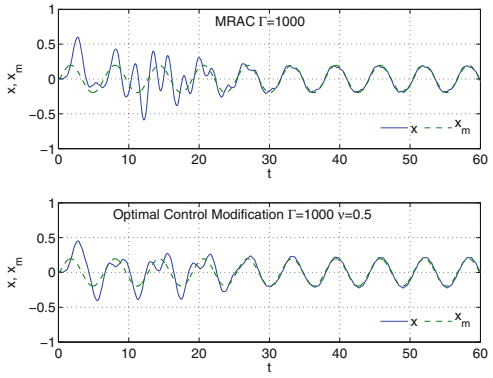

Fig. 9.31 Responses for slow actuator dynamics with MRAC and optimal control modification

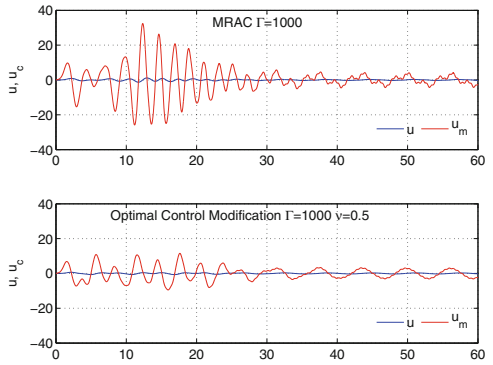

Fig. 9.32 Control and actuator command for slow actuator dynamics with MRAC and optimal control modification

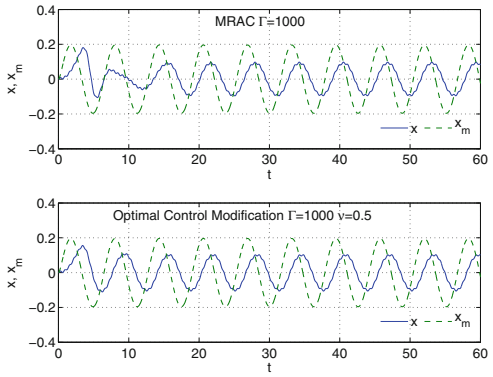

Fig. 9.33 Responses for slow actuator dynamics due to unmodified actuator command

9.13 Optimal Control Modification for Linear Uncertain Systems with Unmodeled Dynamics

Consider the system

$$\dot{x} = Ax + Bu + \Delta(x, z, u) \tag{9.539}$$

$$\dot{z} = f(x, z, u) \tag{9.540}$$

$$y = Cx \tag{9.541}$$

where $z(t)$ is an internal state vector, $\Delta(x, z, u)$ is the plant model error that is unknown and not accounted for, $\dot{z}(t)$ is the unmodeled dynamics, and $y(t)$ is the plant output vector.

When the tracking error based on only the output signal $y(t)$ is used for MRAC, such a class of adaptive control is called output feedback adaptive control. If a stable first-order reference model $y_m(t)$ is specified for the output $y(t)$ to track, then model-reference adaptive control is feasible if the plant transfer function satisfies a certain property called strictly positive real (SPR) condition. Therefore, an essential requirement for output feedback adaptive control is the SPR condition that the transfer function must satisfy. In Chap. 8, we see that the standard MRAC is unstable for non-minimum phase plants (see Example 8.3). Non-minimum phase systems do not have SPR transfer functions. Therefore, output feedback adaptive control of systems with non-SPR transfer functions can be challenging.

The strictly positive real condition is defined as follows:

Definition 9.1 Consider a proper SISO transfer function

$$G(s) = \frac{Z(s)}{R(s)} \tag{9.542}$$

where $Z(s)$ and $R(s)$ are polynomials of degrees m and n, respectively, with $n > m$. The relative degree is defined as $n - m$. If the relative degree of $G(s)$ is not greater than 1 and the real part of $G(s)$ is at least positive for all $\sigma \geq 0$ where $s = \sigma + j\omega$, that is, $\Re(G(s)) \geq 0$ for $\sigma \geq 0$, then the transfer function is said to be positive real (PR). Furthermore, if $G(s - \varepsilon)$ is positive real for some $\varepsilon > 0$, then $G(s)$ is strictly positive real (SPR) [30].

Example 9.19 • Consider the transfer function in Example 8.2

$$G(s) = \frac{s + 1}{s^2 + 5s + 6}$$

Expressing in the complex variables σ and ω, we get

$$G(s) = \frac{\left(\sigma^3 + 6\sigma^2 + \sigma\omega^2 + 11\sigma + 4\omega^2 + 6\right) + j\omega\left(-\sigma^2 - 2\sigma - \omega^2 + 1\right)}{\left(\sigma^2 + 5\sigma - \omega^2 + 6\right)^2 + \omega^2(2\sigma + 5)^2}$$

We see that $\Re\left(\left(G\left(s\right)\right)\right) > 0$ for all $\sigma \geq 0$ and $\omega \geq 0$. If we let $\sigma = -\varepsilon$ and $\omega = 0$, then $\Re\left(G\left(s\right)\right) \geq 0$ for $0 < \varepsilon \leq 1$. So, $G\left(s\right)$ is SPR and is a minimum phase, stable transfer function with relative degree 1.

- Consider the transfer function

$$G\left(s\right) = \frac{s}{s^2 + 5s + 6} = \frac{\left(\sigma^3 + 5\sigma^2 + \sigma\omega^2 + 6\sigma + 5\omega^2\right) + j\omega\left(-\sigma^2 - \omega^2 + 6\right)}{\left(\sigma^2 + 5\sigma - \omega^2 + 6\right)^2 + \omega^2\left(2\sigma + 5\right)^2}$$

We see that $\Re\left(G\left(s\right)\right) \geq 0$ for all $\sigma \geq 0$ and $\omega \geq 0$. So, $G\left(s\right)$ is only PR but not SPR. Note that $G\left(s\right)$ is a stable transfer function with a zero on the $j\omega$ axis.

- The transfer function in Example 8.2

$$\begin{aligned} G\left(s\right) &= \frac{s - 1}{s^2 + 5s + 6} \\ &= \frac{\left(\sigma^3 + 4\sigma^2 + \sigma\omega^2 + \sigma + 6\omega^2 - 6\right) + j\omega\left(-\sigma^2 + 2\sigma - \omega^2 + 11\right)}{\left(\sigma^2 + 5\sigma - \omega^2 + 6\right)^2 + \omega^2\left(2\sigma + 5\right)^2} \end{aligned}$$

is not SPR since $\Re\left(G\left(s\right)\right)$ can be negative for some values of $\sigma \geq 0$ and $\omega \geq 0$. Note that $G\left(s\right)$ is non-minimum phase.

- The transfer function

$$\begin{aligned} G\left(s\right) &= \frac{s + 1}{s^2 - 5s + 6} \\ &= \frac{\left(\sigma^3 - 4\sigma^2 + \sigma\omega^2 + \sigma - 6\omega^2 + 6\right) + j\omega\left(-\sigma^2 - 2\sigma - \omega^2 + 11\right)}{\left(\sigma^2 - 5\sigma - \omega^2 + 6\right)^2 + \omega^2\left(2\sigma - 5\right)^2} \end{aligned}$$

is not SPR since $\Re\left(G\left(s\right)\right)$ can be negative for some values of $\sigma \geq 0$ and $\omega \geq 0$. Note that $G\left(s\right)$ is unstable.

- The transfer function

$$\begin{aligned} G\left(s\right) &= \frac{1}{s^2 + 5s + 6} \\ &= \frac{\left(\sigma^2 + 5\sigma - \omega^2 + 6\right) - j\omega\left(2\sigma + 5\right)}{\left(\sigma^2 + 5\sigma - \omega^2 + 6\right)^2 + \omega^2\left(2\sigma + 5\right)^2} \end{aligned}$$

is not SPR since $\Re\left(G\left(s\right)\right)$ can be negative for some values of $\sigma \geq 0$ and $\omega \geq 0$. Note that $G\left(s\right)$ has relative degree 2.

■

Research in robust adaptive control was motivated by instability phenomena of adaptive control. In fact, instability of adaptive control in the early 1960s which contributed to the crash of one of the NASA X-15 hypersonic vehicles caused a great deal of concern about the viability of adaptive control. Rohrs et al. investigated

various instability mechanisms of adaptive control due to unmodeled dynamics [1]. The Rohrs counterexample demonstrates the weakness of MRAC in its lack of robustness. Let us revisit the topic of unmodeled dynamics as discussed in Sect. 8.4 [20].

The open-loop transfer function of a first-order SISO plant with a second-order unmodeled actuator dynamics is given by

$$\frac{y(s)}{u(s)} = \frac{b\omega_n^2}{(s-a)\left(s^2 + 2\zeta\omega_n s + \omega_n^2\right)} \tag{9.543}$$

where $a < 0$ is unknown, b is unknown, but $b > 0$ is known, and ζ and ω_n are known.

The system has relative degree 3 and therefore is not SPR.

The transfer function of the reference model is specified as

$$\frac{y_m(s)}{r(s)} = \frac{b_m}{s - a_m} \tag{9.544}$$

The reference model is SPR with relative degree 1. Since the relative degree of the reference model is less than the relative degree of the plant, perfect tracking is not possible. Adaptive control of systems with relative degrees greater than 1 is generally much more difficult to handle since the model reference cannot be chosen to be SPR [30].

The controller is given by

$$u = k_y(t)\, y + k_r(t)\, r \tag{9.545}$$

$$\dot{k}_y = \gamma_x y e \tag{9.546}$$

$$\dot{k}_r = \gamma_r r e \tag{9.547}$$

where $e(t) = y_m(t) - y(t)$.

$k_y(t)$ and $k_r(t)$ are initialized with $k_y(0) = -1$ and $k_r(0) = 1$.

The reference command signal is given by

$$r = r_0 \sin \omega_0 t \tag{9.548}$$

where $r_0 = 1$ and $\omega_0 = \sqrt{30}$ rad/s is the frequency at which the closed-loop transfer function has zero phase margin.

The closed-loop system is unstable as shown in Fig. 9.34.

The underlying cause of instability is the lack of robustness of the closed-loop system. Changing either the initial condition of $k_y(t)$ and or the frequency in the reference command signal can result in stabilization of the closed-loop system if it has a sufficient phase margin.

The optimal control modification adaptive law can be designed to handle linear systems with unmodeled dynamics by utilizing the linear asymptotic property.

Suppose the open-loop plant is expressed in general by the following transfer function:

$$\frac{y(s)}{u(s)} \triangleq W_p(s) = k_p \frac{Z_p(s)}{R_p(s)} \tag{9.549}$$

where k_p is a high-frequency gain, and $Z_p(s)$ and $R_p(s)$ are monic Hurwitz polynomials of degrees m_p and n_p, respectively, and $n_p - m_p > 0$ is the relative degree of the plant.

The reference model is given by a transfer function

$$\frac{y_m(s)}{r(s)} \triangleq W_m(s) = k_m \frac{Z_m(s)}{R_m(s)} \tag{9.550}$$

where k_m is a high-frequency gain, and $Z_m(s)$ and $R_m(s)$ are monic Hurwitz polynomials of degrees m_m and n_m, respectively, and $n_m - m_m > 0$ is the relative degree of the reference model.

Let $n_p - m_p > n_m - m_m$. So the SPR condition is no longer possible to ensure tracking of the reference model. Stability of the closed-loop system cannot also be guaranteed with the standard MRAC.

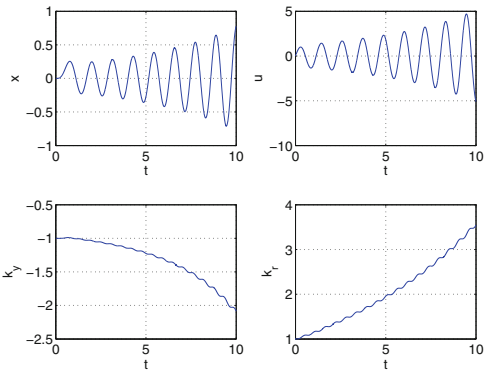

Fig. 9.34 Instability of MRAC by Rohrs counterexample

Suppose the adaptive controller is redesigned with the optimal control modification as

$$u = k_y y + k_r r \tag{9.551}$$

where

$$\dot{k}_y = \gamma_y \left(ye - \nu y^2 k_y \right) \tag{9.552}$$

$$\dot{k}_r = \gamma_r \left(re - \nu r^2 k_r \right) \tag{9.553}$$

Using the linear asymptotic property of the optimal control modification, the asymptotic value of the adaptive controller u can be computed as $\gamma_y \to \infty$ and $\gamma_r \to \infty$ in the limit. Then,

$$\bar{u} = \frac{2y_m - 2y}{\nu} \tag{9.554}$$

The asymptotic closed-loop transfer function can now be computed as

$$\frac{\bar{y}}{r} = \frac{2W_p(s)\,W_m(s)}{\nu + 2W_p(s)} = \frac{2k_m k_p Z_p(s)\,Z_m(s)}{R_m(s)\left(\nu R_p(s) + 2k_p Z_p(s)\right)} \tag{9.555}$$

By a suitable selection of the modification parameter ν, the asymptotic closed-loop transfer function can be designed to have the closed-loop stability. Once the modification parameter ν is chosen, the adaptation rates γ_y and γ_r can be selected to be any reasonable values without compromising the closed-loop stability of the adaptive laws.

Referring back to the first-order plant with the second-order unmodeled actuator dynamics, the adaptive controller asymptotically tends to

$$\bar{u} = \frac{2y_m - 2y}{\nu} = \frac{2b_m r}{\nu(s - a_m)} - \frac{2y}{\nu} \tag{9.556}$$

as $\gamma_y \to \infty$ and $\gamma_r \to \infty$.

Then, the asymptotic closed-loop transfer function is obtained as

$$\frac{\bar{y}}{r} \triangleq G(s) = \frac{2b\omega_n^2 b_m}{\nu(s - a_m)\left[(s - a)\left(s^2 + 2\zeta\omega_n s + \omega_n^2\right) + \frac{2b\omega_n^2}{\nu}\right]} \tag{9.557}$$

Note that the closed-loop transfer function has a relative degree 4 while the transfer function of the reference model has a relative degree 1. This prevents the output $y(t)$ from tracking $y_m(t)$.

The characteristic equation of the transfer function $G(s)$ with an input time delay is computed as

$$s^3 + (2\zeta\omega_n - a)s^2 + \left(\omega_n^2 - 2a\zeta\omega_n\right)s - a\omega_n^2 + \frac{2b\omega_n^2}{\nu}e^{-t_d s} = 0 \tag{9.558}$$

Substituting $s = j\omega$ yields

$$-j\omega^3 - (2\zeta\omega_n - a)\omega^2 + \left(\omega_n^2 - 2a\zeta\omega_n\right)j\omega - a\omega_n^2 + \frac{2b\omega_n^2}{\nu}(\cos\omega t_d - j\sin\omega t_d) = 0 \tag{9.559}$$

This results in two frequency equations

$$-\left(2\zeta\omega_n - a\right)\omega^2 - a\omega_n^2 + \frac{2b\omega_n^2}{\nu}\cos\omega t_d = 0 \tag{9.560}$$

$$-\omega^3 + \left(\omega_n^2 - 2a\zeta\omega_n\right)\omega - \frac{2b\omega_n^2}{\nu}\sin\omega t_d = 0 \tag{9.561}$$

We then obtain the cross-over frequency and phase margin as functions of the modification parameter ν in the following expressions:

$$\omega^6 + \left(a^2 + 4\zeta^2\omega_n^2 - 2\omega_n^2\right)\omega^4 + \left(\omega_n^2 + 4a^2\zeta^2 - 2a^2\right)\omega_n^2\omega^2 + \left(a^2 - \frac{4b^2}{\nu^2}\right)\omega_n^4 = 0 \tag{9.562}$$

$$\phi = \omega t_d = \tan^{-1}\left[\frac{-\omega^3 + \left(\omega_n^2 - 2a\zeta\omega_n\right)\omega}{\left(2\zeta\omega_n - a\right)\omega^2 + a\omega_n^2}\right] \tag{9.563}$$

Note that the cross-over frequency at zero phase margin $\omega_0 = \sqrt{\omega_n^2 - 2a\zeta\omega_n}$ is still the same as that without modification (see Sect. 8.4). However, this cross-over frequency corresponds to a modification parameter ν_{min}. By choosing a modification $\nu > \nu_{min}$ that meets a certain phase margin requirement, the closed-loop adaptive system can be made robustly stable.

Example 9.20 Consider Example 8.5 with the following parameters: $a = -1$, $b = 1$, $a_m = -2$, $b_m = 2$, $\omega_n = 5$ rad/s, and $\zeta = 0.5$. The cross-over frequency at zero phase margin is computed to $\omega_0 = \sqrt{30}$ rad/s. The cross-over frequency and phase margin as a function of the modification parameter ν are shown in Fig. 9.35.

The modification parameter ν corresponding to zero phase margin and 90° phase margin are $\nu_{min} = \nu_0 = 0.3226$ and $\nu_{max} = \nu_{90^\circ} = 0.9482$, respectively. So, the adaptive systems with the unmodeled dynamics can be stabilized with the selection of the modification parameter ν between these two values. The cross-over frequencies at the zero phase margin and 90° phase margin are $\omega_0 = \sqrt{\omega_n^2 - 2a\zeta\omega_n} = \sqrt{30}$ rad/s and $\omega_{90^\circ} = \sqrt{-\frac{a\omega_n^2}{2\zeta\omega_n - a}} = \sqrt{\frac{25}{6}}$ rad/s, respectively. So, robustness is achieved with the optimal control modification by reducing the cross-over frequency of the closed-loop system.

Suppose a 45° phase margin is selected. Then, the cross-over frequency can be computed from Eq. (9.563) as the root of the following equation:

$$\omega^3 + \left(2\zeta\omega_n - a\right)\omega^2 + \left(2a\zeta\omega_n - \omega_n^2\right)\omega + a\omega_n^2 = 0$$

which yields $\omega_{45^\circ} = 3.7568$ rad/s. Then, the modification parameter ν is computed from Eq. (9.562) to be $\nu_{45^\circ} = 0.5924$.

The asymptotic closed-loop transfer function with $\nu_{45^\circ} = 0.5924$ is computed to be

$$G(s) = \frac{\frac{100}{\nu_{45^\circ}}}{s^4 + 8s^3 + 42s^2 + \left(85 + \frac{50}{\nu_{45^\circ}}\right)s + 50 + \frac{100}{\nu}}$$

If $r(t)$ is a constant command signal, then in the limit as $t \to \infty$, $G(0) = \frac{2}{2+\nu_{45^o}} = 0.7715$ as compared to the steady-state value of the transfer function of the reference model $\frac{y_m(s)}{r(s)} = 1$. Thus, tracking of the reference model is not achieved, but in return the closed-loop adaptive system is robustly stable.

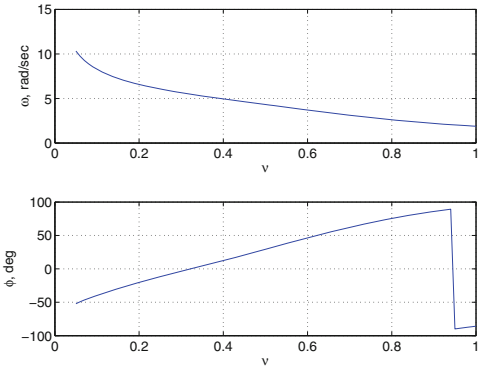

Fig. 9.35 Asymptotic phase margin and cross-over frequency as functions of ν

For the simulations, the time step is chosen to be 1×10^{-6} sec to permit the adaptation rates γ_x and γ_r to be set at 1×10^6 to simulate fast adaptation. The reference command signal is $r(t) = \sin\sqrt{30}t$. The asymptotic response $\bar{y}(t)$ and control signal $\bar{u}(t)$ evaluated analytically agree very well with the simulation results of $y(t)$ and $u(t)$, respectively, as shown in Fig. 9.36. The control signal $u(t)$ exhibits sharp spikes due to the adaptive gain $k_r(t)$ but otherwise tracks the asymptotic control signal $\bar{u}(t)$ very well. Thus, the linear asymptotic property of the optimal control modification is demonstrated to be able to facilitate the stability analysis of linear uncertain systems with unmodeled dynamics, time delay, or non-minimum phase behaviors. In this study, the optimal control modification can handle systems with relative degrees greater than 1 with relative ease.

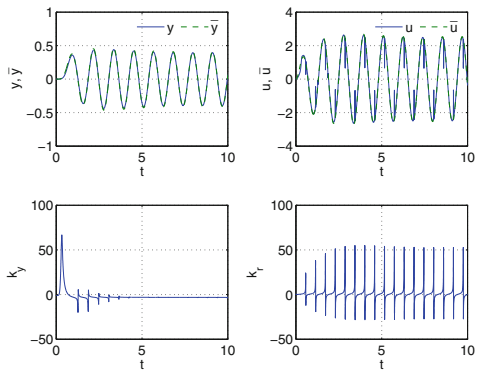

Fig. 9.36 Closed-loop response with optimal control modification ($\nu = 0.5924$, $\gamma_x = \gamma_r = 10^6$)

Example 9.21 Consider the Rohrs' counterexample problem in Example 8.6 [1]. The cross-over frequency and phase margin as a function of the modification parameter ν are shown in Fig. 9.37. The cross-over frequency at the zero phase margin and 90° phase margin are $\omega_0 = \sqrt{259}$ rad/s and $\omega_{90^\circ} = \sqrt{\frac{229}{31}}$ rad/s, respectively. The corresponding modification parameters are $\nu_0 = 0.1174$ and $\nu_{90^\circ} = 1.3394$.

We select $\nu_{45^\circ} = 0.4256$ corresponding to a 45° phase margin and a cross-over frequency $\omega_{45^\circ} = 7.5156$ rad/s for the optimal control modification adaptive laws. The closed-loop response is shown in Fig. 9.38. The closed-loop adaptive system is robustly stable.

All the three robust modification schemes, namely σ modification, e modification, and optimal control modification exhibit minimum values of the modification parameters at which the plant in the Rohrs counterexample begins to stabilize. The σ and e modification parameters can be found by trial-and-error. In contrast, the modification parameter ν is found analytically by taking advantage of the linear asymptotic property of the optimal control modification method.

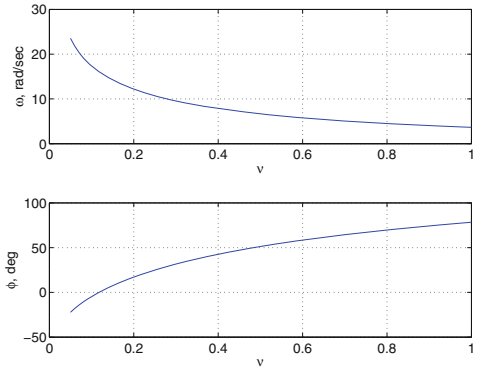

Fig. 9.37 Asymptotic phase margin and cross-over frequency of Rohrs counterexample with optimal control modification

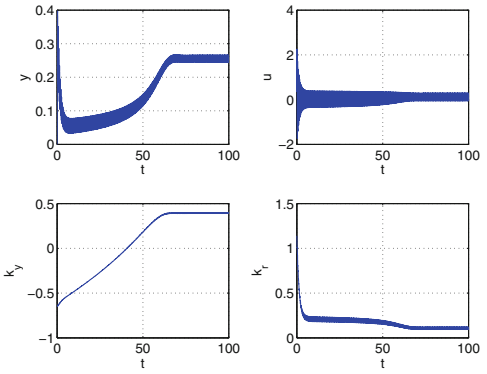

Fig. 9.38 Closed-loop response of Rohrs counterexample with optimal control modification ($\nu = 0.4256$, $\gamma_x = \gamma_r = 1$)

9.14 Adaptive Control of Non-Minimum Phase Plants with Relative Degree 1

Non-minimum phase plants generally pose more difficulty to model-reference adaptive control than minimum phase plants. Output feedback adaptive control generally relies on the SPR property to ensure stability. Non-minimum phase plants do not possess SPR transfer functions. Therefore, adaptive control for non-minimum phase plants cannot be designed using the SPR property. The difficulty with adaptive control design for non-minimum phase plants is due to the ideal property of model-reference adaptive control which attempts to seek asymptotic tracking. This results in a pole-zero cancellation in the right half plane for non-minimum phase systems which leads to unbounded signals.

The linear asymptotic property of the optimal control modification can be used for adaptive control of non-minimum phase plants. By modifying the standard MRAC, the pole-zero cancellation in the right half plane can be prevented. This then results in bounded tracking as opposed to asymptotic tracking. Closed-loop stability can be obtained by a judicious choice of the modification parameter ν. In this section, we will demonstrate an adaptive control method for non-minimum phase plants with a relative degree 1 using the optimal control modification method [20].

Consider the following SISO plant:

$$\dot{x} = ax + bu + gz \tag{9.564}$$

$$\dot{z} = hz + lx + mu \tag{9.565}$$

$$y = x \tag{9.566}$$

where $z(t)$ is the unmeasurable state with internal dynamics, a unknown but all the other parameters are known, and $h < 0$.

The objective is to design an output feedback adaptive controller to track the following reference model:

$$y_m = W_m(s) r = k_m \frac{Z_m(s)}{R_m(s)} r = \frac{b_m r}{s - a_m} \tag{9.567}$$

where $a_m < 0$ and $k_m = b_m$.

The transfer functions of the plant is expressed as

$$\frac{y}{u} = W_p(s) = k_p \frac{Z_p(s)}{R_p(s)} = \frac{b(s-h) + gm}{(s-a)(s-h) - gl} \tag{9.568}$$

where $k_p = b$.

Note that $W_m(s)$ is SPR with a relative degree 1. The plant also has a relative degree 1 and is assumed to be stable. So, $R_p(s) = (s-a)(s-h) - gl$ is Hurwitz.

The ideal output feedback adaptive controller is designed to be of the form

$$u^* = -b^{-1}\theta_1^* y^* - \frac{b^{-1}\theta_2^* y^*}{s-\lambda} - \frac{b^{-1}\theta_3^* u^*}{s-\lambda} + b^{-1}b_m r \tag{9.569}$$

where $\lambda < 0$ is a chosen parameter, and θ_1^*, θ_2^*, and θ_3^* are unknown constants.

$u^*(s)$ is obtained explicitly as

$$u^* = \frac{b^{-1}\left[-\theta_1^*(s-\lambda) - \theta_2^*\right] y^* + b^{-1}b_m(s-\lambda) r}{s-\lambda+b^{-1}\theta_3^*} \tag{9.570}$$

Then, the ideal output $y^*(s)$ is written as

$$y^* = \frac{Z_p(s)}{R_p(s)} \frac{\left[-\theta_1^*(s-\lambda) - \theta_2^*\right] y^* + b_m(s-\lambda) r}{s-\lambda+b^{-1}\theta_3^*} \tag{9.571}$$

We consider the following cases:

9.14.1 Minimum Phase Plant

If the plant is minimum phase, then $Z_p(s)$ is Hurwitz.

Then, the pole-zero cancellation can take place in the left half plane. Therefore, it follows that

$$Z_p(s) = s - \lambda + b^{-1}\theta_3^* \tag{9.572}$$

This results in

$$\theta_3^* = b(\lambda - h) + gm \tag{9.573}$$

The ideal controller $u^*(s)$ then becomes

$$u^* = \frac{b^{-1}\left[-\theta_1^*(s-\lambda) - \theta_2^*\right] y^* + b^{-1}b_m(s-\lambda) r}{Z_p(s)} \tag{9.574}$$

The ideal output $y^*(s)$ is then obtained as

$$y^* = \frac{\left[-\theta_1^*(s-\lambda) - \theta_2^*\right] y^* + b_m(s-\lambda) r}{(s-a)(s-h) - gl} \tag{9.575}$$

This results in the following ideal closed-loop transfer function:

$$\frac{y^*}{r} = \frac{b_m(s-\lambda)}{s^2 - \left(a+h-\theta_1^*\right)s + ah - gl - \lambda\theta_1^* + \theta_2^*} \tag{9.576}$$

We want the ideal closed-loop plant to track the reference model. So, the ideal closed-loop transfer function must be equal to the reference model transfer function $W_m(s)$. Thus,

$$\frac{b_m(s-\lambda)}{s^2-\left(a+h-\theta_1^*\right)s+ah-gl-\lambda\theta_1^*+\theta_2^*}=\frac{b_m}{s-a_m} \tag{9.577}$$

This leads to the following model matching conditions:

$$a+h-\theta_1^*=\lambda+a_m \tag{9.578}$$

$$ah-gl-\lambda\theta_1^*+\theta_2^*=\lambda a_m \tag{9.579}$$

θ_1^* and θ_2^* are then obtained as

$$\theta_1^*=a-a_m+h-\lambda \tag{9.580}$$

$$\theta_2^*=gl-ah+\lambda(a+h-\lambda) \tag{9.581}$$

The adaptive controller is now established as

$$u=-b^{-1}\theta_1 y-\frac{b^{-1}\theta_2 y}{s-\lambda}-\frac{b^{-1}\theta_3 u}{s-\lambda}+b^{-1}b_m r \tag{9.582}$$

where $\theta_1(t)$, $\theta_2(t)$, and $\theta_3(t)$ are the estimates of θ_1^*, θ_2^*, and θ_3^*, respectively.

Let $\tilde{\theta}_1(t)=\theta_1(t)-\theta_1^*$, $\tilde{\theta}_2(t)=\theta_2(t)-\theta_2^*$, and $\tilde{\theta}_3(t)=\theta_3(t)-\theta_3^*$. Then, the output $y(s)$ is expressed as

$$y=W_m(s)r-\frac{W_m(s)}{b_m}\left(\tilde{\theta}_1 y+\frac{\tilde{\theta}_2 y}{s-\lambda}+\frac{\tilde{\theta}_3 u}{s-\lambda}\right) \tag{9.583}$$

Define the tracking error as $e(t)=y_m(t)-y(t)$. Then, the tracking error equation is obtained as

$$\dot{e}=a_m e+\tilde{\Theta}^\top\Phi(t) \tag{9.584}$$

where $\tilde{\Theta}(t)=\left[\tilde{\theta}_1(t)\ \tilde{\theta}_2(t)\ \tilde{\theta}_3(t)\right]^\top$ and $\Phi(t)=\left[\phi_1(t)\ \phi_2(t)\ \phi_3(t)\right]^\top$.

The adaptive law is given by

$$\dot{\tilde{\Theta}}=-\Gamma\Phi(t)e \tag{9.585}$$

where

$$\phi_1=y \tag{9.586}$$

$$\dot{\phi}_2=\lambda\phi_2+y \tag{9.587}$$

$$\dot{\phi}_3 = \lambda \phi_3 + u \tag{9.588}$$

Therefore, all signals are bounded, and the tracking error is asymptotically stable.

9.14.2 Non-Minimum Phase Plant

For non-minimum phase plants, because the standard MRAC attempts to seek asymptotic tracking by performing a pole-zero cancellation in the right half plane, the resulting adaptive controller will become unbounded. Thus, if the adaptive law can be modified to seek only bounded tracking instead of asymptotic tracking, then this would prevent a pole-zero cancellation in the right half plane. The plant then can be stabilized.

For non-minimum phase plants, we consider two possible adaptive controllers.

1. We use the same adaptive controller in Eq. (9.582), but with the optimal control modification adaptive law

$$\dot{\Theta} = -\Gamma \Phi (t) \left[e - \nu \Phi^{\top} (t) \Theta a_m^{-1} \right] \tag{9.589}$$

By invoking the linear asymptotic property of the optimal control modification as $\Gamma \to \infty$, we get

$$\Theta^{\top} \Phi (t) = \frac{a_m (y_m - y)}{\nu} \tag{9.590}$$

Then, the asymptotic linear controller tends to

$$u = \frac{a_m y}{\nu b} + \frac{[\nu b_m - a_m W_m (s)] r}{\nu b} \tag{9.591}$$

Comparing the ideal controller with the asymptotic linear controller, we see that the adaptive controller does not attempt to cancel the unstable zero of $W_p (s)$ since it has a stable pole at $s = a_m$ due to the term $W_m (s)$. Otherwise, the pole-zero cancellation would take place in the right half plane since $Z_p (s)$ is unstable. Therefore, the stability of the adaptive controller is no longer affected by the non-minimum phase behavior of $W_p (s)$. The stability of the closed-loop plant is then determined by a proper selection of the modification parameter ν such that $\nu > 0$ and the closed-loop transfer function is stable.

The asymptotic closed-loop transfer function is expressed as

$$\frac{y}{r} = \frac{W_p (s) [\nu b_m - a_m W_m (s)]}{\nu b - a_m W_p (s)} \tag{9.592}$$

As $\Gamma \to \infty$, the equilibrium value of $y (t)$ tends to

$$\bar{y} = \frac{W_p(0)\left[\nu b_m - a_m W_m(0)\right]}{\nu b - a_m W_p(0)} r \tag{9.593}$$

Thus, the tracking is bounded regardless whether or not $W_p(s)$ is minimum phase. The closed-loop plant therefore is robustly stable with the optimal control modification. However, poor tracking will result if ν is too large to guarantee the closed-loop stability.

2. We use a simple adaptive controller for the first-order SISO plant as if the non-minimum phase dynamics do not exist with $z(t) = 0$

$$u(t) = k_y(t) y + k_r r \tag{9.594}$$

where $k_r = b^{-1} b_m$ and $k_y(t)$ is computed by the optimal control modification adaptive law

$$\dot{k}_y = \gamma_y y \left(e + \nu y k_y b a_m^{-1}\right) b \tag{9.595}$$

By invoking the linear asymptotic property of the optimal control modification, we get

$$k_y y = \frac{a_m (y - y_m)}{\nu b} \tag{9.596}$$

Then, the asymptotic linear controller tends to

$$u = \frac{a_m y}{\nu b} + \frac{\left[\nu b_m - a_m W_m(s)\right] r}{\nu b} \tag{9.597}$$

Note that this asymptotic linear controller is the same as that with the first adaptive controller. Thus, even though both adaptive controllers are different, the closed-loop plants for both controllers behave the same in the limit.

We now will formalize the proof of the optimal control modification for the non-minimum phase plant with relative degree 1 described by Eqs. (9.564) and (9.565) with a unknown but all the other parameters are known and $h < 0$. The adaptive controller is given by Eqs. (9.594) and (9.595).

The closed-loop plant becomes

$$\dot{y} = a_m y + b_m r + b\tilde{k}_y y + g z \tag{9.598}$$

$$\dot{z} = h z + \left(l + m k_y^*\right) y + m\tilde{k}_y y + m k_r r \tag{9.599}$$

where $\tilde{k}_y(t) = k_y(t) - k_y^*$ and $k_y^* = \frac{a_m - a}{b}$.

The tracking error equation is given by

$$\dot{e} = a_m e - b\tilde{k}_y y - g z \tag{9.600}$$

We define the reference internal state dynamics as

$$\dot{z}_m = hz_m + \left(l + mk_y^*\right) y_m + mk_r r \tag{9.601}$$

Let $\varepsilon(t) = z_m(t) - z(t)$ be the internal state tracking error. Then, the internal state tracking error equation is given by

$$\dot{\varepsilon} = h\varepsilon + \left(l + mk_y^*\right) e - m\tilde{k}_y y \tag{9.602}$$

Proof Choose a Lyapunov candidate function

$$V\left(e, \varepsilon, \tilde{k}_y\right) = \alpha e^2 + \beta\varepsilon^2 + \alpha\gamma_y^{-1}\tilde{k}_y^2 \tag{9.603}$$

where $\alpha > 0$ and $\beta > 0$.
$\dot{V}\left(e, \varepsilon, \tilde{k}_y\right)$ is evaluated as

$$\begin{aligned}\dot{V}\left(e, \varepsilon, \tilde{k}_y\right) =& 2\alpha a_m e^2 - 2\alpha g\left(z_m - \varepsilon\right) e + 2\beta h\varepsilon^2 + 2\beta\left(l + mk_y^*\right) e\varepsilon - 2\beta m\tilde{k}_y y\varepsilon \\ &+ 2\alpha\nu b^2 a_m^{-1}\tilde{k}_y\left(\tilde{k}_y + k_y^*\right) y^2 \leq -2\alpha\left|a_m\right|\|e\|^2 + 2\alpha|g|\,\|z_m\|\,\|e\| \\ &- 2\beta|h|\,\|\varepsilon\|^2 + 2\left|\alpha g + \beta\left(l + mk_y^*\right)\right|\|e\|\,\|\varepsilon\| + 2\beta|m|\,\|y\|\left\|\tilde{k}_y\right\|\|\varepsilon\| \\ &- 2\alpha\nu b^2\left|a_m^{-1}\right|\|y\|^2\left\|\tilde{k}_y\right\|^2 + 2\alpha\nu b^2\left|a_m^{-1}\right|\left|k_y^*\right|\|y\|^2\left\|\tilde{k}_y\right\|\end{aligned} \tag{9.604}$$

Using the inequality $2\|a\|\,\|b\| \leq \delta^2\|a\|^2 + \frac{\|b\|^2}{\delta^2}$, we get

$$\begin{aligned}\dot{V}\left(e, \varepsilon, \tilde{k}_y\right) \leq& -2\alpha\left|a_m\right|\|e\|^2 + 2\alpha|g|\,\|z_m\|\,\|e\| - 2\beta|h|\,\|\varepsilon\|^2 \\ &+ \left|\alpha g + \beta\left(l + mk_y^*\right)\right|\left(\delta_1^2\|e\|^2 + \frac{\|\varepsilon\|^2}{\delta_1^2}\right) \\ &+ \beta|m|\left(\delta_2^2\|y\|^2\left\|\tilde{k}_y\right\|^2 + \frac{\|\varepsilon\|^2}{\delta_2^2}\right) \\ &- 2\alpha\nu b^2\left|a_m^{-1}\right|\|y\|^2\left\|\tilde{k}_y\right\|^2 \\ &+ 2\alpha\nu b^2\left|a_m^{-1}\right|\left|k_y^*\right|\|y\|^2\left\|\tilde{k}_y\right\|\end{aligned} \tag{9.605}$$

Note that the negative definite term $-2\alpha\nu b^2\left|a_m^{-1}\right|\|y\|^2\left\|\tilde{k}_y\right\|^2$ of the optimal control modification can be made to dominate the positive definite term $\beta|m|\,\delta_2^2\|y\|^2\left\|\tilde{k}_y\right\|^2$ to enable $\dot{V}\left(e, \varepsilon, \tilde{k}_y\right)$ to be negative definite.

Let $c_1 = 2\alpha\left|a_m\right| - \left|\alpha g + \beta\left(l + mk_y^*\right)\right|\delta_1^2$, $c_2 = 2\beta|h| - \frac{\left|\alpha g + \beta\left(l + mk_y^*\right)\right|}{\delta_1^2} - \frac{\beta|m|}{\delta_2^2}$, $c_3 = 2\alpha\nu b^2\left|a_m^{-1}\right| - \beta|m|\,\delta_2^2$, and $c_4 = \frac{\alpha\nu b^2\left|a_m^{-1}\right|\left|k_y^*\right|}{c_3}$. Then,

$$\dot{V}\left(e,\varepsilon,\tilde{k}_y\right) \le -c_1\|e\|^2 + 2\alpha|g|\|z_m\|\|e\| - c_2\|\varepsilon\|^2 - c_3\|y\|^2\left(\left\|\tilde{k}_y\right\| - c_4\right)^2 + c_3c_4^2\|y\|^2 \tag{9.606}$$

We note that $\|y\|^2 \le \|e\|^2 + 2\|e\|\|y_m\| + \|y_m\|^2$. The ultimate bounds of $\|y_m\|$ and $\|z_m\|$ can be shown to be $\|y_m\| \le c_y r_0$ and $\|z_m\| \le c_z r_0$ where $c_y = \left|a_m^{-1}b_m\right|$, $c_z = \left|h^{-1}mk_r\right| + \left|h^{-1}\left(l + mk_y^*\right)\right|\left|a_m^{-1}b_m\right|$, and $r_0 = \|r\|$. Let $c_5 = c_1 - c_3c_4^2$, $c_6 = \frac{(\alpha|g|c_z + c_3c_4^2c_y)r_0}{c_5}$, and $c_7 = c_5c_6^2 + c_3c_4^2c_y^2r_0^2$. Then,

$$\dot{V}\left(e,\varepsilon,\tilde{k}_y\right) \le -c_5\left(\|e\| - c_6\right)^2 - c_2\|\varepsilon\|^2 - c_3\|y\|^2\left(\left\|\tilde{k}_y\right\| - c_4\right)^2 + c_7 \tag{9.607}$$

ν, α, β, δ_1, and δ_2 are chosen such that $c_2 > 0$, $c_3 > 0$, and $c_5 > 0$. Then, it follows that $\dot{V}\left(e,\varepsilon,\tilde{k}_y\right) \le 0$ if

$$\|e\| \ge c_6 + \sqrt{\frac{c_7}{c_5}} = p \tag{9.608}$$

$$\|\varepsilon\| \ge \sqrt{\frac{c_7}{c_2}} = q \tag{9.609}$$

$$\left\|\tilde{k}_y\right\| \ge c_4 + \sqrt{\frac{c_7}{c_3\left(p + c_yr_0\right)^2}} = \kappa \tag{9.610}$$

Thus, the closed-loop non-minimum phase system is stable with output feedback adaptive control with the optimal control modification. The ultimate bound of $\|e\|$ is then obtained as

$$\|e\| \le \sqrt{p^2 + \frac{\beta}{\alpha}q^2 + \gamma_y^{-1}\kappa^2} \tag{9.611}$$

■

It should be noted that the aforementioned output feedback adaptive control design is feasible only if the knowledge of the plant transfer function is mostly known with the exception of the parameter a. This requirement imposes a severe restriction on the design of output feedback adaptive control for non-minimum phase plants since in many cases such knowledge may not exist if the plants are uncertain. Another drawback with this approach is that the desired tracking performance is not guaranteed. In practical situations, this poor tracking performance can be a major issue.

Example 9.22 Consider the system

$$\dot{x} = ax + bu + gz$$

$$\dot{z} = -z + u$$

$$y = x$$

where $a < 0$ is unknown but $a = -2$ for simulation purposes, and $b = 1$ is known.

The reference model is given by the transfer function $W_m(s)$ with $a_m = -1$ and $b_m = 1$.

The open-loop transfer function is

$$W_p(s) = \frac{s + 1 + g}{(s - a)(s + 1)}$$

The system is minimum phase if $g > -1$. Consider a minimum phase plant with $g = 2$. Then, we design the output feedback adaptive controller according to Eq. (9.582). Let $\lambda = -1$, $\Gamma = I$, and $r(t) = 1$. Figure 9.39 shows the response of the closed-loop plant which tracks the reference model very well in the limit as $t \to \infty$.

Consider a non-minimum phase plant with $g = -2$. We use both adaptive controllers given by Eqs. (9.582) and (9.594).

The asymptotic closed-loop transfer function is given by

$$\frac{y}{r} = \frac{(s - 1)[\nu b_m (s - a_m) - a_m b_m]}{(s - a_m)[\nu (s - a)(s + 1) - a_m (s - 1)]}$$

The steady-state closed-loop transfer function is equal to

$$\frac{\bar{y}}{r} = \frac{b_m (\nu + 1)}{\nu a - a_m}$$

For $a = -2$ and $a_m = -1$, the transfer function is stable for $\nu > 0.5$. Choose $\nu = 2$ and $\gamma_y = 1$. The steady-state closed-loop output is equal to $\bar{y}(t) = -1$. Figure 9.40 shows the stable closed-loop responses of the non-minimum phase plant with both the adaptive controllers. The adaptive controller 1 with the adaptive parameter $\Theta(t)$ has a faster response than the adaptive controller 2 with the adaptive parameter $k_y(t)$. Both adaptive controllers tend to the same steady-state closed-loop response.

The closed-loop plant tracks the reference model very poorly as expected, but the response is stable and tends to an equilibrium value $\bar{y} = -1$ which agrees with the analytical result from the steady-state closed-loop transfer function. The poor tracking performance is typical of a non-minimum phase system with the output generally exhibiting an opposite response to the input.

■

As can be seen from Example 9.22, while the optimal control modification can stabilize a non-minimum phase plant, the tracking performance is quite unacceptable. The issue at hand is the requirement for a non-minimum phase plant to track

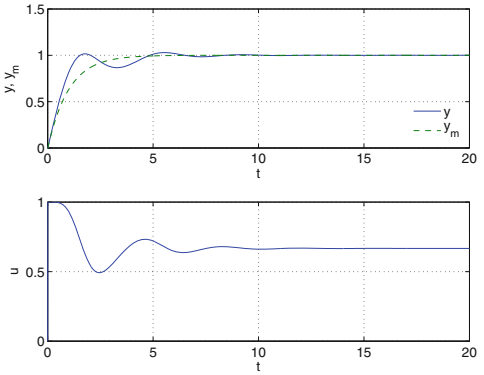

Fig. 9.39 Closed-loop response of minimum phase plant with MRAC

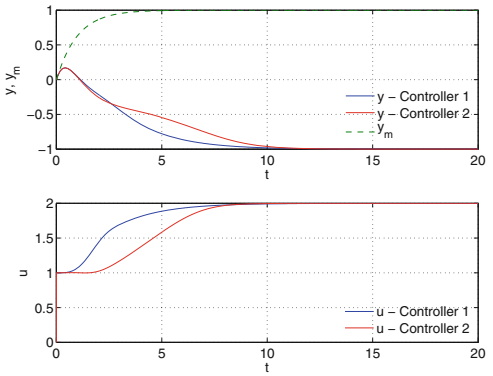

Fig. 9.40 Closed-loop response of non-minimum phase plant with optimal control modification

a minimum phase reference model with the same relative degree. This is a very demanding and perhaps unrealistic requirement. As a consequence, MRAC attempts to seek asymptotic tracking which results in an unstable pole-zero cancellation. If the reference model could be redesigned so that the unstable pole-zero cancellation cannot occur while the tracking performance can still be met, then the output feedback adaptive control design would be more acceptable. One such approach is to design an observer state feedback adaptive control using the Luenberger observer design.

Consider a MIMO system as

$$\dot{x} = Ax + Bu \Leftrightarrow \begin{bmatrix} \dot{x}_1 \\ \dot{x}_2 \end{bmatrix} = \begin{bmatrix} A_{11} & A_{12} \\ A_{21} & A_{22} \end{bmatrix} \begin{bmatrix} x_1 \\ x_2 \end{bmatrix} + \begin{bmatrix} B_1 \\ B_2 \end{bmatrix} u \tag{9.612}$$

$$y = Cx = \begin{bmatrix} C_1 & 0 \end{bmatrix} \begin{bmatrix} x_1 \\ x_2 \end{bmatrix} = C_1 x_1 \tag{9.613}$$

where $x_1(t) \in \mathbb{R}^p$, $x_2(t) \in \mathbb{R}^{n-p}$, $u(t) \in \mathbb{R}^m$, $y(t) \in \mathbb{R}^p$ with $p > m$, $A_{11} \in \mathbb{R}^{p\times p}$ is unknown, $A_{12} \in \mathbb{R}^{p\times(n-p)}$ and $A_{21} \in \mathbb{R}^{(n-p)\times p}$ are known, $A_{22} \in \mathbb{R}^{(n-p)\times(n-p)}$ is known and assumed to be Hurwitz, $B_1 \in \mathbb{R}^{p\times m}$ and $B_2 \in \mathbb{R}^{(n-p)\times m}$ are known, and $C_1 \in \mathbb{R}^{p\times p}$ is known and has full rank. We assume the pair (A, B) is controllable and the pair (A, C) is observable. This partitioned form of the plant can be used advantageously to design an output feedback adaptive control. The system expressed in this form is sufficiently general for many practical applications. For example, systems with unmodeled dynamics could be expressed in this form with $x_1(t)$ being the plant state variable and $x_2(t)$ being the unmodeled state variable.

The Kalman-Yakubovich lemma [30] can be used to determine if the transfer function matrix $G(s) = C(sI - A)^{-1}B$ is SPR. If A is Hurwitz and there exist $P = P^\top \in \mathbb{R}^{n\times n} > 0$ and $Q = Q^\top > 0 \in \mathbb{R}^{r\times n}$ such that

$$PA + A^\top P = -Q \tag{9.614}$$

$$B^\top P = C \tag{9.615}$$

then $G(s)$ is SPR.

We assume that $A = A_0 + \Delta A$ where A_0 is known and ΔA is a small unknown perturbation of A_0 due to the uncertainty in A_{11}. The transfer function $G(s) = C(sI - A)^{-1}B$ is assumed to be non-SPR. The Luenberger observer design constructs an observer state-space model of the plant as

$$\dot{\hat{x}} = \hat{A}\hat{x} + L\left(y - \hat{y}\right) + Bu \tag{9.616}$$

where $\hat{x}(t)$ is the observer state which estimates the plant state $x(t)$, $\hat{A}(t)$ is the estimate of A, $\hat{y}(t) = C\hat{x}(t)$ is the observer output which estimates the plant output $y(t)$, and L is the Kalman filter gain matrix computed using A_0.

A full-state feedback controller can be designed to enable the output $y(t)$ to track a reference command signal $r(t)$. For example, we can use the LQR method to design the full-state feedback controller using the following cost function for tracking a constant reference command signal $r(t)$:

$$J = \lim_{t_f\to\infty} \frac{1}{2}\int_0^{t_f} \left[(Cx - r)^\top Q(Cx - r) + u^\top Ru\right] dt \tag{9.617}$$

Then, the control gains can be computed as

$$K_x^* = -R^{-1}B^\top W \tag{9.618}$$

$$K_r = -R^{-1}B^\top \left(A^\top - WBR^{-1}B^\top\right)^{-1} C^\top Q \tag{9.619}$$

where W is the solution of the Riccati equation

$$WA + A^\top W - WBR^{-1}B^\top W + C^\top QC = 0 \tag{9.620}$$

Then, a reference model is constructed from this LQR design with $A_m = A + BK_x^*$ and $B_m = BK_r$.

If A is unknown, then we can design the following adaptive controller:

$$u = K_x(t)\hat{x} + K_r r \tag{9.621}$$

where the observer state $\hat{x}(t)$ replaces the plant state.

The tracking error is defined as $e(t) = x_m(t) - \hat{x}(t)$. We also define the state estimation error as $e_p(t) = x(t) - \hat{x}(t)$. Then, the error equations are

$$\dot{e} = A_m e - LCe_p - \tilde{A}\hat{x} - B\tilde{K}_x\hat{x} \tag{9.622}$$

$$\dot{e}_p = \left(A_p + \Delta A\right)e_p - \tilde{A}\hat{x} \tag{9.623}$$

where $\tilde{A}(t) = \hat{A}(t) - A$, $\tilde{K}_x(t) = K_x(t) - K_x^*$, $A_p = A_0 - LC$, and $A_p + \Delta A$ is Hurwitz by a suitable choice of L.

Note that the state estimation error signal $e_p(t)$ is generally not available, but for the class of MIMO systems under consideration, it can be constructed. Since C_1 is invertible, then $x_1(t)$ can be constructed from $y(t)$. Let $z(t) = x_2(t)$ be the internal state, then $z(t)$ can be computed from the following equation:

$$\dot{z} = A_{22}z + A_{21}C_1^{-1}y + B_2 u \tag{9.624}$$

with $z(0) = z_0$ and A_{21}, A_{22}, and B_2 known.

Then, the plant state can be constructed as $x(t) = \left[y^\top(t)\, C_1^{-\top}\, z^\top(t)\right]^\top$.

A stable adaptation of the non-SPR plant of Eqs. (9.612) and (9.613) can be achieved by the optimal control modification adaptive laws based on the observer state $\hat{x}(t)$ and the constructed state $x(t)$ from the output $y(t)$ and the internal state $z(t)$

$$\dot{K}_x^\top = \Gamma_x \hat{x}\left(e^\top P + \nu\hat{x}^\top K_x^\top B^\top P A_m^{-1}\right)B \tag{9.625}$$

$$\dot{\hat{A}}^\top = \Gamma_A \hat{x}\left(e^\top P + e_p^\top W + \eta\hat{x}^\top\hat{A}^\top P A_m^{-1}\right) \tag{9.626}$$

where $P = P^\top > 0$ and $W = W^\top > 0$ are solutions to the Lyapunov equations

$$PA_m + A_m^\top P = -Q \tag{9.627}$$

$$WA_p + A_p^\top W = -R \tag{9.628}$$

with $Q = Q^\top > 0$ and $R = R^\top > 0$.

The stability of the observer output feedback adaptive control using the optimal control modification is provided as follows:

Proof Choose a Lyapunov candidate function

$$V\left(e, e_p, \tilde{K}_x, \tilde{A}\right) = e^\top Pe + e_p^\top We_p + \text{trace}\left(\tilde{K}_x \Gamma_x^{-1} \tilde{K}_x^\top\right) + \text{trace}\left(\tilde{A}\Gamma_A^{-1}\tilde{A}^\top\right) \tag{9.629}$$

Then, $\dot{V}\left(e, e_p, \tilde{K}_x, \tilde{A}\right)$ is evaluated as

$$\begin{aligned}\dot{V}\left(e, e_p, \tilde{K}_x, \tilde{A}\right) =& -e^\top Qe - e_p^\top \bar{R}e_p - 2e^\top PLCe_p + 2\nu\hat{x}^\top K_x^\top B^\top PA_m^{-1}B\tilde{K}_x\hat{x} \\ &+ \eta\nu\hat{x}^\top\hat{A}^\top PA_m^{-1}\tilde{A}\hat{x} \leq -c_1\|e\|^2 - c_2\left\|e_p\right\|^2 + 2c_3\|e\|\left\|e_p\right\| \\ &- \nu c_4\left\|\hat{x}\right\|^2\left(\left\|\tilde{K}_x\right\| - c_5\right)^2 + \nu c_4 c_5^2\left\|\hat{x}\right\|^2 \\ &- \eta c_6\left\|\hat{x}\right\|^2\left(\left\|\tilde{A}\right\| - c_7\right)^2 + \eta c_6 c_7^2\left\|\hat{x}\right\|^2 \end{aligned} \tag{9.630}$$

where $\bar{R} = R - W\Delta A - \Delta A^\top W$, $c_1 = \lambda_{min}(Q)$, $c_2 = \lambda_{min}\left(\bar{R}\right)$, $c_3 = \|PLC\|$, $c_4 = \lambda_{min}\left(B^\top A_m^{-\top} QA_m^{-1}B\right)$, $c_5 = \frac{\left\|K_x^{*\top}B^\top PA_m^{-1}B\right\|}{c_4}$, $c_6 = \lambda_{min}\left(A_m^{-\top}QA_m^{-1}\right)$, $c_7 = \frac{\left\|\Delta A^\top PA_m^{-1}\right\|}{c_6}$.

We utilize the inequality $2\|a\|\|b\| \leq \|a\|^2 + \|b\|^2$ and also note that $\left\|\hat{x}\right\|^2 \leq \|e\|^2 + 2\|e\|\|x_m\| + \|x_m\|^2$. Then, $\dot{V}\left(e, e_p, \tilde{K}_x, \tilde{A}\right)$ is bounded by

$$\begin{aligned}\dot{V}\left(e, e_p, \tilde{K}_x, \tilde{A}\right) \leq& -\left(c_1 - c_3 - \nu c_4 c_5^2 - \eta c_6 c_7^2\right)\|e\|^2 + 2\left(\nu c_4 c_5^2\right. \\ &\left.+\eta c_6 c_7^2\right)\|e\|\|x_m\| - (c_2 - c_3)\left\|e_p\right\|^2 - \nu c_4\left\|\hat{x}\right\|^2\left(\left\|\tilde{K}_x\right\| - c_5\right)^2 - \eta c_6\left\|\hat{x}\right\|^2 \\ &\left(\left\|\tilde{A}\right\| - c_7\right)^2 + \left(\nu c_4 c_5^2 + \eta c_6 c_7^2\right)\|x_m\|^2 \end{aligned} \tag{9.631}$$

Note that the ultimate bound of $\|x_m\|$ can be expressed as $\|x_m\| \leq c_x r_0$. Let $c_8 = c_1 - c_3 - \nu c_4 c_5^2 - \eta c_6 c_7^2$, $c_9 = \frac{\left(\nu c_4 c_5^2 + \eta c_6 c_7^2\right)c_x r_0}{c_8}$, $c_{10} = c_2 - c_3$, and $c_{11} = c_8 c_9^2 + \left(\nu c_4 c_5^2 + \eta c_6 c_7^2\right)c_x^2 r_0^2$. Then, $\dot{V}\left(e, e_p, \tilde{K}_x, \tilde{A}\right) \leq 0$ outside the compact set

$$\begin{aligned}\mathscr{S} =& \left\{e(t) \in \mathbb{R}^n,\ e_p(t) \in \mathbb{R}^n,\ \tilde{K}_x(t) \in \mathbb{R}^{n\times m},\ \tilde{A}(t) \in \mathbb{R}^{n\times n} : c_8\left(\|e\| - c_9\right)^2\right. \\ &\left. + c_{10}\left\|e_p\right\|^2 + \nu c_4\left\|\hat{x}\right\|^2\left(\left\|\tilde{K}_x\right\| - c_5\right)^2 + \eta c_6\left\|\hat{x}\right\|^2\left(\left\|\tilde{A}\right\| - c_7\right)^2 \leq c_{11}\right\} \end{aligned} \tag{9.632}$$

by choosing L, Q, R, ν, and η appropriately such that $c_8 > 0$ and $c_{10} > 0$.

By setting $\nu = 0$ and $\eta = 0$, we recover the standard MRAC. Then, it can be shown by Barbalat's lemma that $\dot{V}\left(e, e_p, \tilde{K}_x, \tilde{A}\right)$ is uniformly continuous since $\ddot{V}\left(e, e_p, \tilde{K}_x, \tilde{A}\right)$ is bounded. It follows that $e(t) \to 0$ and $e_p \to 0$ as $t \to \infty$. ■

Note that if the reference model is not derived from the ideal controller of the non-SPR plant, the standard MRAC will not be able to stabilize the plant. On the other hand, the optimal control modification adaptive law can handle the mismatch between the plant and the reference model. Therefore, for a stable adaptation using the standard MRAC for output feedback adaptive control, the reference model must be established from the ideal controller design of the non-SPR plant. The mismatch between the reference model and the non-SPR plant causes MRAC to continue to seek a high-gain control in order to achieve asymptotic tracking. This would lead to instability.

Suppose a reference model is specified as

$$\dot{x}_m = A_m^* x_m + B_m r \tag{9.633}$$

where A_m^* is not established from the non-SPR plant. Then, the model matching condition cannot be satisfied since there exists no solution of K_x^*. To show this, we see that suppose K_x^* exists and can be solved using the pseudo-inverse of B with $m < p < n$ as

$$K_x^* = \left(B^\top B\right)^{-1} B^\top \left(A_m^* - A\right) \tag{9.634}$$

But

$$A + BK_x^* = A + B\left(B^\top B\right)^{-1} B^\top \left(A_m^* - A\right) \neq A_m^* \tag{9.635}$$

For the standard MRAC, the tracking error equation in the presence of the mismatch between the reference model and the non-SPR plant is established as

$$\dot{e} = A_m^* e + \left(A_m^* - A_m\right)\hat{x} - LCe_p - \tilde{A}\hat{x} - B\tilde{K}_x\hat{x} \tag{9.636}$$

Because the optimal control modification only seeks bounded tracking, so the model matching condition is not satisfied. Using the linear asymptotic property of the optimal control modification, the asymptotic value of $K_x(t)$ and $\hat{A}(t)$ can be computed from Eqs. (9.625) and (9.626) by letting $\Gamma \to \infty$. Then, $K_x(t) \to \bar{K}_x$ and $\hat{A}(t) \to \bar{A}$ for a constant reference command signal $r(t)$. From the linear asymptotic property, we get

$$\bar{K}_x\hat{x} = -\frac{1}{\nu}\left(B^\top A_m^{*-\top} PB\right)^{-1} B^\top Pe \tag{9.637}$$

$$\bar{A}\hat{x} = -\frac{1}{\eta} P^{-1} A_m^{*\top}\left(Pe + We_p\right) \tag{9.638}$$

where $P = P^\top > 0$ now solves the Lyapunov equation

$$PA_m^* + A_m^{*\top} P = -Q \tag{9.639}$$

We redefine the estimation errors as $\tilde{K}_x(t) = K_x(t) - \bar{K}_x$ and $\tilde{A}(t) = \hat{A}(t) - \bar{A}$. Then, the error equations are established as

$$\begin{aligned}\dot{e} = &\left[A_m^* + \frac{1}{\nu} B\left(B^\top A_m^{*-\top} P B\right)^{-1} B^\top P + \frac{1}{\eta} P^{-1} A_m^{*\top} P\right] e \\ &- \left(LC - \frac{1}{\eta} P^{-1} A_m^{*\top} W\right) e_p + A_m^* \hat{x} - \tilde{A}\hat{x} - B\tilde{K}_x \hat{x}\end{aligned} \tag{9.640}$$

$$\dot{e}_p = \frac{1}{\eta} P^{-1} A_m^{*\top} P e + \left(A_p + \frac{1}{\eta} P^{-1} A_m^{*\top} W\right) e_p + A\hat{x} - \Delta\tilde{A}\hat{x} \tag{9.641}$$

The standard MRAC results in instability due to the mismatch between the reference model and the non-SPR plant if $A + BK_x^* = A_m \neq A_m^*$ and $PA_m + A_m^\top P \not< 0$, whereas a stable adaptation of the plant can be achieved with the optimal control modification.

Proof Choose the same Lyapunov candidate function in Eq. (9.627). Then, for the standard MRAC, $\dot{V}\left(e, e_p, \tilde{K}_x, \tilde{A}\right)$ is evaluated as

$$\begin{aligned}\dot{V}\left(e, e_p, \tilde{K}_x, \tilde{A}\right) = &e^\top \left(PA_m^* + A_m^{*\top} P\right) e + e^\top P\left(A_m^* - A_m\right)\hat{x} \\ &+ \hat{x}^\top \left(A_m^{*\top} - A_m^\top\right) Pe \\ &- 2e^\top PLCe_p - e_p^\top \bar{R} e_p\end{aligned} \tag{9.642}$$

Upon substituting $\hat{x}(t) = x_m(t) - e(t)$, we get

$$\dot{V}\left(e, e_p, \tilde{K}_x, \tilde{A}\right) = e^\top \left(PA_m + A_m^\top P\right) e + 2e^\top P\left(A_m^* - A_m\right) x_m - 2e^\top PLCe_p - e_p^\top \bar{R} e_p \tag{9.643}$$

Note that $PA_m + A_m^\top P$ is not necessarily negative definite. Therefore,

$$\begin{aligned}\dot{V}\left(e, e_p, \tilde{K}_x, \tilde{A}\right) \leq &\left\|PA_m + A_m^\top P\right\| \|e\|^2 + \left\|P\left(A_m^* - A_m\right)\right\| \left(\|e\|^2 + \|x_m\|^2\right) \\ &+ c_3\left(\|e\|^2 + \left\|e_p\right\|^2\right) - c_2\left\|e_p\right\|^2\end{aligned} \tag{9.644}$$

Thus, $\dot{V}\left(e, e_p, \tilde{K}_x, \tilde{A}\right) \not\leq 0$. Therefore, the tracking error is unbounded and the closed-loop system is unstable.

On the other hand, for the optimal control modification, $\dot{V}\left(e, e_p, \tilde{K}_x, \tilde{A}\right)$ is evaluated as

$$\begin{aligned}\dot{V}\left(e, e_p, \tilde{K}_x, \tilde{A}\right) = e^\top & \left\{-\frac{1}{\eta}Q + \frac{1}{\nu}PB\left[\left(B^\top A_m^{*-\top} PB\right)^{-1} + \left(B^\top A_m^{*-\top} PB\right)^{-\top}\right]B^\top P\right\} e^\top \\ & + 2e^\top PA_m^* x_m - 2e^\top \left[PLC - \frac{1}{\eta}\left(A_m^{*\top} + PA_m^* P^{-1}\right)W + A^\top W\right] e_p \\ & + e_p^\top \left[-\bar{R} + \frac{1}{\eta}W\left(P^{-1}A_m^{*\top} + A_m^* P^{-1}\right)W\right] e_p + 2e_p^\top WAx_m \\ & + 2\nu\hat{x}^\top K_x^\top B^\top PA_m^{-1} B\tilde{K}_x\hat{x} + \eta\nu\hat{x}^\top \Delta\hat{A}^\top PA_m^{-1}\Delta\tilde{A}\hat{x} \end{aligned} \tag{9.645}$$

Note that $P^{-1}A_m^{*\top} + A_m^* P^{-1} = -P^{-1}QP^{-1}$. Then,

$$\begin{aligned}\dot{V}\left(e, e_p, \tilde{K}_x, \tilde{A}\right) \le & -c_{12}\|e\|^2 - c_{13}\left\|e_p\right\|^2 + 2c_{14}\|e\|\left\|e_p\right\| + 2c_{15}\|e\| + 2c_{16}\left\|e_p\right\| \\ & -\nu c_4\left\|\hat{x}\right\|^2\left(\left\|\tilde{K}_x\right\| - c_5\right)^2 + \nu c_4 c_5^2\left\|\hat{x}\right\|^2 - \eta c_6\left\|\hat{x}\right\|^2\left(\left\|\tilde{A}\right\| - c_7\right)^2 + \eta c_6 c_7^2\left\|\hat{x}\right\|^2 \end{aligned} \tag{9.646}$$

where $c_{12} = \lambda_{min}\left(\frac{1}{\eta}Q - \frac{1}{\nu}PB\left[\left(B^\top A_m^{*-\top} PB\right)^{-1} + \left(B^\top A_m^{*-\top} PB\right)^{-\top}\right]B^\top P\right)$, $c_{13} = \lambda_{min}\left(\bar{R} - \frac{1}{\eta}WP^{-1}QP^{-1}W\right)$, $c_{14} = \left\|PLC + \frac{1}{\eta}QP^{-1}W + A^\top W\right\|$, $c_{15} = \left\|PA_m^*\right\| c_x r_0$, $c_{16} = \|WA\| c_x r_0$, and $c_{4,5,6,7}$ are defined previously.

Further simplification using $\left\|\hat{x}\right\|^2 \le \|e\|^2 + 2\|e\|\|x_m\| + \|x_m\|^2$ leads to

$$\begin{aligned}\dot{V}\left(e, e_p, \tilde{K}_x, \tilde{A}\right) \le & -c_{17}\left(\|e\| - c_{18}\right)^2 - c_{19}\left(\left\|e_p\right\| - c_{20}\right)^2 - \nu c_4\left\|\hat{x}\right\|^2 \\ & \left(\left\|\tilde{K}_x\right\| - c_5\right)^2 - \eta c_6\left\|\hat{x}\right\|^2\left(\left\|\tilde{A}\right\| - c_7\right)^2 + c_{21} \end{aligned} \tag{9.647}$$

where $c_{17} = c_{12} - c_{14} - \nu c_4 c_5^2 - \eta c_6 c_7^2$, $c_{18} = \frac{c_{15} + \left(\nu c_4 c_5^2 + \eta c_6 c_7^2\right) c_x r_0}{c_{17}}$, $c_{19} = c_{13} - c_{14}$, $c_{20} = \frac{c_{16}}{c_{19}}$, and $c_{21} = c_{17}c_{18}^2 + c_{19}c_{20}^2 + \left(\nu c_4 c_5^2 + \eta c_6 c_7^2\right) c_x^2 r_0^2$.

Choose L, Q, R, ν, and η such that $c_{17} > 0$ and $c_{19} > 0$. Then, $\dot{V}\left(e, e_p, \tilde{K}_x, \tilde{A}\right) \le 0$ outside a compact set. Therefore, the closed-loop system is uniformly ultimately bounded with the optimal control modification.

■

Using the linear asymptotic property of the optimal control modification, L, Q, ν and η can also be chosen such that the closed-loop matrix formed by $\left(\dot{x}(t), \dot{\hat{x}}(t)\right)$

$$A_c = \begin{bmatrix} A & \frac{1}{\nu} B \left(B^\top A_m^{*-\top} P B \right)^{-1} B^\top P \\ LC - \frac{1}{\eta} P^{-1} A_m^{*\top} W & -LC + \frac{1}{\nu} B \left(B^\top A_m^{*-\top} P B \right)^{-1} B^\top P \\ & + \frac{1}{\eta} P^{-1} A_m^{*\top} (P + W) \end{bmatrix} \tag{9.648}$$

is Hurwitz.

To demonstrate the observer state feedback adaptive control, we return to Example 9.22.

Example 9.23 The non-minimum phase plant in Example 9.22 is defined by the following matrices:

$$A = \begin{bmatrix} a & g \\ 0 & -1 \end{bmatrix}, \; B = \begin{bmatrix} b \\ 1 \end{bmatrix}, \; C = \begin{bmatrix} 1 & 0 \end{bmatrix}$$

where $a = -2$, $b = 1$, and $g = -2$.

The Kalman filter gain is computed as

$$L = \begin{bmatrix} 0.4641 \\ -0.2679 \end{bmatrix}$$

Using $Q = 100$ and $R = 1$, the LQR control gains are obtained as

$$K_x^* = \begin{bmatrix} -2.7327 & -5.4654 \end{bmatrix}, \; k_r = -9.8058$$

Choose $\Gamma_x = I$, $\Gamma_A = 0.1I$, $Q = I$, and $R = I$. Figure 9.41 shows the closed-loop response with the standard MRAC of the plant output $y(t)$ which tracks the redesigned reference model very well. Notice that the reference model now has a non-minimum phase behavior as evidenced by the reversal in the initial response. All the control and adaptive parameter signals are bounded.

Suppose, instead of the reference model computed from the LQR, we use the ideal minimum phase first-order reference model described by the following matrices:

$$A_m^* = \begin{bmatrix} a_m & 0 \\ 0 & -1 \end{bmatrix}, \; B = \begin{bmatrix} b_m \\ 0 \end{bmatrix}$$

Figure 9.42 shows the unstable closed-loop response with the standard MRAC which no longer tracks the reference model. The adaptive parameters are unbounded and drifting as $t \to \infty$.

The optimal control modification is then used with $\nu = 0.13$ selected. Figure 9.43 shows the closed-loop response with the optimal control modification which is able to track the ideal reference model very well. All the control and adaptive parameter signals are bounded.

■

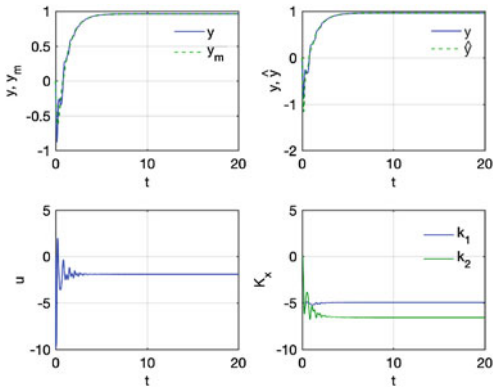

Fig. 9.41 Closed-loop output response to LQR non-minimum phase reference model with observer state feedback MRAC

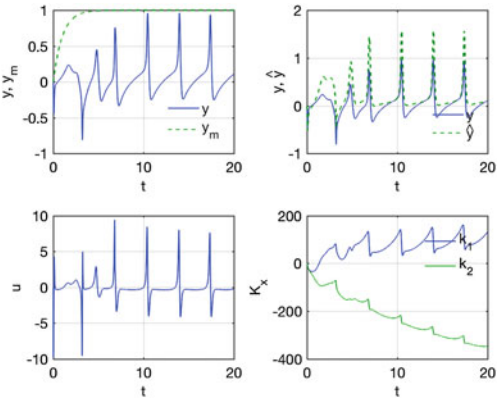

Fig. 9.42 Closed-loop output response to ideal minimum phase reference model with observer state feedback MRAC

Example 9.23 illustrates the significance of the reference model in adaptive control of non-minimum phase plants. If the reference model can be redesigned to be non-minimum phase, then the standard MRAC can achieve asymptotic tracking, albeit with a non-minimum phase behavior. Otherwise, even with the observer state feedback adaptive control design, if the reference model is minimum phase, instability will still result with the standard MRAC. On the other hand, the optimal control modification can produce bounded tracking for both types of reference models.

We have simplified the analysis of the Luenberger observer state feedback adaptive control. There are some excellent textbooks that cover in-depth the subject of output feedback adaptive control. The reader is referred to the textbooks by Ioannu [5] and by Narendra and Annaswamy [35]. The textbook by Lavretsky and Wise presents a

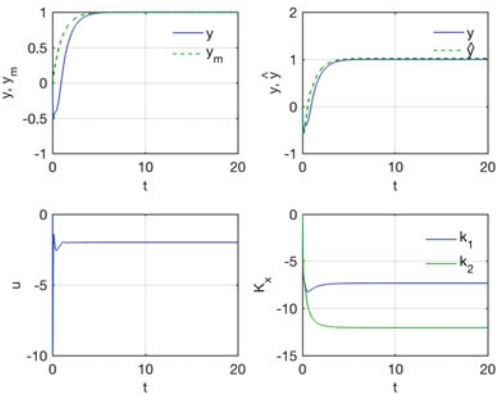

Fig. 9.43 Closed-loop output response to ideal minimum phase reference model with optimal control modification

Luenberger observer state feedback adaptive control method based on squaring up the control input matrix to satisfy the SPR condition for MIMO systems [36]. This section illustrates the general challenges with adaptive control design for systems with only output information.

9.15 Summary

Robust adaptive control is a well-researched topic. The primary objective of robust adaptive control is to improve robustness of adaptive control systems to the parameter drift, time delay, unmodeled dynamics, and other destabilizing effects. Various robust modification schemes have been developed to ensure boundedness of adaptive parameters in the last several decades. The principle of robust modification is based on two central themes: (1) limiting adaptive parameters and (2) adding damping mechanisms to model-reference adaptive control. The robustness issues with the parameter drift, non-minimum phase behaviors, time delay, unmodeled dynamics, and fast adaptation are largely ameliorated with these robust modification schemes, but are not entirely eliminated if the nature of the uncertainty is not completely known.

The standard techniques for robust adaptive control include the dead-zone method, the projection method, the σ modification, and the e modification. Normalization and covariance adaptive gain adjustments are two other techniques common to all adaptive control methods. More recent methods include the optimal control modification, the adaptive loop recovery modification, and the $\mathscr{L}_1$ adaptive control, and many others which have been developed in the recent years. These new methods add more richness to this fertile field of endeavor. In particular, the optimal control modification is an adaptive optimal control method that seeks to minimize a $\mathscr{L}_2$ tracking error norm bounded away from the origin to provide improved robustness. The linear asymptotic property of the optimal control modification for linear uncertain plants

results in asymptotic linear plants in the limit which can be exploited in adaptive control system design and analysis using many existing linear control techniques. For systems with input uncertainty, the bi-objective optimal control modification provides an adaptation mechanism based on both the tracking error and the predictor error using a predictor model that approximates the plant dynamics. For systems with slow first-order actuator dynamics, a singular perturbation method is developed by scaling the adaptive law to allow the plant to track a reference model. An output feedback adaptive control approach based on the optimal control modification method is shown to be able to stabilize first-order plants with unmodeled dynamics having relative degree greater than 1 by taking advantage of the linear asymptotic property. This approach is extended to non-minimum phase plants with relative degree 1. For these non-minimum phase plants, the optimal control modification adaptive law can be designed by a suitable selection of the modification parameter to ensure the closed-loop stability by preventing an unstable pole-zero cancellation typically occurred with the standard MRAC. The potential degraded tracking performance of the output feedback adaptive control for non-minimum phase systems can be addressed by observer state feedback adaptive control using the Luenberger observer design.

9.16 Exercises

1. Consider a time-delay second-order SISO system

$$\ddot{y} + 2\zeta\omega_n \dot{y} + \omega_n^2 y = bu\left(t - t_d\right)$$

where $b = 1$, $t_d = \frac{1}{3}$ s, and ζ and ω_n are unknown but their actual values are -0.5 and 1 rad/s, respectively.
The system is designed to track a second-order reference model

$$\ddot{y}_m + 2\zeta_m\omega_m \dot{y}_m + \omega_m^2 y_m = b_m r\left(t\right)$$

where $\zeta_m = 0.5, \omega_m = 2$ rad/s, $b_m = 4$, and $r\left(t\right) = 1$, with an adaptive controller

$$u = K_x\left(t\right) x + k_r r$$

where $x\left(t\right) = \left[\, y\left(t\right)\ \dot{y}\left(t\right) \,\right]^\top$ and $K_x\left(t\right) = \left[\, k_p\left(t\right)\ k_d\left(t\right) \,\right]$.

   a. Calculate the fixed-gain values of $k_{p_{min}}$ and $k_{d_{min}}$ to achieve a phase margin of 60^o and a time-delay margin of 1/3 s.
   b. Define a convex set described by an ellipse that contains $k_p\left(t\right)$ and $k_d\left(t\right)$

$$g\left(k_p, k_d\right) = \left(\frac{k_p}{a}\right)^2 + \left(\frac{k_d}{b}\right)^2 - 1 \leq 0$$

where a and b are to be determined from $k_{p_{min}}$ and $k_{d_{min}}$. Design a projection method for the adaptive controller to ensure robustness in the presence of time delay. Write down the adaptive law. Implement the adaptive controller in Simulink using the following information: $y(0) = 0, \dot{y}(0) = 0, K_x(0) = 0$, and $\Gamma_x = 0.2I$ with a time step $\Delta t = 0.001$ s. Plot the time histories of $y(t)$, $u(t)$, $k_p(t)$, and $k_d(t)$ for $t \in [0, 600]$ s. What happens when the projection method is removed from the adaptive law?

2. Implement in Simulink the σ modification and e modification for the Rohrs' counterexample with the reference command

$$r = 0.3 + 1.85 \sin 16.1t$$

using the same initial conditions $k_y(0)$ and $k_r(0)$ with $\gamma_x = \gamma_r = 1$, $\sigma = 0.2$, and $\mu = 0.2$ and $\Delta t = 0.001$ s. Plot the time histories of $y(t)$, $u(t)$, $k_y(t)$, and $k_r(t)$ for $t \in [0, 100]$ s. Experiment with different values of σ and μ and determine by trial-and-error the values of σ and μ at which the system begins to stabilize.

3. Consider a first-order SISO system

$$\dot{x} = ax + bu + w$$

where a is unknown, b is known, and w is an unknown disturbance.
To prevent the parameter drift, the σ modification is used in an adaptive regulator design

$$u = k_x(x)\, x$$

$$\dot{k}_x = -\gamma_x \left(x^2 b + \sigma k_x\right)$$

Suppose $x(t)$ is a sinusoidal response where $x(t) = \sin t$.

   a. Derive the general time-varying disturbance $w(t)$ that produces the given response $x(t)$ in terms of a, b, γ_x, σ, and $k_x(0)$. Let $a = 1, b = 1, \gamma_x = 10$, $\sigma = 0.1$, $x(0) = 0$, and $k_x(0) = 0$. Express $w(t)$.
   b. Implement in Simulink the control system with a time step $\Delta t = 0.001$ sec. Plot the time histories of $x(t)$, $u(t)$, $w(t)$, and $k_x(t)$ for $t \in [0, 20]$ sec.
   c. Repeat part (b) with the standard MRAC by setting $\sigma = 0$. Does the system exhibit the parameter drift?

4. Consider a linear system

$$\dot{x} = Ax + Bu$$

$$y = Cx$$

Design a reference model for tracking the output $y(t)$ with a constant reference command $r(t)$ using the optimal control approach and the following cost

function:

$$J = \lim_{t_f \to \infty} \frac{1}{2} \int_0^{t_f} \left[(Cx - r)^\top Q (Cx - r) + u^\top R u \right] dt$$

Derive the expressions for the optimal control gain matrices K_x and K_r for the closed-loop system

$$\dot{x} = (A + BK_x) x + BK_r r$$

Given

$$\dot{x} = \begin{bmatrix} 1 & 2 \\ 1 & -1 \end{bmatrix} + \begin{bmatrix} 2 \\ 1 \end{bmatrix} u$$

$$y = \begin{bmatrix} 1 & 0 \end{bmatrix}$$

$$r = \sin t - 2 \cos 4t - 2e^{-t} \sin^2 4t$$

Implement in Simulink the control system. Let $Q = q$ and $R = \frac{1}{q}$. Determine a suitable value of q, K_x, and K_r such that $\sqrt{\frac{1}{t_f} \int_0^{t_f} (y - r)^2 \, dt} \leq 0.05$ for $t \in [0, 10]$ s. Initialize with $x(0) = \begin{bmatrix} -2 & 1 \end{bmatrix}^\top$. Plot the time histories of $y(t)$ and $r(t)$ on the same plot, and $e(t) = y(t) - r(t)$.

5. Consider a time delay second-order SISO system

$$\ddot{y} - \dot{y} + y = u (t - t_d)$$

where $t_d = 0.1$ s is a time delay.
The unstable open-loop plant is stabilized with an adaptive controller

$$u = K_x x$$

where $x(t) = \begin{bmatrix} y(t) & \dot{y}(t) \end{bmatrix}^\top \in \mathbb{R}^2$ and $K_x(t) = \begin{bmatrix} k_p(t) & k_d(t) \end{bmatrix}$, to achieve an ideal reference model

$$\ddot{y}_m + 6\dot{y}_m + y_m = 0$$

a. Express the optimal control modification adaptive law for $K_x(t)$. Let $\Gamma \to \infty$ and $Q = I$, calculate the equilibrium values of $K_x(t)$ as a function of the modification parameter ν.
b. Determine numerically the value of the modification parameter ν to achieve the maximum time-delay margin to within 0.001. Compute the equilibrium values of $K_x(t)$ corresponding to this modification parameter ν. Implement the adaptive controller in Simulink with this modification parameter using the following information: $\Gamma = 10I$, $y(0) = 1$, $\dot{y}(0) = 0$, and $K_x(0) = 0$ with a time step $\Delta t = 0.001$ s. Plot the time histories of $x(t)$, $u(t)$, and $K_x(t)$ for $t \in [0, 10]$ s.

c. Increase the adaptation rate to $\Gamma = 10000I$. Repeat the simulations with a time step $\Delta t = 0.0001$ s. Compare the steady-state values of $K_x(t)$ at 10 s with those results computed in part (b).

6. Consider a first-order SISO plant as

$$\dot{x} = ax + b\left(u + \theta^* x + w\right)$$

with $a = -1$, $b = 1$, $\theta^* = 2$, and

$$w = \cos t + 4\sin t - 4e^{-t}\sin t - (\cos 2t + 2\sin 2t)\sin t$$

This disturbance will cause a parameter drift when the standard MRAC is used in a regulator design.
An adaptive controller is designed as

$$u = k_r r - \theta(t)\, x - \hat{w}(t)$$

to enable the plant to follow a reference model

$$\dot{x}_m = a_m x_m + b_m r$$

where $a_m = -2$, $b_m = 2$, and $r(t) = 1$.

a. Calculate k_r. Express the adaptive loop recovery modification adaptive laws for $\theta(t)$ and $\hat{w}(t)$ using a modification parameter $\eta = 0.1$.
b. Implement the adaptive controller in Simulink using the following information: $x(0) = 0$, $\theta(0) = 0$, $\hat{d}(0) = 0$, and $\gamma = \gamma_d = 100$ with a time step $\Delta t = 0.001$ s. Plot the time histories of $x(t)$, $u(t)$, $\theta(t)$, and $d(t)$ and $\hat{d}(t)$ together on the same plot for $t \in [0, 100]$ s.

7. Consider a second-order SISO plant

$$\ddot{y} + 2\zeta\omega_n\dot{y} + \omega_n^2 y = bu(t - t_d)$$

where $\zeta = -0.5$ and $\omega_n = 1$ rad/s are unknown, $b = 1$ is known, and t_d is a known time delay.
Design an adaptive controller using the normalized MRAC without the projection method to allow the plant to follow a reference model

$$\ddot{y}_m + 2\zeta_m\omega_m\dot{y}_m + \omega_m^2 y_m = b_m r(t)$$

where $\zeta_m = 3$, $\omega_m = 1$, $b_m = 1$, and $r(t) = r_0 \sin t$.

a. Implement the adaptive controller in Simulink using the following information: $t_d = 0$, $x(0) = 0$, $K_x(0) = 0$, and $\Gamma_x = 100I$ with a time step $\Delta t = 0.001$ s for the standard MRAC by setting $R = 0$ with $r_0 = 1$ and $r_0 = 100$. Plot the time histories of $y(t)$ and $y_m(t)$, $e_1(t) = y_m(t) - y(t)$, $u(t)$, and $K_x(t)$ for $t \in [0, 100]$ s. Comment on the effect of the amplitude of the reference command signal on MRAC.
b. Repeat part (a) for the normalized MRAC with $R = I$ and $r_0 = 100$ for $t_d = 0$ and $t_d = 0.1$ s. Comment on the effect of normalization on the amplitude of the reference command signal and time delay.

8. For the Rohrs' counterexample, design a standard MRAC with the covariance adjustment method without the projection method.

a. Implement the adaptive controller in Simulink using the following information: $y(0) = 0$, $k_y(0) = -0.65$, $k_r(0) = 1.14$, $\gamma_y(0) = \gamma_r(0) = 1$, and $\eta = 5$ with a time step $\Delta t = 0.01$ s. Plot the time histories of $k_y(t)$, $k_r(t)$, $\gamma_y(t)$, and $\gamma_r(t)$ for $t \in [0, 100]$ s. Note: plot $\gamma_y(t)$ and $\gamma_r(t)$ with the logarithmic scale in the y axis for better visualization.
b. Repeat part (a) with $t \in [0, 1000]$ s. Do $k_y(t)$ and $k_r(t)$ reach their equilibrium values or do they exhibit a parameter drift behavior?

9. Consider a first-order SISO plant

$$\dot{x} = ax + b\lambda\left[u(t - t_d) + \theta^* \phi(x)\right] + w$$

where $a = -1$ and $b = 1$ are known, $\lambda = -1$ and $\theta^* = 0.5$ are unknown, but the sign of λ is known, $\phi(x) = x^2$, $t_d = 0.1$ s is a known time delay, and $w(t) = 0.02 + 0.01 \cos 2t$.
The reference model is given by

$$\dot{x}_m = a_m x_m + b_m r$$

where $a_m = -2$, $b_m = 2$, and $r(t) = \sin t$.

a. Design an adaptive controller using the standard tracking error-based optimal control modification method. Express the adaptive laws.
b. Implement the adaptive controller in Simulink using the following information: $x(0) = k_x(0) = k_r(0) = \theta(0) = 0$ and $\gamma_x = \gamma_r = \gamma_\theta = 20$ with a time step $\Delta t = 0.001$ sec for the standard MRAC with $\nu = 0$ and for the optimal control modification with $\nu = 0.2$. Plot the time histories of $x(t)$ and $x_m(t)$ on the same plot, $u(t)$, $k_x(t)$, $k_r(t)$, and $\theta(t)$ for $t \in [0, 60]$ sec.

10. For Exercise 9.9, suppose λ is completely unknown.

    a. Design an adaptive controller using the bi-objective optimal control modification method. Express the adaptive laws.
    b. Implement the adaptive controller in Simulink using $\gamma_\lambda = \gamma_w = 20$, $\eta = 0$, and the rest of the information in Exercise 9.9 along with the initial conditions $\hat{\lambda}(t) = 1$ and $\hat{w}(t) = 0$. Plot the time histories of $x(t)$ and $x_m(t)$ on the same plot, $u(t)$, $k_x(t)$, $k_r(t)$, $\theta(t)$, $\hat{\lambda}(t)$ and $\hat{w}(t)$ and w on the same plot for $t \in [0, 60]$ s.
    c. Comment on the results of Exercises 9.9 and 9.10. Which method seems to work better?

References

1. Rohrs, C. E., Valavani, L., Athans, M., & Stein, G. (1985). Robustness of continuous-time adaptive control algorithms in the presence of unmodeled dynamics. *IEEE Transactions on Automatic Control*, *AC-30*(9), 881–889.
2. Ioannou, P., & Kokotovic, P. (1984). Instability analysis and improvement of robustness of adaptive control. *Automatica*, *20*(5), 583–594.
3. Ioannu, P. A. and Sun, J., (1996). *Robust Adaptive Control*, Prentice-Hall, Inc., 1996
4. Narendra, K. S., & Annaswamy, A. M. (1987). A new adaptive law for robust adaptation without persistent excitation. *IEEE Transactions on Automatic Control*, *AC-32*(2), 134–145.
5. Ioannu, P. A., & Sun, J. (1996). *Robust adaptive control*. Upper Saddle River: Prentice-Hall, Inc.
6. Calise, A. J., & Yucelen, T. (2012). Adaptive loop transfer recovery. *AIAA Journal of Guidance, Control, and Dynamics*, *35*(3), 807–815.
7. Lavretsky, E. (2009). Combined/composite model reference adaptive control. *IEEE Transactions on Automatic Control*, *54*(11), 2692–2697.
8. Hovakimyan, N., & Cao, C. (2010). *$\mathscr{L}_1$ Adaptive control theory: Guaranteed robustness with fast adaptation*. Philadelphia: Society for Industrial and Applied Mathematics.
9. Nguyen, N. (2012). Optimal control modification for robust adaptive control with large adaptive gain. *Systems and Control Letters*, *61*(2012), 485–494.
10. Yucelen, T., & Calise, A. J. (2011). Derivative-free model reference adaptive control. *AIAA Journal of Guidance, Control, and Dynamics*, *34*(4), 933–950.
11. Nguyen, N., Krishnakumar, K., & Boskovic, J. (2008). An optimal control modification to model-reference adaptive control for fast adaptation. In *AIAA Guidance, Navigation, and Control Conference, AIAA 2008-7283, August 2008*.
12. Campbell, S., Kaneshige, J., Nguyen, N., & Krishnakumar, K. (2010). An adaptive control simulation study using pilot handling qualities evaluations. In *AIAA Guidance, Navigation, and Control Conference, AIAA-2010-8013, August 2010*.
13. Campbell, S., Kaneshige, J., Nguyen, N., & Krishnakumar, K. (2010). Implementation and evaluation of multiple adaptive control technologies for a generic transport aircraft simulation. In *AIAA Infotech@Aerospace Conference, AIAA-2010-3322, April 2010*.

14. Hanson, C., Johnson, M., Schaefer, J., Nguyen, N., & Burken, J. (2011). Handling qualities evaluations of low complexity model reference adaptive controllers for reduced pitch and roll damping scenarios. In *AIAA Guidance, Navigation, and Control Conference, AIAA-2011-6607, August 2011*.
15. Hanson, C., Schaefer, J., Johnson, M., & Nguyen, N. Design of Low Complexity Model Reference Adaptive Controllers, NASA-TM-215972.
16. Nguyen, N., Hanson, C., Burken, J., & Schaefer, J. (2016). Normalized optimal control modification and flight experiments on NASA F/A-18 Aircraft. *AIAA Journal of Guidance, Control, and Dynamics*.
17. Schaefer, J., Hanson, C., Johnson, M., & Nguyen, N. (2011). Handling qualities of model reference adaptive controllers with varying complexity for pitch-roll coupled failures. *AIAA Guidance, Navigation, and Control Conference, AIAA-2011-6453, August 2011*.
18. Bryson, A. E., & Ho, Y. C. (1979). *Applied optimal control: Optimization, estimation, and control*. John Wiley & Sons, Inc.
19. Bryson, A. E., & Ho, Y. C. (1979). *Applied optimal control: Optimization, estimation, and control*. New Jersey: Wiley Inc.
20. Nguyen, N. (2013). Adaptive control for linear uncertain systems with unmodeled dynamics revisited via optimal control modification. In *AIAA Guidance, Navigation, and Control Conference, AIAA-2013-4988, August 2013*.
21. Nguyen, N. (2010). Asymptotic linearity of optimal control modification adaptive law with analytical stability margins. In *AIAA Infotech@Aerospace Conference, AIAA-2010-3301, April 2010*.
22. Calise, A. J., Yucelen, T., Muse, J., & Yang, B. (2009). A loop recovery method for adaptive control. In *AIAA Guidance, Navigation, and Control Conference, AIAA-2009-5967, August 2009*.
23. Cao, C., & Hovakimyan, N. (2007). Guaranteed transient performance with $\mathscr{L}_1$ adaptive controller for systems with unknown time-varying parameters and bounded disturbances: Part I. In *American Control Conference, July 2007*.
24. Cao, C., & Hovakimyan, N. (2008). Design and analysis of a novel $\mathscr{L}_1$ adaptive control architecture with guaranteed transient performance. *IEEE Transactions on Automatic Control*, *53*(2), 586–591.
25. Nguyen, N., Burken, J., & Hanson, C. (2011). Optimal control modification adaptive law with covariance adaptive gain adjustment and normalization. In *AIAA Guidance, Navigation, and Control Conference, AIAA-2011-6606, August 2011*.
26. Nguyen, N. (2014). Multi-objective optimal control modification adaptive control method for systems with input and unmatched uncertainties. In *AIAA Guidance, Navigation, and Control Conference, AIAA-2014-0454, January 2014*.
27. Nguyen, N. and Balakrishnan, S. N. (2014). Bi-objective optimal control modification adaptive control for systems with input uncertainty. *IEEE/CAA Journal of Automatica Sinica*, *1*(4), 423–434.
28. Nguyen, N. (2012). Bi-objective optimal control modification adaptive control for systems with input uncertainty. In *AIAA Guidance, Navigation, and Control Conference, AIAA-2012-4615, August 2012*.
29. Nguyen, N. (2013). Bi-objective optimal control modification adaptive law for unmatched uncertain systems. In *AIAA Guidance, Navigation, and Control Conference, AIAA-2013-4613, August 2013*.
30. Slotine, J.-J., & Li, W. (1991). *Applied nonlinear control*. Upper Saddle River: Prentice-Hall, Inc.
31. Nguyen, N., Krishnakumar, K., Kaneshige, J., & Nespeca, P. (2008). Flight dynamics modeling and hybrid adaptive control of damaged asymmetric aircraft. *AIAA Journal of Guidance, Control, and Dynamics*, *31*(3), 751–764.
32. Nguyen, N., Ishihara, A., Stepanyan, V., & Boskovic, J. (2009). Optimal control modification for robust adaptation of singularly perturbed systems with slow actuators. In *AIAA Guidance, Navigation, and Control Conference, AIAA-2009-5615, August 2009*.

33. Kokotovic, P., Khalil, H., & O'Reilly, J. (1987). *Singular perturbation methods in control: analysis and design*. Philadelphia: Society for Industrial and Applied Mathematics.
34. Ardema, M. (1981). Computational singular perturbation method for dynamical systems. *AIAA Journal of Guidance, Control, and Dynamics*, *14*, 661–663.
35. Narendra, K. S., & Annaswamy, (2005). *Stable adaptive systems*. New York: Dover Publications.
36. Lavretsky, E., & Wise, K. (2012). *Robust and adaptive control*. Berlin: Springer.

Chapter 10
Aerospace Applications

Abstract This chapter presents several adaptive control applications with a particular focus on aerospace flight control applications. Two relatively simple pendulum applications are used to illustrate a nonlinear dynamic inversion adaptive control design method for tracking a linear reference model. The rest of the chapter presents several adaptive flight control applications for rigid aircraft and flexible aircraft. The chapter concludes with an application of the optimal control modification to a F-18 aircraft model. The flight control applications for rigid aircraft include the σ modification, e modification, bi-objective optimal control modification, least-squares adaptive control, neural network adaptive control, and hybrid adaptive control which combines model-reference adaptive control with a recursive least-squares parameter identification method. An adaptive control design for a flexible aircraft is presented using a combined adaptive law with the optimal control modification and adaptive loop recovery modification to suppress the dynamics of the aircraft flexible modes. An adaptive linear quadratic gaussian (LQG) design based on the optimal control modification for flutter suppression is presented. By taking advantage of the linear asymptotic property, the adaptive flutter suppression can be designed to achieve a closed-loop stability with output measurements.

Adaptive control is a potentially promising technology that can improve performance and stability of a conventional fixed-gain controller. In recent years, adaptive control has been receiving a significant amount of attention. In aerospace applications, adaptive control technology has been demonstrated successfully in both unmanned aircraft and man-rated aircraft arenas. During 2002 to 2006, NASA conducted the intelligent flight control system (IFCS) program to demonstrate the ability of a neural network intelligent flight control system onboard a NF-15B research aircraft (tail number 837), shown in Fig. 10.1 for enhanced aircraft flight control performance under faults and failures [1, 2]. The flight demonstration program was a joint collaboration between NASA Ames Research Center, NASA Armstrong Flight Research Center, the Boeing Company, and other organizations. The intelligent flight control system was based on the e modification [3] with the sigma-pi neural network based on the work by Calise [4]. The first phase of the flight test program revealed that the intelligent flight control system did not perform as well as it was in simulations.

N.T. Nguyen, *Model-Reference Adaptive Control*, Advanced Textbooks
in Control and Signal Processing, https://doi.org/10.1007/978-3-319-56393-0_10

In some instances, the intelligent flight control system generated large commands that caused load limit excursions. A subsequent modification to simplify the neural network demonstrated an improvement in the intelligent flight control system in simulations. However, during the final phase of the flight test experiment, mixed results were obtained. Lateral pilot-induced oscillations were experienced during an in-flight simulated stabilator failure. Consequently, a further study was conducted at the conclusion of the IFCS program in 2006. It was noted during this study that the normalization method performed well in simulations.

Fig. 10.1 NASA NF-15B research aircraft (tail number 837)

During 2010 to 2011, NASA conducted a follow-on flight test program of adaptive control onboard a F/A-18A aircraft (tail number 853) shown in Fig. 10.2. The adaptive controllers were a simplified MRAC with $\Phi(x) = x$ and the optimal control modification with and without normalization [5–8]. Prior to the flight test program, several adaptive controllers were evaluated by eight NASA test pilots in the Advanced Flight Concept Simulator at NASA Ames Research Center in 2009 [9, 10]. The evaluation study showed that the optimal control modification performed well across different failure scenarios [7, 9]. NASA Armstrong Flight Research Center conducted a further investigation of the optimal control modification and simulation experiments in a F-18 flight simulator [11]. The simulation results supported the improved performance with the optimal control modification in a simplified adaptive control design. In addition, the normalization method was also implemented in conjunction with the optimal control modification based on the previous study during the IFCS program [12]. The flight test program showed improvements in the adaptation process under most failure scenarios [5–8].

The use of adaptive control potentially could help reduce the development cost of production flight control systems for aerospace vehicles. Typically, in aerospace production systems, accurate plant models must be developed to ensure high confidence in a flight control design. The model development of a typical aerospace system in general can be quite expensive since extensive experimental validation in wind tunnel facilities and in flight is often required. Adaptive control may permit the use of less accurate plant models since the adaptation process can accommodate

Fig. 10.2 NASA F/A-18A research aircraft (tail number 853)

the uncertainty in the plants. For this to happen, certification barriers for adaptive control must be overcome.

In aerospace applications, the ability of an adaptive controller to modify a predesigned control system is viewed as a strength and a weakness at the same time. On the one hand, the premise of being able to accommodate system failures is a major advantage of adaptive control. On the other hand, potential problems with adaptive control exist with regard to robustness. Therefore, in spite of the many recent advances in adaptive control, currently there are no adaptive controllers that have yet been certified for mission-critical or safety-critical systems. This is not to say that adaptive control is generally not considered as a viable option. Quite the contrary, in a number of major aerospace systems, adaptive control has been viewed as an option in the recent years.

The development of certifiable adaptive flight control systems represents a major challenge to overcome. Adaptive control will never become part of the future unless it can be proven that it is is highly safe and reliable. Technical challenges are continued to be addressed by the research community.

To demonstrate the potential benefits of adaptive control, this chapter presents some example adaptive control applications with a particular focus on aerospace flight control. The learning objectives of this chapter are:

- To be able to design adaptive controllers for a variety of applications;
- To be able to design nonlinear dynamic inversion adaptive controllers for nonlinear systems;
- To develop a familiarity with various aircraft applications and a basic understanding of aircraft flight control;
- To learn how to design adaptive controllers for systems with partial-state information using the Kalman filter; and
- To be able to combine both direct MRAC and indirect least-squares parameter estimation to improve effectiveness of adaptive controllers.

10.1 Inverted Pendulum

An inverted pendulum, shown in Fig. 10.3, is an unstable nonlinear system that is fairly analogous to a launch vehicle. When the pendulum is in equilibrium at the top,

a slight perturbation will cause the pendulum to swing down to the stable equilibrium in the vertically downward position.

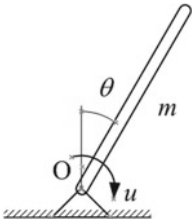

Fig. 10.3 Inverted pendulum

Consider the equation of motion of a simple inverted pendulum

$$\frac{1}{3}mL^2\ddot{\theta} - \frac{1}{2}mgL\sin\theta + c\dot{\theta} = u\left(t - t_d\right) \tag{10.1}$$

where m is the mass of the pendulum, L is the length, g is the gravity constant, c is the damping coefficient which is assumed to be unknown, $\theta\left(t\right)$ is the angular position of the pendulum, $u\left(t\right)$ is the control input which represents the motor torque, and t_d is a time delay which represents the motor actuator dynamics.

Let $x_1\left(t\right) = \theta\left(t\right)$, $x_2\left(t\right) = \dot{\theta}\left(t\right)$, and $x\left(t\right) = \left[\, x_1\left(t\right)\ x_2\left(t\right) \,\right]^\top$. Then,

$$\dot{x} = f\left(x\right) + B\left[u\left(t - t_d\right) - cx_2\right] \tag{10.2}$$

where

$$f\left(x\right) = \begin{bmatrix} x_2 \\ \frac{3g}{2L}\sin x_1 \end{bmatrix} \tag{10.3}$$

$$B = \begin{bmatrix} 0 \\ \frac{3}{mL^2} \end{bmatrix} \tag{10.4}$$

We want to design an adaptive controller that enables the closed-loop plant to follow a reference model

$$\dot{x}_m = A_m x_m + B_m r \tag{10.5}$$

Using the pseudo-inverse, the adaptive controller is obtained as

$$u = \left(B^\top B\right)^{-1} B^\top \left[A_m x + B_m r - f\left(x\right)\right] + \hat{c}\left(t\right) x_2 \tag{10.6}$$

The delay-free closed-loop plant is described by

$$\dot{x} = A_m x + B_m r + B\tilde{c}x_2 \tag{10.7}$$

The delay-free tracking error equation is expressed as

$$\dot{e} = A_m e - B\tilde{c}x_2 \tag{10.8}$$

The standard MRAC adaptive law for $\hat{c}\,(t)$ is then given by

$$\dot{\hat{c}} = \gamma x_2 e^\top PB \tag{10.9}$$

However, in the presence of time delay, the adaptive law may be modified to include the optimal control modification as

$$\dot{\hat{c}} = \gamma \left(x_2 e^\top PB + \nu x_2^2 \hat{c} B^\top P A_m^{-1} B \right) \tag{10.10}$$

ν can be chosen to guarantee stability in the presence of the time delay by using the linear asymptotic property of the optimal control modification which yields

$$B\hat{c}x_2 = -\frac{1}{\nu} \left(B^\top A_m^{-\top} P \right)^{-1} B^\top Pe \tag{10.11}$$

as $\gamma \to \infty$.

The closed-loop plant with the time delay is expressed as

$$\dot{x} = f\,(x) - f\,(x\,(t - t_d)) + A_m x\,(t - t_d) + B_m r\,(t - t_d) + B\hat{c}\,(t - t_d)\, x_2\,(t - t_d) - Bcx_2 \tag{10.12}$$

The nonlinear term $f\,(x)$ does create a problem since linear stability analysis cannot be used. However, consider the case when t_d is small, then

$$f\,(x) - f\,(x\,(t - t_d)) = \begin{bmatrix} x_2 - x_2\,(t - t_d) \\ \frac{3g}{2L} \sin x_1 - \frac{3g}{2L} \sin x_1\,(t - t_d) \end{bmatrix} \tag{10.13}$$

If t_d is small, then using a first-order finite-difference method, we obtain

$$\frac{\sin x_1 - \sin x_1\,(t - t_d)}{t_d} \approx \frac{d \sin x_1}{dt} = \dot{x}_1 \cos x_1 = x_2 \cos x_1 \tag{10.14}$$

Therefore,

$$f\,(x) - f\,(x\,(t - t_d)) \approx \begin{bmatrix} x_2 - x_2\,(t - t_d) \\ \frac{3g}{2L} t_d x_2 \cos x_1 \end{bmatrix} \tag{10.15}$$

The worst case for linear stability is when $\cos x_1 = 1$. So,

$$\begin{aligned} \dot{x} = {} & A\,(t_d)\, x - A\,(0)\, x\,(t - t_d) + \left[A_m + \frac{1}{\nu} \left(B^\top A_m^{-\top} P \right)^{-1} B^\top P \right] x\,(t - t_d) + B_m r\,(t - t_d) \\ & - \frac{1}{\nu} \left(B^\top A_m^{-\top} P \right)^{-1} B^\top P x_m\,(t - t_d) - Bcx_2 \end{aligned} \tag{10.16}$$

where

$$A(t) = \begin{bmatrix} 0 & 1 \\ 0 & \frac{3g}{2L}t \end{bmatrix} \tag{10.17}$$

It is noted that this approach is a bounded linear approximation for stability analysis. It is not always possible to bound a nonlinear system with a linear system for stability analysis. In general, the Lyapunov stability theory for time delay systems must be used if a system is nonlinear. However, the Lyapunov stability theory for nonlinear time delay systems can be very challenging and generally produces very conservative results [13].

Example 10.1 Let $m = 0.1775$ slug, $L = 2$ ft, $c = 0.2$ slug-ft^2/s, $t_d = 0.05$ s, and $\theta(0) = \dot{\theta}(0) = 0$. The reference model is specified by

$$\ddot{\theta}_m + 2\zeta_m \omega_m \dot{\theta}_m + \omega_m^2 \theta_m = \omega_m^2 r$$

where $\zeta_m = 0.5$, $\omega_m = 2$, and $r(t) = 15°$.

The response of the closed-loop system with the optimal control modification using $\gamma = 100$ and $\nu = 0.5$ is shown in Fig. 10.4.

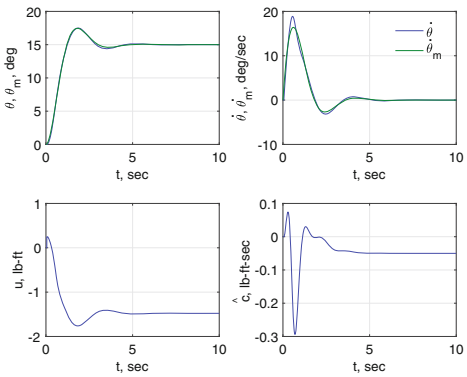

Fig. 10.4 Closed-loop response with optimal control modification

10.2 Double Pendulum in Robotic Applications

Robotic arms are usually modeled as a double linkage pendulum as shown in Fig. 10.5. The control objective of the double pendulum is to achieve a certain configuration described by the angular positions of the linkages.

The equations of motion of a double pendulum are given by

$$\frac{1}{3}\left(m_1+3m_2\right)L_1^2\ddot{\theta}_1+\frac{1}{2}m_2L_1L_2\ddot{\theta}_2\cos\left(\theta_2-\theta_1\right)-\frac{1}{2}m_2L_1L_2\theta_2^2\sin\left(\theta_2-\theta_1\right)$$
$$+\frac{1}{2}\left(m_1+2m_2\right)gL_1\sin\theta_1+\left(c_1+c_2\right)\dot{\theta}_1-c_2\dot{\theta}_2=u_1\left(t-t_d\right)+u_2\left(t-t_d\right) \tag{10.18}$$

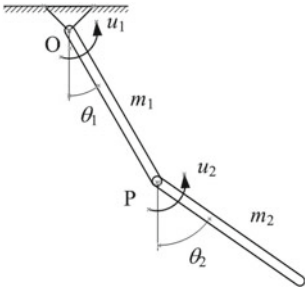

Fig. 10.5 Double pendulum

$$\frac{1}{3}m_2L_2^2\ddot{\theta}_2+\frac{1}{2}m_2L_1L_2\ddot{\theta}_1\cos\left(\theta_2-\theta_1\right)+\frac{1}{2}m_2L_1L_2\theta_1^2\sin\left(\theta_2-\theta_1\right)$$
$$+\frac{1}{2}m_2gL_2\sin\theta_2+c_2\dot{\theta}_2=u_2\left(t-t_d\right) \tag{10.19}$$

where m_1 and m_2 are the masses of the linkages, L_1 and L_2 are the lengths, c_1 and c_2 are the friction coefficients at the joints which are assumed to be unknown, g is the gravity constant, $\theta_1(t)$ and $\theta_2(t)$ are the angular positions of the double pendulum, $u_1(t)$ and $u_2(t)$ are the control variables which represent the motor torques at the joints, and t_d is the time delay due to the motor actuator dynamics.

These equations can be recast as

$$\underbrace{\begin{bmatrix}\frac{\left(m_1+3m_2\right)L_1^2}{3} & \frac{m_2L_1L_2\cos\left(\theta_2-\theta_1\right)}{2}\\ \frac{m_2L_1L_2\cos\left(\theta_2-\theta_1\right)}{2} & \frac{m_2L_2^2}{3}\end{bmatrix}}_{p(x_1)}\begin{bmatrix}\ddot{\theta}_1\\ \ddot{\theta}_2\end{bmatrix}$$
$$=\underbrace{\begin{bmatrix}\frac{m_2L_1L_2\theta_2^2\sin\left(\theta_2-\theta_1\right)}{2}-\frac{\left(m_1+2m_2\right)gL_1\sin\theta_1}{2}\\ -\frac{m_2L_1L_2\theta_1^2\sin\left(\theta_2-\theta_1\right)}{2}-\frac{m_2gL_2\sin\theta_2}{2}\end{bmatrix}}_{f(x_1)}$$
$$+\underbrace{\begin{bmatrix}1 & 1\\ 0 & 1\end{bmatrix}}_{C}\begin{bmatrix}u_1\left(t-t_d\right)\\ u_2\left(t-t_d\right)\end{bmatrix}+\underbrace{\begin{bmatrix}-c_1-c_2 & c_2\\ 0 & -c_2\end{bmatrix}}_{D}\begin{bmatrix}\dot{\theta}_1\\ \dot{\theta}_2\end{bmatrix} \tag{10.20}$$

Let $x_1(t) = \left[\theta_1(t)\ \theta_2(t)\right]^\top$, $x_2(t) = \left[\dot{\theta}_1(t)\ \dot{\theta}_2(t)\right]^\top$, and $u(t) = \left[u_1(t)\ u_2(t)\right]^\top$. Then, the equations of motion become

$$\dot{x}_2 = p^{-1}(x_1) f(x_1) + p^{-1}(x_1) Cu(t - t_d) + p^{-1}(x_1) Dx_2 \tag{10.21}$$

We want to design an adaptive controller that enables the closed-loop plant to follow a reference model

$$\begin{bmatrix} \dot{x}_{m_1} \\ \dot{x}_{m_2} \end{bmatrix} = \underbrace{\begin{bmatrix} 0 & I \\ K_p & K_d \end{bmatrix}}_{A_m} \begin{bmatrix} x_{m_1} \\ x_{m_2} \end{bmatrix} + \underbrace{\begin{bmatrix} 0 \\ -K_p \end{bmatrix}}_{B_m} r \tag{10.22}$$

where K_p and K_d are the proportional and derivative control gain matrices such that

$$K_p = \begin{bmatrix} -\omega_{m_1}^2 & 0 \\ 0 & -\omega_{m_2}^2 \end{bmatrix} = \text{diag}\left(-\omega_{m_1}^2, -\omega_{m_2}^2\right) \tag{10.23}$$

$$K_d = \begin{bmatrix} -2\zeta_{m_1}\omega_{m_1} & 0 \\ 0 & -2\zeta_{m_2}\omega_{m_2} \end{bmatrix} = \text{diag}\left(-2\zeta_{m_1}\omega_{m_1}, -2\zeta_{m_2}\omega_{m_2}\right) \tag{10.24}$$

The adaptive controller can be found by inverting the delay-free equations of motion with $t_d = 0$ such that

$$K_p x_1 + K_d x_2 - K_p r = \dot{x}_2 = p^{-1}(x_1) f(x_1) + p^{-1}(x_1) Cu + p^{-1}(x_1) \hat{D}(t) x_2 \tag{10.25}$$

This yields

$$u = C^{-1} p(x_1) \left(K_p x_1 + K_d x_2 - K_p r\right) - C^{-1} f(x_1) - C^{-1} \hat{D}(t) x_2 \tag{10.26}$$

The delay-free closed-loop plant is then described by

$$\dot{x}_2 = K_p x_1 + K_d x_2 - K_p r - p^{-1}(x_1) \tilde{D}(t) x_2 \tag{10.27}$$

The term $p^{-1}(x_1) \tilde{D}(t) x_2(t)$ can be evaluated as

$$\begin{aligned} p^{-1}(x_1) \tilde{D}(t) x_2 &= \frac{1}{\det p(x_1)} \begin{bmatrix} \frac{m_2 L_2^2}{3} & -\frac{m_2 L_1 L_2 \cos(\theta_2 - \theta_1)}{2} \\ -\frac{m_2 L_1 L_2 \cos(\theta_2 - \theta_1)}{2} & \frac{(m_1 + 3m_2) L_1^2}{3} \end{bmatrix} \\ &\quad \begin{bmatrix} -\tilde{c}_1 - \tilde{c}_2 & \tilde{c}_2 \\ 0 & -\tilde{c}_2 \end{bmatrix} \begin{bmatrix} \dot{\theta}_1 \\ \dot{\theta}_2 \end{bmatrix} \\ &= \underbrace{\begin{bmatrix} -\frac{m_2 L_2^2 (\tilde{c}_1 + \tilde{c}_2)}{3} & \frac{m_2 L_2^2 \tilde{c}_2}{3} & 0 & \frac{m_2 L_1 L_2 \tilde{c}_2}{2} \\ 0 & -\frac{(m_1 + 3m_2) L_1^2 \tilde{c}_2}{3} & \frac{m_2 L_1 L_2 (\tilde{c}_1 + \tilde{c}_2)}{2} & -\frac{m_2 L_1 L_2 \tilde{c}_2}{2} \end{bmatrix}}_{\tilde{\Theta}^\top} \end{aligned}$$

$$\underbrace{\begin{bmatrix} \frac{\dot{\theta}_1}{\det p(x_1)} \\ \frac{\dot{\theta}_2}{\det p(x_1)} \\ \frac{\dot{\theta}_1 \cos(\theta_2-\theta_1)}{\det p(x_1)} \\ \frac{\dot{\theta}_2 \cos(\theta_2-\theta_1)}{\det p(x_1)} \end{bmatrix}}_{\Phi(x_1,x_2)} = \tilde{\Theta}^\top \Phi(x_1, x_2) \tag{10.28}$$

Then, this implies

$$\hat{D}(t)\, x_2 = p(x_1)\, \Theta^\top \Phi(x_1, x_2) \tag{10.29}$$

So, the adaptive controller becomes

$$u = C^{-1} p(x_1) \left(K_p x_1 + K_d x_2 - K_p r\right) - C^{-1} f(x_1) - C^{-1} p(x_1)\, \Theta^\top \Phi(x_1, x_2) \tag{10.30}$$

Thus, the closed-loop plant can be expressed as

$$\begin{bmatrix} \dot{x}_1 \\ \dot{x}_2 \end{bmatrix} = \underbrace{\begin{bmatrix} 0 & I \\ K_p & K_d \end{bmatrix}}_{A_m} \begin{bmatrix} x_1 \\ x_2 \end{bmatrix} + \underbrace{\begin{bmatrix} 0 \\ -K_p \end{bmatrix}}_{B_m} r - \underbrace{\begin{bmatrix} 0 \\ I \end{bmatrix}}_{B} \tilde{\Theta}^\top \Phi(x_1, x_2) \tag{10.31}$$

Let $e(t) = \left[x_{m_1}^\top(t) - x_1^\top(t)\ x_{m_2}^\top(t) - x_2^\top(t)\right]^\top$, then the tracking error equation is obtained as

$$\dot{e} = A_m e + B\tilde{\Theta}^\top \Phi(x_1, x_2) \tag{10.32}$$

where

$$A_m = \begin{bmatrix} 0 & 0 & 1 & 0 \\ 0 & 0 & 0 & 1 \\ -\omega_{m_1}^2 & 0 & -2\zeta_{m_1}\omega_{m_1} & 0 \\ 0 & -\omega_{m_2}^2 & 0 & -2\zeta_{m_2}\omega_{m_2} \end{bmatrix} \tag{10.33}$$

$$B = \begin{bmatrix} 0\ 0 \\ 0\ 0 \\ 1\ 0 \\ 0\ 1 \end{bmatrix} \tag{10.34}$$

Due to the presence of the time delay which represents the motor actuator dynamics, the adaptive law for $\Theta(t)$ should include a robust modification scheme or the projection method. For example, the adaptive law for $\Theta(t)$ with the σ modification is given by

$$\dot{\Theta} = -\Gamma\left[\Phi(x_1, x_2)\, e^\top P B + \sigma\Theta\right] \tag{10.35}$$

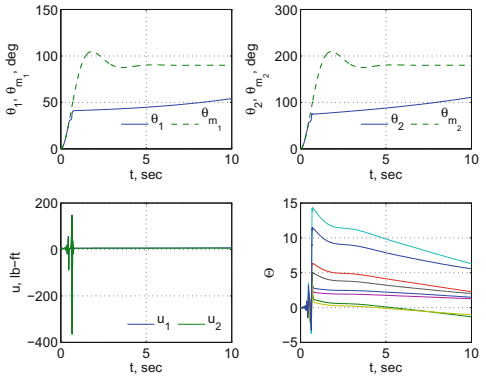

Fig. 10.6 Closed-loop response with MRAC

Example 10.2 Let $m_1 = m_2 = 0.1775$ slug, $L_1 = L_2 = 2$ ft, $c_1 = c_2 = 0.2$ slug-ft^2/s, $t_d = 0.005$ s, and $\theta_1(0) = \dot{\theta}_1(0) = \theta_2(0) = \dot{\theta}_2(0) = 0$. The reference model is specified by $\omega_{m_1} = \omega_{m_2} = 2$ rad/s, $\zeta_{m_1} = \zeta_{m_2} = 0.5$, and $r(t) = \begin{bmatrix} 90^\circ & 180^\circ \end{bmatrix}^\top$ rad. Let $\Gamma = 10I$ and $\sigma = 1$.

The responses of the closed-loop system with the standard MRAC and σ modification are shown in Figs. 10.6 and 10.7. The closed-loop response with the standard MRAC is very poor due to the time delay. The adaptive control signals are very large, and the adaptive parameters appear to be drifting. In other words, the closed-loop system is on the verge of instability. On the other hand, the σ modification produces a very good closed-loop response. The adaptive control signals exhibit some initial high-frequency oscillations but then settle to steady-state values. The adaptive parameters all converge to zero.

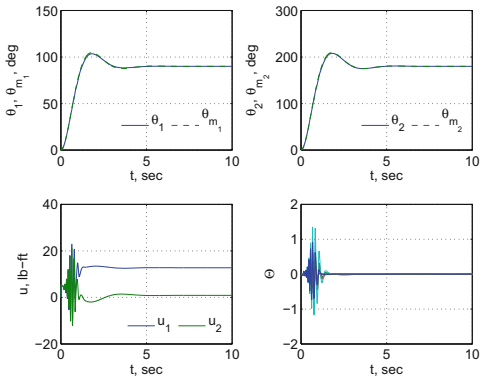

Fig. 10.7 Closed-loop response with σ modification

10.3 Adaptive Control of Aircraft Longitudinal Dynamics

The motion of an aircraft is unconstrained in a three-dimensional space. Therefore, aircraft dynamics possess all six degrees of freedom involving translational and angular velocities in the roll, pitch, and yaw axes. The combined motion of aircraft can be decomposed into a symmetric or longitudinal motion in the pitch axis and asymmetric or lateral-directional motion in roll and yaw axes.

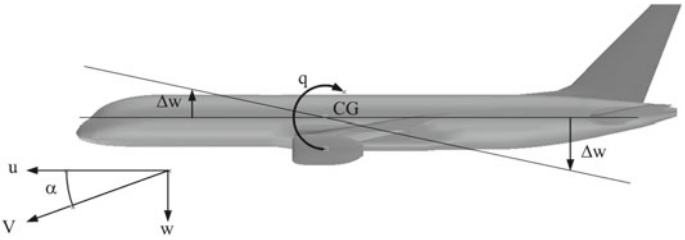

Fig. 10.8 Aircraft longitudinal dynamics

The longitudinal dynamics of an aircraft are described by the airspeed V, the angle of attack α, and the pitch rate q as shown in Fig. 10.8. There are two longitudinal modes: the phugoid mode and the short-period mode. The short-period mode involves the angle of attack and pitch rate that affect the aircraft longitudinal stability.

The equations of motion for a symmetric flight are given by [14]

$$mV\dot{\alpha} = -C_L\bar{q}S - T\sin\alpha + mg\cos(\theta - \alpha) + mVq \tag{10.36}$$

$$I_{yy}\dot{q} = C_m\bar{q}S\bar{c} + Tz_e \tag{10.37}$$

where $m(t)$ is the aircraft mass, $\bar{q}(t)$ is the dynamic pressure, S is the wing reference area, $\bar{c}$ is the mean aerodynamic chord, $T(t)$ is the engine thrust, $V(t)$ is the airspeed, $\alpha(t)$ is the angle of attack, $\theta(t)$ is the pitch attitude, $q(t) = \dot{\theta}(t)$ is the pitch rate, $I_{yy}(t)$ is the mass moment of inertia about the aircraft pitch axis, $C_L(t)$ is the lift coefficient, and $C_m(t)$ is the pitching moment coefficient about the aircraft center of gravity. Note that the aircraft mass and inertia properties as well as aerodynamic coefficients are time-varying due to the fuel burn.

The motion can be decomposed into a trim motion and a perturbed motion. The trim motion is a motion when the aircraft is in an equilibrium for a steady-level flight for which $V(t) = \bar{V}$, $\alpha(t) = \bar{\alpha}$, and $q(t) = \bar{q} = 0$. The perturbed motion is a small amplitude motion about the trim condition. Because the amplitudes are assumed to be small, linearization of the equations of motion can be performed to derive the linear equations of motion for the perturbed motion. The equations of motion are linearized as

$$m\bar{V}\dot{\alpha} = -\left(C_{L_\alpha}\alpha + C_{L_{\dot{\alpha}}}\frac{\dot{\alpha}\bar{c}}{2\bar{V}} + C_{L_q}\frac{q\bar{c}}{2\bar{V}} + C_{L_{\delta_e}}\delta_e\right)\bar{q}S + mg\sin\bar{\gamma}\,(\alpha-\theta) + m\bar{V}q \tag{10.38}$$

$$I_{yy}\dot{q} = \left(C_{m_\alpha}\alpha + C_{m_{\dot{\alpha}}}\frac{\dot{\alpha}\bar{c}}{2\bar{V}} + C_{m_q}\frac{q\bar{c}}{2\bar{V}} + C_{m_{\delta_e}}\delta_e\right)\bar{q}S\bar{c} \tag{10.39}$$

where $\bar{\gamma} = \bar{\theta} - \bar{\alpha}$ is the trim flight path angle; $\delta_e\,(t)$ is the elevator control surface deflection; C_{L_α}, $C_{L_{\dot{\alpha}}}$, C_{L_q}, and $C_{L_{\delta_e}}$ are stability and control derivatives of C_L; and C_{m_α}, $C_{m_{\dot{\alpha}}}$, C_{m_q}, and $C_{m_{\delta_e}}$ are stability and control derivatives of C_m.

Assuming $\bar{\gamma} = 0$ and neglecting $C_{L_{\dot{\alpha}}}$ and C_{L_q} which are generally small, then the equations of motion can be written as

$$\underbrace{\begin{bmatrix}\dot{\alpha}\\ \dot{\theta}\\ \dot{q}\end{bmatrix}}_{\dot{x}} = \underbrace{\begin{bmatrix}\frac{Z_\alpha}{\bar{V}} & 0 & 1\\ 0 & 0 & 1\\ M_\alpha + \frac{M_{\dot{\alpha}}Z_\alpha}{\bar{V}} & 0 & M_q + M_{\dot{\alpha}}\end{bmatrix}}_{A}\underbrace{\begin{bmatrix}\alpha\\ \theta\\ q\end{bmatrix}}_{x}$$
$$+\lambda\underbrace{\begin{bmatrix}\frac{Z_{\delta_e}}{\bar{V}}\\ 0\\ M_{\delta_e} + \frac{M_{\dot{\alpha}}Z_{\delta_e}}{\bar{V}}\end{bmatrix}}_{B}\left(\underbrace{\delta_e\,(t-t_d)}_{u(t-t_d)} + \underbrace{\begin{bmatrix}\theta_\alpha^* & 0 & \theta_q^*\end{bmatrix}}_{\Theta^{*\top}}\underbrace{\begin{bmatrix}\alpha\\ \theta\\ q\end{bmatrix}}_{x}\right) + \begin{bmatrix}w_\alpha\\ w_\theta\\ w_q\end{bmatrix} \tag{10.40}$$

where $Z_\alpha = -\frac{C_{L_\alpha}\bar{q}S}{m}$ and $Z_{\delta_e} = \frac{C_{L_{\delta_e}}\bar{q}S}{m}$ are the normal force derivatives (positive down); $M_\alpha = \frac{C_{m_\alpha}\bar{q}S\bar{c}}{I_{yy}}$, $M_{\delta_e} = \frac{C_{m_{\delta_e}}\bar{q}S\bar{c}}{I_{yy}}$, $M_{\dot{\alpha}} = \frac{C_{m_{\dot{\alpha}}}\bar{q}S\bar{c}^2}{2I_{yy}\bar{V}}$, and $M_q = \frac{C_{m_q}\bar{q}S\bar{c}^2}{2I_{yy}\bar{V}}$ are the pitching moment derivatives (positive nose up); θ_α^* and θ_q^* are the uncertainty in $\alpha\,(t)$ and $q\,(t)$ due to failures; λ is the uncertainty in the control effectiveness of the elevator control surface; and t_d is a time delay which represents the elevator control surface actuator dynamics.

Suppose an adaptive pitch attitude controller is to be designed to enable the pitch attitude to follow a reference model specified as

$$\ddot{\theta}_m + 2\zeta_m\omega_m\dot{\theta}_m + \omega_m^2\theta_m = \omega_m^2 r \tag{10.41}$$

For perfect tracking, the pitch attitude should have the same dynamics. Therefore,

$$\ddot{\theta} = -2\zeta_m\omega_m q - \omega_m^2\,(\theta - r) \tag{10.42}$$

The delay-free pitch rate equation is written as

$$\ddot{\theta} - \left(M_\alpha + \frac{M_{\dot{\alpha}}Z_\alpha}{\bar{V}}\right)\alpha - \left(M_q + M_{\dot{\alpha}}\right)\dot{\theta} = \left(M_{\delta_e} + \frac{M_{\dot{\alpha}}Z_{\delta_e}}{\bar{V}}\right)\left(\delta_e + \Theta^{*\top}x\right) \tag{10.43}$$

where $\Theta^* = \left[\theta_\alpha^* \; 0 \; \theta_q^*\right]^\top$ and $x(t) = \left[\alpha(t) \; \theta(t) \; q(t)\right]^\top$.

Therefore, the elevator control surface deflection $\delta_e(t)$ can be designed by inverting the pitch rate equation. This yields

$$\delta_e = k_\alpha \alpha + k_\theta (\theta - r) + k_q q - \Theta^\top(t) x \tag{10.44}$$

where

$$k_\alpha = -\frac{M_\alpha + \frac{M_{\dot\alpha} Z_\alpha}{\bar V}}{M_{\delta_e} + \frac{M_{\dot\alpha} Z_{\delta_e}}{\bar V}} \tag{10.45}$$

$$k_\theta = -\frac{\omega_m^2}{M_{\delta_e} + \frac{M_{\dot\alpha} Z_{\delta_e}}{\bar V}} \tag{10.46}$$

$$k_q = -\frac{2\zeta_m \omega_m + M_q + M_{\dot\alpha}}{M_{\delta_e} + \frac{M_{\dot\alpha} Z_{\delta_e}}{\bar V}} \tag{10.47}$$

Thus, the attitude controller is a proportional-integral (PI) controller of the pitch rate, where k_p is the proportional gain and k_θ is the integral gain. The feedback gain k_α in $\alpha(t)$ is designed to cancel out the angle-of-attack dynamic in the pitch rate equation.

Using the nominal controller with no adaptation, i.e., $\Theta(t) = 0$, the full-state reference model can be established as

$$\underbrace{\begin{bmatrix}\dot\alpha_m \\ \dot\theta_m \\ \dot q_m\end{bmatrix}}_{\dot x_m} = \underbrace{\begin{bmatrix}\frac{Z_\alpha + Z_{\delta_e} k_\alpha}{\bar V} & \frac{Z_{\delta_e} k_\theta}{\bar V} & 1 + \frac{Z_{\delta_e} k_q}{\bar V} \\ 0 & 0 & 1 \\ 0 & -\omega_m^2 & -2\zeta_m \omega_m\end{bmatrix}}_{A_m} \underbrace{\begin{bmatrix}\alpha_m \\ \theta_m \\ q_m\end{bmatrix}}_{x_m} + \underbrace{\begin{bmatrix}-\frac{Z_{\delta_e} \omega_m^2}{M_{\delta_e} \bar V + M_{\dot\alpha} Z_{\delta_e}} \\ 0 \\ \omega_m^2\end{bmatrix}}_{B_m} r \tag{10.48}$$

The delay-free tracking error equation is

$$\dot e = A_m e + B \tilde\Theta^\top x \tag{10.49}$$

The optimal control modification can be used for the adaptive law to take advantage of the linear asymptotic property that allows the modification parameter ν to be computed to guarantee stability of the closed-loop system in the presence of time delay.

The adaptive controller is designed using the bi-objective optimal control modification adaptive laws as follows:

$$u = K_x x + k_r r + u_{ad} \tag{10.50}$$

where

$$u_{ad} = \Delta K_x(t) x + \Delta k_r(t) r - \Theta^\top(t) x \tag{10.51}$$

Then, $\Delta K_x(t)$, $\Delta k_r(t)$, and $\Theta^\top(t)$ are computed from the following bi-objective optimal control modification adaptive laws:

$$\Delta \dot{K}_x^\top = \Gamma_{K_x} x \left(e^\top P + \nu u_{ad}^\top \hat{\lambda} B^\top P A_m^{-1} \right) B \hat{\lambda} \tag{10.52}$$

$$\Delta \dot{k}_r = \gamma_{k_r} r \left(e^\top P + \nu u_{ad}^\top \hat{\lambda} B^\top P A_m^{-1} \right) B \hat{\lambda} \tag{10.53}$$

$$\dot{\Theta} = -\Gamma_\Theta x \left(e^\top P + \nu u_{ad}^\top \hat{\lambda} B^\top P A_m^{-1} + e_p^\top P - \eta \left\{ \left[u + 2\Theta^\top \Phi(x) \right]^\top \hat{\lambda} B^\top + \hat{w}^\top \right\} P A_m^{-1} \right) B \hat{\lambda} \tag{10.54}$$

$$\dot{\hat{\lambda}} = -\gamma_\lambda \left[u + \Theta^\top x \right] \left(e_p^\top P - \eta \left\{ \left[u + 2\Theta^\top \Phi(x) \right]^\top \hat{\lambda} B^\top + \hat{w}^\top \right\} P A_m^{-1} \right) B \tag{10.55}$$

$$\dot{\hat{w}}^\top = -\gamma_w \left(e_p^\top P - \eta \left\{ \left[u + 2\Theta^\top \Phi(x) \right]^\top \hat{\lambda} B^\top + \hat{w}^\top \right\} P A_m^{-1} \right) \tag{10.56}$$

Example 10.3 The short-period mode dynamics of a transport aircraft at Mach 0.8 and 30,000 ft are described by

$$\dot{x} = Ax + B\lambda \left[u(t - t_d) + \Theta^{*\top} x \right]$$

where $\lambda = 0.5$ represents an uncertainty in the effectiveness of the elevator control surface, $t_d = 0.05$ s is the time delay which the elevator actuator dynamics, and the matrices A, B, and Θ^* are

$$A = \begin{bmatrix} -0.7018 & 0 & 0.9761 \\ 0 & 0 & 1 \\ -2.6923 & 0 & -0.7322 \end{bmatrix}, \; B = \begin{bmatrix} -0.0573 \\ 0 \\ -3.5352 \end{bmatrix}, \; \Theta^* = \begin{bmatrix} 0.5 \\ 0 \\ -0.4 \end{bmatrix}$$

The reference model is specified by $\zeta_m = 0.75$ and $\omega_m = 1.5$ rad/s to give a desired handling quality. A nominal controller is designed with $k_\alpha = -0.7616$, $k_\theta = -k_r = 0.6365$, and $k_q = 0.4293$. The closed-loop eigenvalues of the nominal plant are -0.6582 and $-1.2750 \pm 0.7902i$. The reference model is then established from the closed-loop nominal plant with

$$A_m = \begin{bmatrix} -0.6582 & -0.0365 & 0.9466 \\ 0 & 0 & 1 \\ 0 & -2.2500 & -2.5500 \end{bmatrix}, \; B_m = \begin{bmatrix} 0.0365 \\ 0 \\ 2.2500 \end{bmatrix}$$

The parametric uncertainty Θ^* and the control input uncertainty λ result in a short-period mode damping ratio of 0.2679, which is 34% less than the nominal short-period mode damping ratio of 0.4045.

The adaptive flight control architecture for the bi-objective optimal control modification is illustrated in Fig. 10.9 [15].

Figure 10.10 shows the aircraft response due to the baseline controller. With no adaptation, the closed-loop plant does not track the reference model well.

Figure 10.11 is the plot of the aircraft response with the standard MRAC for the adaptation rates $\Gamma_x = \Gamma_\Theta = 50I$ and $\gamma_r = 50$. The attitude angle command tracking has improved considerably. However, there are large initial transients in the pitch rate response as well as high-frequency oscillations.

Figure 10.12 shows the aircraft response with the bi-objective MRAC for the adaptation rates $\Gamma_x = \Gamma_\Theta = 50I$ and $\gamma_r = \gamma_\lambda = \gamma_w = 50$ by setting $\nu = \eta = 0$ in the bi-objective optimal control modification adaptive laws. The closed-loop becomes unstable after 14 s. The instability of the adaptive laws is consistent with the theory which shows that η cannot be zero when an external disturbance $w(t)$ exists due to the term c_8 in the stability theorem. Moreover, it is also consistent with the MRAC theory which establishes that the standard MRAC generally exhibits a parameter drift in the presence of a disturbance. To prevent a parameter drift, the disturbance estimate $\hat{w}(t)$ must be bounded by setting $\eta > 0$. If the disturbance $w(t)$ is not estimated by setting $\gamma_w = 0$, then the bi-objective MRAC is stable as shown in Fig. 10.13 since the term c_8 becomes bounded when the adaptive law for $\hat{w}(t)$ is not present. The bi-objective MRAC with $\gamma_w = 0$ has a very similar tracking performance to that with the standard MRAC.

Figure 10.14 shows the aircraft response with the bi-objective optimal control modification for the same adaptation rates with $\nu = \eta = 0.4$. The closed-loop response with the bi-objective optimal control modification is significantly improved with a very good tracking performance and no high-frequency oscillations.

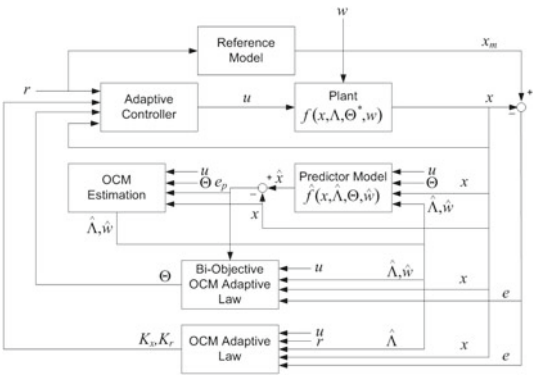

Fig. 10.9 Adaptive flight control architecture for bi-objective optimal control modification

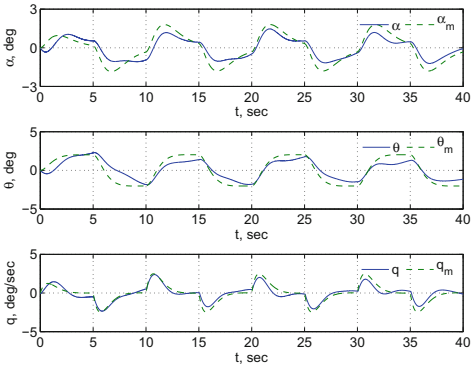

Fig. 10.10 Aircraft response with baseline controller

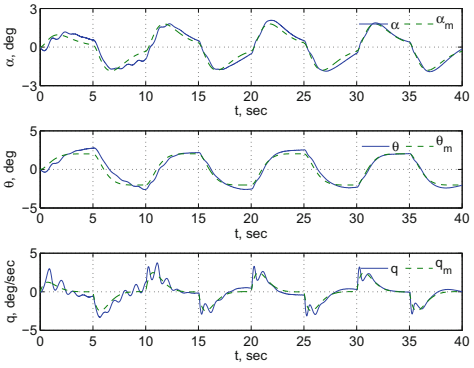

Fig. 10.11 Aircraft response with standard MRAC

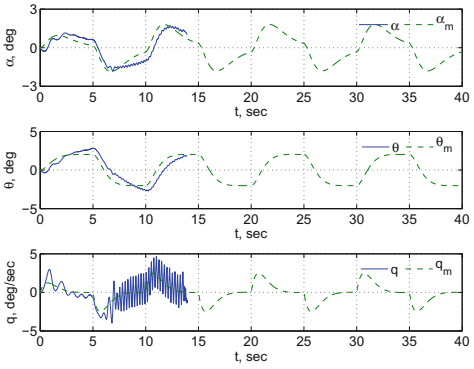

Fig. 10.12 Aircraft response with bi-objective MRAC ($\gamma_w > 0$)

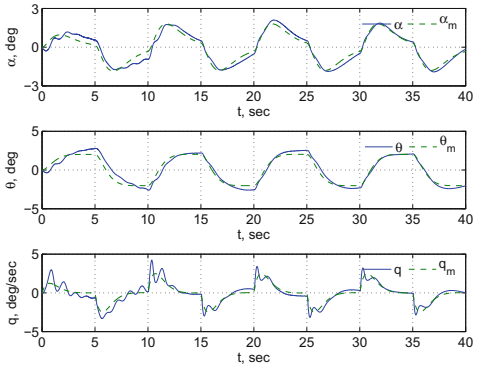

Fig. 10.13 Aircraft response with bi-objective MRAC ($\gamma_w = 0$)

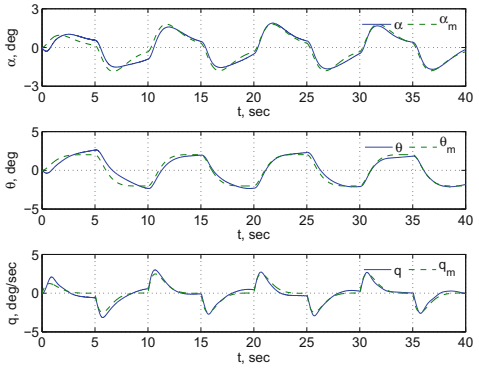

Fig. 10.14 Aircraft response with bi-objective optimal control modification

Figure 10.15 compares the elevator deflections produced by all the various controllers. The elevator deflections with the standard MRAC and bi-objective MRAC with $\gamma_w = 0$ exhibit significant high-frequency oscillations and high amplitudes. The elevator deflection with the bi-objective MRAC with $\gamma_w > 0$ is in full saturation before the controller goes unstable at 14 s. In contrast, the bi-objective optimal control modification produces a well-behaved control signal for the elevator deflection with no discernible saturation or high-frequency oscillations. The amplitude of the elevator deflection produced by the bi-objective optimal control modification is roughly double that for the baseline controller to account for the 50% reduction in the control effectiveness of the elevator.

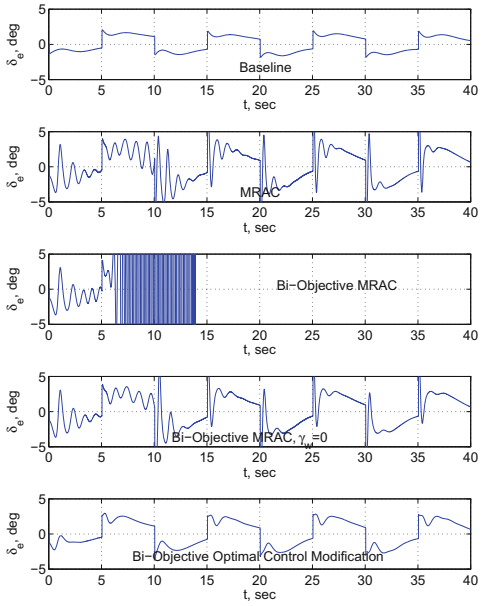

Fig. 10.15 Elevator deflections

10.4 Recursive Least-Squares and Neural Network Pitch Attitude Adaptive Flight Control

Consider the short-period dynamics of an aircraft with a matched unstructured uncertainty $f(\alpha)$ as a function of the angle of attack due to nonlinear aerodynamics [16]

$$\begin{bmatrix} \dot{\alpha} \\ \dot{\theta} \\ \dot{q} \end{bmatrix} = \begin{bmatrix} \frac{Z_\alpha}{\bar{u}} & 0 & 1 \\ 0 & 0 & 1 \\ M_\alpha + \frac{M_{\dot{\alpha}} Z_\alpha}{\bar{u}} & 0 & M_q + M_{\dot{\alpha}} \end{bmatrix} \begin{bmatrix} \alpha \\ \theta \\ q \end{bmatrix} + \begin{bmatrix} \frac{Z_{\delta_e}}{\bar{u}} \\ 0 \\ M_{\delta_e} + \frac{M_{\dot{\alpha}} Z_{\delta_e}}{\bar{u}} \end{bmatrix} [\delta_e + f(\alpha)] \tag{10.57}$$

A pitch attitude controller is designed to track a desired second-order pitch attitude dynamics. The pitch rate equation is written as

$$\ddot{\theta} - \left(M_\alpha + \frac{M_{\dot{\alpha}} Z_\alpha}{\bar{u}} \right) \alpha - \left(M_q + M_{\dot{\alpha}} \right) \dot{\theta} = \left(M_{\delta_e} + \frac{M_{\dot{\alpha}} Z_{\delta_e}}{\bar{u}} \right) [\delta_e + f(\alpha)] \tag{10.58}$$

The elevator input is designed with the following proportional-integral (PI) control law:

$$\delta_e = k_\alpha \alpha + k_\theta (\theta - r) + k_q q - \hat{f}(\alpha) \tag{10.59}$$

where $x(t) = \left[\alpha(t)\ \theta(t)\ q(t)\right]^\top$, $K_x = \left[k_\alpha\ k_\theta\ k_q\right]^\top$, and $\hat{f}(\alpha)$ is the function approximation of the unstructured uncertainty $f(\alpha)$.

The plant modeling error is computed as $\varepsilon(t) = \dot{x}_d(t) - \dot{x}(t) = A_m x(t) + B_m r(t) - \dot{x}(t)$, where $\dot{x}(t)$ is estimated by a backward finite-difference method. The uncertainty is modeled with the first four terms of the Chebyshev orthogonal polynomials

$$\hat{f}(\alpha) = \Theta^\top \Phi(\alpha) = \theta_0 + \theta_1 \alpha + \theta_2\left(2\alpha^2 - 1\right) + \theta_3\left(4\alpha^3 - 3\alpha\right) \tag{10.60}$$

$\Theta(t)$ is estimated by both the least-squares gradient adaptive law

$$\dot{\Theta} = -\Gamma \Phi(\alpha)\varepsilon^\top B\left(B^\top B\right)^{-1} \tag{10.61}$$

and the RLS adaptive laws

$$\dot{\Theta} = -R\Phi(\alpha)\varepsilon^\top B\left(B^\top B\right)^{-1} \tag{10.62}$$

$$\dot{R} = -\eta R\Phi(\alpha)\Phi^\top(\alpha)R \tag{10.63}$$

Note that the adaptive laws are implemented with the scaling of the B matrix by $\left(B^\top B\right)^{-1}$ to keep the RLS parameter $\eta < 2$ (see Sect. 7.3.2).

As discussed in Sect. 6.6, the signal $\dot{x}(t)$ may not be necessarily available and therefore needs to be estimated. The predictor model of the plant can be implemented to estimate the signal $\dot{x}(t)$ as follows:

$$\dot{\hat{x}} = A_m \hat{x} + (A - A_m)x + B\left[u + \Theta^\top \Phi(\alpha)\right] \tag{10.64}$$

Then, the predictor-based least-squares gradient and RLS adaptive laws are given by

$$\dot{\Theta} = -\Gamma \Phi(\alpha)\varepsilon_p^\top B\left(B^\top B\right)^{-1} \tag{10.65}$$

$$\dot{\Theta} = -R\Phi(\alpha)\varepsilon_p^\top B\left(B^\top B\right)^{-1} \tag{10.66}$$

where $\varepsilon_p(t) = \dot{x}_d(t) - \dot{\hat{x}}(t)$.

For comparison, the least-squares gradient adaptive controller is replaced by the standard MRAC using the same Chebyshev orthogonal polynomials

$$\dot{\Theta} = -\Gamma \Phi(\alpha)e^\top PB \tag{10.67}$$

where $e(t) = x_m(t) - x(t)$.

In addition, instead of using the Chebyshev orthogonal polynomials, a two-layer neural network with a sigmoidal activation function is used to approximate the unstructured uncertainty as

$$\hat{f}(\alpha) = \Theta^{\top}\sigma\left(W^{\top}\bar{\alpha}\right) \tag{10.68}$$

where $\bar{\alpha}(t) = \left[1\ \alpha(t)\right]^{\top}$ and $\sigma()$ is the sigmoidal activation function.

The neural network adaptive controller is specified by the following adaptive laws:

$$\dot{\Theta} = -\Gamma_{\Theta}\Phi\left(W^{\top}\bar{\alpha}\right)e^{\top}PB \tag{10.69}$$

$$\dot{W} = -\Gamma_{W}\bar{\alpha}e^{\top}PBV^{\top}\sigma'\left(W^{\top}\bar{\alpha}\right) \tag{10.70}$$

where $\Theta^{\top}(t) = \left[V_0(t)\ V^{\top}(t)\right]$.

Example 10.4 The numerical model of the short-period dynamics for a transport aircraft at Mach 0.8 and 30,000 ft is given by

$$\begin{bmatrix}\dot{\alpha}\\ \dot{\theta}\\ \dot{q}\end{bmatrix} = \begin{bmatrix}-0.7018 & 0 & 0.9761\\ 0 & 0 & 1\\ -2.6923 & 0 & -0.7322\end{bmatrix}\begin{bmatrix}\alpha\\ \theta\\ q\end{bmatrix} + \begin{bmatrix}-0.0573\\ 0\\ -3.5352\end{bmatrix}\left[\delta_e + f(\alpha)\right]$$

For simulation purposes, the unstructured uncertainty that represents nonlinear aerodynamics is described by

$$f(\alpha) = 0.1\cos\alpha^3 - 0.2\sin 10\alpha + 0.05e^{-\alpha^2}$$

The least-squares gradient and RLS adaptive controllers are implemented with $\eta = 0.2$ and $\Gamma = R(0) = I$. The aircraft longitudinal responses with the nominal controller and with the least-squares gradient and RLS adaptive controllers are shown in Figs. 10.16, 10.17 and 10.18.

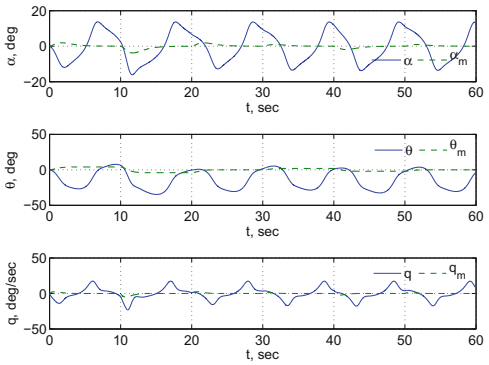

Fig. 10.16 Aircraft response with nominal controller

The aircraft response with the nominal controller is seen to be extremely poor with the maximum angle of attack of almost 14^{o} which is well into stall. The benefit of the least-squares gradient adaptive control is clearly demonstrated by the simulation results which show a very good tracking performance. However, the RLS adaptive control does not perform well. This could be due to the slow parameter convergence of the RLS adaptive control which can improve stability robustness of adaptive control in the presence of time delay or unmodeled dynamics at the expense of the tracking performance.

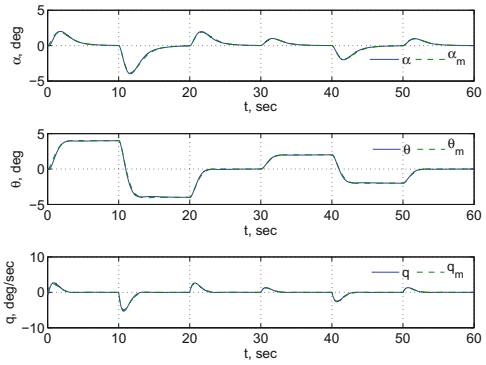

Fig. 10.17 Aircraft response with least-squares gradient adaptive control

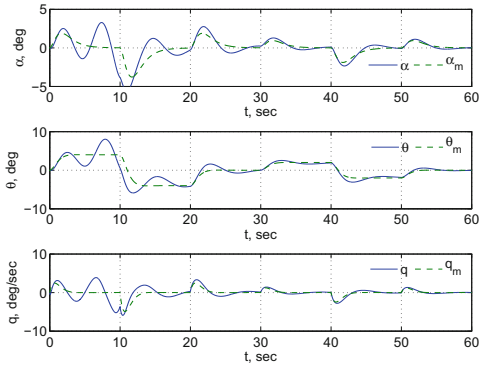

Fig. 10.18 Aircraft response with RLS adaptive control ($\eta = 0.2$)

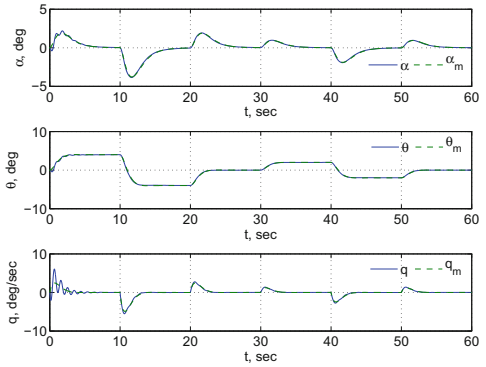

Fig. 10.19 Aircraft response with predictor-based least-squares gradient adaptive control

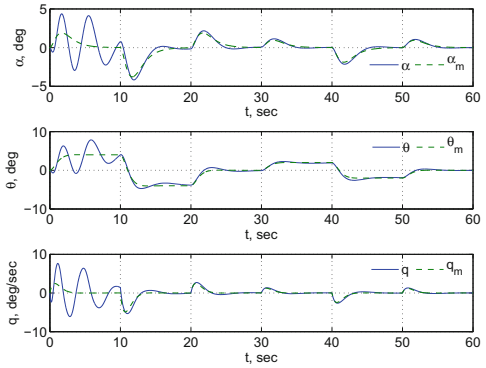

Fig. 10.20 Aircraft response with predictor model-based RLS adaptive control ($\eta = 0.2$)

Figures 10.19 and 10.20 illustrate the use of the predictor-based plant modeling error $\varepsilon_p(t)$ in the least-squares gradient and RLS adaptive control instead of the true plant modeling error $\varepsilon(t)$. The predictor-based least-squares gradient adaptive controllers provide a very good tracking performance as compared to its counterpart using the true plant modeling error. The pitch rate response exhibits some small initial high-frequency oscillations. The predictor-based RLS adaptive controller is observed to provide much better tracking after 20 s than the original RLS adaptive controller, but overall both the RLS adaptive controllers perform worse than the least-squares gradient adaptive controllers. The results indicate that the predictor model can provide a good estimation of the signal $\dot{x}(t)$ without differentiation which can introduce noise in practical applications.

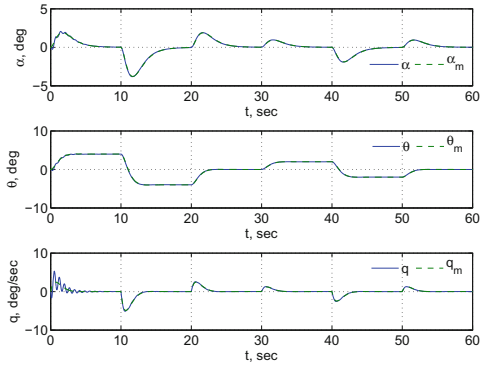

Fig. 10.21 Aircraft response with MRAC

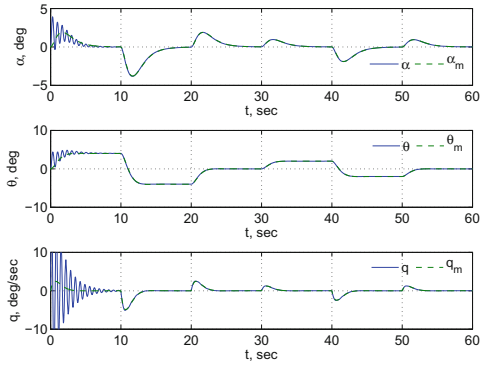

Fig. 10.22 Aircraft response with neural network MRAC

The aircraft responses with MRAC ($\Gamma = \Gamma_\Theta = \Gamma_W = 10I$) using the Chebyshev orthogonal polynomial and the neural network are shown in Figs. 10.21 and 10.22. The responses in Figs. 10.21 and 10.22 both exhibit initial high-frequency oscillations, but the subsequent tracking performance is very good. The neural network MRAC has much more pronounced high-frequency oscillations which are due to the initialization of the neural network weights with random numbers that range between -1 and 1. As a result, a saturation in the elevator is encountered.

The elevator commands for all four adaptive controllers are shown in Fig. 10.23. Both the MRAC and neural network MRAC produce high-frequency control input signals in the first 10 s. This is generally undesirable and therefore should be avoided.

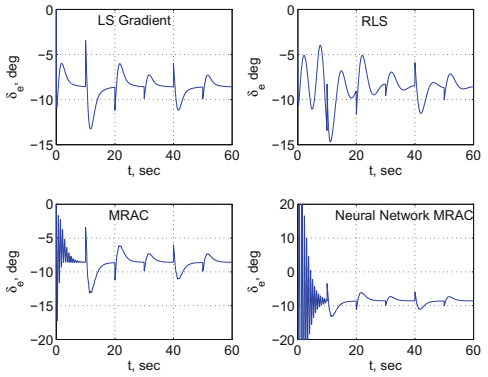

Fig. 10.23 Elevator deflections

To illustrate the issue of robustness and show that the RLS adaptive controller is actually better able to handle time delay or unmodeled dynamics than the least-squares gradient adaptive controller or MRAC, a numerical evidence of the time-delay margin is computed for each of the four adaptive controllers using a time step of 0.001 s. The results are shown in Table 10.1.

Table 10.1 Estimated time-delay margins

Adaptive law	Numerical evidence of time delay Margin
Least-squares gradient	0.073 s
Predictor-based least-squares gradient	0.032 s
RLS with $\eta = 0.2$	0.269 s
Predictor-based RLS with $\eta = 0.2$	0.103 s
MRAC	0.020 s
Neural network MRAC	0.046 s

The RLS adaptive controller has the best time-delay margin than the other three adaptive controllers. The standard MRAC has very poor robustness which is a well-known fact [17]. Generally, the standard MRAC has to be modified to improve robustness using the projection method or various modification techniques, such as the σ modification [18], e modification [3], optimal control modification [19], and adaptive loop recovery modification [20]. The time-delay margin for the neural network MRAC varies with the initialization of the neural network weights. It should be noted that both the predictor-based least-squares adaptive controllers suffer a significant reduction in the time-delay margin by a factor of more than 2.

The aircraft responses due to a 0.020 s time delay for the four adaptive controllers are shown in Figs. 10.24, 10.25, 10.26, and 10.27. As shown, the least-squares gradient adaptive controller maintains a very good tracking performance with a 0.020 s time delay. The MRAC and neural network MRAC exhibit high-frequency oscillations. The RLS adaptive controller exhibits low-frequency transients as it is much more robust than the other three adaptive controllers. Thus, overall, the least-squares gradient adaptive controller seems to perform the best among all of the adaptive controllers.

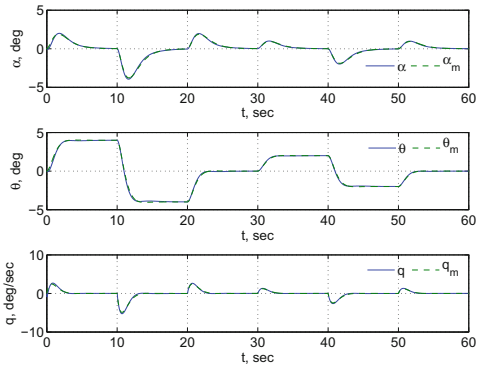

Fig. 10.24 Aircraft response with least-squares gradient with 0.020 s time delay

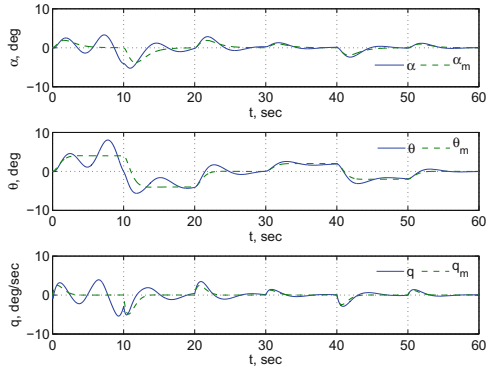

Fig. 10.25 Aircraft response with RLS with 0.020 s time delay ($\eta = 0.2$)

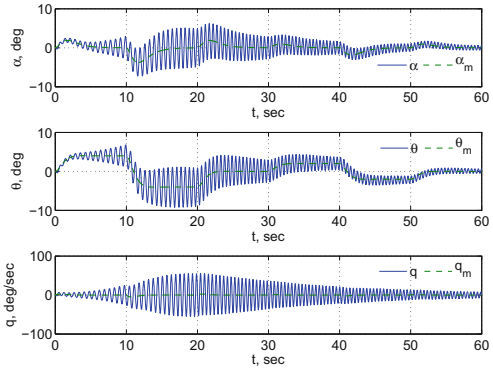

Fig. 10.26 Aircraft response with MRAC with 0.020 s time delay

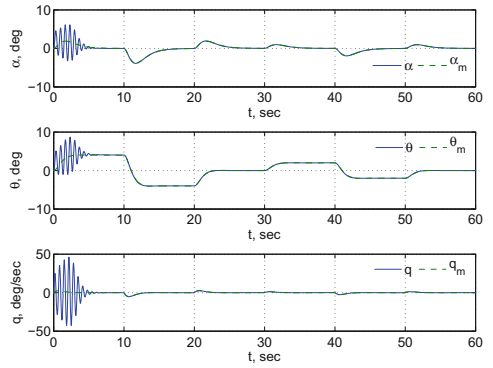

Fig. 10.27 Aircraft response with neural network MRAC with 0.020 s time delay

10.5 Adaptive Control of Flexible Aircraft

Lightweight aircraft design has received a considerable attention in recent years as a means for improving cruise efficiency. Reducing aircraft weight results in lower lift requirement which directly translates into lower drag, hence reduced engine thrust requirement during cruise. The use of lightweight materials such as advanced composite materials has been adopted by airframe manufacturers in many current and future aircraft. Modern lightweight materials can provide less structural rigidity while maintaining the required load-carrying capacity. As structural flexibility increases, aeroelastic interactions with aerodynamic forces and moments become an increasingly important consideration in aircraft design. Understanding aeroelastic effects can improve the prediction of aircraft aerodynamic performance and provide an insight into how to design an aerodynamically efficient flexible airframe to

reduce the fuel consumption. Structural flexibility of airframes can also cause significant aeroelastic interactions that can degrade vehicle stability margins, potentially leading to degraded flying qualities. There exists a trade-off between the desire of having lightweight, flexible structures for weight savings and the need for maintaining sufficient robust stability margins in consideration of flight dynamics, stability, and control.

It is of interest to examine the effect of aeroelasticity on the short-period mode of an aircraft. The aeroelastic effect on an aircraft is assumed to be contributed only by the flexible wing structures. Aeroelastic contributions by the fuselage and tail empennage are assumed to be negligible. For simplicity, only the first symmetric bending mode (1B) and first symmetric torsion mode (1T) are considered. Quasi-steady aerodynamics assumption is invoked to simplify the model. The coupled aeroelastic flight dynamic model of an aircraft that accounts for interactions between wing bending and torsion on aircraft performance and stability in the pitch axis can be expressed in the following state-space form [21]:

$$
\begin{bmatrix} \dot{\alpha} \\ \dot{q} \\ \dot{w}_1 \\ \dot{\theta}_1 \\ \ddot{w}_1 \\ \ddot{\theta}_1 \end{bmatrix} = \begin{bmatrix} -\frac{1}{m_{\alpha\alpha}} C_{L_\alpha} & \frac{1}{m_{\alpha\alpha}} \left(\frac{mV_\infty}{q_\infty S} - \frac{C_{L_q} \bar{c}}{2\bar{V}_\infty} \right) & -\frac{1}{m_{\alpha\alpha}} \frac{C_{L_{w_1}}}{\bar{c}} \\ \frac{1}{m_{qq}} \left(C_{m_\alpha} + \frac{m_{q\alpha}}{m_{\alpha\alpha}} C_{L_\alpha} \right) & \frac{1}{m_{qq}} \left[\frac{C_{m_q} \bar{c}}{2\bar{V}_\infty} + \frac{m_{q\alpha}}{m_{\alpha\alpha}} \left(\frac{C_{L_q} \bar{c}}{2\bar{V}_\infty} - \frac{mV_\infty}{q_\infty S} \right) \right] & \frac{1}{m_{qq}} \left(\frac{C_{m_{w_1}}}{\bar{c}} + \frac{m_{q\alpha}}{m_{\alpha\alpha}} \frac{C_{L_{w_1}}}{\bar{c}} \right) \\ 0 & 0 & 0 \\ 0 & 0 & 0 \\ -\frac{1}{m_{w_1 w_1}} h_{w_1 \alpha} & -\frac{1}{m_{w_1 w_1}} h_{w_1 q} & -\frac{1}{m_{w_1 w_1}} k_{w_1 w_1} \\ -\frac{1}{m_{\theta_1 \theta_1}} h_{\theta_1 \alpha} & -\frac{1}{m_{\theta_1 \theta_1}} h_{\theta_1 q} & -\frac{1}{m_{\theta_1 \theta_1}} k_{\theta_1 w_1} \end{bmatrix}
$$

$$
\begin{bmatrix} -\frac{1}{m_{\alpha\alpha}} C_{L_{\theta_1}} & -\frac{1}{m_{\alpha\alpha}} \frac{C_{L_{\dot{w}_1}}}{\bar{V}_\infty} & -\frac{1}{m_{\alpha\alpha}} \frac{C_{L_{\dot{\theta}_1}} \bar{c}}{2\bar{V}_\infty} \\ \frac{1}{m_{qq}} \left(C_{m_{\theta_1}} + \frac{m_{q\alpha}}{m_{\alpha\alpha}} C_{L_{\theta_1}} \right) & \frac{1}{m_{qq}} \left(\frac{C_{m_{\dot{w}_1}}}{\bar{V}_\infty} + \frac{m_{q\alpha}}{m_{\alpha\alpha}} \frac{C_{L_{\dot{w}_1}}}{\bar{V}_\infty} \right) & \frac{1}{m_{qq}} \left(\frac{C_{m_{\dot{\theta}_1}} \bar{c}}{2\bar{V}_\infty} + \frac{m_{q\alpha}}{m_{\alpha\alpha}} \frac{C_{L_{\dot{\theta}_1}} \bar{c}}{2\bar{V}_\infty} \right) \\ 0 & 1 & 0 \\ 0 & 0 & 1 \\ -\frac{1}{m_{w_1 w_1}} k_{w_1 \theta_1} & -\frac{1}{m_{w_1 w_1}} c_{w_1 w_1} & -\frac{1}{m_{w_1 w_1}} c_{w_1 \theta_1} \\ -\frac{1}{m_{\theta_1 \theta_1}} k_{\theta_1 \theta_1} & -\frac{1}{m_{\theta_1 \theta_1}} c_{\theta_1 w_1} & -\frac{1}{m_{\theta_1 \theta_1}} c_{\theta_1 \theta_1} \end{bmatrix} \begin{bmatrix} \alpha \\ q \\ w \\ \theta \\ \dot{w} \\ \dot{\theta} \end{bmatrix}
$$

$$
+ \begin{bmatrix} -\frac{1}{m_{\alpha\alpha}} C_{L_{\delta_e}} & -\frac{1}{m_{\alpha\alpha}} C_{L_\delta} \\ \frac{1}{m_{qq}} \left(C_{m_{\delta_e}} + \frac{m_{q\alpha}}{m_{\alpha\alpha}} C_{L_{\delta_e}} \right) & \frac{1}{m_{qq}} \left(C_{m_\delta} + \frac{m_{q\alpha}}{m_{\alpha\alpha}} C_{L_\delta} \right) \\ 0 & 0 \\ 0 & 0 \\ 0 & \frac{1}{m_{w_1 w_1}} g_{w_1 \delta_1} \\ 0 & -\frac{1}{m_{w_1 w_1}} g_{\theta_1 \delta_1} \end{bmatrix} \begin{bmatrix} \delta_e \\ \delta_f \end{bmatrix} \tag{10.71}
$$

where $\delta_f\ (t)$ is a symmetric flap control surface deflection on the wing and $m_{\alpha\alpha}, m_{q\alpha}$, and m_{qq} are defined as

$$
m_{\alpha\alpha} = \frac{m\bar{V}_\infty}{q_\infty S} + \frac{C_{L_{\dot{\alpha}}} \bar{c}}{2\bar{V}_\infty} \tag{10.72}
$$

$$
m_{q\alpha} = -\frac{C_{m_{\dot{\alpha}}} \bar{c}}{2\bar{V}_\infty} \tag{10.73}
$$

$$m_{qq} = \frac{I_{YY}}{q_\infty S\bar{c}} \tag{10.74}$$

The subscripts w_1 and θ_1 denote the first bending and first torsion quantities, respectively. The symbols m, c, and k denote the generalized mass, generalized damping which includes both structural and aerodynamic damping, and generalized stiffness, respectively. The subscripts α and q denote the angle of attack and pitch rate, respectively. The symbols h and g denote the generalized forces acting on the wing structure due to the rigid aircraft states $\alpha\,(t)$ and $q\,(t)$ and due to the symmetric flap control surface deflection $\delta_f\,(t)$, respectively.

Example 10.5 Consider a flexible wing aircraft at a midpoint cruise condition of Mach 0.8 and 30,000 ft with 50% fuel remaining. For the configuration with 50% fuel remaining and assuming a structural damping of $\zeta_1 = 0.01$, the A matrix is given by

$$A = \begin{bmatrix} -8.0134 \times 10^{-1} & 9.6574 \times 10^{-1} & 1.2608 \times 10^{-2} & 5.0966 \times 10^{-1} & 5.4634 \times 10^{-4} & -2.4249 \times 10^{-3} \\ -2.4526 \times 10^{0} & -9.1468 \times 10^{-1} & 4.6020 \times 10^{-2} & 2.1726 \times 10^{0} & 3.5165 \times 10^{-3} & -6.2222 \times 10^{-2} \\ 0 & 0 & 0 & 0 & 1 & 0 \\ 0 & 0 & 0 & 0 & 0 & 1 \\ 1.4285 \times 10^{3} & 1.5869 \times 10^{1} & -3.1602 \times 10^{1} & -1.4029 \times 10^{3} & -2.4360 \times 10^{0} & 5.2088 \times 10^{0} \\ -3.9282 \times 10^{2} & -1.8923 \times 10^{0} & 5.6931 \times 10^{0} & -2.8028 \times 10^{2} & 3.2271 \times 10^{-1} & -6.1484 \times 10^{0} \end{bmatrix}$$

The eigenvalues of the short-period mode of the rigid aircraft can be computed from the 2×2 upper left matrix partition of the A matrix. These eigenvalues are stable as shown

$$\lambda_{SP} = -0.8580 \pm 1.5380i$$

The eigenvalues of the 4×4 lower right matrix partition corresponding to the 1B and 1 T modes are also stable as shown

$$\lambda_{1B} = -2.0955 \pm 8.2006i$$

$$\lambda_{1T} = -2.1967 \pm 15.1755i$$

The eigenvalues of the flexible aircraft are also stable, but with a reduced damping in the 1 T mode, as shown

$$\lambda_{SP} = -0.5077 \pm 0.5229i$$

$$\lambda_{1B} = -3.1878 \pm 8.3789i$$

$$\lambda_{1T} = -1.4547 \pm 15.1728i$$

The computed frequencies and damping ratios of the short-period mode, and the 1B and 1 T modes with 50% fuel remaining are shown in Table 10.2. The short-period mode can be seen to be significantly affected by the aeroelastic coupling of the rigid

aircraft flight dynamics with the 1B and 1 T modes. The frequency of the coupled short-period mode is significant reduced, but the damping increases.

Table 10.2 Frequencies and damping ratios at Mach 0.8 and 30,000 ft for flexible aircraft

Mode	Short period	1B	1T
Uncoupled frequency, rad/s	1.761	8.4641	15.3337
Coupled frequency, rad/s	0.7288	8.9648	15.2424
Uncoupled damping ratio	0.4872	0.2476	0.1433
Coupled damping ratio	0.6966	0.3556	0.0954

The frequencies and damping ratios as a function of the airspeed at the same altitude of 30,000 ft are shown in Figs. 10.28 and 10.29. Generally, the frequencies of the short-period mode and 1B mode increase with increasing the airspeed, while the frequency of the 1 T mode decreases precipitously with increasing the airspeed. The divergence speed is the airspeed at which the torsion modal frequency becomes zero.

The damping ratios for both the short-period mode and 1B mode generally increase with increasing airspeed. The damping ratio for the 1 T mode increases with increasing the airspeed up to Mach 0.7 and thereafter decreases rapidly. The flutter speed is the airspeed at which the damping ratio of any aeroelastic modes becomes zero. It is apparent that the 1 T mode would exhibit a zero damping at a flutter speed of about Mach 0.85. The low damping ratio of the 1 T mode can be a problem for aircraft stability. Uncertainty in aeroelastic properties can adversely affect the performance and stability of a flexible aircraft. Active feedback control can potentially help improve the stability margins of the aeroelastic modes.

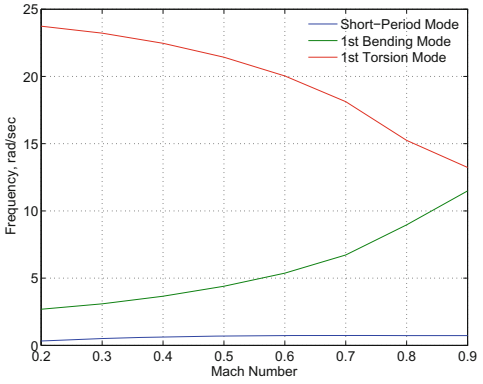

Fig. 10.28 Frequencies of flexible aircraft modes

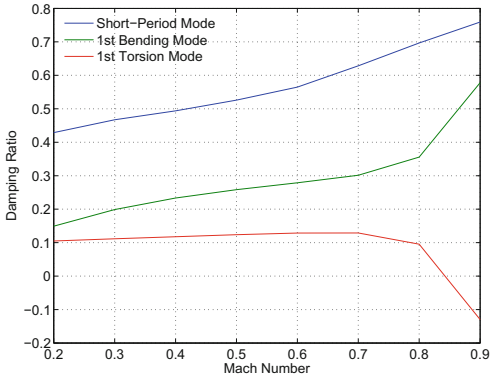

Fig. 10.29 Damping ratios of flexible aircraft modes

■

Consider a linearized model of a flexible aircraft with a matched uncertainty

$$\dot{x} = Ax + B\left[u + \Theta^{*\top}\Phi\left(x_r\right)\right] \tag{10.75}$$

$$x_r = Cx \tag{10.76}$$

where $x(t) \in \mathbb{R}^n$ is a state vector that is composed of a rigid aircraft state vector $x_r(t) \in \mathbb{R}^{n_r}$ and an elastic wing state vector $x_e(t) \in \mathbb{R}^{n_e = n - n_r}$, $u(t) \in \mathbb{R}^m$ is a control vector, $A \in \mathbb{R}^n \times \mathbb{R}^n$ and $B \in \mathbb{R}^n \times \mathbb{R}^m$ are constant and known matrices, $\Theta^* \in \mathbb{R}^{p \times m}$ is a constant and unknown matrix that represents a matched parametric uncertainty in the rigid aircraft state, and $\Phi(x_r) \in \mathbb{R}^p$ is a vector of known regressor functions of the rigid aircraft states.

Assuming that there is a sufficient frequency separation between the "slow" rigid aircraft dynamics and "fast" elastic wing dynamics, then the fast and slow dynamics can be decoupled using the standard singular perturbation method. The fast dynamics of the elastic wing modes are assumed to approach the equilibrium solution infinitely fast. Therefore, the rigid aircraft dynamics with approximately zero-order elastic wing dynamics can be obtained by setting $\dot{x}_e(t) = \varepsilon(x)$, where $\varepsilon(x)$ is a small parameter [22]. Thus,

$$\begin{bmatrix} \dot{x}_r \\ \varepsilon \end{bmatrix} = \begin{bmatrix} A_{rr} & A_{re} \\ A_{er} & A_{ee} \end{bmatrix} \begin{bmatrix} x_r \\ x_e \end{bmatrix} + \begin{bmatrix} B_r \\ B_e \end{bmatrix} \left[u + \Theta^{*\top}\Phi\left(x_r\right)\right] \tag{10.77}$$

Then, the elastic wing dynamics are approximated by

$$x_e = A_{ee}^{-1}\varepsilon(x) - A_{ee}^{-1}A_{er}x_r - A_{ee}^{-1}B_e\left[u + \Theta^{*\top}\Phi(x_r)\right] \tag{10.78}$$

Substituting $x_e(t)$ into the rigid aircraft dynamics yields

$$\dot{x}_r = A_p x_r + B_p\left[u + \Theta^{*\top}\Phi(x_r)\right] + \Delta(x) \tag{10.79}$$

where

$$A_p = A_{rr} - A_{re}A_{ee}^{-1}A_{er} \tag{10.80}$$

$$B_p = B_r - A_{re}A_{ee}^{-1}B_e \tag{10.81}$$

$$\Delta(x) = A_{re}A_{ee}^{-1}\varepsilon(x) \tag{10.82}$$

The term $\Delta(x)$ represents the effect of unmodeled dynamics of the elastic wing modes. The reduced-order plant matrix A_p is assumed to be Hurwitz. Otherwise, an output feedback adaptive control design would be necessary.

The objective is to design an adaptive control that enables the rigid aircraft state vector $x_r(t)$ to tracks a reference model

$$\dot{x}_m = A_m x_m + B_m r \tag{10.83}$$

where $A_m \in \mathbb{R}^{n_r} \times \mathbb{R}^{n_r}$ is a known Hurwitz matrix, $B_m \in \mathbb{R}^{n_r} \times \mathbb{R}^r$ is a known matrix, and $r(t) \in \mathbb{R}^r$ is a piecewise continuous bounded reference command vector.

The adaptive controller is designed with

$$u = K_x x_r + K_r r - \Theta^{\top}\Phi(x_r) \tag{10.84}$$

where $\Theta(t)$ is an estimate of Θ^* and it is assumed that K_x and K_r can be found such that the following model matching conditions are satisfied:

$$A_p + B_p K_x = A_m \tag{10.85}$$

$$B_p K_r = B_m \tag{10.86}$$

Defining the tracking error as $e(t) = x_m(t) - x_r(t)$, then the tracking error equation becomes

$$\dot{e} = A_m e + B\tilde{\Theta}^{\top}\Phi(x_r) - \Delta(x) \tag{10.87}$$

where $\tilde{\Theta}(t) = \Theta(t) - \Theta^*$ is the estimation error.

Because of the presence of unmodeled dynamics, the standard model-reference adaptive law that adjusts $\Theta(t)$ which is given by

$$\dot{\Theta} = -\Gamma \Phi(x_r) e^{\top} P B \tag{10.88}$$

is not robust. As the adaptive gain Γ increases, the adaptive law becomes increasingly sensitive to the unmodeled dynamics $\Delta(x)$ that can lead to instability [17].

To improve robustness to unmodeled dynamics, we use the optimal control modification adaptive law to estimate the unknown parameter Θ^* [19]. The optimal control modification adaptive law is given by

$$\dot{\Theta} = -\Gamma \left[\Phi(x_r) e^{\top} P B - \nu \Phi(x_r) \Phi^{\top}(x_r) \Theta B^{\top} P A_m^{-1} B \right] \tag{10.89}$$

where $\Gamma = \Gamma^{\top} > 0 \in \mathbb{R}^p \times \mathbb{R}^p$ is the adaptation rate matrix, $\nu > 0 \in \mathbb{R}$ is the modification parameter, and P is the solution of the Lyapunov equation

$$P A_m + A_m^{\top} P = -Q \tag{10.90}$$

Alternatively, the adaptive loop recovery modification adaptive law [20] can be used to adjust $\Theta(t)$ as

$$\dot{\Theta} = -\Gamma \left[\Phi(x_r) e^{\top} P B + \eta \frac{d\Phi(x_r)}{dx_r} \frac{d\Phi^{\top}(x_r)}{dx_r} \Theta \right] \tag{10.91}$$

where $\eta > 0 \in \mathbb{R}$ is the modification parameter.

Both the optimal control modification and the adaptive loop recovery modification adaptive laws can also be blended together in a combined adaptive law as follows:

$$\dot{\Theta} = -\Gamma \left[\Phi(x_r) e^{\top} P B - \nu \Phi(x_r) \Phi^{\top}(x_r) \Theta B^{\top} P A_m^{-1} B + \eta \frac{d\Phi(x_r)}{dx_r} \frac{d\Phi^{\top}(x_r)}{dx_r} \Theta \right] \tag{10.92}$$

Example 10.6 The reduced-order model of the flexible aircraft in Example 10.5 that retains only the rigid aircraft states is given by

$$\begin{bmatrix} \dot{\alpha} \\ \dot{q} \end{bmatrix} = \begin{bmatrix} -0.2187 & 0.9720 \\ -0.4053 & -0.8913 \end{bmatrix} \begin{bmatrix} \alpha \\ q \end{bmatrix} + \begin{bmatrix} -0.0651 \\ -3.5277 \end{bmatrix} \left(\delta_e + \begin{bmatrix} \theta_{\alpha}^* & \theta_q^* \end{bmatrix} \begin{bmatrix} \alpha \\ q \end{bmatrix} \right) + \begin{bmatrix} \Delta_{\alpha}(x) \\ \Delta_q(x) \end{bmatrix} + \begin{bmatrix} f_{\alpha}(t) \\ f_q(t) \end{bmatrix}$$

where $\theta^* = 0.4$ and $\theta_q^* = -0.3071$ represent a parametric uncertainty corresponding to a short-period frequency of 1.3247 rad/s and a damping ratio of 0.0199 which is close to neutral pitch stability.

The time-varying functions $f_\alpha(t)$ and $f_q(t)$ are disturbances due to a moderate vertical wind gust modeled by the Dryden turbulence model [14] with a vertical velocity amplitude of about 10 ft/s and a pitch rate amplitude of 1.5 deg/s as shown in Fig. 10.30.

A desired reference model of the pitch attitude is given by

$$\ddot{\theta}_m + 2\zeta\omega_m\dot{\theta}_m + \omega_m^2\theta_m = \omega_n^2 r$$

where $\zeta_m = 0.85$ and $\omega_m = 1.5$ rad/s are chosen to give a desired handling characteristic.

Let $x_r(t) = \left[\alpha(t)\ \theta(t)\ q(t)\right]^\top$, $u(t) = \delta_e(t)$, and $\Theta^{*\top} = \left[\theta_\alpha^*\ 0\ \theta_q^*\right]$. A nominal controller is designed as $\bar{u}(t) = K_x x(t) + k_r r(t)$ where $K_x = -\frac{1}{b_3}\left[a_{31}\ \omega_n^2\ 2\zeta\omega_n + a_{33}\right] = \left[-0.1149\ 0.6378\ 0.4702\right]$ and $k_r = \frac{1}{b_3}\omega_n^2 = -0.6378$. The closed-loop eigenvalues are -0.2112 and $-1.2750 \pm 0.7902i$. The nominal closed-loop plant is then chosen to be the reference model as

$$\underbrace{\begin{bmatrix}\dot{\alpha}_m\\ \dot{\theta}_m\\ \dot{q}_m\end{bmatrix}}_{\dot{x}_m} = \underbrace{\begin{bmatrix}-0.2112 & -0.0415 & 0.9414\\ 0 & 0 & 1\\ 0 & -2.2500 & -2.5500\end{bmatrix}}_{A_m}\underbrace{\begin{bmatrix}\alpha_m\\ \theta_m\\ q_m\end{bmatrix}}_{x_m} + \underbrace{\begin{bmatrix}0.0415\\ 0\\ 2.2500\end{bmatrix}}_{B_m} r$$

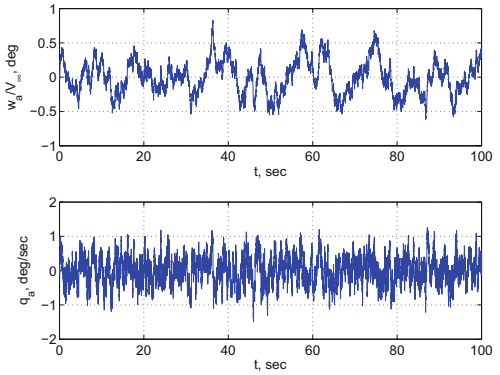

Fig. 10.30 Vertical wind gust model

An adaptation rate $\Gamma = 100I$ is used for the adaptive controller with the input function chosen as $\Phi(x_r) = \left[1\ \alpha\ \theta\ q\right]^\top$ whereby the bias input is needed to handle the time-varying wind gust disturbances.

For the optimal control modification, the modification parameter is set to $\nu = 0.2$. For the adaptive loop recovery modification, the modification parameter is set to $\eta = 0.2$. Also, the Jacobian of the input function $d\Phi(x_r)/dx_r$ is simply an

identity matrix, thereby making the adaptive loop recovery modification effectively a σ modification adaptive law [18].

A pitch attitude doublet is commanded. The response of the flexible aircraft without adaptive control is shown in Fig. 10.31. It is clear that the aircraft response does not track well with the reference model. Moreover, the high-frequency oscillations in the pitch rate response due to the aeroelastic interactions with the bending and torsion modes are highly objectionable from the pilot handing quality perspective.

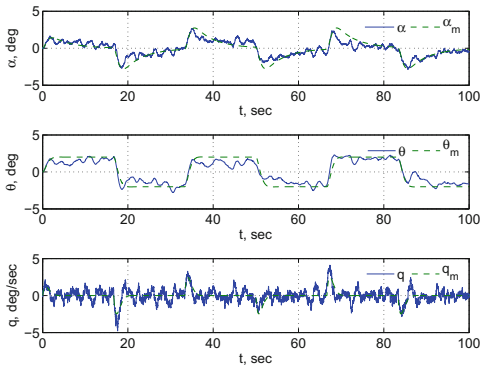

Fig. 10.31 Longitudinal response of flexible aircraft with no adaptive control

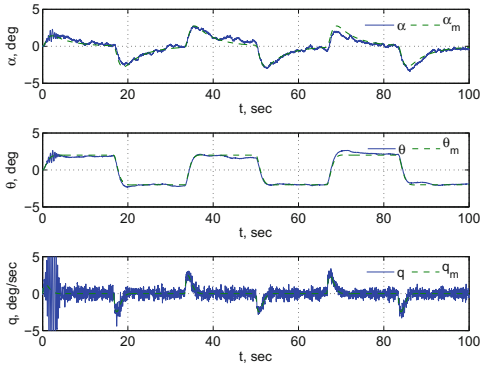

Fig. 10.32 Longitudinal response of flexible aircraft with standard MRAC ($\Gamma = 100I$)

Using the standard model-reference adaptive control (MRAC) by setting $\nu = \eta = 0$, the pitch attitude tracking is much improved as shown in Fig. 10.32. However, the initial transient in the pitch rate is quite large and is characterized by high-frequency oscillations in the pitch rate response.

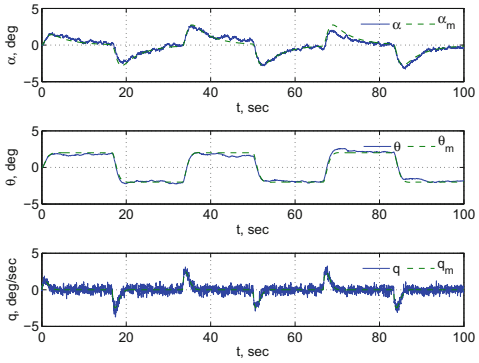

Fig. 10.33 Longitudinal response of flexible aircraft with optimal control modification (OCM) ($\Gamma = 100I$, $\nu = 0.2$)

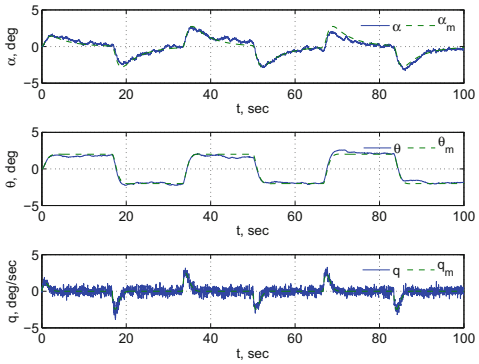

Fig. 10.34 Longitudinal response of flexible aircraft with adaptive loop recovery modification (ALR) ($\Gamma = 100I$, $\eta = 0.2$)

In contrast, Fig. 10.33 shows that the optimal control modification adaptive law is able to suppress the large initial transient of the pitch rate and the amplitude of the high-frequency oscillations. The response of the aircraft due to the adaptive loop recovery modification adaptive law as shown in Fig. 10.34 is very similar to that with the optimal control modification adaptive law.

The aeroelastic wing tip bending deflection and torsional twist are shown in Figs. 10.35 and 10.36 for the four different controllers: baseline nominal controller, standard MRAC, optimal control modification, and adaptive loop recovery modification. The aeroelastic wing is modeled to be rather flexible to demonstrate the aeroelastic effects on adaptive control. The rigid aircraft pitch attitude command and wind gust result in a bending deflection amplitude of 5 ft and a torsional twist amplitude of about 3 deg at the wing tip. The aeroelastic deflections are quite significant since the flight condition at Mach 0.8 is approaching the flutter speed at Mach

0.85. It is noted that the standard MRAC results in a very large initial transient of the torsional twist. This large torsional twist is clearly not realistic and in practice would result in excessive wing loading and wing stall. These effects are not taken into account in the simulations. Nonetheless, this illustrates the undesirable behavior of the standard MRAC in the flight control implementation for flexible aircraft.

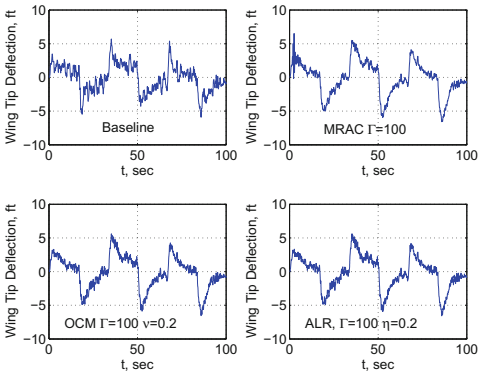

Fig. 10.35 Wing tip deflection of first bending mode

Figure 10.37 is the plot of the elevator deflections for the four controllers. The standard MRAC produces a significant control saturation during the initial transient. This saturation leads to an undesirable rigid aircraft response and aeroelastic deflections. Both the optimal control modification and adaptive loop recovery modification adaptive laws produce quite similar elevator deflections. Also, it is observed that the elevator deflection for the baseline controller has a lower-frequency content than those corresponding to the optimal control modification and adaptive loop recovery modification adaptive laws. This indicates that the adaptive controllers effectively account for the aeroelastic wing dynamics in the elevator deflection commands to suppress the responses of the aeroelastic wing modes, whereas the baseline controller has no knowledge of the effect of the aeroelastic wing dynamics.

This study shows that adaptive control can be used to accommodate uncertainty for flexible aircraft. The effect of aeroelasticity is captured in the reduced-order model as unmodeled dynamics. The results show that the standard MRAC is neither sufficiently robust nor able to produce well-behaved control signals. Excessive torsional twist and control saturation due to the standard MRAC are noted. Both the optimal control modification and adaptive loop recovery modification adaptive laws are seen to be more effective in reducing the tracking error while maintaining the aeroelastic deflections to within reasonable levels.

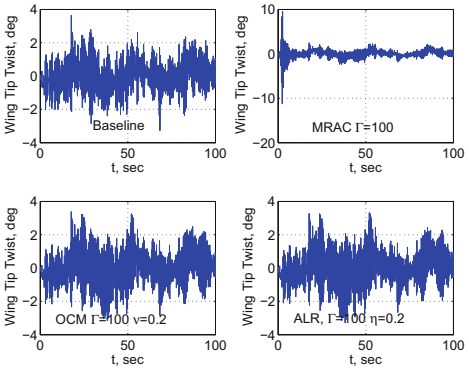

Fig. 10.36 Wing tip twist of first torsion mode

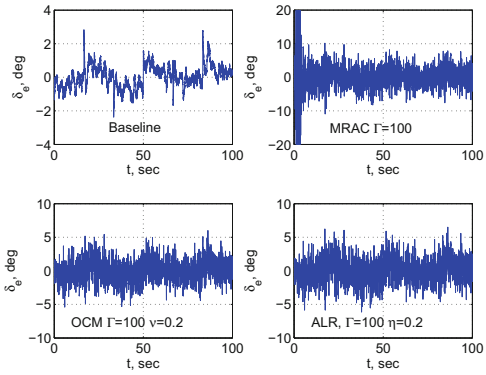

Fig. 10.37 Elevator deflection

10.6 Adaptive Linear Quadratic Gaussian Flutter Suppression Control

Flutter is a structural dynamic phenomenon in aircraft flight dynamics that manifests itself as an aeroelastic instability which can result in structural failures. Aircraft are designed to ensure that their flutter boundaries are far away from their flight envelopes. As modern aircraft begin to employ lightweight materials in aircraft structures for improved fuel efficiency, increased aeroelastic interactions and reduced flutter margins become a definite possibility. Active flutter suppression control is a structural feedback control that suppresses structural vibration and increases aeroelastic stability of aircraft structures. This study illustrates an application of adaptive augmentation Linear Quadratic Gaussian (LQG) control for flutter suppression for a new type of aircraft flight control surfaces. Optimal control modification adaptive law will be used as the adaptive augmentation controller.

In the recent years, NASA has developed a new type of aircraft flight control surfaces called the Variable Camber Continuous Trailing Edge Flap (VCCTEF) [23–25]. The VCCTEF, illustrated in Fig. 10.38, is a wing shaping control device designed to reshape a flexible aircraft wing in-flight to improve the aerodynamic performance while suppressing any adverse aeroelastic interactions. It employs three chordwise flap segments to provide a variable camber to change the wing shape for increasing the aerodynamic performance. The flap is also made up of individual spanwise sections which enable different flap settings at each flap spanwise position. This results in the ability to control the wing shape as a function of the wing span, thereby resulting in a change to the wing twist to establish the best lift-to-drag ratio at any aircraft gross weight or mission segment. The individual spanwise flap sections are connected with a flexible elastomer material to form a continuous trailing edge with no flap gaps in the wing planform for drag and noise reduction purposes.

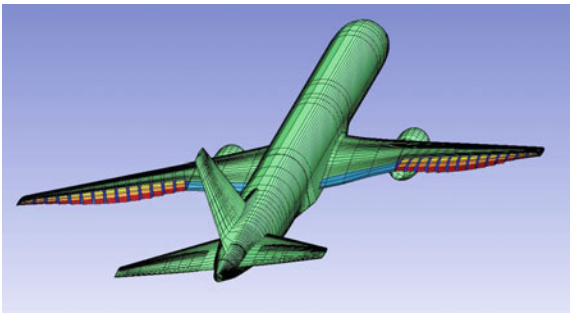

Fig. 10.38 Variable camber continuous trailing edge flap concept

Consider a notional aircraft equipped with highly flexible wings. The flexibility of modern transport wings can cause a reduction in the flutter margin which can compromise the stability of an aircraft. A flutter analysis is conducted to examine the effect of the increased flexibility of a conventional aircraft wing based on a NASA Generic Transport Model (GTM) [26]. The baseline stiffness of the GTM wing is reduced by 50%. This configuration is referred to as the flexible wing GTM. The flutter analysis computes the aeroelastic frequencies and damping ratios over a range of the airspeed as shown in Figs. 10.39 and 10.40 [27]. When the damping ratio of an aeroelastic mode encounters a zero crossing, a flutter speed is noted. The lowest flutter speed establishes a flutter boundary.

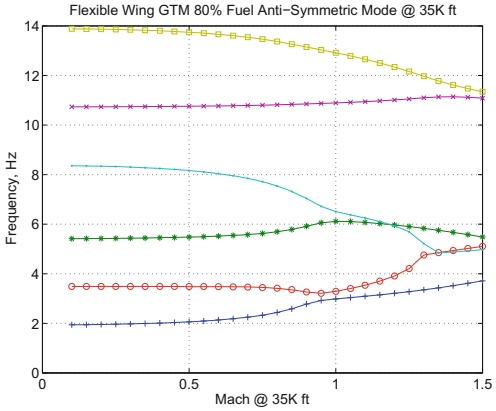

Fig. 10.39 Natural frequencies of antisymmetric modes of flexible wing GTM

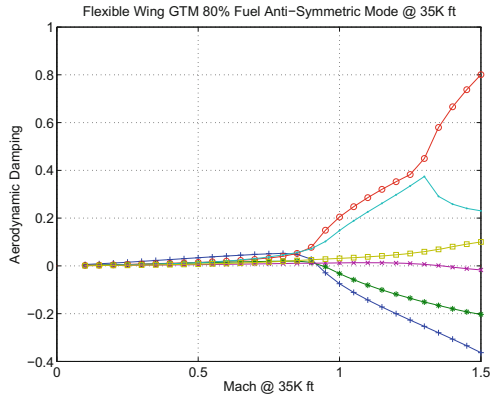

Fig. 10.40 Damping ratios of antisymmetric modes of flexible wing GTM

Table 10.3 shows the flutter speed prediction at 35,000 ft for the stiff wing GTM and the flexible wing GTM. The critical flutter mode is an antisymmetric mode. The flutter boundary is significantly reduced by 31% with the flexible wing GTM.

The FAA (Federal Aviation Administration) requires the aircraft certification to demonstrate a flutter margin of at least 15% above the dive speed which is normally determined from flight testing. For a maximum operating Mach 0.8, the dive speed may be estimated to be about 15% over the maximum operating Mach, or Mach 0.92. Thus, the flutter clearance for this notional aircraft would require a minimum flutter speed of Mach 1.06 at 35,000 ft. The stiff wing GTM meets this flutter clearance, but the flexible wing GTM does not. To increase the flutter speed, active flutter suppression is an option. Currently, active flutter suppression has not been certified for transport aircraft, but this situation may change as the FAA has begun to investigate

certification requirements for active flutter suppression control for commercial transport aircraft.

Table 10.3 Flutter speed prediction

	Symmetric mode	Antisymmetric mode
Flutter Mach @ 35K ft (Stiff Wing)	1.358	1.310
Flutter Mach @ 35K ft (Flexible Wing)	0.938	0.925

Consider a general aeroservoelastic (ASE) state-space model of the form

$$\begin{bmatrix} \dot{\eta} \\ \dot{\mu} \end{bmatrix} = \begin{bmatrix} A_{11} & A_{12} \\ A_{21} & A_{22} \end{bmatrix} \begin{bmatrix} \eta \\ \mu \end{bmatrix} + \begin{bmatrix} B_{11} & B_{12} & B_{13} \\ B_{21} & B_{22} & B_{23} \end{bmatrix} \begin{bmatrix} \delta \\ \dot{\delta} \\ \ddot{\delta} \end{bmatrix} \tag{10.93}$$

$$y = C_1\eta + C_2\mu + D_1\delta + D_2\dot{\delta} + D_3\ddot{\delta} \tag{10.94}$$

where $\mu(t)$ is a fast state vector that contains the generalized aeroelastic states for high-frequency aeroelastic modes, $\eta(t)$ is a slow state vector that contains the generalized aeroelastic states for lower-frequency aeroelastic modes as well as the rigid aircraft states, $\delta(t)$ is the control surface deflection vector, and $y(t)$ is the output vector.

Note that the aeroelastic states are dependent on the velocity and acceleration of the control surface deflection vector $\delta(t)$. This dependency is usually neglected in rigid aircraft flight dynamics, but can be significant in aeroservoelasticity especially for flutter suppression.

The quality of fast and slow states can be examined by the eigenvalues of the partitioned matrices A_{11} and A_{22}. Since $\mu(t)$ is a fast state vector, then we can write $\varepsilon \|A_{11}\| < \|A_{22}\|$, where ε is a small quantity.

In general, an ASE state-space model contains both the rigid aircraft modes, which usually have low frequencies, and the aeroelastic modes which are at much higher frequencies than the rigid aircraft modes. Flutter modes are usually associated with those aeroelastic modes in the low-frequency range. As a result, high-frequency aeroelastic modes normally do not participate in a flutter response. In a control design, it is usually expedient to remove high-frequency modes in order to simplify a controller design. By removing the high-frequency aeroelastic modes, the ASE state-space model is reduced in the model order. We will employ the singular perturbation method to reduce the order of an ASE state-space model [28]. The advantage of the singular perturbation method is that the physical modes are properly retained for a flutter suppression control design.

Using the singular perturbation approach, the fast and slow dynamics can be decoupled. To decouple the fast and slow states, we perform a time scale separation

by applying the singular perturbation method. Toward that end, we consider the usual slow or stretched time transformation

$$\tau = \varepsilon t \tag{10.95}$$

where τ is a slow time variable.

Then, the fast and slow state-space models are transformed into a singularly perturbed system as

$$\dot{\eta} = A_{11}\eta + A_{12}\mu + B_{11}\delta + B_{12}\dot{\delta} + B_{13}\ddot{\delta} \tag{10.96}$$

$$\varepsilon\frac{d\mu}{d\tau} = A_{21}\eta + A_{22}\mu + B_{21}\delta + B_{22}\dot{\delta} + B_{23}\ddot{\delta} \tag{10.97}$$

The Tikhonov's theorem can be used to approximate the solution of the singularly perturbed system with the solution of a "reduced-order" system by setting $\varepsilon = 0$ [22]. Thus, the reduced-order system is given by

$$\dot{\eta}_0 = A_{11}\eta_0 + A_{12}\mu_0 + B_{11}\delta + B_{12}\dot{\delta} + B_{13}\ddot{\delta} \tag{10.98}$$

$$A_{21}\eta_0 + A_{22}\mu_0 + B_{21}\delta + B_{22}\dot{\delta} + B_{23}\ddot{\delta} = 0 \tag{10.99}$$

where $\eta_0(\tau)$ and $\mu_0(\tau)$ are the "outer" solution of the singularly perturbed system.

The term "outer" is in connection with the concept of "inner" or "boundary layer" and "outer" solutions which have the origin in the boundary layer theory due to Prandtl. The "inner" or "boundary layer" solution for this system is obtained from

$$A_{11}\eta_i + A_{12}\mu_i + B_{11}\delta + B_{12}\dot{\delta} + B_{13}\ddot{\delta} = 0 \tag{10.100}$$

$$\dot{\mu}_i = A_{21}\eta_i + A_{22}\mu_i + B_{21}\delta + B_{22}\dot{\delta} + B_{23}\ddot{\delta} \tag{10.101}$$

The solution is then expressed as

$$\eta = \eta_0 + \eta_i - \eta_{MAE} \tag{10.102}$$

$$\mu = \mu_0 + \mu_i - \mu_{MAE} \tag{10.103}$$

where $\eta_{MAE}(t)$ and $\mu_{MAE}(t)$ are correction terms by a matched asymptotic expansion method applied to both the inner and outer solutions [29]. The outer solution is in fact the asymptotic solution of the original system as $t \to \infty$.

Since the asymptotic behavior of a closed-loop system is an important consideration for stability implication, the outer solution of the singularly perturbed system is of significant importance. Thus, we obtain the outer solution as the reduced-order model using only the outer solution of the slow state vector $\eta_0(t)$ as

$$\dot{\eta}_0 = \left(\underbrace{A_{11} - A_{12}A_{22}^{-1}A_{21}}_{\bar{A}_{11}} \right) \eta_0 + \left[\underbrace{B_{11} - A_{12}A_{22}^{-1}B_{21}}_{\bar{B}_{11}} \; \underbrace{B_{12} - A_{12}A_{22}^{-1}B_{22}}_{\bar{B}_{12}} \; \underbrace{B_{13} - A_{21}A_{22}^{-1}B_{23}}_{\bar{B}_{13}} \right] \begin{bmatrix} \delta \\ \dot{\delta} \\ \ddot{\delta} \end{bmatrix} + \Delta\dot{\eta}_0 \tag{10.104}$$

$$y = \left(\underbrace{C_1 - C_2A_{22}^{-1}A_{21}}_{\bar{C}_1} \right) \eta_0 + \left(\underbrace{D_1 - C_2A_{22}^{-1}B_{21}}_{\bar{D}_1} \right) \delta + \left(\underbrace{D_2 - C_2A_{22}^{-1}B_{22}}_{\bar{D}_2} \right) \dot{\delta} + \left(\underbrace{D_3 - C_2A_{22}^{-1}B_{23}}_{\bar{D}_3} \right) \ddot{\delta} + \Delta y \tag{10.105}$$

We will use the slow state vector $\eta_0(t)$ as the approximation of the actual slow state vector $\eta(t)$.

Now, consider a simplified second-order actuator model

$$\ddot{\delta} + 2\zeta\omega_n\dot{\delta} + \omega_n^2\delta = \omega_n^2\delta_c \tag{10.106}$$

The state-space representation then becomes

$$\underbrace{\begin{bmatrix} \dot{\eta} \\ \dot{\delta} \\ \ddot{\delta} \end{bmatrix}}_{\dot{x}} = \underbrace{\begin{bmatrix} \bar{A}_{11} & \bar{B}_{11} - \bar{B}_{13}\omega_n^2 & \bar{B}_{12} - 2\bar{B}_{13}\zeta\omega_n \\ 0 & 0 & I \\ 0 & -\omega_n^2 & -2\zeta\omega_n \end{bmatrix}}_{A} \underbrace{\begin{bmatrix} \eta \\ \delta \\ \dot{\delta} \end{bmatrix}}_{x} + \underbrace{\begin{bmatrix} \bar{B}_{13}\omega_n^2 \\ 0 \\ \omega_n^2 \end{bmatrix}}_{B} \underbrace{\delta_c}_{u} + \underbrace{\begin{bmatrix} \Delta\dot{\eta} \\ 0 \\ 0 \end{bmatrix}}_{\Delta\dot{x}} \tag{10.107}$$

$$y = \underbrace{\begin{bmatrix} \bar{C}_1 & \bar{D}_1 - \bar{D}_3\omega_n^2 & \bar{D}_2 - 2\bar{D}_3\zeta\omega_n \end{bmatrix}}_{C} \underbrace{\begin{bmatrix} \eta \\ \delta \\ \dot{\delta} \end{bmatrix}}_{x} + \underbrace{\bar{D}_3\omega_n^2}_{D} \underbrace{\delta_c}_{u} + \Delta y \tag{10.108}$$

which can be expressed in the canonical form

$$\dot{x} = Ax + Bu + \Delta \tag{10.109}$$

$$y = Cx + Du \tag{10.110}$$

where Δ is the residual high-order dynamics of the high-frequency aeroelastic modes.

Example 10.7 To illustrate the model reduction, the ASE state-space models with 22 modes at various flight conditions are developed for the flexible wing GTM roll dynamics coupled to the wing antisymmetric modes [30]. The open-loop ASE model has two unstable modes at Mach 0.86 and an altitude of 10,000 ft. Using the model reduction method above, it can be shown in Table 10.4 that a reduced-order model using only the first 8 modes can capture all the unstable modes and approximate the first 6 modes of the higher-order ASE model quite well [28].

Table 10.4 Antisymmetric modes of ESAC wing @ Mach 0.86 and Altitude 10,000 ft

Mode	$n = 6$	$n = 7$	$n = 8$	$n = 22$ (Full)
Rigid	-2.7392	-2.7395	-2.7385	-2.7385
1	$2.7294 \pm 19.8683i$	$2.7512 \pm 19.8529i$	$2.7804 \pm 19.8561i$	$2.7842 \pm 19.8513i$
2	$-0.1553 \pm 24.3565i$	$-0.1557 \pm 24.3562i$	$-0.1547 \pm 24.3553i$	$-0.1549 \pm 24.3552i$
3	$-6.3434 \pm 24.0892i$	$-6.3272 \pm 24.0739i$	$-6.4220 \pm 23.9949i$	$-6.4174 \pm 23.9920i$
4	$-0.3902 \pm 37.1580i$	$-0.3782 \pm 37.1461i$	$0.0571 \pm 37.4423i$	$0.0584 \pm 37.4846i$
5	$-20.0160 \pm 32.3722i$	$-20.2813 \pm 32.3013i$	$-20.4217 \pm 32.4999i$	$-20.4833 \pm 32.5445i$

■

Suppose we introduce an uncertainty into the nominal ASE state-space model as

$$\dot{x} = (A + \Delta A)\, x + (B + \Delta B)\, u \tag{10.111}$$

$$y = Cx + Du \tag{10.112}$$

where $A \in \mathbb{R}^n \times \mathbb{R}^n$, $B \in \mathbb{R}^n \times \mathbb{R}^m$, $C \in \mathbb{R}^p \times \mathbb{R}^n$, $D \in \mathbb{R}^p \times \mathbb{R}^m$ with $p \geq m$, $\Delta A = \delta_A A$, and $\Delta B = \delta_B B$ are known perturbations of the A and B matrices, and δ_A and δ_B are assumed to be small parameters that represent multiplicative model variations.

Observer state feedback control based on output measurements is generally used for flutter suppression control since the full-state information is not measurable. The idea is to design an adaptive augmentation controller that is robust to the perturbation in the nominal plant model due to the model variation. Toward that end, we assume the pair (A, B) is controllable, and the pair (A, C) is observable.

In general, output feedback adaptive control of MIMO systems can be quite difficult. The SPR condition for a system transfer function matrix is required as is the case with a SISO system for stable adaptive control. In general, the system transfer function matrix from $u(t)$ to $y(t)$ can be non-square, hence non-SPR, if the number of inputs and the number of outputs are different. The Kalman–Yakubovich lemma [31] can be used to determine whether the transfer function $G(s) = C(sI - A)^{-1} B$ is SPR by the following conditions:

$$PA + A^{\top} P = -Q \tag{10.113}$$

$$PB = C^{\top} \tag{10.114}$$

for any $P = P^{\top} > 0$ and $Q = Q^{\top} > 0$.

Equation (10.114) leads to the following necessary and sufficient condition for a SPR transfer function matrix [32]:

$$B^{\top} PB = B^{\top} C^{\top} = CB > 0 \tag{10.115}$$

Therefore, the condition $CB > 0$ requires CB to be a symmetric positive-definite square matrix. This condition requires as a minimum that rank $(CB) = m$. This implies that the number of inputs is equal to number of outputs. If the numbers of inputs and outputs are not equal, we will assume that the number of outputs is greater than the number of inputs m. This condition will lead to an easier output feedback adaptive control design by employing various methods of squaring up a non-square matrix [33, 34]. These methods are used in a number of adaptive output feedback control approaches such as the observer state feedback adaptive control method by Lavretsky and Wise [35].

As shown in Sects. 9.13 and 9.14, the optimal control modification method can be used to control non-SPR SISO systems with non-minimum phase behaviors or with relative degree greater than 1. We will extend this approach to MIMO systems by taking advantage of the linear asymptotic property of the optimal control modification.

The LQG method is a standard technique for control design of systems with output or partial-state information. A Luenberger state observer is constructed to estimate the nominal plant model using the Kalman filter optimal estimation method as

$$\dot{\hat{x}} = A\hat{x} + L\left(y - \hat{y}\right) + Bu \tag{10.116}$$

where $\hat{x}(t)$ is the observer state vector, L is the Kalman filter gain, and $\hat{y}(t)$ is the observer output given by

$$\hat{y} = C\hat{x} + Du \tag{10.117}$$

A loop transfer recovery technique can be applied to improved the closed-loop stability margin of the observer system.

We employ the separation principle of control and estimation by invoking an assumption that a full-state feedback design provides a stabilizing controller for the observer system.

Consider an ideal full-state observer controller

$$u^* = K_x^* \hat{x} + K_y^* \left(y - \hat{y}\right) + K_r^* r \tag{10.118}$$

The ideal closed-loop observer model is then expressed as

$$\dot{\hat{x}} = A\hat{x} + L\left(y - \hat{y}\right) + BK_x^* \hat{x} + BK_y^* \left(y - \hat{y}\right) + BK_r^* r \tag{10.119}$$

The objective is to design a closed-loop full-state observer model that track a reference model

$$\dot{x}_m = A_m x_m + B_m r \tag{10.120}$$

where

$$A + BK_x^* = A_m \tag{10.121}$$

$$BK_r^* = B_m \tag{10.122}$$

$$BK_y^* = -L \tag{10.123}$$

Then, the adaptive controller is designed as

$$u = K_x(t)\,\hat{x} + K_y(t)\left(y - \hat{y}\right) + K_r(t)\,r \tag{10.124}$$

Let $\tilde{K}_x(t) = K_x(t) - K_x^*$, $\tilde{K}_y(t) = K_y(t) - K_y^*$, and $\tilde{K}_r(t) = K_r(t) - K_r^*$ be the estimation errors of $K_x(t)$, $K_y(t)$, and $K_r(t)$, respectively. Then, the closed-loop plant is written as

$$\dot{\hat{x}} = A_m\hat{x} + B_m r + B\tilde{K}_x\hat{x} + B\tilde{K}_y\left(y - \hat{y}\right) + B\tilde{K}_r r \tag{10.125}$$

Let $e_p(t) = x(t) - \hat{x}(t)$ be the state estimation error. Then, the state estimation error equation is computed as

$$\dot{e}_p = A_p e_p + \Delta A\left(e_p + \hat{x}\right) + \Delta B\left(K_x\hat{x} + K_y C e_p + K_r r\right) \tag{10.126}$$

where $A_p = A - LC$ is Hurwitz.

Let $e(t) = x_m(t) - \hat{x}(t)$ be the tracking error, then the tracking equation is expressed as

$$\dot{e} = A_m e - B\tilde{K}_x\hat{x} - B\tilde{K}_y C e_p - B\tilde{K}_r r \tag{10.127}$$

The adaptive laws for $K_x(t)$, $K_y(t)$, and $K_r(t)$ using the optimal control modification [28] are given by

$$\dot{K}_x^\top = \Gamma_x\hat{x}\left(e^\top P + \nu_x\hat{x}^\top K_x^\top B^\top P A_m^{-1}\right)B \tag{10.128}$$

$$\dot{K}_y^\top = \Gamma_y\left(y - \hat{y}\right)\left[e^\top P + \nu_y\left(y - \hat{y}\right)^\top K_y^\top B^\top P A_m^{-1}\right]B \tag{10.129}$$

$$\dot{K}_r^\top = \Gamma_r r\left(e^\top P + \nu_r r^\top K_r^\top B^\top P A_m^{-1}\right)B \tag{10.130}$$

with the initial conditions $K_x(0) = \bar{K}_x$, $K_y(0) = \bar{K}_y$, and $K_r(0) = \bar{K}_r$, where $\Gamma_x = \Gamma_x^\top > 0$, $\Gamma_y = \Gamma_y^\top > 0$, and $\Gamma_r = \Gamma_r^\top > 0$ are the adaptation rate matrices; $\nu_x > 0$ $\nu_y > 0$, and $\nu_r > 0$ are the modification parameters; and $P = P^\top > 0$ is the solution of the Lyapunov equation

$$PA_m + A_m^\top P + Q = 0 \tag{10.131}$$

where $Q = Q^\top > 0$.

As discussed in Sect. 9.14, if the reference model is SPR and the plant is non-SPR, then an adaptive control design with the standard MRAC is infeasible unless the reference model is modified to be non-SPR from the ideal control design for the non-SPR plant. The optimal control modification has been shown to be able to handle non-SPR plants with either SPR or non-SPR reference models. For an adaptive augmentation design, the robust baseline controller can also serve to reduce the sensitivity of the closed-loop plant to the non-minimum phase behavior if a robust modification or the projection method is used.

Consider an adaptive augmentation regulator design with the following adaptive controller:

$$u = \bar{K}_x\hat{x} + \Delta K_x\hat{x} + K_y\left(y - \hat{y}\right) \tag{10.132}$$

where $\bar{K}_x$ is obtained from the Linear Quadratic Regulator (LQR) design of the full-state equation, and the adaptive laws for $\Delta K_x(t)$ and $K_y(t)$ are given by

$$\Delta\dot{K}_x^\top = -\Gamma_x\hat{x}\hat{x}^\top\left(P - \nu_x\Delta K_x^\top B^\top P A_m^{-1}\right)B \tag{10.133}$$

$$\dot{K}_y^\top = -\Gamma_y\left(y - \hat{y}\right)\left[\hat{x}^\top P - \nu_y\left(y - \hat{y}\right)^\top K_y^\top B^\top P A_m^{-1}\right]B \tag{10.134}$$

The adaptive laws can be shown to be stable as follows:

Proof Choose a Lyapunov candidate function

$$V\left(\hat{x}, e_p, \Delta\tilde{K}_x, \tilde{K}_y\right) = \hat{x}^\top P\hat{x} + e_p^\top W e_p + \text{trace}\left(\Delta\tilde{K}_x \Gamma_x^{-1} \Delta\tilde{K}_x^\top\right) + \text{trace}\left(\tilde{K}_y \Gamma_y^{-1} \tilde{K}_y^\top\right) \tag{10.135}$$

where

$$WA_p + A_p^\top W = -R < 0 \tag{10.136}$$

Then, evaluating $\dot{V}\left(\hat{x}, e_p, \Delta\tilde{K}_x, \tilde{K}_y\right)$ yields

$$\begin{aligned}
&\dot{V}\left(\hat{x}, e_p, \Delta\tilde{K}_x, \tilde{K}_y\right) \\
&= -\hat{x}^\top Q\hat{x} - e_p^\top R e_p + 2e_p^\top W\Delta A\left(e_p + \hat{x}\right) + 2e_p^\top W\Delta B\left(\bar{K}_x\hat{x} + \Delta K_x\hat{x} + K_y C e_p\right) \\
&\quad + 2\nu_x\hat{x}^\top\Delta K_x^\top B^\top P A_m^{-1} B\Delta\tilde{K}_x\hat{x} + 2\nu_y e_p^\top C^\top K_y^\top B^\top P A_m^{-1} B\tilde{K}_y C e_p \\
&= -\hat{x}^\top Q\hat{x} - e_p^\top R e_p - \nu_x\hat{x}^\top\Delta\tilde{K}_x^\top B^\top A_m^{-\top} Q A_m^{-1} B\Delta\tilde{K}_x\hat{x} \\
&\quad - \nu_y e_p^\top C^\top\tilde{K}_y^\top B^\top A_m^{-\top} Q A_m^{-1} B\tilde{K}_y C e_p + 2\nu_x\hat{x}^\top\Delta K_x^{*\top} B^\top P A_m^{-1} B\Delta\tilde{K}_x\hat{x} \\
&\quad + 2\nu_y e_p^\top C^\top K_y^{*\top} B^\top P A_m^{-1} B\tilde{K}_y C e_p \\
&\quad + 2e_p^\top W\left(\underbrace{\Delta A + \Delta B K_y^* C}_{\Delta A_p}\right) e_p \\
&\quad + 2e_p^\top W\left(\underbrace{\Delta A + \Delta B\bar{K}_x + \Delta B\Delta K_x^*}_{\Delta A_m}\right)\hat{x} + 2e_p^\top W\Delta B\Delta\tilde{K}_x\hat{x} + 2e_p^\top W\Delta B\tilde{K}_y C e_p
\end{aligned} \tag{10.137}$$

$\dot{V}\left(\hat{x}, e_p, \Delta\tilde{K}_x, \tilde{K}_y\right)$ is bounded by

$$\begin{aligned}
\dot{V}\left(\hat{x}, e_p, \Delta\tilde{K}_x, \tilde{K}_y\right) \leq &- c_1\left\|\hat{x}\right\|^2 - \nu_x c_2\left\|\hat{x}\right\|^2\left\|\Delta\tilde{K}_x\right\|^2 \\
&+ 2\nu_x c_2 c_3\left\|\hat{x}\right\|^2\left\|\Delta\tilde{K}_x\right\| - (c_4 - 2c_7)\left\|e_p\right\|^2 \\
&- \nu_y c_5\left\|e_p\right\|^2\left\|\tilde{K}_y\right\|^2 + 2\nu_y c_5 c_6\left\|e_p\right\|^2\left\|\tilde{K}_y\right\| + 2c_8\left\|\hat{x}\right\|\left\|e_p\right\| \\
&+ 2c_9\left\|\hat{x}\right\|\left\|e_p\right\|\left\|\Delta\tilde{K}_x\right\| + 2c_{10}\left\|e_p\right\|^2\left\|\tilde{K}_y\right\|
\end{aligned} \tag{10.138}$$

where $c_1 = \lambda_{min}(Q)$, $c_2 = \lambda_{min}\left(B^\top A_m^{-\top} Q A_m^{-1} B\right)$, $c_3 = \frac{\left\|B^\top P A_m^{-1} B\right\|\left\|\Delta K_x^*\right\|}{c_2}$, $c_4 = \lambda_{min}(R)$, $c_5 = c_2\|C\|^2$, $c_6 = \frac{\left\|B^\top P A_m^{-1} B\right\|\left\|K_y^*\right\|\|C\|}{c_5}$, $c_7 = \left\|W\Delta A_p\right\|$, $c_8 = \|W\Delta A_m\|$, $c_9 = \|W\Delta B\|$, and $c_{10} = c_9\|C\|$.

Using the inequality $2\|a\|\|b\| \leq \|a\|^2 + \|b\|^2$, we obtain

$$\dot{V}\left(\hat{x}, e_p, \Delta\tilde{K}_x, \tilde{K}_y\right) \leq -(c_1 - c_8)\left\|\hat{x}\right\|^2 - (\nu_x c_2 - c_9)\left\|\hat{x}\right\|^2\left\|\Delta\tilde{K}_x\right\|^2 + 2\nu_x c_2 c_3\left\|\hat{x}\right\|^2\left\|\Delta\tilde{K}_x\right\| - (c_4 - 2c_7 - c_8 - c_9)\left\|e_p\right\|^2 - \nu_y c_5\left\|e_p\right\|^2\left\|\tilde{K}_y\right\|^2 + 2\left(\nu_y c_5 c_6 + c_{10}\right)\left\|e_p\right\|^2\left\|\tilde{K}_y\right\| \tag{10.139}$$

With further simplification, we get

$$\dot{V}\left(\hat{x}, e_p, \Delta\tilde{K}_x, \tilde{K}_y\right) \leq -\left(c_1 - c_8 - \frac{\nu_x^2 c_2^2 c_3^2}{\nu_x c_2 - c_9}\right)\left\|\hat{x}\right\|^2 - (\nu_x c_2 - c_9)\left\|\hat{x}\right\|^2\left(\left\|\Delta\tilde{K}_x\right\| - \frac{\nu_x c_2 c_3}{\nu_x c_2 - c_9}\right)^2 - \left[c_4 - 2c_7 - c_8 - c_9 - \frac{\left(\nu_y c_5 c_6 + c_{10}\right)^2}{\nu_y c_5}\right]\left\|e_p\right\|^2 - \nu_y c_5\left\|e_p\right\|^2\left(\left\|\tilde{K}_y\right\|^2 - \frac{\nu_y c_5 c_6 + c_{10}}{\nu_y c_5}\right)^2 \tag{10.140}$$

We choose Q, R, ν_x, and ν_y to satisfy the following inequalities:

$$c_1 - c_8 - \frac{\nu_x^2 c_2^2 c_3^2}{\nu_x c_2 - c_9} > 0 \tag{10.141}$$

$$\nu_x c_2 - c_9 > 0 \tag{10.142}$$

$$c_4 - 2c_7 - c_8 - c_9 - \frac{\left(\nu_y c_5 c_6 + c_{10}\right)^2}{\nu_y c_5} > 0 \tag{10.143}$$

Then, $\dot{V}\left(\hat{x}, e_p, \Delta\tilde{K}_x, \tilde{K}_y\right) \leq 0$. Therefore, the adaptive regulator design is stable.

■

Note that this adaptive augmentation controller is designed to tolerate the uncertainty due to the plant model variation, but does not attempt to accommodate the uncertainty by canceling the uncertainty. The goal is to enable the adaptive control design to have a sufficient robustness due to the plant model variation. In the event the plant model variation is zero, then $c_7 = 0$, $c_8 = 0$, $c_9 = 0$, and $c_{10} = 0$. This implies $\nu_x \leq \frac{c_1}{c_2 c_3^2}$ and $\nu_y \leq \frac{c_4}{c_5 c_6^2}$. On the other hand, if the plant model variation is large, it is possible that there are no suitable values of ν_x and ν_y that can stabilize the plant.

The Lyapunov stability analysis shows how the modification parameters ν_x and ν_y could be selected to ensure a stable adaptation. As discussed in Sect. 9.5.3, the Lyapunov stability analysis often results in a high degree of conservatism that could render the selection of the modification parameters infeasible. Therefore, in practice,

the linear asymptotic property of the optimal control modification can be invoked to find suitable values of ν_x and ν_y to ensure the closed-loop stability. In the limit as $\Gamma \to \infty$, the following adaptive parameters tend to:

$$B\Delta K_x \to \frac{1}{\nu_x} B \left(B^\top A_m^{-\top} P B \right)^{-1} B^\top P \tag{10.144}$$

$$BK_y y \to \frac{1}{\nu_y} B \left(B^\top A_m^{-\top} P B \right)^{-1} B^\top P \hat{x} \tag{10.145}$$

Using this linear asymptotic property, it is possible to estimate stability margins of the closed-loop system in the limit as shown in Sects. 9.13 and 9.14. The closed-loop system then tends to an asymptotic linear system in the limit as

$$\dot{x} = (1+\delta_A) Ax + (1+\delta_B) B\bar{K}_x \hat{x} + \left(\frac{1}{\nu_x} + \frac{1}{\nu_y} \right) (1+\delta_B) B \left(B^\top A_m^{-\top} P B \right)^{-1} B^\top P \hat{x} \tag{10.146}$$

$$\dot{\hat{x}} = \left[A - LC + B\bar{K}_x + \left(\frac{1}{\nu_x} + \frac{1}{\nu_y} \right) B \left(B^\top A_m^{-\top} P B \right)^{-1} B^\top P \right] \hat{x} + LCx \tag{10.147}$$

Thus, stability margins can be determined for the closed-loop plant matrix which is given by

$$A_c = \begin{bmatrix} (1+\delta_A) A & (1+\delta_B) B\bar{K}_x + \left(\frac{1}{\nu_x} + \frac{1}{\nu_y} \right) (1+\delta_B) B \left(B^\top A_m^{-\top} P B \right)^{-1} B^\top P \\ LC & A - LC + B\bar{K}_x + \left(\frac{1}{\nu_x} + \frac{1}{\nu_y} \right) B \left(B^\top A_m^{-\top} P B \right)^{-1} B^\top P \end{bmatrix} \tag{10.148}$$

Then, ν_x and ν_y can be chosen to provide the closed-loop stability.

It is noted that $K_y(t)$ accounts for the model variation in the Luenberger state observer design. Alternatively, $K_y(t)$ could be eliminated if the observer design is sufficiently robust using the loop transfer recovery method. Then, the observer feedback adaptive control with the optimal control modification comes down to selecting a suitable value of ν_x to ensure the closed-loop stability.

Example 10.8 The ASE state-space model in Example 10.7 contains 45 states, 64 outputs, and 4 inputs. The states include the aircraft roll rate $p(t)$ and two generalized states for each of the 22 aeroelastic modes. The outputs include the aircraft airspeed $V(t)$, angle of attack $\alpha(t)$, sideslip angle $\beta(t)$, aircraft angular rates $\left[p(t)\ q(t)\ r(t) \right]^\top$, aircraft position $\left[x(t)\ y(t)\ h(t) \right]^\top$, aircraft attitude $\left[\phi(t)\ \theta(t)\ \psi(t) \right]^\top$, accelerations in the three axes $\left(N_x, N_y, N_z \right)$ at the forward and aft locations of the wing tip, and the four hinge moments of the control surfaces. The control surfaces are the four outboard third camber segments of the VCCTEF. All these surfaces are blended together to provide a single input to address the relative constraints imposed by the elastomer material. For the flutter suppression

control design, only the two N_z acceleration measurements are used as the outputs. Figure 10.41 illustrates the input and output locations [28].

All the control surfaces are not entirely independent in their motions due to the physical constraints imposed by the elastomer material. This material has certain displacement and rate limits. Thus, any adjacent control surfaces will also have relative displacement and rate limits. These limits are in addition to the normal position and rate limits that each of the control surfaces is subjected to. Thus, these relative constraints can cause challenges in a control design of this system.

Consider the following relative displacement and rate constraints:

$$|\delta_{i+1} - \delta_i| \leq \Delta\delta \tag{10.149}$$

$$\left|\dot{\delta}_{i+1} - \dot{\delta}_i\right| \leq \Delta\dot{\delta} \tag{10.150}$$

where $i = 1, 2, 3$.

For the VCCTEF design, the relative motion between any adjacent flap sections is allowed to be within two degrees. The rate constraint imposed by the elastomer material is not yet defined and thus is assumed to be large. The actuator dynamics are modeled as a second-order system. This actuator model is highly simplified since it does not take into account the hinge moment which is a function of the states and the dynamics of the elastomer material in the overall actuator model.

To address the relative displacement limit, a concept of virtual control is introduced [36]. The control surface deflections are described by a shape function. This shape function can be any reasonable shape function with a smooth and gradual slope. One simple function is a linear function. The control surface deflections are then parametrized as a linear function

$$\delta_i = \frac{i\,\delta_v}{4} \tag{10.151}$$

where $i = 1, 2, 3, 4$ such that $\delta_1(t)$ is the inboard flap and $\delta_4(t)$ is the outboard flap, and $\delta_v(t)$ is the virtual control surface deflection.

Since the inboard flap section $\delta_1(t)$ cannot deflect more than two degrees relative to the stationary flap adjacent to it, then $\delta_v(t) \leq 8$ deg. Also, the outboard flap deflection $\delta_4(t)$ is the same as the virtual control surface deflection. Thus, one can think that the outboard flap $\delta_4(t)$ is a master control input, while the other three control surfaces are slave control inputs since their motions are dependent on the master control input.

Thus, the virtual control derivatives are computed as

$$B_{jk} = \sum_{i=1}^{4} \frac{i\,B_{ijk}}{4} \tag{10.152}$$

where B_{jk_i} is the control derivative of mode jth with respect to the displacement ($k = 1$), velocity ($k = 2$), and acceleration ($k = 3$) of flap section ith.

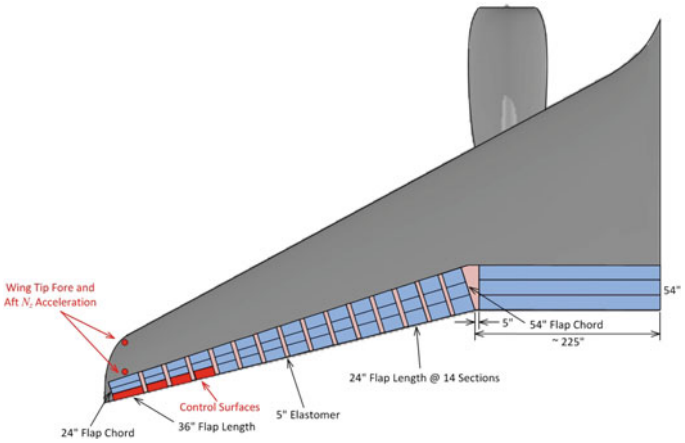

Fig. 10.41 Flutter suppression control surfaces and accelerometer locations

The simulation is conducted with only the reduced-order aeroservoelastic state-space model for a flight condition at Mach 0.86 and an altitude of 10,000 ft. There are two unstable aeroelastic modes: mode 1 and mode 4, as shown in Table 10.4. Process noise and sensor noise are introduced to simulate the structural response to atmospheric turbulence. The baseline full-state feedback controller is designed with a LQR controller tuned to give good performance. A LQG output feedback controller is then designed using the ideal full-state feedback gain. The adaptive augmentation controller is then turned on. The adaptation rate matrices and modification parameters are selected to be $\Gamma_x = \Gamma_y = 1$ and $\eta_x = \eta_y = 0.1$.

The root locus of the open-loop transfer functions between the accelerometers and the virtual control are shown in Figs. 10.42 and 10.43. It is shown that the individual transfer functions have two unstable poles corresponding to the two unstable modes and zeros on the right half plane. However, the transmission zeros of the MIMO system transfer function actually are stable.

An initial roll rate of 0.1 rad/s is specified. Figures 10.44, 10.45, and 10.46 show the responses of the roll rate, the generalized displacement of mode 1, and the generalized displacement of mode 4, respectively, without the process and sensors noises for the baseline full-state feedback LQR controller and the output feedback LQG controller with and without the adaptive augmentation controller. The full-state feedback LQR controller performs much better than the output feedback LQG controller with and without the adaptive augmentation controller using only the two accelerometers at the wing tip. The LQG controller does seem to need further tuning. The adaptive augmentation controller causes an increase in the overshoot of the responses due to the output feedback LQG controller as well as injects high-frequency contents into the modal responses. Nonetheless, all the controllers are able to suppress the two unstable aeroelastic modes.

The effects of process and sensor noises are examined. Figures 10.47, 10.48, and 10.49 show the responses of the roll rate, the generalized displacement of mode 1, and the generalized displacement of mode 4, respectively, with the process and

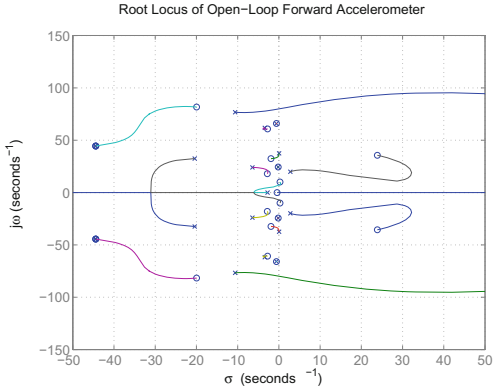

Fig. 10.42 Root locus of open-loop transfer function of forward accelerometer

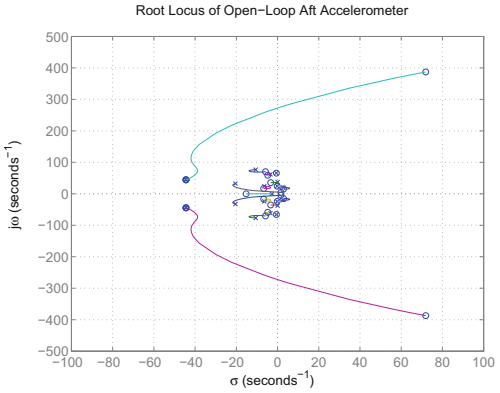

Fig. 10.43 Root locus of open-loop transfer function of aft accelerometer

sensor noises for the baseline full-state feedback LQR controller and the output feedback LQG controller with and without the adaptive augmentation controller. All the controllers are able to maintain good performance in the presence of the process and sensor noises.

Figures 10.50 and 10.51 show the root locus plots of the closed-loop transfer functions of the accelerometers with the adaptive augmentation controller using the final gain matrix. As can be seen, the closed-loop transfer functions are completely stable. Figures 10.52 and 10.53 are the frequency response plots for the open-loop and closed-loop transfer functions of the accelerometers. The largest frequency response is due to mode 4. The closed-loop frequency response is significantly less than the open-loop frequency response, indicating the effectiveness of the aeroelastic mode suppressioncontroller.

Next, the plant model variation is introduced into the aeroservoelastic state-space model by specifying $\Delta A = 0.05A$ and $\Delta B = -0.1B$. The process and sensor

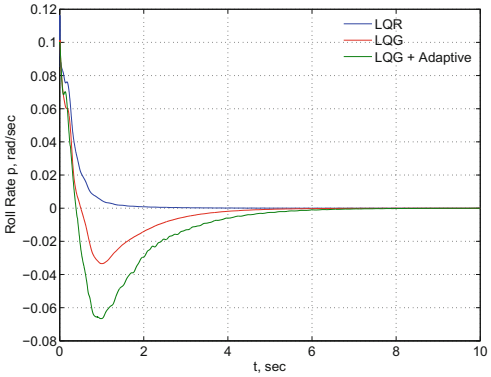

Fig. 10.44 Roll rate response for LQR and LQG controllers without process and sensor noises

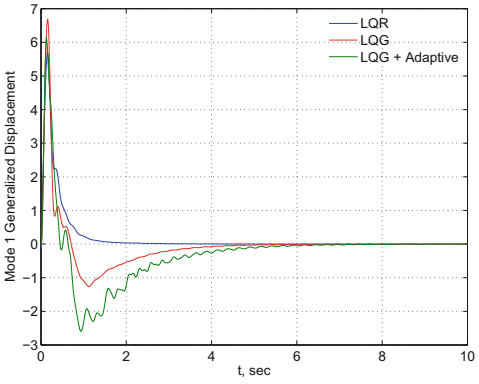

Fig. 10.45 Mode 1 generalized displacement response for LQR and LQG controllers without process and sensor noises

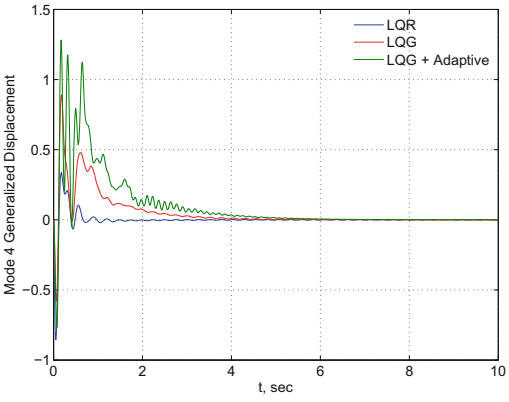

Fig. 10.46 Mode 4 generalized displacement response for LQR and LQG controllers without process and sensor noises

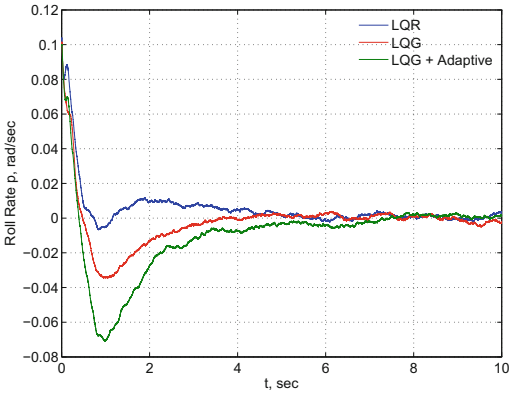

Fig. 10.47 Roll rate response for LQR and LQG controllers with process and sensor noises

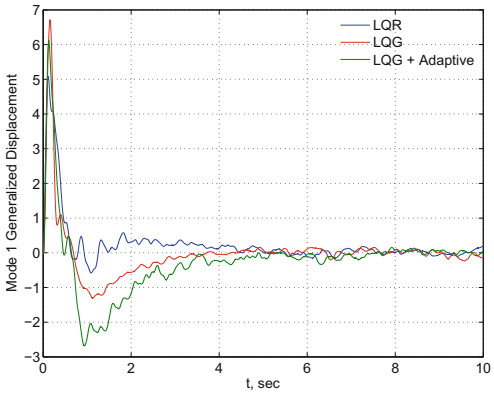

Fig. 10.48 Mode 1 generalized displacement response for LQR and LQG controllers with process and sensor noises

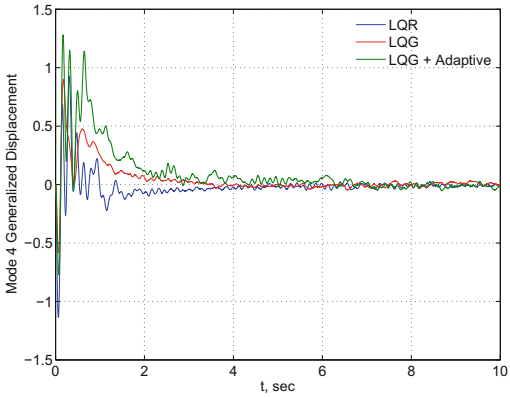

Fig. 10.49 Mode 4 generalized displacement response for LQR and LQG controllers with process and sensor noises

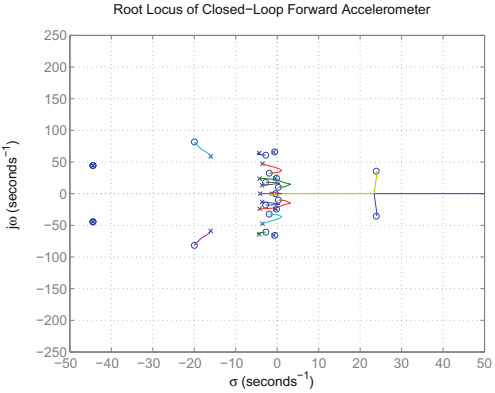

Fig. 10.50 Root locus of closed-loop transfer function of forward accelerometer

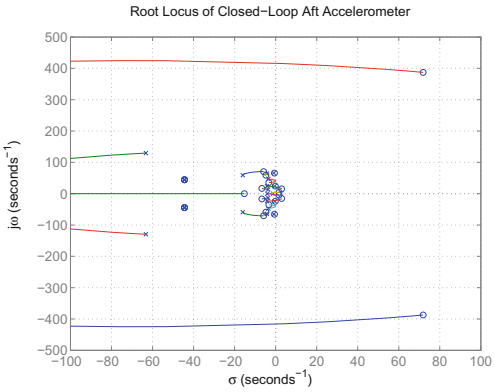

Fig. 10.51 Root locus of closed-loop transfer function of aft accelerometer

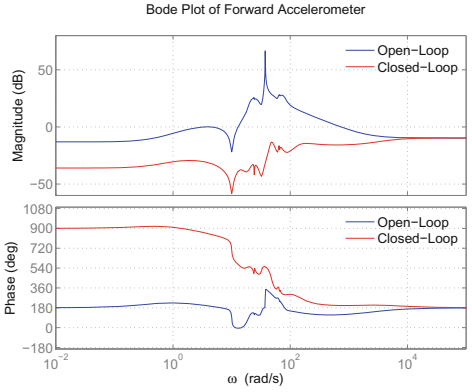

Fig. 10.52 Frequency response of forward accelerometer

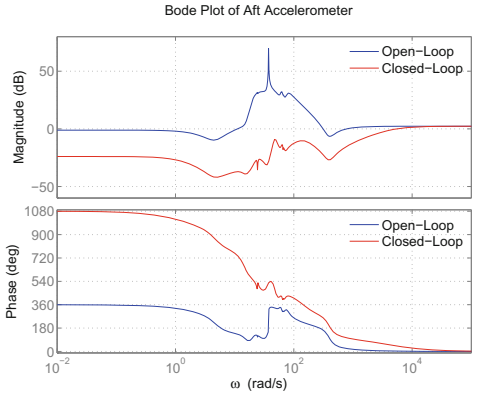

Fig. 10.53 Frequency response of aft accelerometer

noises are also included. The output feedback LQG controller without the adaptive augmentation controller is unstable as shown in Figs. 10.54, 10.55, and 10.56. On the other hand, the adaptive augmentation controller is able to stabilize the aeroelastic modes in the presence of the plant model variation. The closed-loop plant matrix without the adaptive augmentation controller is in fact unstable. Stability of the closed-loop plant is restored in the presence of the adaptive augmentation controller.

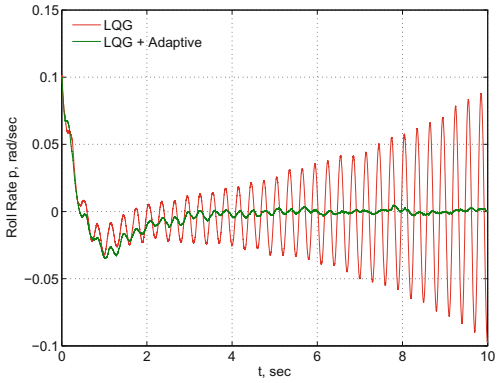

Fig. 10.54 Roll rate response with and without adaptive augmentation controller

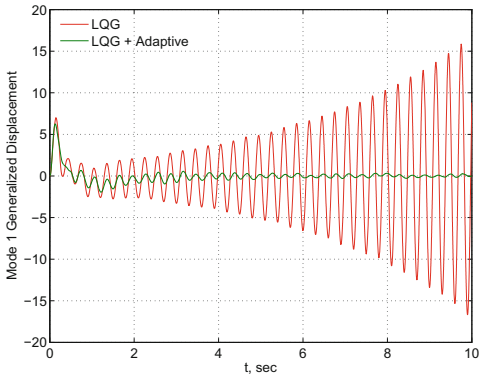

Fig. 10.55 Mode 1 generalized displacement response with and without adaptive augmentation controller

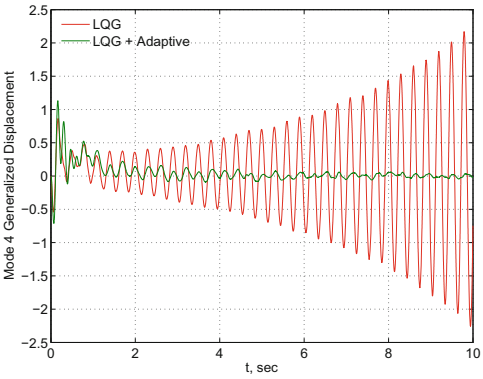

Fig. 10.56 Mode 4 generalized displacement response with and without adaptive augmentation controller

Figure 10.57 is the plot of the time history of the virtual control command for the output feedback LQG controller with and without the adaptive augmentation controller. The largest amplitude of the stabilizing virtual control command for the adaptive augmentation controller is 6.22°. The linear mapping between the virtual control command and the physical control commands results in 1.56° which meets the physical constraint of 2° on the relative deflection of the VCCTEF.

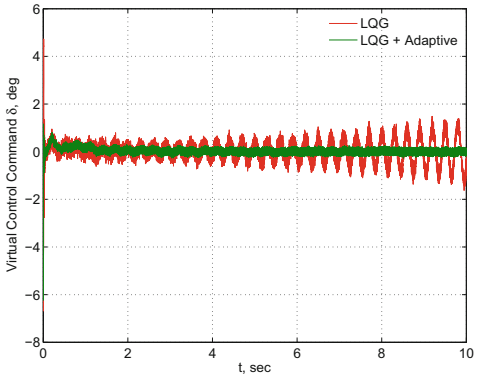

Fig. 10.57 Virtual control command with and without adaptive augmentation controller

10.7 Adaptive Flight Control

Flight control is an important aircraft system that provides many critical functions to enable safe operations of an aircraft. A pilot controls an aircraft by moving a control input device such as a control yoke, rudder pedal, or side stick. A pilot command signal is sent to a flight control system which processes the signal further and converts it into an actuator command signal. This signal is then sent to an actuator system that drives the position of a flight control surface such as the aileron, elevator, or rudder. This flight control feature is called a pilot command tracking task. Another important flight control feature is to enhance aircraft stability via a stability augmentation system (SAS). The SAS provides the additional damping to the rigid aircraft modes by feedback control. A typical SAS on an aircraft is a yaw damper.

Connections between control input devices to flight control surfaces can be made via mechanical linkages which exist in older aircraft. Hydraulic flight control systems use hydraulic fluid circuits in conjunction with partial mechanical flight control systems to drive flight control surfaces. Hydraulic flight control systems are still found in many aircraft in operation nowadays. Modern aircraft usually employ fly-by-wire (FBW) flight control systems which replace mechanical systems with electronics. A pilot command is converted into an electrical signal transmitted to a flight control computer for processing. The flight control computer computes actuator command signals and transmits these signals to hydraulic actuators to drive flight control surfaces.

A typical flight control system consists of an inner-loop stability augmentation system and an outer-loop autopilot system as illustrated in the Fig. 10.58. The command input into a flight control system can be accomplished via a pilot's direct mechanical input or an autopilot. When engaged, the autopilot generates an attitude command of the attitude angles or an altitude command for a selected autopilot task such as cruise or landing. This command is processed as a feedforward signal and then is summed with the SAS to form a control signal. The SAS uses feedback of

aircraft's sensed angular rate variables, such as the roll rate, pitch rate, and yaw rate to provide the additional damping to the aircraft dynamics. The control signal is transmitted to flight control actuators that drive flight control surfaces to change the aircraft dynamics.

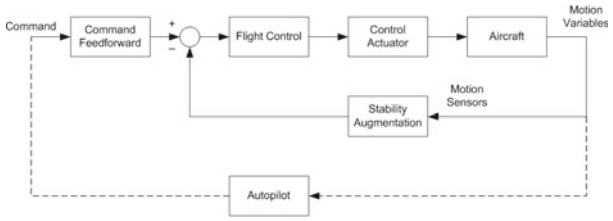

Fig. 10.58 Flight control system

Most conventional flight control systems utilize extensive gain-scheduling schemes via table-lookups in order to achieve desired handling qualities throughout a flight envelope. While this approach has proven to be very successful, the development process can be expensive and often results in aircraft-specific implementations. In rare occurrences when a failure or damage occurs to an aircraft, a conventional flight control system may no longer perform pilot command tracking tasks as intended since the aircraft flight dynamics may deviate from its design characteristics substantially, thereby causing a degradation in the performance of the flight control system. Adaptive flight control can offer a possibility for restoring the performance of a flight control system in an event of failure or damage to an aircraft.

The linearized equations of the angular motion for an aircraft with failures or damage can be expressed in general as [19]

$$\dot{x} = (C + \Delta C)\, x + (D + \Delta D)\, u + (E + \Delta E)\, z \tag{10.153}$$

where $x(t) = \left[\, p(t)\ q(t)\ r(t) \,\right]^{\top}$ is an inner-loop state vector comprising the roll, pitch, and yaw rates; $u(t) = \left[\, \delta_a(t)\ \delta_e(t)\ \delta_r(t) \,\right]^{\top}$ is a control vector comprising the aileron, elevator, and rudder control surface deflections; $z(t) = \left[\, \phi(t)\ \alpha(t)\ \beta(t)\ V(t)\ h(t)\ \theta(t) \,\right]^{\top}$ is an outer-loop state vector comprising the bank angle, angle of attack, sideslip angle, airspeed, altitude, and pitch angle; $C \in \mathbb{R}^3 \times \mathbb{R}^3$, $D \in \mathbb{R}^3 \times \mathbb{R}^3$, and $E \in \mathbb{R}^3 \times \mathbb{R}^6$ are the nominal aircraft plant matrices for the inner-loop dynamics; and ΔC, ΔD, and ΔE are the changes in the inner-loop plant matrices due to failures or damage.

In general, the inner-loop state variables; namely, the angular rates have faster dynamics than the outer-loop variables. This frequency separation allows the inner-loop dynamics to be decoupled from the outer-loop dynamics in a flight control design. This can simplify the design significantly. The outer-loop dynamics are described by the following equation:

$$\dot{z} = (F + \Delta F)\, z + (G + \Delta G)\, u + (H + \Delta H)\, x \tag{10.154}$$

where $F \in \mathbb{R}^6 \times \mathbb{R}^6$, $G \in \mathbb{R}^6 \times \mathbb{R}^3$, and $H \in \mathbb{R}^6 \times \mathbb{R}^3$ are the nominal outer-loop aircraft plant matrices; and ΔF, ΔG, and ΔH are the changes in the outer-loop plant matrices due to failures or damage.

Consider the following inner-loop rate command adaptive flight control architecture as shown in Fig. 10.59. The control architecture comprises: (1) a reference model that translates a rate command $r\,(t)$ into a reference acceleration command $\dot{x}_m\,(t)$, (2) a proportional-integral (PI) feedback control for stability augmentation and tracking, (3) a dynamic inversion controller that computes actuator commands $u_c\,(t)$ to achieve a desired acceleration command $\dot{x}_d\,(t)$, and (4) an adaptive control augmentation that computes an adaptive signal $u_{ad}\,(t)$ that augments the reference acceleration command to form a desired acceleration command for the dynamic inversion controller. The adaptive control augmentation is the standard MRAC with any robust modification schemes, such as the projection method, σ modification, e modification, optimal control modification, and adaptive loop recovery modification with or without the normalization and covariance adjustment methods.

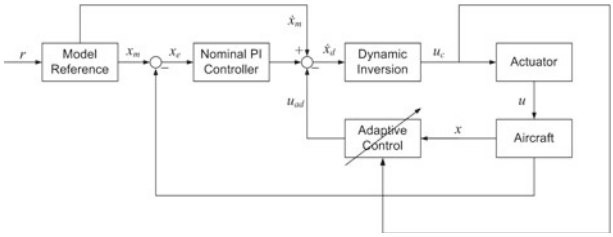

Fig. 10.59 Adaptive flight control architecture

For rate command attitude hold (ACAH) flight control, a first-order reference model is used to filter the rate command $r\,(t)$ into a reference acceleration command $\dot{x}_m\,(t)$ as

$$\dot{x}_m = -\Omega\,(x_m - r) \tag{10.155}$$

where $\Omega = \text{diag}\left(\omega_p, \omega_q, \omega_r\right)$ is a diagonal matrix of the reference model frequencies.

The nominal controller is then specified as

$$\bar{u} = K_p\,(x_m - x) + K_i \int_0^t (x_m - x)\, d\tau \tag{10.156}$$

where $K_p = \text{diag}\left(2\zeta_p\omega_p, 2\zeta_q\omega_q, 2\zeta_r\omega_r\right)$ is the proportional gain matrix and $K_i = \text{diag}\left(\omega_p^2, \omega_q^2, \omega_r^2\right)$ is the integral gain matrix [37].

For transport aircraft, typical values of the reference model frequencies ω_p, ω_q, and ω_r are 3.5, 2.5, and 2.6, respectively; and typical values of the reference model damping ratios ζ_p, ζ_q, and ζ_r are $\frac{1}{\sqrt{2}}$.

The desired acceleration is computed as

$$\dot{x}_d = \dot{x}_m + \bar{u} - u_{ad} \tag{10.157}$$

The adaptive signal $u_{ad}(t)$ is designed to estimate the uncertainty in the aircraft plant dynamics.

The desired acceleration is the ideal response of the nominal aircraft plant dynamics. Therefore, the ideal aircraft dynamics can be expressed as

$$\dot{x}_d = Cx + Du + Ez \tag{10.158}$$

The dynamic inversion controller then computes the actuator command from the closed-loop plant model of the ideal aircraft dynamics [37]

$$u_c = D^{-1}\left(\dot{x}_d - Cx - Ez\right) \tag{10.159}$$

Substituting $u_c(t)$ for $u(t)$ into the aircraft model, then the closed-loop plant model of the aircraft is obtained as

$$\dot{x} = \dot{x}_m + \bar{u} - u_{ad} + \Delta Cx + \Delta Du_c + \Delta Ez \tag{10.160}$$

Let $\Theta^{*\top} = \left[\begin{array}{ccc}\Delta C & \Delta D & \Delta E\end{array}\right]$ and $\Phi(x, u_c, z) = \left[\begin{array}{ccc}x^\top(t) & u_c^\top(t) & z^\top(t)\end{array}\right]^\top$. Then, the adaptive signal $u_{ad}(t)$ can be designed as

$$u_{ad} = \Delta\hat{C}(t)\,x + \Delta\hat{D}(t)\,u_c + \Delta\hat{E}(t)\,z = \left[\begin{array}{ccc}\Delta\hat{C} & \Delta\hat{D} & \Delta\hat{E}\end{array}\right]\left[\begin{array}{c}x\\u_c\\z\end{array}\right] = \Theta^\top(t)\,\Phi(x, u_c, z) \tag{10.161}$$

Then,

$$\dot{x} = \dot{x}_m + K_p\left(x_m - x\right) + K_i\int_0^t \left(x_m - x\right)d\tau - \tilde{\Theta}^\top\Phi(x, u_c, z) \tag{10.162}$$

where $\tilde{\Theta}(t) = \Theta(t) - \Theta^*$ is the estimation error of the unknown matrices.

The tracking error equation is expressed as

$$\dot{x}_m - \dot{x} = -K_p\left(x_m - x\right) - K_i\int_0^t \left(x_m - x\right)d\tau + \tilde{\Theta}^\top\Phi(x, u_c, z) \tag{10.163}$$

Let $e(t) = \left[\begin{array}{cc}\int_0^t\left[x_m^\top(t) - x^\top(t)\right]d\tau & x_m^\top(t) - x^\top(t)\end{array}\right]^\top$. Then,

$$\dot{e} = A_m e + B\tilde{\Theta}^\top\Phi(x, u_c, z) \tag{10.164}$$

where

$$A_m = \begin{bmatrix} 0 & I \\ -K_i & -K_p \end{bmatrix} \tag{10.165}$$

$$B = \begin{bmatrix} 0 \\ I \end{bmatrix} \tag{10.166}$$

Then, the adaptive law can be designed with any robust adaptive control scheme such as the e modification

$$\dot{\Theta} = -\Gamma \left[\Phi (x, u_c, z)\, e^\top P B + \mu \left\| e^\top P B \right\| \Theta \right] \tag{10.167}$$

Alternatively, if the optimal control modification is used, then

$$\dot{\Theta} = -\Gamma \Phi (x, u_c, z) \left[e^\top P - \nu \Phi^\top (x, u_c, z)\, \Theta B^\top P A_m^{-1} \right] B \tag{10.168}$$

Note that actuator dynamics can affect the closed-loop stability of an aircraft. Therefore, a suitable selection of the modification parameter should be made to ensure sufficient robustness. An actuator system must have a higher frequency bandwidth than the frequency of a given mode in consideration. Roughly speaking, the frequency bandwidth of an actuator should be at least several times greater than the highest frequency of the aircraft modes. For example, the short-period mode is about 2.5 rad/s and then the frequency of the actuator for the elevator could be about 10 times larger or 25 rad/s. The damping ratio should be sufficiently large to provide a well-damped control surface deflection.

For example, a second-order actuator system is modeled as

$$\ddot{u} + 2\zeta_a \omega_a \dot{u} + \omega_a^2 u = \omega_a^2 u_c \tag{10.169}$$

where $\omega_a \gg \max\left(\omega_p, \omega_q, \omega_r\right)$.

The response of an actuator is subject to both position and rate limits. Since flight control surfaces are generally of a flap-type design, as the flap deflection increases beyond a certain limit, the performance of the flap becomes degraded due to flow separation. This would result in nonlinear aerodynamics. Therefore, flight control surface positions are generally designed to operate within a linear range. Typically, for the elevator and aileron, the position limits are maintained between $\pm 20^{\circ}$. For the rudder, the position limit is smaller since the rudder is a powerful flight control surface that can generate a significant structural loading on the vertical tail at a high rudder deflection. The rudder position limit is also scheduled with the altitude and airspeed. As the airspeed and altitude increase, the rudder position limit becomes smaller.

Typically, the rate limit of an actuator system is established by the design of the actuator. A typical rate limit is about 60°/s for transport aircraft. If an actuator is operating normally, a pilot command would translate into an expected response. However, when a rate limit occurs due to a degraded actuator performance, the actuator would not produce a sufficiently fast response to meet the pilot command.

Consequently, the pilot would tend to apply a greater command to try to overcome the lag in the actuator dynamics. This actuator lag and the pilot positive feedback can result in an adverse consequence known as pilot-induced oscillations (PIO), which could lead to a catastrophic loss of control.

Example 10.9 Adaptive flight control is an effective method for controlling a damaged aircraft. A transport aircraft with wing damage is shown in Fig. 10.60. The wing damage is modeled as a 28% loss of the left wing [37]. Since the damage is asymmetric, the motion of the damaged aircraft is fully coupled in the roll, pitch, and yaw axes.

Fig. 10.60 Transport aircraft with left wing damaged

A level flight condition of Mach 0.6 at 15,000 ft is selected. The remaining right aileron control surface is the only roll control effector available. The reference model is specified by $\omega_p = 2.0$ rad/s, $\omega_q = 1.5$ rad/s, $\omega_r = 1.0$ rad/s, and $\zeta_p = \zeta_q = \zeta_r = 1/\sqrt{2}$.

The pilot pitch rate command is simulated with a series of ramp input longitudinal stick command doublets, corresponding to the reference pitch angle $\pm 3.81^{\circ}$ from trim. The tracking performance of the nominal controller without adaptation is compared against the standard MRAC, the e modification with $\mu = 0.1$, and the optimal control modification with $\nu = 0.1$. The adaptive gains are selected to be as large as possible within the numerical stability limit of the adaptive laws. This results in $\Gamma = 60$ for the standard MRAC, $\Gamma = 800$ for the e modification, and $\Gamma = 2580$ for the optimal control modification. Thus, it can be seen that the optimal control modification can tolerate a much larger adaption rate than the standard MRAC. This large adaptation rate allows the optimal control modification to achieve fast adaptation to better adapt to uncertainty than the standard MRAC.

The aircraft angular rate responses are shown in Fig. 10.61. The nominal controller without adaptation produces a rather poor tracking of the reference pitch rate. Both the standard MRAC and e modification improve the tracking performance significantly.

The optimal control modification (OCM) is able to provide a better tracking than both the standard MRAC and *e* modification. Due to the asymmetric wing damage, the roll axis is most affected. With the nominal controller, there is a significant roll rate of as high as 20°/s. Both the standard MRAC and *e* modification reduce the maximum amplitude of the roll rate to about 10°/s. The optimal control modification further reduces the roll rate to a maximum value of about 4°/s. All the three adaptive controllers significantly reduce the yaw rate to a very low level. The *e* modification is observed to perform slightly better than the standard MRAC and optimal control modification in the yaw axis.

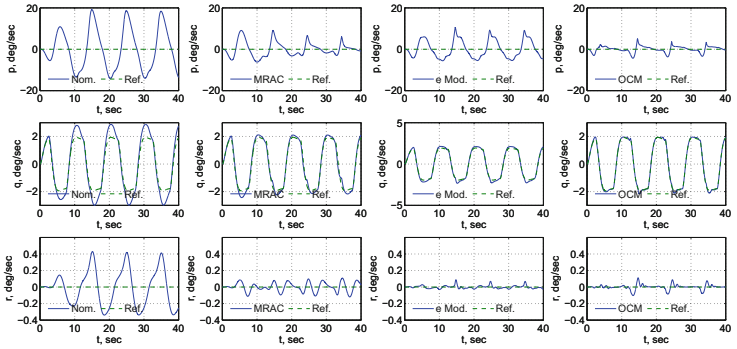

Fig. 10.61 Closed-loop responses of roll, pitch, and yaw rates

The aircraft attitude responses are shown in Fig. 10.62. When there is no adaptation, the reference pitch attitude could not be followed accurately. With adaptive control, the tracking is much improved and the optimal control modification produces the pitch angle tracking better than both the standard MRAC and *e* modification. Without adaptation, as expected the damaged aircraft exhibits a rather severe roll behavior with a large bank angle between -30^{o} and 20^{o}. Both the standard MRAC and *e* modification reduce the bank angle significantly. However, the optimal control modification shows a drastic improvement in the arrest of the roll motion with the bank angle maintained very close to the trim value. All the three adaptive controllers produce similar angle-of-attack responses. With the optimal control modification, the sideslip angle is reduced to near zero, while both the standard MRAC and *e* modification still produce considerable sideslip angle responses.

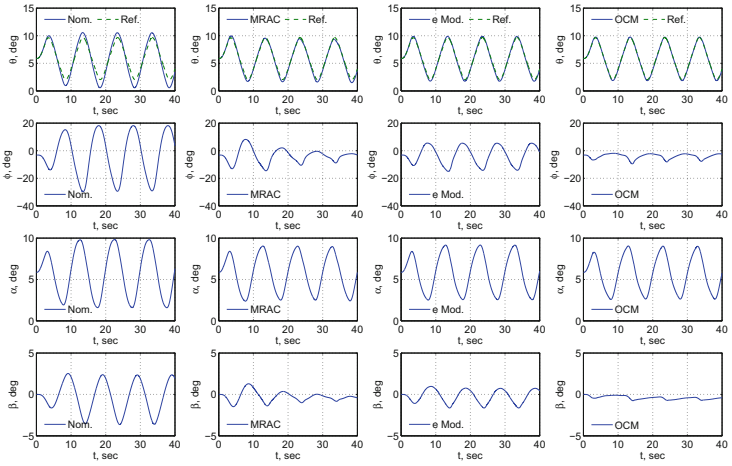

Fig. 10.62 Closed-loop responses of pitch angle, bank angle, angle of attack, and sideslip angle

The control surface deflections are shown in Fig. 10.63. Because of the wing damage, the damaged aircraft has to be trimmed with a rather large aileron deflection. This causes the roll control authority to be severely limited. Therefore, a roll control saturation is present in all cases. The elevator deflection is nominally similar for all the four controllers and is well within its control authority. The rudder deflection produced by the baseline controller is quite significant. Generally, it is desired to keep the rudder deflection as small as possible in normal operation. Typically, the rudder deflection limit is reduced as the airspeed and altitude increase. Both the standard MRAC and *e* modification reduce the baseline rudder deflection to some extent, but the optimal control modification is observed to produce the smallest rudder deflection.

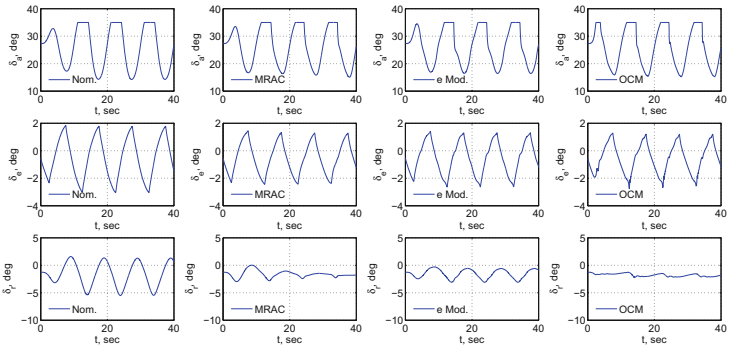

Fig. 10.63 Closed-loop responses of aileron, elevator, and rudder deflections

10.8 Hybrid Adaptive Flight Control

In the adaptive flight control design in Sect. 10.7, MRAC is used to estimate the plant uncertainty due to ΔC, ΔD, and ΔE. However, it is well known that MRAC is designed to drive the tracking error to zero, but is not designed with the primary objective of parameter estimation. Least-squares methods on the hand are well-known techniques for parameter estimation. It is possible to combine both the least-squares parameter estimation and MRAC into a control architecture. This approach for flight control is called hybrid adaptive flight control [37].

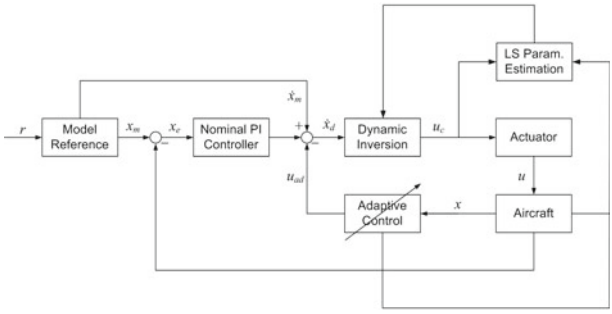

Fig. 10.64 Hybrid adaptive flight control system

The hybrid adaptive flight control architecture is shown in Fig. 10.64. The architecture includes an indirect adaptive control that uses a least-squares parameter estimation technique to estimate the true plant model of the aircraft in conjunction with a direct MRAC designed to reduce the tracking error.

In the hybrid adaptive flight control approach, the dynamic inversion controller computes the actuator command from a predictor or estimated plant model of the aircraft dynamics rather than the ideal plant model. The estimated plant model is expressed as

$$\dot{\hat{x}} = \left(C + \Delta\hat{C}\right) x + \left(D + \Delta\hat{D}\right) u + \left(E + \Delta\hat{E}\right) z \tag{10.170}$$

Setting the desired acceleration $\dot{x}_d(t)$ equal to $\dot{\hat{x}}(t)$, the actuator command is computed from the estimated plant model by the dynamic inversion controller as

$$u_c = \left(D + \Delta\hat{D}\right)^{-1}\left[\dot{x}_d - \left(C + \Delta\hat{C}\right)x - \left(E + \Delta\hat{E}\right)z\right] \tag{10.171}$$

The actuator command now depends on the estimates of the plant matrices ΔC, ΔD, and ΔD which are computed from the indirect adaptive control using a least-squares parameter estimation method. The plant modeling error $\varepsilon(t)$ is computed by subtracting the plant model from the estimated plant model as

$$\varepsilon = \dot{x}_d - \dot{x} = \left(\Delta\hat{C} - \Delta C\right)x + \left(\Delta\hat{D} - \Delta D\right)u_c + \left(\Delta\hat{E} - \Delta E\right)z = \tilde{\Theta}^\top \Phi(x, u_c, z) \tag{10.172}$$

The recursive least-squares (RLS) indirect adaptive laws for computing $\Theta(t)$ are given by

$$\dot{\Theta} = -R\Phi(x, u_c, z)\,\varepsilon^\top \tag{10.173}$$

$$\dot{R} = -R\Phi(x, u_c, z)\,\Phi^\top(x, u_c, z)\,R \tag{10.174}$$

where $R(t) = R^\top(t) > 0$ is the covariance matrix that acts as a time-varying adaptation rate matrix.

Alternatively, the least-squares gradient indirect adaptive law can be used by setting $R(t)$ to be a constant.

The matrices $\Delta\hat{C}(t)$, $\Delta\hat{D}(t)$, and $\Delta\hat{E}(t)$ are computed from $\Theta(t)$ at each time step and then are used in the dynamic inversion controller to compute the actuator command.

Using Eq. (10.157), the closed-loop plant is expressed as

$$\dot{x} = \dot{x}_m + K_p(x_m - x) + K_i\int_0^t (x_m - x)\,d\tau - u_{ad} - \varepsilon \tag{10.175}$$

where $u_{ad}(t)$ is a direct adaptive control signal computed as

$$u_{ad} = \Delta\Theta^\top \Phi(x, u_c, z) \tag{10.176}$$

where $\Delta\Theta(t)$ is the residual estimate of the unknown plant matrices.

The tracking error equation is expressed as

$$\dot{e} = A_m e + B(u_{ad} + \varepsilon) \tag{10.177}$$

The direct MRAC law for computing $\Delta\Theta(t)$ can be selected to be any robust modification scheme such as the e modification given by

$$\Delta\dot{\Theta} = -\Gamma\left[\Phi(x, u_c, z)\,e^\top PB + \mu\left\|e^\top PB\right|\Delta\Theta\right] \tag{10.178}$$

The hybrid adaptive flight control thus uses the RLS indirect adaptive control to estimate the plant uncertainty. The goal of the RLS indirect adaptive control is to

drive the plant modeling error to zero. This information is then used in the dynamic inversion controller to compute the actuator command. The control signal from the actuator command produces a closed-loop aircraft response which is then compared with the reference model to form the tracking error. However, because the plant modeling error is reduced by the RLS indirect adaptive control, the resulting tracking error will be smaller than if the RLS indirect adaptive control is not present. The MRAC law further drives the residual tracking error to zero. Because the residual tracking error is small, the adaptation rate for the direct MRAC can be set to a small value to improve robustness. The RLS parameter estimation method is inherently robust, so, together with the direct MRAC, the hybrid adaptive flight control architecture can provide a very effective and robust adaptation mechanism.

Example 10.10 For the same wing-damage aircraft simulation in Example 10.9, the hybrid adaptive flight control is implemented using the RLS indirect adaptive control in conjunction with the direct adaptive control using the e modification. The covariance matrix is initialized with $R(0) = 100I$. The closed-loop response of the damaged aircraft due to the hybrid adaptive flight control is shown in Fig. 10.65. The closed-loop response is exceedingly well-behaved. Both the roll and yaw rates are much smaller than those with the e modification alone. The pitch rate and pitch attitude both track the reference model extremely well. The bank angle and sideslip angle are reduced close to zero as shown in Fig. 10.66. The saturation in the aileron is still present, but the rudder deflection is much smaller than that with the e modification alone as shown in Fig. 10.67. Thus, the performance of the hybrid adaptive flight control is much better than the e modification alone.

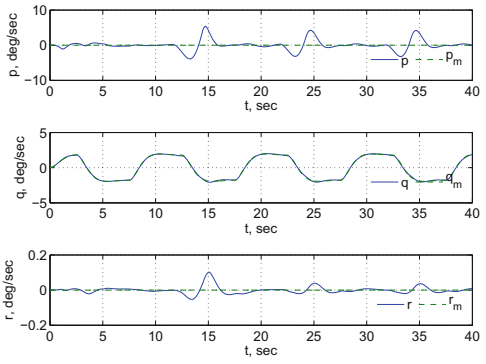

Fig. 10.65 Closed-loop responses of roll, pitch, and yaw rates

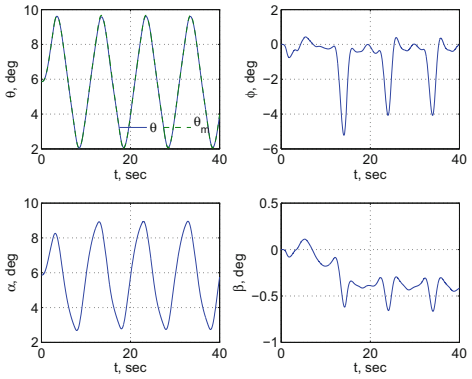

Fig. 10.66 Closed-loop responses of pitch angle, bank angle, angle of attack, and sideslip angle

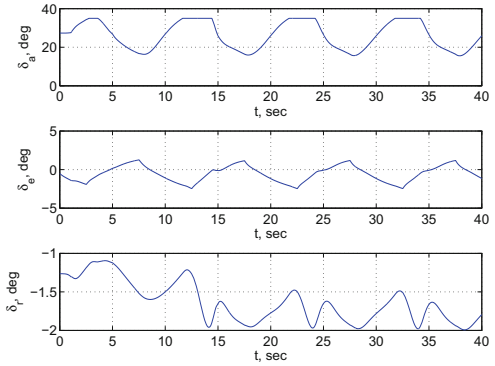

Fig. 10.67 Closed-loop responses of aileron, elevator, and rudder deflections

10.9 Adaptive Flight Control for F-18 Aircraft with Optimal Control Modification

Adaptive flight control can be used to provide consistent handling qualities and restore stability of aircraft under off-nominal flight conditions such as those due to failures or damage. Suppose an aircraft plant is described by

$$\dot{x} = A_{11}x + A_{12}z + B_1u + f_1(x, z) \tag{10.179}$$

$$\dot{z} = A_{21}x + A_{22}z + B_2u + f_2(x, z) \tag{10.180}$$

where A_{ij} and B_i, $i = 1, 2$, $j = 1, 2$ are nominal aircraft matrices which are assumed to be known; $x(t) = \left[p(t)\ q(t)\ r(t) \right]^\top$ is an inner-loop state vector of roll, pitch, and yaw rates; $z(t) = \left[\Delta\phi(t)\ \Delta\alpha(t)\ \Delta\beta(t)\ \Delta V(t)\ \Delta h(t)\ \Delta\theta(t) \right]^\top$ is an outer-loop state vector of aircraft attitude angles, airspeed, and altitude; $u(t) = \left[\Delta\delta_a(t)\ \Delta\delta_e(t)\ \Delta\delta_r(t) \right]^\top$ is a control vector of aileron, elevator, and rudder deflections; and $f_i(x, z)$, $i = 1, 2$ is an unstructured uncertainty due to off-nominal events which can be approximated as

$$f_i(x, z) = \Theta_i^{*\top} \Phi(x, z) + \delta(x, z) \tag{10.181}$$

where Θ_i^* is an unknown, constant ideal weight matrix, and $\Phi(x, z)$ is the input regressor function vector chosen to be

$$\Phi(x, z) = \left[x^\top\ px^\top\ qx^\top\ rx^\top\ z^\top\ u^\top(x, z) \right]^\top \tag{10.182}$$

The inner-loop rate feedback control is designed to improve aircraft rate response characteristics such as the short-period mode and Dutch roll mode. The reference model is a second-order model that specifies desired handling qualities with good damping and natural frequency characteristics as

$$\left(s^2 + 2\zeta_p \omega_p s + \omega_p^2\right) \phi_m = g_p \delta_{lat} \tag{10.183}$$

$$\left(s^2 + 2\zeta_q \omega_q s + \omega_q^2\right) \theta_m = g_q \delta_{lon} \tag{10.184}$$

$$\left(s^2 + 2\zeta_r \omega_r s + \omega_r^2\right) \beta_m = g_r \delta_{rud} \tag{10.185}$$

where $\phi_m(t)$, $\theta_m(t)$, and $\beta_m(t)$ are the reference bank, pitch, and sideslip angles; ω_p, ω_q, and ω_r are the natural frequencies for desired handling qualities in the roll, pitch, and yaw axes; ζ_p, ζ_q, and ζ_r are the desired damping ratios; $\delta_{lat}(t)$, $\delta_{lon}(t)$, and $\delta_{rud}(t)$ are the lateral stick input, longitudinal stick input, and rudder pedal input; and g_p, g_q, and g_r are the input gains.

Let $p_m(t) = \dot{\phi}_m(t)$, $q_m(t) = \dot{\theta}_m(t)$, and $r_m(t) = -\dot{\beta}_m(t)$, then the reference model can be represented as

$$\dot{x}_m = -K_p x_m - K_i \int_0^t x_m(\tau)\, d\tau + Gr \tag{10.186}$$

where $x_m(t) = \left[p_m(t)\ q_m(t)\ r_m(t) \right]^\top$, $K_p = \text{diag}\left(2\zeta_p\omega_p, 2\zeta_q\omega_q, 2\zeta_r\omega_r\right)$, $K_i = \text{diag}\left(\omega_p^2, \omega_q^2, \omega_r^2\right) = \Omega^2$, $G = \text{diag}\left(g_p, g_q, g_r\right)$, and $r(t) = \left[\delta_{lat}(t)\ \delta_{lon}(t)\ \delta_{rud}(t) \right]^\top$.

For the roll axis, the reference model could also be a first-order model

$$\left(s + \omega_p\right) p_m = g_p \delta_{lat} \tag{10.187}$$

Assuming the pair (A_{11}, B_1) is controllable and the outer-loop state vector $z(t)$ is stabilizable, then the nominal PI feedback controller, defined by $\bar{u}(t)$, is given by

$$\bar{u} = K_p (x_m - x) + K_i \int_0^t [x_m(\tau) - x(\tau)] d\tau \tag{10.188}$$

and the adaptive controller, defined by $u_{ad}(t)$, is given by

$$u_{ad} = \Theta_1^\top \Phi(x, z) \tag{10.189}$$

Assuming B_1 is invertible, then the dynamic inversion controller is computed as

$$u = B_1^{-1} (\dot{x}_m - A_{11}x - A_{12}z + \bar{u} - u_{ad}) \tag{10.190}$$

In a more general case when the control vector has more inputs than the number of states to be controlled, then an optimal control allocation strategy using a pseudo-inverse method is used to compute the dynamic inversion controller as

$$u = B_1^\top \left(B_1 B_1^\top\right)^{-1} (\dot{x}_m - A_{11}x - A_{12}z + \bar{u} - u_{ad}) \tag{10.191}$$

Let $e(t) = \left[\int_0^t \left[x_m^\top(t) - x^\top(t)\right] d\tau \; x_m^\top(t) - x^\top(t)\right]^\top$ be the tracking error, then the tracking error equation is given by

$$\dot{e} = A_m e + B \left[\Theta_1^\top \Phi(x, z) - f_1(x, z)\right] \tag{10.192}$$

where

$$A_m = \begin{bmatrix} 0 & I \\ -K_i & -K_p \end{bmatrix} \tag{10.193}$$

$$B = \begin{bmatrix} 0 \\ I \end{bmatrix} \tag{10.194}$$

Let $Q = 2cI$, where $c > 0$ is a weighting constant and I is an identity matrix, then it can be shown that

$$P = c \begin{bmatrix} K_i^{-1} K_p + K_p^{-1}(K_i + I) & K_i^{-1} \\ K_i^{-1} & K_p^{-1}\left(I + K_i^{-1}\right) \end{bmatrix} > 0 \tag{10.195}$$

$$PB = c \begin{bmatrix} K_i^{-1} \\ K_p^{-1}\left(I + K_i^{-1}\right) \end{bmatrix} \tag{10.196}$$

$$B^\top P A_m^{-1} B = -cK_i^{-2} < 0 \tag{10.197}$$

Then, the optimal control modification adaptive law for a nominal PI feedback controller is specified by

$$\dot{\Theta}_1 = -\Gamma\left[\Phi(x,z)\, e^{\top} PB + c\nu\Phi(x,z)\,\Phi^{\top}(x,z)\,\Theta_1 K_i^{-2}\right] \tag{10.198}$$

which can also be expressed as

$$\dot{\Theta}_1 = -\Gamma\left[\Phi(x,z)\, e^{\top} PB + c\nu\Phi(x,z)\,\Phi^{\top}(x,z)\,\Theta_1 \Omega^{-4}\right] \tag{10.199}$$

Suppose the tracking error equation is of a proportional-derivative (PD) type

$$\ddot{e} = -K_d\dot{e} - K_p e + \tilde{\Theta}_2^{\top}\Phi(x,z) \tag{10.200}$$

where $e(t) = x_m(t) - x(t)$

Then, the optimal control modification adaptive law for a nominal PD feedback controller is specified by

$$\dot{\Theta}_2 = -\Gamma\left[\Phi(x,z)\, e^{\top} PB + c\nu\Phi(x,z)\,\Phi^{\top}(x,z)\,\Theta_2 K_p^{-2}\right] \tag{10.201}$$

where

$$PB = c\begin{bmatrix} K_p^{-1} \\ K_d^{-1}\left(I + K_p^{-1}\right) \end{bmatrix} \tag{10.202}$$

Furthermore, if the tracking error equation is of a proportional type

$$\dot{e} = -K_p e + \tilde{\Theta}_3^{\top}\Phi(x,z) \tag{10.203}$$

then the optimal control modification adaptive law for a nominal proportional controller is specified by

$$\dot{\Theta}_3 = -c\Gamma\left[\Phi(x,z)\, e^{\top} K_p^{-1} + \nu\Phi(x,z)\,\Phi^{\top}(x,z)\,\Theta_3 K_p^{-2}\right] \tag{10.204}$$

An adaptive flight control design is implemented on an F-18 aircraft model of NASA F/A-18 research aircraft (tail number 853) as shown in Fig. 10.2, with both the standard baseline dynamic inversion controller and the adaptive controller with the optimal control modification adaptive law [11]. The flight condition is a test point of Mach 0.5 and an altitude of 15,000 ft. All of the pilot inputs used in the simulations are from pre-selected piloted stick inputs for comparison purposes. A time delay of 0.01 s is injected at the actuators to account for the actuator lag.

The first simulation scenario is called an A matrix failure which is emulated by a center of gravity (CG) shift so as to reduce the amplitude of the pitch stability derivative C_{m_α} which is normally negative for a stable aircraft in pitch. Figure 10.68 shows the responses of the aircraft. The failure is inserted at 13 s. Upon the failure insertion, the closed-loop plant with the nominal controller can no longer track the reference model. Excessive overshoots in the pitch rate and angle of attack are observed. With the adaptive controller, the pitch rate tracks the reference pitch rate command quite well and the overshoots are significantly reduced.

Figure 10.69 shows the tracking errors in the roll, pitch, and yaw axes along with the adaptation weights. With the adaptive controller, the roll rate tracking error is essentially reduced to zero. Both the pitch rate tracking error and yaw rate tracking error are reduced to no more than about 2°/s with the adaptive controller. The weights exhibit some large initial transients but then converge to their steady-state values quickly after 28 s.

Figure 10.70 shows the control surface deflections with the nominal controller and the adaptive controller. The actuator models are high-fidelity fourth-order models with time delays. The control surface deflections with the adaptive controller are well-behaved and smaller in amplitudes than the control surface deflections with the nominal controller.

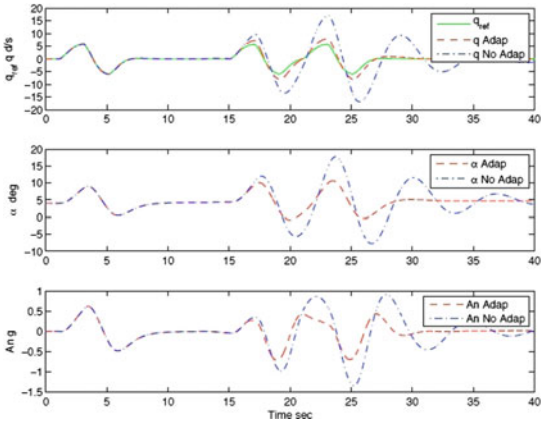

Fig. 10.68 Longitudinal states due to an A matrix failure (C_{m_α} shift at 13 s) with and without optimal control modification

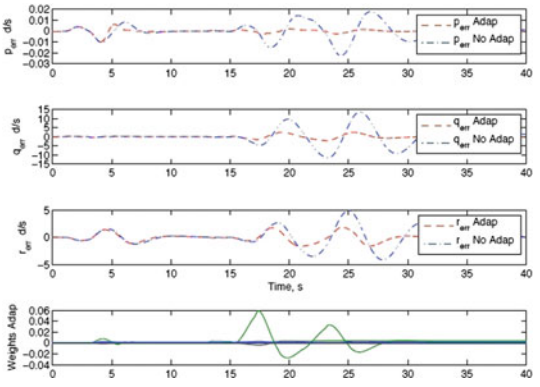

Fig. 10.69 Tracking errors due to an A matrix failure (C_{m_α} shift at 13 s) with and without optimal control modification

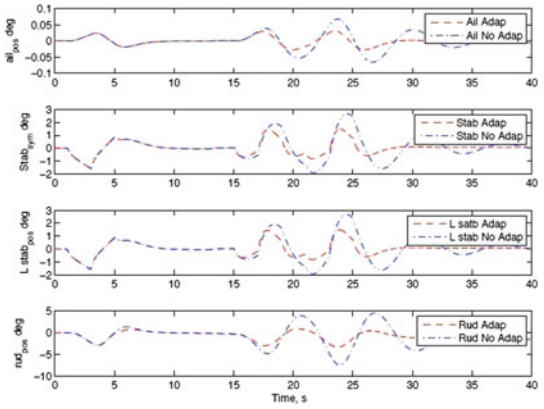

Fig. 10.70 Control surfaces due to an A matrix failure (C_{m_α} shift at 13 s) with and without optimal control modification

The second simulation scenario is called a B matrix failure which is emulated by a jammed left stabilator at +2.5° from trim. Figure 10.71 and 10.72 show the responses of the aircraft in the pitch, roll, and yaw axes. The failure is inserted at 13 s. Upon the failure insertion, the closed-loop plant with the nominal controller is unable to follow the reference model. The pitch rate can longer track the reference pitch rate command. The roll and yaw rates are quite large. With the adaptive controller, the pitch, roll, and yaw rates are significantly reduced. The bank angle is also significantly reduced from 12° with the nominal controller to about 5°. The sideslip angle is reduced from 8° to 4°.

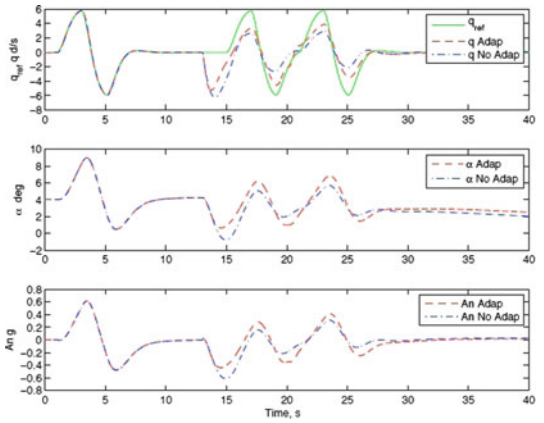

Fig. 10.71 Longitudinal states due to a B matrix failure (Stabilator Jammed at 2.5° at 13 s) with and without optimal control modification

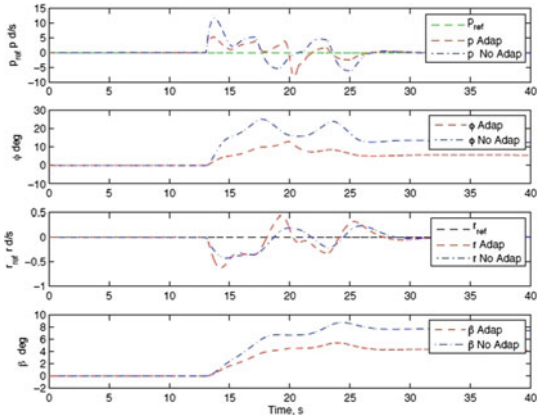

Fig. 10.72 Lateral-directional states due to a B matrix failure (Stabilator Jammed at 2.5° at 13 s with and without optimal control modification

Figure 10.73 shows the tracking errors in the roll, pitch, and yaw axes along with the adaptation weights. The roll rate tracking error and pitch rate tracking error are generally smaller with the adaptive controller than with the nominal controller. The yaw rate tracking error is about the same for both the nominal controller and the adaptive controller. The weights converge after about 20 s.

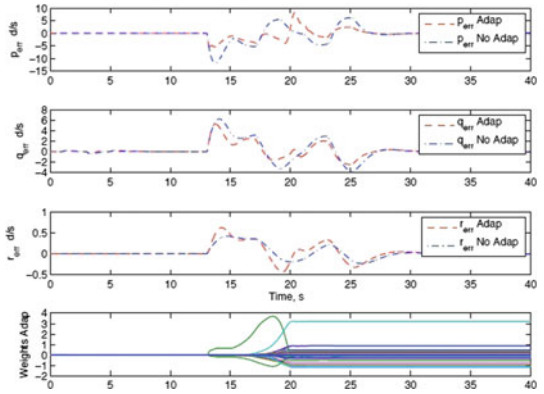

Fig. 10.73 Tracking errors due to a B matrix failure (Stabilator Jammed at 2.5° at 13 s) with and without optimal control modification

The optimal control modification adaptive control is shown to be able to achieve fast adaptation with a good damping characteristic. The simulation scenario with the A matrix failure is conducted with the adaptation rate changed from $\Gamma = 0.5$ to $\Gamma = 50$ while keeping the modification parameter $\nu = 1$ constant. The failure

is inserted at 2 s. Figure 10.74 shows the pitch rate tracking error for $\Gamma = 0.5$ and $\Gamma = 50$. Increasing the adaptation rate Γ from 0.5 to 50 results in a significantly smaller tracking error. This is as expected. The response is nicely damped with $\Gamma = 50$ without any high-frequency oscillations. The weights converge faster with increasing the adaptation rate Γ. Thus, the simulation shows that a larger adaptation rate can produce better tracking with the optimal control modification without causing any high-frequency oscillations.

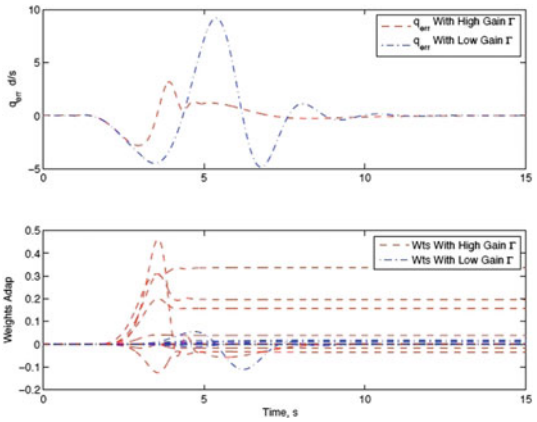

Fig. 10.74 Pitch rate error and weights due to an A-matrix failure (C_{m_α} Shift at 2 s) with optimal control modification ($\Gamma = 0.5$ and $\Gamma = 50$ with fixed $\nu = 1$)

The modification parameter ν provides the damping to the adaptive controller. The same simulation scenario with the A matrix failure is conducted with the modification parameter changed from $\nu = 0.25$ to $\nu = 1$ while keeping the adaptation rate $\Gamma = 5$ constant. Figure 10.75 shows the pitch rate tracking errors for $\nu = 0.25$ and $\nu = 1$. Increasing the modification parameter ν from 0.25 to 1 adds more damping to the adaptive controller. As a result, the pitch rate tracking error is well-damped with $\nu = 1$ without any oscillations. All the weights converge faster with increasing the modification parameter ν. Thus, this simulation shows that a larger modification parameter can help improved the performance of the adaptive controller.

This F-18 aircraft simulation study validates the effectiveness of adaptive control in general and the optimal control modification in particular in improving the flight control performance of a degraded aircraft. The study coupled with a piloted high-fidelity F-18 flight simulator experiment established the basis for a flight test program on NASA F/A-18 research aircraft (tail number 853) in 2010 and 2011.

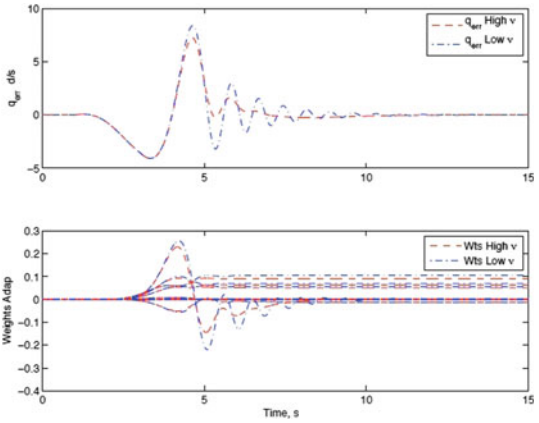

Fig. 10.75 Pitch rate error and weights due to an A-matrix failure (C_{m_α} shift at 2 s) with optimal control modification (fixed $\Gamma = 5$ with $\nu = 0.25$ and $\nu = 1$)

10.10 Summary

Adaptive control enjoys many applications in aerospace. It has a long history dated back to the 1950s with the first adaptive control deployed on NASA X-15 hypersonic vehicles. Applications of adaptive control in other domains are numerous. Adaptive flight control applications for aircraft longitudinal dynamics using the bi-objective optimal control modification and least-squares adaptive control with Chebyshev polynomial approximation and neural networks are illustrated. Adaptive flight control for flexible aircraft with aeroelastic interactions using the optimal control modification and adaptive loop recovery modification is presented. An adaptive LQG control method is developed for a flutter suppression of a flexible wing. A general adaptive flight control architecture based on a dynamic inversion with adaptive augmentation control is outlined. Robust modification schemes based on σ modification, e modification, and optimal control modification are used in the adaptive augmentation control to improve robustness. Hybrid adaptive flight control is a robust adaptive flight control architecture that blends both direct MRAC and indirect adaptive control using least-squares parameter identification together. This technique can significantly improve the performance of a flight control system under off-nominal operation of an impaired or damaged aircraft. Finally, an adaptive flight control design for a F/A-18A NASA aircraft based on the optimal control modification is implemented in simulations. This implementation was later used in the actual flight testing in 2010 and 2011.

10.11 Exercises

1. Consider the equation of motion of an inverted pendulum

$$\frac{1}{3}mL^2\ddot{\theta} - \frac{1}{2}mgL\sin\theta + c\dot{\theta} = u\left(t - t_d\right)$$

   a. Expand $\sin\theta$ using the Taylor series expansion about $\theta\left(t\right) = 0$ for the first two terms. Then, express the equation of motion in the form of

$$\dot{x} = Ax + B\left[u\left(t - t_d\right) + \Theta^{*\top}\Phi\left(x\right)\right]$$

   where $x_1\left(t\right) = \theta\left(t\right)$, $x_2\left(t\right) = \dot{\theta}\left(t\right)$, $x\left(t\right) = \left[\begin{array}{cc} x_1\left(t\right) & x_2\left(t\right)\end{array}\right]^\top$, $\Phi\left(x\right)$ is comprised of the function in the nonlinear term of the Taylor series expansion of $\sin\theta$ and the function in the damping term, and Θ^* is a vector of parameters associated with $\Phi\left(x\right)$ which are assumed to be unknown.

   b. Let $m = 0.1775$ slug, $L = 2$ ft, $c = 0.2$ slug-ft^2/s, $t_d = 0.05$ sec, and $\theta\left(0\right) = \dot{\theta}\left(0\right) = 0$. Using the equation of motion in part (a), design an adaptive controller using the optimal control modification to enable the closed-loop plant to track a reference model specified by

$$\ddot{\theta}_m + 2\zeta_m\omega_m\dot{\theta}_m + \omega_m^2\theta_m = \omega_m^2 r$$

   where $\zeta_m = 0.5$, $\omega_m = 2$, and $r = \frac{\pi}{12}$. Calculate K_x and k_r.

   c. Implement the adaptive controller in Simulink using the nonlinear plant with $\Theta^\top\left(0\right) = \left[\begin{array}{cc}\theta_1^* & 0\end{array}\right]$ and a time step $\Delta t = 0.001$ s for the standard MRAC with $\Gamma = 100$ and the optimal control modification with $\Gamma = 100$ and $\nu = 0.5$. Plot the time histories of $x\left(t\right)$ and $x_m\left(t\right)$ on the same plot, $u\left(t\right)$, and $\Theta\left(t\right)$ for $t \in [0, 10]$ s. Compare the closed-loop response with the optimal control modification to that in Example 10.1. Does the linear nominal controller design in this problem appear to work as well as the nonlinear nominal controller design in Example 10.1?

2. Implement a longitudinal dynamic model of an aircraft.

$$\dot{x} = Ax + B\left[u\left(t - t_d\right) + \Theta^{*\top}x\right]$$

   where $x\left(t\right) = \left[\begin{array}{ccc}\alpha\left(t\right) & \theta\left(t\right) & q\left(t\right)\end{array}\right]^\top$, $u\left(t\right) = \delta_e\left(t\right)$, and $\Theta^* = \left[\begin{array}{ccc}\theta_\alpha^* & 0 & \theta_q^*\end{array}\right]^\top$, with the following information: $\bar{V} = 795.6251$ ft/s, $\bar{\gamma} = 0$, $Z_\alpha = -642.7855$ ft/s^2, $Z_{\delta_e} = -55.3518$ ft/s^2, $M_\alpha = -5.4898$ s^{-2}, $M_{\delta_e} = -4.1983$ s^{-2}, $M_q = -0.6649$ s^{-1}, $M_{\dot{\alpha}} = -0.2084$ s^{-1}, $\theta_\alpha^* = 0.5$, $\theta_q^* = -0.5$, and $t_d = 0.1$ s.

   a. Design an adaptive pitch attitude controller using the optimal control modification to enable the closed-loop plant to follow a second-order reference model of the pitch attitude specified by $\zeta_m = \frac{1}{\sqrt{2}}$ and $\omega_m = 2$ rad/s. Express

the adaptive controller with the feedback gain values and the reference model.

b. Implement the adaptive controller in Simulink using the following information: $x(0) = 0$ and $\Theta(0) = 0$ with a time step $\Delta t = 0.01$ s for: 1) the nominal controller, 2) the standard MRAC with $\Gamma = 500$, and 3) the optimal control modification with $\Gamma = 500$ and $\nu = 0.5$. The reference command signal $r(t)$ is a pitch attitude doublet specified in the following plot.

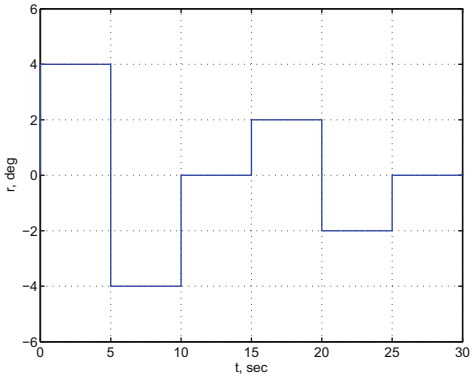

For each controller, plot the time histories of each of the elements of $x(t)$ and $x_m(t)$ on the same plot, and $u(t)$ for $t \in [0, 30]$ s. Plot in units of deg for $\alpha(t)$, $\theta(t)$, and $\delta_e(t)$, and deg/s for $q(t)$. Comment on the simulation results.

References

1. Bosworth, J., & Williams-Hayes, P. S. (2007). Flight test results from the NF-15B IFCS project with adaptation to a simulated stabilator failure. In *AIAA Infotech@Aerospace Conference, AIAA-2007-2818, May 2007*.
2. Williams-Hayes, P. S. Flight test implementation of a second generation intelligent flight control system. In: *NASA TM-2005-213669*.
3. Narendra, K. S., & Annaswamy, A. M. (1987). A new adaptive law for robust adaptation without persistent excitation. *IEEE Transactions on Automatic Control*, *AC-32*(2), 134–145.
4. Calise, A. J., & Rysdyk, R. T. (1998). Nonlinear adaptive flight control using neural networks. *IEEE Control System Magazine*, *18*(6):14–25.
5. Hanson, C., Johnson, M., Schaefer, J., Nguyen, N., & Burken, J. (2011). Handling qualities evaluations of low complexity model reference adaptive controllers for reduced pitch and roll damping scenarios. In *AIAA Guidance, Navigation, and Control Conference, AIAA-2011-6607, August 2011*.
6. Hanson, C., Schaefer, J., Johnson, M., & Nguyen, N. Design of low complexity model reference adaptive controllers. In: *NASA-TM-215972*.
7. Nguyen, N., Hanson, C., Burken, J., & Schaefer, J. (2016). Normalized optimal control modification and flight experiments on NASA F/A-18 aircraft. In: *AIAA Journal of Guidance, Control, and Dynamics*.
8. Schaefer, J., Hanson, C., Johnson, M., & Nguyen, N. (2011). Handling qualities of model reference adaptive controllers with varying complexity for pitch-roll coupled failures. In *AIAA Guidance, Navigation, and Control Conference AIAA-2011-6453, August 2011*.

9. Campbell, S., Kaneshige, J., Nguyen, N., & Krishnakumar, K. (2010) An adaptive control simulation study using pilot handling qualities evaluations. In *AIAA Guidance, Navigation, and Control Conference, AIAA-2010-8013, August 2010*.
10. Campbell, S., Kaneshige, J., Nguyen, N., & Krishnakumar, K. (2010). Implementation and evaluation of multiple adaptive control technologies for a generic transport aircraft simulation. In *AIAA Infotech@Aerospace Conference, AIAA-2010-3322, April 2010*.
11. Burken, J., Nguyen, N., & Griffin, B. (2010). Adaptive flight control design with optimal control modification for f- 18 aircraft model. In *AIAA Infotech@Aerospace Conference, AIAA-2010-3364, April 2010*.
12. Nguyen, N., Burken, J., & Hanson, C. (2011). Optimal control modification adaptive law with covariance adaptive gain adjustment and normalization. In *AIAA Guidance, Navigation, and Control Conference, AIAA-2011-6606, August 2011*.
13. Nguyen, N., & Summers, E. (2011). On time delay margin estimation for adaptive control and robust modification adaptive laws. In *AIAA Guidance, Navigation, and Control Conference, AIAA-2011-6438, August 2011*.
14. Nelson, R. C. (1989). *Flight stability and automatic control*. New York: McGraw-Hill
15. Nguyen, N., & Balakrishnan, S. N. (2014). Bi-objective optimal control modification adaptive control for systems with input uncertainty. *IEEE/CAA Journal of Automatica Sinica*, **1**(4), 423–434.
16. Nguyen, N. (2013). Least-squares model reference adaptive control with chebyshev orthogonal polynomial approximation. *AIAA Journal of Aerospace Information Systems*, *10*(6), 268–286.
17. Rohrs, C. E., Valavani, L., Athans, M., & Stein, G. (1985). Robustness of continuous-time adaptive control algorithms in the presence of unmodeled dynamics. *IEEE Transactions on Automatic Control*, *AC-30*(9), 881–889.
18. Ioannou, P., & Kokotovic, P. (1984). Instability analysis and improvement of robustness of adaptive control. *Automatica*, *20*(5), 583–594.
19. Nguyen, N. (2012). Optimal control modification for robust adaptive control with large adaptive gain. *Systems & Control Letters*, *61*(2012), 485–494.
20. Calise, A. J., & Yucelen, T. (2012). Adaptive loop transfer recovery. *AIAA Journal of Guidance, Control, and Dynamics*, *35*(3), 807–815.
21. Nguyen, N., Tuzcu, I., Yucelen, T., & Calise, A. (2011). Longitudinal dynamics and adaptive control application for an aeroelastic generic transport model. In *AIAA Atmospheric Flight Mechanics Conference, AIAA-2011-6319, August 2011*.
22. Kokotovic, P., Khalil, H., & O'Reilly, J. (1987). *Singular perturbation methods in control: analysis and design*. Philadelphia: Society for Industrial and Applied Mathematics.
23. Nguyen, N. (2010). Elastically Shaped Future Air Vehicle Concept," NASA Innovation Fund Award 2010 Report, October 2010, Submitted to NASA Innovative Partnerships Program. http://ntrs.nasa.gov/archive/nasa/casi.ntrs.nasa.gov/20110023698.pdf.
24. Nguyen, N., Trinh, K., Reynolds, K., Kless, J., Aftosmis, M., Urnes, J., & Ippolito, C., Elastically shaped wing optimization and aircraft concept for improved cruise efficiency. In *AIAA Aerospace Sciences Meeting, AIAA-2013-0141, January 2013*.
25. Urnes, J., Nguyen, N., Ippolito, C., Totah, J., Trinh, K., & Ting, E., A mission adaptive variable camber flap control system to optimize high lift and cruise lift to drag ratios of future N+3 transport aircraft. In *AIAA Aerospace Sciences Meeting, AIAA-2013-0214, January 2013*.
26. Jordan, T., Langford, W., Belcastro, C., Foster, J., Shah, G., Howland, G., et al. (2004). Development of a dynamically scaled generic transport model testbed for flight research experiments. In *AUVSI Unmanned Unlimited, Arlington, VA*.
27. Nguyen, N., Ting, E., Nguyen, D., & Trinh, K., Flutter analysis of mission-adaptive wing with variable camber continuous trailing edge flap. In *55th AIAA/ASME/ASCE/AHS/ASC Structures, Structural Dynamics, and Materials Conference, AIAA-2014-0839, January 2014*.
28. Nguyen, N., Swei, S., & Ting, E. (2015). Adaptive linear quadratic gaussian optimal control modification for flutter suppression of adaptive wing. In *AIAA Infotech@Aerospace Conference, AIAA 2015-0118, January 2015*.

29. Ardema, M. (1981). Computational singular perturbation method for dynamical systems. *AIAA Journal of Guidance, Control, and Dynamics*, *14*, 661–663.
30. Dykman, J., Truong, H., & Urnes, J. (2015). Active control for elastic wing structure dynamic modes. In *56th AIAA/ASCE/AHS/ASC Structures, Structural Dynamics, and Materials Conference, AIAA-2015-1842, January 2015*.
31. Slotine, J.-J., & Li, W. (1991) *Applied Nonlinear Control*. Englewood Cliffs: Prentice-Hall, Inc.
32. Hsu, L., Teixeira, M. C. M., Costa, R. R., & Assunčao, E. (2011). Necessary and sufficient condition for generalized passivity, passification and application to multivariable adaptive systems. In *18th International Federation of Automatic Control World Congress, August 2011*.
33. Misra, P. (1993). Numerical algorithms for squaring-up non- square systems part II: general case. In *American Control Conference, June 1993*.
34. Qu, Z., Wiese, D., Annaswamy, A. M., & Lavretsky, E. (2014). Squaring-up method in the presence of transmission zeros. In *19th International Federation of Automatic Control World Congress, August 2014*.
35. Lavretsky, E., & Wise, K. (2012). *Robust and adaptive control*. Berlin: Springer.
36. Nguyen, N., & Urnes, J. (2012). Aeroelastic modeling of elastically shaped aircraft concept via wing shaping control for drag reduction. In: *AIAA Atmospheric Flight Mechanics Conference, AIAA-2012-4642, August 2012*.
37. Nguyen, N., Krishnakumar, K., Kaneshige, J., & Nespeca, P. (2008). Flight dynamics modeling and hybrid adaptive control of damaged asymmetric aircraft. *AIAA Journal of Guidance, Control, and Dynamics*, *31*(3), 751–764.

Suggested Exam Questions

1. For the following systems, determine the equilibrium points. Use the Lyapunov's direct method to determine the type of Lyapunov stability for each of the equilibrium points. Determine all the invariant sets and the values of the Lyapunov function on the sets. If an equilibrium point is stable, conclude if it is asymptotically stable, and if so, show whether or not it is also exponentially stable.

   a.
   $$\begin{bmatrix} \dot{x}_1 \\ \dot{x}_2 \end{bmatrix} = \begin{bmatrix} (x_2 - x_1)\left(x_1^2 + x_2^2 - 1\right) \\ -(x_1 + x_2)\left(x_1^2 + x_2^2 - 1\right) \end{bmatrix}$$

   b.
   $$\begin{bmatrix} \dot{x}_1 \\ \dot{x}_2 \end{bmatrix} = \begin{bmatrix} x_2^2 - x_2 \\ -x_1 - x_2 + 1 \end{bmatrix}$$

   c.
   $$\begin{bmatrix} \dot{x}_1 \\ \dot{x}_2 \end{bmatrix} = \begin{bmatrix} x_2 \\ -x_1 - (1 + \sin x_1)\, x_2 \end{bmatrix}$$

2. Linearize the systems in problem 2 and determine the types of equilibrium points. Plot phase portraits.

3. Given the following system
   $$\begin{bmatrix} \dot{x}_1 \\ \dot{x}_2 \end{bmatrix} = \begin{bmatrix} -2 + \sin^2 x_1 & 1 - \sin x_1 \cos x_2 \\ -1 + \sin x_1 \cos x_2 & -2 - \cos^2 x_2 \end{bmatrix} \begin{bmatrix} x_1 \\ x_2 \end{bmatrix}$$
   Determine the stability of this system about the origin using the Lyapunov candidate function
   $$V(x) = \frac{1}{2} x^\top x$$
   If asymptotically stable, determine if the origin is exponentially stable and find the rate of convergence of $\|x\|$, where $x(t) = \left[x_1(t)\ x_2(t) \right]^\top$.

N.T. Nguyen, *Model-Reference Adaptive Control*, Advanced Textbooks in Control and Signal Processing, https://doi.org/10.1007/978-3-319-56393-0

4. Given a linear system

$$\dot{x} = Ax + Bh(t)$$

where $x(t) = \left[x_1(t)\ x_2(t) \right]^\top \in \mathbb{R}^2$ and

$$A = \begin{bmatrix} -1 & 2 \\ -4 & -2 \end{bmatrix},\ B = \begin{bmatrix} 1 \\ 1 \end{bmatrix},\ h(t) = \left(1 + e^{-t}\right)(\sin t + \cos t)$$

   a. Compute P that solves the Lyapunov equation

$$PA + A^\top P = -I$$

   and also compute the eigenvalues of P to verify that P is positive definite.

   b. Use the following Lyapunov candidate function

$$V(x) = x^\top Px$$

   to compute $\dot{V}(x)$. Establish an upper bound on $\dot{V}(x)$ in terms of $\|x\|$, and then determine a lower bound on $\|x\|$ that satisfies $\dot{V}(x) \leq 0$ using the $\mathcal{L}_\infty$ norm and the Cauchy–Schwartz inequality

$$\|CD\| \leq \|C\|\,\|D\|$$

   c. Find an analytical solution of an upper bound of the Lyapunov function $V(t)$ as an explicit function of t from $\dot{V}(x)$ in part (b), given $V(0) = 2$, by utilizing the following relationship for a positive definite function

$$\lambda_{min}(P)\,\|x\|^2 \leq V(x) = x^\top Px \leq \lambda_{max}(P)\,\|x\|^2$$

   and the following variable transformation

$$W(t) = \sqrt{V(t)}$$

   d. Find the ultimate bound of $\|x\|$ by finding the limit of $V(t)$ as $t \to \infty$. If an ultimate bound exists, then the solution of $x(t)$ is uniformly ultimately bounded.

5. Consider a first-order nonlinear SISO system with a matched uncertainty

$$\dot{x} = ax + b\left(u + \theta^* x^2\right)$$

where a is unknown but b is known, and θ^* is unknown.
A reference model is specified by

$$\dot{x}_m = a_m x_m + b_m r$$

where $a_m < 0$ and b_m are known, and $r(t)$ is a bounded command signal.

a. Design a direct adaptive controller that enables the plant output $x(t)$ to track the reference model signal $x_m(t)$. Show by Lyapunov stability analysis that the tracking error is asymptotically stable; i.e., $e(t) \to 0$ as $t \to \infty$.
b. Implement the adaptive controller in Simulink, given $b = 2$, $a_m = -1$, $b_m = 1$, and $r(t) = \sin t$. For adaptation rates, use $\gamma_x = 1$ and $\gamma = 1$. For simulation purposes, assume $a = 1$ and $\theta^* = 0.2$ for the unknown parameters. Plot $e(t)$, $x(t)$, $x_m(t)$, $u(t)$, and $\theta(t)$ for $t \in [0, 50]$.
c. Repeat part (b) for $\gamma_x = 10$ and $\gamma = 10$. Plot the same sets of data as in part (b). Comment on the simulation results for parts (b) and (c) regarding the tracking of the reference model, the quality of the signal in terms of the relative frequency content, and the convergence of $k_x(t)$ and $\theta(t)$ as the adaptation rates increase.
d. Repeat part (b) for $r(t) = 1(t)$ where $1(t)$ is the unit-step function. Plot the same sets of data as in part (b). Comment on the convergence of $k_x(t)$ and $\theta(t)$ to the ideal values k_x^* and θ^*.

6. Given a first-order nonlinear system

$$\dot{x} = ax + Bu + cx^2$$

where $x(t) \in \mathbb{R}$, $u(t) \in \mathbb{R}^2$, a is an unknown constant, $B = \begin{bmatrix} 1 & 2 \end{bmatrix}$ is known, and c is an unknown constant.
The reference model is specified as

$$\dot{x}_m = a_m x_m + b_m r$$

where $a_m = -1$, $b_m = 1$, and $r(t) = \sin t$.
Express the system in the form of a matched uncertainty

$$\dot{x} = ax + B\left[u + \Theta^{*\top} \Phi(x)\right]$$

Determine K_x^*, K_r^*, and Θ^*. Write down the adaptive laws for $K_x(t)$ and $\Theta(t)$. Implement the controller in Simulink. Use $\gamma_x = \gamma_\Theta = 1$. Assume all initial conditions to be zero and $a = 1$, $c = 0.2$ for simulation purpose. Plot $e(t)$, $x(t)$ versus $x_m(t)$, $K_x(t)$, and $\Theta(t)$ for $t \in [0, 40]$.

7. The symmetric sigmoidal function

$$\sigma(x) = \frac{1 - e^{-x}}{1 + e^{-x}}$$

can be used to model a control actuator saturation, which frequently exists in real systems.

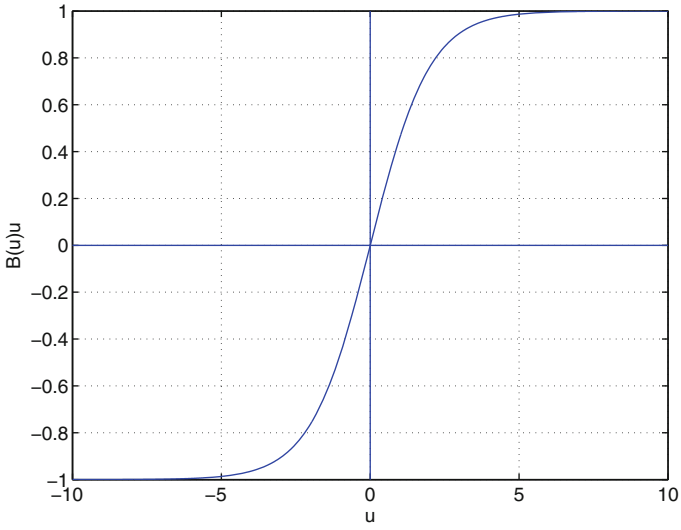

Saturation occurs when a control actuator ceases to be effective. When there are more inputs than commands, a control allocation strategy should be developed to allocate redundant control effectors in an optimal manner so as to produce an output that tracks a command. Define $y(u)$ as the output of a control allocator as

$$y = V^{\top}\sigma\left(W^{\top}u\right)$$

where $y(u) \in \mathbb{R}^n$, $V \in \mathbb{R}^m \times \mathbb{R}^n$, $W \in \mathbb{R}^p \times \mathbb{R}^m$, and $u \in \mathbb{R}^p$, $p \geq n$.
V can be used to specify a saturation limit, while $V^{\top}W^{\top}$ plays the role of a nonlinear $B(u)$ matrix. Develop an optimal control allocation strategy by computing the gradient of the following cost function with respect to u, i.e., ∇J_u

$$J(u) = \frac{1}{2}\epsilon^{\top}\epsilon$$

where $\epsilon = y - r$ and $r \in \mathbb{R}^n$ are a command vector for which an optimal control vector u is to be found to minimize the cost function.
Given $r = 1$ and

$$V = \begin{bmatrix} 0.75 \\ 0.5 \end{bmatrix}, \quad W = \begin{bmatrix} 1.2 & 0.8 \\ 0.5 & 1.5 \end{bmatrix}$$

Write a MATLAB code to compute u using the steepest descent method with an adaptation rate $\varepsilon = 0.1$ and a number of iteration of $n = 1000$. Indicate the final value of u and plot u.

8. Adaptive control can be used for disturbance rejection. Disturbances are usually time signals that may have multiple frequency contents. Unlike unstructured uncertainty in the form of an unknown function $f(x)$, an unknown function of

time $f(t)$ should be approximated by a bounded function. This prevents adaptive signals from blowing up in time. Both the sigmoidal and radial basis functions are bounded functions, but a polynomial function is not. Consider a first-order system with an unknown disturbance

$$\dot{x} = ax + b[u + f(t)]$$

where a and $f(t)$ are unknown, but $b = 2$. For simulation purpose, $a = 1$ and $f(t) = 0.1\sin 2.4t - 0.3\cos 5.1t + 0.2\sin 0.7t$.
The reference model is given by

$$\dot{x}_m = a_m x_m + b_m r$$

where $a_m = -1$, $b_m = 1$, and $r(t) = \sin t$.
Implement in Simulink a direct adaptive control using the least-squares gradient method to approximate $f(t)$ by a sigmoidal neural network with $\Theta(t) \in \mathbb{R}^5$, $W(t) \in \mathbb{R}^2 \times \mathbb{R}^4$ using the activation function $\sigma(x) = \frac{1}{1+e^{-x}}$. Write down the neural net adaptive laws for $k_x(t)$, $\Theta(t)$, and $W(t)$. All initial neural net weights are randomized between 0 and 1. The initial condition for $k_x(t)$ is zero. Use $\Gamma_x = 10I$. Plot $e(t)$, $\epsilon(t)$, $x(t)$ versus $x_m(t)$ with disturbance rejection, $x(t)$ versus $x_m(t)$ without disturbance rejection, $k_x(t)$, $\Theta(t)$, and $W(t)$ for $t \in [0, 40]$.

9. Given the following plant

$$\dot{x} = -2x - z + u + w$$

$$\dot{z} = -3z + 4u$$

$$y = x$$

where $x(t)$ is the plant output, $z(t)$ is an internal state, and $w(t) = 1$ is a constant disturbance.

   a. If a linear controller $u(t) = k_x x(t)$ is used, where k_x is constant, express the transfer function from $w(t)$ to $x(t)$. Find all values of k_x for which the closed-loop plant is stable.
   b. Find the equilibrium state $\bar{x}$ as a function of k_x from part (a). Suppose an adaptive regulator controller is designed with the σ modification

$$u = k_x(t)\, x$$

$$\dot{k}_x = -\gamma\left(x^2 + \sigma k_x\right)$$

   Find the minimum value of the modification parameter σ_{min} to within 0.01 by finding the roots of a polynomial in terms of $\bar{k}_x$ for which one or more roots satisfy the values of k_x in part (a). Calculate $\bar{k}_x$ and $\bar{x}$.

c. Implement the adaptive controller in Simulink with $\sigma = \sigma_{min} - 0.05$ and $\sigma = 0.5$ using the following information: $x(0) = 0$, $z(0) = 0$, $k_x(0) = 0$, and $\gamma = 10$ using a time step $\Delta t = 0.001$ s. Plot the time histories of $x(t)$ and $\theta(t)$ for $t \in [0, 10]$ s for both values of σ. Comment on the two responses. Calculate $\bar{k}_x$ and $\bar{x}$ for $\sigma = 0.5$ analytically and compare them with the simulation results.

10. Given a first-order SISO system with a matched uncertainty

$$\dot{x} = ax + b\left(u + \theta^* x^2\right)$$

subject to $x(0) = x_0$, where $a = 1$ and $b = 1$ are known, and $\theta^* = 2$ is unknown.
An adaptive controller is designed using the optimal control modification adaptive law to enable the plant to follow a reference model

$$\dot{x}_m = a_m x_m + b_m r$$

where $a_m = -1$, $b_m = 1$, and $r(t) = 1$
The adaptive controller is given by

$$u = k_x x + k_r r - \theta(t) x^2$$

a. Express the closed-loop system with the nominal (non-adaptive) controller $u = k_x x$ in terms of the reference model parameters a_m and b_m. Determine whether or not the closed-loop system with the nominal controller is unconditionally (globally) stable by explicitly integrating the plant model to find the solution of $x(t)$. If the closed-loop plant is not globally stable, find the stability condition imposed on x_0.
b. Express the optimal control modification adaptive law for $\theta(t)$. Use Sect. 9.5.3 to estimate the limiting value of the modification parameter ν_{max} to within 0.001. If applicable, express $\varphi(\|x\|, \|x_m\|, \nu, \theta^*)$. Then, ν_{max} can be found by trial and error to be the largest value for which $\varphi(\|x\|, \|x_m\|, \nu_{max}, \theta^*) = 0$ such that $\|x\| > \|x_m\|$. Express the ultimate bound of $\|e\|$ and $\left\|\tilde{\theta}\right\|$ as a function $\|x\|$, ν, and γ. Evaluate them for $\gamma = 500$.
c. Implement the adaptive controller in Simulink with MRAC for which $\nu = 0$ and the optimal control modification with $\nu = \nu_{max}$ determined from part (b) using the following information: $x(0) = 1$, $\theta(0) = 0$, and $\gamma = 500$ with a time step $\Delta t = 0.001$ s. Plot the time histories of $x(t)$, $u(t)$, and $\theta(t)$ for $t \in [0, 10]$ s for both MRAC and the optimal control modification. Comment on the responses of the two adaptive controllers and compare the maximum tracking error $\|e\|$ and maximum parameter estimation error $\left\|\tilde{\theta}\right\|$ due to the optimal control modification to those determined from part (b).

11. Consider the equation of motion of an inverted pendulum constrained to move horizontally by a control force $u\,(t)$

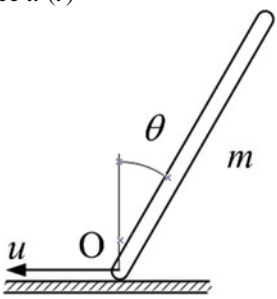

$$\frac{1}{12}mL^2\left(4-3\cos^2\theta\right)\ddot{\theta}-\frac{1}{2}mgL\sin\theta+\frac{1}{8}mL^2\dot{\theta}^2\sin 2\theta+c\dot{\theta}=\frac{1}{2}L\cos\theta u\,(t-t_d)$$

where m is the mass of the pendulum, L is the length, g is the gravity constant, c is the damping coefficient which is assumed to be unknown, $\theta\,(t)$ is the angular position, $u\,(t)$ is the control input which represents the horizontal force at point O, and t_d is a time delay which represents the motor actuator dynamics.

a. Let $x_1\,(t)=\theta\,(t)$, $x_2\,(t)=\dot{\theta}\,(t)$, and $x\,(t)=\left[x_1\,(t)\;x_2\,(t)\right]^\top$. Derive the expressions for the nonlinear dynamic inversion adaptive controller and the σ modification adaptive law to estimate the unknown coefficient c in order to enable the closed-loop plant to track a reference model specified by

$$\ddot{\theta}_m+2\zeta_m\omega_m\dot{\theta}_m+\omega_m^2\theta_m=\omega_m^2 r$$

which can be expressed in general as

$$\dot{x}_m=A_m x_m+B_m r$$

b. Given $m=0.1775$ slug, $g=32.174$ ft/s, $L=2$ ft, $c=0.2$ slug-ft^2/s, $\zeta_m=0.75$, $\omega_m=2$, and $r=\frac{\pi}{12}\sin 2t$. Implement the adaptive controller in Simulink with the following information: $x\,(0)=0$, $\hat{c}\,(0)=0$, $\gamma=100$, and a time step $\Delta t=0.001$ s for the following cases: (1) the standard MRAC with $t_d=0$, (2) the standard MRAC with $t_d=0.01$ s, and (3) the σ modification with $\sigma=0.1$. For each case, plot the time histories of $x\,(t)$ and $x_m\,(t)$ on the same plot, $u\,(t)$, and $\hat{c}\,(t)$ for $t\in[0,\,10]$ s. Plot in the units of deg for $x_1\,(t)$, deg/s for $x_2\,(t)$, lb for $u\,(t)$, lb-ft-sec for $\hat{c}\,(t)$.

12. Given a longitudinal dynamic model of an aircraft with a matched uncertainty

$$\begin{bmatrix} \dot{\alpha} \\ \dot{q} \end{bmatrix} = \begin{bmatrix} \frac{Z_\alpha}{\bar{V}} & 1 \\ M_\alpha + \frac{M_{\dot{\alpha}} Z_\alpha}{\bar{V}} & M_q + M_{\dot{\alpha}} \end{bmatrix} \begin{bmatrix} \alpha \\ q \end{bmatrix} + \begin{bmatrix} \frac{Z_{\delta_e}}{\bar{V}} \\ M_{\delta_e} + \frac{M_{\dot{\alpha}} Z_{\delta_e}}{\bar{V}} \end{bmatrix} \left(\delta_e (t - t_d) + \begin{bmatrix} \theta_\alpha^* & \theta_q^* \end{bmatrix} \begin{bmatrix} \theta \\ q \end{bmatrix} \right)$$

with the following information: $\bar{V} = 795.6251$ ft/s, $\bar{\gamma} = 0$, $Z_\alpha = -642.7855$ ft/s^2, $Z_{\delta_e} = -55.3518$ ft/s^2, $M_\alpha = -5.4898$ sec^{-2}, $M_{\delta_e} = -4.1983\,\text{s}^{-2}$, $M_q = -0.6649$ sec^{-1}, $M_{\dot{\alpha}} = -0.2084\,\text{s}^{-1}$, $\theta_\alpha^* = -5.4$, $\theta_q^* = -0.3$, and $t_d = 0.01$ sec.

a. Design a nominal proportional–integral control

$$\delta_e = k_p \alpha + k_i \int_0^t (\alpha - r)\, d\tau + k_q q$$

by finding the general expressions and the numerical values for k_p, k_i, and k_q to enable the aircraft to track a reference model of the angle of attack

$$\ddot{\alpha}_m + 2\zeta_m \omega_m \dot{\alpha}_m + \omega_m^2 \alpha_m = \omega_m^2 r$$

where $\zeta_m = 0.75$ and $\omega_m = 1.5$ rad/s.

b. Let $z(t) = \int_0^t (\alpha(t) - r(t))\, d\tau$, provide the general expression and the numerical value for the reference model of the aircraft as

$$\dot{x}_m = A_m x_m + B_m r$$

where $x(t) = \begin{bmatrix} z(t) & \alpha(t) & q(t) \end{bmatrix}^\top$.

c. Let $\Theta^* = \begin{bmatrix} 0 & \theta_\alpha^* & \theta_q^* \end{bmatrix}^\top$. Design an adaptive angle-of-attack controller using the optimal control modification to enable the closed-loop plant to track the reference model. Express the adaptive controller and the adaptive law. Given $Q = 100I$, select the modification parameter to guarantee stability of the closed-loop plant by using the linear asymptotic property of the optimal control modification and the following formulas to compute the crossover frequency and time delay margin for MIMO systems. Plot ν versus t_d for $\nu \in [0, 5]$ and determine ν to within 0.01 for $t_d = 0.01$ s
For a general time delay system

$$\dot{x} = Ax + Bu(t - t_d)$$

with a linear controller

$$u = K_x x$$

the crossover frequency and time delay margin can be estimated as

$$\omega = \overline{\mu}\left(-jA\right) + \left\|BK_x\right\|$$

$$t_d = \frac{1}{\omega}\cos^{-1}\frac{\overline{\mu}\left(A\right)}{\overline{\mu}\left(-BK_x\right)}$$

where $\bar{\mu}$ is a matrix measure quantity defined as

$$\overline{\mu}\left(C\right) = \max_{1\le i\le n}\lambda_i\left(\frac{C+C^*}{2}\right)$$

for a general complex-value matrix C with its conjugate transpose C^*.

d. Implement the adaptive controller in Simulink using the following information: $x\left(0\right) = 0$, $\Theta\left(0\right) = 0$, $\Gamma = 1000I$, and ν determined from part (c) with a time step $\Delta t = 0.001$ s. The reference command signal $r\left(t\right)$ is a pitch attitude doublet specified in the following plot.

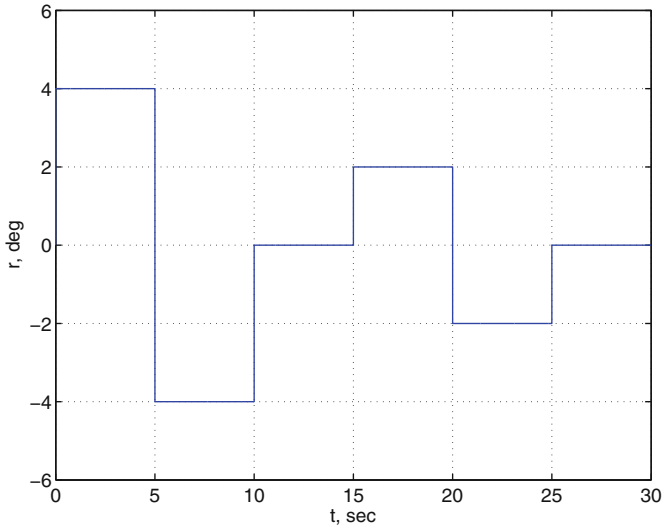

Plot the time histories of each of the elements of $x\left(t\right)$ and $x_m\left(t\right)$ on the same plot, and $u\left(t\right)$ for $t \in [0, 30]$ s. Plot in the units of deg–sec for $z\left(t\right)$, deg for $\alpha\left(t\right)$ and $\delta_e\left(t\right)$, and deg/s for $q\left(t\right)$.

13. Given a longitudinal dynamic model of a damaged aircraft

$$\dot{\alpha} = \left(\frac{Z_\alpha}{\bar{V}} + \Delta A_{\alpha\alpha}\right)\alpha + q + \left(\frac{Z_{\delta_e}}{\bar{V}} + \Delta B_\alpha\right)\delta_e\left(t - t_d\right)$$

$$\dot{q} = \left(M_\alpha + \frac{M_{\dot{\alpha}}Z_\alpha}{\bar{V}} + \Delta A_{q\alpha}\right)\alpha + \left(M_q + M_{\dot{\alpha}} + \Delta A_{qq}\right)q$$
$$+ \left(M_{\delta_e} + \frac{M_{\dot{\alpha}}Z_{\delta_e}}{\bar{V}} + \Delta B_q\right)\delta_e\left(t - t_d\right)$$

a. Design an ACAH hybrid adaptive flight controller for the pitch axis to enable the aircraft to follow a reference model

$$\dot{q}_m = -\omega_q \left(q_m - r\right)$$

by providing the expressions for the hybrid adaptive controller, the least-squares gradient parameter estimation of $\Delta A_{q\alpha}$, ΔA_{qq}, ΔB_q, and the optimal control modification adaptive law to handle the residual tracking error.

b. Implement the hybrid adaptive flight controller in Simulink using the same aircraft parameters from Exam Problem 12 and the following additional information: $t_d = 0.02\,\text{s}$, $\zeta_q = 0.75$, $\omega_q = 2.5$ rad/s, $\Delta A_{\alpha\alpha} = 0.1616/\text{s}$, $\Delta A_{q\alpha} = 2.1286\ /\text{s}^2$, $\Delta A_{qq} = 0.5240\ /\text{s}$, $\Delta B_\alpha = -0.0557\ /\text{s}$, $\Delta B_q = -2.5103\ /\text{s}^2$, $\alpha(0) = 0$, $q(0) = 0$, $\Delta\hat{A}_{q\alpha}(0) = 0$, $\Delta\hat{A}_{\alpha\alpha}(0) = 0$, $\Delta\hat{B}_q(0) = 0$, $R = 1000I$, $\Gamma = 1000I$, and $\nu = 0.1$ with a time step $\Delta t = 0.001\,\text{s}$. The reference command signal $r(t)$ is a pitch rate doublet specified in the following plot.

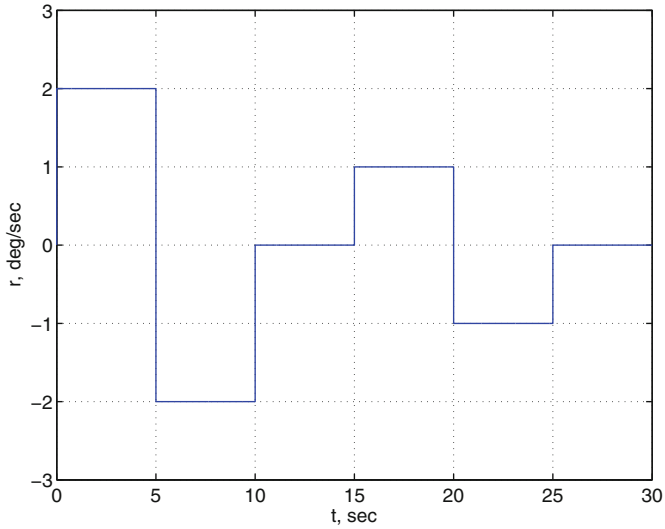

c. Simulate three cases: (1) nominal controller, (2) only direct MRAC, and (3) hybrid adaptive control with both direct MRAC and indirect least-squares gradient adaptive control. For each case, plot the time histories of each of the elements of $\alpha(t)$, $\theta(t)$, $q(t)$ and $q_m(t)$ on the same plot, and $u(t)$ for $t \in [0, 30]\,\text{s}$. In addition, plot $\Theta(t)$ for case 2; and $\Delta\hat{A}_{q\alpha}(t)$, $\Delta\hat{A}_{qq}(t)$, $\Delta\hat{B}_q(t)$ for case 3. Plot in the units of deg for $\alpha(t)$, $\theta(t)$, and $\delta_e(t)$, and deg/s for $q(t)$.

Index

A
Actuator Dynamics
  Robustness Issues, 196, 200
  Slow Actuator, 307–313
Adaptive Flight Control
  Dynamic Inversion Control, 355, 359, 409
  e Modification, 350–354
  F-18 Aircraft, 358–365
  Hybrid, 350–354
  Inner Loop, 407, 408
  Optimal Control Modification, 350–354, 359–365
  Outer Loop, 408
  Rate Command Attitude Hold, 349
  Stability Augmentation System, 406
Adaptive Linear Quadratic Gaussian
  Adaptive Flutter Suppression, 337–344
  Adaptive Law, 332, 394, 410
Adaptive Loop Recovery Modification
  Adaptive Law, 261–263, 265, 266
  Combined with Optimal Control Modification, 381, 383–385
  Flexible Aircraft Adaptive Control, 384, 386–388
Adjoint Equation, 236, 239, 241, 242, 294, 295
Aircraft Adaptive Control
  Adaptive Flight Control, 408–427
  Bi-Objective Optimal Control Modification, 363–368
  e Modification, 411–416
  Least-Squares Adaptive Control, 369
  Longitudinal Dynamics, 360–364
  Neural Network Adaptive Control, 370
  Optimal Control Modification, 411–416, 421–427
  Pitch Attitude Control, 362–364
Amplitude Saturation, 20, 21
Autonomous Systems, 18–21, 47–67

B
Barbalat's Lemma, 74–79
Barbashin–Krasovskii Theorem, 61, 62
Bi-Objective Optimal Control Modification
  Adaptive Law, 290–307
  Aircraft Adaptive Control, 310–312, 363–368
  Singularly Perturbed Systems, 309, 312

C
Cauchy Theorem, 38, 39
Chebyshev Orthogonal Polynomial Approximation, 153, 154, 367, 371
Compact Set, 37
Controllability, 111
Covariance Adjustment, 280–285
Cross-Over Frequency, 194, 197, 200, 201, 319

D
Dead-Zone Method, 212–213
Dynamic Inversion Control, 411, 413, 421

E
e Modification
  Adaptive Flight Control, 410–413
  Adaptive Law, 228–233
  Hybrid Adaptive Flight Control, 415
Energy Function, 52, 53

N.T. Nguyen, *Model-Reference Adaptive Control*, Advanced Textbooks in Control and Signal Processing, https://doi.org/10.1007/978-3-319-56393-0

Equilibrium, 23
Error Signals
  Approximation, 126
  Plant Modeling, 138, 139, 369
  Predictor, 287
  State Estimation, 129, 130
  Tracking, 88, 89

F
F-18 Aircraft Adaptive Flight Control
  Flight Validation, 353
  Optimal Control Modification, 417, 424
Fast Adaptation, 200, 201
Finite Escape Time, 27
Flexible Aircraft Adaptive Control, 382–386
  Adaptive Flutter Suppression, 387–408
  Adaptive Linear Quadratic Gaussian, 391–408
  Adaptive Loop Recovery Modification, 382–386
  Coupled Aeroelastic Flight Dynamic Model, 376–380
  Flutter Speed, 380, 387–391
  Model Reduction, 391–394
  Optimal Control Modification, 382–386, 397–399
  Singular Perturbation, 381, 391–394
Flight Validation, 4, 5, 351, 353
Function Approximation, 151–159

G
Generic Transport Model
  Damaged Aircraft, 412–419
  Flexible Aircraft, 377–380, 382
  Longitudinal Dynamics, 364, 370

H
Hamiltonian Function, 235, 239, 241, 242, 294
Hybrid Adaptive Flight Control, 414, 416

K
Kalman-Yakubovich Lemma, 331, 394

L
$\mathcal{L}_1$ Adaptive Control, 267–274
Lagrange Multiplier, 235
LaSalle's Invariant Set Theorem, 63–66
Least-Squares
  Gradient Method, 130
  Recursive, 134–137
  Regression, 126–128
Least-Squares Gradient Adaptive Control
  Aircraft Adaptive Control, 369
  Combined with Model-Reference Adaptive Control, 133–141
  Direct Adaptive Control, 168–173
  Direct Adaptive Control with Neural Network, 173–175
  Indirect Adaptive Control, 137, 139
  Predictor-Based, 369
Limit Cycle, 28
Linearization, 22, 24
Lipschitz Condition
  Global, 39
  Local, 40
Luenberger Observer Design, 330, 394
Lyapunov Equation
  Algebraic, 59, 68, 101, 242, 294
  Differential, 67–69, 242
Lyapunov Function
  Candidate, 56
  Decrescent, 71
  Definition, 55, 56
Lyapunov's Direct Method
  Autonomous Systems, 52–57
  Non-Autonomous Systems, 70
Lyapunov Theorem
  Exponential Stability, 60
  Local Stability, 57, 60

M
Model Matching Condition, 90, 100, 111
Model-Reference Adaptive Control
  Composition, 85–90
  Direct, 85, 89–96, 98–107, 109–118
  Indirect, 95–99, 105–110, 117–120
  Neural Network, 179–183, 369–370
  Nonlinear Integral Control, 197–204
  Overview, 83–85
  Robustness Issues, 186–204
  Time-Delay Margin, 257

N
Negative Definiteness, 24–27
Neural Network
  Aircraft Adaptive Control, 370
  Learning Law, 156–158
  Radial Basis Function, 155–157
  Sigmoidal Function, 155–158, 369–370
Non-Autonomous Systems, 18–20, 69–79

Nonlinear Systems, 17–28
Non-Minimum Phase Systems
  Optimal Control Modification, 322–332
  Robustness Issues, 190–193
Norm
  Matrix, 34–38
  Vector, 31–35
Normalization, 274–281

O
Optimal Control, 234–241
Optimal Control Allocation, 421
Optimal Control Modification
  Adaptive Flight Control, 411–416
  Adaptive Flutter Suppression, 396–399
  Adaptive Law, 234–254
  F-18 Aircraft, 421–427
  Flexible Aircraft Adaptive Control, 382–386
  Linear Asymptotic Property, 253–261, 317–321, 354–356, 398–399
  Output Feedback of Non-SPR and Non-Minimum Phase Systems, 314–343
  Singularly Perturbed Systems, 310–311
  Systems with Control Input Uncertainty, 285–291
Output Feedback Adaptive Control
  Observer-Based Design, 329–343, 393–399
  Single-Input-Single-Output Plant of Relative Degree 1, 322–332

P
Parameter Convergence
  Combined Least-Squares Model-Reference Adaptive Control, 145
  Least-Squares, 131–135
  Model-Reference Adaptive Control, 104–105, 177–178
Parameter Drift, 177–178
Parameter Identification, 125–148
Pendulum
  Double, 357–361
  Inverted, 354–356
Persistent Excitation, 131–135
Phase Margin, 197, 198, 200, 202, 319
Phase Plane Analysis, 24–27
Polynomial Approximation, 151–153
Pontryagin's Minimum Principle, 236
Positive Definiteness, 40–43
Predictor Model, 147, 287, 292
Projection Method, 97–99, 110, 119, 213–221

R
Radial Unbounded Functions, 60–63
Rate Limiting, 20
Rate of Convergence, 51, 52, 133
Recursive Least-Squares Adaptive Control
  Aircraft Adaptive Control, 369
  Combined with Model-Reference Adaptive Control, 141–143
  Direct Adaptive Control, 160–169
  Hybrid Adaptive Flight Control, 417
  Indirect Adaptive Control, 137–139, 143–145
  Predictor-Based, 369
Reference Model
  Model Mismatch, 333–343
  Overview, 88–90
Relative Degree, 314–318
Riccati Equation
  Algebraic, 240
  Differential, 240, 332
Robust Adaptive Control, 209, 211
Rohrs' Counterexample
  Optimal Control Modification Redesign, 320–321
  Robustness, 199, 200

S
σ Modification, 220–228
  Switching, 227, 228
Singular Perturbation
  Adaptive Control, 307–314
  Flexible Aircraft, 381–382, 390–394
  Inner Solution, 391–393
  Outer Solution, 307–310
  Tikhonov's Theorem, 308, 391–393
Spectral Radius, 36, 37
Stability, 47–79
  Asymptotic, 50–52, 60–63
  Autonomous Systems, 47–67
  Definition, 49
  Exponential, 51–53, 59–61
  Global, 60–63
  Local, 24–27, 56–59
  Lyapunov, 49
  Non-Autonomous Systems, 69–79
  Uniform, 70, 71
Steepest Descent, 130, 238
Strictly Positive Real, 314–318
Sweep Method, 239, 242

T
Time-Delay Margin, 202, 203, 257, 258
Time-Delay Systems, 193–195
Trace Operator, 35, 108
Tranversality Condition, 236, 239–241
Two-Point Boundary Value Problem, 236, 237

U
Uncertainty
  Control Input, 88, 286, 291
  Matched, 86, 87, 90
  Parametric, 85–87
  Structured, 86, 90
  Unmatched, 87
  Unstructured, 86, 176
Uniform Boundedness, 71
Uniform Continuity, 74–76
Uniform Ultimate Boundedness, 72–75
Unmodeled Dynamics
  Definition, 86, 95
  Robustness Issues, 195–200

V
Van der Pol Oscillator, 28
Verification and Validation, 6–9
Virtual Control, 399–400